Biotechnology Studies of Sulfatase 2 as a Novel Target for the Treatment of Hepatocellular Carcinoma

Sari Faisal Alhasan, BPharm, MPhil

PhD Thesis

A thesis submitted for the degree of Doctor of Philosophy in the Northern Institute for Cancer Research (NICR), Medical School, Newcastle University

January 2014

Abstract

Hepatocellular carcinoma (HCC) often arises on the background of chronic liver disease, and effective systemic treatments for HCC are limited. The disease is common globally and the majority of those affected survive less than 1 year. Expression of Sulfatase 2 (SULF2), an extracellular heparan sulfate 6-O-endosulfatase which modulates growth factor/receptor tyrosine kinase and Wnt signalling, has been reported to be increased at the mRNA level in advanced HCC. This thesis has explored the potential of SULF2 as a candidate for targeted anti-cancer therapy.

Expression of SULF2 was compared at the mRNA and protein levels in 6 HCC cell lines. The impact of SULF2 silencing on signalling pathways and cell growth was assessed *in vitro* and *in vivo* using shRNA.

Three of the 6 HCC cell lines showed high SULF2 expression at both the mRNA and protein level. The effect of SULF2 gene silencing in HCC cells was cell line-dependent, with inhibition of Wnt-3a-induced β-catenin-dependent transcriptional activity in the HuH-7 cell line and inhibition of FGF-1/2-stimulated phosphorylation of ERK, and IGF-II-stimulated phosphorylation of AKT, in the SNU-182 cell line. SULF2 suppression significantly reduced cell growth and proliferation in both cell lines. Xenograft implantation using HuH-7 cells was completely abrogated by silencing of SULF2. Microarray gene expression analysis of HuH-7 cell lines showed that SULF2 suppression dramatically upregulated catalytically active angiotensin converting enzyme 2 (ACE2) at the mRNA and protein level. The level of the ACE2 product, the hepta-peptide angiotensin 1-7 that has been reported to have anti-proliferative and anti-angiogenic activities, was also increased.

Recombinant SULF2 enzyme was produced and purified, and commercially available sulfatases were characterised, for screening of potential small-molecule inhibitors of SULF2. Together, the studies described in this thesis have shown that SULF2 is an attractive and tractable target for the treatment of HCC.

Acknowledgements

It would not have been possible to write this PhD thesis without the generous help and support of the amazing people around me, to only some of whom it is possible to give particular mention here.

Above all, I would like to thank my supervisors, Professor Herbie Newell, Doctor Helen Reeves and Doctor Gary Beale for their remarkable support throughout for which my mere expression of thanks does not suffice. Herbie, the boss, has been always an inspiration to me with his marvellous enthusiasm and passion for cancer research, not to mention his advice and unsurpassed knowledge of almost everything. The helpful advice and support of my lovely supervisor, Helen, has been invaluable on both an academic and a personal level, for which I am extremely grateful. I am also very thankful to the tremendous assistance of Gary throughout my PhD studies, where he was always available to help and give advice.

I would like to acknowledge the academic and technical support of staff in the Northern Institute for Cancer Research (NICR) in Newcastle University, particularly the support of our exceptional collaborators from the chemistry department that provided all the necessary materials and advice that proved to be indispensable throughout my research. The computer facilities of the NICR have been outstanding and always satisfied my needs.

I cannot thank enough my parents, brother, sister and relatives for all their love and support throughout, as always, for which I will be in debt for them for the rest of my life. All words of appreciation and gratitude in the world are not enough to express my thanks to these wonderful people.

Last, but by no means least, I thank Doctor Michael J. Tilby who generously helped me during my MPhil degree and recommended this brilliant project to me. I also would like to thank my friends and colleagues, especially Huw Thomas, for their support and encouragement throughout.

Table of Contents

List of Figures and Tables

A. List of Figures

B. List of Tables

List of Abbreviations

4-MUS	4-methylumbelliferyl sulfate
aa	amino acids
Ab	antibody
ABC	active β-catenin
ACE	angiotensin I converting enzyme (peptidyl-dipeptidase A) 1
ACE2	angiotensin I converting enzyme (peptidyl-dipeptidase A) 2
ACEi	ACE inhibitor
AFP	α-fetoprotein
Ang-(1-7)	angiotensin 1-7
Ang-(1-9)	angiotensin 1-9
Ang II	angiotensin II
APC	adenomatous polyposis coli
ARB	angiotensin II type 1 receptor blocker
ARS	arylsulfatase
ARSA	arylsulfatase A
ARSB	arylsulfatase B
ARSC	arylsulfatase C
ARSD	arylsulfatase D
ARSE	arylsulfatase E
ARSF	arylsulfatase F
ARSG	arylsulfatase G
AT1R	angiotensin II type 1 receptor
B2M	β2 microglobulin
BIO	6-bromo-indirubin-3'-oxime
BSA	bovine serum albumin
cDNA	complementary deoxyribonucleic acid
CK-1α	casein kinase 1α
CM	conditioned medium
CMV	cytomegalovirus

Ct	cycle threshold
DLK1	delta-like 1 homolog (Drosophila)
DNA	deoxyribonucleic acid
Dvl	dishevelled
ECM	extracellular matrix
ECRs	evolutionarily constrained regions
EGFP	enhanced green fluorescent protein
ELISA	enzyme-linked immunosorbent assay
EMATE	oestrone 3-O-sulfamate
ER	endoplasmic reticulum
ERK	extracellular signal-regulated kinase
ESCC	oesophageal squamous cell carcinoma
FBS	foetal bovine serum
FGE	Cα-formylglycine-generating enzyme
FGF	fibroblast growth factor
FGFR	fibroblast growth factor receptor
FGly	Cα-formylglycine
FI	fluorescence intensity
FZD	frizzled
GAGs	glycosaminoglycans
GALNS	N-acetylgalactosamine-6-sulfatase
GlcA	glucuronic acid
GlcNAc	N-acetylglucosamine
GlcNS	N-sulfoglucosamine
GlcNS6S	N-sulfoglucosamine-6-O-sulfate
GNS	N-acetylglucosamine-6-sulfatase
GPC3	glypican 3
GPI	glycosylphosphatidylinositol
GSK-3β	glycogen synthase kinase 3β
HB-EGF	heparin binding-epidermal growth factor
HBV	hepatitis B virus
HCC	hepatocellular carcinoma

HCT	Human Colon Tumour
HCV	hepatitis C virus
HD	hydrophilic domain
HEK 293T	Human Embryonic Kidney 293T
HGF	hepatocyte growth factor
hr	hour
hrs	hours
HS	heparan sulfate
HS6STs	heparin sulfate 6-O-sulfotransferases
HSCs	hepatic stellate cells
HSPGs	heparin sulfate proteoglycans
ICC	immunocytochemistry
IdoA	iduronic acid
IdoA2S	iduronic acid-2-O-sulfate
IDS	iduronate-2-sulfatase
IGF	insulin-like growth factor
IHC	immunohistochemistry
IPs	Immunoprecipitates
IPTG	isopropyl β-D-thiogalactoside
Km	Michaelis constant
LacI	lac repressor
LacO	lac operator
MasR	Mas receptor
min	minutes
MMP	matrix metalloproteinase
MOI	multiplicity of infection
MOIs	multiplicities of infection
MSulf1/2	mouse Sulf1/2
MU-Gal	4-Methylumbelliferyl β-D-galactopyranoside
MU-Gal,6S	4-methylumbelliferyl β-D-galactopyranoside-6-sulfate
MU-GlcNAc	4-methylumbelliferyl-N-acetyl-β-D-glucosaminide
MU-GlcNAc,6S	4-Methylumbelliferyl-6-sulfo-N-acetyl-β-D-glucosaminide

MYCN	v-myc myelocytomatosis viral related oncogene, neuroblastoma derived (avian)
NSCLC	non-small-cell lung carcinoma
NSG	NOD scid gamma
NT shRNA	Non-targeting short hairpin RNA
O.D.	optical density
ORF	open reading frame
OS	overall survival
OSCC	oral squamous cell carcinoma
p-AKT	phospho-AKT
PCDH20	protocadherin 20
PDGF	platelet-derived growth factor
p-ERK	phospho-extracellular signal-regulated kinase
qPCR	quantitative polymerase chain reaction
QSulf1	quail Sulf1
RAS	rennin-angiotensin system
rhACE2	recombinant human ACE2
RNA	ribonucleic acid
RT	room temperature
RTK	receptor tyrosine kinase
RT-PCR	reverse transcription- polymerase chain reaction
RT-qPCR	reverse transcription-quantitative polymerase chain reaction
SCCHN	squamous cell carcinoma of the head and neck
SDS-PAGE	sodium dodecyl sulfate polyacrylamide gel electrophoresis
SGSH	N-sulfoglucosamine sulfohydrolase
SLPI	secretory leukocyte peptidase inhibitor
SRB	sulforhodamine B
STS	steroid sulfatase
SULF1	sulfatase 1
SULF2	sulfatase 2
SULF1/2	SULF1 and SULF2
SUMF1	sulfatase modifying factor 1

TCF	T-cell factor
TFPI2	tissue factor pathway inhibitor 2
VEGF	vascular endothelial growth factor
Vmax	maximum rate
v/v	volume/volume
WB	western blot
WNT5A	wingless-type MMTV integration site family, member 5A
w/v	weight/volume
w/w	weight/weight

Chapter 1. Introduction

1.1. Hepatocellular Carcinoma

1.1.1. Incidence

Hepatocellular carcinoma (HCC) is the leading primary malignancy of the liver in adults and accounts for about 85% of primary liver cancers. Globally, HCC is the fifth most widespread solid tumour and the third leading cause of cancer death (Parkin et al., 2005). During the last 30 years, the incidence and deaths from liver cancer have progressively increased in the United States and other western countries (Edwards et al., 2010).

1.1.2. Aetiology

HCC arises in the background of chronic hepatitis or cirrhosis in approximately 80% of cases. Chronic infection with hepatitis B virus (HBV) or hepatitis C virus (HCV) are the commonest causes of chronic liver disease worldwide (Bosch et al., 2005), while non-alcoholic fatty liver disease (NAFLD) is now the commonest cause in western societies (Starley et al. 2010). Other factors also contribute to the aetiology of liver disease and/or HCC, including alcohol ingestion (Ribes et al., 2008), dietary exposure to aflatoxin B1 (AFB) (Wild and Gong, 2010) (Liu and Wu, 2010), obesity, diabetes mellitus (Regimbeau et al., 2004), and oral contraceptives (El-Serag and Rudolph, 2007). All these risk factors either cause genetic aberrations and lead to the formation of HCC, or create an environment where the growth of cells with genetic aberrations conferring a survival advantage is encouraged.

1.1.3. Chronologic sequence of HCC development

Hepatocarcinogenesis in humans progresses through a process that could require >30 years following the first diagnosis of chronic infection with HBV or HCV (Figure 1.1). Only a proportion of patients with chronic hepatitis develop cirrhosis or HCC.

An increased incidence of HCC occurs in the setting of cirrhosis or chronic hepatitis (Figure 1.1), and in these two conditions several events are ongoing, including the presence of a large number of dead hepatocytes, infiltration of inflammatory cells and excessive deposition of connective tissue into the liver. All these events lead to highly modified matrix structure and hepatic microenvironment (Thorgeirsson and Grisham, 2002).

Figure 1.1 depicts the sequence of events that precede the development of HCC. This sequence involves the formation of phenotypically altered hepatocytes that is followed by the development of dysplastic hepatocytes that form preneoplastic foci or nodules (Thorgeirsson and Grisham, 2002).

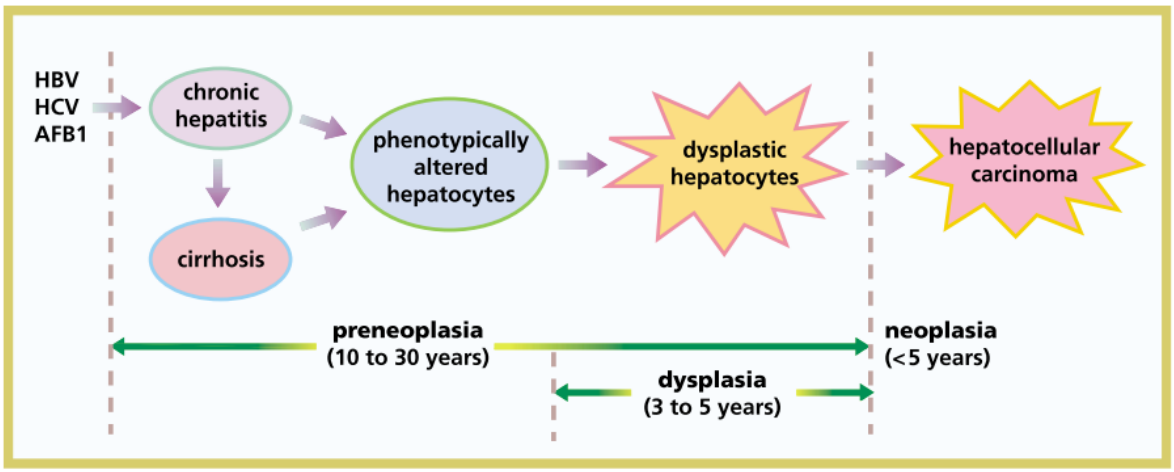

Figure 1.1: Sequential changes in the human liver that lead to the development of HCC (adapted from Thorgeirsson and Grisham, 2002).

1.1.4. Staging

In general, staging is an essential process for predicting the prognosis and guiding the management of patients with cancer. A number of staging and prognostic systems for HCC are being used currently, though none is universally adopted or regularly employed in clinical trials. This diversity in staging systems is partly attributable to the heterogeneity of the disease, but also the significant impact that the underlying liver disease and function can have on outcome. A range of clinical and radiologic parameters are encompassed into HCC scoring schemes that define specific staging systems, such as the CLIP or CUPI scores, for example

(Table 1.1) (Gallo et al., 1998) (Clark et al., 2005). These systems are proposed replacements for the traditional TNM stage used commonly in other cancer types, and there are currently three well-validated systems, namely, BCLC, JIS and CLIP (Pons et al., 2005). All these three systems depend on the Child-Pugh score which is utilized to evaluate the prognosis of chronic liver disease, particularly cirrhosis. Table 1.1 lists the different staging systems of HCC with their evaluated parameters and classifications.

Table 1.1: HCC staging systems and their evaluated variables (adapted from Pons et al., 2005).

Classification	**Type**	**Stages**	**Variables**	
			Tumour Stage	**Liver Function**
Barcelona-Clinic Liver Cancer (BCLC)	Staging	0: Very Early A: Early B: Intermediate C: Advanced D: End-Stage	Portal invasion Metastases Morphology Okuda Performance status	Child-Pugh Portal hypertension Bilirubin
The Cancer of the Liver Italian Program (CLIP)	Score	0, 1, 2, 3, 4, 5, 6	Portal invasion </> 50% liver involvement Alpha-fetoprotein	Child-Pugh
Chinese University Prognostic Index (CUPI)	Score	Low risk: ≤1 Intermediate: 2-7 High: ≥8	TNM Alpha-fetoprotein	Ascites Bilirubin Alkaline phosphatase
Estrogen Receptor (E.R.)	System	E.R. wild-type E.R. variant	Oestrogen receptor	-
French	Score	A: 0 points; B: 1-5 Points; C: ≥6 Points	Portal invasion Alpha-fetoprotein	Bilirubin Alkaline phosphatase
Japan Integrated Staging (JIS)	Score	Stage I, II, III, IV	TNM	Child-Pugh
Okuda Stage	System	Stage I, II, III	50% liver involvement	Bilirubin Albumin Ascites
Tumour-Node-Metastasis (TNM)	System	Stage I, II, III	Morphology Vascular invasion Metastases	Fibrosis

1.1.5. Treatment approaches

There have been many improvements in the prevention and management of HCC, including enhanced treatment of HCV (Tokita et al., 2005) (Kulik et al., 2006), lower frequency of HBV infection due to vaccination programs in some countries (Chang et al., 2009) (Beasley, 2009), improved screening and early detection of HCC in patients at high risk of developing the disease (Schutte et al., 2009), as well as the FDA approval of the multi-kinase inhibitor sorafenib for the treatment of patients with advanced HCC (Lang, 2008) (Kane et al., 2009).

A number of treatment approaches are available for patients with HCC; however, the only curative treatments are surgical. Resection is often not possible because of the poor regenerative capacity of the underlying chronically diseased liver. Therefore, liver transplantation is often the only potential cure, but it is applicable to only a small percentage of patients. Surgical treatments are limited to those presenting with early stage disease, with little co-morbidity (Thomas et al., 2010).

While liver transplantation is also preferred because it eradicates the risk of developing new primary tumours on the background of cirrhosis, the availability of donor organs is a severe limitation (Taura et al., 2007) (Nuzzo et al., 2007). Thus resection remains an option for those with cirrhosis which is not complicated by significant portal hypertension, and larger resections can be carried out in patients with healthy hepatic parenchyma, who do not have underlying chronic liver disease (Teh et al., 2005) (Cunningham et al., 2009).

In cases where patients are not eligible for resection or transplantation, but with a liver-confined tumour, locoregional modalities might be employed. These modalities include radiofrequency ablation (RFA), percutaneous ethanol injection, transarterial chemoembolization (TACE) and cryotherapy. These approaches are not curative but help reduce or destroy tumour and may enable a more definitive treatment such as liver transplantation at a later stage (Heckman et al., 2008) (Pompili et al., 2008) (Belghiti et al., 2008).

Clinically, HCC is resistant to chemotherapy as evidenced by the poor response to different chemotherapeutic agents. Impairment of liver function further limits the

usefulness of cytotoxic chemotherapy and both factors contribute to the lack of evidence that systemic treatment enhances overall survival (OS) of HCC patients (Simonetti et al., 1997). The multi-kinase inhibitor and anti-angiogenic agent sorafenib, which has manageable treatment-related adverse events (lethargy, gastrointestinal disturbances, hand and feet rash) has been shown to increase OS, albeit by only a few weeks (Llovet et al., 2008) (Cheng et al., 2009), and sorafenib provides “proof of concept” that targeting agents can have useful clinical activity in HCC. Therefore, there is an unequivocal requirement for safer and more effective systemic agents for advanced HCC, especially where there is liver dysfunction or sorafenib intolerance.

One potential way to improve HCC therapy is to identify a cancer-causing gene with a cancer specific expression pattern and a protein product amenable, by virtue of location and biochemistry, to small molecule inhibition. Ideally, targeting the product of this gene would elicit either a cytotoxic tumour response (i.e. partial or complete regression) or sustained tumour growth inhibition (i.e. stable disease). One such promising candidate is sulfatase 2 (SULF2), which is a member of the sulfatase gene family containing 17 different enzymes. SULF2 catalyses the desulfation of its biological substrate heparan sulfate proteoglycans (HSPGs) extracellularly, thereby regulating different signalling pathways. The following four sections will describe the sulfatase family of enzymes, the natural substrate HSPGs of SULF2, the structure and characteristics of SULF2 and the reported role of SULF2 in different types of cancer.

1.2. The Sulfatase Family

Sulfatases are enzymes that catalyse the hydrolysis of sulfate esters ($R\text{-}OSO_3^-$) and sulfamates ($R\text{-}NHSO_3^-$) as illustrated in the reactions below (Diez-Roux and Ballabio, 2005)

$$R\text{-}OSO_3^- + H_2O \rightarrow R\text{-}OH + H^+ + SO_4^{2-}$$

$$R\text{-}NHSO_3^- + H_2O \rightarrow R\text{-}NH_3^+ + SO_4^{2-}$$

This desulfating action is shared by all sulfatases, although each sulfatase has its own substrate specificity extending from complicated glycosaminoglycans (GAGs) to smaller hydroxysteroids and sulfolipids molecules (Diez-Roux and Ballabio, 2005). Currently, studies have uncovered the presence of 17 different human genes coding for genuine sulfatases, while there are only 14 in rodents (Sardiello et al., 2005). Human sulfatases can be categorized into three groups based on their cellular localization and pH-dependent functions (Sardiello et al., 2005) (Buono and Cosma, 2010), and these are listed in Table 1.2.

Table 1.2: Human sulfatases with their cellular localization and pH-dependent functions.

Cellular localization pH-dependency		*Sulfatase name*	*Symbol*	*Cytogenetic location*
Lysosomal Acidic pH-dependent		Arylsulfatase A	ARSA	22q13.3
		Arylsulfatase B	ARSB	5q14.1
		N-acetylgalactosamine-6-sulfatase	GALNS	16q24.3
		N-acetylglucosamine-6-sulfatase	GNS (G6S)	12q14.2–12q14.3
		N-sulfoglucosamine sulfohydrolase (or heparan N-sulfatase)	SGSH	17q25.3
		Iduronate-2-sulfatase	IDS	Xq28
Non-lysosomal Neutral pH-dependent	Microsomal	Arylsulfatase C (or steroid sulfatase)	ARSC (STS)	Xp22.3
	Endoplasmic reticulum	Arylsulfatase D	ARSD	Xp22.3
		Arylsulfatase F	ARSF	Xp22.3
		Arylsulfatase G	ARSG	17q24.2
		Arylsulfatase I	ARSI	5q32
		Arylsulfatase J	ARSJ	4q26
	Golgi	Arylsulfatase E	ARSE	Xp22.3
	Not determined	Arylsulfatase H	ARSH	Xp22.3
		Arylsulfatase K	ARSK	5q15
Extracellular Neutral–basic pH-dependent		Sulfatase 1	SULF1	8q13.2–8q13.3
		Sulfatase 2	SULF2	20q13.1

Regardless of their substrate specificity, sulfatases have sequence homology. Four domains constitute the protein structure: the highly conserved A, B and C and the less conserved D domains. Domains A, B and C contribute to form the N-terminus whereas D contains the C-terminus (Buono and Cosma, 2010). The active site is contained within the B domain where > 90% similarity has been found among all sulfatases, suggesting evolutionarily constrained regions (ECRs) which might be indispensable for the enzymatic activity of sulfatases (Sardiello et al., 2005).

Essential for sulfatase activity and present in the catalytic active site is a Cα-formylglycine (FGly) residue. FGly is produced posttranslationally from a cysteine residue that is contained within a consensus motif (Landgrebe et al., 2003). In eukaryotes, FGly generation occurs in the endoplasmic reticulum by the activity of FGly-generating enzyme (FGE) that is encoded by the SUMF1 (sulfatase modifying factor 1) gene (Dierks et al., 1997) (Dierks et al., 2003) (Cosma et al., 2003).

Sulfatases include asparagines which are glycosylated and are therefore regarded as glycoproteins. N-Glycosylation has been predicted for all sulfatases by bioinformatic methodology through identifying consensus sequences for N-glycosylation (Buono and Cosma, 2010). However, no crystallography data have been generated for the majority of human sulfatases, with the exception of arylsulfatases A, B and C, and no structure biology evidence for glycosylation exists. Nevertheless, it has been reported that N-linked glycosylation can control the appropriate folding, stability and assembly of glycoproteins (Helenius, 1994) (Helenius and Aebi, 2001), and proper folding of human sulfatases could similarly rely on oligosaccharide modification. For example, expression of unglycosylated iduronate-2-sulfatase (IDS) led to unprocessed and catalytically inactive enzyme (Millat et al., 1997).

1.3. Heparan Sulfate Proteoglycans

1.3.1. Structure and characteristics

Heparan sulfate proteoglycans (HSPGs) consist of one or more chains of heparan sulfate (HS) glycosaminoglycans (GAGs) that are attached to a core protein.

HSGAGs are sequences of polysaccharides made up of alternating uronic acid units (iduronic acid (IdoA) or glucuronic acid (GlcA)) and glucosamine units that are N-acetylated or N-sulfated to give N-acetylglucosamine (GlcNAc) and N-sulfoglucosamine (GlcNS), respectively (Figure 1.2) (Lamanna et al., 2007) (Bishop et al., 2007).

The HS chains are assembled in the Golgi apparatus and attached by the activity of different enzymes onto core proteins to form HSPGs. In the course of their formation, HS chains go through numerous modifications including C5 epimerization of GlcA to IdoA, N-deacetylation and N-sulfation of GlcNAc, and O-sulfation of uronic acids at C2 or of glucosamine at C6 and to a less extent at C3 (denoted 2S, 6S and 3S, respectively) (Figure 1.2) (Bernfield et al., 1999) (Perrimon and Bernfield, 2000). Sulfation is catalysed by sulfotransferases in the lumen of Golgi apparatus where 3'-phosphoadenosine 5'-phosphosulfate is the sulfate donor (Abeijon et al., 1997) (Honke and Taniguchi, 2002).

These modifications of HS chains lead to the formation of interspersed sulfated and non-sulfated fragments, and generates a high degree of heterogeneity with respect to chain stretch, location of modified fragments and the degree of epimerization and sulfation inside the fragments. Figure 1.3 depicts the three domains that contribute to HS chain structure with their compositions, namely, the highly-sulfated S domains that are flanked by the less-sulfated transition zones. Both domains are separated by non-sulfated domains (Gallagher, 2006) (Bishop et al., 2007).

HSPGs differ in their cellular localization and can be divided into three groups: the first group spans the cell membrane and includes syndecans and betagylcan, whereas members of the second group are linked to glycosylphosphatidylinositol (GPI) and include glypicans. In contrast, the third group is secreted into the extracellular space and examples include perlecan, collagen XVIII and agrin (Figure 1.4) (Bernfield et al., 1999) (Bishop et al., 2007).

(a) N-Acetylated

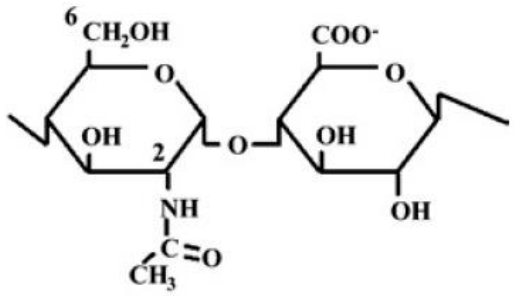

GlcNAc α1-4 GlcA

(b) N-Sulfated

variable O-sulfation

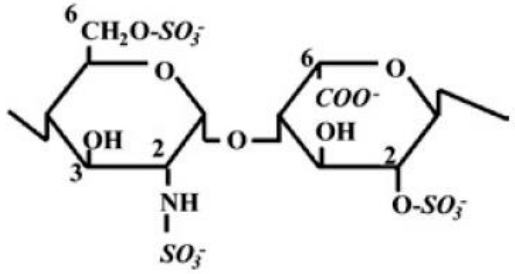

GlcNS,6S α1-4 IdoA,2S

Figure 1.2: HS disaccharide composition: The main disaccharide alternating units are GlcNAc or GlcNS and a uronic acid either GlcA or IdoA. In the case of GlcNAc, it is always connected to GlcA (a). While GlcNS is predominantly linked to IdoA (b) where they are commonly sulfated at C6 and C2, respectively. GlcNAc can also undergo C6 sulfation when neighbouring a GlcNS-containing disaccharide. Additionally, C3 sulfation of GlcNS and C2 sulfation of GlcA may occur but to a less extent (adapted from Gallagher, 2006).

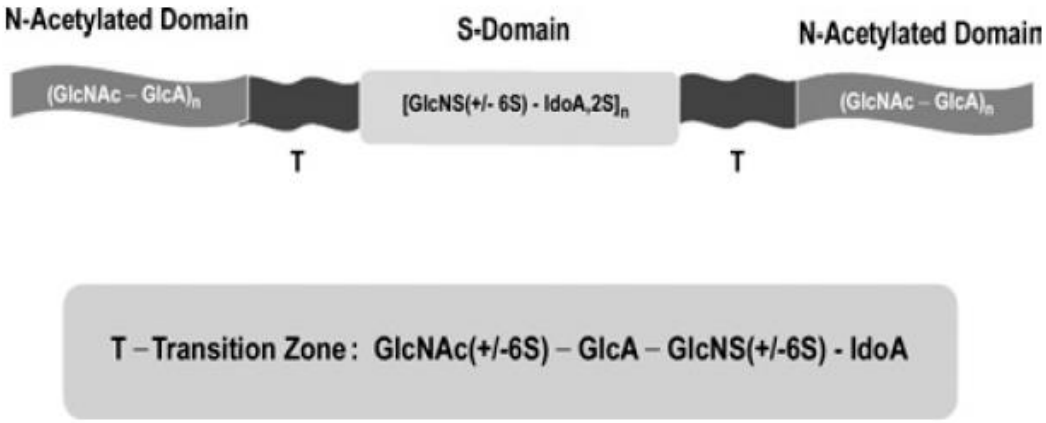

Figure 1.3: HS domain structure: HS chains can undergo different modifications including epimerization, N- and O-sulfation leading to the formation of non-sulfated (NA) domains that disperse highly sulfated (NS) S-domains, and less sulfated (NA/NS) transition zones (adapted from Gallagher, 2006).

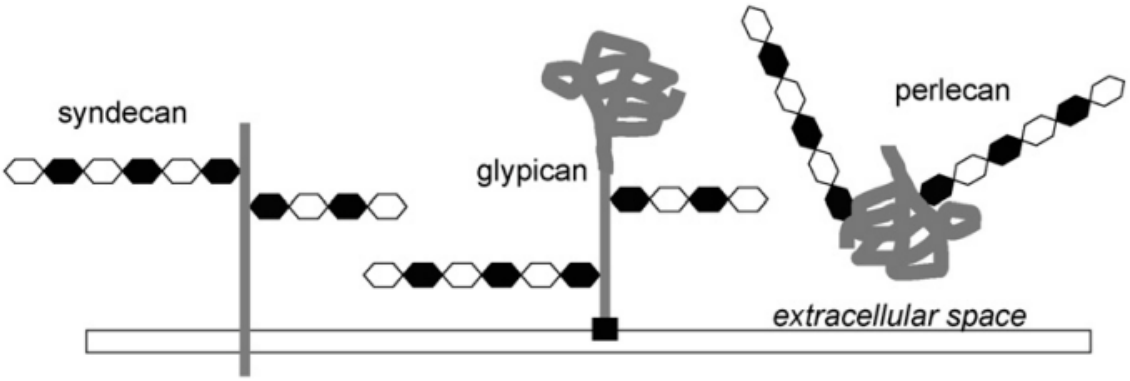

Figure 1.4: HSPG subgroups: HSPGs can be divided according to their cellular localization into three subgroups: the membrane spanning HSPGs such as syndecans, the GPI-linked glypicans, and the secreted extracellular HSPGs like perlecan (adapted from Lamanna et al., 2007).

1.3.2. Functions

The presence of uronic acid moieties and sulfate groups that are negatively charged in HS chains produces binding sites for a number of different proteins with diverse functions, as listed in Table 1.3. Consequently, HSPGs can perform a variety of signalling and structural functions (Bishop et al., 2007). HS can associate with extracellular matrix (ECM) components such as interstitial collagen, laminins and fibronectin, and it has been found to have indispensable roles in mediating interactions between cells or between cells and the ECM. Furthermore, the ability of HS to associate with different protein ligands (Table 1.3) makes the ligands more available to bind to the cell surface or ECM (Bernfield et al., 1999) (Vlodavsky et al., 2002). For example, the role of HS in facilitating the binding of fibroblast growth factors (FGFs) to their cognate receptors has been described extensively (Mohammadi et al., 2005) (Forsten-Williams et al., 2005). In contrast, the binding of HSPGs may also lead to sequestration of bioactive proteins, such as vascular endothelial growth factor (VEGF), thereby inhibiting their function. The association between HS and different ligands can also help to protect the latter from proteolytic cleavage, while in other instances HSPGs serve as co-receptors (Bernfield et al., 1999) (Vlodavsky et al., 2002).

Table 1.3: Protein ligands that interact with HS.

General Class	Examples
Growth factors	FGF-1, FGF-2, HGF, HB-EGF, VEGF, PDGF, amphiregulin
Growth factor receptor	FGFR
ECM molecules	Laminin, fibronectin, thrombospondin, fibrin, collagens, tenascin, vitronectin
Morphogens	TGF-β, BMPs, Wnts, Shh
Enzymes	Urokinase, hyaluronidase, elastase, superoxide dismutase, thrombin
Enzyme inhibitor	Antithrombin (protease inhibitor)
Cytokines	IL-7, IFN-g, IL-3, TNF-a, GM-CSF
Chemokines	IL-8, CXCL12, CCL21
Adhesion molecules	L-selectin, Mac-1, NCAM, PECAM-1

Adapted from Rosen and Lemjabbar-Alaoui, 2010 and Bishop *et al*., 2007.

FGF: fibroblast growth factor, HGF: hepatocyte growth factor, HB-EGF: heparin binding-epidermal growth factor, VEGF: vascular endothelial growth factor, PDGF: platelet-derived growth factor, ECM: extracellular matrix, FGFR: fibroblast growth factor receptor, TGF-β: transforming growth factor-β, BMPs: bone morphogenetic proteins, Shh: sonic hedgehog.

1.3.3. Modifications

Since HSPGs have numerous important functions, modification of HSPG structure provides the cells with a mechanism of response to variations in the extracellular compartment. For example, HSPGs can be modified and hence their function can be altered by the activity of heparanase that can cleave HS at specific sites by endoglycosidic activity (Vlodavsky et al., 2002). As a consequence, ligands sequestered by HSPGs, such as angiogenic factors, are released and access their receptors, thereby leading to phenotypic effects (Figure 1.5).

Another modification of HS chains concerns the sulfate group at the 6-O position of glucosamine which has been reported to be essential for the binding of several proteins to HS (Gallagher, 2001) (Habuchi et al., 2004), and three HS 6-O-sulfotransferases (HS6STs) have been found in humans and mice that catalyse the 6-O sulfation (Figure 1.2) (Habuchi et al., 2000) (Habuchi et al., 2003). Two extracellular glucosamine 6-O endosulfatases SULF1 and SULF2 (collectively, referred to as SULF1/2) counteract the effect of HS6ST by postsynthetically

catalysing the removal of 6-O-sulfate from HS at the cell surface or the ECM (Dhoot et al., 2001) (Morimoto-Tomita et al., 2002) (Ohto et al., 2002). Therefore, the sulfation status at the 6-O position of HSPGs is controlled by two groups of enzymes (the SULF1/2 and HS6STs) whose combined functions modulate a variety of signalling pathways, and a large body of evidence has accumulated indicating the important role of SULF1/2 in cancer (see Section 1.5).

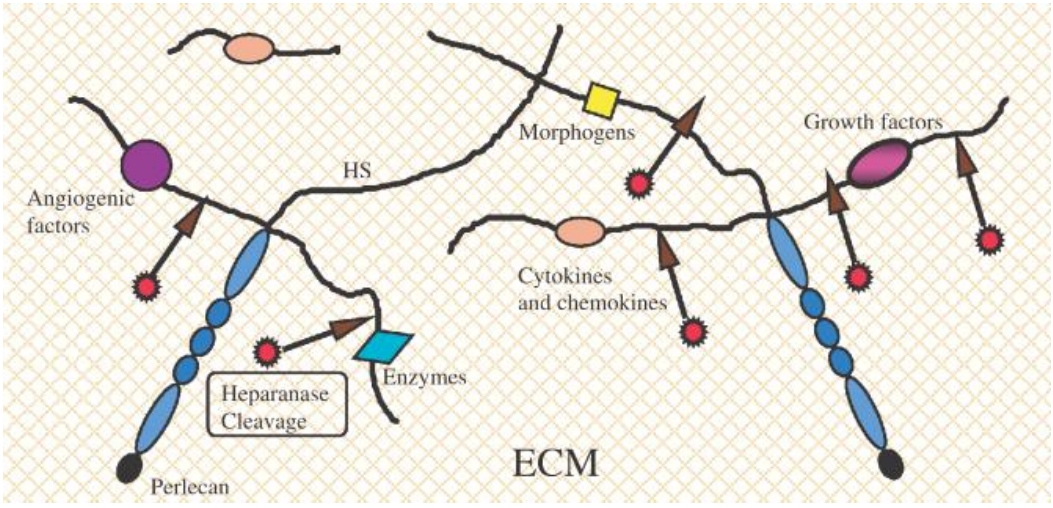

Figure 1.5: Model for the different types of protein ligands that interact with HS and their release by heparanase (adapted from Vlodavsky *et al*., 2002).

1.4. SULF1/2

1.4.1. Cloning and characterisation of SULF1/2

Dhoot *et al*. were the first to describe an avian gene termed QSulf1 in the quail embryo. This gene was thought to encode a sulfatase as it contained a domain similar to human lysosomal N-acetylglucosamine-6-sulfatase (GNS or G6S) enzyme. QSulf1 was subsequently shown to be expressed in somite muscle progenitors and to be involved in muscle specification in the quail embryo (Dhoot et al., 2001). The significance of QSulf1 discovery was underlined by its role in modulating the Wnt signalling pathway. An ortholog of QSulf1 was later identified in the rat embryo which was designated RSulfFP1 (‘floor plate 1’) because of its abundant expression in the floor plate of the evolving nervous system (Ohto et al., 2002). In 2002, Morimoto-Tomita *et al*. reported the cloning of the human and

mouse orthologs SULF1 and MSulf1, and their homologues SULF2 and MSulf2, respectively. These mammalian SULF1/2 and MSulf1/2 proteins were reported to be secreted into the conditioned media of transfected cells and to be enzymatically active (Morimoto-Tomita et al., 2002).

1.4.2. Structure of SULF1/2

As described for QSulf1 (Dhoot et al., 2001), Sulf1 and Sulf2 proteins are comprised of approximately 870 amino acids (aa) in vertebrates. Sulf1/2 genes display 64% sequence similarity (Morimoto-Tomita et al., 2002) (Lamanna et al., 2007) and share similar domain organization structure, which is depicted in Figure 1.6, starting with a secretion signal sequence followed by an N-terminal domain and a C-terminal domain. Spanning the two N- and C-terminal sulfatase domains is a basic hydrophilic domain (HD) of 300-320 aa (Table 1.4) (Figure 1.6) (Figure 1.7) (Morimoto-Tomita et al., 2002) (Rosen and Lemjabbar-Alaoui, 2010).

The N-terminal domain includes the conserved enzymatic domain that is shared by all sulfatases. Residues 415-871 (for SULF1)/416-870 (for SULF2), include the HD domain and C-terminal domain which are unique to SULF1/2 proteins, distinguishing them from other members of the sulfatase family (Figure 1.6). The C-terminal domain, however, shares a high degree of similarity with its counterpart in human lysosomal GNS (that also shares the same substrate with human SULF1/2, i.e., HS chains). This similarity of the C-terminal domain across these three enzymes may indicate a role for this domain in recognizing GlcNS/GlcNAc units of HS chains (Morimoto-Tomita et al., 2002) (Lai et al., 2008 c).

Sulf1/2 orthologs between species also show a high degree of homology with 93% and 94% aa similarity for Sulf1 and Sulf2, respectively, between human and mouse. Sulf1/2 homologues (i.e., Sulf1 and Sulf2) within the same species show 63-64% aa similarity (Morimoto-Tomita et al., 2002). As discussed earlier, the oxidation of a conserved cysteine to FGly is an early posttranslational event required to produce catalytically active SULF1/2, and takes place in a two-step reaction (Figure 1.8) (Dhoot et al., 2001) (Morimoto-Tomita et al., 2002). This

modification is vital for the enzymatic activity of SULF1/2, facilitating the hydrolysis of sulfate esters.

Table 1.4: Structures of human SULF1/2 (Morimoto-Tomita et al., 2002).

	SULF1	**SULF2**
Length (aa)	871	870
Signal peptide	1-22	1-24
N-terminal (sulfatase) domain	42-414	43-415
Hydrophilic domain (HD)	415-735	416-715
GNS-related domain	736-843	717-824
Number of N-glycosylation sites	10	11

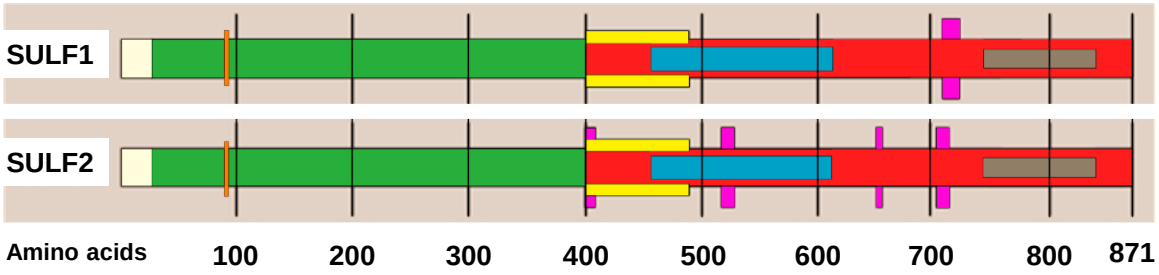

Figure 1.6: Structure of human SULF1/2: (From left to right) white: signal peptide, green: N-terminal sulfatase domain, orange line: FGly, red: HD and C-terminal domains that include: yellow: polypeptide not similar to other sulfatases, blue: region with slight similarity between SULF1/2 proteins, brown: GNS-related region, purple: HS recognition sites, rich in arginine and lysine and mainly in the HD domain, are responsible for binding of SULF1/2 proteins to their sulfated substrates and to the cell surface (Adapted from Lai et al., 2008 c).

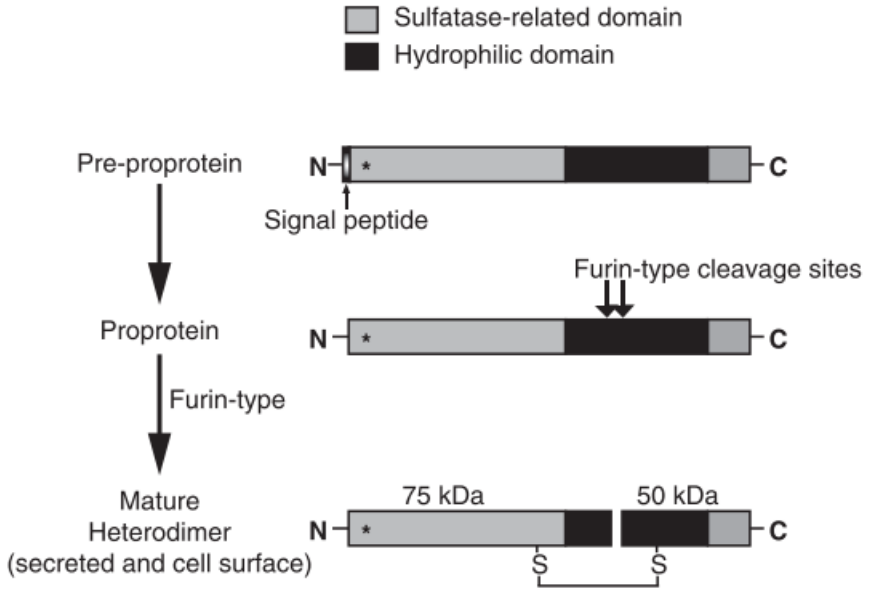

Figure 1.7: Domain organization and processing of SULF1/2: First, the signal peptide is cleaved from the SULF1/2 pre-proprotein. Second, the resulting proprotein is processed by a furin-type proteinase in the HD domain (coloured in black) to give the 75 and 50 kDa domains that are linked by disulfide bonds in the mature protein. The asterisk indicates FGly residue that is essential for activity (adapted from Rosen and Lemjabbar-Alaoui, 2010).

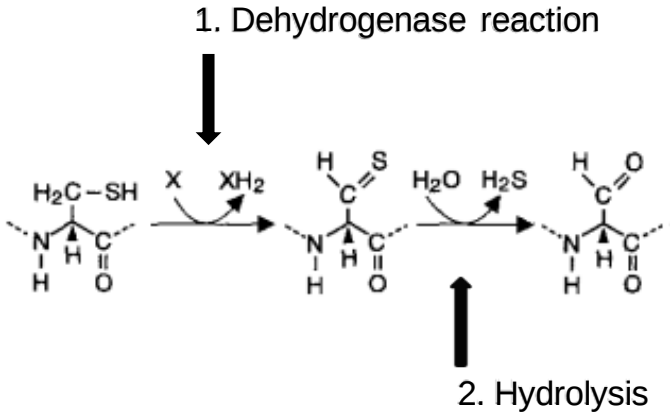

Figure 1.8: Conversion of cysteine to FGly of SULF1/2: The conversion is a two-step reaction starting with a dehydrogenase reaction followed by a hydrolysis step (Schmidt et al. 1995).

SULF1/2 enzymes are first produced as pre-proproteins from which the signal peptide is removed in the endoplasmic reticulum (ER) to give the pro-protein (Figure 1.7) (Tang and Rosen, 2009). Theoretically, the molecular mass of the human SULF1/2 proproteins should be ~ 100 kDa based on their amino acid sequence. However, by protein immunoblot the bands detected were of 132 kDa (Morimoto-Tomita et al., 2002) or 125 kDa (Tang and Rosen, 2009). This increase in mass from 100 to 132 kDa is ascribed to N-glycosylation as treating human SULF1/2 with N-glycanase gives the 100 kDa form (Morimoto-Tomita et al., 2002). Similar results have been reported in the rat after N-glycanase treatment (Nagamine et al., 2010). N-glycosylation of QSulf1 was shown to be necessary for its secretion and membrane targeting, as well as for binding to its substrate and endosulfatase activity (Ambasta et al., 2007), which may also apply to human SULF1/2.

Tang and Rosen have reported that the 125 kDa human proprotein is further proteolytically processed by two furin-type proteinase-mediated cleavages that most probably occur in the trans Glogi (Tang and Rosen, 2009) (Thomas, 2002). The cleavage sites have been identified by Edman sequencing (Figure 1.9) and found to be in the HD domains in both human enzymes (Tang and Rosen, 2009) and those in other species such as the rat (Nagamine et al., 2010). This processing of human SULF1/2 leads to the formation of 75 and 50 kDa fragments that are linked by disulfide bonding to form the 125 kDa heterodimer (Figure 1.7). Therefore, by protein immunoblot and under reducing conditions, SULF1/2 can be detected as 75 and 50 kDa bands (Tang and Rosen, 2009). Notably, many cancer cell lines studied show additional processed forms of the enzymes (Morimoto-Tomita et al., 2005) (Nawroth et al., 2007) (Lemjabbar-Alaoui et al., 2010).

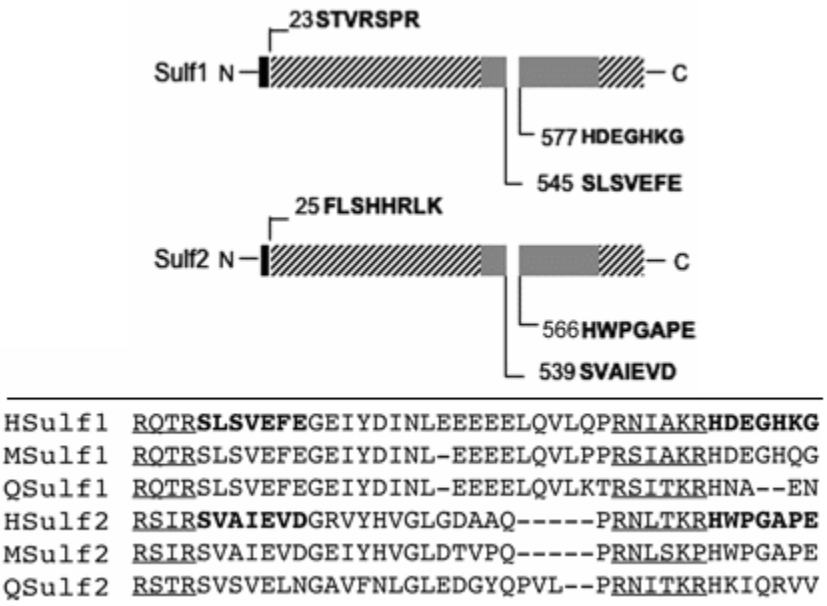


```
HSulf1  RQTRSLSVEFEGEIYDINLEEEEELQVLQPRNIAKRHDEGHKG
MSulf1  RQTRSLSVEFEGEIYDINL-EEEELQVLPPRSIAKRHDEGHQG
QSulf1  RQTRSLSVEFEGEIYDINL-EEEELQVLKTRSITKRHNA--EN
HSulf2  RSIRSVAIEVDGRVYHVGLGDAAQ-----PRNLTKRHWPGAPE
MSulf2  RSIRSVAIEVDGEIYHVGLDTVPQ-----PRNLSKPHWPGAPE
QSulf2  RSTRSVSVELNGAVFNLGLEDGYQPVL--PRNITKRHKIQRVV
```

Figure 1.9: Furin-type cleavage sites of SULF1/2: The underlined amino acid sequences identified by Edman sequencing are furin-type cutting sequences, and the sequence alignment shows that they are conserved among species.

By immunofluorescence and protein immunoblot, the mature Sulf1/2 enzymes have been found to be secreted, but also to be localized to the cell membrane in both human and mouse (Morimoto-Tomita et al., 2002) (Lamanna et al., 2008) (Tang and Rosen, 2009). In contrast, QSulf1/2 enzymes are not secreted, being retained on the cell surface (Dhoot et al., 2001) (Ai et al., 2006). This association with the cell membrane is likely mediated by the HD domains, as deletion mutations in these domains increased the secretion of the enzyme (Dhoot et al., 2001) (Ai el al., 2006) (Frese et al., 2009). Interestingly, membrane association is sensitive to high salt treatment (Morimoto-Tomita et al., 2002), revealing that it is mediated by electrostatic interactions between the negatively charged GAGs and the highly charged HD domains that are rich in arginine (R) and lysine (K), rather than trans-membrane integration (Ai et al., 2006) (Lamanna et al., 2008). The sequences that are highly rich in R and K correspond to heparin-binding motifs and serve as HS recognition sites (Figure 1.6). These HS recognition sites are included in Table 1.5 and are different between human SULF1 and SULF2 (Lai et al., 2008 c). Also, membrane fractionation into detergent-soluble and insoluble fractions showed that SULF1/2 enzymes are enriched, particularly in the insoluble fraction,

suggesting an affinity for lipid raft domains (Lamanna et al., 2008). This localization is noteworthy because lipid rafts are fundamental in several signal transduction pathways (Lingwood and Simons, 2010). Essential for this localization is the furin-type proteinase-mediated cleavage, as deletion mutation of the two furin cleavage sequences caused a significantly lower accumulation of mutant SULF1/2 into lipid rafts, without affecting the amount of secreted versus plasma membrane-retained SULF1/2 proteins (Tang and Rosen, 2009).

Table 1.5: HS recognition sites of human SULF1/2 enzymes with their sequences and locations.

Enzyme	*Sequence*	*Location*
SULF1	RRRKKERKEKRRQRK	721-735 (HD domain)
SULF2	KKKMR	402-406 (N-terminal)
	RRKKLFKKKYK	518-528 (HD domain)
	KKKR	653-656 (HD domain)
	KRKKKLRKLLKR	702-713 (HD domain)

R: arginine, K: lysine, E: glutamic acid, Q: glutamine, M: methionine, L: leucine, F: phenylalanine, Y: tyrosine.

1.4.3. Enzymatic activity of SULF1/2

As reviewed above, SULF1 and SULF2 are glucosamine 6-O endosulfatases which release the sulfate group at position 6-O primarily from trisulfated disaccharide motifs (IdoA2S-GlcNS6S) present in the highly sulfated S-domains of HS chains or in heparin (Figure 1.10) (Morimoto-Tomita et al., 2002) (Ai et al., 2003) (Saad et al., 2005) (Staples et al., 2011).

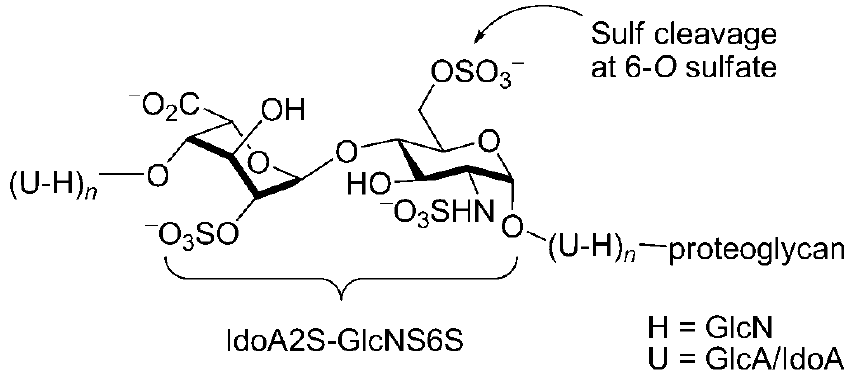

Figure 1.10: SULF1/2 enzymes remove the 6-O-sulfate in preformed HSPGs.

Even though SULF1/2 and some lysosomal sulfatases share the same substrate (i.e., HS chains), there are differences in their activity. Firstly, SULF1/2 proteins are endosulfatases and have intra-chain activity, whereas lysosomal enzymes are exosulfatases and liberate sulfate groups during degradation of proteoglycans from the termini of the chains (Diez-Roux and Ballabio, 2005). However, Staples *et al*. have shown that human SULF2 acts not only on the internal regions of HS, but also on the non-reducing ends (Staples et al., 2011). Secondly, the pH optimum for the activity of SULF1/2 is pH 7 - 8 (i.e., in the neutral-basic range), while the lysosomal sulfatases work at an acidic pH (Morimoto-Tomita et al., 2002). These pH values are consistent with the cellular localization of these two types of enzymes, namely, the cell surface and the lysosomes, respectively. However, apart from SULF1/2, there are other non-lysosomal sulfatases that have maximal activity at neutral pH. These reside in the ER or Golgi (Table 1.2) (Hanson et al., 2004) (Sardiello et al., 2005).

SULF1/2 enzymes, like most sulfatases, are capable of hydrolysing 4-methylumbelliferyl sulfate (4-MUS), which is a synthetic fluorogenic arylsulfatase substrate (Morimoto-Tomita et al., 2002). However, the affinity of 4-MUS for SULF1/2 is very low. The Michaelis constant (Km) defines an enzyme's affinity for a substrate, and is the substrate concentration at which the reaction rate is half its maximum rate (Vmax). Thus, a high Km value means that the enzyme has a low affinity for the substrate, and a high concentration is needed for the reaction to operate at half its maximum rate. Accordingly, the Km of SULF1/2 4-MUS reaction was found to be approximately 10 mM (Uchimura et al., 2006 b) (Rosen and Lemjabbar-Alaoui, 2010). Nevertheless, an arylsulfatase activity assay using 4-MUS as a substrate offers a method to measure the activity of SULF1/2 and could be used to screen for small-molecule inhibitors. In summary, SULF1/2 enzymes have both endosulfatase and arylsulfatase activities, where the former makes them unique and distinguishes them from other sulfatases.

Although the catalytic active site of SULF1/2 is located in the 75 kDa N-terminal subunit (Morimoto-Tomita et al., 2002), this subunit has been reported to be inactive when expressed alone (Tang and Rosen et al., 2009). This observation

indicates that the 50 kDa C-terminal subunit is also essential for both enzymatic activities of SULF1/2 (i.e., endosulfatase and arylsulfatase activities). This is because the N-terminal subunit lacks the most C-terminal of the ECRs that are shared by all sulfatases (Tang and Rosen et al., 2009).

With respect to the role of HD domains of SULF1/2, these are implicated in binding to the cell surface (Ai et al., 2006) (Frese et al., 2009). Also, the HD domains are involved in binding to the substrate HS; endosulfatase activity against HSPG is dependent on HS binding, as mutant SULF1/2 proteins that lack the HD domain demonstrate arylsulfatase activity against 4-MUS but not endosulfatase activity (Ai et al., 2006) (Frese et al., 2009) (Tang and Rosen, 2009). This binding of HD domains to the substrate was reported to be particularly dependent on 6-O sulfation, and hence sulfate hydrolysis facilitates the release of SULF1/2 enzymes enabling access to other regions (Frese et al., 2009).

Endosulfatase assays using heparin or HSPGs as substrates have shown similar enzymatic activity of SULF1/2 (Morimoto-Tomita et al., 2002) (Lamanna et al., 2008). Intriguingly, mutant SULF1/2 enzymes that cannot be cleaved by deletion of their furin cleavage sites maintain both arylsulfatase and endosulfatase activities, suggesting that processing of SULF1/2 proteins into their two subunits is not necessary for function (Tang and Rosen, 2009) (Nagamine et al., 2010). Nonetheless, unprocessed SULF1/2 proteins are rendered incapable of potentiating Wnt signalling, possibly due to impaired distribution of mutant SULF1/2 into membranous lipid rafts, where many components of Wnt signalling are also localized (Tang and Rosen, 2009).

Purified recombinant human SULF2 has been shown to have pro-angiogenic activity, promoting angiogenesis as evidenced by the chick chorioallantoic membrane assay. This activity of SULF2 was equivalent to that of $VEGF_{165}$, used as a positive control (Morimoto-Tomita et al., 2005), and was suggested to be due to the mobilization of HSPG-sequestered angiogenic factors in the ECM, through desulfation of HS chains by SULF2. Thus, these factors become available to bind to their signal-transducing receptors and exert their biological activity. This result is consistent with the ability of human SULF2 to mobilize $VEGF_{165}$ and reverse its

binding with immobilized heparin in an enzyme-linked immunosorbent assay (ELISA) (Uchimura et al., 2006 a).

HS chains of HSPGs have been reported to be involved in binding to a number of growth factors (Table 1.3) and their associated receptor tyrosine kinases. Also, a requirement for 6-O sulfation of HS chains for cell-surface signalling by growth factors such as FGF-1 and FGF-2 has been described (Pye et al., 1998) (Pye et al., 2000). Using X-ray crystallography analysis, DiGabriele *et al*. demonstrated a direct role of 6-O sulfation and 2-O sulfation of heparin in its binding to FGF-1 (DiGabriele et al., 1998), while no such requirement for 6-O sulfation was revealed for binding of FGF-2 to heparin (Faham et al., 1996). However, the 6-O sulfation of HS was shown to be necessary for promotion of FGF-2 activity (Guimond et al., 1993) (Pye et al., 1998), indicating a role in the interaction between HS and FGFR1 (Kan et al., 1993) (Panteliano et al., 1994). In this latter case, it is envisaged that HS works as a bridge to form the ternary complex FGF-2/HS/FGFR (Rusnati et al., 1994). Also, it has been found that both chain length and sulfation pattern (including 6-O sulfation status) of HS is involved in differential activation of FGF-1/FGF-2 signalling (Pye et al., 2000). These data were further confirmed by the ability of human SULF2 to greatly reduce FGF-1 but not FGF-2 binding to immobilized heparin (Uchimura et al., 2006 a).

Thus, 6-O sulfation of HSPGs can be modified by SULF1/2 enzymes which regulate different signalling pathways with implications for normal and pathological processes, including embryonic development, growth, chronic disease and cancer.

1.5. SULF1/2 in Cancer

1.5.1. SULF1 in cancer

The binding of a growth factor to its receptor can be inhibited by 6-O desulfation of HS chains of HSPGs by SULF1, and inhibition can abolish growth factor signalling in different types of cancers. Thus, overexpression of SULF1 in the human myeloma cell line CAG reduced tumour growth *in vivo* but not *in vitro*. This effect was attributed to inhibition of the assembly of the FGF-2 ternary signalling complex as shown *in vitro* (Dai et al., 2005). SULF1 expression was reported to be undetectable or extremely low in 77% (23 of 30) of primary ovarian carcinomas and in 71% (5 of 7) of ovarian cancer cell lines. SULF1 re-expression in ovarian cancer cell lines reduced proliferation *in vitro* and response to treatment with FGF-2 and HB-EGF, but not the response to heparinated FGF-2 or EGF (Lai et al., 2003). SULF1 expression in squamous cell carcinoma of the head and neck (SCCHN) cell lines downregulated MAPK/extracellular signal-regulated kinase (ERK) signalling pathway activation by either FGF-2 or HGF, and PI3K/AKT signalling pathway activation by HGF, with a subsequent reduction of proliferation and invasion *in vitro* (Lai et al., 2004 a). Also, SULF1 was downregulated in 60% of primary invasive breast cancer specimens, and SULF1 expression in MDA-MB-468 breast cancer cell line inhibited autocrine EGFR-mediated activation of ERK *in vitro*, which was restored after targeting SULF1 with shRNA (Narita et al., 2007). Also, in the same cell line, SULF1 expression reduced tumourigenicity and inhibited angiogenesis in nude mice *in vivo* (Narita et al., 2006).

In hepatocellular carcinoma (HCC), SULF1 was found to be downregulated in 82% (9 of 11) of HCC cell lines as evidenced by RT-PCR (reverse transcription-polymerase chain reaction), and in 29% (9 of 31) of primary HCCs as revealed by RT-qPCR (reverse transcription-quantitative polymerase chain reaction). This downregulation of SULF1 was shown to be due to loss of one allele and/or DNA (deoxyribonucleic acid) hypermethylation, as treatment of SULF1-negative HCC cell lines with a DNA methylase inhibitor reactivated SULF1 expression (Lai et al., 2004 b). As in SCCHN cell lines, SULF1 expression in HCC cell lines abrogated FGF-2- and HGF-mediated growth signalling pathways and increased sensitivity to

apoptosis (Lai et al., 2004 b). In another study, expression of SULF1 in two HCC cell lines (HuH-7 and Hep 3B) was shown to reduce tumourigenicity in xenograft models *in vivo*, while shRNA-mediated knockdown of the recombinant SULF1 in these two cell lines led to increased ERK and AKT phosphorylation (Lai et al., 2006). Collectively, these results suggest that SULF1 is a negative regulator of MAPK/ERK and PI3K/AKT signalling pathways in HCC cell lines.

Contrary to HCC, ovarian cancer and breast cancer, pancreatic cancer showed upregulation of SULF1 expression in 71% (22 of 31) of specimens by RT-qPCR, while SULF1 expression was absent in 50% (4 of 8) of pancreatic cancer cell lines. In spite of this pattern of expression, SULF1 re-expression in one of these SULF1-negative cell lines reduced basal (uninduced) and FGF-2-mediated growth and invasion *in vitro* (Li et al., 2005). The role of SULF1 was also studied in oesophageal squamous cell carcinoma (ESCC). Membranous SULF1 staining by immunohistochemistry (IHC) was positive in 48% (42 of 87) of ESCC samples as opposed to the negative staining of neighbouring benign epithelium. RT-PCR showed an absence of SULF1 expression in 3 of 7 ESCC cell lines (Liu et al., 2013). SULF1 re-expression in one of the SULF1-negative cell lines inhibited HGF signalling, as evidenced by western blot (WB), which showed inhibition of phosphorylation of the HGF receptor c-Met and the downstream mediator ERK1/2 in response to exogenous HGF (Liu et al., 2013). This effect on HGF signalling was translated into reduced proliferation and dramatically diminished HGF-mediated invasiveness of SULF1-transfected cells. Clinically, SULF1 staining was found to be inversely correlated with both tumour size and invasion, but not tumour grading or metastasis (Liu et al., 2013).

The aforementioned studies suggest that desulfation of HSPG by SULF1 abolishes growth factor signalling through interfering with the binding of growth factors with their receptors. Thus, SULF1 has a tumour suppressor effect in most types of cancer studied including myeloma, ovarian, head and neck, breast, liver, pancreatic and oesophageal cancers, even though it was found to be upregulated in pancreatic cancer and ESCC.

In another study, SULF1 mRNA was shown to be expressed in 50% (12 of 24) of pancreatic adenocarcinoma cell lines while the protein was detected only in one (HS766T) out of three cell lines that expressed SULF1 mRNA (messenger ribonucleic acid) as determined by WB. Also, SULF1 protein could be detected in the detergent lysate but not in the conditioned medium (CM) of HS766T cells (Nawroth et al., 2007). In the same study, a recombinant SULF1 protein was shown to promote Wnt signalling in SULF1-transfected Human Embryonic Kidney 293T (HEK 293T) cells in response to either Wnt-1 or Wnt-4. Interestingly, the catalytically inactive form of SULF1 that was generated by a mutation in two cysteine residues in the active site (S1ΔCC) reduced Wnt signalling by half in three cell lines that demonstrated autocrine Wnt activity even though native SULF1 protein was only detected in one of these cell lines. However, all three cell lines expressed SULF2 protein and catalytically inactive SULF2 (S2ΔCC) had the same effect of reducing Wnt signalling (Nawroth et al., 2007). These data suggest that SULF1 is a potentiator of autocrine Wnt signalling and that a functional redundancy between SULF1/2 enzymes exists at least in pancreatic cancer cell lines. The effect of SULF1 silencing on cell growth and tumourigenicity was not investigated in this latter study, and hence the role of SULF1 in pancreatic cancer has not been fully elucidated.

Similar to pancreatic cancer, in non-small-cell lung carcinoma (NSCLC), SULF1 expression was upregulated in 100% (10 of 10) of lung squamous carcinoma samples with an 18-fold change compared with the neighbouring non-malignant tissues as determined by microarray analysis. In line with the microarray data, RT-qPCR of other cases showed SULF1 upregulation in both squamous carcinoma and adenocarcinoma by 12- and 3-fold, respectively. Also, SULF1 was expressed in 19% (3 of 16) of NSCLC cell lines (Lemjabbar-Alaoui et al., 2010). However, no further studies of SULF1 in this particular type of cancer have been performed. In another study, SULF1 expression was assessed in chondrosarcoma patient samples by IHC and was found to be strongly expressed in most cases but with no statistically significant relationship to the histological grade of tumour (Waaijer et al., 2012).

The role of SULF1 in gastric cancer has also been studied. Hur *et al*. showed upregulation of SULF1 mRNA levels in gastric cancer cell lines and in 30/30 tumour tissues compared to their neighbouring benign tissues as assessed by RT-qPCR, and this was attributed to hypomethylation of SULF1 promoter (Hur et al., 2012). Also Tang *et al*. reported the upregulation of SULF1 in gastric cancer tissues at the mRNA level including cases that were Epstein-Barr virus-infected (Tang et al., 2012). Overexpression of SULF1 in one gastric cancer cell line increased tumourigenicity *in vivo* (Hur et al., 2012). Interestingly, SULF1 protein expression studied by IHC was found to be highly expressed in the stroma surrounding cancer cells, but only weakly expressed by the cancer cells themselves while very weakly or not expressed by normal mucosal cells. Furthermore, this study showed that SULF1 expression is a poor prognostic indicator for gastric cancer and correlates with increased recurrence rates and lymph node metastases (Hur et al., 2012).

Overall, SULF1 has been reported to be upregulated in certain types of cancer including pancreatic, lung, chondrosarcoma and gastric cancer. However, it was not mechanistically studied in gastric cancer where it was found to have tumour-promoting activity. Nevertheless, SULF1 acts a tumour suppressor in the majority of cancers and the effects of SULF1 are clearly tumour type- and cell line-dependent.

1.5.2. SULF2 in cancer

1.5.2.1. SULF2 in myeloma, chondrosarcoma, breast, lung, pancreatic, glioblastoma, gastric and oesophageal cancers

Similar to SULF1, SULF2 was shown to be an inhibitor of myeloma tumour growth, as forced expression in one human myeloma cell line reduced tumour growth *in vivo* but not *in vitro* through inhibiting the assembly of the FGF-2 ternary signalling complex, as evidenced by staining of tumour sections originating from injecting empty vector- or SULF2-transfected cells into immunocompromised mice (Dai et al., 2005). Also, SULF2 protein expression was found to be absent in most cases

of chondrosarcoma patient samples as assessed by IHC and staining was only focal in a small number of cases (Waaijer et al., 2012).

In contrast to SULF1, SULF2 is upregulated 7-fold in ductal carcinoma (7 samples) compared with normal breast tissues (4 samples) as evidenced by SAGE analysis, and in 30% (6 of 20) of breast carcinomas as determined by complementary DNA (cDNA) microarray. Also, SULF2 was upregulated in mouse models of breast cancer and was expressed in 38% (3 of 8) of breast carcinoma cell lines as measured by RT-PCR. SULF2 protein was secreted into the medium of the SULF2-positive cell lines as determined by WB. The secreted SULF2 in one of these cell lines, namely, MCF-7 was purified and tested and was found to be enzymatically active as shown by arylsulfatase (ARS) activity assay using 4-MUS as a substrate. However, no further investigation of the function of the endogenously expressed SULF2 was carried out in these cell lines (Morimoto-Tomita et al., 2005). In another study, SULF2 suppression in two breast adenocarcinoma cell lines (including MCF-7) and one mammary epithelial cell line was found to enhance proliferation and survival of the three cell lines and colony formation in the two adenocarcinoma cell lines (Hampton et al., 2009). Collectively, two studies (Dai et al., 2005) (Hampton et al., 2009) suggest that SULF2 works as a tumour suppressor, even though it is upregulated in breast cancer. However, as discussed below, studies suggesting that SULF2 is a tumour suppressor are in the minority.

In NSCLC, SULF2 expression was upregulated in 80% (8 of 10) of lung squamous carcinoma samples with a 3-fold change compared with the adjacent non-malignant tissues as determined by microarray analysis. In line with the microarray data, RT-qPCR of other samples showed SULF2 upregulation in both squamous carcinoma and adenocarcinoma, 4- and 3-fold upregulation, respectively. Also, SULF2 was expressed at the mRNA and protein levels in 31% (5 of 16) of NSCLC cell lines (Lemjabbar-Alaoui et al., 2010). Immunocytochemistry for SULF2 showed variable staining in 10 squamous cell carcinomas while no staining was seen in 10 adenocarcinomas or in normal airway epithelium (Lemjabbar-Alaoui et al., 2010). Knockdown of SULF2 in NSCLC cell lines by shRNA decreased cell growth *in vitro*

and tumourigenicity *in vivo*. Expression of a dominant-negative form of SULF2, in which SULF2 is mutated at two cysteine residues in the catalytic domain (S2ΔCC) that render it catalytically inactive, had the same effect of reducing cell growth *in vitro*. Also, either shRNA-mediated SULF2 knockdown or dominant-negative S2ΔCC reduced autocrine Wnt signalling, comparable to the inhibition of Wnt signalling induced by soluble Wnt antagonists such as sFRP or WIF-1. SULF2 overexpression in SULF2-positive NSCLC cell lines did not cause an increase in Wnt signalling activity while SULF2 expression in a SULF2-negative background showed a marked increase (Lemjabbar-Alaoui et al., 2010). Together, these data suggest a role for SULF2 in positively modulating Wnt signalling.

In pancreatic adenocarcinoma, IHC showed that SULF2 was expressed in 57% (4 of 7) of patient samples while RT-PCR showed that 88% (21 of 24) of pancreatic adenocarcinoma cell lines expressed SULF2 mRNA. Also, SULF2 protein was detected in four cell lines tested and was found in both the detergent lysate and the CM (Nawroth et al., 2007). As with SULF1, a recombinant SULF2 protein was shown to promote Wnt signalling in SULF2-transfected HEK 293T cells in response to either Wnt-1 or Wnt-4. Moreover, shRNA-mediated SULF2 knockdown or transfection with S2ΔCC in 3 pancreatic adenocarcinoma cell lines with an active autocrine Wnt pathway reduced Wnt signalling, cell growth *in vitro* and tumourigenicity *in vivo* (Nawroth et al., 2007). Therefore, both studies (Lemjabbar-Alaoui et al., 2010) (Nawroth et al., 2007) suggested that SULF2, like SULF1, is a potentiator of autocrine Wnt signalling.

Consistent with the lung and pancreatic cancer data, SULF2 expression was shown to be upregulated by at least 2-fold in 46% (197 of 424) of human glioblastomas as compared to normal brain. Also, SULF2 protein was expressed in 50% (29 of 57) of primary glioblastomas as demonstrated by IHC and in 67% (4 of 6) astrocytoma cell lines as evidenced by WB. SULF2 suppression in one of these cell lines by shRNA decreased cell growth and viability *in vitro* and tumourigenicity *in vivo*. By using a human phospho-receptor tyrosine kinase array, it was found that SULF2 suppression reduced the phosphorylation of several receptor tyrosine kinases of which the most affected ones were PDGFRα and

insulin-like growth factor (IGF) receptor, IGF1Rβ. On the contrary, phospho-FGFR3 was slightly increased and no effect on Wnt signalling was detected. SULF2 suppression in another cell line caused the same effect of reduced phosphorylation of PDGFRα (Phillips et al., 2012).

Similar to SULF1, SULF2 expression was found to be upregulated in gastric cancer cell lines and in tumour tissues as a result of hypomethylation of SULF2 promoter. Overexpression of SULF2 in one gastric cancer cell line increased tumourigenicity *in vivo* (Hur et al., 2012). Interestingly, this upregulation of SULF2 expression in gastric cancer and the effect on the tumourigenicity of gastric cells was less marked than for SULF1 (Hur et al., 2012).

Lastly, SULF2 has been studied by IHC in invasive oesophageal cancer and found to be expressed in all squamous cell carcinoma cases (25 of 25) and in 91% of adenocarcinoma cases (68 of 75), with 49% and 36% of tumour cells staining positive for SULF2, respectively (Lui et al., 2012). Clinically, there was an inverse correlation between the percentage of SULF2-positive tumour cells and survival of patients (Lui et al., 2012).

Taken together, the above studies demonstrate upregulation of expression and an oncogenic role for SULF2 in many types of cancer including lung, pancreatic, glioblastoma, gastric and oesophageal cancers, in addition to hepatocellular carcinoma which is discussed in detail below.

1.5.2.2. SULF2 in HCC

1.5.2.2.1. *In vitro* data

SULF2 mRNA has been reported to be upregulated in 57% (79 of 139) of HCC specimens compared with neighbouring benign tissues and in 73% (8 of 11) of HCC cell lines as assessed by microarray and RT-qPCR (Lai et al., 2008 a). SULF2 protein was also upregulated in HCC as assessed by IHC and WB (Lai et al., 2010 a).

By microarray analyses of gene expression, Lee *et al*. were able to define two discrete HCC subclasses (A and B) which were related to HCC patient survival.

Subclass A was associated with a poorer prognosis than subclass B (Lee et al., 2004). In an independent study of SULF2 expression in the two HCC prognostic subclasses, tumours with a cluster A profile were predominant in the high SULF2 group (93%) compared with the low SULF2 group (12.5%) (Lai et al., 2008 a). Also, the high SULF2 group was associated with higher proliferation and lower apoptosis indices as assessed by IHC using Ki-67 proliferation assay and TUNEL-based apoptosis assay (Lai et al., 2008 a). Consistent with these results, forced SULF2 expression in the SULF2-negative Hep 3B cell line increased proliferation and migration while the opposite effect was shown after knockdown of SULF2 in SULF2-positive HuH-7 cell line using shRNA (Lai et al., 2008 a).

SULF2 was reported to upregulate glypican 3 (GPC3) as shown by immunocytochemistry (ICC) and WB, and to promote both FGF-2 growth factor and Wnt/β-catenin signalling pathways (Lai et al., 2008 a) (Lai et al., 2010 b). With respect to FGF-2 signalling, forced expression of SULF2 was shown to increase FGF-2 binding to the cell surface as evidenced by flow cytometry. This binding was demonstrated to be significantly inhibited by heparin suggesting specific binding of FGF-2 to HS chains. Also, forced SULF2 expression increased the phosphorylation of FGF-2 signalling downstream mediators, ERK and AKT either at the basal level or after stimulation with FGF-2 (Lai et al., 2008 a), while SULF2 knockdown decreased AKT phosphorylation as shown by WB (Lai et al., 2010 a). Regarding the Wnt signalling pathway, the binding of Wnt-3a to Hep 3B cells was shown to be dependent on HS chains as demonstrated by flow cytometry (Lai et al., 2010 b). Forced expression of SULF2 in these cells upregulated Wnt-3a and promoted Wnt/β-catenin signalling pathway activity as shown by increased levels of Wnt-3a, β-catenin, cyclin D1 and the inactive phosphorylated form of GSK-3β (glycogen synthase kinase 3β) using WB and ICC. Wnt activation was assessed using the T-cell factor (TCF)-luciferase reporter system. This role of SULF2 in promoting Wnt signalling was confirmed by downregulation of SULF2 in HuH-7 cells using shRNA, which showed inhibition of basal Wnt signalling (Lai et al., 2010 b). Interestingly, both FGF-2 and Wnt-3a binding to HCC cells was shown to be mediated by GPC3 as shRNA-mediated knockdown of GPC3 decreased binding (Lai et al., 2008 a)

(Lai et al., 2010 b). This latter result suggests a requirement for GPC3 in the SULF2-mediated enhancement of FGF-2 and Wnt signalling pathways *in vitro*.

Forced expression of SULF2 in HCC cells was also shown to improve their resistance to drug-induced apoptosis, whereas SULF2 knockdown demonstrated the opposite effect including downregulation of the anti-apoptotic protein Bcl-2 and upregulation of the pro-apoptotic protein BAD (Lai et al., 2010 a).

1.5.2.2.2. *In vivo* data

SULF2 expression in the SULF2-negative Hep 3B cells was found to increase tumourigenicity after implantation into immunocompromised mice as demonstrated by the faster growth of the tumours derived from SULF2-transfected cells compared to those established from empty vector-transfected cells. There was also upregulation of GPC3 levels as evidence by IHC analysis of xenograft sections from SULF2-transfected tumour (Lai et al., 2008 a).

1.5.2.2.3. Clinical data

Increased SULF2 expression was found to be associated with high proliferation and low apoptosis indices, and related to poor prognosis and high recurrence rate after resection (Lai et al., 2008 a).

In summary SULF2, unlike SULF1, has an oncogenic effect in the majority of the cancer types studied, including HCC. This effect is ascribed to activation of two signalling pathways in particular, the first of which is growth factor and receptor tyrosine kinase (RTK) signalling leading to activation of downstream kinases ERK and AKT. The second is Wnt signalling which leads to β-catenin-dependent transcriptional activation (Figure 1.11).

Unexpectedly, even though SULF1 and SULF2 demonstrate differing effects on RTK signalling, both activate Wnt signalling. While SULF1/2 proteins have a conserved N-terminal sulfatase domain, they diverge in the rest of their structures which contain distinct HS recognition sites between SULF1/2 enzymes as described earlier. These sites are implicated in binding to HS chains and could explain the dissimilarity in the functional activities of SULF1/2 enzymes in cancer.

This suggestion is in line with the reported effects of murine MSulf1/2 enzymes in knockout mouse models where, in spite of the existence of some degree of functional redundancy between MSulf1/2 enzymes, single knockouts have similar, but not equal, effect on phenotype and HS structure (Lamanna et al., 2008) (Kalus et al., 2009) (Nagamine et al., 2012). Neither MSulf1- nor MSulf2-knockout mice exhibited significant phenotypic or developmental abnormalities. In contrast, double knockout mice showed neonatal lethality accompanied with mild skeletal and renal defects (Holst et al., 2007) (Ratzka et al., 2008). MSulf2-knockout mice were in general viable and fertile but with strain-specific reduced body mass and mild lung or brain defects (Lum et al., 2007) (Kalus et al., 2009).

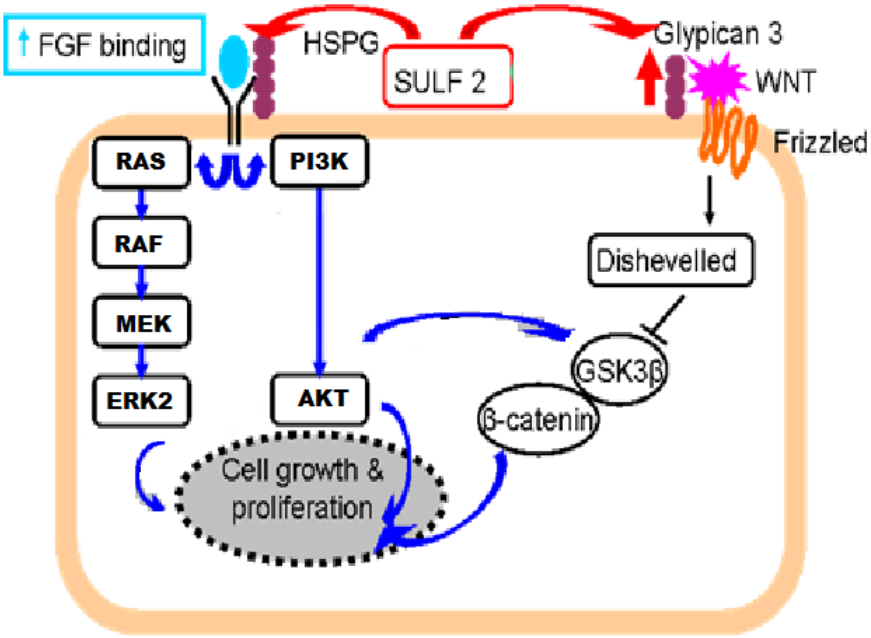

Figure 1.11: The role of human SULF2 on signalling pathways in HCC: SULF2 promotes FGF binding to the cell-surface, and FGF-induced ERK and AKT activation, and upregulates glypican 3 (GPC3) which promotes Wnt signalling.

1.6. Project Objective

Molecular biology and functional studies were undertaken to further validate SULF2 as a therapeutic target in HCC, investigate mechanisms by which SULF2 promotes cancer cell proliferation and tumourigenicity, and develop cell-free and cell-based assays to support the discovery and development of SULF2 inhibitors.

Hypotheses to be tested

- SULF2 knockdown in human cancer cells inhibits proliferation *in vitro* and tumourigenicity *in vivo*.
- SULF2 inhibition inhibits signalling pathways in a cell-type dependent manner.

Plan of investigation – 4 components

1. ***Definition of the relative contributions of SULF1 and SULF2 to proliferation and tumourigenicity in HCC cell lines:***

SULF2 is one of two cell surface sulfatases. In contrast to SULF2, SULF1 can prevent cell growth in a tumour type dependent manner, i.e. SULF1 can reduce growth factor/receptor binding and signalling, cell growth and *in vivo* tumour growth. The role of SULF1 in liver cancer has not been clearly defined. While SULF1 mRNA is often undetectable in liver cancer cell lines, this most likely occurs as a result of acquired DNA methylation as loss of SULF1 mRNA expression is a relatively uncommon event in resected primary tumours (Lai et al., 2008 c). The possibility, however, that in some instances SULF1 loss contributes to loss of tumour suppressor activity in liver cancers (Lai et al., 2004 b) (Lai et al., 2006) needs to be carefully considered. SULF1 or SULF2 shRNA were transfected into HCC cell lines with pre-established SULF1 and SULF2 backgrounds, and effects on proliferation and tumourigenicity determined. An understanding of the relative roles of SULF2 and SULF1 in liver tumour cell proliferation and survival was used to inform the target compound profile for SULF2 inhibitor design, i.e. is a selective SULF2 or a dual SULF1/2 inhibitor preferable?

2. ***Investigation of the cellular signalling pathways relevant to SULF2-mediated proliferation and tumourigenicity:***

SULF2 has been implicated in the regulation of two key cell signalling pathways that are involved in multiple tumour types: HSPG-binding growth factor signalling, notably FGF signalling, and the Wnt pathway. Small molecule FGF receptor tyrosine kinase, MEK and Wnt signalling inhibitors were used as positive controls in experiments to probe the role of FGF or Wnt signalling in SULF2-regulated HCC cell growth and survival. The HCC cell lines were selected from an existing panel (SNU-182, SNU-475, HuH-7, HepG2, Hep 3B, PLC/PRF/5) and includes those that have already been shown to be sensitive to SULF2 knockdown (Lai et al., 2008 a).

3. ***Development of cell-free and cell-based assays to support the discovery and development of SULF2 inhibitors:***

The evaluation of potential small molecule SULF2 inhibitors developed by the CR UK Programme requires SULF1 and SULF2 enzyme assays and counter screens which were established using the fluorogenic substrate 4-methylumbelliferyl sulfate (Morimoto-Tomita et al., 2005) (Uchimura et al., 2006 b). Assays to study the effects of compounds on cell growth and tumourigenicity were established, supported by mechanistic studies.

4. ***Development of predictive and pharmacodynamic biomarkers to support the preclinical and clinical development of SULF2 inhibitors:***

The successful development of targeted therapies requires a well-defined biomarker strategy and the cellular assays developed will be translated into biomarker assays as SULF1/2 inhibitors suitable for *in vivo* evaluation become available. Specifically, a microarray gene expression analysis was conducted after SULF2 knockdown to define possible markers.

Chapter 2. Materials and Methods

2.1. Reagents

4-Methylumbelliferyl sulfate (4-MUS) potassium salt (Sigma) (purity ≥ 99.95%, impurity ≤ 0.05% (w/w) by free 4-methylumbelliferone) was dissolved in H_2O to give a stock solution at 15 mM. 4-Methylumbelliferyl-6-sulfo-N-acetyl-β-D-glucosaminide (MU-GlcNAc,6S) (Merck), 4-methylumbelliferyl-N-acetyl-β-D-glucosaminide (MU-GlcNAc) (Merck) and 4-methylumbelliferyl β-D-galactopyranoside-6-sulfate (MU-Gal,6S) (Sigma) were dissolved in H_2O to give a stock solution at 10 mM. 4-Methylumbelliferyl β-D-galactopyranoside (MU-Gal) (Sigma) was dissolved in DMSO at 100 mM. Oestrone 3-O-sulfamate (EMATE) (purity ≥ 98%, Sigma) was dissolved in DMSO to give a stock solution at 2 mM. P-Nitrocatechol sulfate (PNCS) (Sigma) was dissolved in H_2O to give a stock solution at 6 mM. β-Glucosidase was from almonds (Sigma) and β-galactosidase was from *Escherichia coli* (*E. coli*) (Sigma). FGF-1, FGF-2, IGF-I, IGF-II and VEGF-165 were from Cell Signalling. Angiotensin 1-7 and angiotensin II acetate salt hydrates (Sigma) were dissolved in PBS.

2.2. Cell Culture

Cells were incubated in a SANYO CO_2 incubator (5% CO_2, 37°C and 100% humidity) and were handled in a class II laminar flow BioMAT^2 hood under sterile conditions. All HCC cell lines were cultured in DMEM (Dulbecco's modified Eagle's medium) nutrient mixture F-12 HAM with 15 mM HEPES (Sigma). All culture media were supplemented with 10% (v/v) foetal bovine serum (FBS) (Sigma), 2 mM L-glutamine (Sigma), antibiotics (100 unit/ml penicillin and 100 µg/ml streptomycin) (Sigma). The medium was changed every two days and the cells were subcultured once a week. For the cell-based arylsulfatase (ARS) activity assay, the cells were cultured in phenol red-free DMEM with 1000 mg glucose/L (Sigma) with all the other supplements as described above. For transfection, Opti-MEM I reduced-serum medium with GlutaMAX (Invitrogen) and without antibiotics was used.

Subculturing cells: The medium was aspirated and the adherent cells were washed with PBS followed by detaching the cells using trypsin-EDTA solution (Sigma) (0.5 g trypsin/L and 0.2 g EDTA/L in PBS). After incubation for 5 minutes (min), culture medium was added to block the trypsin and the cells were resuspended diluted and transferred into new culture plates or flasks.

Freezing cells: After trypsinization and blocking trypsin, the cells were centrifuged at 1,000 xg for 5 min (Mistral 3000i, DJB Labcare) and the supernatant was aspirated. The cell pellet was resuspended in freezing medium (10% (v/v) DMSO in culture medium; freshly prepared), pipetted into cryovials (1 ml per vial each containing $1x10^6$ cells), put in cryochamber filled with isopropyl alcohol (Cryo 1C freezing container, Nalgene) to achieve -1°C/min rate of cooling, stored at -70°C freezer for short-term storage and then transferred into liquid nitrogen for long-term storage.

2.3. Transformation, Plasmid Propagation and Purification

Transformation: 0.5 µg of plasmid DNA was mixed with one vial of One Shot TOP10 chemically competent *E. coli* (Invitrogen). The mixture was kept on ice for 25 min, incubated for 1 min at 37°C and then placed on ice. 200 µl of S.O.C (Super Optimal broth with Catabolite repression) medium (Novagen) was added and following incubation for 1 hour at 37°C with shaking, transformed bacteria were streaked on an agar petri dish containing the appropriate selective antibiotic (25 µg/ml kanamycin or 100 µg/ml ampicillin) and incubated overnight at 37°C. A single colony was picked and transferred into 2 ml LB (Luria Bertani) medium containing the appropriate antibiotic. LB medium was prepared by suspending 20 g of LB broth powder (Sigma) in 1 liter of distilled water followed by autoclaving. After an overnight incubation at 37°C in an orbital shaker, the culture was diluted 1:500 in 200 ml LB medium with the selective antibiotic and incubated overnight with shaking. Bacteria were centrifuged at 6000 xg for 15 min at 4°C and then stored at -20°C after discarding the supernatant.

Plasmid purification: This was performed using HiSpeed plasmid purification maxi kit (Qiagen) and according to the manufacturer's protocol.

2.4. Transfection of Cells Using SULF1/2 Plasmids

TrueORF Myc-DDK-tagged ORF clones of human SULF1 (RC216632) and human SULF2 (RC212675) were used as transfection-ready DNA (OriGene). The open reading frames (ORF) of SULF1 (ORF Size: 2616 bp) or SULF2 (ORF Size: 2613 bp) were inserted at the multiple cloning site of the PrecisionShuttle pCMV6-Entry vector (Figure 2.1). Sgf I and Mlu I restriction enzymes were used for cloning. The ORF was inserted under a cytomegalovirus (CMV) promoter to allow for constitutive expression of the protein which was fused with a C-terminal MYC/DDK tag that can be used for antibody-based detection and purification. The plasmid confers resistance to neomycin (and its analogue, G418) and is used as a selectable marker.

Lipofectamine (Invitrogen) or FuGENE HD (Promega) transfection reagents were used to transfect cells. A pCI-neo/EGFP plasmid that constitutively expresses EGFP (enhanced green fluorescent protein) was used for optimisation of transfection conditions. Transfection was performed by testing different ratios of transfection reagent to DNA and by scaling up the whole transfection mixture (i.e., transfection reagent plus DNA) to choose the condition that gave the highest transfection efficiency for each single cell line.

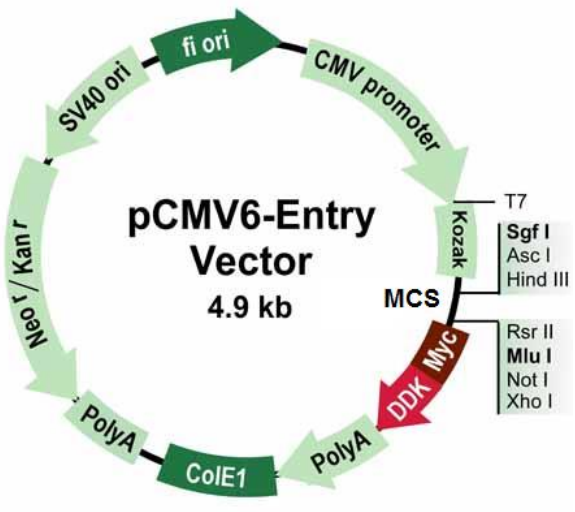

Figure 2.1: Map for PrecisionShuttle pCMV6-Entry vector. The open reading frame of SULF1 or SULF2 were inserted at the multiple cloning site (MCS) of the vector.

Stable transfection: cells were cultured until they reach 80% confluency. The transfection reagent or the plasmid DNA were incubated separately for 5 minutes in 100 µl of serum- and antibiotic-free medium or Opti-MEM medium that was pre-warmed to room temperature (RT). After incubating the transfection reagent/DNA mixture at RT for 25-45 minutes for lipofectamine or for up to 10 min for FuGENE, the mixture was added to the wells containing serum- and antibiotic-free culture medium which was changed into normal culture medium after 24 hours. G418 was used for selection at a concentration of 800 µg/ml and was added after 48 hours. The medium was changed every 3 days and the antibiotic was replenished with every medium change. At the end of the selection period, determined by the death of all control untransfected cells, different colonies were picked either by cloning cylinders (for HuH-7 and Hep 3B) or by dislodging colonies using the tip of 20 µl pipette set at 10 µl (for HepG2). The colonies were expanded under a selection pressure of 400 µg/ml G418.

Transient transfection: The same protocol for stable transfection was performed where the transfection reagent/DNA mixture was added into Opti-MEM medium. The medium was changed into serum-containing medium after 24 hours.

2.5. Generation of SULF2 Lentiviral Particles and Their Transduction into Cells

Generation of SULF2 lentiviral particles: Three constructs were used for the generation of SULF2 recombinant vesicular stomatitis virus G protein (VSV-G)-pseudotyped lentiviral particles. These were: (1) Precision LentiORF SULF2 clone (Open Biosystems) where SULF2 ORF was inserted into the pLOC vector with dual marker cassette that allows for the expression of SULF2, nuclear localized TurboGFP and blasticidin resistance gene from the same CMV promoter (Figure 2.2); (2) envelope plasmid (pMD2.G*);* and (3) packaging plasmid (pCMV_dR8.91). The maps of all constructs are shown in Figure 2.2. Plasmid-containing bacteria were first amplified from glycerol stocks using 100 µg/ml ampicillin (Sigma) as a bacterial selection marker and then the plasmids were propagated and purified as described in Section 2.3.

HEK 293T cells were used to produce the lentiviral particles according to a published protocol (Naldini et al., 1996). $3x10^5$ cells were cultured in a 10 cm dish and then co-transfected with a mixture of the three aforementioned plasmids (20 µg of LentiORF SULF2 plasmid, 5 µg pMD2.G plasmid and 15 µg pCMV_dR8.91 plasmid) using the calcium phosphate transfection method. After overnight incubation, cells were washed with PBS and fresh medium was added. Lentiviral particles-containing conditioned medium was collected after 3 days which approximately contains 10^6 transducing units (TU)/ml. Following centrifugation at 1,800 xg for 15 min at 4°C and filtration using a 0.45 µm filter to remove cell debris, the viral supernatant was concentrated 10-fold by centrifugation at 120,000 xg for 2 hours at 4°C in an Optima XL-100K ultracentrifuge (Beckman Coulter). The supernatant was discarded and viral pellet was resuspended in serum-containing medium and stored as aliquots at -80 °C.

Transduction of SULF2 lentiviral particles into cells: $3x10^5$ Hep 3B cells/well were seeded in a 6-well plate. Different volumes of lentiviral particles-containing medium with 8 µg/ml hexadimethrine bromide (Polybrene, Sigma) were added. After overnight incubation, the medium was replaced by a fresh medium and 24 hours later cells were selected using 1 µg/ml blasticidin S hydrochloride (Sigma) until formation of colonies. Colonies were then picked by dislodging using the tip of 20 µl pipette set at 10 µl and after bulk cultures were established analysed using WB, immunocytochemistry and ARS activity assay.

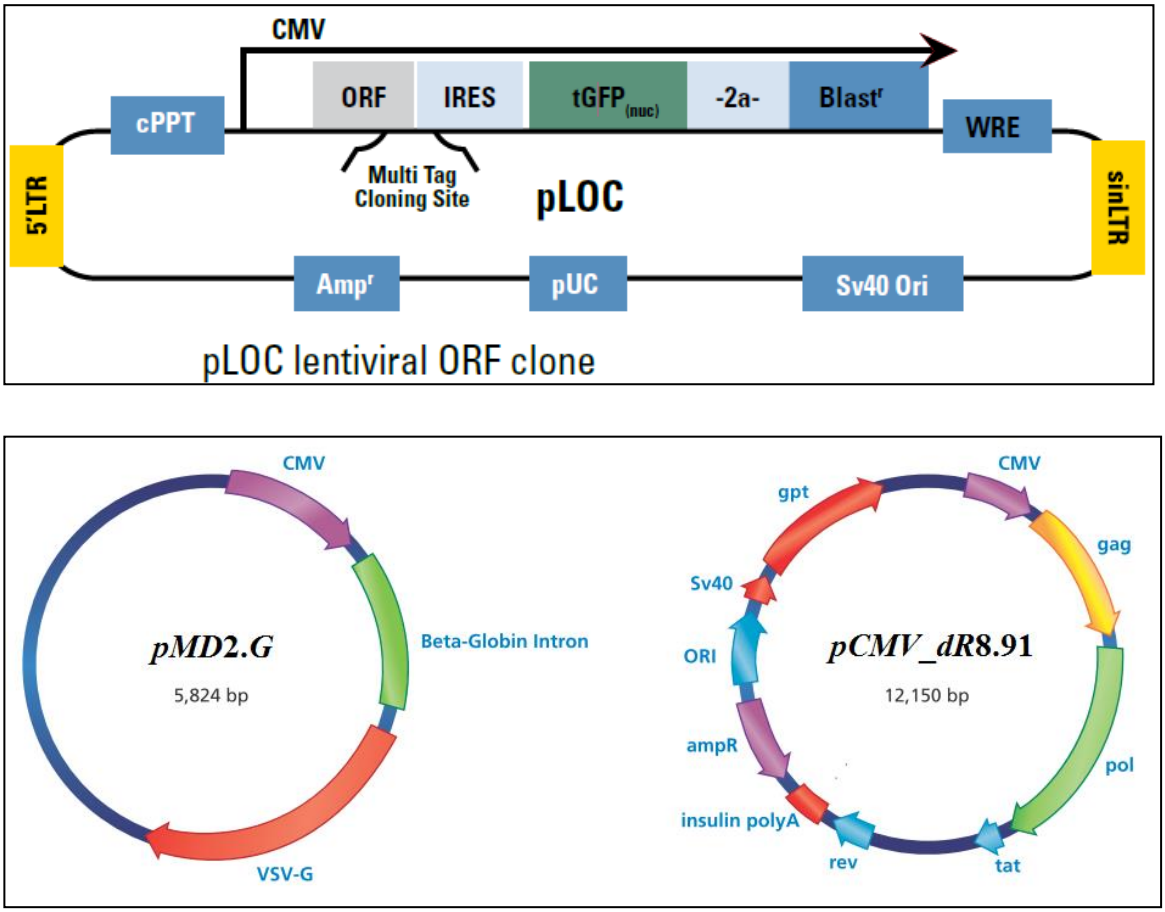

Figure 2.2: Maps of the plasmids used to generate SULF2 lentiviral particles: Top: Precision LentiORF SULF2 clone where the open reading frame of SULF2 was inserted at the multiple cloning site of the pLOC vector. Bottom panel left: envelope plasmid (pMD2.G). Bottom panel right: packaging plasmid (pCMV_dR8.91).

2.6. SULF1 and SULF2 Knockdown Using shRNA Lentiviral Particles

A target set of 5 individual clones of mission TRC1 or TRC2 shRNA lentiviral particles (Sigma) for either SULF1 or SULF2 was used for gene silencing where different shRNA sequences (listed in Table 2.1 and Table 2.2) were inserted into the TRC1.5-pLKO.1-puro or TRC2-pLKO-puro vector and directed by the human U6 promoter. Figure 2.3 shows the map of the TRC2 vector which is only different from the TRC1.5 vector in that it contains the Woodchuck hepatitis virus post-transcriptional regulatory element (WPRE) which enables enhanced expression of the shRNA (Zufferey et al., 1999). For inducible shRNA lentiviral particles, the

pLKO vector was designed to include a LacI (repressor) and a modified U6 promoter with three LacO (operator) sequences (2 in the promoter and one 3' of it) (Figure 2.4).

$1x10^5$ cells/well in a 12-well plate were infected with different multiplicities of infection (MOIs) values of either individual SULF1 or SULF2 shRNA lentiviral particles or TRC2-pLKO-puro non-targeting shRNA control transduction particles (Sigma) in the presence of 8 µg/ml hexadimethrine bromide (Sigma). For stable transduction, the medium was replaced after overnight incubation by a fresh medium. 1 day later, the transduced cells were selected using 1 µg/ml (for SNU-182) or 2 µg/ml (for HuH-7 or HepG2) puromycin dihydrochloride (Sigma) until all control untransduced cells were killed.

Non-targeting shRNA (NT shRNA) sequences have four base pair mismatches to any known human gene. The sequences of both constitutive and inducible NT shRNAs used are listed in Table 2.3.

Table 2.1: shRNA sequences of mission TRC1 or TRC2 SULF1 shRNA lentiviral particles.

TRC number	Region	Sequence
TRCN0000051098*	CDS	CCGGCCCAAATATGAACGGGTCAAACTCGAGTTTGACC CGTTCATATTTGGGTTTTTG
TRCN0000051099*	CDS	CCGGCCAACACATAACTCCTAGTTACTCGAGTAACTAGG AGTTATGTGTTGGTTTTTG
TRCN0000373588	CDS	CCGGGCGAGAATGGCTTGGATTAATCTCGAGATTAATCC AAGCCATTCTCGCTTTTTG
TRCN0000373589	3′ UTR	CCGGTCTGGTGGACTGGACTAATTACTCGAGTAATTAGT CCAGTCCACCAGATTTTTG
TRCN0000373658	CDS	CCGGGCCGACCATGGTTACCATATTCTCGAGAATATGGT AACCATGGTCGGCTTTTTG

Clones marked by asterisks are TRC1-version lentiviral particles while the rest are TRC2-version lentiviral particles. CDS: coding sequence; 3′ UTR: 3′ untranslated region.

Table 2.2: shRNA sequences of mission TRC2 SULF2 shRNA lentiviral particles.

TRC number	Region	Sequence
TRCN0000364454	CDS	CCGGCCCACATCGTCCTCAACATTGCTCGAGCAATGTTGAGGACGATGTGGGTTTTTG
TRCN0000364517	CDS	CCGGGGACAACACGTACATCGTATACTCGAGTATACGATGTACGTGTTGTCCTTTTTG
TRCN0000364518	3′ UTR	CCGGGGGCGAAAGTCATTGGAATTTCTCGAGAAATTCCAATGACTTTCGCCCTTTTTG
TRCN0000369076	CDS	CCGGTGCACATCGACCACGAGATTGCTCGAGCAATCTCGTGGTCGATGTGCATTTTTG
TRCN0000376409	CDS	CCGGTGCGGATATGGACGGGAAATCCTCGAGGATTTCCCGTCCATATCCGCATTTTTG

CDS: coding sequence; 3′ UTR: 3′ untranslated region.

Table 2.3: shRNA sequences of mission TRC2 non-targeting shRNA lentiviral particles.

TRC number	Sequence
Constitutive NT shRNA	CCGGCAACAAGATGAAGAGCACCAACTCGAGTTGGTGCTCTTCATCTTGTTGTTTTT
Inducible iNT.shRNA	CCGGGCGCGATAGCGCTAATAATTTCTCGAGAAATTATTAGCGCTATCGCGCTTTTT

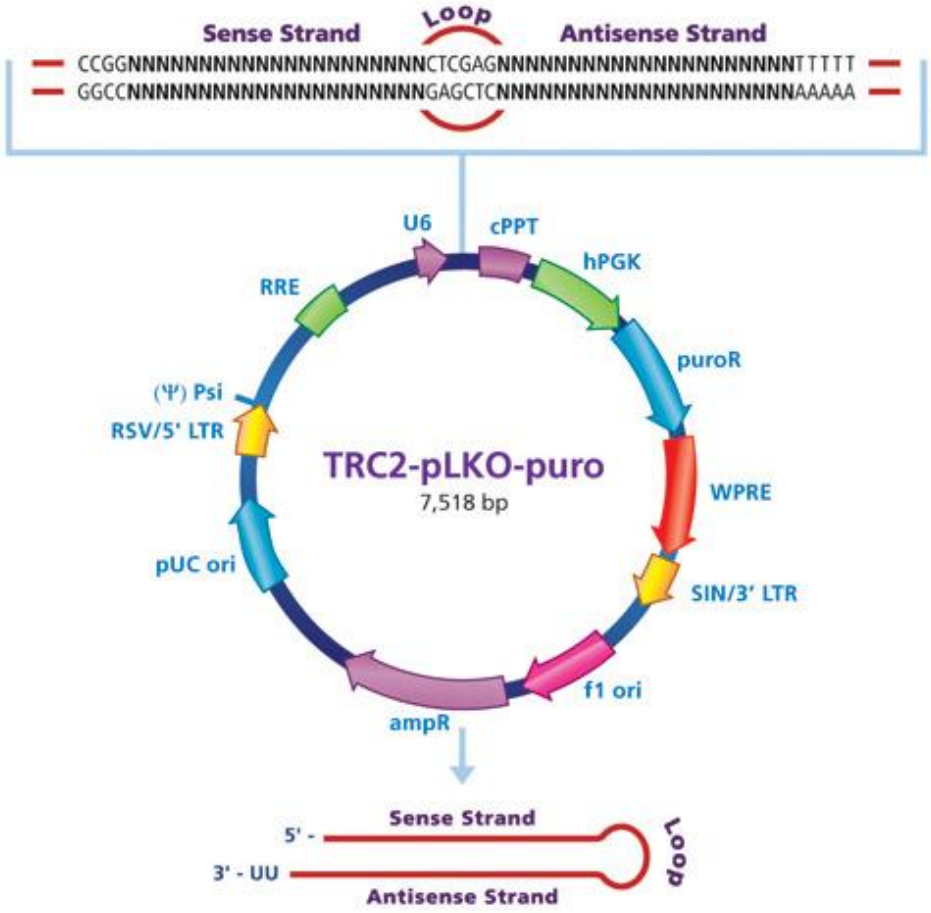

Figure 2.3: TRC2-pLKO-puro vector map.

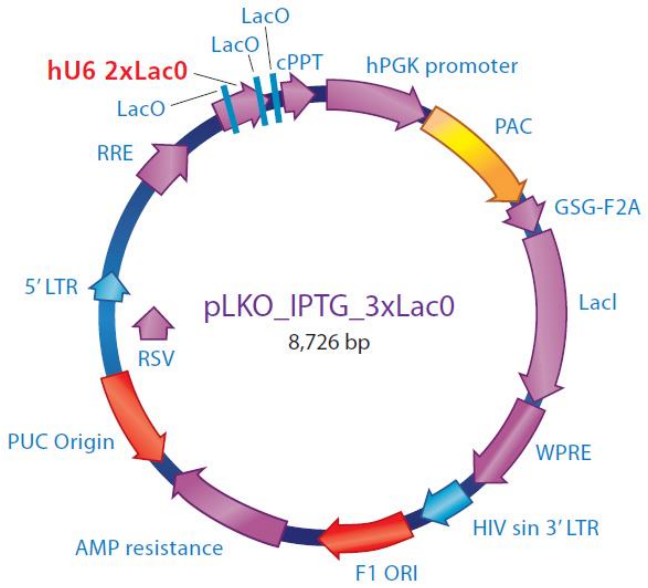

Figure 2.4: Inducible shRNA (pLKO-puro-IPTG-3xLacO) vector map.

2.7. RNA Extraction, Reverse Transcription and Polymerase Chain Reaction

RNA extraction: RNA (ribonucleic acid) was extracted during the exponential phase of cell proliferation. After seeding $2x10^5$ cells/well for 24 hours, the medium was removed and the cells were washed with PBS. RNA was isolated using RNeasy mini kit (Qiagen) and according to the manufacturer's protocol. During the extraction and before RNA cleanup, contaminating DNA was removed by on-column digestion using the RNase-free DNase set (Qiagen) and according to the manufacturer's protocol. The RNA concentration was determined by measuring the optical density at 260 nm by Nanodrop, and the tubes were stored at -80°C.

Reverse transcription: Reverse transcription system (Promega) was used to prepare cDNA according to the manufacturer's protocol. 1 µg of RNA was incubated at 70°C for 10 min and then put on ice. The RNA was added to a 20 µl reaction mixture consisted of 4 µl of 25 mM $MgCl_2$, 2 µl of reverse transcription 10x buffer, 2 µl of 10 mM dNTP mixture, 0.5 µl (20 u) of RNasin ribonuclease inhibitor, 0.6 µl (15 u) of AMV reverse transcriptase, 1 µl (0.5 µg) of oligo-dT primer and the volume was adjusted to 20 µl with nuclease-free water. The samples were incubated at 42°C for 1 hour and at 95°C for 5 minutes, and then placed on ice for 5 min. The samples were diluted 10 times in nuclease-free water and then stored at -20°C.

Quantitative polymerase chain reaction (qPCR): cDNA was thawed on ice and a master mix was prepared for each set of primers which consisted of the following components for each 10 µl single reaction: 5 µl Platinum SYBR Green qPCR SuperMix-UDG with ROX (Invitrogen), 0.2 µl (final concentration 0.2 µM) of each primer (forward and reverse) and 3.6 µl of nuclease-free H_2O. 1 µl of cDNA was added to each single reaction. The samples were loaded onto 384-well reaction plate (MicroAmp optical plate, Applied Biosystems) and the qPCR reaction was performed using the 7900HT Fast Real-Time PCR System (Applied Biosystems) equipped with the SDS 2.3 software. The standard program was used (50°C for 2 min, 95°C for 10 min followed by 40 cycles of 95°C for 15 sec and 60°C for 1 min). Each sample was prepared in triplicate and the results were analysed by the SDS RQ Manager software. The primer sequences are listed in Table 2.4 and the

SULF1 primer set was from Eurofines MWG Operon. All other primer sets were from Sigma.

Polymerase chain reaction (PCR): The AmpliTaq Gold 360 DNA polymerase kit (Applied Biosystems) was used for this purpose. A master mix for each set of primers was prepared by adding the following components for each 25 µl reaction: 2.5 µl of 25 mM $MgCl_2$, 2.5 µl of 10x PCR buffer, 0.5 µl of 10 mM dNTP mixture, 0.5 µl of 10 µM of each primer (forward and reverse), 0.5 µl of DNA polymerase and 15.5 µl of nuclease-free H_2O (Ambion). 2.5 µl of cDNA samples were added into each PCR tube with 22.5 µl of the PCR master mix. The PCR reaction was performed using the GeneAmp PCR system 2700 thermal cycler (Applied Biosystems) and the standard program (94°C for 10 min followed by 20-40 cycles of 94°C for 1 min, 55°C for 1 min and 72°C for 1 min, and terminated by one hold at 72°C for 10 min).

Agarose nucleic acid gel electrophoresis: 1% (w/v) agarose gel was prepared by adding 1.5 g of agarose (Fisher Scientific) to 150 ml of 0.5x TBE buffer. 5x TBE buffer was prepared by adding 57 g Tris base, 27.5 g boric acid and 20 ml of 0.5 M EDTA (pH 8) and adjusting the volume to 1 L with water. After dissolving agarose with heat using a microwave, 15 µl of 10,000x GelRed nucleic acid gel stain (Biotium) was added and the mixture was poured into a gel tray and left to cool at RT. Five µl of 6x loading dye was added to the 25 µl PCR reaction volume and the samples were loaded onto the gel with 5 µl of a 100 bp DNA ladder (Invitrogen). After running the samples at 153 V for 1 hour using a horizontal gel electrophoresis system (Horizon 11-14, Life Technologies), the gel was viewed using Bio-Rad imager equipped with Quantity One 4.5.2 software.

2.8. Concentration of Conditioned Medium

The conditioned medium (CM) was enriched 20 times using a Centricon-10 centrifugal filter devise (Millipore) and according to the manufacturer's protocol. In brief, 2 ml of CM was added into the sample reservoir attached to the filtrate vial and centrifuged at 5000 xg for 1 hour (hr). Subsequently, the filtrate vial was removed and the retentate vial was attached to the sample reservoir. The retentate was recovered by inverting the device and centrifuging at 1000 xg for 2 min.

Table 2.4: Primer sequences used for RT-PCR and RT-qPCR.

GENE	F Primer	R Primer
SULF2	ATGAGTTTGACATCAGGGTCCCGT	ATGGATTTCCCGTCCATATCCGCA
SULF1	GGTCCAAGTGTAGAACCAGGATC	GACAGACTTGCCGTCCACATCA
GAPDH	CAATGACCCCTTCATTGACC	GATCTCGCTCCTGGAAGATG
B2M	TGCTCGCGCTACTCTCTCTTT	TCTGCTGGATGACGTGAGTAAAC
SUMF1	CTCAACTGGCTATTTGACAGAGG	TTTCACAGGTAACCACCAGGG
GPC3	CCTTTGAAATTGTTGTTCGCCA	CCTGGGTTCATTAGCTGGGTA
CCND1	GCTGCGAAGTGGAAACCATC	CCTCCTTCTGCACACATTTGAA
MYC	CAAATGCAACCTCACAACCTTGGC	GCCCAAAGTCCAATTTGAGGCAGT
TP53	CAGCACATGACGGAGGTTGT	TCATCCAAATACTCCACACGC
VEGFA	AGGGCAGAATCATCACGAAGT	AGGGTCTCGATTGGATGGCA
FLT1	TTTGCCTGAAATGGTGAGTAAGG	TGGTTTGCTTGAGCTGTGTTC
KDR	GGCCCAATAATCAGAGTGGCA	CCAGTGTCATTTCCGATCACTTT
GLI1	AACGCTATACAGATCCTAGCTCG	GTGCCGTTTGGTCACATGG
PTCH1	ACTTCAAGGGGTACGAGTATGT	TGCGACACTCTGATGAACCAC
PTCH2	GCTTCGTGCTTACTTCCAGGG	CATGCGGAGACCTAATGCCA
HHIP	CCCTGCATAGTGGGGATGG	AGGCTTAGCAGTCCTCTTTCAT
FOXF1	CCCAGCATGTGTGACCGAAA	ATCACGCAAGGCTTGATGTCT
FOXM1	CGTCGGCCACTGATTCTCAAA	GGCAGGGGATCTCTTAGGTTC
BCL2	GGTGGGGTCATGTGTGTGG	CGGTTCAGGTACTCAGTCATCC
ACE2	ACAGTCCACACTTGCCCAAAT	TGAGAGCACTGAAGACCCATT
CEACAM7	GTTACCCACAATGACGCAGGA	TCCACCGGATTGAAGTTGTTG
HEPH	TGCGATATGAAGCCTTTCAAGAT	GGAGGCACGGTTGTAGAAGA
PCDH20	AAAATGCACCTGTAAACACCCG	GCGATAGGTCTGTACCCCATTA
HOXB7	CGAGTTCCTTCAACATGCACT	TTTGCGGTCAGTTCCTGAGC
CTBP2	GAATTGCCGTGTGCAACATCC	CGTGTTCCTCCGGTACAGG
SLPI	GAGATGTTGTCCTGACACTTGTG	AGGCTTCCTCCTTGTTGGGT
EDIL3	AGCATACCGAGGGGATACATT	CAAGGCTCAACTTCGCATTCA
SLFN11	AACCCCAACGCCCGATAAC	TCATGCAAGCATAGCCATAGAG
PRSS3	CCACCCTAAATACAACAGGGAC	TCAGCACCAAAGCTCAGAGTG
CEACAM6	TCAATGGGACGTTCCAGCAAT	CACTCCAATCGTGATGCCGA
TFPI2	CTGGGGCTGTCGATTCTGC	TCTCCGCGTTATTTCCTGTTG
BEX1	GCAGTAAACAGTCTCAGCATGG	GGCTCCCCTTTATTAGCAACTT
CTSE	AGGCATCCGTCCCTCAAGAA	CCTTGGCACTCTGGTCCATTG
DLK1	CTTTCGGCCACAGCACCTAT	TGTCATCCTCGCAGAATCCAT
AHSG	CTTCAACGCTCAGAACAACGG	CCACATAGGTAGAAGGTGGGA
MYCN	CACGTCCGCTCAAGAGTGTC	GTTTCTGCGACGCTCACTGT
WNT5A	TCGACTATGGCTACCGCTTTG	CACTCTCGTAGGAGCCCTTG
DKK1	ATAGCACCTTGGATGGGTATTCC	CTGATGACCGGAGACAAACAG
GPC4	GTGGGAAATGTGAACCTGGAA	CGAGGGACATCTCCGAAGG
MMP2	CCCACTGCGGTTTTCTCGAAT	CAAAGGGGTATCCATCGCCAT
MMP9	TGTACCGCTATGGTTACACTCG	GGCAGGGACAGTTGCTTCT
AGTR1	ATTTAGCACTGGCTGACTTATGC	CAGCGGTATTCCATAGCTGTG
ACE	AACATGCAAATAGCCAACCACA	TGCCCGTTCTAGGTCCTGAA
CUX2	AGCGGGTGTTTGGGCATTA	CCAGTACATTCTGCTCATCCG
MAS1	ATGGATGGGTCAAACGTGACA	CGATGTGCATTCCCGACTG
FOXO1	TGATAACTGGAGTACATTTCGCC	CGGTCATAATGGGTGAGAGTCT

2.9. Protein Extraction and Quantitation

Protein extraction: Protein was extracted during the exponential phase of cell proliferation. $2x10^5$ cells/well in a 6-well plate were cultured for 24 hours, medium removed and the cells washed with PBS. The PBS was aspirated completely and the plate was placed on ice. Two different protein extraction reagents were used depending on the downstream applications. For western blot application, PhosphoSafe extraction reagent (Novagen) (containing 4 phosphatase inhibitors, sodium fluoride, sodium vanadate, β-glycerophosphate and sodium pyrophosphate) to which protease inhibitor cocktail (Sigma) added in the ratio 250:1 was used, while for immunoprecipitation applications, a non-denaturing NP-40 buffer was used. This buffer consisted of 50 mM Tris (pH 7.4), 1% (v/v) NP-40, 0.15 M NaCl, 2 mM EDTA, 10 mM sodium fluoride, 1 mM PMSF (phenylmethylsulfonyl fluoride) and 200 µl/50ml protease inhibitor cocktail. After adding the extraction reagent, the plate surface was scraped with a cell scraper and the content was transferred into an eppendorf tube. The samples were further lysed by sonication using Soniprep 150 plus at an amplitude of 4 for 10 seconds. The samples were then centrifuged at 16,100 xg for 10 min at 4°C using a table-top eppendorf centrifuge 5415D to remove cell debris and the supernatant was stored at -70°C.

Protein quantitation: protein was quantified using the bicinchoninic acid (BCA) assay. This is a colorimetric assay based on the ability of proteins (particularly the amino acids cysteine, cystine, tryptophan and tyrosine) to reduce cupric ion Cu^{+2} (in reagent B) into cuprous ion Cu^{+1} in an alkaline solution (the biuret reaction). This is followed by detecting Cu^{+1} ions using BCA (in reagent A), leading to the formation of a purple colour that is proportional to protein concentration. First, diluted bovine serum albumin (BSA) standards of different concentrations ranging from 0.25 - 2 mg/ml were prepared and working reagent (WR) was prepared by mixing reagent A with reagent B in the ratio 50:1 (Pierce BCA protein assay kit, Thermo Scientific). Protein samples were diluted 1:5 and 10 µl of each sample or standard was added in triplicate in 96-well plate. 10 µl of H_2O was added into the blank wells and 190 µl of the WR was added to each well. After mixing on a plate

shaker for 30 seconds, the plate was incubated at RT for 15 minutes and then the absorbance at 562 nm was read by FLUOstar Omega (BMG Labtech) plate reader using the Omega data analysis software.

2.10. SDS-PAGE and Western Blot

Sodium dodecyl sulfate polyacrylamide gel electrophoresis (SDS-PAGE): Denaturing and reducing gel electrophoreses was performed using NuPAGE Novex 4-12% Bis-Tris Gel 1.0 mm (Invitrogen). Samples were prepared by adding 4x NuPAGE LDS (lithium dodecyl sulfate) sample buffer (Invitrogen), 10x NuPAGE sample reducing agent (Invitrogen) and incubation at 70°C for 10 min to denature and reduce the protein. After the denaturation step, the samples were placed on ice to prevent proteins from folding again and centrifuged shortly before loading onto the gel. The gel cassette was placed in the XCell SureLock Mini-Cell system (Invitrogen). The upper and lower buffer chambers of the system were filled with 1x SDS running (electrophoresis) buffer. The 20x NuPAGE MOPS SDS running buffer (Invitrogen) was used and the upper (inner) chamber was filled with 200 ml of 1x SDS running buffer containing 500 µl of NuPAGE antioxidant (Invitrogen). The samples and protein standard were loaded onto the gel which then ran at 200 V. The protein standard used was either the Novex sharp pre-stained protein standard (Invitrogen) or the HiMark pre-stained high molecular weight protein standard (Invitrogen).

Western blot (WB): One nitrocellulose transfer membrane (HyBond-C Extra, Amersham Biosciences) and 4 filter papers were cut for each gel and soaked in transfer buffer (6.06 g Tris base, 28.28 g glycine, 200 ml methanol and dH_2O made up to 2 liters). The gel was removed from its cassette and wetted in transfer buffer and then the following were placed in order over the cathode (black) core: 1 blotting pad, 2 filter papers, the gel, transfer membrane and 2 filter papers. Air bubbles were removed by passing a roller and then another blotting pad was put on top and the transfer cassette was closed tightly using the anode (transparent) core. The cassette was slid into a transfer tank (Geneflow) and the tank was filled with transfer buffer. After running at 300 mAs for 90 min, the membrane was removed from its cassette and blocked in blocking buffer composed of 5% (w/v)

milk and 3% (w/v) BSA in Tris-buffered saline-Tween (TBS-T) for 1 hour with gentle agitation. 10x TBS-T was prepared by dissolving 60 g of Tris, 90 g of NaCl and 5 ml of Tween 20 in 1 L of H_2O and the final pH was adjusted to 7.5 with concentrated HCl. Following blocking, the membrane was incubated with 1:1000 (1:500 for SULF1) diluted primary antibody in blocking buffer overnight on a roller mixer (Stuart SRT6).

Table 2.5 lists the different primary antibodies used. After decanting the primary antibody, the membrane was washed 3 times in TBS-T for 15 min each time and then incubated with 1:1000 diluted secondary antibody in blocking buffer for 1 hour. The secondary antibodies used were: polyclonal goat anti-rabbit immunoglobulins/ horseradish peroxidase (HRP) (dakocytomation), polyclonal goat anti-mouse immunoglobulins/HRP (dakocytomation) or donkey anti-goat IgG-HRP (Santa Cruz Biotechnology). After decanting the secondary antibody, the membrane was washed 4 times in TBS-T for 10 min each time. The chemiluminescence substrate, either Pierce ECL Western Blotting Substrate or SuperSignal West Dura Extended Duration Substrate (Thermo Scientific), was prepared by mixing the stable peroxide solution and the luminol/enhancer solution at a ratio of 1:1. Following incubation with the substrate for 2-5 min, the excess substrate was drained and the membrane was placed under a clear plastic cover in a film cassette and exposed to X-ray film. The film was developed using developing solution (RG X-ray developer, Champion) and fixative (RG X-ray fixer, Champion) in the Mediphot 937 developing system.

The membrane was stripped and reprobed when necessary. For stripping, the membrane was incubated with 10 ml stripping buffer at 50°C for 45 min with rotation using the Hybridiser HB-1 (Techne). Stripping buffer was prepared in a fume hood by adding 20 ml of 10% (w/v) SDS, 12.5 ml Tris HCl (pH 6.8) of the concentration 0.5 M and 0.8 ml β-mercaptoethanol and the volume was adjusted to 100 ml with dH_2O. After rinsing the membrane with water, it was washed once with TBS-T, blocked with blocking buffer for 1 hour and then reprobed with another primary antibody.

Table 2.5: List of the different primary antibodies used.

Antibody	**Raised in /Clonality**	**Immunogen**	**Band size** (kDa)
SULF2 (Abcam)	Rabbit Polyclonal	SULF2 C terminal amino acids 823-870	50
SULF2 (Abnova)	Rabbit Polyclonal	Rat SULF2	75-100
SULF2 (Thermo)	Rabbit Polyclonal	Synthetic peptide corresponding to SULF2	
SULF2 (Aviva)	Rabbit Polyclonal	SULF2 C terminal amino acids 802-851	
SULF2 (Sigma)	Goat Polyclonal	Internal region between the two furin cleavage sites (amino acids 545-560) of SULF2	
SULF2 (LR)	Rabbit Polyclonal	SULF2 HD amino acids 421-444	
SULF2 (NCL)	Rabbit Polyclonal	SULF2 HD amino acids 421-435	
SULF2 (AbD Serotec)	Mouse Monoclonal	Epitope within SULF2 C-terminal subunit	37, 50, 135
SULF1 (Abcam)	Rabbit Polyclonal	Amino acid 850 to the C-terminus of SULF1	58, 132
SULF1 (Abnova)	Goat Polyclonal	N-terminal amino acids 391-406 of mouse Sulf1 that contains L^{392} instead of P^{392} in human SULF1	
β-Actin (Sigma)	Mouse monoclonal	β-Actin C-terminal peptide: Ser-Gly-Pro-Ser-Ile-Val-His-Arg-Lys-Cys-Phe	42
STS/ARSC (Abcam)	Rabbit Polyclonal	Synthetic peptide corresponding to a region within internal sequence amino acids 396-445 of STS/ARSC	63
Total β-catenin (Cell Signalling)	Rabbit Polyclonal	Synthetic peptide corresponding to residues around Ser37 of β-catenin	92
Total β-catenin (Cell Signalling)	Mouse Monoclonal	Synthetic peptide corresponding to the carboxy terminus of β-catenin	92
Non-phospho-β-catenin (Cell Signalling)	Rabbit Polyclonal	Synthetic peptide corresponding to a region surrounding residue Ser37 of β-catenin	92
Phospho-ERK1/2 (Cell Signalling)	Rabbit Monoclonal	Synthetic phosphopeptide corresponding to residues surrounding Thr202/Tyr204 of human p44 MAP kinase (ERK1)	42, 44
ERK1/2 (Cell Signalling)	Mouse Monoclonal	Synthetic peptide corresponding to the sequence of p44/42 MAP kinase (ERK1/2)	42, 44
Phospho-AKT (Cell Signalling)	Rabbit Monoclonal	Synthetic phosphopeptide corresponding to residues around Ser473 of AKT	60
AKT (Cell Signalling)	Rabbit Monoclonal	Synthetic peptide corresponding to residues in the carboxy-terminal sequence of AKT	60
GAPDH (Cell Signalling)	Rabbit Monoclonal	Synthetic peptide corresponding to residues near the carboxy terminus of GAPDH	37
ACE2 (Cell Signalling)	Rabbit Polyclonal	Synthetic peptide corresponding to residues near the amino terminus of ACE2	120
DLK1 (R and D Systems)	Mouse Monoclonal	Recombinant human DLK1 long isoform Ala124-Pro297	47

Antibody	**Raised in /Clonality**	**Immunogen**	**Band size** (kDa)
PCDH20 (Santa Cruz)	Rabbit Polyclonal	Peptide mapping within an N-terminal extracellular domain of human PCDH20	102
Wnt-5a (R and D Systems)	Rat Monoclonal	Recombinant mouse Wnt-5a (Gln38-Lys380)	49
TFPI2 (R and D Systems)	Mouse Monoclonal	Recombinant human TFPI2 (Asp23-Phe235)	27
SLPI (R and D Systems)	Mouse Monoclonal	Recombinant human SLPI	14

2.11. Immunocytochemistry (ICC)

$4x10^5$ cells/well were grown on glass coverslips in a 6-well plate. After 48 hours, the cells were rinsed with PBS and fixed in ice-cold methanol for 15 min at RT. The cells were washed twice with PBS and permeabilized by incubation with TBS-T for 10 min. Following washing with PBS three times for 5 min each, the cells were incubated for 30 min with a blocking buffer composed of 3% (w/v) BSA and 10% (v/v) FBS in PBS. After that the cells were incubated with 1:100 diluted primary antibody in blocking buffer for 1 hr at RT. The antibody was decanted and the cells were washed in TBS-T three times for 5 min each. Cells were then incubated with the secondary antibody in blocking buffer (1:800 of Alexa Fluor 546 or Alexa Fluor 488 goat anti-mouse or Alexa Fluor 488 goat anti-rabbit, Invitrogen) at RT for 1 hr in the dark followed by washing the cells in the dark with TBS-T three times for 5 min each. The coverslips were then mounted with Vectashield mounting medium with DAPI (Vector Laboratories), sealed with nail polish and stored at 4°C.

2.12. Immunoprecipitation

200 µl of protein A agarose bead slurry (Calbiochem) was centrifuged at 400 xg for 10 min. After discarding the supernatant, the remaining 100 µl of beads were washed with 1 ml of 1x HEPES (pH 8) and then centrifuged again. The supernatant was removed and an excess of SULF1 or 2 antibody (4 µg) was added. Following overnight incubation at 4°C under rotary agitation, the beads were centrifuged and the excess antibody was removed. Equal amounts of HCC cell lysates extracted by

NP-40 extraction buffer (1 mg for each 100 µl of beads) were added and incubated overnight at 4°C under rotary agitation. The beads were then centrifuged, the supernatant discarded, and the beads were washed twice with HEPES (1 ml each time), and resuspended in 100 µl of HEPES and stored at 4°C.

2.13. Arylsulfatase Activity Assay

The assay is based on the ability of sulfatase to convert 4-methylumbelliferyl sulfate (4-MUS) into the fluorescent product 4-methylumbelliferone (4-MU) by desulfation as shown in the reaction below.

4-Methylumbelliferyl sulfate (4-MUS) 4-Methylumbelliferone (4-MU)

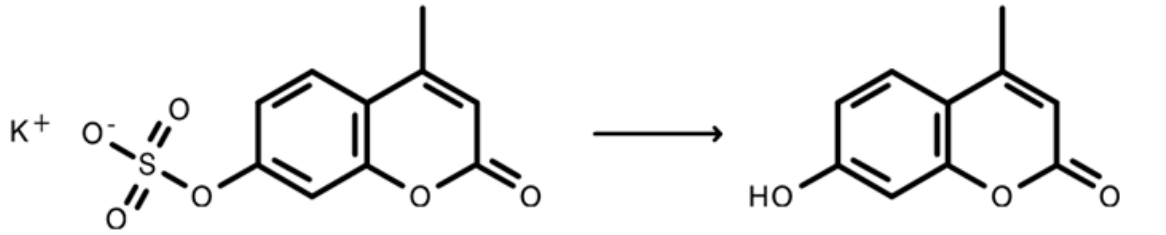

Fluorescence λ_{ex} 355 nm; λ_{em} 460 nm

Cell-based assay: Cells were seeded in a 96-well plate. After 24 hours, the medium was removed and replaced by 100 µl phenol-free medium, and STS/ARSC was inhibited with 10 - 50 µM of oestrone 3-O-sulfamate (Sigma) for 1 hour at 37°C. The remaining sulfatase activity was measured by incubation with the substrate 4-MUS for different time periods at 37°C after which the fluorescence of the product 4-MU was read at 460 nm following excitation at 355 nm using FLUOstar Omega (BMG Labtech) plate reader using the Omega data analysis software.

Cell lysate- and immunoprecipitated enzyme-based assay: HCC cell lysates or SULF1/2-antibody immunoprecipitates (IPs) prepared in Section 2.12 were used in this assay by adding equal amounts of cell lysates or bead slurry in a 96-well black plate (Sterilin) in 50 µl reaction mixture of the following components: 5 µl of 10x (500 mM) HEPES reaction buffer (pH 8), 5 µl of 10x (100 mM) $CaCl_2$, 4-MUS at the required concentration and made up to 50 µl with dH_2O. The plate was incubated

for different time points at 37°C after which the fluorescence of the product 4-MU was read as described above.

Recombinant sulfatase assays: Commercially available recombinant human sulfatases (ARSA and ARSB from R and D Systems, STS/ARSC, ARSD, ARSF, ARSG, IDS, GNS and GALNS from Origene) were diluted in reaction buffer as indicated above at different pH values and 4-MUS concentrations. After incubation at 37°C, the reaction was stopped using 100 µl of 1 M Tris (pH 10.5) and the fluorescence of 4-MU was read.

2.14. Crystal Violet Staining

Crystal violet is a protein dye that gives a reading at 595 nm that is proportional to cell count. For staining cells in 96-well plates, medium was removed and the plate was tapped onto paper towel to drain the medium completely. Each well was covered with 100 µl of crystal violet solution (0.4% (w/v) in distilled water). After incubation for 30 min at RT, the wells were washed under tap water flowing gently and then 3 times with 200 µl PBS with shaking on a plate shaker (Heidolph, Titramax 1000) for 5 min each time. Cells were solubilized by adding 100 µl/well of 1% (w/v) SDS solution with shaking for 30 min at RT and the optical density at 595 nm was measured using a FLUOstar Omega (BMG Labtech) plate reader.

2.15. TCF Luciferase Reporter Assay

Two different reporter plasmids were used. For transient transfection, the TCF reporter plasmid kit (Upstate, Millipore) was used to measure Wnt signalling. This kit contained two plasmids: a) TOPflash including 3 wild-type TCF binding sites and b) FOPflash including 2 wild-type and 1 mutated TCF binding site upstream of the thymidine kinase (TK) minimal promoter and luciferase ORF (Figure 2.5). $6x10^4$ cells/well in 24-well plates were transiently co-transfected in a reverse manner in Opti-MEM with 200 ng of either TOPflash or FOPflash along with 200 ng of β-galactosidase reporter plasmid using FuGENE in the ratio 1:2 (µg total DNA: µl FuGENE). The β-galactosidase plasmid was used for internal normalization to correct for variable transfection efficiencies.

For stable transduction, the 7TFP lentiviral construct was used which was obtained from Addgene and was made and deposited by Prof. Roel Nusse (Fuerer and Nusse, 2010). This construct contains 7 TCF binding sites upstream of luciferase ORF in addition to puromycin as a selectable marker (Figure 2.6). Lentiviral particles were made using this construct as described in Section 2.5 and were used to infect HCC cells. Subsequently, cells were selected using puromycin. 7TFP-transduced cells were seeded into 96-well plates at 10,000 cells/well.

After overnight incubation of either transiently transfected or stably transduced cells in serum-free medium, cells were treated with recombinant human Wnt-3a (R and D Systems), 6-bromo-indirubin-3'-oxime (BIO) (Sigma) and/or the dishevelled (Dvl)-PDZ domain inhibitor II, compound 3289-8625 (Calbiochem) for different time periods. For TOPflash-transfected cells, cell lysates were prepared using reporter lysis buffer (RLB) (Promega) and luciferase and β-galactosidase activities were measured using a luciferase assay system (Promega) and a β-galactosidase enzyme assay system (Promega), according to the manufacturer's protocol. For luciferase activity, a 96-well plate containing 10 µl cell lysate per well was placed in FLUOstar Omega plate reader which was programmed to dispense 50 µl of luciferase assay reagent per well followed immediately by reading the light produced for 10 seconds. For β-galactosidase activity, 10 µl of assay 2x buffer was added to a 96-well plate containing 10 µl cell lysate per well and incubated for 5 min at 37°C or until the formation of a faint yellow colour. After that the reaction was stopped using 50 µl of 1 M sodium carbonate and the optical density at 420 nm was measured. For 7TFP-transduced cells, luciferase activity was measured using ONE-Glo luciferase assay system (Promega) which uses 5'-fluoroluciferin as a substrate that is more stable than luciferin and gives more consistent luminescence following the reaction below.

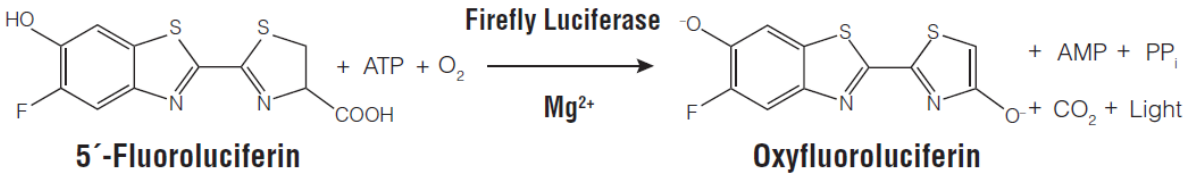

100 µl of the reagent was added to the wells and incubated for 3 min at RT before measuring the luminescence using a FLUOstar Omega plate reader.

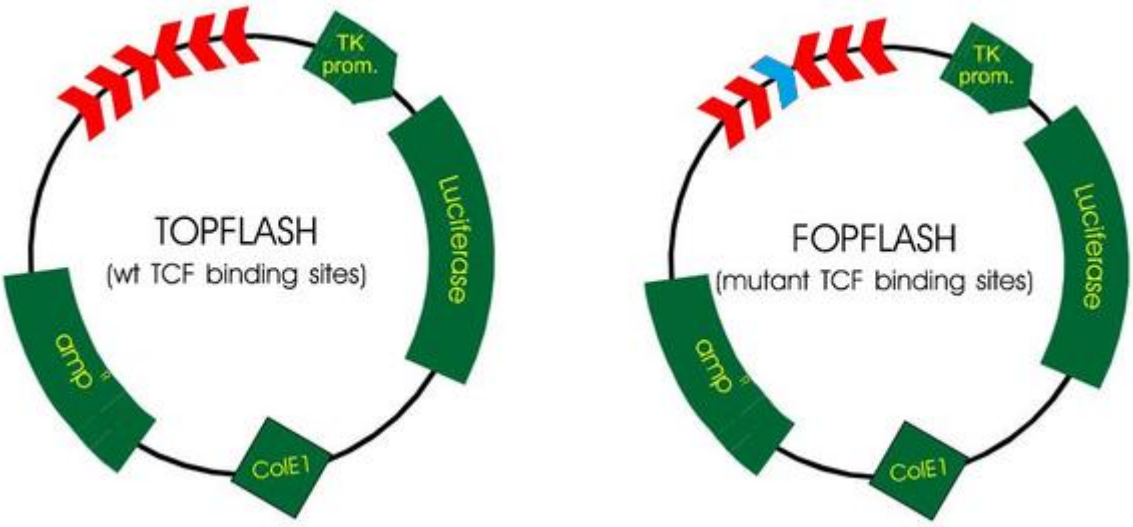

Figure 2.5: TOPflash/FOPflash plasmid maps: *Left*: TOPflash plasmid including two sets of three copies of the full (wild-type) TCF binding site with the second set in the reverse orientation and *Right*: FOPflash plasmid including two full (in red) and one incomplete (mutated) copy (in blue) of the TCF binding site followed by three full copies in the reverse orientation. These two sets in each plasmid were upstream of the TK minimal promoter and luciferase ORF.

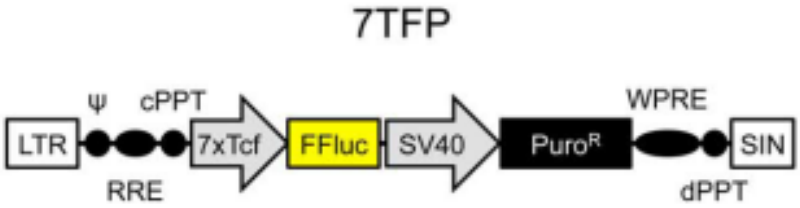

Figure 2.6: 7TFP plasmid map: The plasmid includes 7 copies of the full (wild-type) TCF binding site upstream of Firefly luciferase (FFluc) ORF. The puromycin resistance gene ($Puro^R$) is under the SV40 promoter.

2.16. Phospho-ERK, Phospho-AKT and Total β-catenin ELISA

The ELISA assays were performed using PathScan phospho-p44/42 MAPK (Thr202/Tyr204), PathScan phospho-AKT1 (Ser473) or PathScan total β-catenin sandwich ELISA kits (Cell Signalling) that use 96-well plates coated with a capture antibody and according to the manufacturer's protocol. In brief, 50 µg of cell lysates

were loaded into each well of the ELISA plate and the volume was completed to 100 µl using sample diluent. The wells were sealed and incubated at 4°C overnight. The wells were then washed 4 times with washing buffer and incubated with 100 µl of detection antibody for 1 hr at 37°C. After washing the wells again as before, 100 µl of HRP-linked secondary antibody was added for 30 min at 37°C. The wells were washed and 100 µl of TMB substrate was added for 10 - 20 min at RT. The reaction was stopped by adding 100 µl of stop solution and the optical density at 450 nm was read using a FLUOstar Omega plate reader.

2.17. Sulforhodamine B (SRB) Cell Growth Assay

SRB stains proteins where the intensity of the staining is proportional to the number of cells. Cells were grown in 96-well plates (100 µl medium/well) for different periods and then fixed using 25 µl/well of ice-cold 50% (w/v) trichloroacetic acid (TCA). After incubation for 1 hour at 4°C, the liquid was removed and the wells were washed 5 times with dH_2O. The plates were left to dry and then stored at 4°C until required. For SRB staining, the plates were allowed to reach room temperature and then stained with 100 µl of 0.4% (w/v) SRB solution in 1% (v/v) acetic acid for 30 min. Subsequently, the unbound dye was discarded and the wells were washed 5 times with 1% acetic acid. The plates were left to dry overnight and then the dye was dissolved by adding 100 µl/well of 10 mM Tris (pH 10.5). The plates were shaked for 20 min on a vibrating platform shaker (Titramax 1000, Heidolph) and the absorbance at 510 or 570 nm was read using a FLUOstar Omega plate reader.

2.18. Cell Proliferation Assay

Cells were cultured in 96-well plates (100 µl medium/well) for different time points and then washed with PBS and trypsinized by 100 µl trypsin. The trypsin was blocked by adding 100 µl of serum-containing medium and the cells were transferred into counter pots, diluted 10 times using Isoton II solution and then counted using the Coulter Z1 (dual-threshold model) cell counter (Beckman Coulter) where the upper and lower size levels were set at 24 and 8 µm, respectively.

2.19. ELISA for RB4CD12-Based Detection of SULF1/2 Activity

100 µl/well of 50 µg/ml biotinylated heparin was immobilized on streptavidin-coated 96-well microplate (R and D systems, Minneapolis MN, USA). After incubation at 4°C overnight, the plate was washed with PBS-T (0.1% (v/v) Tween-20 in PBS) three times and blocked with 200 µl of 3% (w/v) BSA for 2 hours at RT. The plate was washed again as indicated above and incubated with enzyme-antibody IPs of cell lysate for 2 hours at 37°C with 1x HEPES and 1x $MgCl_2$ in 100 µl reaction mixture. Then the plate was washed and the c-Myc tagged RB4CD12 antibody (1:100 dilution in blocking solution) was added. RB4CD12 antibody was provided by Toin van Kuppevelt, Nijmegen, The Netherlands. After incubation for 1 hour at RT, the plate was washed 5 times in PBS-T for 10 minutes each with shaking and incubated with HRP-conjugated mouse monoclonal antibody to c-Myc (Abcam) (1:100 dilution of 1 mg/ml stock solution in blocking buffer) for 1 hour at RT. The plate was washed again and 100 µl/well of 1-Step Ultra TMB-ELISA (Thermo scientific) was added and incubated at RT until a blue colour developed. 50 µl of 2 M sulfuric acid was added and the optical density at 450 nm was measured using a FLUOstar Omega plate reader.

2.20. Tumourigenicity Assay

All of the *in vivo* experiments were reviewed and approved by the local institutional animal welfare committee, and were performed according to the United Kingdom Coordinating Committee on Cancer Research Guidelines for the Welfare of Animals in Experimental Neoplasia (Second Edition) (Workman et al., 1998) and national law. 8 - 10 week-old female CD-1 athymic nude mice (Charles River Laboratories) or in house bred NOD scid gamma (NSG) mice (Comparative Biology Center, Medical School, Newcastle University) were implanted with a suspension of $1x10^7$ HCC cells in 50 µl of culture medium or Matrigel basement membrane matrix (BD Biosciences) subcutaneously (s.c.) on the right flank. For inducible shRNA-transduced HuH-7 cells, 10 mice were implanted for each cell line (i.e., iNT.shRNA or iSULF2.shRNA-transduced cells). Half of the mice of each group were maintained on drinking water containing 12.5 mM IPTG (isopropyl β-D-thiogalactoside).

Mice were monitored for tumour growth for 100 days post implantation and the size of any tumour that arose was measured in 2 dimensions using a digital caliper three times a week. Tumour volumes were determined from the two measurements using the formula (longest dimension/2) x (shortest dimension^2).

2.21. Quantification of small RNAs

The QuantiMir RT system (Cambridge Bioscience) was used. The system converts small non-coding RNAs into quantifiable cDNA by tagging small RNA with poly A tag followed by annealing anchor oligo dT adaptor and reverse transcription reaction to create the first strand cDNA that can be used as a template for qPCR reaction using a 3' universal reverse primer and a forward primer corresponding to the siRNA effector sequence of the shRNA of interest. The 5' human U6 small nuclear RNA (snRNA) forward primer was used as an endogenous control. The sequences of the forward primers used in this assay are shown in Table 2.6. The assay was performed according to the manufacturer's instructions. Total RNA was extracted from cell pellets by adding 100 µl of chilled cells-to-Cts lysis buffer followed by incubation at 45°C for 10 min. Samples were then chilled on ice and 2 µl of DNase I was added and samples incubated at 37°C for 15 min followed by inactivation of DNase by heating at 75°C for 5 min. Five µl of each sample was then used in the reverse transcription reaction that was initiated by adding a poly A tail by incubating samples with 2 µl of 5x poly A buffer, 1 µl of 25 mM MnCl2, 1.5 µl of 5 mM ATP and 0.5 µl of poly A polymerase at 37°C for 30 min. A 0.5 µl of oligo dT adaptor was then added and samples heated at 60°C for 5 min. cDNA was synthesized by adding 4 µl of 5x RT buffer, 2 µl of dNTP mix, 1.5 µl of 0.1 M DTT, 1.5 µl of RNase-free H2O and 1 µl of reverse transcriptase followed by incubation at 42°C for 60 min. Samples were then heated at 95°C for 10 min and resulting cDNAs stored at -20°C or used in qPCR reaction as described in Section 2.7.

Table 2.6: Forward primer sequences used for QuantiMir small RNA quantification.

Forward primer	Sequence
5' Human U6 snRNA	CGCAAGGATGACACGCAAATTC
Constitutive NT shRNA	CAACAAGATGAAGAGCACCAA
Constitutive and inducible SULF2 shRNA	GGGCGAAAGTCATTGGAA
Constitutive and inducible SULF1 shRNA	TCTGGTGGACTGGACTAAT
Inducible iNT.shRNA	GCGATAGCGCTAATAATTT

2.22. Affymetrix Microarray Gene Expression Analysis

Biologically independent quadruplicates each containing $5x10^6$ cells of HuH-7 control untransduced cells or HuH-7 transduced with either NT shRNA or S2.shRNA_18 were harvested and resuspended in 300 µl RNAprotect Cell Reagent (Qiagen) and sent at RT for Affymetrix microarray analysis to the Center of Physiology and Pathophysiology, Institute of Neurophysiology, Cologne, Germany. The RNA was extracted and DNase-treated and then the quality of the RNA was tested by measuring the optical density (O.D.) at 260 nm/O.D. 280 nm and O.D. 260 nm/O.D. 230 nm ratios, RIN (RNA integrity number) using an Agilent Bioanalyzer 2100 and running RNA on a denaturing agarose gel to measure the ribosomal RNA species 28S/18S ratio.

For transcriptional profiling, Affymetrix Human Genome U133 plus 2.0 arrays were used. Array hybridization and analysis were conducted by the Center of Physiology and Pathophysiology, Institute of Neurophysiology, Cologne, Germany as described in Appendix C.

Analysis of affected pathways was completed by determining gene ontologies (GO) enriched with differentially expressed transcripts and by using Kegg pathways database (http://www.genome.jp/kegg/tool/search_pathway.html) and GeneSpring 12.6 software (Agilent Technologies).

2.23. Flow Cytometry Analysis

ImageStream^X (Amnis, Seattle) imaging flow cytometer was used, which has a high-speed automated microscope that can capture images of cells in flow and quantify the intensity and location of fluorescent probes. After trypsinization and blocking trypsin, the cells were centrifuged at 1,000 xg for 5 min, the supernatant aspirated and the cell pellet washed with PBS. The cells were then fixed in 1% (v/v) formalin in PBS for 20 min at RT. After centrifugation at 500 xg for 5 min, formalin was removed and cells resuspended in saponin-containing perm/wash buffer (BD Biosciences) for 1 hr at RT to permeabilize cells. Cells were centrifuged and gently resuspended in 100 µl of perm/wash buffer containing the primary antibody at dilution 1:100. After overnight incubation at 4°C, cells were centrifuged and resuspended in 100 µl of perm/wash buffer containing Texas Red secondary antibody (Invitrogen) at dilution 1:1000 for 1 hr at RT in the dark. Cells were then centrifuged and resuspended in 100 µl of perm/wash buffer and DAPI (1 µg/ml final concentration) was added to stain nuclei for 1 hr at RT. Cells were centrifuged at 500 xg and re-suspended in an appropriate volume of PBS so that the sample ran at < 1000 objects/sec. Texas Red was excited at 561 nm and the emission at 595-660 nm was measured. DAPI was excited at 405 nm and the emission was measured at 430-505 nm. Analysis was performed using the IDEAS software (version 5.0, Amnis, Seattle). To compensate for spectral overlap, cells labelled with a single-colour positive control for each fluorochrome were used. Round single cells (RSCs) were gated using a scatter plot of area versus aspect ratio of the brightfield image. The RSC population was then assessed for a sub-population of cells in best focus using the gradient Root Mean Square (RMS) feature. Gradient RMS calculates large changes in pixel values in the image. Cells with a gradient RMS > 50 are generally considered to be in best focus .The sub-population of RSCs in best focus was then assessed for the level of expression of proteins of interest by measuring the mean pixel intensity.

2.24. Measurement of ACE2 Activity

Two fluorogenic peptide substrates were used, Mca-Tyr-Val-Ala-Asp-Ala-Pro-Lys(Dnp)-OH (R and D systems) and Mca-Ala-Pro-Lys(Dnp)-OH (Enzo Life Sciences). The assay depends on the ability of ACE2 enzyme to cleave the amide bond between proline (Pro) and lysine (Lys) amino acids leading to the release of the fluorochrome Mca (7-methoxycoumarin-4-yl acetyl) from its quencher Dnp (2,4-dinitrophenyl) group. Fifty µl of substrate diluted to 40 µM in 2x assay buffer (150 mM Tris, 2M NaCl, pH 7.5) was added to 50 µl of cell lysates prepared in RLB buffer, or recombinant human ACE2 (R and D systems) and the fluorescence of the reaction was read at 405 nm after excitation at 320 nm using a FLUOstar Omega plate reader.

2.25. Measurement of Ang-(1-7) Level

The Ang-(1-7) ELISA (Uscn Life Science) was used which is a competitive inhibition enzyme immunoassay using a 96-well plate pre-coated with an Ang-(1-7) specific antibody. The Ang-(1-7) in the samples or the standards competes with a biotin-labelled Ang-(1-7) (reagent A) for binding to the Ang-(1-7) antibody. After washing the unbound conjugate, HRP-conjugated avidin (reagent B) is added where the bound amount of avidin is reversely proportional to Ang-(1-7) concentration. The assay was performed according to the manufacturer's instructions. Fifty µl of each sample was added in each well to which equal volume of reagent A was added immediately. After incubation for 1 hr at 37°C, the wells were washed with 1x wash solution four times, 100 µl of detection reagent B added and the plate incubated for 30 min at 37°C. The wells were washed as before and 90 µl of substrate solution added followed by incubation for 10 - 15 min at 37°C. Fifty µl of stop solution was added and the optical density at 450 nm was measured using a FLUOstar Omega plate reader.

2.26. Statistical Analysis

All graphs were generated using GraphPad Prism 6.00 software. To calculate *p* values after SULF1/2 knockdown, Minitab 16 statistical software was used. 2-

sample t-test or one-way ANOVA were used for normally distributed samples. Homogeneity of variances was first determined using Levene's test before conducting one-way ANOVA. When overall significant difference in group means was shown by one-way ANOVA, post-hoc pairwise comparisons tests were performed, including Tukey's and Fisher's tests.

Chapter 3. SULF1/2 Expression and Activity in HCC Cell Lines

To study the biology of SULF1 and SULF2 in hepatocellular carcinoma, six HCC cell lines were chosen. The expression levels of SULF1/2 enzymes were first investigated at the mRNA and protein levels followed by measuring the sulfatase enzymatic activity of these cell lines.

3.1. SULF1/2 mRNA Expression in HCC Cell Lines

In order to characterise SULF1 and SULF2 mRNA levels in HCC cell lines, RT-PCR was performed. DNA gel electrophoresis suggested that SULF2 was expressed at higher levels in three cell lines (SNU-182, HuH-7 and HepG2), lower levels in SNU-475, and was absent in Hep 3B and PLC/PRF/5 cell lines (Figure 3.1). For quantification of gene expression levels of SULF1 and SULF2, RT-qPCR was conducted. GAPDH and β2 microglobulin (B2M) were used as reference genes. Sequences of the primers used are listed in Table 2.1. First, the primers of GAPDH, B2M, SULF1 and SULF2 were validated using different quantities of cDNA for the HS766T pancreatic cancer cell line that is known to express high levels of both SULF1 and SULF2. The results showed that triplicate measurements of each gene had identical Ct (cycle threshold) values that inversely correlated with cDNA volumes (Figure 3.2; A) and the ratios of Ct values for each gene relative to that of GAPDH, used for normalization, remained constant (Figure 3.2; B). Also, the dissociation curve showed that the triplicate measurements for each gene had identical melting temperatures of the amplicon and no primer dimers were formed (Figure 3.2; C). Therefore, these primers were considered as suitable for measuring the expression level of SULF1 and SULF2.

The RT-qPCR experiment presented in Figure 3.3 showed that SULF1 was only strongly expressed in 1 of 6 HCC cell lines (SNU-182) and weakly expressed in SNU-475 (Figure 3.3; B), while SULF2 was strongly expressed in 3 of 6 HCC cell lines (SNU-182, HuH-7 and HepG2), moderately expressed in SNU-475, weakly expressed in PLC/PRF/5 and was undetectable in Hep 3B cells (Figure 3.3; A). It was noteworthy that in SNU-182 cells SULF1 expression was 4-fold higher than

that of SULF2 as indicated by the Ct value of 22 for SULF1 compared with 24 for SULF2. In SNU-475 cells, Ct values were 33 for SULF1 compared with 29 for SULF2, i.e., the SULF2 transcript was 16-fold higher than the SULF1 transcript.

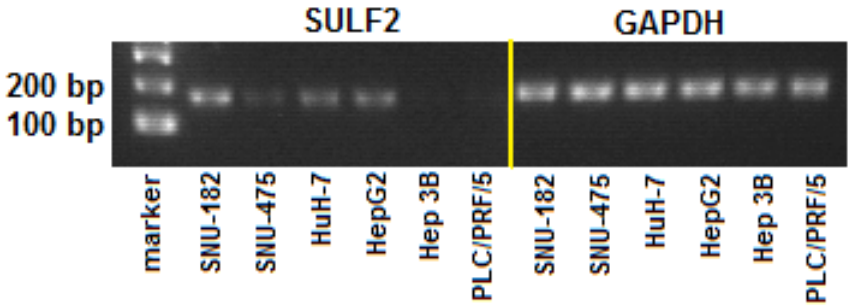

Figure 3.1: Representative gel showing SULF2 mRNA levels in HCC cell lines: mRNA was harvested from 6 HCC cell lines and RT-PCR was performed using SULF2 primers, and the products were separated by agarose gel electrophoresis. GAPDH was used as the control. The experiment was performed in duplicate and a representative gel is shown. Data generated using the method described in Section 2.7.

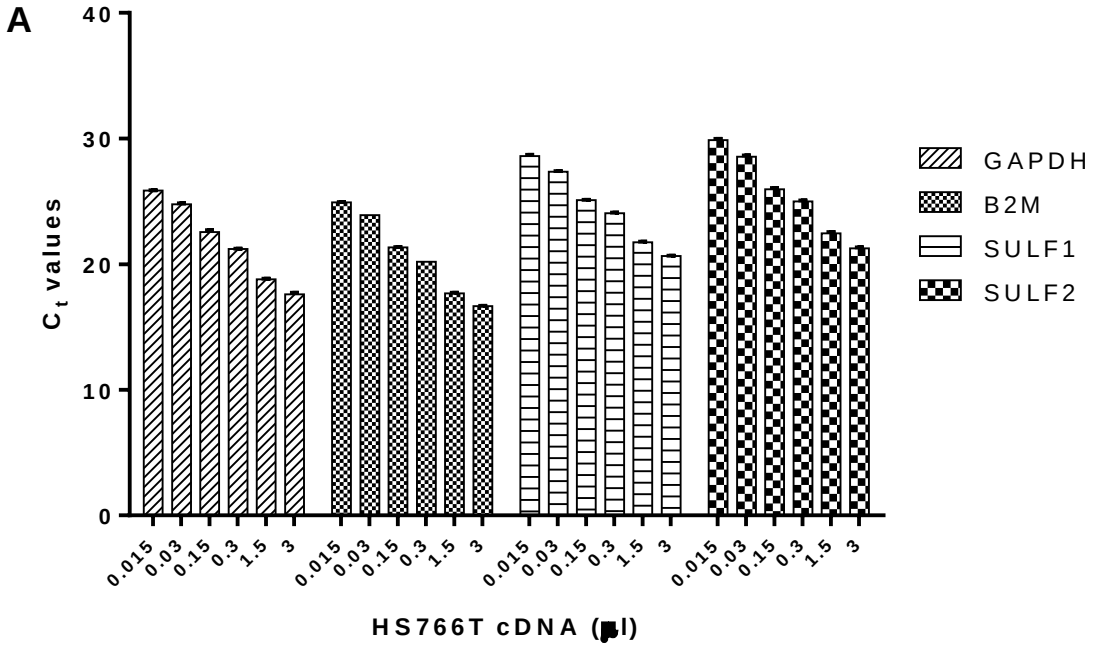

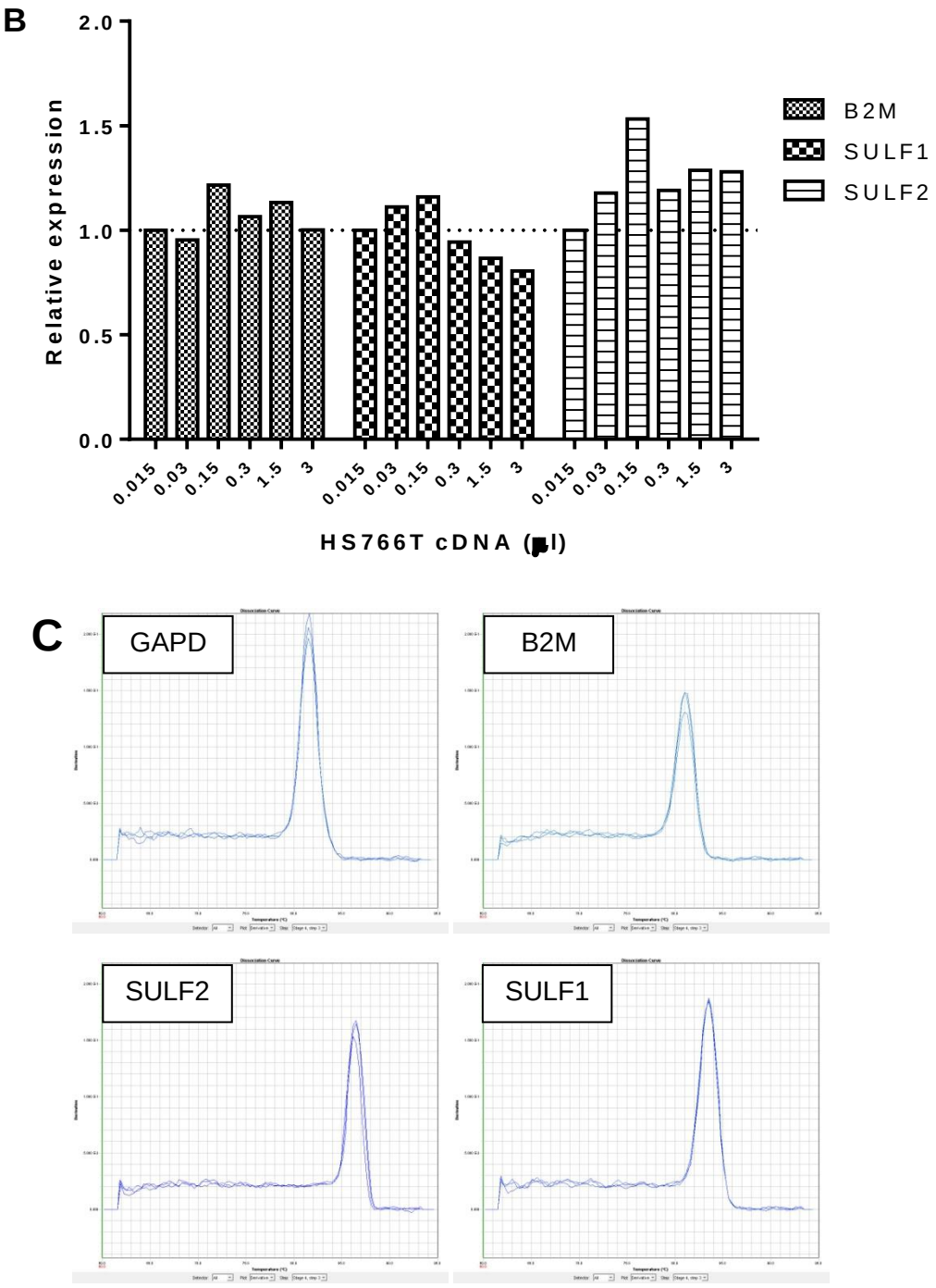

Figure 3.2: Validation of RT-qPCR primers: A + B: RT-qPCR was performed using a range of HS766T cDNA volumes in triplicate. **(A)** The raw Ct values were plotted against the cDNA volume. Values are the mean of triplicates and error bars represent the standard error. **(B)** The relative expression of B2M, SULF1 and SULF2 using GAPDH as a reference gene. **(C)** Derivative dissociation curve of 1 µl of cDNA. The experiment was performed once. Data generated using the method described in Section 2.7.

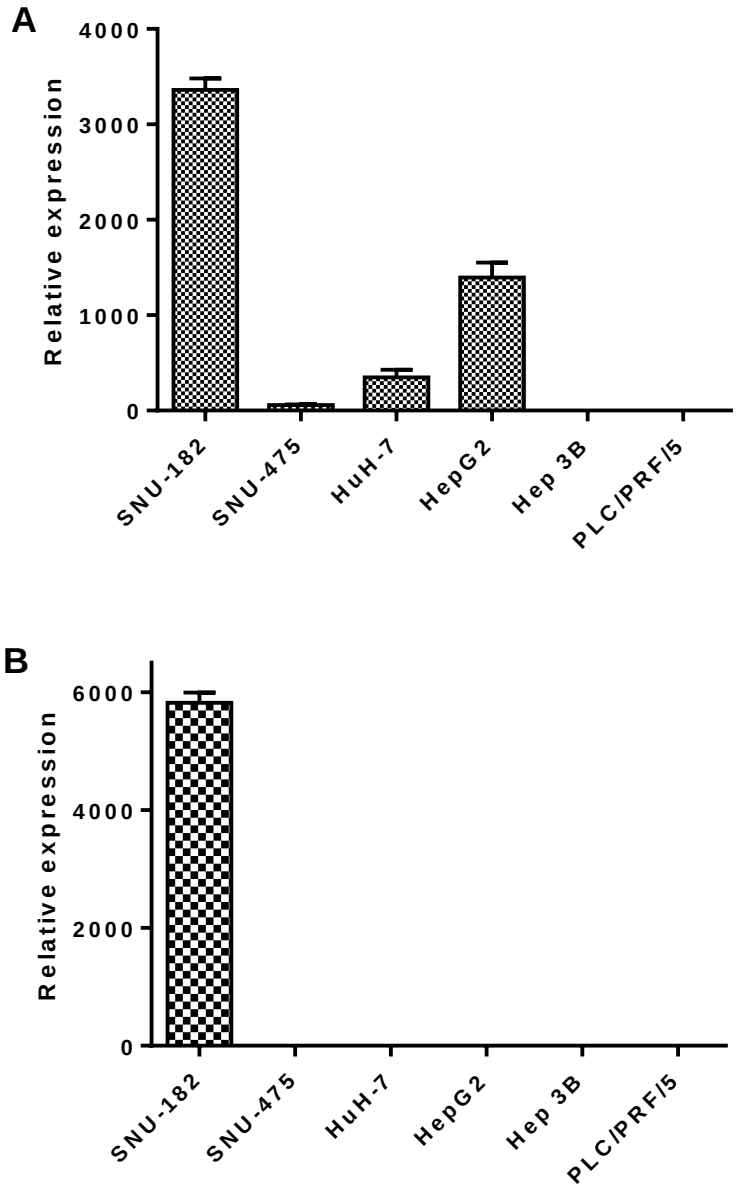

Figure 3.3: Quantification of SULF1/2 mRNA levels by RT-qPCR in HCC cell lines: Data were normalized to the expression of GAPDH and presented relative to the expression level of PLC/PRF/5 cell line for SULF2 **(A)** or SNU-475 cell line for SULF1 **(B)**. Values are the mean of three experiments each containing three biological replicates and error bars represent the standard error. Data generated using the method described in Section 2.7.

3.2. SULF1/2 Protein Expression in HCC Cell Lines

To investigate whether SULF1/2 mRNA is translated into protein in HCC cell lines and to determine the localization of SULF1/2 proteins, western blot (WB) and immunocytochemistry (ICC) experiments were performed, respectively.

3.2.1. SULF1/2 protein expression measured using western blot

The performance of five commercially available antibodies (listed in Table 2.5) reportedly detecting SULF2 protein under reducing conditions was tested. However, none of these antibodies detected the appropriate SULF2 bands, namely the full-length protein along with one of its subunits (i.e., 75 or 50 kDa), depending on the immunogen to which the antibody (Ab) was raised. SULF2 Ab (LR) (kindly provided by Prof. Lewis Roberts, USA), raised against HD amino acids 421-444, gave better results. Blotting with this antibody was predicted to identify both the full-length 125 kDa and the 75 kDa bands that encompass the N-terminal domain. The 125 kDa band was detected in five HCC cell lines except Hep 3B cells (Figure 3.4; right), while the 75 kDa band was indistinguishable from a non-specific protein smear that appeared around that region.

To generate a new SULF2 antibody, namely SULF2 Ab (NCL), the SULF2 HD amino acids 421-435 were used to which a cysteine residue was added as an immunogen in an attempt to generate a similar result to that obtained using SULF2 Ab (LR). The peptide was designed and the antibody was raised in two rabbits by Eurogentec. The company provided the sera from the two rabbits, 1271 and 1272. After purification and testing the antibody specificity by ELISA, the antibody failed to detect the correct SULF2 bands by WB and gave unspecific binding.

A new SULF2 Ab (Serotec) that was first reported by Lemjabbar-Alaoui *et al.* in 2010 became commercially available. WB using this antibody showed the expression of SULF2 protein in the cell lines that expressed high levels of SULF2 mRNA, namely SNU-182, HuH-7 and HepG2 (Figure 3.4; left). Moreover, this antibody gave less unspecific binding compared with SULF2 Ab (LR). However, the 50 kDa subunit could not be detected in any of the cells that endogenously expressed SULF2.

Regarding SULF1, two antibodies were tested and only the SULF1 antibody that was raised against the C-terminal domain, SULF1 Ab (Abcam), detected a 125 kDa band, although not the 50 kDa band that encompasses the C-terminal domain (Figure 3.5). The results in Figure 3.5 were in line with the RT-qPCR data as a 125 kDa band could be detected in the SNU-182 cell line but not the other HCC cell lines. HS766T pancreatic cancer cell line was used as a positive control for SULF1.

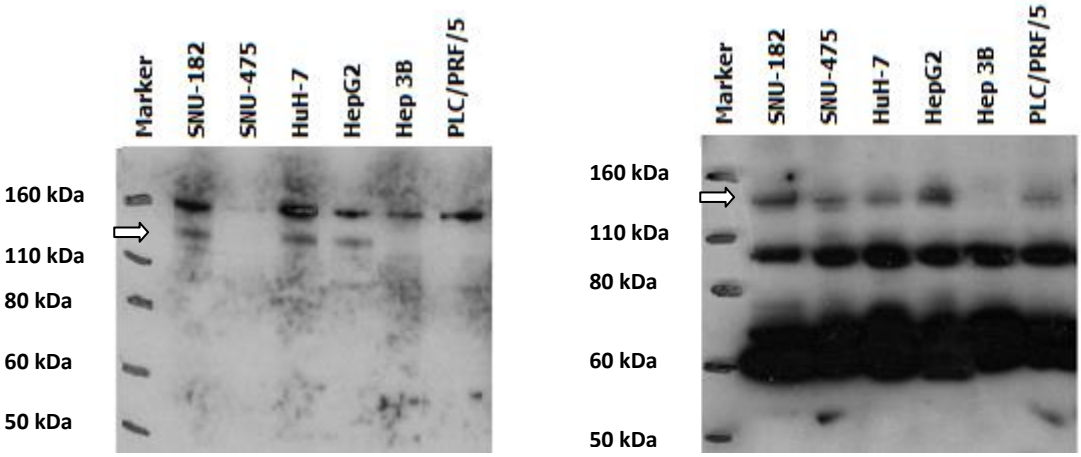

Figure 3.4: SULF2 protein expression in HCC cell lines: Protein immunoblotting was performed on whole cell lysates with SULF2 Ab (Serotec) (Left), or SULF2 Ab (LR) (Right). The white arrows point to the band with the appropriate molecular weight for full-length SULF2 protein. The experiment was performed in triplicate and representative blots are shown. Data generated using the method described in Section 2.10.

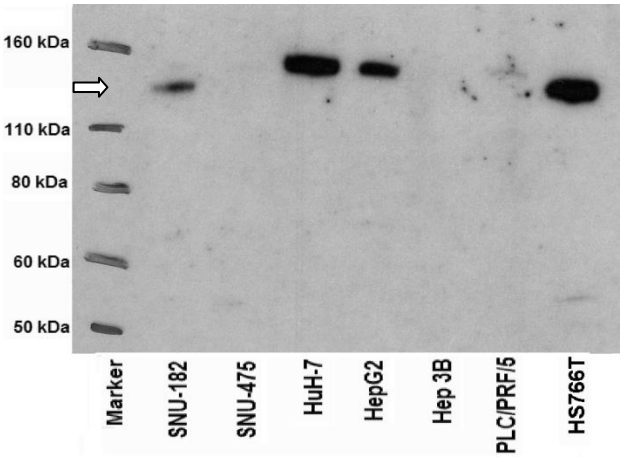

Figure 3.5: SULF1 protein expression in HCC cell lines: Protein immunoblotting was performed on whole cell lysates with SULF1 Ab (Abcam). The white arrow points to the band with the appropriate molecular weight for the full-length SULF1 protein. The experiment was performed in triplicate and a representative blot is shown. Data generated using the method described in Section 2.10.

3.2.2. SULF1/2 protein expression analysed using immunocytochemistry

In order to investigate the subcellular localization of SULF1/2 in HCC cell lines, ICC was performed. Three HCC cell lines (HuH-7, HepG2 and Hep 3B) and the HS766T pancreatic cancer cell line were studied using SULF2 Ab (LR) or SULF2 Ab (Serotec) for SULF2 and SULF1 Ab (Abcam) for SULF1. These were the antibodies that gave the best results by WB. SULF2 Ab (LR) showed positive cytoplasmic and membranous staining for SULF2 in HuH-7 (Figure 3.6; 1B), HepG2 (Figure 3.6; 2B) and HS766T (data not shown) cells. However, this staining was similar to that in SULF2 non-expressing Hep 3B cells (Figure 3.6; 3B) indicating that this antibody is not suitable for ICC.

In contrast, SULF2 Ab (Serotec) produced dotted-like staining of HuH-7 and HepG2 cells (Figure 3.7; 1-2B) rather than widespread staining of the whole cells. This pattern is in line with other studies reporting the enrichment of SULF2 in lipid raft domains on the cell surface (Tang and Rosen, 2009). Hep 3B cells were completely negative with this antibody (Figure 3.7; 3B).

With respect to SULF1, no staining was detected in any of the tested cell lines except for weak staining in HS766T cells (data not shown), despite the very high level of protein expression of SULF1 in this cell line as measured by WB. Therefore, SULF1 Ab (Abcam) was regarded as unsuitable for ICC. Negative control samples stained with secondary antibody in the absence of primary antibody did not show staining in any of the cell lines (data not shown).

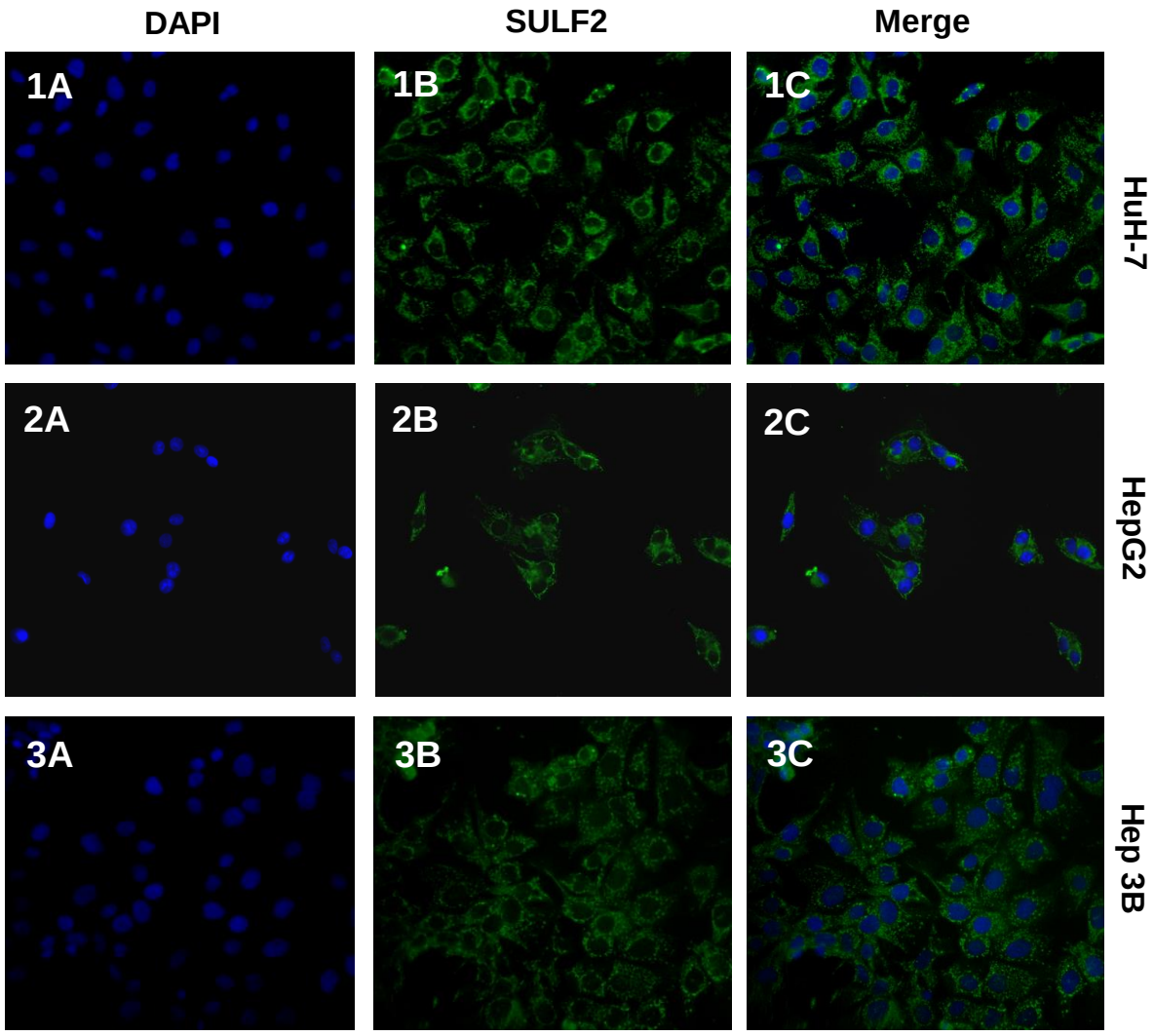

Figure 3.6: ICC staining of SULF2 in HCC cell lines using SULF2 Ab (LR): HCC cells were grown on glass coverslips and incubated with SULF2 Ab (LR) which was then stained green with Alexa Fluor 488 conjugated secondary antibody. Mounting medium with DAPI was used to counter-stain the nuclei in blue. **(1)** HuH-7, **(2)** HepG2, **(3)** Hep3B. **(A)** blue channel for DAPI, **(B)** green channel for Alexa Fluor 488, **(C)** merge picture. The experiment was performed in duplicate. Data generated using the method described in Section 2.11.

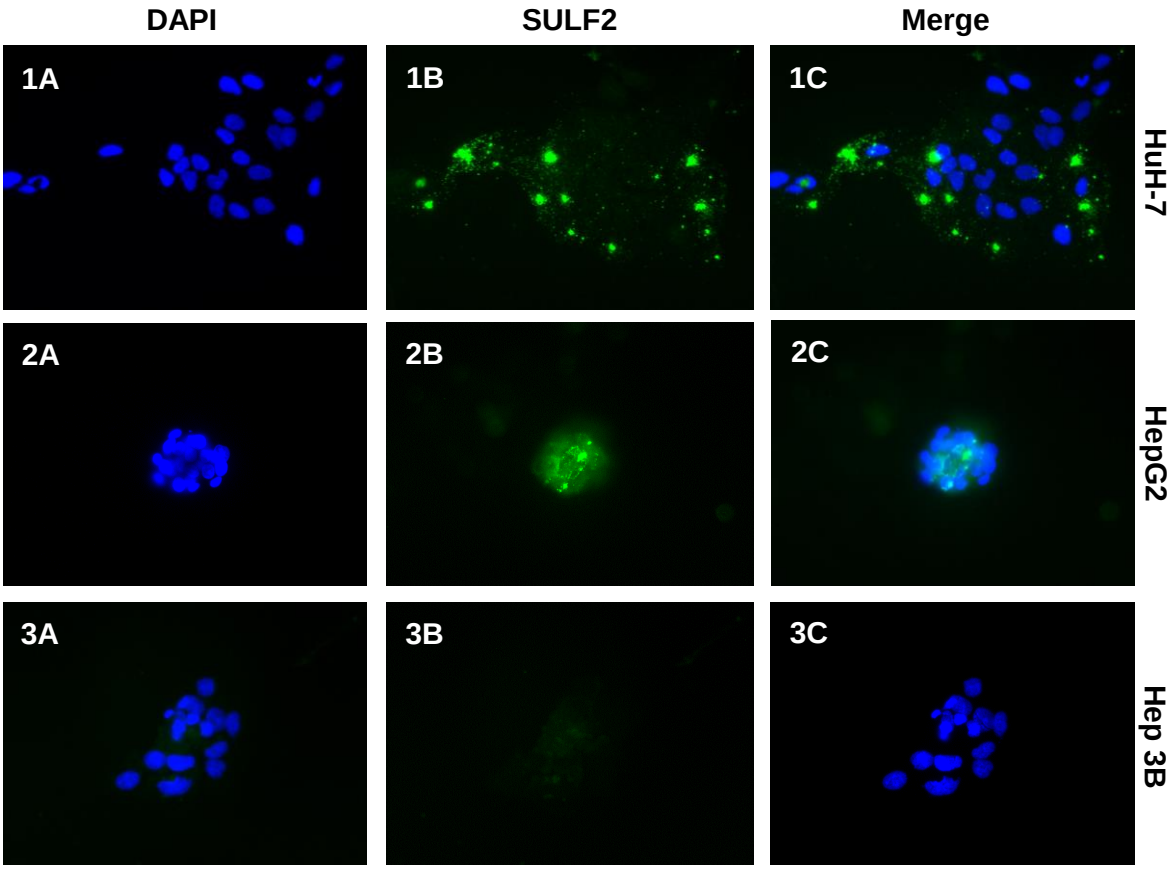

Figure 3.7: ICC staining of SULF2 in HCC cell lines using SULF2 Ab (Serotec): HCC cells were grown on glass coverslips and incubated with SULF2 Ab (Serotec) which was then stained green with Alexa Fluor 488 conjugated secondary antibody. Mounting medium with DAPI was used to counter-stain the nuclei in blue. **(1)** HuH-7, **(2)** HepG2, **(3)** Hep3B. **(A)** blue channel for DAPI, **(B)** green channel for Alexa Fluor 488, **(C)** merge picture. The experiment was performed in duplicate. Data generated using the method described in Section 2.11.

3.3. Arylsulfatase Activity Assay in HCC Cell Lines

SULF1/2 enzymes have been reported to have both endosulfatase as well as arylsulfatase (ARS) activities. To determine whether SULF1/2 proteins expressed in the different HCC cell lines were enzymatically active, their ARS activity was measured using the pseudo-substrate 4-MUS. 4-MUS is converted into the fluorescent product 4-MU by desulfation as described in Section 2.13.

3.3.1. Optimisation of the conditions of the ARS activity assay

The fluorescence of the product 4-MU is affected by the pH of the reaction mixture, with maximal fluorescence in alkaline solutions. This can be problematic if the pH optimum of the enzymes under investigation is in the acidic or neutral range. In such a case, the reaction would need to be stopped by increasing the pH of the reaction mixture to read the fluorescence of 4-MU, and as a result the assay would be discontinuous. Therefore, it was necessary to determine the sensitivity of 4-MU fluorescence at different pH values, as a continuous assay is optimal for studying the kinetics of SULF1/2 enzymatic reactions and the effects of inhibitors.

Therefore, serial dilutions of 4-MU were added to HEPES solutions of different pH values ranging from 7 to 11, and the fluorescence intensity (FI) was measured. The results in Figure 3.8 show that FI values increased with increasing 4-MU concentrations to a peak of 4-MU fluorescence at a pH of 10 (Figure 3.8; A). However, 4-MU fluorescence could be detected at concentrations ≥ 0.1 µM 4-MU at all pH values studied (Figure 3.8; B). As the pH optimum for SULF1/2 activity is at 7 – 8, and in order to develop a continuous assay, the following conditions were used in all subsequent experiments: a pH of 7.4 was used for the cell-based assay which is the pH value of cell culture medium, and for all other cell-free assays a pH of 8 was used.

The results presented in Figure 3.9 show that 4-MU readings are stable over at least a two-hour period, which was considered sufficient for performing a continuous assay and kinetic studies.

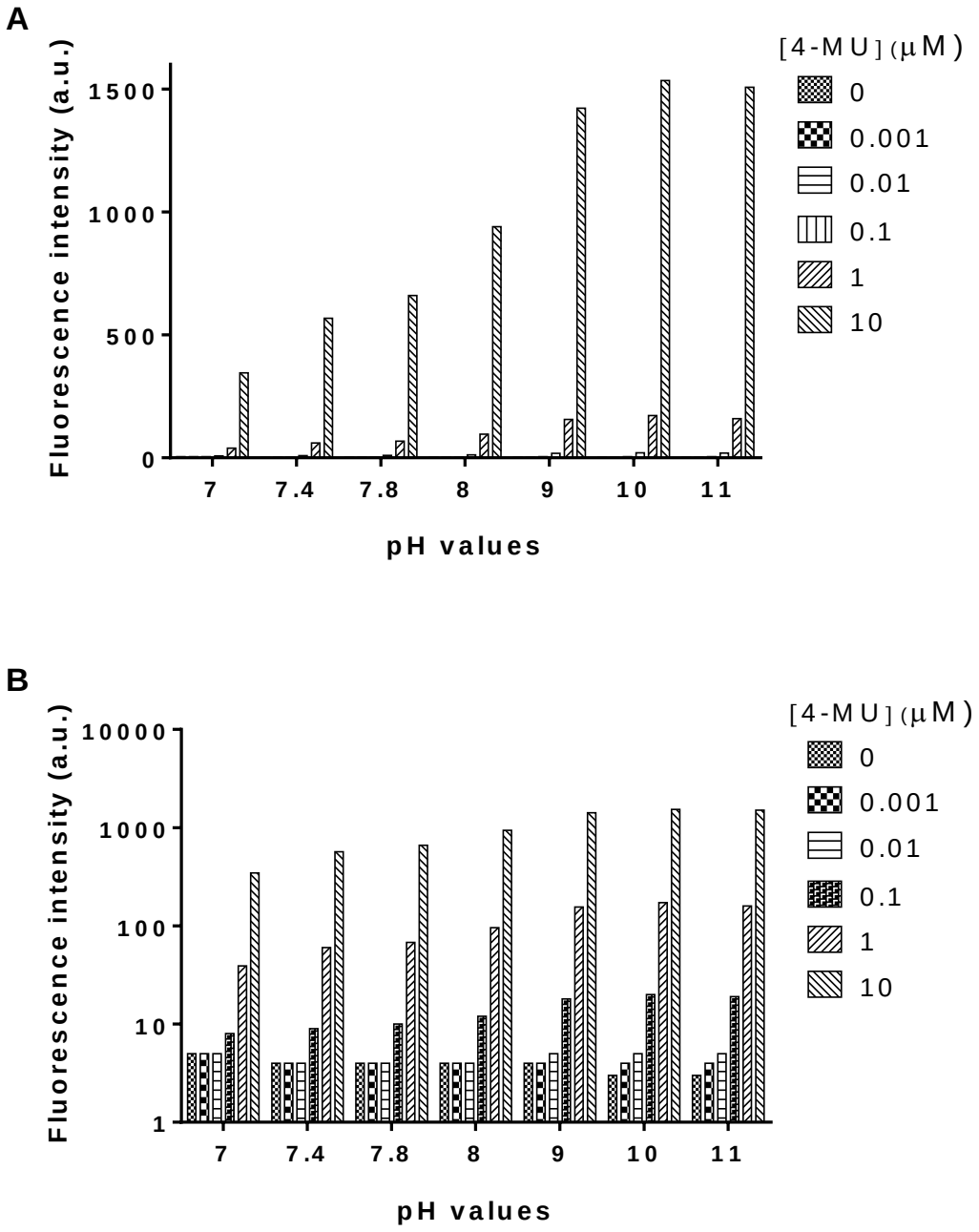

Figure 3.8: Effect of pH on the fluorescence of 4-MU: Serial dilutions of 4-MU were prepared in HEPES solutions of different pH and the fluorescence of 4-MU was measured at 460 nm following excitation at 355 nm. **(A)** Normal scale. **(B)** Logarithmic scale. The experiment was performed in triplicate. Data generated using the method described in Section 2.13.

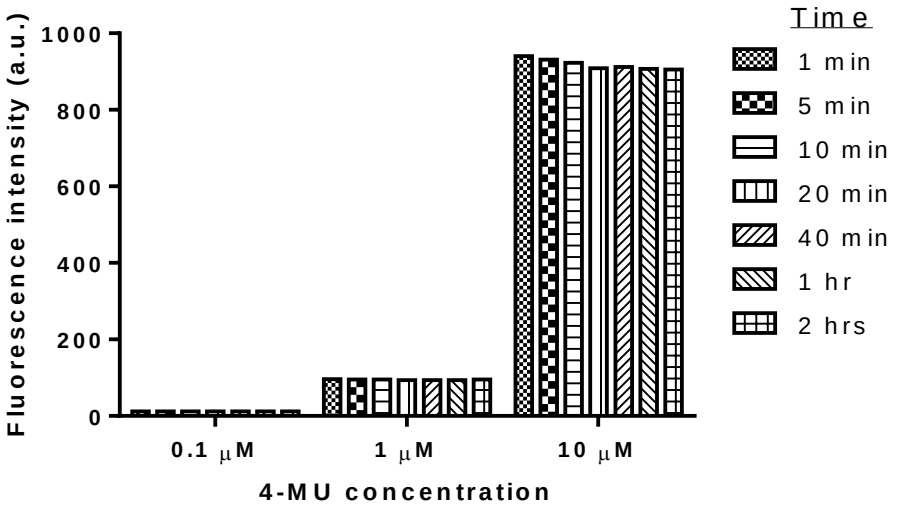

Figure 3.9: Stability of the fluorescence of 4-MU over time: Serial dilutions of 4-MU was prepared in pH 8 HEPES solution and the fluorescence of 4-MU was measured at 460 nm following excitation at 355 nm at different time points. The experiment was performed in triplicate. Data generated using the method described in Section 2.13.

3.3.2. Cell-based assay

In this assay, total ARS activity was measured and no differentiation was possible for either SULF1 or SULF2. Moreover, if other members of the sulfatase family are secreted outside the cells, or if 4-MUS is internalized into the cells and hydrolysed, the ARS activity measured could be due to other sulfatases in addition to the two extracellular SULF1/2 enzymes. However, it was possible to inhibit the activity of one of these alternative sulfatases, namely, steroid sulfatase/arylsulfatase C (STS/ARSC), using the well-validated irreversible inhibitor oestrone 3-O-sulfamate (EMATE) (Howarth et al., 1994) (Poirier et al, 1999).

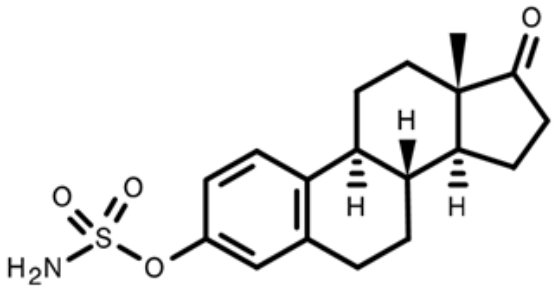

Oestrone 3-O-sulfamate (EMATE)

For the cell-based assay, equal numbers of cells were cultured and then STS/ARSC was inhibited by incubation with EMATE. Remaining ARS activity was determined by incubation with the substrate 4-MUS and measurement of the fluorescent product 4-MU. The results in Figure 3.10 show that only two cell lines out of 6 tested exhibited ARS activity. HuH-7 had very high activity and HepG2 had lower but detectable activity while no significant activity was detected in any of the other four cell lines. These results suggested a poor correlation between SULF1/2 mRNA and protein levels and sulfatase activity in HCC cell lines. Possible explanations include poor affinity of the substrate 4-MUS for SULF1/2 enzymes, or that SULF1/2 enzymes are present in some HCC cell lines in an inactive form.

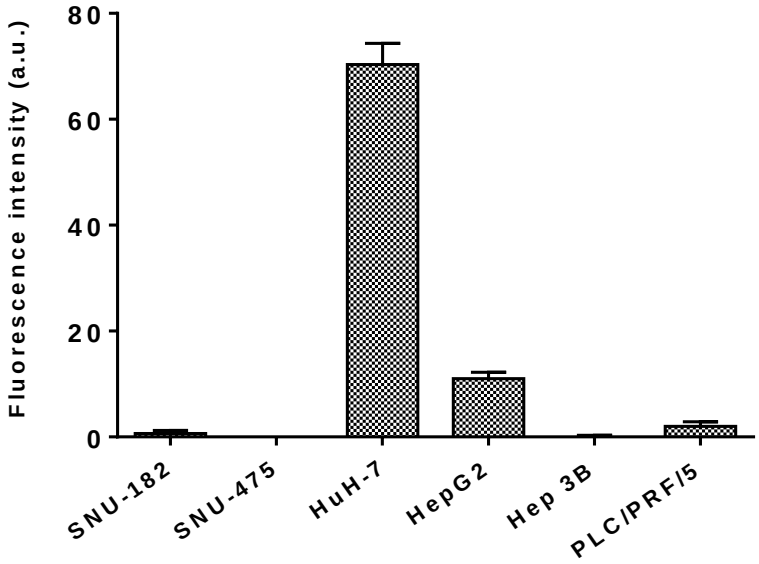

Figure 3.10: Cell-based arylsulfatase activity assay in HCC cell lines: 10,000 cells/well were cultured in 96-well plate for 24 hours. STS/ARSC was then inhibited by incubation with 10 µM EMATE for 1 hour, and remaining sulfatase activity was measured by incubation with 0.5 mM 4-MUS for 4 hours after which the fluorescence of the product 4-MU was read at 460 nm following excitation at 355 nm. Values are the mean of triplicates and error bars represent the standard error. The experiment was performed in triplicate. Data generated using the method described in Section 2.13.

To determine the level of STS/ARSC activity based on the effect of EMATE on cell-based ARS activity assay in HCC cell lines, the two cell lines that showed ARS activity (i.e., HuH-7 and HepG2) as well as Hep 3B that had no activity, as a negative control, were studied. The cells were incubated with or without EMATE

and ARS activity was measured by incubation with the substrate 4-MUS and 4-MU fluorescence measured at different time points (Figure 3.11; A). The results showed that the majority of the sulfatase activity in HCC cell lines could be inhibited by the STS/ARSC inhibitor EMATE and only a low level of activity was not inhibited in both HuH-7 and HepG2 cell lines. Cell number at the time of the analysis was similar in the 3 cell lines and not affected by EMATE, as measured by crystal violet staining (Figure 3.11; B)

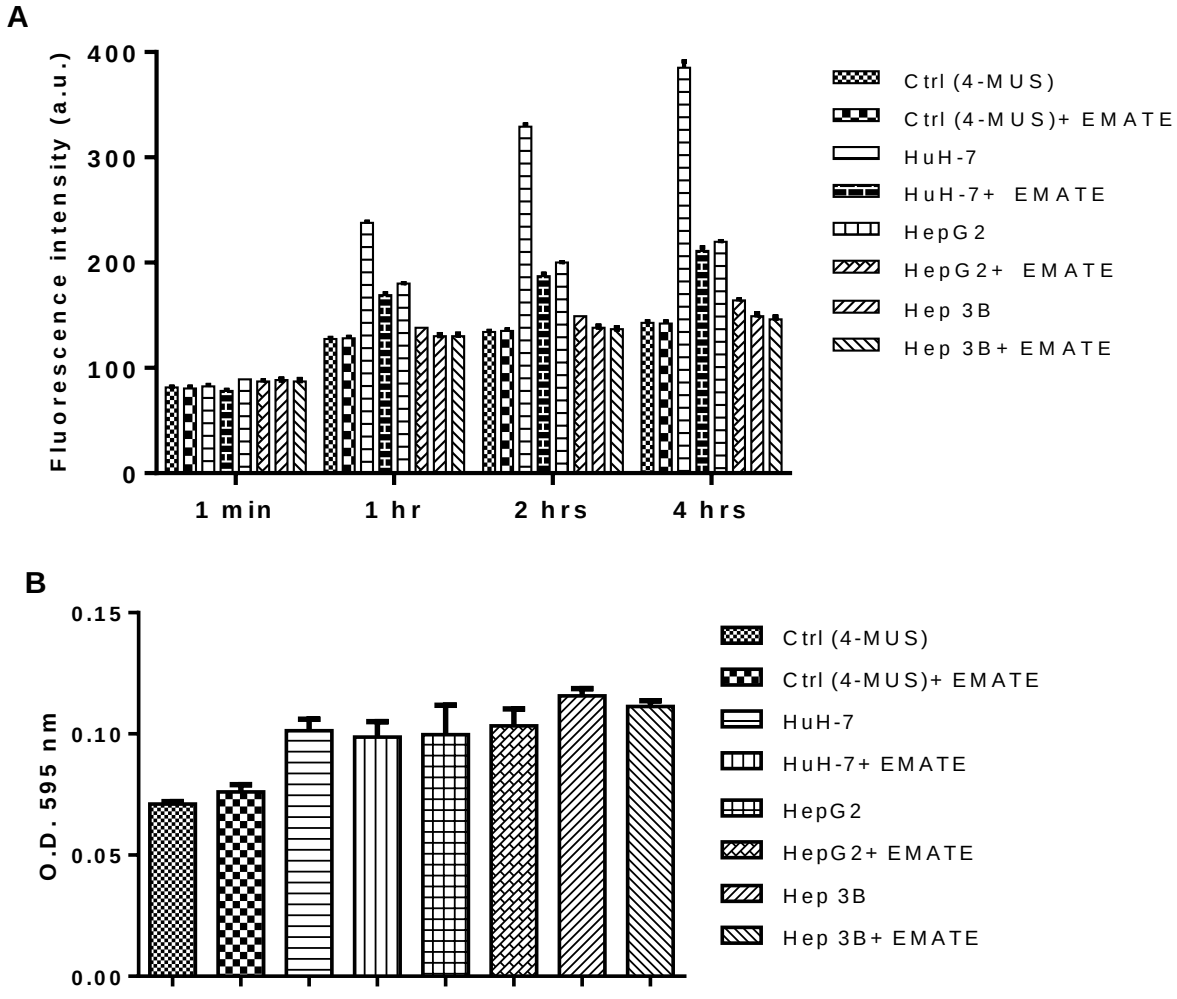

Figure 3.11: Effect of EMATE on arylsulfatase activity assay in HCC cell lines: 10,000 cells/well were cultured in a 96-well plate for 24 hours. Cells were then incubated with or without 10 µM EMATE for 1 hour. **(A)** Arylsulfatase activity was measured by incubation with 2.6 mM 4-MUS and reading the fluorescence of the product 4-MU at 460 nm following excitation at 355 nm. **(B)** Crystal violet staining of the same cells at the end of the ARS activity assay. Values are the mean of triplicates and error bars represent the standard error. The experiment was performed in triplicate. Data generated using the methods described in Section 2.13 and Section 2.14.

3.3.3. Relationship between ARS activity and cell number

To investigate the effect of cell number on the ARS activity, different numbers of HCC cells were seeded in 96-well plates and the EMATE-uninhibitable ARS activity was measured using the substrate 4-MUS, followed by staining of the cells with crystal violet. The results in Figure 3.12 show that the ARS activity of HuH-7 and HepG2 cells is proportional to the number of seeded cells. No ARS activity was detected in the other 4 HCC cell lines (SNU-182, SNU-475, Hep 3B and PLC/PRF/5) even at $1x10^5$ cells/well (data not shown).

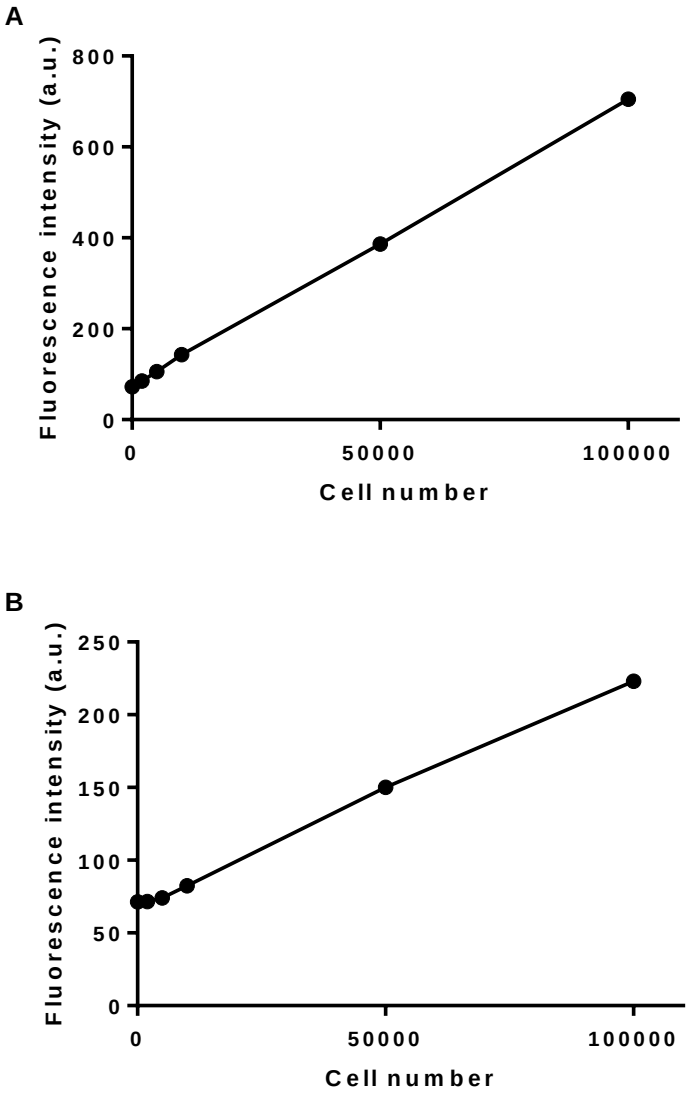

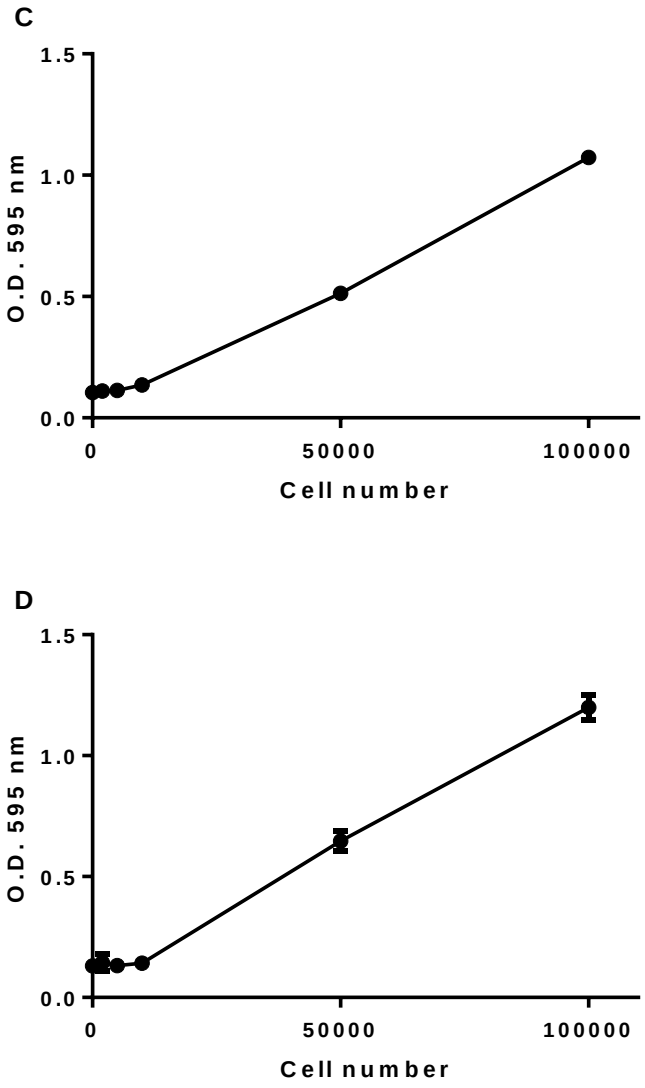

Figure 3.12: Effect of cell number on arylsulfatase activity in HCC cell lines: Increasing numbers of cells/well were cultured in 96-well plates for 24 hours. Steroid STS/ARSC was then inhibited by incubation with 10 µM EMATE for 1 hour, and remaining sulfatase activity was measured by incubation with 0.5 mM 4-MUS for 4 hours. 100 µl of CM of HuH-7 **(A)** and HepG2 **(B)** was transferred into a new plate and 50 µl of 1 M Tris solution (pH 10.4) was added to increase 4-MU fluorescence which was read at 460 nm following excitation at 355 nm. Cells were then stained with crystal violet and the absorbance at 595 nm was read for HuH-7 **(C)** and HepG2 **(D)**. Values are the mean of triplicates and error bars represent the standard error. The experiment was performed in triplicate. Data generated using the methods described in Section 2.13 and Section 2.14.

3.3.4. ARS activity of HCC conditioned media

Mature SULF1/2 can be retained on the cell surface or secreted into the extracellular fluid. To determine whether SULF1/2 proteins were secreted into the conditioned medium (CM), and whether the secreted proteins were enzymatically active, equal numbers of cells from the different cell lines (HuH-7, HepG2, Hep 3B and HS766T) were cultured in phenol red-free medium. After 48 hours, the CM was collected and concentrated 20 times. Then ARS activity was measured using 4-MUS as a substrate. However, none of the cell lines tested showed any significant activity relative to control wells containing the substrate 4-MUS only (data not shown).

3.3.5. ARS activity of HCC cell lysates

In addition to the extracellular SULF1/2, enzymatically active SULF1/2 can be found in the ER and Golgi apparatus (Ai et al., 2003). Therefore, to compare the total level of SULF1/2 that could be present in different cellular compartments across HCC cell lines, ARS activity assays were performed using total cell lysates. Equal quantities of lysates were pre-incubated with EMATE to inhibit STS/ARSC before measuring the ARS activity using 4-MUS. The results in Figure 3.13 show that only HuH-7 and HepG2 cell lines had ARS activity and that no activity was detected in the other four cell lines. These results were consistent with the cell-based assay data (Figure 3.10). The EMATE-uninhibitable activity of the cell lysates was ~ 40% and 60% of the total activity for HuH-7 and HepG2 cell lines, respectively (Figure 3.13).

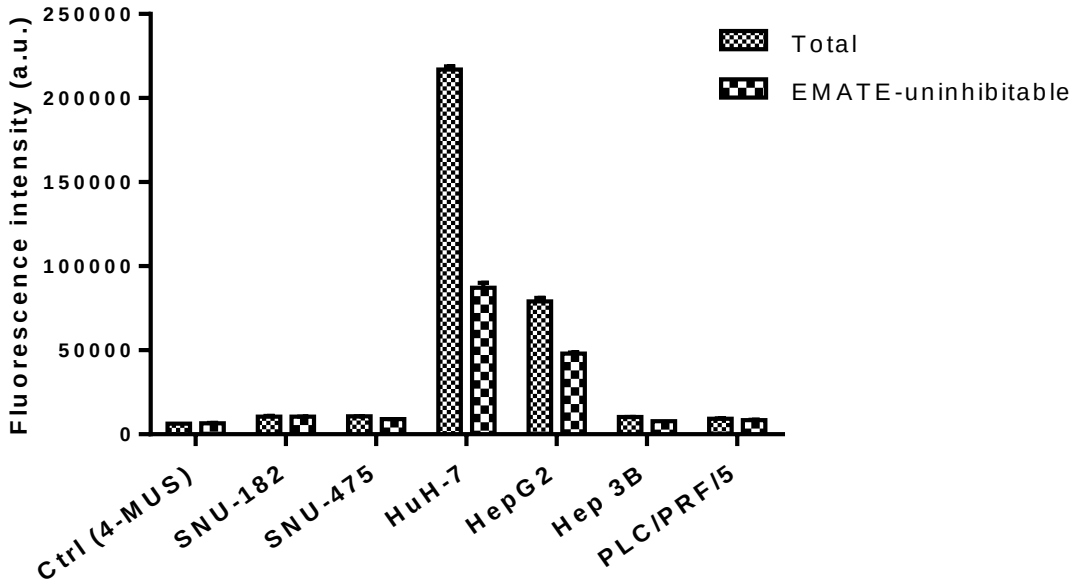

Figure 3.13: Arylsulfatase activity assay of HCC cell lysates: 20 µg of HCC cell lysates extracted in RLB were incubated with or without 100 µM EMATE for 1 hour to inhibit STS/ARSC. After incubation with 3 mM 4-MUS for 3 hours at pH 7.5 the reaction was stopped and the fluorescence of the product 4-MU was read at 460 nm following excitation at 355 nm. Values are the mean of triplicates and error bars represent the standard error. The experiment was performed in triplicate. Data generated using the method described in Section 2.13.

3.3.6. ARS activity of SULF-antibody immunoprecipitates of HCC cell lysates

ARS activity that was detected using cells or cell lysates could be due to the enzymatic activity of other members of the sulfatase family in addition to SULF1/2, as 4-MUS is a broad spectrum sulfatase substrate as discussed earlier. Therefore, SULF1/2 enzymes in HCC lysates were isolated by immunoprecipitation using SULF1 or SULF2 antibodies. Equal amounts of protein from lysates of HCC cell lines were incubated with protein A agarose beads that were pre-loaded with excess SULF1 Ab (Abcam) or SULF2 Ab (Abcam) to form SULF1/2-Ab immunoprecipitates (IPs) (see Section 2.12). These two antibodies were raised against the C-terminal domain of the corresponding SULF. The SULF2 Ab (Abcam) was initially chosen to avoid interference of the antibody-bead complex with the catalytic active site which is present in the N terminal domain of the SULF2 enzyme. ARS activity of equal volumes of bead slurry was measured using the

substrate 4-MUS. For the SULF2-Ab (Abcam) IPs, the results showed that HuH-7 cell lysate had the highest activity followed by HepG2 cell lysate while no activity was detected with the other HCC cell lysates (Figure 3.14; A).

To confirm these results, the immunoprecipitation of SULF2 from HuH-7 and HepG2 cell lysates was repeated using a different antibody, namely SULF2 Ab (LR) that was raised against the HD domain. The results using the SULF2-Ab (LR) IPs were in line with the previous data using SULF2-Ab (Abcam) IPs and showed that both HuH-7 and HepG2 IPs had ARS activity which was higher in HuH-7 cell line (Figure 3.14; B). Furthermore, SULF2-Ab (Serotec) IPs showed similar results to SULF2-Ab (Abcam) IPs (data not shown). In all subsequent experiments SULF2-Ab (Abcam) IPs were used.

With respect to SULF1, immunoprecipitation was performed using SNU-182 cell lysate only as this was the only HCC cell line that expressed SULF1. The HS766T cell line was also used as a positive control. No ARS activity was detected using SULF1-Ab IPs of SNU-182 cell lysate (data not shown), while a slight activity was detected for HS766T cell line (Figure 3.15).

To investigate whether the ARS activity of SULF2-Ab IPs was lysate protein concentration dependent, SULF2 was immunoprecipitated by incubation of increasing quantities of HuH-7 cell lysate with the same volume of SULF2 antibody-loaded beads. The HuH-7 cell line was used for this purpose as it had the highest ARS activity. The results in Figure 3.15 show that ARS activity increased with increasing quantities of lysate.

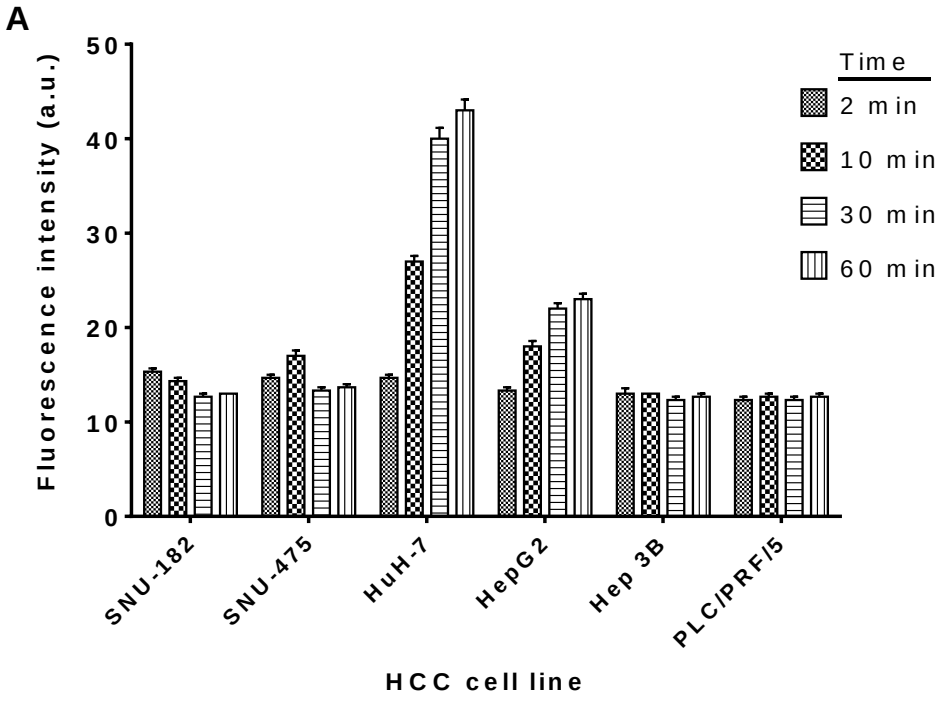
A
Fluorescence intensity (a.u.)
50
40
30
20
10
0
Time
2 min
10 min
30 min
60 min
SNU-182
SNU-475
HuH-7
HepG2
Hep 3B
PLC/PRF/5
HCC cell line

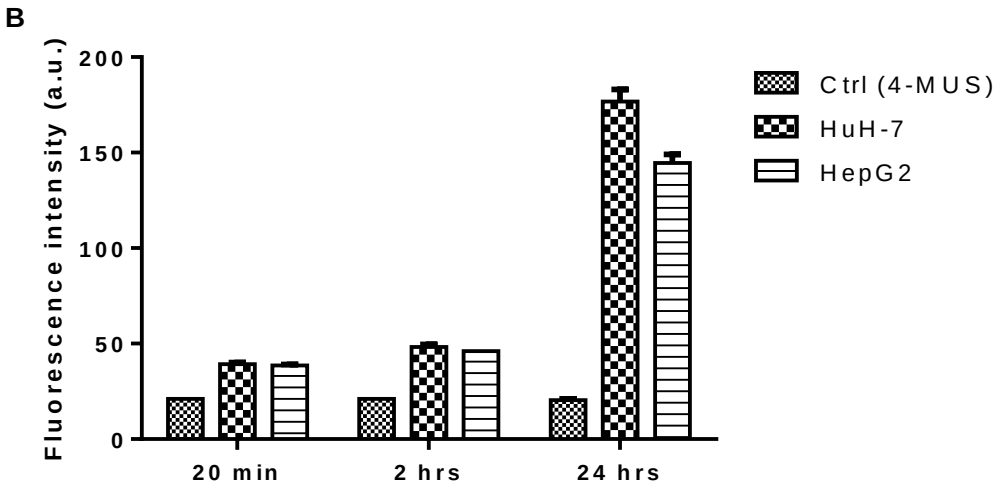
B
Fluorescence intensity (a.u.)
200
150
100
50
0
Ctrl (4-MUS)
HuH-7
HepG2
20 min
2 hrs
24 hrs

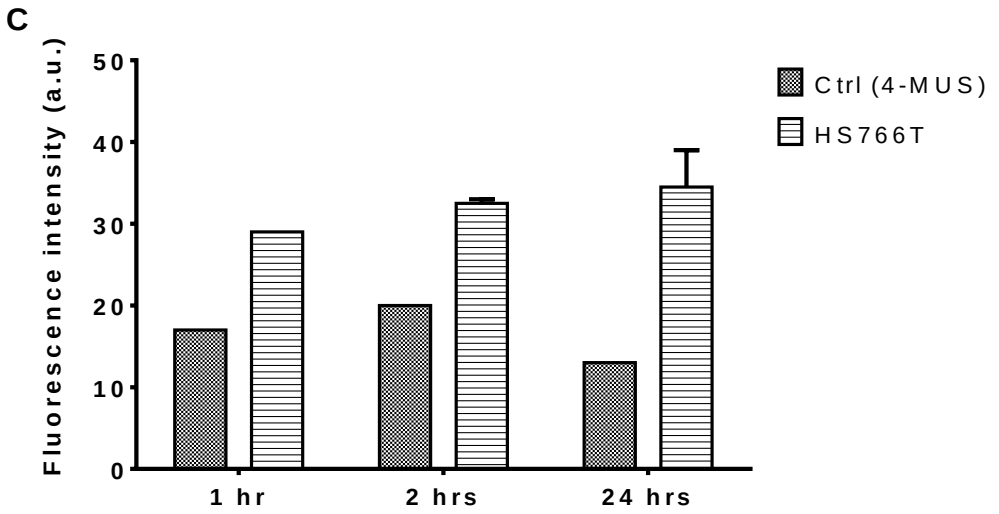

Figure 3.14: Arylsulfatase activity assay of SULF2-Ab IPs of HCC cell lysates: 1 mg of HCC cell lysates was incubated with protein A agarose beads that were pre-loaded with excess SULF2 Ab (Abcam) **(A)**, SULF2 Ab (LR) **(B)** or SULF1 Ab (Abcam) **(C)**. Equal volumes of bead slurry were added to a 96-well plate and arylsulfatase activity was measured by incubation with 4-MUS for the time period indicated and reading the fluorescence of the product 4-MU at 460 nm following excitation at 355 nm. Values are the mean of triplicates and error bars represent the standard error. Each experiment was performed in triplicate. Data generated using the methods described in Section 2.12 and Section 2.13.

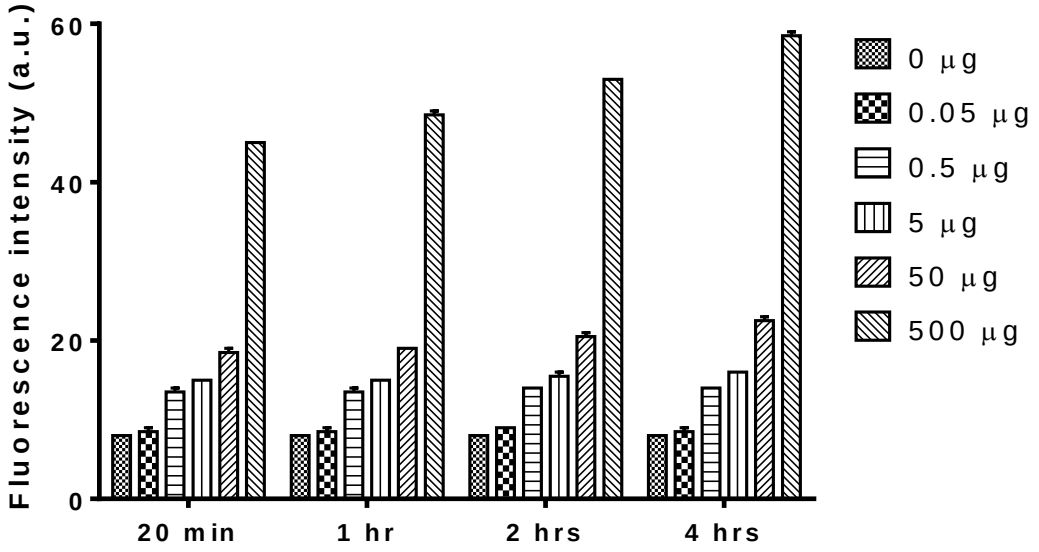

Figure 3.15: Arylsulfatase activity of SULF2-Ab IPs generated using different quantities of HuH-7 cell lysate: Different amounts of HuH-7 cell lysate (0 - 500 µg) were incubated with 25 µl of protein A agarose beads that were pre-loaded with excess SULF2 Ab (Abcam).The beads were washed and 1 mM 4-MUS was added and arylsulfatase activity was measured by reading the fluorescence of the product 4-MU at 460 nm following excitation at 355 nm. Values are the mean of duplicates and error bars represent the standard error. Data are from a single experiment. Data generated using the method described in Section 2.12 and Section 2.13.

3.3.7. Kinetics of the arylsulfatase activity of SULF2 using the substrate 4-MUS

One aim of these studies was to evaluate the use of the ARS activity assay of SULF2 with 4-MUS as a substrate in the screening of small-molecule inhibitors of SULF2. Therefore, it was important to study the kinetics of SULF2 with 4-MUS and to calculate the Michaelis constant (Km) of the reaction. For this purpose, SULF2-Ab IPs of HuH-7 cell lysate were used and equal volumes of bead slurry were used and incubated with different concentrations of 4-MUS, and the fluorescence of the product 4-MU was read at different time points (Figure 3.16; A-G). The initial rates of the reactions were calculated and plotted against the substrate concentrations (Figure 3.16; H). The Km, defined as the concentration at half the maximum initial rate, was found to be 2.6 mM. The calculated Km was relatively high and indicates that 4-MUS is a poor SULF2 substrate.

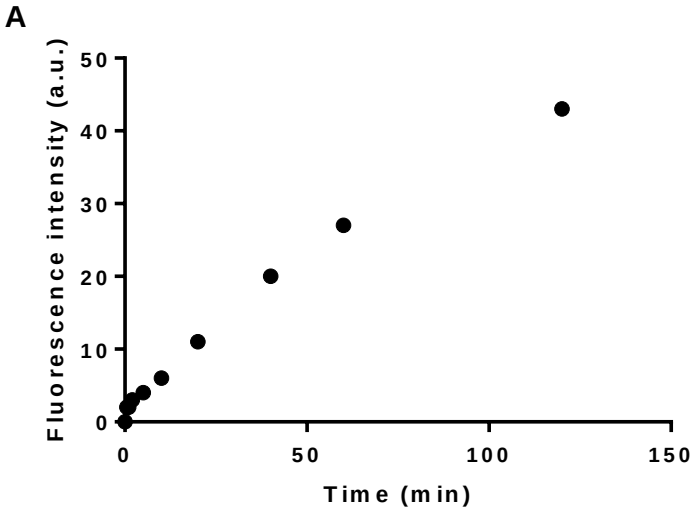

B

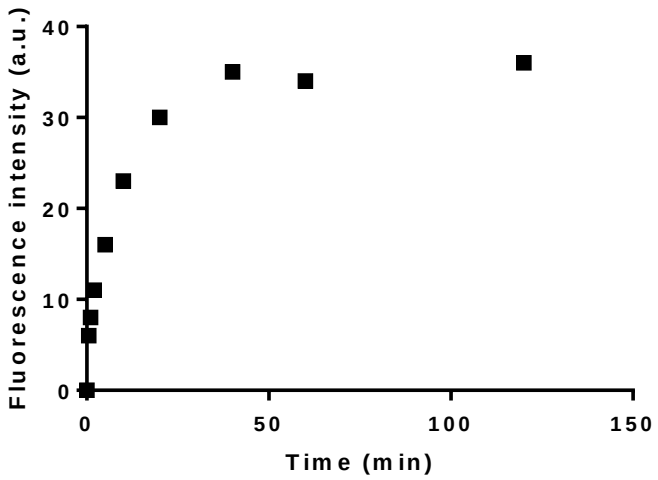
Fluorescence intensity (a.u.)
40
30
20
10
0
0
50
100
150
Time (min)

C

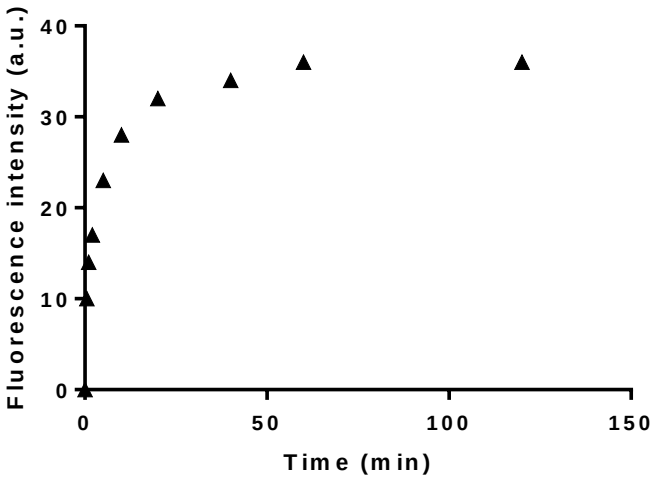
Fluorescence intensity (a.u.)
40
30
20
10
0
0
50
100
150
Time (min)

D

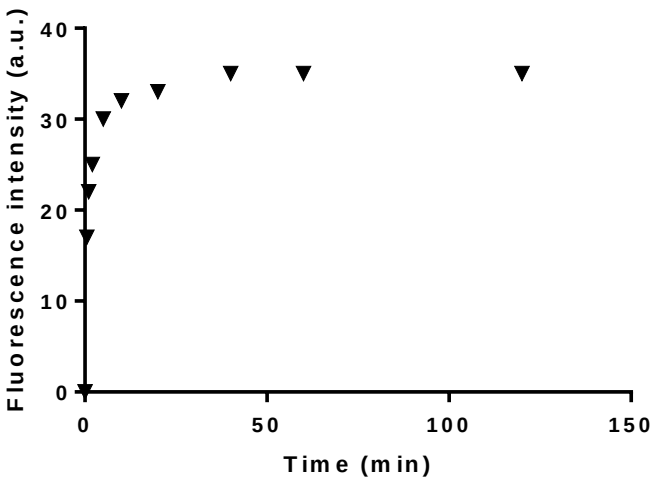
Fluorescence intensity (a.u.)
40
30
20
10
0
0
50
100
150
Time (min)

E

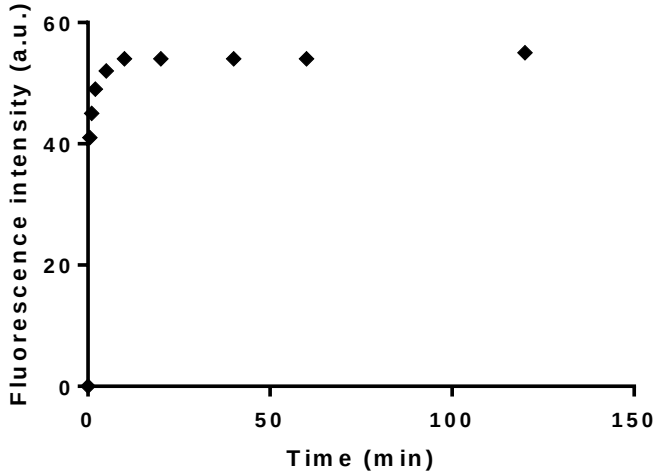
Fluorescence intensity (a.u.)
0
20
40
60
0
50
100
150
Time (min)

F

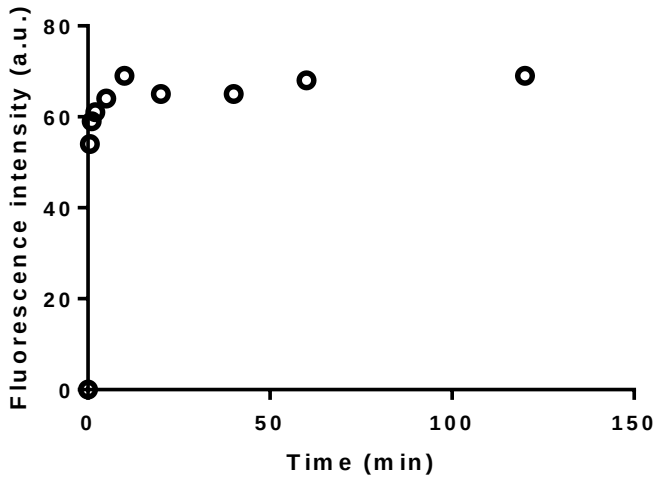
Fluorescence intensity (a.u.)
0
20
40
60
80
0
50
100
150
Time (min)

G

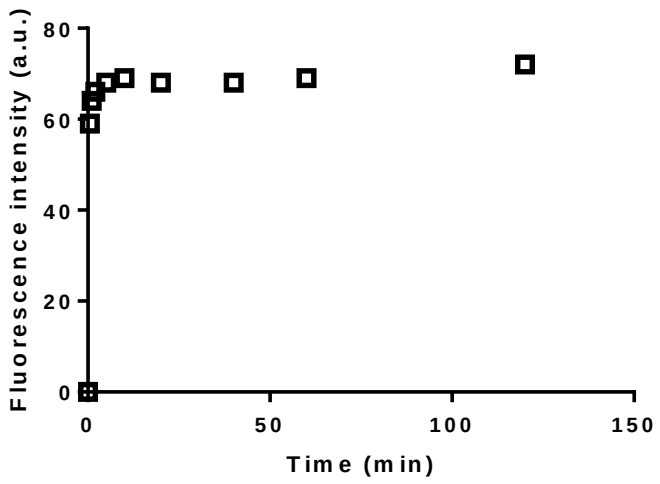
Fluorescence intensity (a.u.)
0
20
40
60
80
0
50
100
150
Time (min)

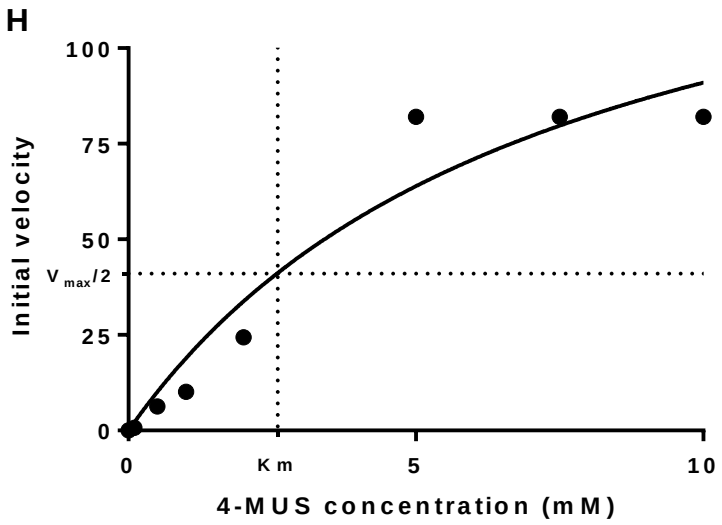

Figure 3.16: Kinetics of arylsulfatase activity of SULF2-Ab IPs using 4-MUS: Equal volumes of bead slurry of SULF2-Ab IPs of HuH-7 cell lysate were added to a 96-well plate and arylsulfatase activity was measured by incubation with different concentrations of 4-MUS (**A**: 0.1 mM; **B**: 0.5 mM; **C**: 1 mM; **D**: 2 mM; **E**: 5 mM; **F**: 7.5 mM; **G**: 10 mM) and reading the fluorescence of the product 4-MU at 460 nm following excitation at 355 nm. **H**: The initial velocity was plotted against 4-MUS concentration. GraphPad Prism was used to determine the Km using the model: Y = Vmax*X/(Km + X). The experiment was performed in duplicate. Data generated using the methods described in Section 2.12 and Section 2.13.

3.3.8. Effect of EMATE on ARS activity of SULF2

3.3.8.1. Effect of EMATE on ARS activity of SULF2-Ab IPs

To investigate whether the enzyme purified by immunoprecipitation of HuH-7 cell lysate using SULF2 antibody was contaminated with STS/ARSC, a major component of cellular sulfatase activity in this cell line (Figure 3.13), SULF2-Ab IPs of HuH-7 cell lysate were pre-incubated with different concentrations of the STS/ARSC inhibitor EMATE for 1 hour, and the ARS activity measured using 4-MUS as a substrate at different time points. The results showed no inhibition of the SULF2-Ab IP ARS activity even at 100 µM of EMATE (Figure 3.17). The results also showed that there was no linear increase of product formation over time (Figure 3.17).

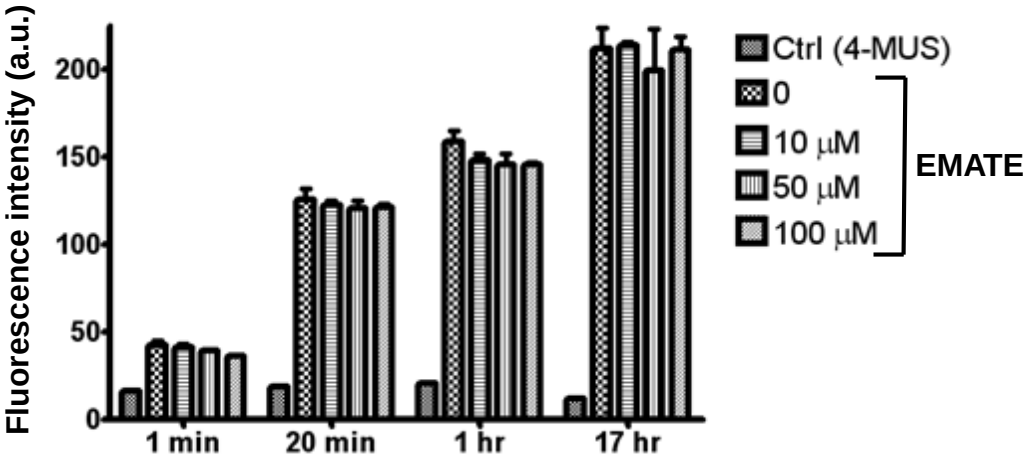

Figure 3.17: Effect of EMATE on arylsulfatase activity of SULF2-Ab IPs: Equal volumes of bead slurry of SULF2-Ab IPs of HuH-7 cell lysate were incubated with EMATE for 1 hour and arylsulfatase activity measured by incubation with 2.6 mM 4-MUS and reading the fluorescence of the product 4-MU at 460 nm following excitation at 355 nm. Values are the mean of triplicates and error bars represent the standard error. The experiment was performed in triplicate. Data generated using the methods described in Section 2.12 and Section 2.13.

3.3.8.2. Effect of EMATE on the kinetics of ARS activity of SULF2 using 4-MUS

To confirm that EMATE was not an inhibitor of SULF2, the effect of EMATE on the kinetics of SULF2 using 4-MUS as a substrate was investigated. Equal volumes of SULF2-Ab IPs of HuH-7 cell lysate were pre-incubated with EMATE followed by incubation with 4-MUS. The fluorescence of the product 4-MU was determined and the kinetics of the reaction was studied as described in Section 3.3.7. The results showed no effect of EMATE on the kinetics of the reaction as the slope after plotting the initial rate against the substrate concentration did not change in the presence (slope = 14.7) or absence (slope = 15.6) of EMATE (Figure 3.18).

A

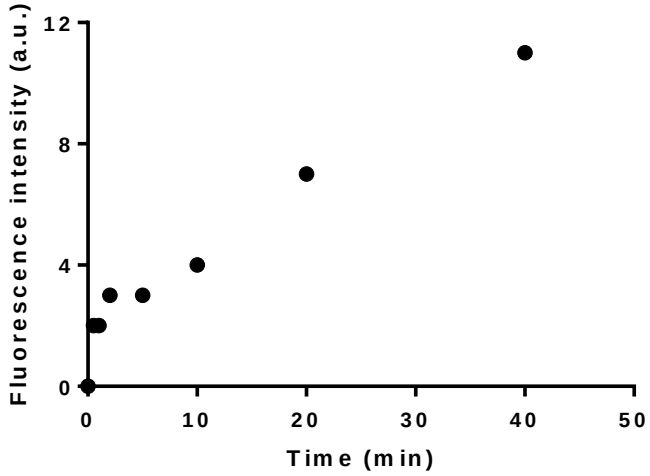
Fluorescence intensity (a.u.)
0
4
8
12
0
10
20
30
40
50
Time (min)

B

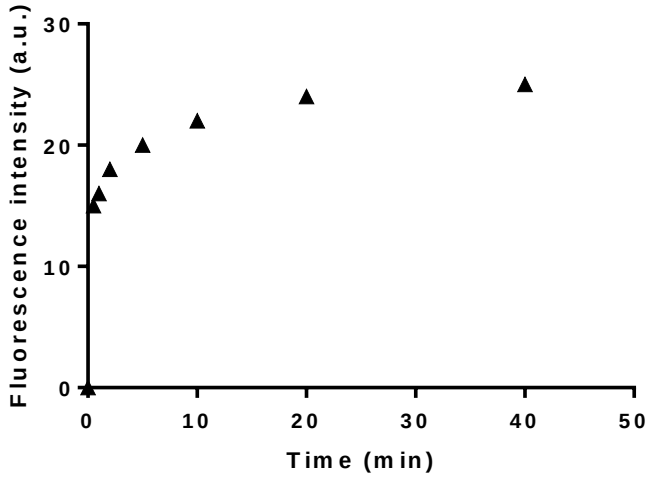
Fluorescence intensity (a.u.)
0
10
20
30
0
10
20
30
40
50
Time (min)

C

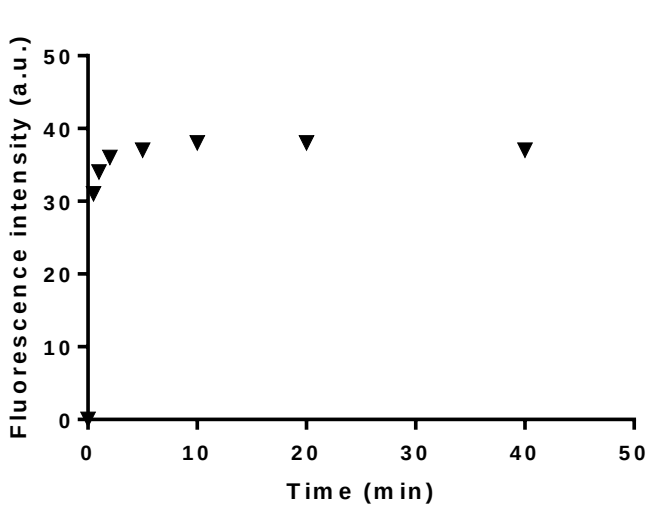
Fluorescence intensity (a.u.)
0
10
20
30
40
50
0
10
20
30
40
50
Time (min)

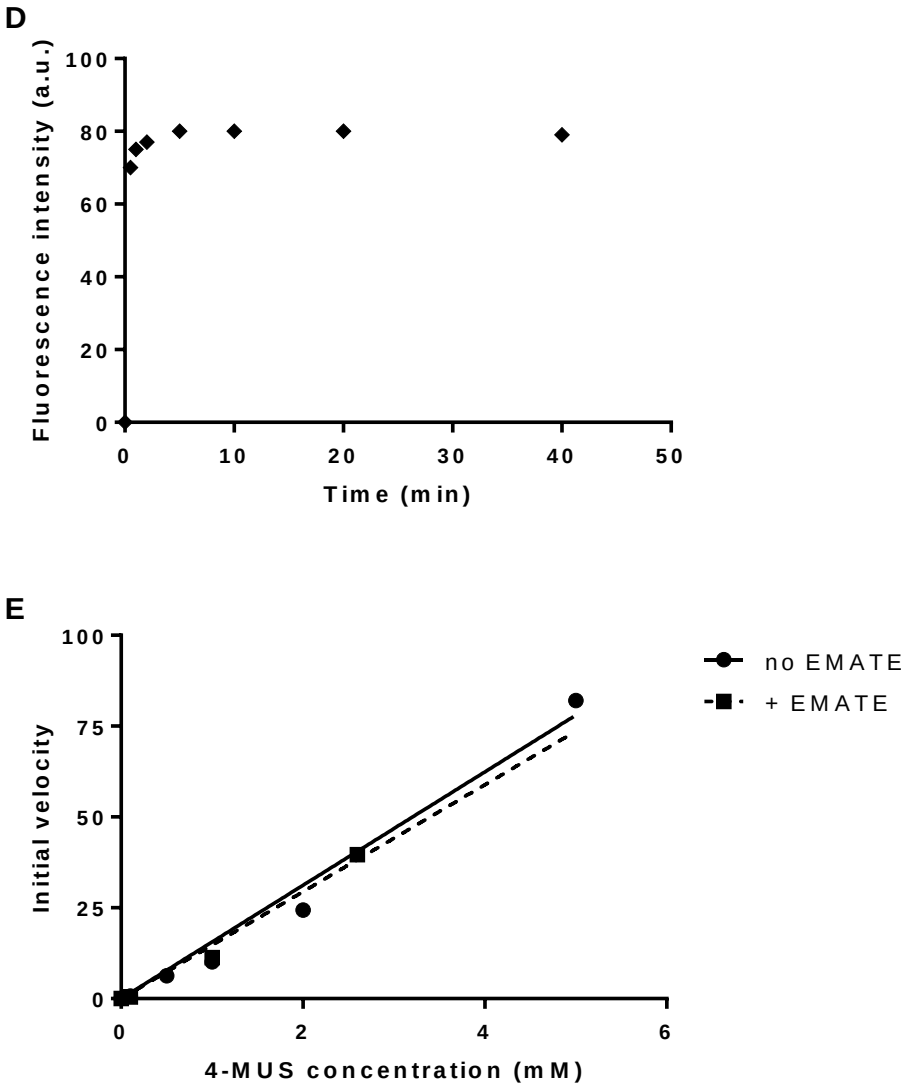

Figure 3.18: EMATE effect on the kinetics of arylsulfatase activity of SULF2-Ab IPs using 4-MUS: Equal volumes of bead slurry of SULF2-Ab IPs of HuH-7 cell lysate were added to a 96-well plate and incubated with 10 µM of EMATE for 1 hour. After that ARS activity was measured by incubation with different concentrations of 4-MUS (**A**: 0.1 mM; **B**: 1 mM; **C**: 2.6 mM; **D**: 5 mM) and reading the fluorescence of the product 4-MU at 460 nm following excitation at 355 nm. **E**: The initial velocity was plotted against 4-MUS concentration. The experiment was performed in duplicate. Data generated using the methods described in Section 2.12 and Section 2.13.

3.3.8.3. Effect of EMATE on ARS activity of whole cell lysate

To determine the concentration of EMATE that should be used to inhibit STS/ARSC in all subsequent experiments, the effect of different concentrations of EMATE on ARS activity of whole cell lysate was investigated. HuH-7 cell lysate was used and the results in Figure 3.19 show that EMATE concentrations of 10-50 µM inhibited the majority of the STS/ARSC activity. EMATE concentrations > 50 µM did not markedly increase inhibition of STS/ARSC.

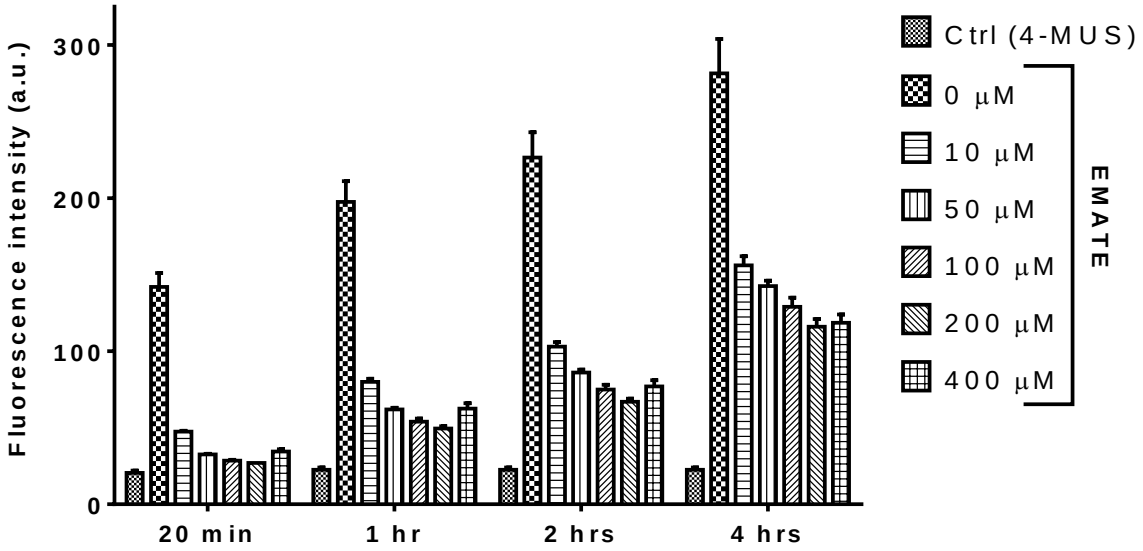

Figure 3.19: Effect of EMATE on arylsulfatase activity of HuH-7 whole cell lysate: Equal quantities of HuH-7 cell lysate were incubated with EMATE for 1 hour, and sulfatase activity measured by incubation with 2.6 mM 4-MUS and reading the fluorescence of the product 4-MU at 460 nm following excitation at 355 nm. Values are the mean of triplicates and error bars represent the standard error. The experiment was performed in triplicate. Data generated using the method described in Section 2.13.

3.4. Determination of the Endosulfatase Activity of SULF1/2 Using the RB4CD12-Based ELISA

In addition to the arylsulfatase activity of SULF1/2 enzymes, they possess oligosaccharide endosulfatase activity. To measure endosulfatase activity against heparin, the anti-HS phage display antibody RB4CD12 was used in an ELISA application as described in Section 2.19. The preferred sequence for RB4CD12 binding is the trisulfated disaccharide composed of iduronic acid 2-O-sulfate and N-sulfo-glucosamine-6-O-sulfate (Uchimura et al., 2010). Therefore, the binding of cMyc-tagged RB4CD12 primary antibody to immobilized heparin is inhibited on reduction of 6-O sulfation by SULF1/2. Reduced RB4CD12 binding leads to decreased levels of HRP-conjugated anti-cMyc secondary antibody binding and hence to less oxidization of the HRP substrate, TMB, which leads to lower optical density readings at 450 nm compared with untreated control wells.

SULF1, SULF2 and STS/ARSC enzymes purified by immunoprecipitation were used in this assay. For SULF2, two different antibodies were used for immunoprecipitation, namely, the polyclonal SULF2 Ab (Abcam) and the more specific monoclonal SULF2 Ab (Serotec). Both STS/ARSC and SULF2 enzymes were purified from HuH-7 cell lysate as these cells had the highest ARS activity (Figure 3.10). SULF1 enzyme was purified from SNU-182 cell lysate as it is the only HCC cell line that expresses high level of SULF1.

The ELISA results depicted in Figure 3.20 showed a decrease in the binding of RB4CD12 antibody as indicated by the optical density readings at 450 nm with increasing volumes of both SULF2-Ab IPs, but no change in the readings of the wells treated with STS/ARSC-Ab IPs. These results suggest that the SULF2-Ab IPs, but not STS/ARSC-Ab IPs, exhibited a concentration-dependent endosulfatase activity on immobilized heparin. Interestingly, the SULF1-Ab (Abcam) IPs also showed concentration-dependent endosulfatase activity (Figure 3.20). SULF2-Ab IPs from HepG2 or SNU-182 cell lysates were not tested due to the limited availability of the RB4CD12 antibody.

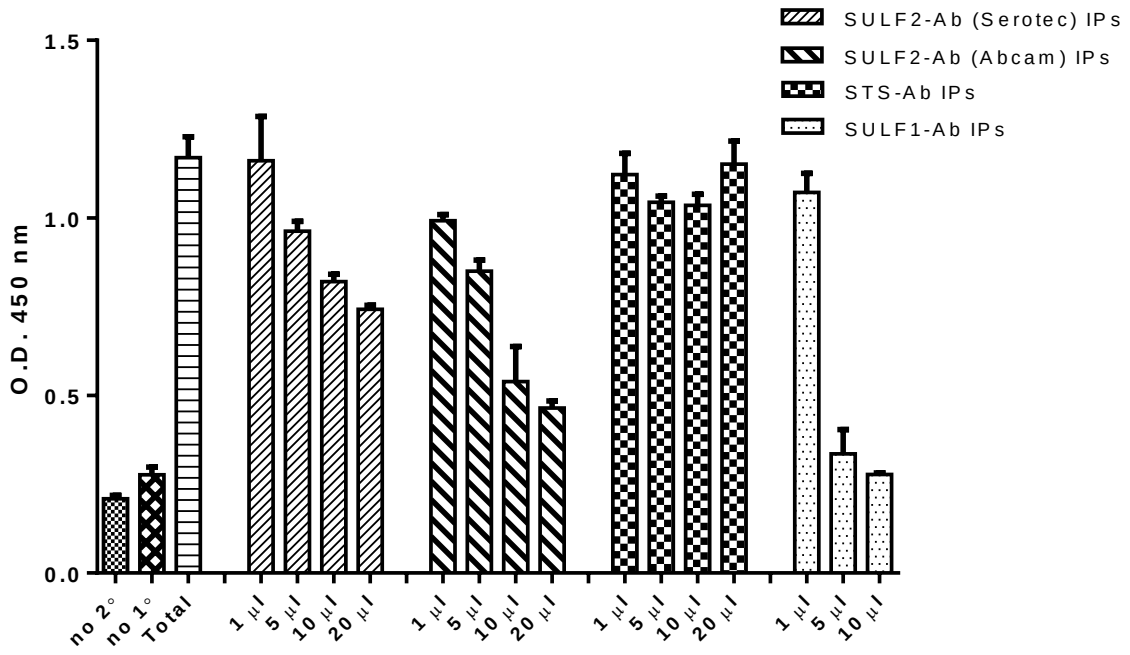

Figure 3.20: Endosulfatase activity measured using RB4CD12-based ELISA: SULF2-Ab (Serotec) IPs, SULF2-Ab (Abcam) IPs and STS/ARSC-Ab IPs from HuH-7 cell lysate and SULF1-Ab (Abcam) IPs from SNU-182 cell lysate were added in increasing volumes (1, 5, 10, 20 µl) to immobilised heparin in an ELISA plate. Following incubation with RB4CD12 antibody, the plate was incubated with HRP-conjugated cMyc antibody. HRP activity was detected by adding TMB substrate and reading the absorbance of the oxidized product at 450 nm. Total: untreated heparin. No 2^{o}: cMyc secondary antibody omitted. No 1^{o}: RB4CD12 primary antibody omitted. Values are the mean of triplicates and error bars represent the standard error. The experiment was performed in duplicate. Data generated using the methods described in Section 2.12 and Section 2.19.

3.5. Summary

In summary, a panel of six HCC cell lines were characterised for expression of SULF1 and SULF2 at the mRNA and protein levels and for arylsulfatase and endosulfatase enzymatic activities. Based on the pattern of expression, these cell lines constitute three groups, namely, SULF1 and SULF2-positive (SNU-182 and SNU-475), SULF2-positive (HuH-7 and HepG2) and SULF1 and SULF2 negative (Hep 3B and PLC/PRF/5). This allows studying the biology of SULF1/2 enzymes in different backgrounds.

The arylsulfatase activity assay using 4-MUS as a substrate was also characterised. Only HuH-7 and HepG2 cells and cell lysates had arylsulfatase activity. Immunoprecipitated SULF2 from HuH-7 and HepG2 cell lysates but not SNU-182 cell lysate had arylsulfatase activity, and activity was not inhibited by the STS/ARSC inhibitor, EMATE. Immunoprecipitated SULF2 from HuH-7 cell lysate and immunoprecipitated SULF1 from SNU-182 cell lysate showed endosulfatase activity demonstrating that endogenous SULF1/2 proteins are enzymatically active in HCC cell lines.

Chapter 4. Generating Recombinant SULF1/2 Proteins and Characterisation of Commercially Available Sulfatases

For screening small-molecule inhibitors of SULF2, it is important to generate recombinant SULF2 protein that can be easily and reliably purified, and used in an enzymatic assay or ELISA to screen inhibitors and to avoid contamination with other members of the sulfatase family. To generate recombinant protein, two different approaches were used to deliver the exogenous SULF2 DNA. The first approach was transfection of a SULF2 construct into cells. However, due to a low transfection efficiency, another approach was used, namely, transduction with SULF2-containing lentiviral particles.

4.1. Gene Delivery of SULF2 by Transfection

For transfection, the SULF1 or SULF2 open reading frame (ORF) was inserted under a CMV promoter to allow for constitutive expression of the protein which was fused with a C-terminal MYC/DDK tag for antibody detection and purification. Five different cell lines were transfected with these two constructs. Three of these were SULF1- and SULF2-negative, including Human Colon Tumour (HCT) cells and two HCC cell lines, Hep 3B and PLC/PRF/5. SULF1/2 expression in a negative background was designed to enable cell-based screening of inhibitors, by comparing effects in SULF1/2 non-expressing versus over-expressing cells, as well as to generate the recombinant SULF1/2 proteins. Two SULF2-positive HCC cell lines, HuH-7 and HepG2, were also evaluated, as these cells were known to be capable of producing and processing SULF2 protein (Chapter 3). As discussed earlier (Chapter 1), SULF1/2 enzymes are complex proteins that require different processing steps.

4.1.1. Optimisation of transfection conditions

Before attempting transfection of SULF1/2 constructs, transfection conditions were optimised. A pCI-neo/EGFP plasmid that constitutively expressed the fluorescent protein EGFP was used for this purpose. Transfection was performed by lipofection

using two different transfection reagents, namely, lipofectamine and FuGENE as described in Section 2.4. Optimisation was carried out by testing different ratios of transfection reagent to DNA, and by scaling up the whole transfection mixture (i.e., transfection reagent plus DNA) to identify the conditions that gave the highest transfection efficiency for each single cell line. The transfection efficiency was assessed by fluorescence microscopy and characterised by two criteria i.e., percentage of green cells to total cells and fluorescence intensity. In all tested cell lines, FuGENE was superior to lipofectamine but nevertheless overall transfection efficiency was low. Of the HCC cell lines, HuH-7 was the easiest cell line to transfect with 5% green cells (Figure 4.1) and more intense fluorescence than other cell lines followed by Hep 3B, while HepG2 was poorly transfected. For all cell lines, the ratio 2:1 (FuGENE:DNA) gave the best results.

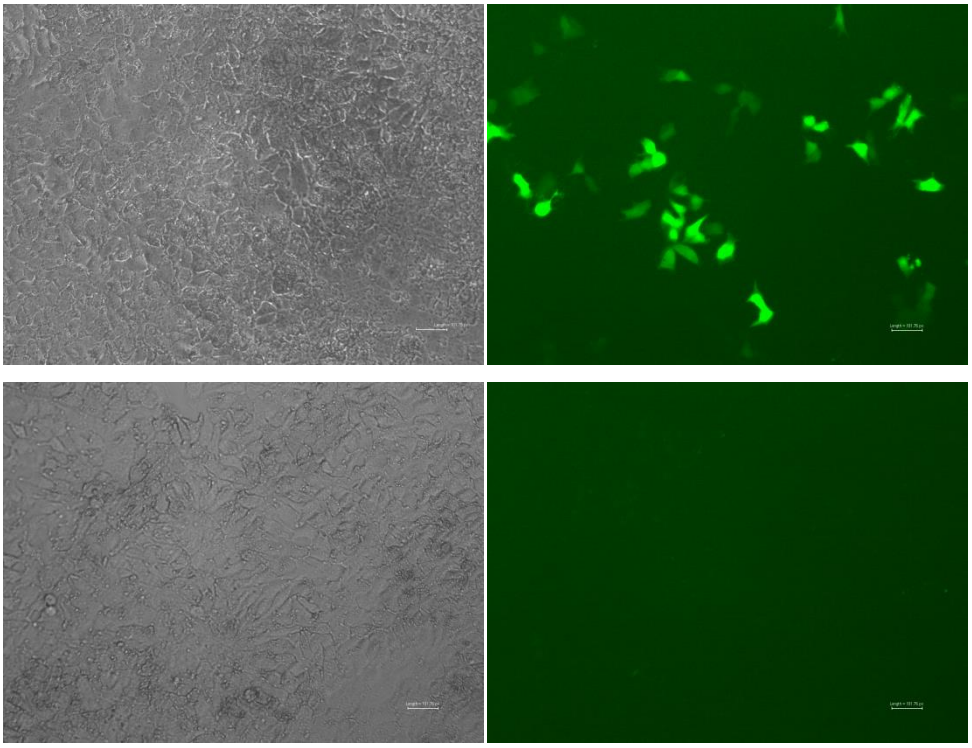

Figure 4.1: Optimisation of transfection conditions: HuH-7 cells were transfected in a 96-well plate with different ratios of FuGENE:DNA. After 24 hrs, the cells were examined under a fluorescence microscope. Right panel is EGFP channel: cells transfected in the ratio 2:1 (top); untransfected cells (bottom). Left panel is bright field of transfected (top) and untransfected (bottom) cells. The bar represents 100 pixels. Data are from a single experiment. Data generated using the method described in Section 2.4.

4.1.2. Screening of colonies

After transfection with SULF1 or SULF2 constructs, G418 antibiotic was used to select for the successfully transfected antibiotic-resistant cells. Whole resistant HCT or PLC/PRF/5 cells were collected while for the other three HCC cell lines, resistant colonies were picked up: 20 colonies of each SULF1- or SULF2-transfected HepG2, 9 colonies of each SULF1- or SULF2-transfected HuH-7 or Hep 3B. The colonies were expanded and screened using different methods. Only examples of the screened colonies are shown below.

4.1.2.1. Screening of colonies using RT-qPCR

mRNA was extracted from colonies of SULF1- or SULF2-transfected cells and SULF1/2 mRNA levels compared with those of control untransfected cells. Figure 4.2 shows a sample of screened HepG2 colonies. SULF2 expression was 4-fold and 80-fold higher in SULF2-transfected clone 13 and clone 15 cells, respectively, than in control untransfected HepG2 cells. SULF1-transfected cells had no increase in SULF2 expression over control.

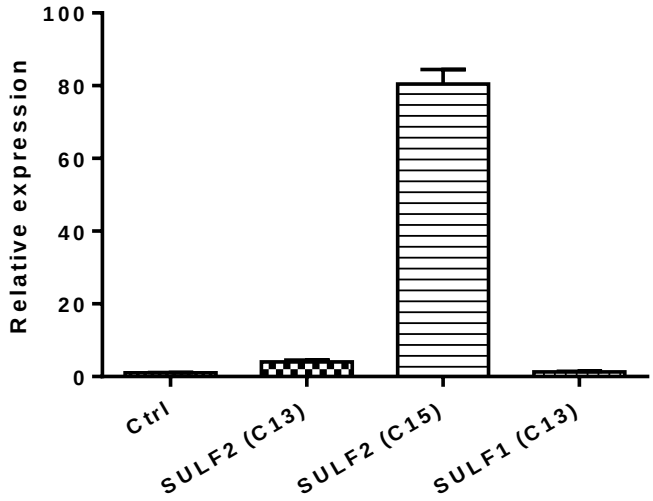

Figure 4.2: Screening of colonies using RT-qPCR: mRNA was extracted from control untransfected (Ctrl), SULF1- and SULF2-transfected HepG2 cells. RT-qPCR was performed using SULF2 primers, and the data were normalized to the expression level of the control untransfected cells used as a calibrator. GAPDH was used as a reference gene. SULF2 (C13) and SULF2 (C15) are SULF2-transfected clones 13 and 15. SULF1 (C13) is SULF1-transfected clone 13. Values are the mean of triplicates and error bars represent the standard error. Data are from a single experiment. Data generated using the methods described in Section 2.4 and Section 2.7.

4.1.2.2. Screening of colonies using western blot

Transfected cells were also screened for recombinant SULF1/2 proteins using WB. Two types of antibodies were used for this purpose; an anti-SULF1/2 antibody (either SULF2 or SULF1) or an anti-DDK antibody, as the recombinant proteins were C-terminally tagged with DDK. Both the CM and the cell lysate were screened. Figure 4.3 shows WB of the SULF2-transfected HCT cell line. In this case, the recombinant protein was purified from the conditioned medium using an anti-FLAG (DDK) M2 affinity column. A weak band corresponding to the full length SULF2 protein was detected in the first eluate. This result suggested the successful translation of the recombinant SULF2 protein and its secretion into the CM. However, no arylsulfatase activity was detected in any of the eluates using 4-MUS as a substrate. The presence of recombinant proteins was also studied in the cell lysate, and Figure 4.4 depicts the analysis of a sample of HepG2 colonies transfected with SULF1 or SULF2 constructs and blotted using either SULF2 Ab (LR) or anti-DDK antibody. The results show the presence of the full-length protein in SULF2-transfected HepG2 clone 15, which had the highest SULF2 protein expression among all screened colonies, but not in the control untransfected HepG2 cells. However, ICC data showed that not all clone 15 cells were expressing SULF2 protein (Figure 4.5), consistent with the low transfection efficiency of HCC cells.

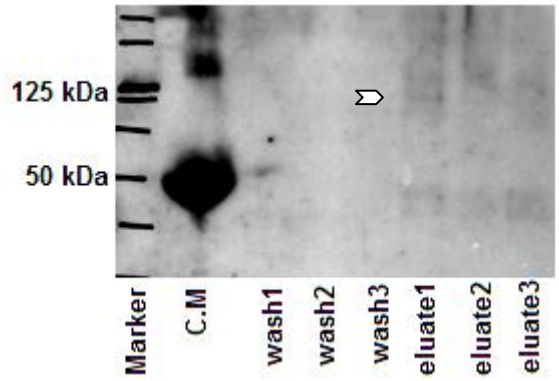

Figure 4.3: Screening of SULF2-transfected HCT cells using WB: DDK-tagged SULF2 recombinant protein from CM of SULF2-transfected HCT cell line was purified using anti-FLAG M2 affinity column followed by WB using an anti-DDK antibody. C.M: the remaining conditioned medium from which the protein was purified. The white arrow points to a band with the appropriate molecular weight for the full-length SULF2 protein. The experiment was performed in duplicate. Data generated using the methods described in Section 2.4 and Section 2.10.

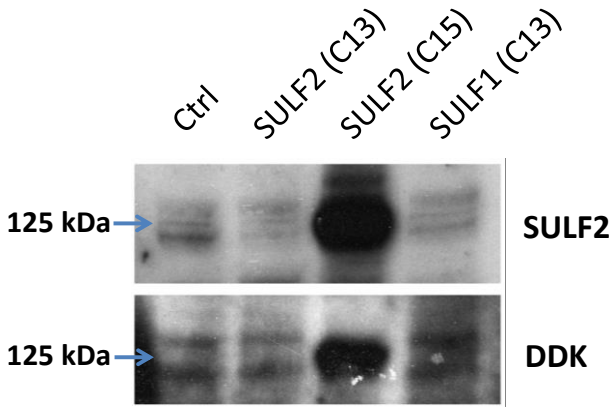

Figure 4.4: Screening of HepG2 colonies using WB: SULF1- or SULF2-transfected HepG2 colonies were blotted with SULF2 Ab (LR) (top) and anti-DDK Ab (bottom). Ctrl: control untransfected HepG2. Data are from a single experiment. Data generated using the methods described in Section 2.4 and Section 2.10.

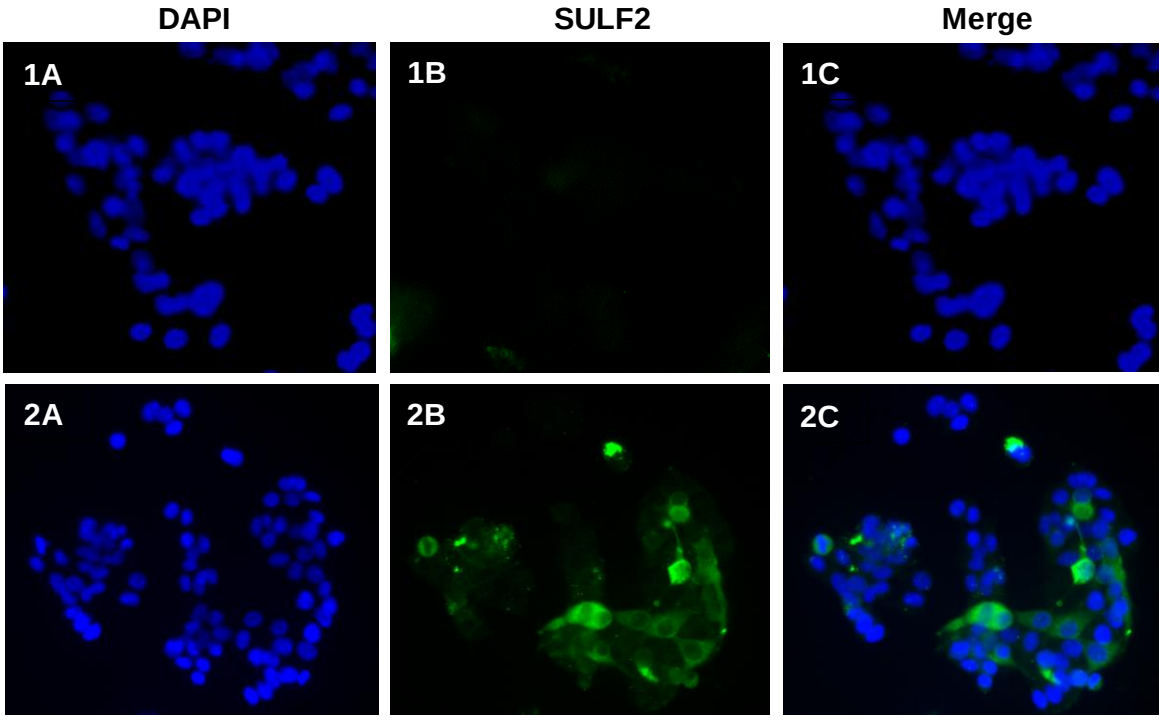

Figure 4.5: ICC staining of SULF2 protein after transfection of the SULF2 plasmid into HCC cells: HepG2 control untransduced cells or SULF2-transfected HepG2 clone 15 cells were grown on glass coverslips and incubated with SULF2 Ab (Serotec) and then stained green with Alexa Fluor 488 conjugated secondary antibody. Mounting medium with DAPI was used to counter-stain the nuclei in blue. **(1)** control untransduced cells, **(2)** Clone 15. **(A)** blue channel for DAPI, **(B)** green channel for Alexa Fluor 488, **(C)** merge picture. Data are from a single experiment. Data generated using the methods described in Section 2.4 and Section 2.11.

4.1.2.3. Screening of colonies using an ARS activity assay

Colonies were also screened using an arylsulfatase activity assay with 4-MUS as the substrate to investigate whether or not the recombinant protein was enzymatically active. Both whole cells and cell lysates were used for this purpose. For cell-based screening, equal numbers of cells from each clonal population were seeded and their ARS activities were compared with that of untransfected cells which served as a control. No significant ARS activity was detected over control in any of the tested colonies.

For cell lysate screening, equal amounts of cell lysates from different clonal populations were screened for their ARS activities, which were compared with that of control untransfected cells. The transfected colonies in SULF-negative background (i.e., Hep 3B colonies) didn't show significant ARS activity over control (data not shown). While transfected colonies in SULF-positive background (i.e., HuH-7 and Hep G2 colonies) showed a modest ≤ 2-fold increase in ARS activity over control.

Notably, the SULF2-transfected HepG2 clone 15 cells that showed high level expression of recombinant SULF2 protein compared with control, still displayed only a 2-fold increase in ARS activity over that in untransfected HepG2 cells (Figure 4.6). Also, ARS activity of clone 15 cells was similar to that of clone 14 cells that had much lower levels of recombinant SULF2 protein.

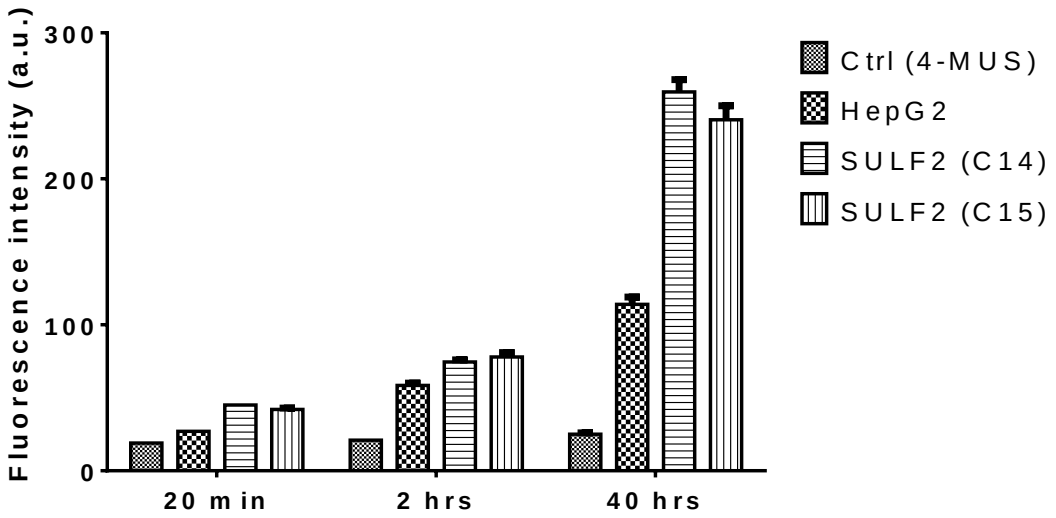

Figure 4.6: Arylsulfatase activity of SULF2-transfected HepG2 clones: 30 µg of cell lysates were incubated with 50 µM EMATE for 1 hr to inhibit STS/ARSC, and then ARS activity was measured by adding 2.6 mM of 4-MUS and reading the fluorescence of the product 4-MU. HepG2: untransfected cells, SULF2 (C14) and SULF2 (C15) are SULF2-transfected clones 14 and 15, respectively. Values are the mean of triplicates and error bars represent the standard error. The experiment was performed in triplicate. Data generated using the method described in Section 2.13.

4.1.2.4. Screening of colonies using SULF1/2-Ab IPs

Screening was performed using SULF2-transfected HepG2 clone 15 to investigate whether or not the recombinant SULF2 protein was active, as the ARS activity assay of the cell lysate showed only a 2-fold increase in activity over control (Figure 4.6). SULF2 Ab (LR) was used for immunoprecipitation, equal volumes of bead slurry were added, and ARS activity was measured using the substrate 4-MUS. The results in Figure 4.7 show no significant difference in the ARS activity of IPs between clone 15 and control cells suggesting that the ARS activity of both cells was due to endogenous SULF2 and that the recombinant SULF2 protein in clone 15 was not active.

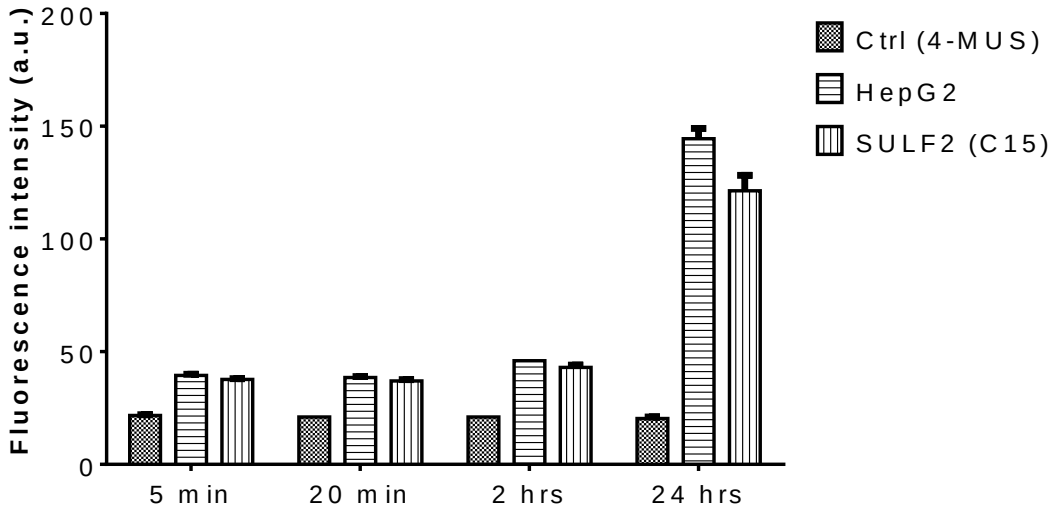

Figure 4.7: Arylsulfatase activity assay of SULF2-Ab IPs of control untransfected HepG2 and SULF2-transfected HepG2 clone 15 cell lysates: 1mg of HCC cell lysates were incubated with protein A agarose beads that were pre-loaded with excess SULF2 Ab (LR). Equal volumes of bead slurry were added to a 96-well plate and arylsulfatase activity was measured by incubation with 2.6 mM 4-MUS and reading the fluorescence of the product 4-MU at 460 nm following excitation at 355 nm. Values are the mean of triplicates and error bars represent the standard error. Data are from a single experiment. Data generated using the methods described in Section 2.12 and Section 2.13.

4.2. Gene Delivery of SULF2 by Transduction

Given the low transfection efficiency of HCC cells, another approach to expressing SULF2 protein was investigated, namely transduction with SULF2 lentiviral particles into HCC cells. SULF2 lentiviral particles were generated as described in Section 2.5 where the expression of both SULF2 and a blasticidin selectable marker were driven by the same promoter. This design allowed for enrichment of SULF2-expressing cells after selection with blasticidin. Hep 3B cells were transduced with different volumes of SULF2 lentiviral particles-containing CM followed by selection of transduced cells using blasticidin. WB analysis was performed using a SULF2 Ab (Serotec) that was raised against a region in the C-terminal domain. WB data revealed the expression of a 125 kDa protein consistent with full-length SULF2 in addition to a 50 kDa protein consistent with the C-terminal subunit of SULF2 protein, in the SULF2-transduced cells. No SULF2 protein was detected in the control untransduced Hep 3B cells. The expression of SULF2

protein was dependent on the volume of SULF2 lentiviral particle-containing CM added to the cells (Figure 4.8). To determine what percentage of cells were expressing SULF2 protein, ICC was performed which confirmed intense staining for SULF2 protein in the majority of the transduced cells, and no visible staining in the control untransduced cells (Figure 4.9). However, no arylsulfatase activity detected of the cell lysates of the transduced cells using 4-MUS as the substrate (data not shown). Therefore, individual colonies were picked to screen for cells enriched in catalytically active SULF2. WB was performed using the SULF2 Ab (Serotec), which identified clones 10 and 26 as the most highly expressing clones followed by clones 17 and 19 (Figure 4.10). This SULF2 expression was confirmed by ICC, and Figure 4.11 shows SULF2 staining in clones 10, 17 and 26 but not in the control untransduced Hep 3B cells. Unfortunately, as for the SULF2-transfected cells, none of the SULF2-transduced clonal population cell lysates showed any detectable activity against 4-MUS in comparison to Hep 3B control untransduced cells. HuH-7 cell lysate was used as positive control in this assay (Figure 4.12)

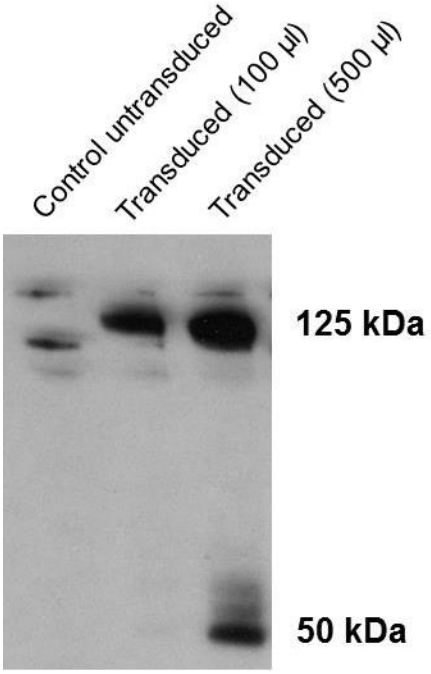

Figure 4.8: WB analysis of SULF2 protein expression after transduction of SULF2 lentiviral particles into HCC cells: Hep 3B cells were transduced with either 100 µl or 500 µl SULF2 lentiviral particle-containing conditioned medium. WB was performed using SULF2 Ab (Serotec). The experiment was performed in triplicate and a representative blot is shown. Data generated using the methods described in Section 2.5 and Section 2.10.

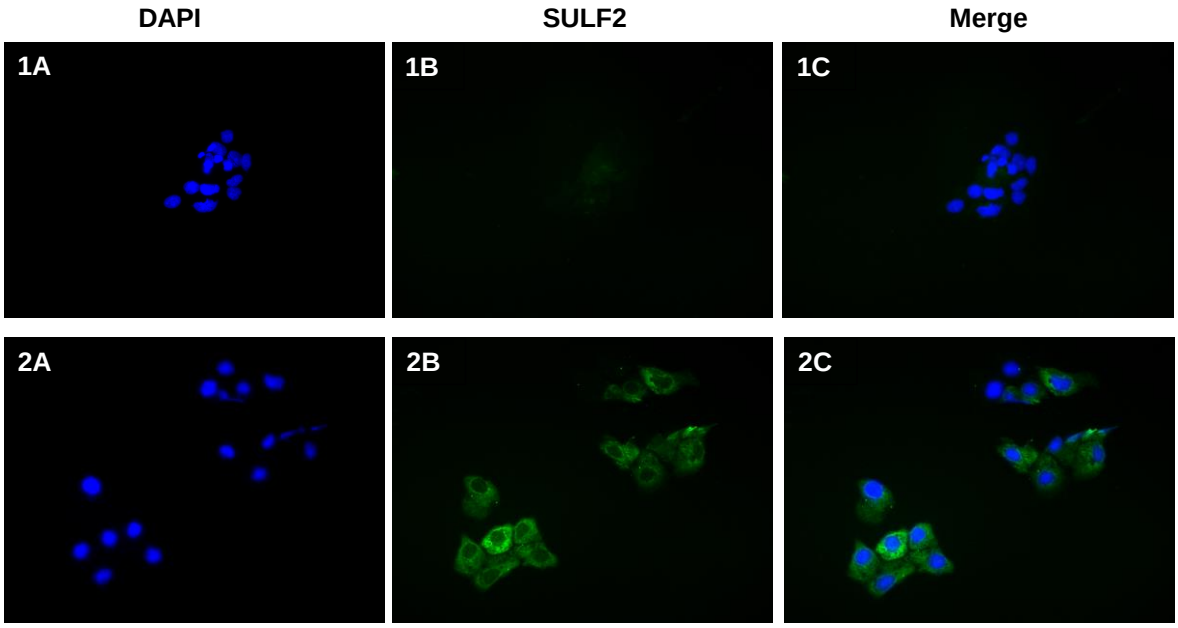

Figure 4.9: ICC staining of SULF2 protein after transduction of SULF2 lentiviral particles into HCC cells: Hep 3B control untransduced cells or those transduced with 500 µl SULF2 lentiviral particle-containing CM were grown on glass coverslips and incubated with SULF2 Ab (Serotec) and then incubated with Alexa Fluor 488 conjugated secondary antibody. Mounting medium with DAPI was used to counter-stain the nuclei in blue. **(1)** control untransduced cells, **(2)** SULF2-transduced cells. **(A)** blue channel for DAPI, **(B)** green channel for Alexa Fluor 488, **(C)** merge picture. The experiment was performed in duplicate. Data generated using the methods described in Section 2.5 and Section 2.11.

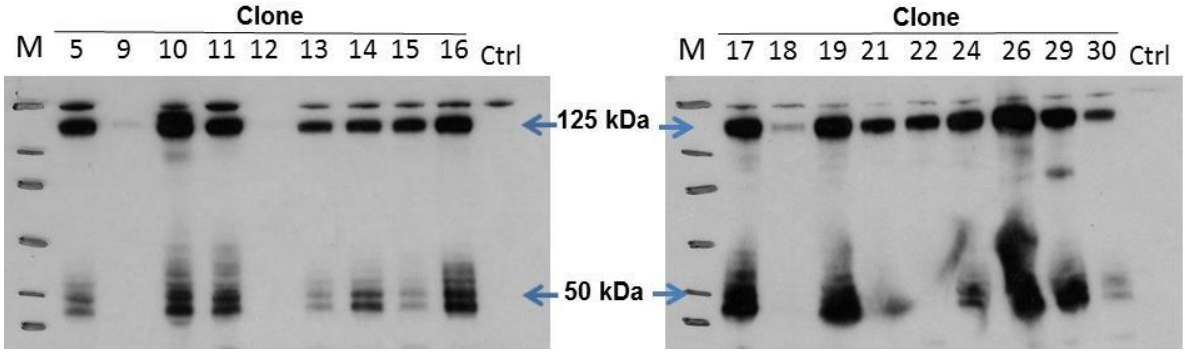

Figure 4.10: SULF2 protein expression in SULF2-transduced clones of Hep3B cells: Hep 3B cells were transduced with SULF2 lentiviral particles followed by selection with blasticidin and picking of colonies. WB was performed using SULF2 Ab (Serotec). M: Marker, Ctrl: control untransduced cells. The experiment was performed in duplicate and representative blots are shown. Data generated using the methods described in Section 2.5 and Section 2.10.

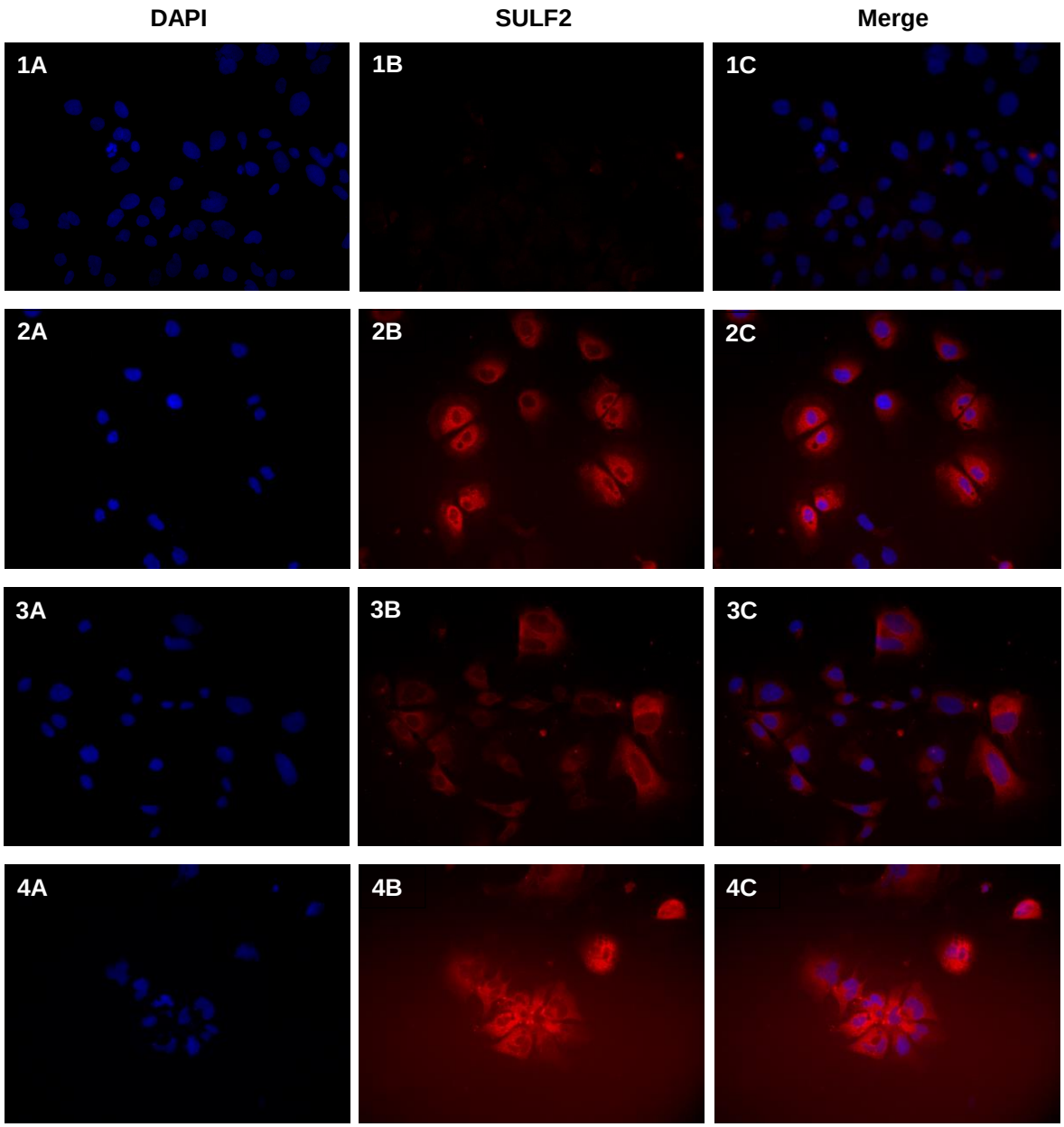

Figure 4.11: ICC staining of SULF2-transduced clones of Hep3B cells: Cells were grown on glass coverslips and incubated with SULF2 Ab (Serotec) and then incubated with Alexa Fluor 546 conjugated secondary antibody. Mounting medium with DAPI was used to counter-stain the nuclei in blue. **(1)** control untransduced cells, **(2)** Clone 10, **(3)** Clone 17, **(4)** Clone 26. **(A)** blue channel for DAPI, **(B)** red channel for Alexa Fluor 546, **(C)** merge picture. The experiment was performed in duplicate. Data generated using the method described in Section 2.11.

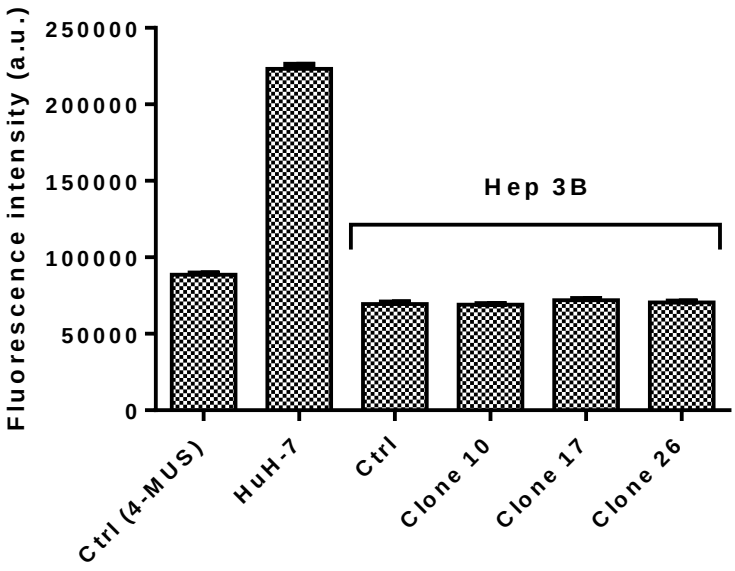

Figure 4.12: Arylsulfatase activity of SULF2-transduced Hep 3B clones: 30 µg cell lysates were incubated with 50 µM EMATE for 1 hr to inhibit STS/ARSC, and ARS activity was then measured by adding 2.6 mM of 4-MUS and reading the fluorescence of the product 4-MU. Ctrl: control untransduced Hep 3B cells. Ctrl (4-MUS): substrate control with no lysate added. Values are the mean of triplicates and error bars represent the standard error. The experiment was performed in triplicate. Data generated using the method described in Section 2.13.

The lack of enzymatic activity of the SULF2 protein generated was potentially due to the production of an inactive form due to insufficient Cα-formylglycine generating enzyme (FGE) activity that is required for the conversion of a cysteine residue in the catalytic active site into Cα-formylglycine. To test this hypothesis the SUMF1 gene that encodes for the FGE enzyme was co-expressed.

4.3. Overexpression of SUMF1 in SULF2-Expressing Cells

Prior to attempting overexpression of SUMF1, the endogenous level of SUMF1 in HCC cell lines was investigated by RT-qPCR. The results showed that all six HCC cell lines express a similar level of SUMF1 ranging from 2^5 - 2^8 fold higher than the GAPDH endogenous control gene (Figure 4.13).

To investigate whether SUMF1 co-expression could activate the over-expressed recombinant SULF2 protein, a SUMF1 construct was transfected into cells. However, the SUMF1 construct has no selectable marker, thus it was either

transiently transfected or co-transfected with the SULF2 construct for stable transfection.

Both Hep 3B and HEK 293T cells were transfected, the latter having a relatively high transfection efficiency, and expression of SUMF1 was investigated at the mRNA level by RT-PCR. The results showed the successful expression of SUMF1 mRNA after transient transfection in both HEK 293T and Hep 3B cells; however, SUMF1 was lost when it was stably transfected with the SULF2 construct in Hep 3B cells (Figure 4.14). Therefore, SULF2 and SUMF1 constructs were transiently co-transfected into HEK 293T cells and the expression of both proteins was confirmed at the protein level by WB (Figure 4.14). Also, SULF2-expressing HepG2 clone 15 was transiently transfected with the SUMF1 construct. However, none of these cells showed any arylsulfatase activity in cell lysates or conditioned medium (data not shown).

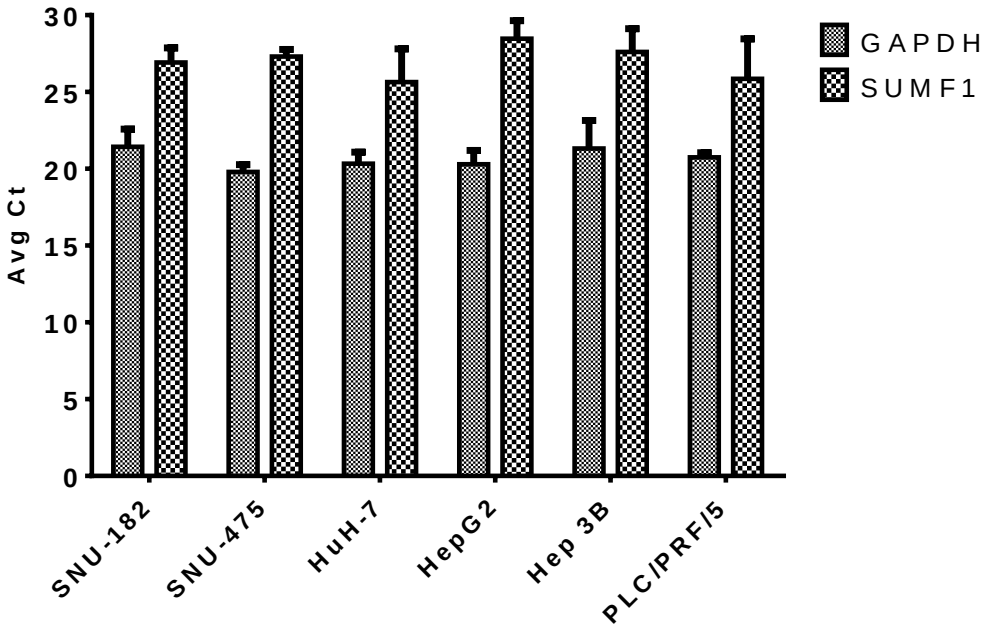

Figure 4.13: SUMF1 expression in HCC cell lines: RT-qPCR was performed on mRNA extracted from HCC cells. GAPDH was used as a reference gene. Error bars represent standard error of the mean of triplicates. Values are the mean of triplicates and error bars represent the standard error. Data are from a single experiment. Data generated using the method described in Section 2.7.

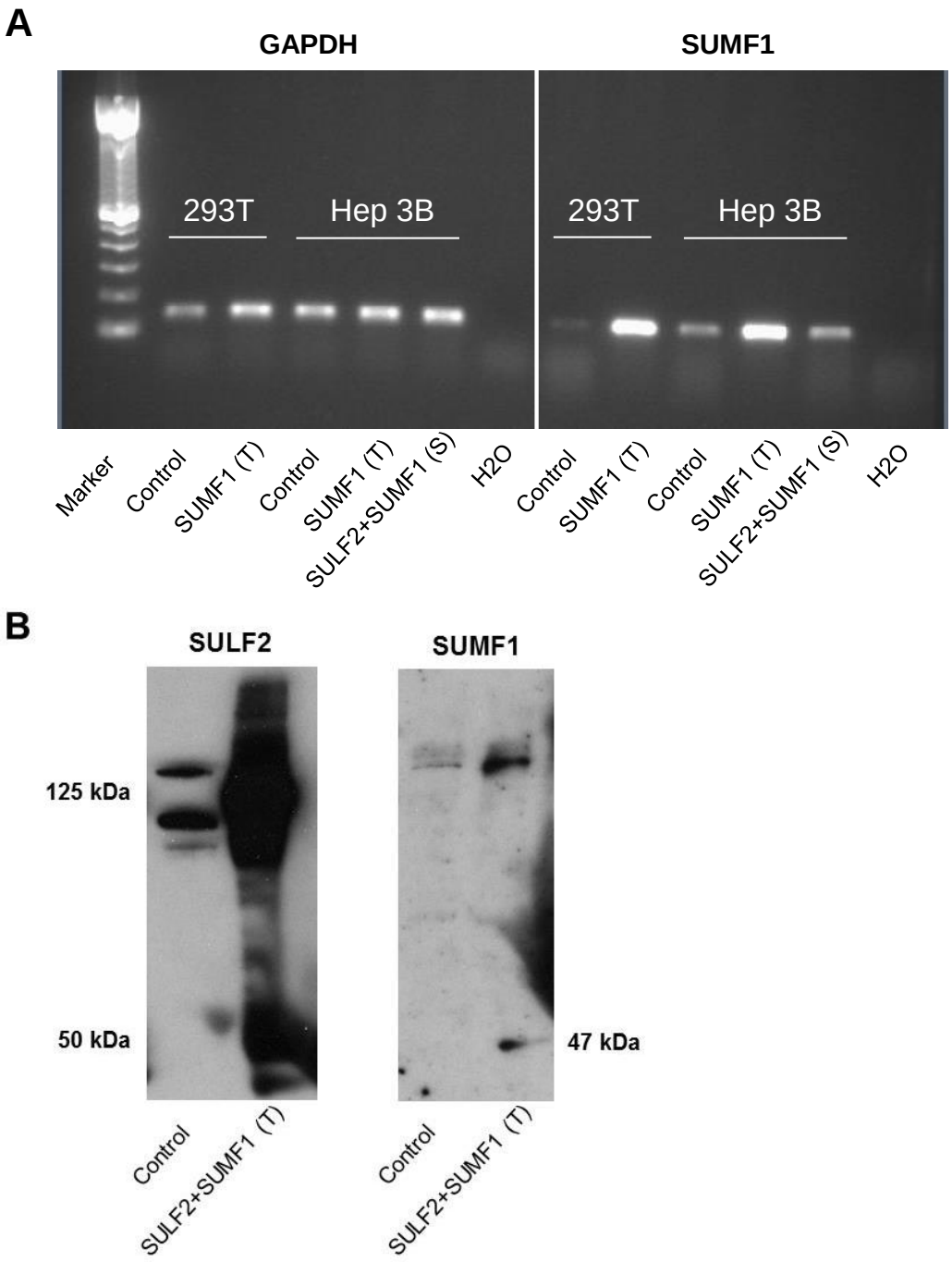

Figure 4.14: Overexpression of SUMF1 in HEK 293T and Hep 3B cells: **(A)** RT-PCR of HEK 293T or Hep 3B cells that were transfected with the SUMF1 construct. The reaction was performed for 30 cycles using SUMF1 primers (right) or GAPDH (left) as a reference gene. **(B)** WB of control untransfected or SULF2 and SUMF1-transiently co-transfected HEK 293T cells using SULF2 (left) or SUMF1 (right) antibodies. Control: untransfected cells, SUMF1 (T): SUMF1-transiently transfected cells, SULF2+SUMF1 (S): SULF2 and SUMF1-stably co-transfected cells, SULF2+SUMF1 (T): SULF2 and SUMF1-transiently co-transfected cells. All experiments were performed in duplicate and representative images and blots are shown. Data generated using the methods described in Section 2.4, Section 2.7 and Section 10.

4.4. Transient Transfection and Production of SULF2

The experiments in the preceding sections demonstrated that it was possible to express recombinant SULF2 at very high level. However, there was no enzymatic activity associating with the SULF2 protein. It is plausible that high levels of catalytically active SULF2 enzyme are toxic to the cells, and the focus was changed to transient transfection of other previously reported SULF2 constructs. A simple SULF2 construct was used for this purpose, which was described by the first group that cloned human SULF2. The wild-type SULF2 ORF was cloned into the pcDNA3.1 vector backbone and was tagged by Myc and His (polyhistidine metal-binding tag) at the C-terminal end (Morimoto-Tomita et al., 2002). Also, the catalytically inactive mutated form of SULF2 (also called S2ΔCC) that was generated by conversion of the cysteine at residue 88 in the active site into alanine was used as negative control for enzymatic activity. Both constructs were deposited by Prof. Steven Rosen on Addgene. WB of the conditioned medium of cells transiently transfected with either the wild-type or the mutated SULF2 showed the expression of both full-length protein and the 50 kDa subunit to which the SULF2 Ab (Serotec) was raised (Figure 4.15; A), indicating appropriate processing of the expressed proteins and their secretion into the medium. Arylsulfatase activity assays showed that only the CM of cells transfected with wild-type SULF2 had activity, while no activity was detected for either the mock transfected or the S2ΔCC-transfected cells (Figure 4.15; B). The active SULF2 could be purified and enriched about 160-fold from the CM using nickel affinity gel to which the His tag of the SULF2 protein binds, while no activity was detected in the flow-through (Figure 4.15; C). However, it was not possible to remove the protein from the beads using the standard reagents imidazole or EDTA because both inhibited the ARS reaction. Therefore, the SULF2-bound beads were used for screening SULF2 inhibitors.

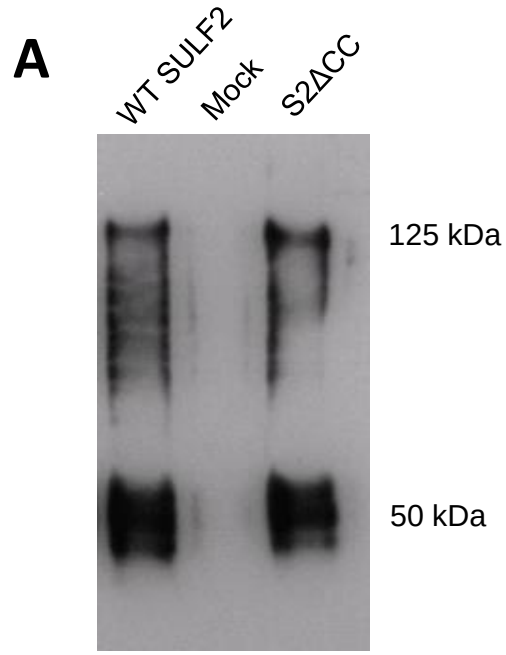
A
WT SULF2
Mock
S2ΔCC
125 kDa
50 kDa

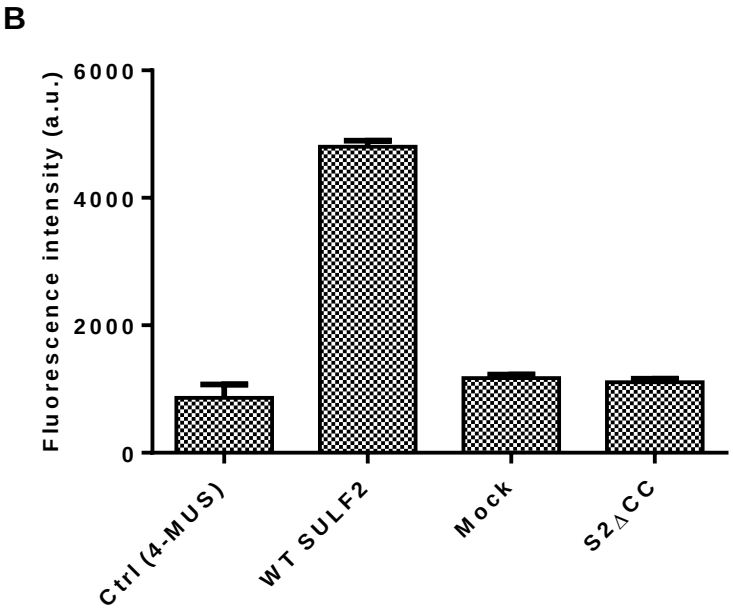
B
Fluorescence intensity (a.u.)
6000
4000
2000
0
Ctrl (4-MUS)
WT SULF2
Mock
S2ΔCC

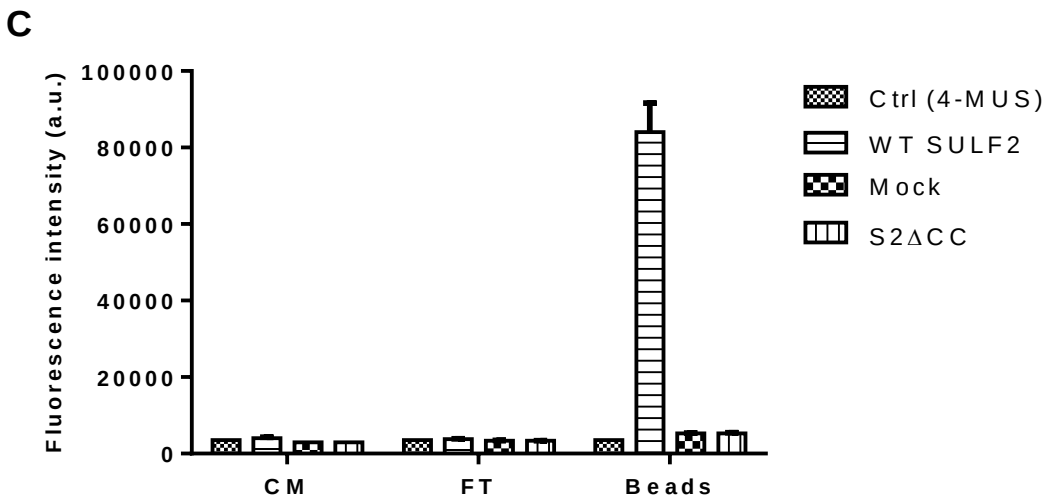

Figure 4.15: Transient expression and enzymatic activity of SULF2 in the CM of transfected HEK 293T cells: HEK 293T cells were transfected with wild-type SULF2 plasmid (lane 1: WT SULF2), mock transfected without plasmid (lane 2: Mock), or transfected with a catalytically inactive SULF2 plasmid (lane 3: S2ΔCC). CM was collected after 3 days. **(A)** WB was performed using SULF2 Ab (Serotec). **(B)** ARS activity of 20 µl CM was measured by adding 8 mM of 4-MUS and reading the fluorescence of the product 4-MU. **(C)** SULF2 was purified using nickel affinity gel, and the ARS activity of CM (starting material before purification), SULF2-bound beads and flow-through (FT) from the column after purification was measured. Ctrl (4-MUS): substrate control with no CM added. For (B and C) values are the mean of triplicates and error bars represent the standard error. All experiments were performed in triplicate and a representative blot is shown for (A). Data generated using the methods described in Section 2.4, Section 2.10 and Section 2.13.

4.5. Characterisation of Commercially Available Sulfatases for Counter-Screening SULF2 Inhibitors

It was anticipated that in addition to testing against active SULF2, potential SULF2 inhibitors would be tested against other members of the sulfatase family to determine selectivity. Therefore, all sulfatases that are commercially available were purchased and their activity with the substrate 4-MUS was characterised in terms of pH optimum, concentration and time dependency. The Km values of the reaction were measured whenever possible and when 4-MUS was a particularly poor substrate, other substrates were used where available.

4.5.1. Characterisation of arylsulfatase A (ARSA)

ARSA activity has an acidic pH optimum (Figure 4.16), which is consistent with its lysosomal subcellular localization. Concentration-dependent activity with 4-MUS exhibited a good dynamic range (Figure 4.17) (Table 4.1). The Km value was calculated as 2.2 mM at pH 4.5 (Figure 4.18), while the reported value is 12.5 mM at pH 5.7 (Hanson et al., 2004).

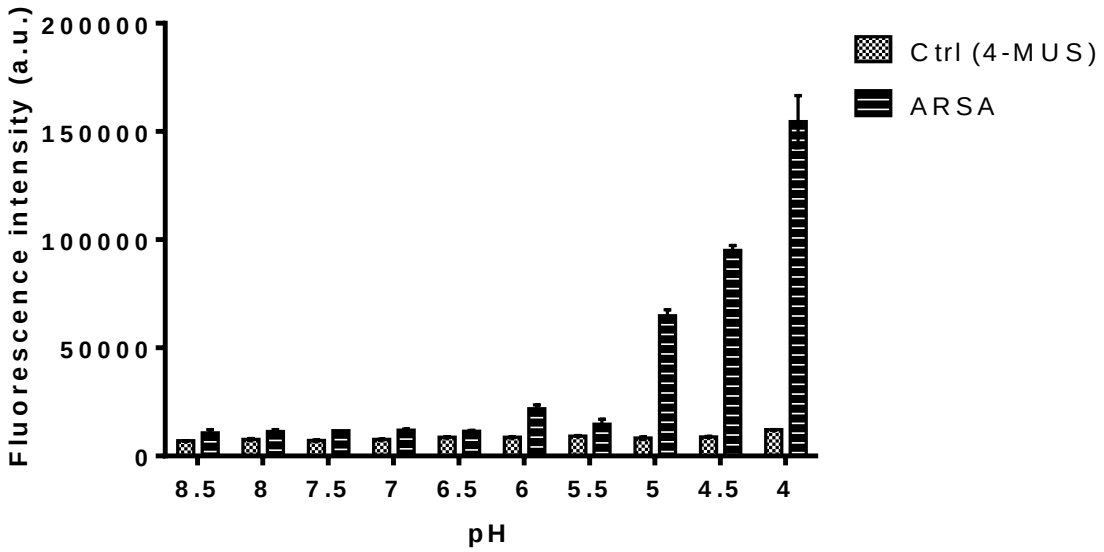

Figure 4.16: pH-dependent ARS activity of ARSA: 100 ng ARSA was incubated with 3 mM 4-MUS at different pH values for 2 hrs. The reaction was stopped using 1 M Tris (pH 10.4) and the fluorescence of the product 4-MU was read at 460 nm after excitation at 355 nm. Values are the mean of triplicates and error bars represent the standard error. The experiment was performed in duplicate. Data generated using the method described in Section 2.13.

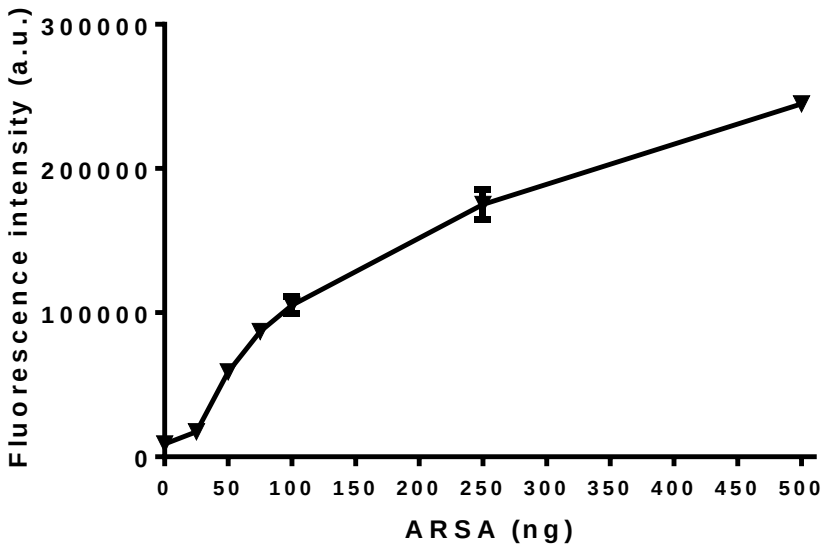

Figure 4.17: Concentration-dependent ARS activity of ARSA: Different concentrations of ARSA were incubated with 3 mM 4-MUS at pH 4.5 for 2 hrs. The reaction was stopped using 1 M Tris (pH 10.4) and the fluorescence of the product 4-MU was read at 460 nm after excitation at 355 nm. Values are the mean of triplicates and error bars represent the standard error. The experiment was performed in duplicate. Data generated using the method described in Section 2.13.

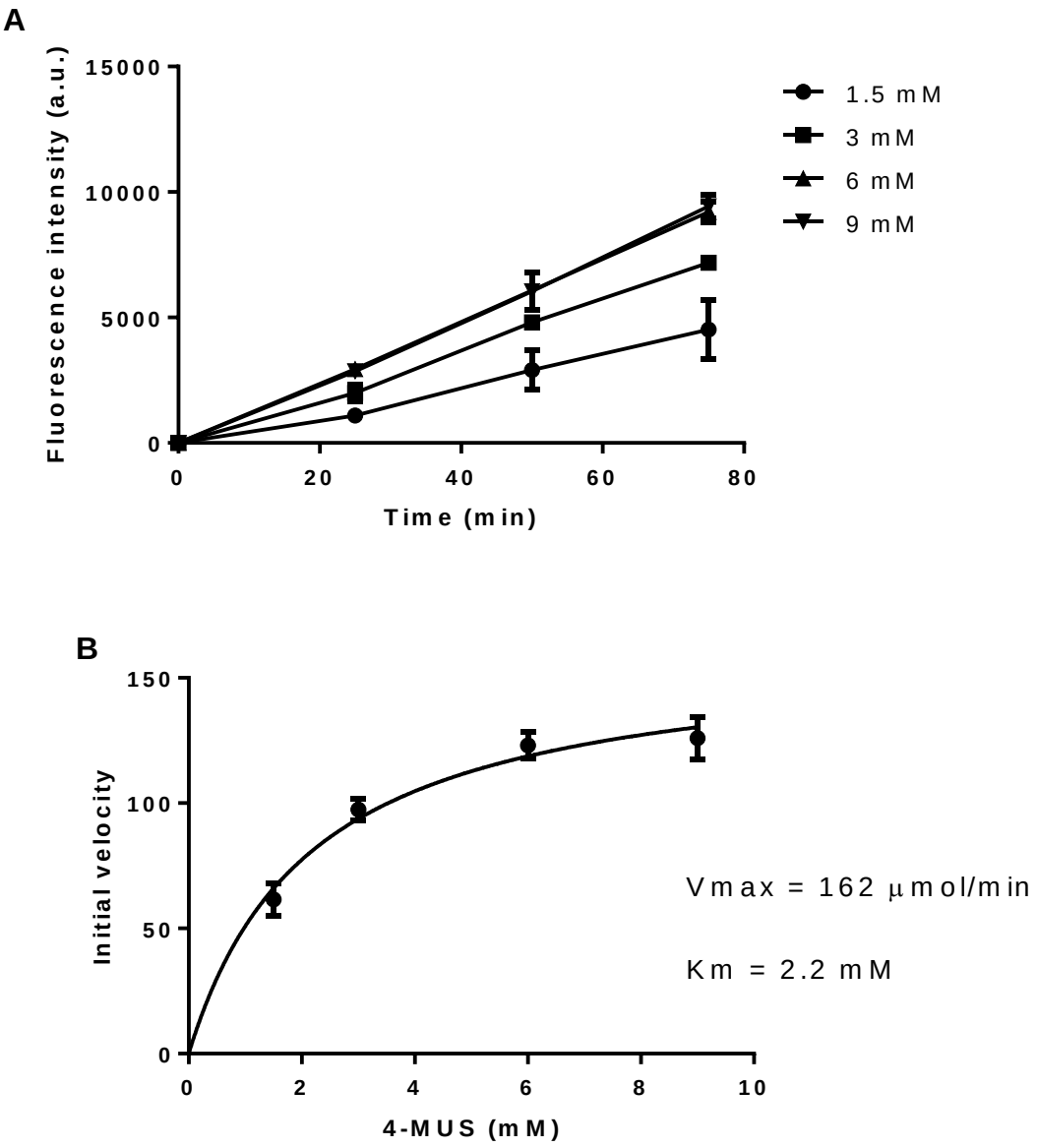

Figure 4.18: Determination of the Km of 4-MUS for ARSA: **(A)** 75 ng ARSA was incubated with different concentrations of 4-MUS at pH 4.5 for different time points. The reaction was stopped using 1 M Tris (pH 10.4) and the fluorescence of the product 4-MU was read at 460 nm after excitation at 355 nm. Values are the mean of triplicates and error bars represent the standard error. **(B)** Initial velocity was plotted against 4-MUS concentration. GraphPad Prism was used to determine the Km using the model: Y = Vmax*X/(Km + X). The experiment was performed in duplicate. Data generated using the method described in Section 2.13.

4.5.2. Characterisation of arylsulfatase B (ARSB)

As for ARSA, ARSB showed an acidic pH optimum (Figure 4.19), consistent with its lysosomal localization. Concentration-dependent activity with 4-MUS also exhibited a good dynamic range (Figure 4.20) (Table 4.1). The Km value was calculated as 415 µM at pH 4.5 (Figure 4.21), whereas the reported value is 1,180 µM at pH 5.6 (Hanson et al., 2004).

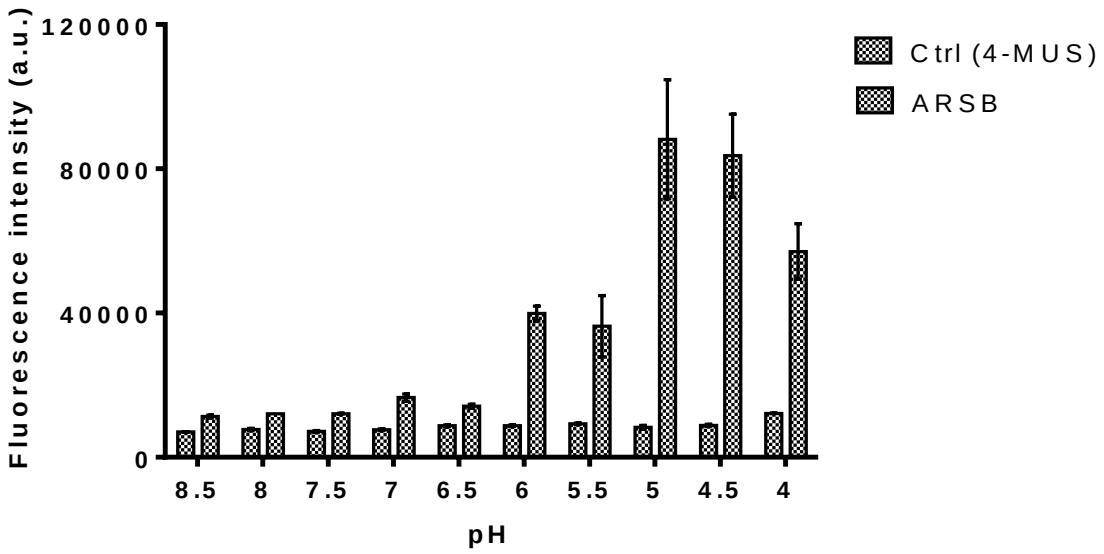

Figure 4.19: pH-dependent ARS activity of ARSB: 100 ng ARSB was incubated with 3 mM 4-MUS at different pH values for 2 hrs. The reaction was stopped using 1 M Tris (pH 10.4) and the fluorescence of the product 4-MU was read at 460 nm after excitation at 355 nm. Values are the mean of triplicates and error bars represent the standard error. The experiment was performed in duplicate. Data generated using the method described in Section 2.13.

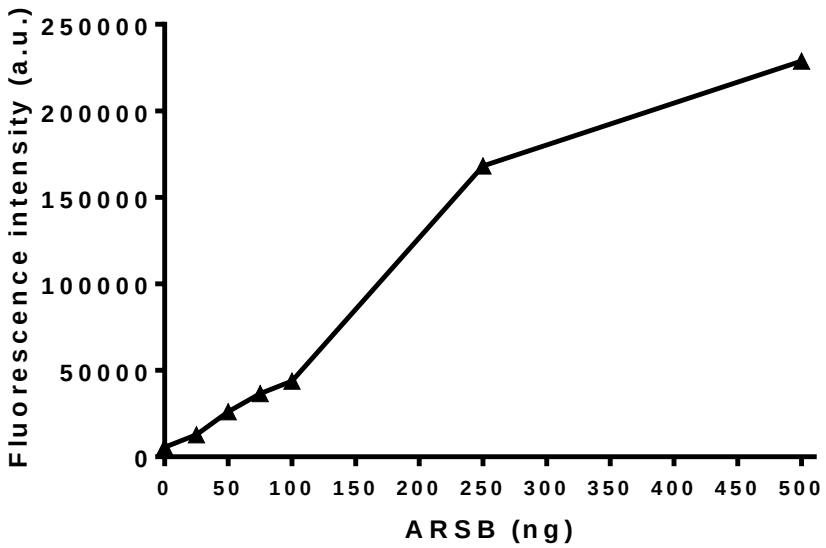

Figure 4.20: Concentration-dependent ARS activity of ARSB: Different concentrations of ARSB were incubated with 3 mM 4-MUS at pH 4.5 for 2 hrs. The reaction was stopped using 1 M Tris (pH 10.4) and the fluorescence of the product 4-MU was read at 460 nm after excitation at 355 nm. Values are the mean of triplicates and error bars represent the standard error. The experiment was performed in duplicate. Data generated using the method described in Section 2.13.

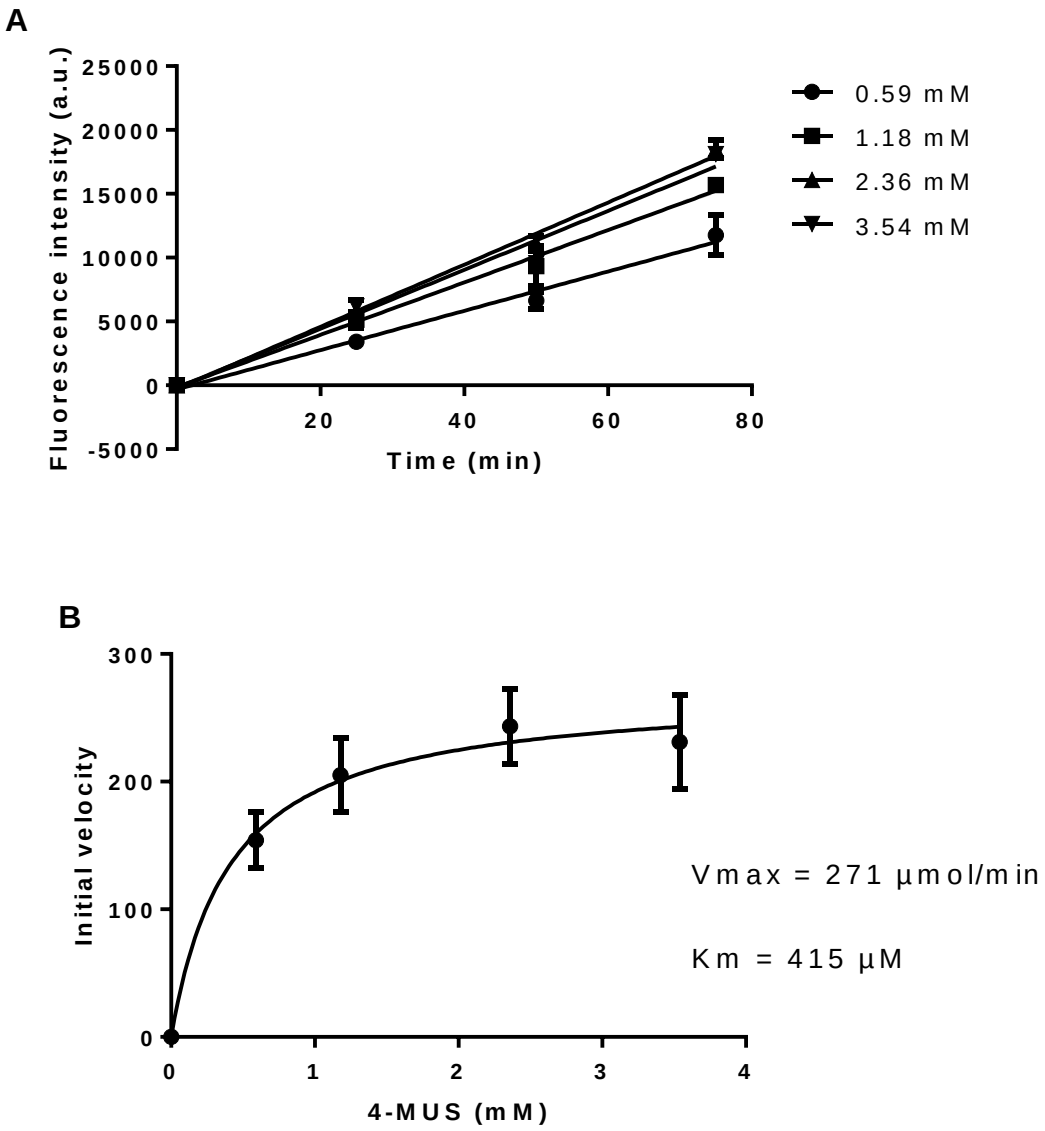

Figure 4.21: Determination of the Km of 4-MUS for ARSB: **(A)** 75 ng ARSB was incubated with different concentrations of 4-MUS at pH 4.5 for different time points. The reaction was stopped using 1 M Tris (pH 10.4) and the fluorescence of the product 4-MU was read at 460 nm after excitation at 355 nm. Values are the mean of triplicates and error bars represent the standard error. **(B)** Initial velocity of the reaction was plotted against 4-MUS concentration. GraphPad Prism was used to determine the Km using the model: Y = Vmax*X/(Km + X). The experiment was performed in duplicate. Data generated using the method described in Section 2.13.

4.5.3. Characterisation of steroid sulfatases/arylsulfatase C (STS/ARSC)

STS/ARSC showed a pH optimum of 7.5 (Figure 4.22), in line with localization in the microsomes. Concentration-dependent activity against 4-MUS exhibited a good dynamic range (Figure 4.23) (Table 4.1). The Km value was 82 µM at pH 7.5 (Figure 4.24), compared to the reported value of 800 µM at pH 7 (Hanson et al., 2004).

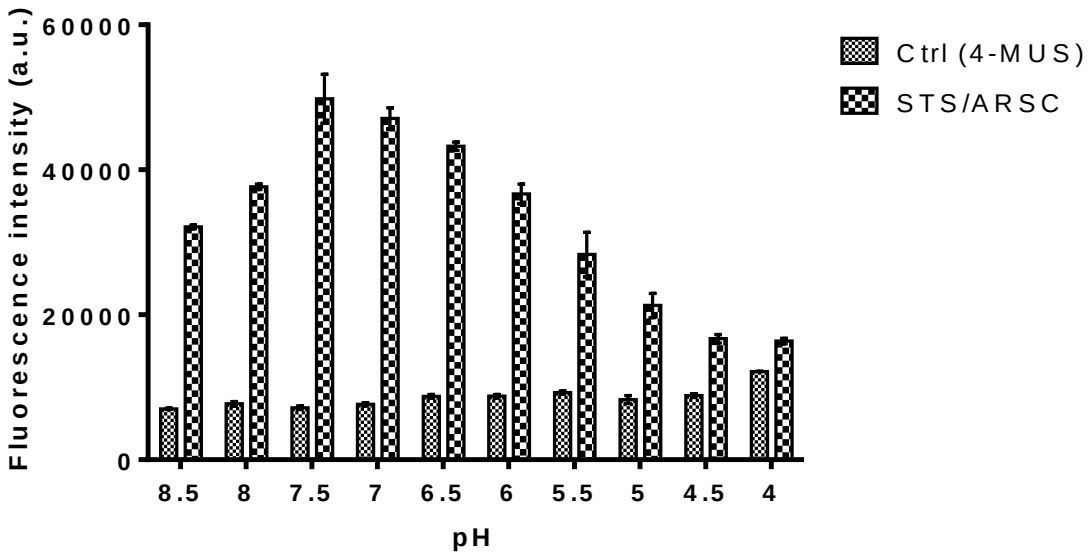

Figure 4.22: pH-dependent ARS activity of STS/ARSC: 100 ng STS/ARSC was incubated with 3 mM 4-MUS at different pH values for 2 hrs. The reaction was stopped using 1 M Tris (pH 10.4) and the fluorescence of the product 4-MU was read at 460 nm after excitation at 355 nm. Values are the mean of triplicates and error bars represent the standard error. The experiment was performed in duplicate. Data generated using the method described in Section 2.13.

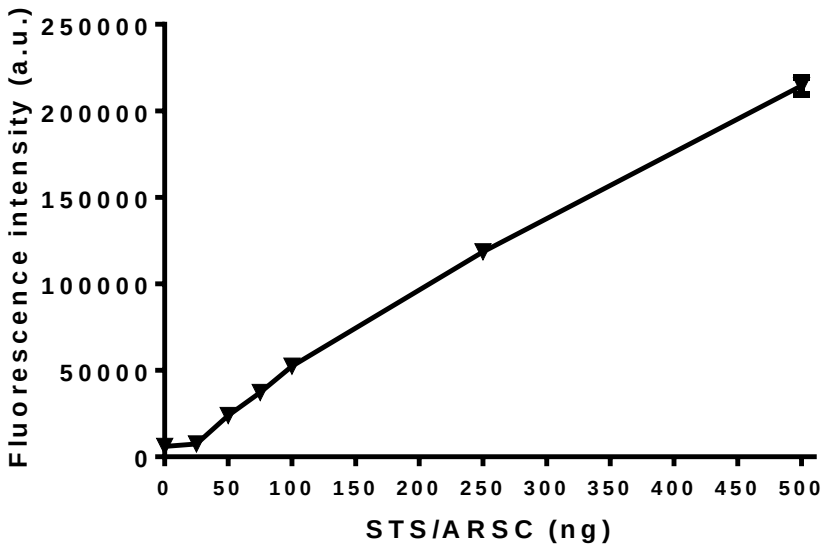

Figure 4.23: Concentration-dependent ARS activity of STS/ARSC: Different concentrations of STS/ARSC were incubated with 3 mM 4-MUS at pH 7.5 for 2 hrs. The reaction was stopped using 1 M Tris (pH 10.4) and the fluorescence of the product 4-MU was read at 460 nm after excitation at 355 nm. Values are the mean of triplicates and error bars represent the standard error. The experiment was performed in duplicate. Data generated using the method described in Section 2.13.

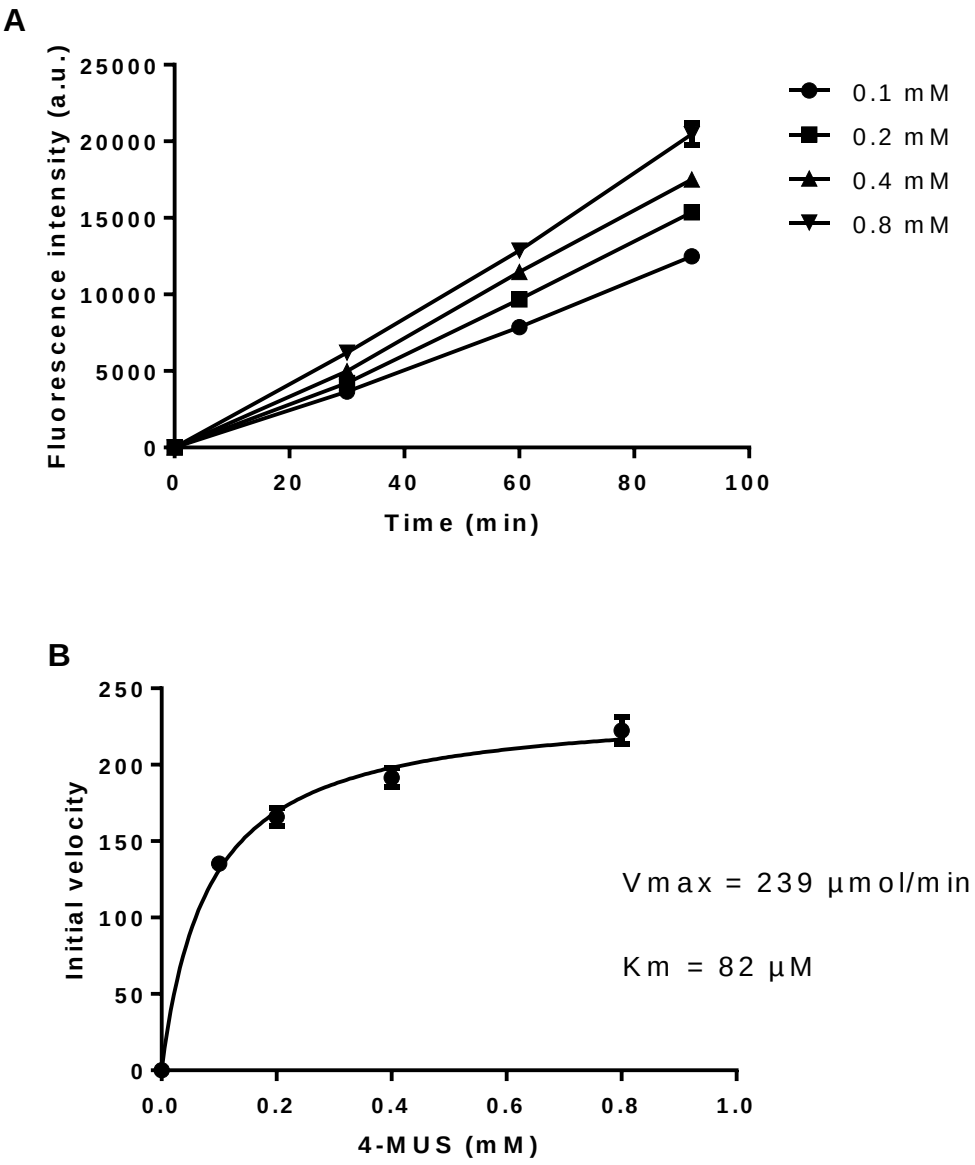

Figure 4.24: Determination of the Km of 4-MUS for STS/ARSC: **(A)** 75 ng STS/ARSC was incubated with different concentrations of 4-MUS at pH 7.5 for different time points. The reaction was stopped using 1 M Tris (pH 10.4) and the fluorescence of the product 4-MU was read at 460 nm after excitation at 355 nm. Values are the mean of triplicates and error bars represent the standard error. **(B)** Initial velocity of the reaction was plotted against 4-MUS concentration. GraphPad Prism was used to determine the Km using the model: Y = Vmax*X/(Km + X). The experiment was performed in duplicate. Data generated using the method described in Section 2.13.

4.5.4. Characterisation of neutral pH-dependent sulfatases

In addition to STS/ARSC, other neutral pH-dependent sulfatases were tested; the ER sulfatases ARSD, ARSF and ARSG. These three enzymes showed very weak activity using 4-MUS (Figure 4.25), with no more than 1.4-, 1.5- and 6.7-fold increase over substrate-only control, using 500 ng of ARSD, ARSF and ARSG, respectively (Table 4.1). This lack of activity made it difficult to measure the Km values for these enzymes. Also, this result indicated that 4-MUS is not a suitable substrate for assaying the activity of these three enzymes.

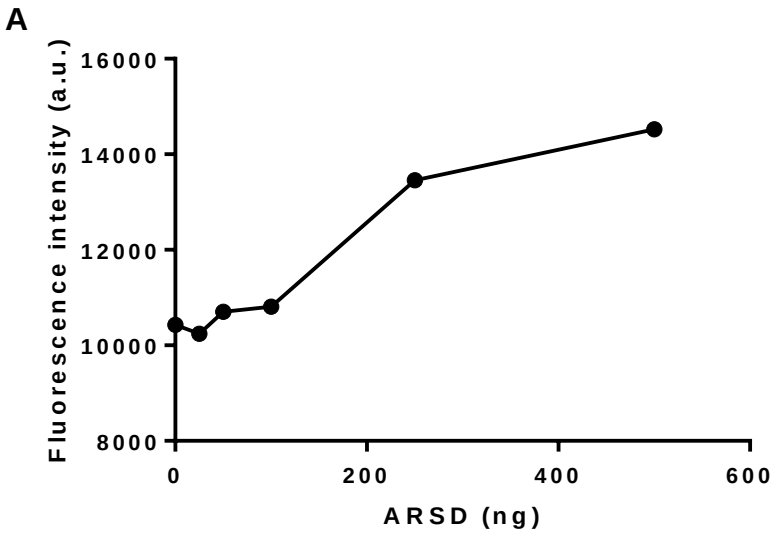

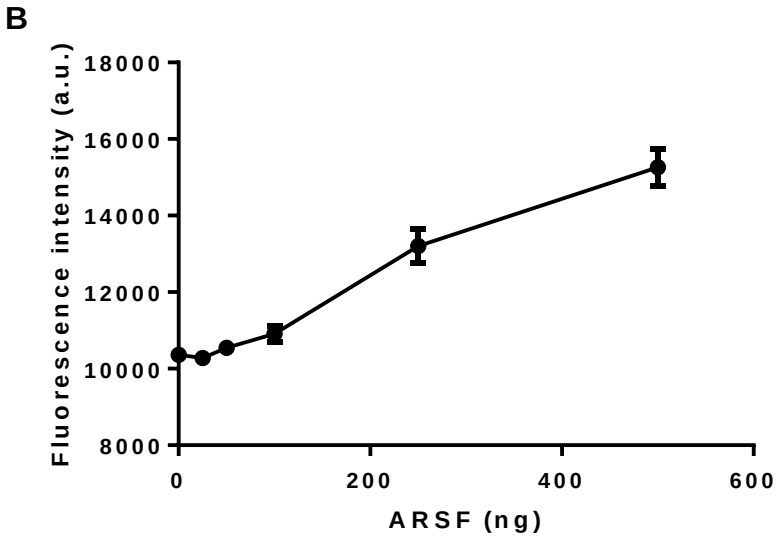

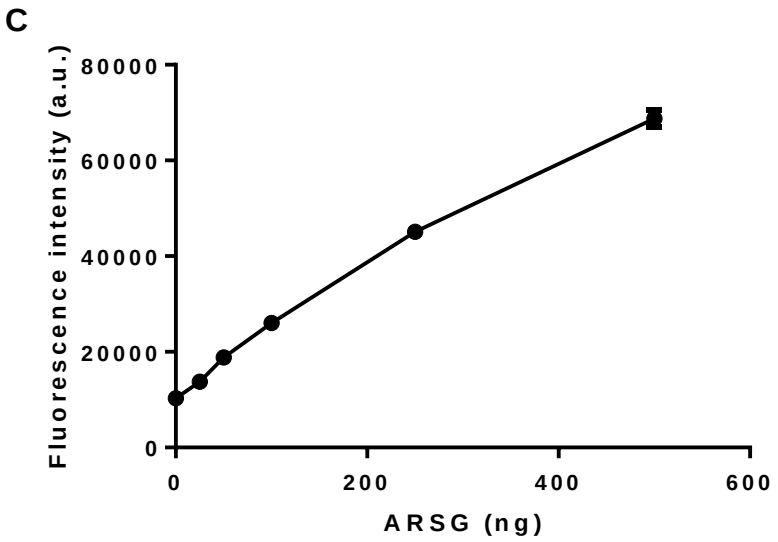

Figure 4.25: Concentration-dependent ARS activity of ARSD (A), ARSF (B) and ARSG (C): Different concentrations of the enzymes were incubated with 3 mM 4-MUS at pH 7.5 for 2 hrs. The reaction was stopped using 1 M Tris (pH 10.4) and the fluorescence of the product 4-MU was read at 460 nm after excitation at 355 nm. Values are the mean of triplicates and error bars represent the standard error. The experiment was performed in duplicate. Data generated using the method described in Section 2.13.

4.5.5. Characterisation of acidic pH-dependent sulfatases

In addition to ARSA and ARSB, the activity of three other lysosomal enzymes, namely, GALNS, GNS and IDS was measured using 4-MUS as the substrate. Of these three enzymes only IDS showed weak activity, with a 2.5-fold increase over control using 500 ng of the enzyme (Figure 4.26) (Table 4.1). No activity was detected for GALNS or GNS using 4-MUS (Figure 4.26). Therefore, other substrates were tested for these lysosomal enzymes. One was the chromogenic substrate p-nitrocatechol sulfate, where the removal of the sulfate groups by lysosomal arylsulfatases (e.g., ARSA and ARSB) leads to the formation of p-nitrocatechol. The absorbance of p-nitrocatechol can be measured in alkaline solution at 510 nm (van der Pal et al., 1991). IDS, GALNS and GNS enzymes failed to show any detectable activity, even at high enzyme concentrations (data not shown). Another indirect assay was therefore explored, which was the glucosidase- and galactosidase-coupled assays for GNS and GALNS, respectively.

A

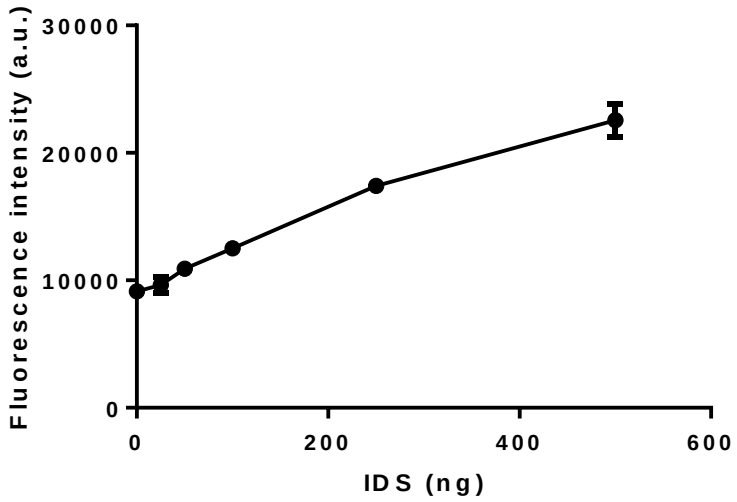
Fluorescence intensity (a.u.)
30000
20000
10000
0
0
200
400
600
IDS (ng)

B

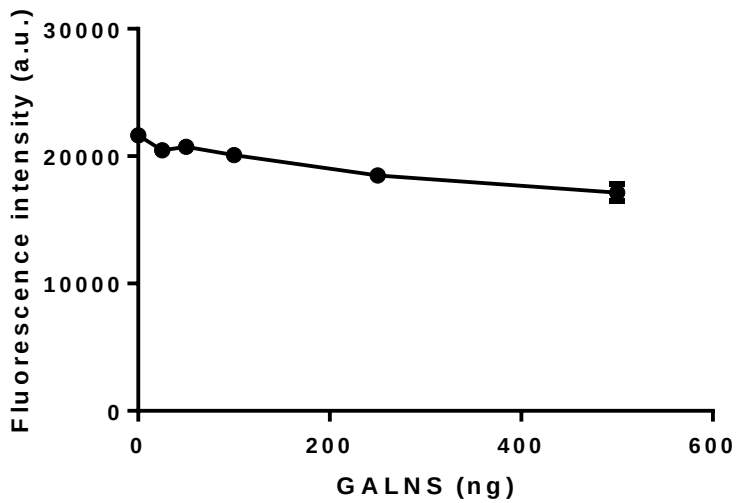
Fluorescence intensity (a.u.)
30000
20000
10000
0
0
200
400
600
GALNS (ng)

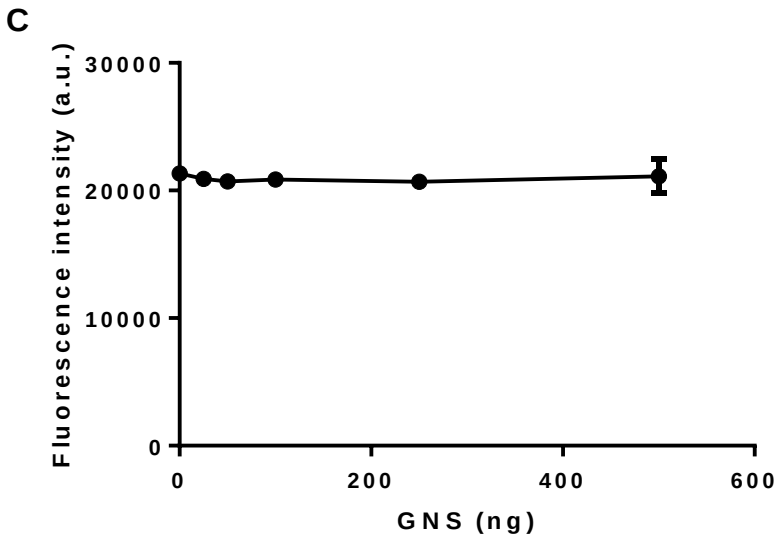

Figure 4.26: Concentration-dependent ARS activity of IDS (A), GALNS (B) and GNS (C): Different concentrations of the enzymes were incubated with 3 mM 4-MUS at pH 4.5 for 2 hrs. The reaction was stopped using 1 M Tris (pH 10.4) and the fluorescence of the product 4-MU was read at 460 nm after excitation at 355 nm. Values are the mean of triplicates and error bars represent the standard error. The experiment was performed in duplicate. Data generated using the method described in Section 2.13.

4.5.5.1. Characterisation of GNS using the glucosidase-coupled assay

GNS is a lysosomal exosulfatase that removes the 6-O-sulfate group from N-sulfated or N-acetylated glucosamine residues at the non-reducing end of HS chains, or N-acetylated glucosamine residues of keratan sulfate (Parenti et al., 1997). To measure GNS activity a glucosidase-coupled assay can be used, which depends on the intrinsically poor ability of β-glucosidase to hydrolyse the glycosidic bond between 4-MU and N-acetyl glucosamine when the latter is modified by a 6-O-sulfate as depicted in Figure 4.27 (Myette et al., 2009). In this assay, 4-methylumbelliferyl-6-sulfo-N-acetyl-β-D-glucosaminide (MU-GlcNAc,6S) is used, with 4-methylumbelliferyl-N-acetyl-β-D-glucosaminide (MU-GlcNAc) serving as a positive control for the activity of β-glucosidase. By performing the glucosidase-coupled assay at pH 4.5, the pH optimum of GNS, an assay was performed to confirm that β-glucosidase had minimal activity against MU-GlcNAc,6S compared with its activity against MU-GlcNAc. GNS alone had no activity against either

substrate (Figure 4.28; A). The minimal activity of β-glucosidase against MU-GlcNAc,6 was slightly increased by pre-incubation of the substrate with 250 ng of GNS for two hours, followed by adding β-glucosidase (Figure 4.28; B). This result suggested that the activity of GNS was the rate-limiting step of the glucosidase-coupled assay, as reported previously (Myette at al., 2009). Therefore, incubation of MU-GlcNAc,6S with high quantities of GNS and for a longer time was required to achieve the dynamic range needed for counter-screening of inhibitors (Figure 4.29; A). Under these conditions, it was found that GNS retained some activity at pH 7.5 (Figure 4.29; B).

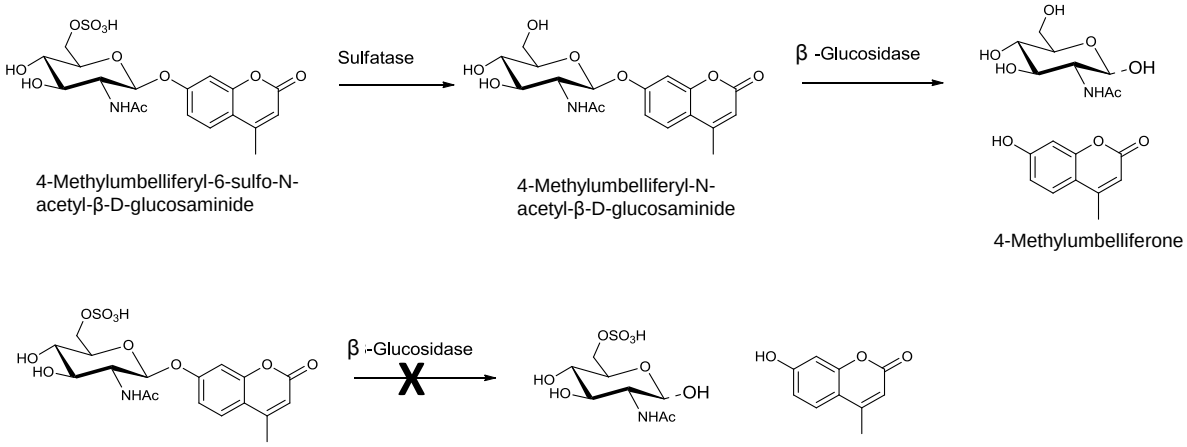

Figure 4.27: Principle of the glucosidase-coupled assay

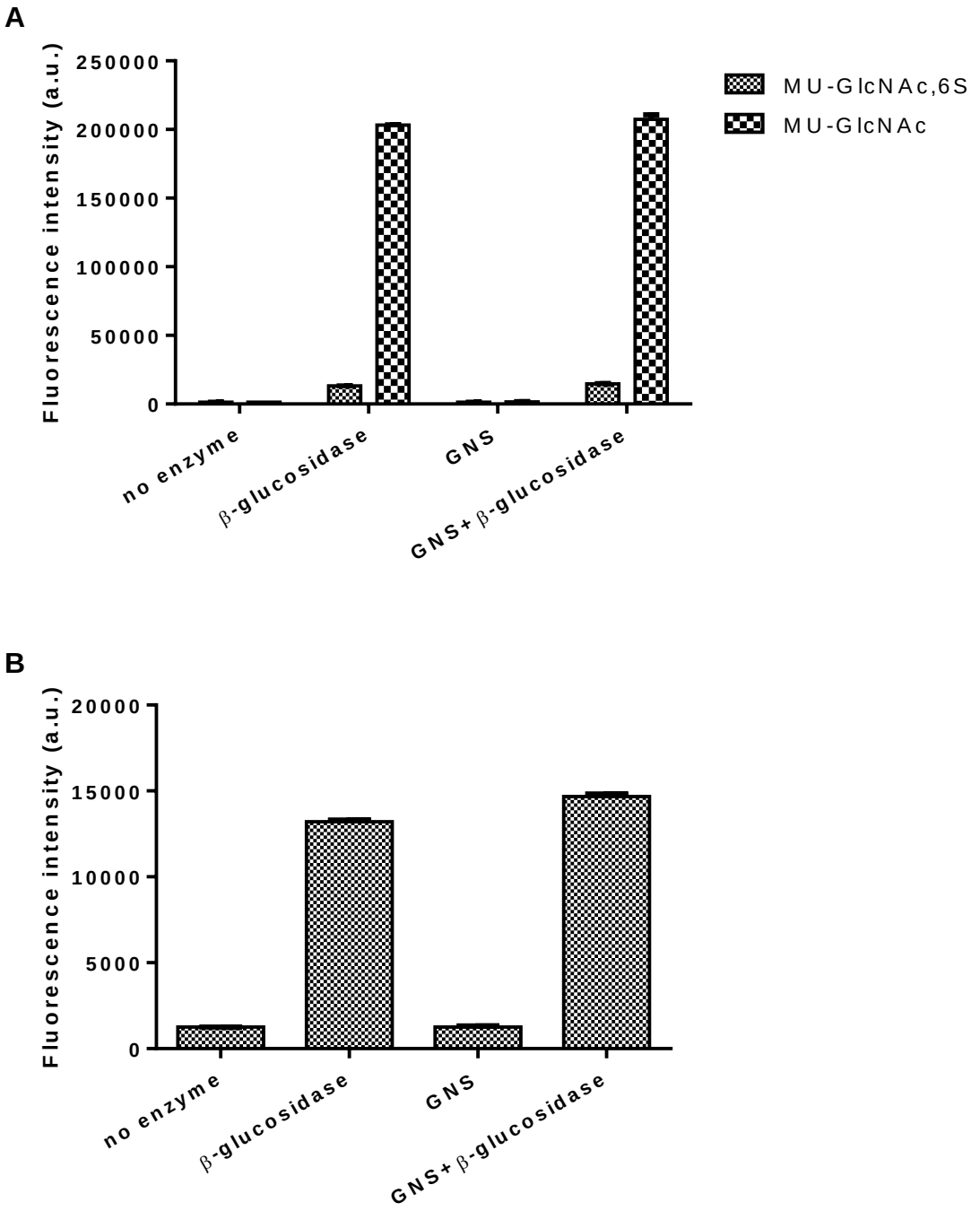

Figure 4.28: Activity of β-glucosidase and/or GNS against MU-GlcNAc,6S and MU-GlcNAc: 2 mM MU-GlcNAc,6S and MU-GlcNAc were incubated with 250 ng GNS for 2 hrs at 37°C in a reaction buffer containing HEPES and $MgCl_2$ followed by adding 40 units of β-glucosidase for 1 hr. The reaction was stopped using 1 M Tris (pH 10.4) and the fluorescence of the product 4-MU was read at 460 nm after excitation at 355 nm. **(B)** is the same as **(A)** with MU-GlcNAc data excluded for clarity. Values are the mean of triplicates and error bars represent the standard error. The experiment was performed in triplicate.

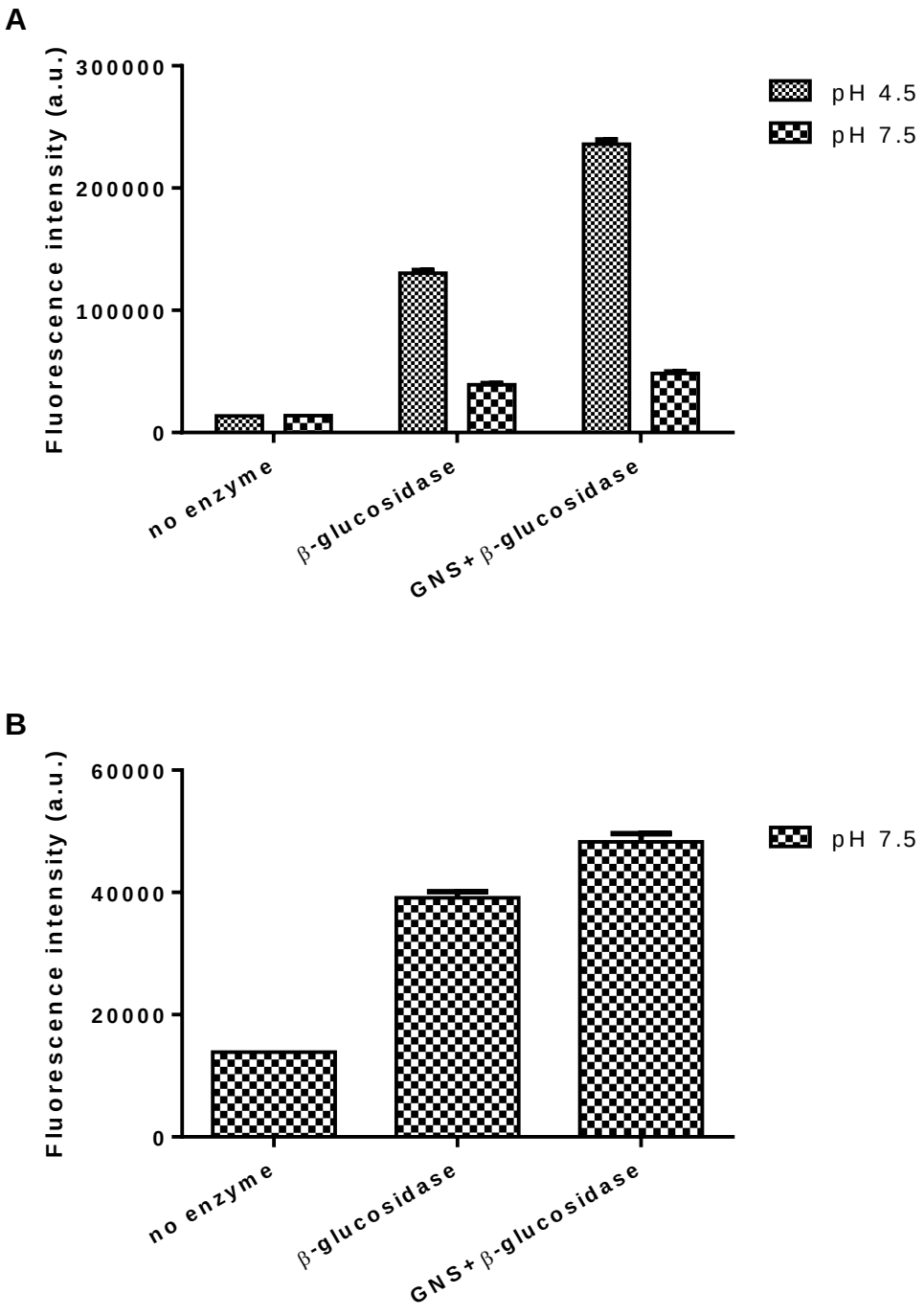

Figure 4.29: Glucosidase-coupled assay of GNS activity: 2 mM MU-GlcNAc,6S was incubated with 500 ng GNS for 3 hrs at 37°C followed by adding 40 units β-glucosidase for 1 hr. The reaction was stopped using 1 M Tris (pH 10.4) and the fluorescence of the product 4-MU was read at 460 nm after excitation at 355 nm. **(B)** is the same as **(A)** with the data at pH 4.5 excluded for clarity. Values are the mean of triplicates and error bars represent the standard error. The experiment was performed in triplicate.

4.5.5.2. Characterisation of GALNS using the galactosidase-coupled assay

GALNS is a lysosomal exosulfatase that removes 6-sulfate group from N-acetylated galactosamine residues of chondroitin sulfate or from galactosamine residues in keratan sulfate (Parenti et al., 1997). In a similar approach to that used for measuring GNS activity, the galactosidase-coupled assay was used for GALNS. This assay depends on the intrinsically poor ability of β-galactosidase to hydrolyse the glycosidic bond between 4-MU and galactosamine when the latter is modified by a 6-O-sulfate (van Diggelen et al., 1990). For this assay, 4-methylumbelliferyl β-D-galactopyranoside-6-sulfate (MU-Gal,6S) was used and 4-methylumbelliferyl β-D-galactopyranoside (MU-Gal) served as a positive control for the activity of β-galactosidase. The assay showed that β-galactosidase has no activity against MU-Gal,6S at pH 4.5, the pH optimum of GALNS, although it has some activity at pH 7.5 (Figure 4.31; A) and very high activity against MU-Gal at pH 4.5 (Figure 4.30; A). GALNS alone had no activity against either substrate (Figure 4.30). Pre-incubation of the MU-Gal,6S with 500 ng GNS at pH 4.5 for 4 hours followed by adding β-galactosidase was not associated with any measurable activity (Figure 4.31; B), suggesting either that this commercial GALNS enzyme is not active, or that MU-Gal,6S is not a substrate for this enzyme.

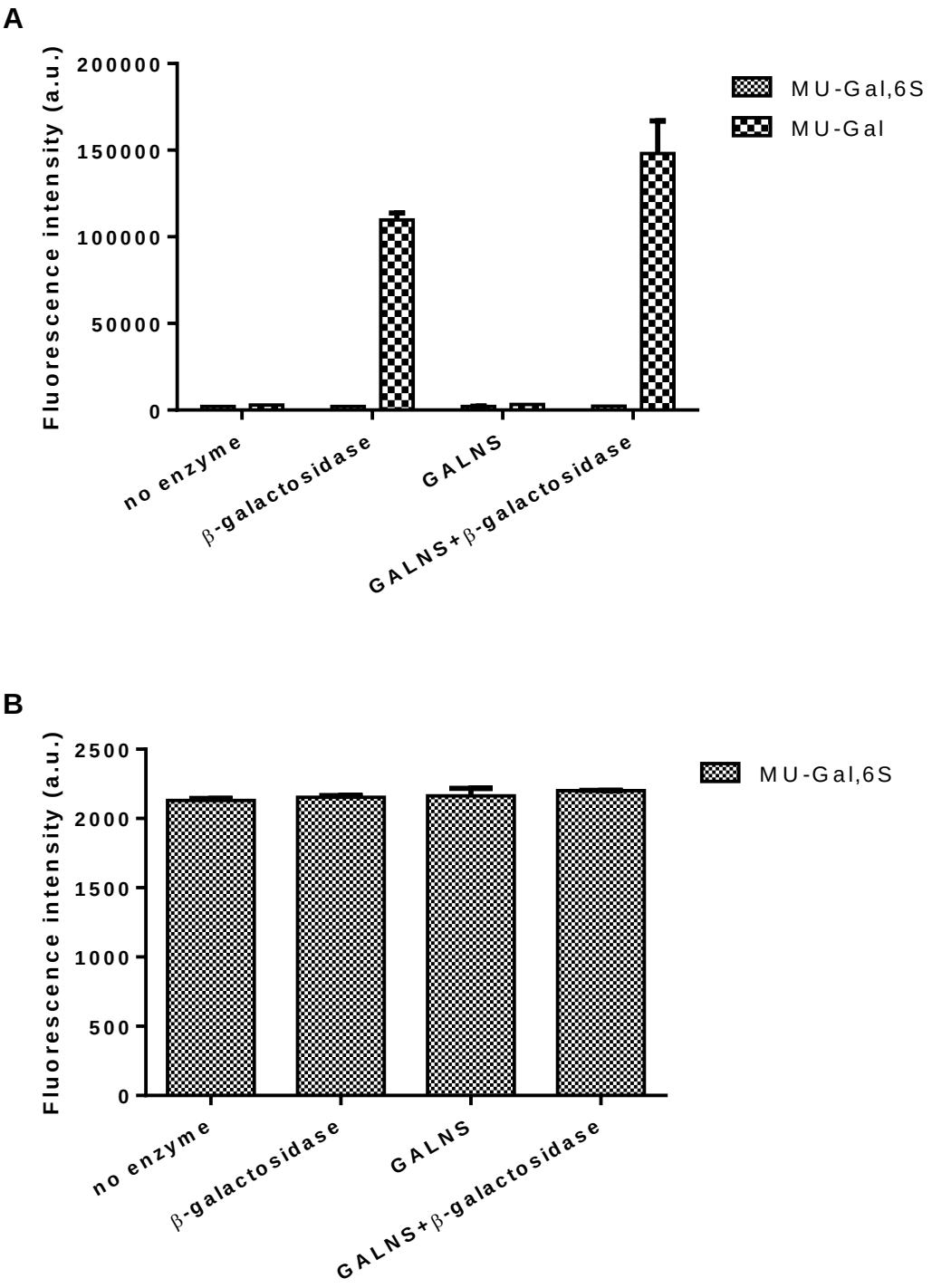

Figure 4.30: Activity of β-galactosidase and/or GALNS against MU-Gal,6S and MU-Gal: 2 mM MU-Gal,6S and MU-Gal were incubated with 250 ng GALNS for 1 hrs at 37°C in a reaction buffer containing HEPES (pH 4.5) and $MgCl_2$ followed by adding 40 units β-galactosidase for 1 hr. The reaction was stopped using 1 M Tris (pH 10.4) and the fluorescence of the product 4-MU was read at 460 nm after excitation at 355 nm. **(B)** is the same as **(A)** with MU-Gal data excluded for clarity. Values are the mean of triplicates and error bars represent the standard error. The experiment was performed in triplicate.

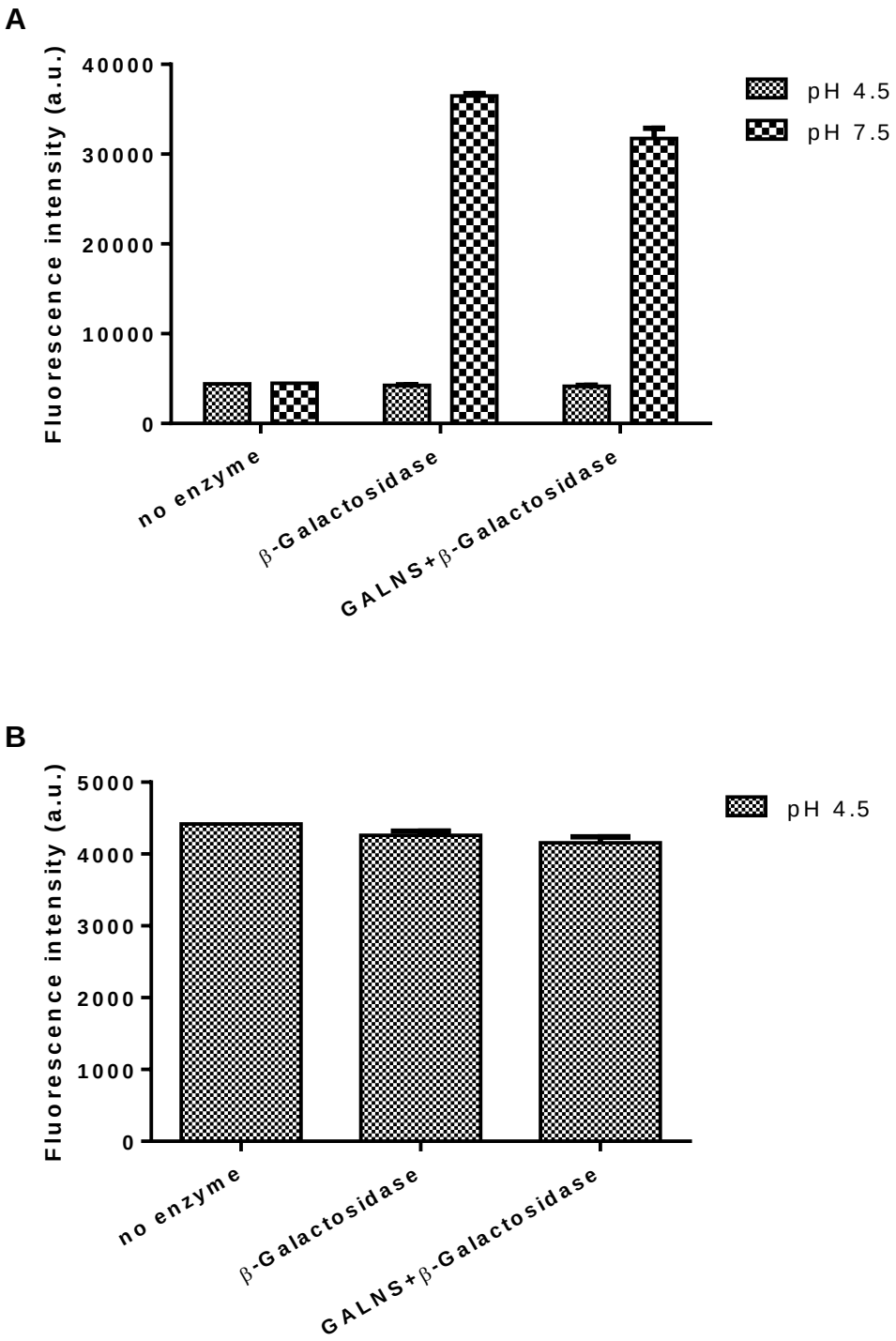

Figure 4.31: Galactosidase-coupled assay of GALNS activity: 2 mM MU-Gal,6S was incubated with 500 ng GALNS for 4 hrs at 37°C followed by adding 40 units β-galactosidase for 1 hr. The reaction was stopped using 1 M Tris (pH 10.4) and the fluorescence of the product 4-MU was read at 460 nm after excitation at 355 nm. **(B)** is the same as **(A)** with the data at pH 7.5 excluded for clarity. Values are the mean of triplicates and error bars represent the standard error. The experiment was performed in triplicate.

Table 4.1: Relative ARS activity of sulfatases against 4-MUS.

Enzyme	**Ratio of activity to control (no enzyme)**								
(ng)	***ARSA***	***ARSB***	***STS/ ARSC***	***ARSD***	***ARSF***	***ARSG***	***IDS***	***GNS***	***GALNS***
0	1	1	1	1	1	1	1	No Activity	No Activity
25	2	3	1	1	1	1.3	1.1		
50	7	6	4	1	1	1.8	1.2		
75	10	9	6						
100	12	11	9	1	1.1	2.5	1.4		
250	20	42	20	1.3	1.3	4.4	1.9		
500	28	59	36	1.4	1.5	6.7	2.5		
Km (μM)	**2,200**	**415**	**82**	**N/A**	**N/A**	**N/A**	**N/A**	**N/A**	**N/A**

4.6. Summary

Recombinant SULF2 protein could be stably expressed at high levels but did not show any catalytic activity using 4-MUS as the substrate even after co-expression with the FGE enzyme that is responsible for sulfatase activation. In contrast, transient expression of SULF2 did produce catalytically active enzyme that was secreted into conditioned medium. The failure to generate SULF2 by stable expression could possibly be due to toxicity resulting from high levels of active SULF2 enzyme in the stably transfected cells, such that only cells with inactive SULF2 and/or low levels of active SULF2 survive. The inactivity of SULF2 could be due to defective post-translational processing independent of the FGE enzyme, and the inability to detect low levels of active SULF2 could be due to the poor affinity of the SULF2 enzyme for the substrate 4-MUS. The transiently expressed active SULF2 could be enriched from CM using affinity binding but could not be eluted. Thus, SULF2 bound to beads was identified as the only viable source of enzyme for screening of inhibitors.

Setting up the sulfatase counter-screens was more straightforward. Three commercially available sulfatases, ARSA, ARSB and STS/ARSC, have high affinity to 4-MUS so these can be used in the initial counter-screening of potential inhibitors of SULF2. ARSD, ARSF, ARSG and IDS did have weak activity against 4-MUS substrate, but as large amounts of enzyme would need to be purchased these sulfatases would only be used for counter-screening of inhibitors inactive in the initial counter screen with ARSA, ARSB and STS/ARSC. A similar approach was proposed for GNS, where the glucosidase-coupled assay could be used for highly selected inhibitors, as a high concentration of the enzyme is required.

Chapter 5. Effects of Constitutive SULF1/2 Suppression in HCC Cell Lines

Numerous signalling pathways are recognized as playing a part in hepatocarcinogenesis. Two of the most important and best characterised are the growth factor/receptor tyrosine kinase (RTK) signalling pathway and the Wnt signalling pathway. Key growth factors involved in the RTK pathway include FGF-1, FGF-2, IGF-I, IGF-II and VEGF-165 (Yang et al., 2011) (Min et al., 2011) (Wu and Zhu, 2011) (Cornellà et al., 2011) (Zhang et al., 2012). The 6-O sulfation of HSPGs is reportedly important for these two signalling pathways and 6-O sulfation is post-synthetically modified by the activity of SULF1/2. Thus, these pathways were characterised in HCC cell lines and the effect of SULF2 gene silencing on these pathways investigated.

5.1. Characterisation of Wnt Signalling in HCC Cell Lines

Secreted Wnt ligands can activate two signalling pathways. The first is the canonical Wnt signalling pathway in which ligands bind to frizzled (FZD) receptors and this leads to activation of T-cell factor/lymphocyte enhancer factor (TCF/LEF) transcription factors (Gordon and Nusse, 2006). The second is the non-canonical signalling pathway, which regulates cytoskeletal reorganization and calcium mobilization (Veerman et al., 2003). The canonical pathway is better characterised and is generally considered the more pertinent to carcinogenesis (Polakis et al., 2012). While a number of ways of measuring the canonical signalling pathway have been developed, there is a shortage of assays to study the non-canonical pathway (van Amerongen and Nusse, 2009). The focus here will be on the canonical Wnt signalling pathway.

Canonical Wnt signalling is mediated by the protein β-catenin. In the absence of Wnt ligands (Figure 5.1; left), β-catenin is kept at a low level through association with the destruction complex composed of the adenomatous polyposis coli (APC) protein, axin and two kinases, namely glycogen synthase kinase 3β (GSK-3β) and

casein kinase 1α (CK-1α). The degradation cascade of β-catenin is initiated after phosphorylation at Ser45 by CK-1α (Amit et al., 2002) (Liu et al., 2002). This initial event leads to its subsequent further phosphorylation at Ser33, Ser37 and Thr41 by GSK-3β (Wu and He, 2006), which leads to degradation of β-catenin by the ubiquitin-proteasome pathway, involving the ubiquitin ligase β-TrCP (Willert and Nusse, 1998) (Nusse, 2012).

Upon signalling (Figure 5.1; right), Wnt ligands bind to fizzled receptors and low-density lipoprotein receptor-related protein 5 and 6 (LRP5/6) co-receptors, and this leads to the rearrangement of the receptors. The LRP tail is phosphorylated by CK-1γ which also requires frizzled and the scaffolding protein dishevelled (Dvl). Subsequently, LRP recruits axin and disrupts the destruction complex (Mao et al., 2001) (Bilic et al., 2007). In another model, it was proposed that frizzled receptors recruit Dvl through binding with the PDZ domain of Dvl (Umbhauer et al., 2000) (Wong et al., 2003) (Cong et al., 2004). The similarity between the N terminus of Dvl and the DIX domain of axin leads to their interaction and to the formation of a Dvl, axin and GSK-3β complex upon Wnt binding (Schwarz-Romond et al., 2007) (Nusse et al., 2012). As a result, β-catenin is no longer phosphorylated by GSK-3β, and it accumulates in the cytoplasm followed by translocation to the nucleus. In the nucleus β-catenin forms a complex with TCF/LEF transcription factors and other elements including BCL9, pygopus (Pygo), and CBP to drive the transcription of downstream genes such as MYC and CCND1 (Willert and Nusse, 1998) (Grigoryan et al., 2008) (Nusse, 2012).

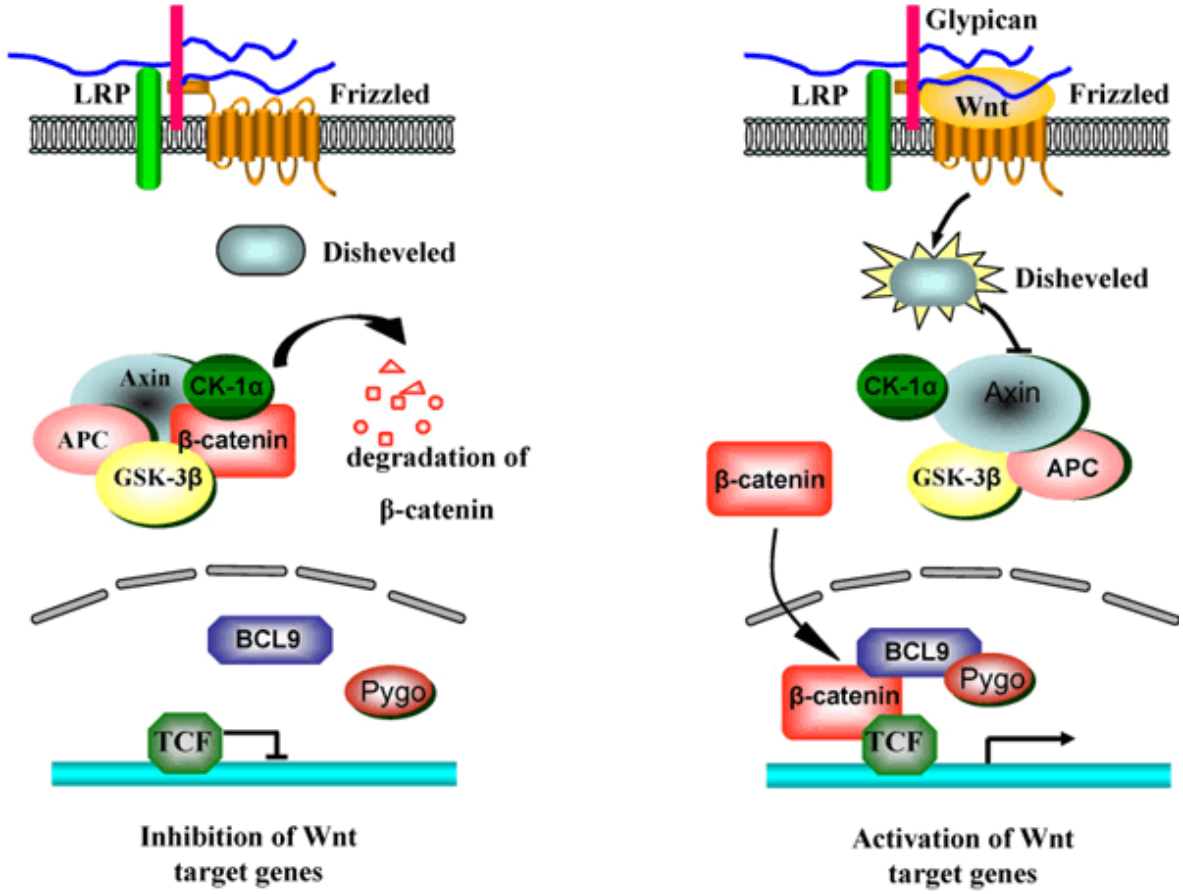

Figure 5.1: Diagram representing the canonical Wnt signalling pathway: **Left**: Inactive Wnt signalling: In the absence of Wnt ligand, β-catenin is targeted for degradation by the destruction complex (axin, APC, CK-1α and GSK-3β). **Right**: Active Wnt signalling: Binding of Wnt ligand to its frizzled receptor and LRP5/6 co-receptor recruits the scaffolding protein dishevelled and this leads to the disruption of the destruction complex and stabilization of β-catenin which translocates to the nucleus and activates transcription of target genes.

There are numerous means of monitoring canonical Wnt signalling. These include detecting changes in the levels or activity of β-catenin as detected by performing WB, ICC or ELISA using antibodies against total β-catenin or active β-catenin (ABC); β-catenin lacking phosphates at Ser33/37/Thr41. Changes in β-catenin/TCF activity can be detected using luciferase reporter assays, as described in Section 2.15. The format can involve transiently transfecting cells with a plasmid vector containing a 'TOPflash' reporter, or stably transducing cells with 7TFP lentiviral particles. The TOPflash plasmid has three TCF binding sites upstream of the luciferase coding sequence, promoting the expression of luciferase following activation of Wnt signalling. The activity of the expressed luciferase is measured by a chemiluminescent reaction using luciferin as the substrate. The 7TFP construct has seven TCF binding sites upstream of Firefly luciferase making it more robust for detecting changes in Wnt signalling, as the greater number of sites available for binding enhances the signal to noise ratio. The 7TFP lentiviral particle reporter has been previously characterised (Fuerer and Nusse, 2010) and offers the advantage of being integrated within the majority of the cells, rather than a subset of cells, as is the case using transient transfection.

For stimulation of Wnt signalling in HCC cell lines, the canonical Wnt-3a ligand was used, which modulates cell proliferation and survival via a β-catenin-dependent signalling pathway (Galli et al., 2006). β-Catenin is not only involved in Wnt signalling but also has other functions in the cells, including a role in cell adhesion at the cell surface (Brembeck et al., 2006). As levels of β-catenin can be very high in HCC cell lines, and only a proportion of β-catenin will be involved in Wnt signalling, subtle or small changes in β-catenin levels were difficult to detect by WB in HuH-7 and Hep 3B cells (data not shown). Furthermore, the functional consequences are unknown. Therefore, the TCF luciferase reporter assay was established. For screening of cell lines the TOPflash construct was used, co-transfected with a β-galactosidase construct. The activity of β-galactosidase was measured and used for normalization, thereby correcting for variation in transfection efficiency. Treatment of HCC cell lines with Wnt-3a showed that only HuH-7 and Hep3B cells were responsive to Wnt-3a treatment, leading to increased luciferase activity, while HepG2 cells were not responsive but had very high basal

level (data not shown). For further studies, the HuH-7 cell line was chosen and the cells were treated with increasing concentrations of Wnt-3a for different durations. The results showed a Wnt-3a concentration-dependent increase in TCF activity at all time points. However, 6 hours of treatment was found to give the highest luciferase activity in response to Wnt-3a (Figure 5.3; A).

As a positive control for stimulation of the canonical Wnt signalling, 6-bromo-indirubin-3'-oxime (BIO) was used, the structure of which is shown in Figure 5.2. BIO is a potent and selective inhibitor of GSK-3α/β (Meijer et al., 2003) (Polychronopoulos et al., 2004). TCF reporter activity showed BIO concentration-dependent stimulation up to 1 µM, while higher concentrations were toxic to cells (Figure 5.3; B). To confirm that the activation of Wnt signalling following Wnt-3a treatment was due to Wnt-3a binding to frizzled receptor, and hence via the canonical Wnt signalling pathway, the Dvl-PDZ domain inhibitor II, compound 3289-8625 was used (structure shown in Figure 5.2). This compound disrupts the interaction between Dvl and FZD and thus blocks Wnt-3a-induced β-catenin-dependent transcriptional activity (Grandy et al., 2009). Also, this compound serves as a positive control for the inhibition of Wnt signalling. HuH-7 cells were incubated with increasing concentrations of compound 3289-8625 for 1 hr, followed by stimulation with 100 ng/ml of Wnt-3a and the results showed concentration-dependent inhibition of luciferase reporter activity (Figure 5.3; C).

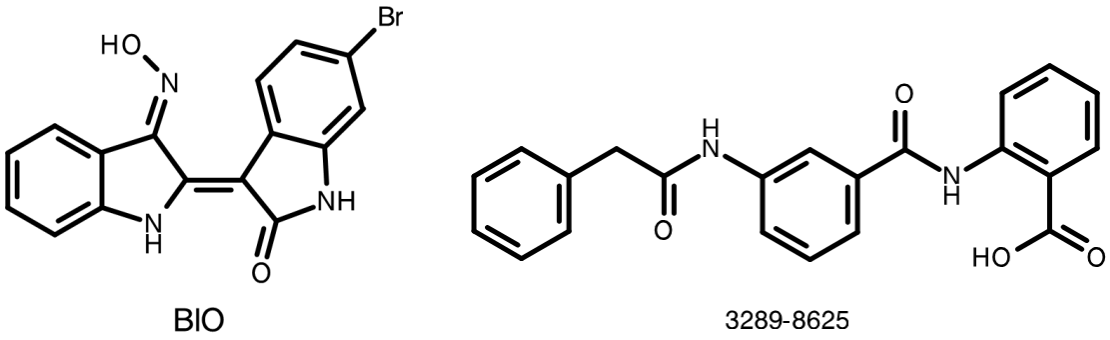

Figure 5.2: The structure of BIO (6-bromo-indirubin-3'-oxime) (Left) and of compound 3289-8625 (Dvl-PDZ Domain Inhibitor II) (Right).

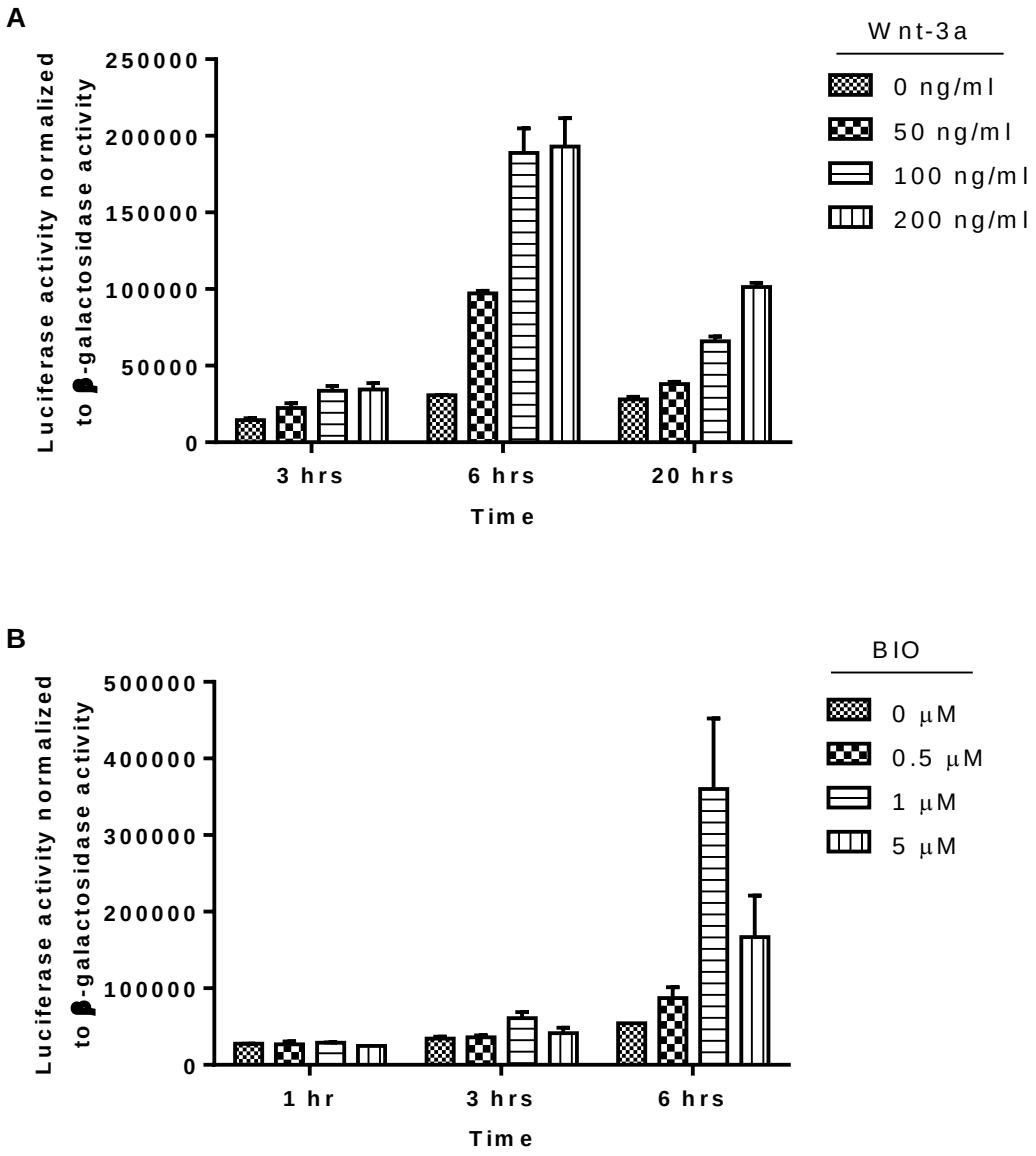
A
Luciferase activity normalized to β-galactosidase activity
250000
200000
150000
100000
50000
0
3 hrs
6 hrs
20 hrs
Time
Wnt-3a
0 ng/ml
50 ng/ml
100 ng/ml
200 ng/ml
B
Luciferase activity normalized to β-galactosidase activity
500000
400000
300000
200000
100000
0
1 hr
3 hrs
6 hrs
Time
BIO
0 μM
0.5 μM
1 μM
5 μM

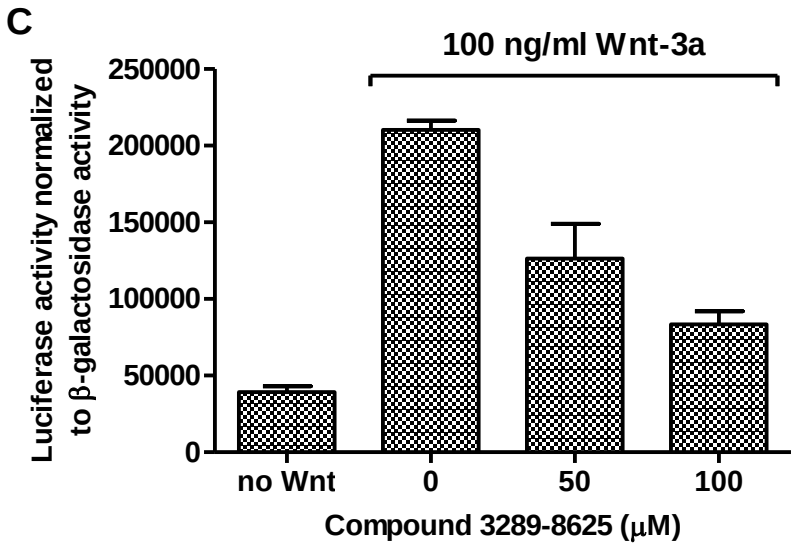

Figure 5.3: Characterisation of the TCF reporter assay in HuH-7 cells: HuH-7 cells were transiently co-transfected with TOPflash and β-galactosidase constructs. The cells were then stimulated with different concentrations of Wnt-3a **(A)** or BIO **(B)** for different time points or treated with different concentrations of compound 3289-8625 for 1 hour followed by treatment with 100 ng/ml Wnt-3a for 6 hours **(C)**. The cell lysates were extracted and the TOPflash luciferase activity was measured and normalized to the activity of β-galactosidase. Values are the mean of triplicates and error bars represent the standard error. The experiment was performed in triplicate. Data generated using the method described in Section 2.15.

5.2. Characterisation of Growth Factor/Receptor Tyrosine Kinase Signalling in HCC Cell Lines

Growth factors act through binding to their cognate receptor tyrosine kinases which then transduce the signal, predominantly via the MEK/MAPK/ERK or the PI3K/AKT cascades, depending on the type of the growth factor and the cells being studied. Transduction leads to the phosphorylation of ERK1/2 and/or AKT that can be detected by WB or quantified by an ELISA for phospho-ERK (p-ERK) or phospho-AKT (p-AKT).

P-ERK and p-AKT stimulation was studied in three cell lines; SNU-182, HuH-7 and Hep 3B. Responsiveness to different growth factors, and the optimal concentration of the growth factor and exposure time were defined.

SNU-182 cells were serum-starved overnight and then stimulated with FGF-1, FGF-2, IGF-I, IGF-II or VEGF-165. These five growth factors were selected given the reported involvement of FGF, IGF and VEGF signalling and downstream mediators (i.e., MAPK/ERK and PI3K/AKT signalling pathways) in HCC (Min et al., 2011) (Wu and Zhu, 2011) (Cornellà et al., 2011).

To determine the optimal concentrations of the growth factors required to achieve maximal phosphorylation of ERK and/or AKT, the cells were treated with a range of growth factor concentrations for 10 min, and then WB was performed. The blots showed that FGF-1, FGF-2, IGF-I cause phosphorylation of both ERK and AKT at concentrations as low as 0.1 nM. Only 10 nM of IGF-II caused phosphorylation of AKT but not ERK after 10 min, while VEGF-165 did not cause any increase in phosphorylation of either ERK or AKT in the SNU-182 cell line even at a high concentration (Figure 5.4).

To determine optimal exposure times for SNU-182 cells to the different growth factors, the cells were treated with 10 nM of the growth factors for different time periods followed by extraction of cell lysates and WB. The blots showed that the stimulation of p-ERK and p-AKT was highest after 10 min exposure to FGF-1, 5-10 min exposure to FGF-2 and 5 min exposure to IGF-I. IGF-II caused phosphorylation of AKT after 10 min and of ERK after 5 min only, possibly explaining why stimulation of ERK phosphorylation could not be detected in the experiment where an exposure time of 10 min was used. Again, VEGF-165 failed to cause any phosphorylation of ERK or AKT up to 10 min exposure to this growth factor (Figure 5.5).

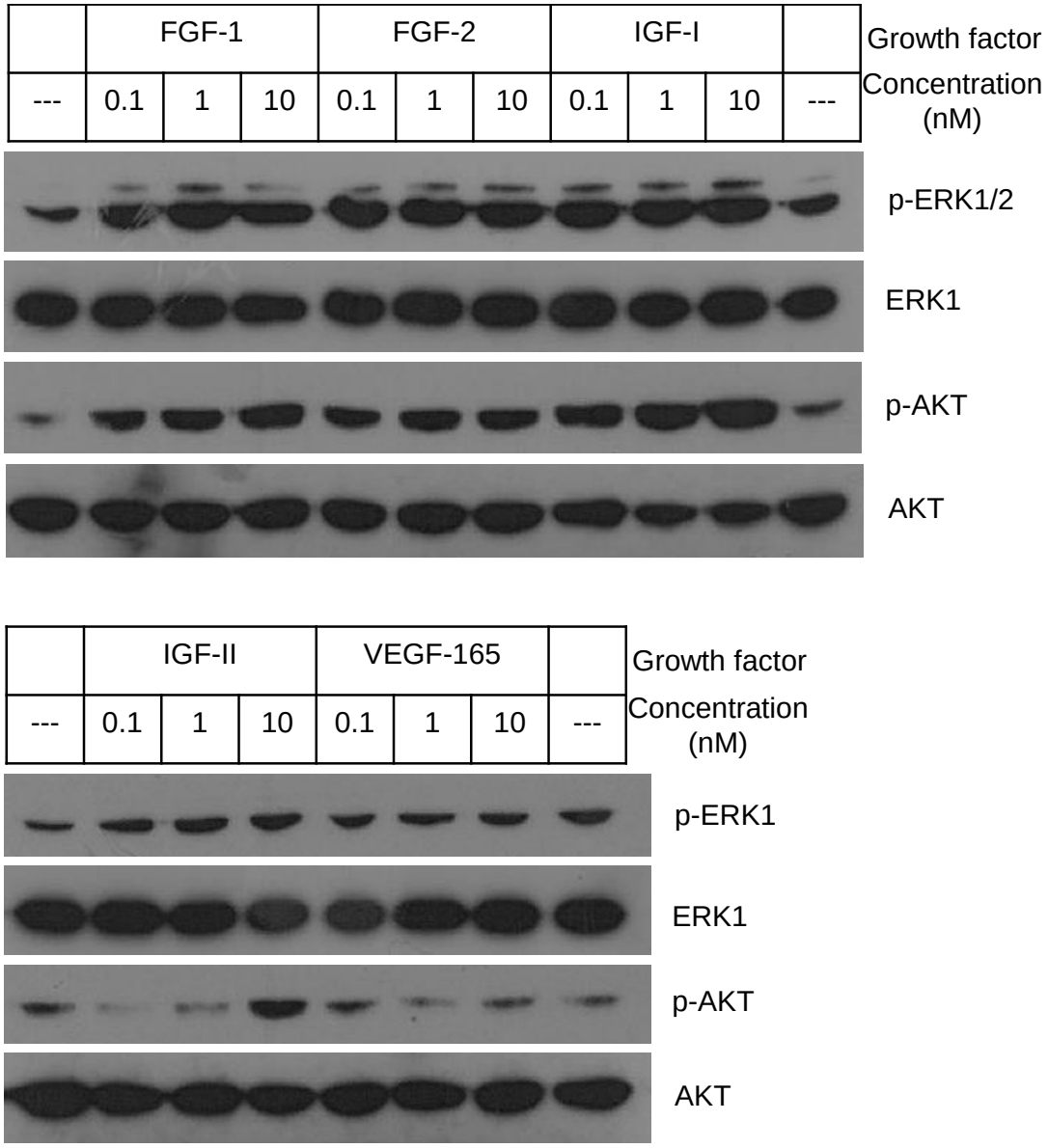

Figure 5.4: Optimisation of p-ERK and p-AKT stimulation in response to different concentrations of growth factors in SNU-182 cells: SNU-182 cells were serum-starved overnight and then treated with 0.1, 1 or 10 nM of FGF-1, FGF-2, IGF-I, IGF-II or VEGF-165 for 10 min. Cell lysates were prepared, 15 µg/lane loaded and WB performed using antibodies against p-ERK and p-AKT. Then WB membranes were stripped and re-probed using total ERK and total AKT antibodies to serve as loading controls. The experiment was performed in duplicate and representative blots are shown. Data generated using the method described in Section 2.10.

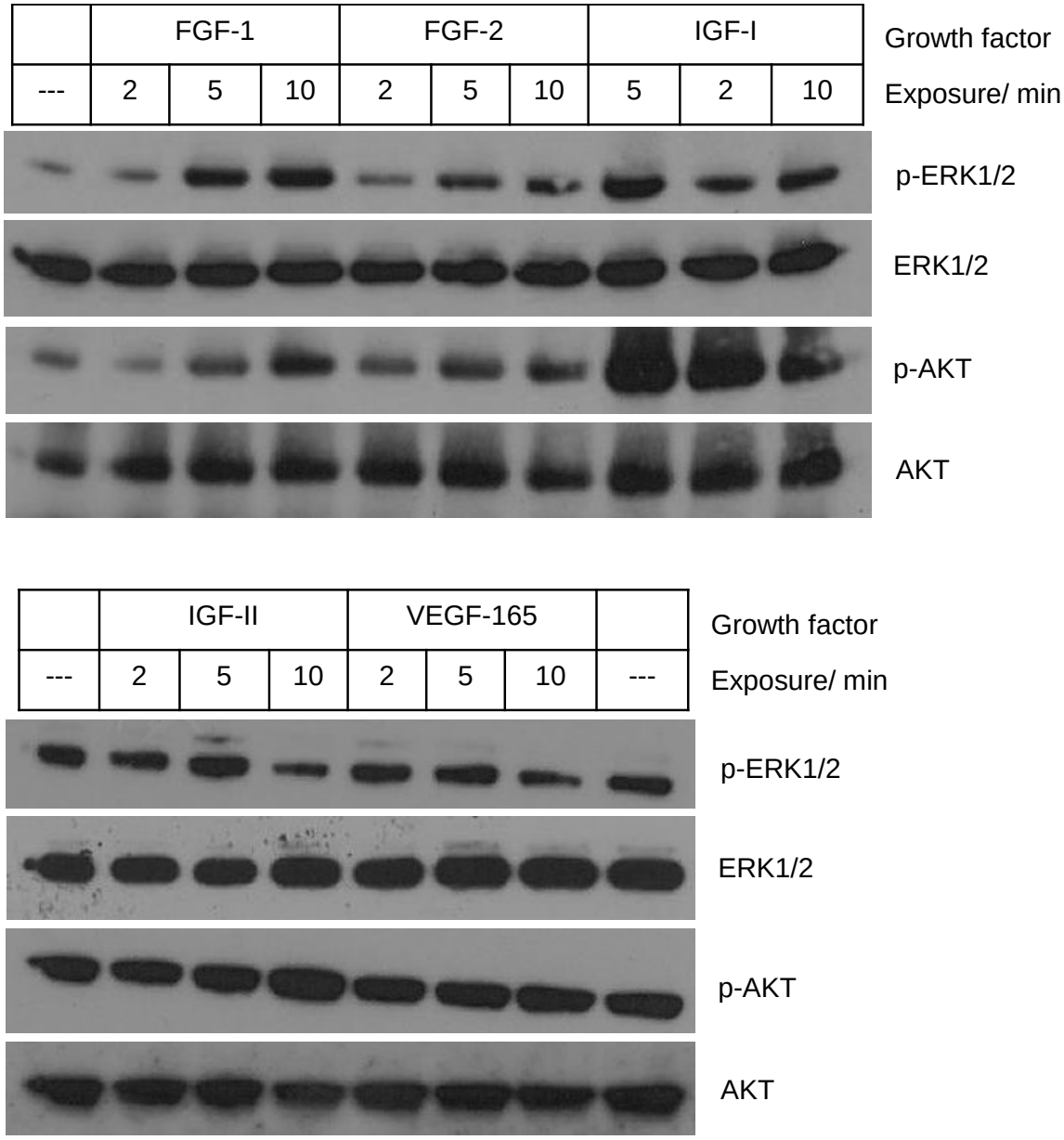

Figure 5.5: Optimisation of p-ERK and p-AKT stimulation in response to different exposure times of growth factors in SNU-182 cells: SNU-182 cells were serum-starved overnight and then treated with 10 nM of FGF-1, FGF-2, IGF-I, IGF-II or VEGF-165 for 2, 5 or 10 min. Cell lysates were prepared, 15 µg/lane loaded and WB performed using antibodies against p-ERK and p-AKT. Then WB membranes were stripped and re-probed using total ERK and total AKT antibodies to serve as loading controls. The experiment was performed in duplicate and representative blots are shown. Data generated using the method described in Section 2.10.

To further characterise growth factor/RTK signalling in SNU-182 cells, the potent and selective inhibitor of the FGF receptor (FGFR1 and FGFR3) PD173074 was used (Mohammadi et al., 1998) (Kunii et al., 2008) (Pardo et al., 2009). The structure of PD173074 is shown in Figure 5.6. SNU-182 cells were incubated with increasing concentrations of PD173074 for 1 hr, followed by treatment with 10 nM of FGF-1 or FGF-2 for 10 min. An ELISA for p-ERK was performed and the results demonstrated concentration-dependent inhibition of basal, FGF-1- and FGF-2-induced ERK phosphorylation (Figure 5.7; A). The IC_{50} for inhibition of FGF-stimulated p-ERK by PD173074 was found to be 84 nM for FGF-1 and 27 nM for FGF-2 (Figure 5.7; B). Also, the MEK inhibitor PD0325901 (Barrett et al., 2008) was used at 1 µM and caused complete inhibition of basal, FGF-1- and FGF-2-induced ERK phosphorylation (data not shown). The structure of PD0325901 is shown in Figure 5.6. HuH-7 and Hep 3B cells showed similar results to SNU-182 cells (G. Beale personal communication).

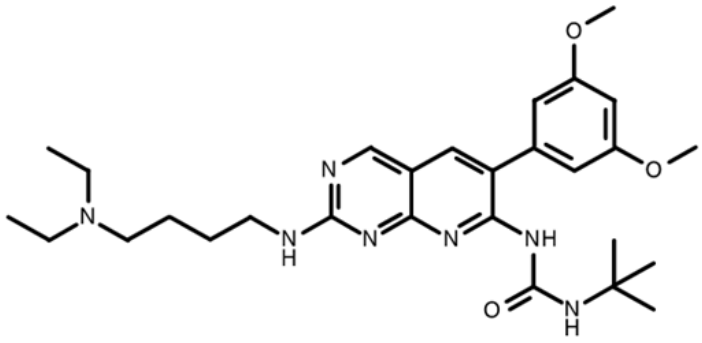

PD173074 PD0325901

Figure 5.6: The structure of the FGFR inhibitor PD173074 (Left) and the MEK inhibitor PD0325901 (Right).

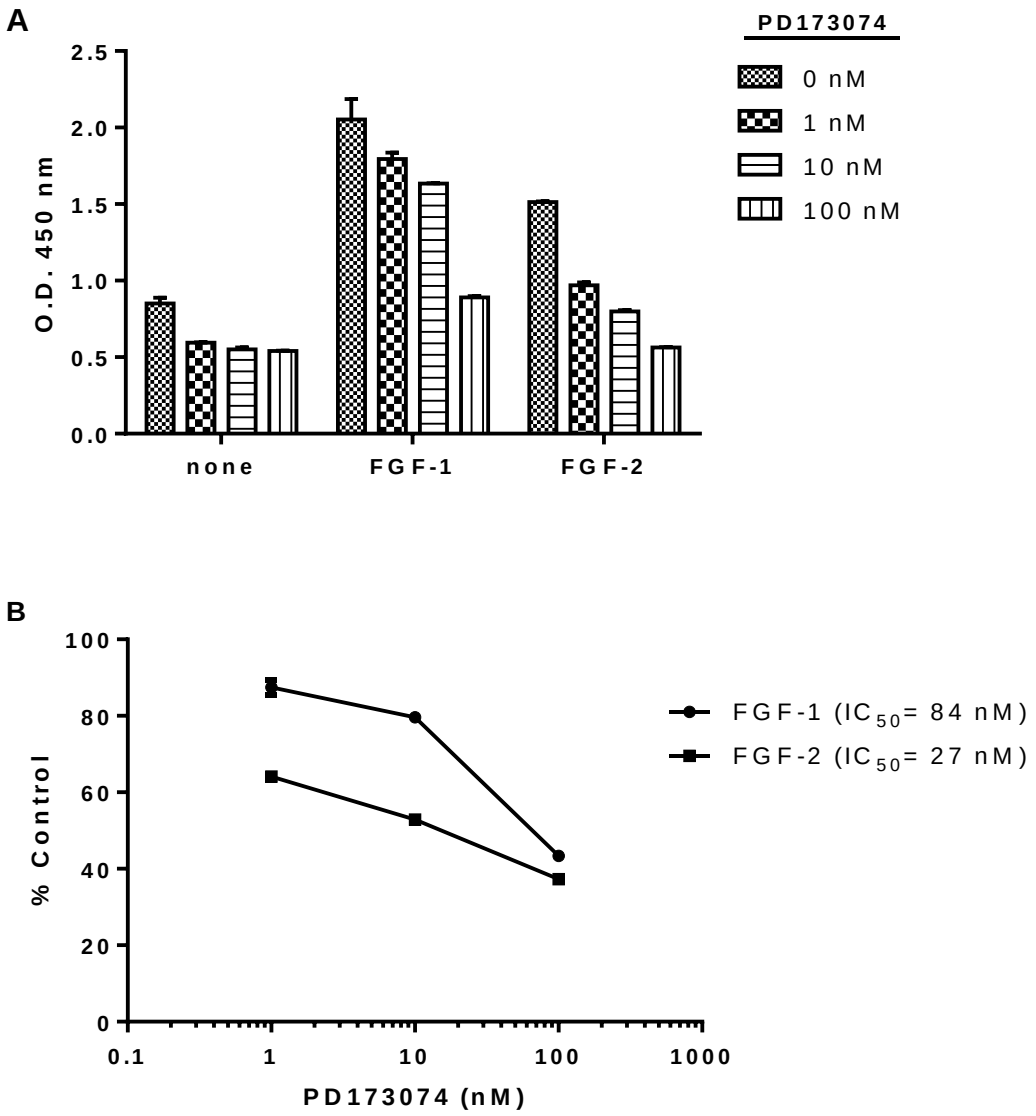

Figure 5.7: Characterisation of p-ERK stimulation in SNU-182 cells in response to FGF-1 and FGF-2 and inhibition by PD173074: SNU-182 cells were serum-starved overnight and treated with different concentrations of PD173074 for 1 hr followed by stimulation with 10 nM of FGF-1 or FGF-2 for 10 min. Cell lysates were prepared and the p-ERK ELISA was performed using 50 µg cell lysate/well. **(A)** Raw data. Values are the mean of triplicates and error bars represent the standard error. **(B)** Data expressed as a percentage of FGF-1- or FGF-2-stimulated PD173074-untreated cells. The experiment was performed in triplicate. Data generated using the method described in Section 2.16.

5.3. Knockdown of SULF1/2 Genes and Effects on Signalling, Cell Growth and Tumourigenicity

To study the biology of SULF1/2 in HCC cell lines, SULF1 and SULF2 were knocked down using shRNA and the subsequent signalling and phenotypic consequences examined. SULF2 suppression can also serve as a positive control or surrogate for SULF2 inhibition using small molecule inhibitors, providing a means of exploring the consequences of inhibition of SULF2 over SULF1 and other sulfatases.

5.3.1. Identification of the optimal shRNA sequence to induce gene silencing

To identify the optimal shRNA sequence to suppress SULF2 expression, HuH-7 cells were used as they endogenously express high level of SULF2 that is also enzymatically active (Chapter 3). Non-targeting shRNA (NT shRNA) (containing four base pair mismatches to any known human gene) or five commercially available clones of SULF2-targeting shRNA lentiviral particles each containing a different shRNA sequence (Table 2.2) were either transiently or stably transduced at different multiplicities of infection (MOIs). All shRNAs were constitutively expressed under the U6 promoter. MOI is defined as the number of lentiviral particles per cell. The MOI was optimised for stable transduction at 0.5 as using a higher MOI caused detrimental effects on infected cells including increased cell death and inability of remaining viable cells to proliferate. This effect could be due to the multiple integration sites per cell at high MOI which could lead to the insertion of the construct within the coding sequences of important genes and hence disruption of their functions.

RNA was extracted after 24 or 48 hrs for transient transduction, or after selection with puromycin until all control untransduced cells were killed for stable transduction. SULF2 expression was quantified using RT-qPCR. The analysis showed that shRNA sequence TRCN0000364518 (S2.shRNA_18) caused the greatest SULF2 gene silencing compared to NT shRNA after either transient or stable transduction (Figure 5.8).

To test the specificity of SULF2 knockdown, the expression levels of B2M, TP53 and KLF6 were analysed after stable SULF2 knockdown in HuH-7 cells using S2.shRNA_18. The RT-qPCR data showed marked suppression of SULF2 expression in the S2.shRNA_18-transduced cells (97% decrease versus NT shRNA-transduced cells) with no effect on the mRNA levels of B2M, TP53 or KLF6 (Figure 5.9). SULF1 mRNA level remained undetectable in HuH-7 cells after SULF2 knockdown as in control cells. The specificity and consistency of SULF2 targeting was also confirmed by knockdown of SULF2 using S2.shRNA_18 in HepG2 cells (Figure 5.10) that do not express SULF1 and in SNU-182 cells (Figure 5.11) that endogenously express both SULF1 and SULF2. Importantly, the results showed no effect on SULF1 expression in SNU-182 cells after SULF2 gene silencing. Collectively, the data of SULF2 gene silencing in the three cell lines tested showed the lack of any stimulation of the expression of SULF1 in response to the loss of SULF2.

A similar procedure was followed to identify the optimal SULF1-targeting shRNA. The SNU-182 cell line was used for this purpose as it was the only HCC cell line that expressed a high level of SULF1. The results showed that shRNA sequence TRCN0000373589 (S1.shRNA_89) caused the greatest gene silencing of SULF1 after transient or stable transduction (Figure 5.12) without affecting the expression level of four other genes including SULF2 (Figure 5.13). The non-targeting (NT) shRNA caused a slight upregulation of SULF2 expression in HuH-7 (Figure 5.9) and HepG2 cells (Figure 5.10), but not in SNU-182 cells (Figure 5.11) (Figure 5.13). Expression levels of all other genes tested were unchanged in NT shRNA cells relative to control untransduced cells in all tested cell lines (Figure 5.9) (Figure 5.10) (Figure 5.11) (Figure 5.13). S2.shRNA_18 and S1.shRNA_89 were used in all subsequent experiments and these are referred to as SULF2 shRNA and SULF1 shRNA, respectively, throughout the rest of the thesis. All resulting stable cell lines which constitutively expressed SULF2 shRNA and SULF1 shRNA were analysed for the downstream consequences of SULF1 or SULF2 gene silencing. The effect of gene silencing on cell functionality was tested using different phenotypic and mechanistic assays according to the cascade shown in Figure 5.144.

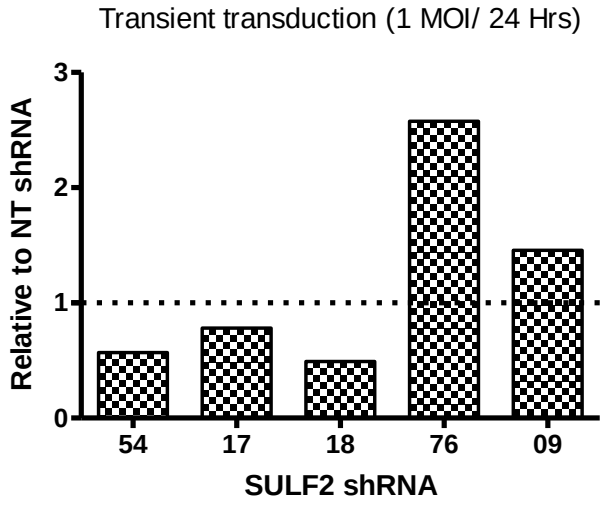
Transient transduction (1 MOI/ 24 Hrs)
Relative to NT shRNA
3
2
1
0
54
17
18
76
09
SULF2 shRNA

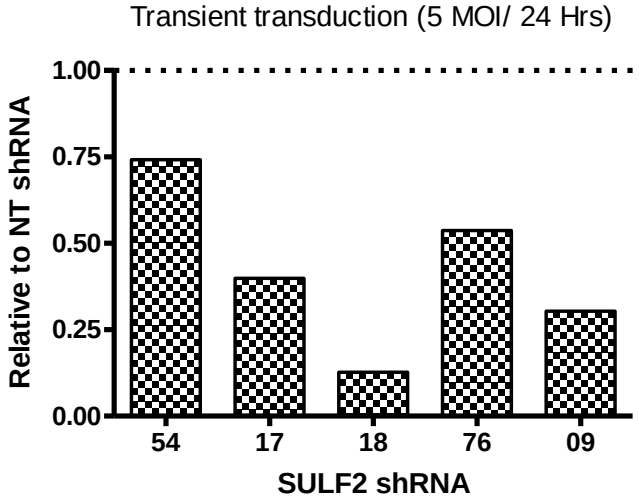
Transient transduction (5 MOI/ 24 Hrs)
Relative to NT shRNA
1.00
0.75
0.50
0.25
0.00
54
17
18
76
09
SULF2 shRNA

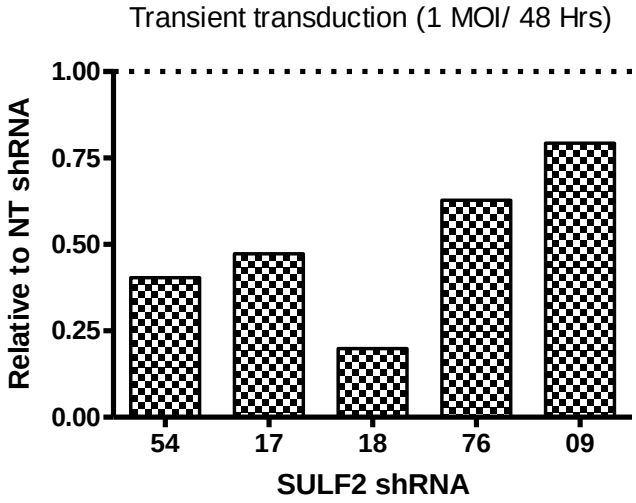
Transient transduction (1 MOI/ 48 Hrs)
Relative to NT shRNA
1.00
0.75
0.50
0.25
0.00
54
17
18
76
09
SULF2 shRNA

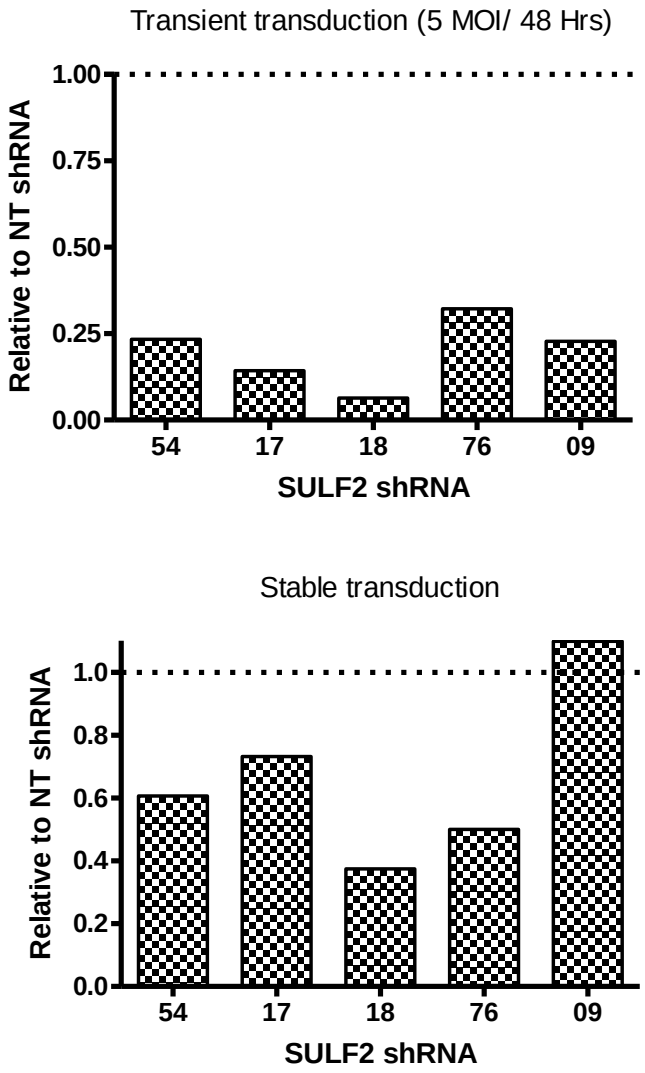

Figure 5.8: Identification of the optimal SULF2-targeting shRNA: HuH-7 cells were transiently transduced with 1 or 5 MOI for 24 or 48 hrs or stably transduced with different SULF2 targeting shRNA lentiviral particles or NT shRNA lentiviral particles. RT-qPCR was performed and the data normalized to the expression of GAPDH and presented relative to the SULF2 mRNA expression level in cells transduced with NT shRNA. Data are from a single experiment. Data generated using the methods described in Section 2.6 and Section 2.7.

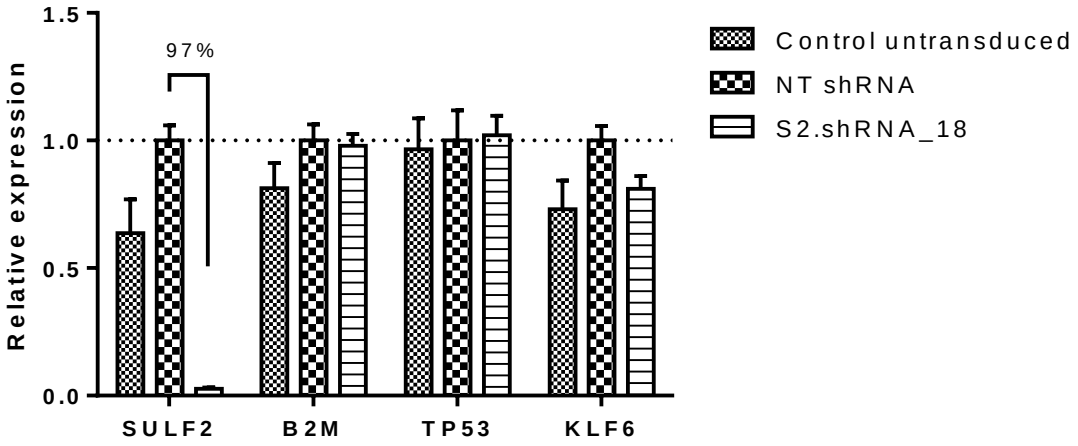

Figure 5.9: Effect of SULF2 gene silencing on the expression of selected genes in the HuH-7 cell line: HuH-7 cells were stably transduced with either S2.shRNA_18 or NT shRNA lentiviral particles. RT-qPCR was performed and the data normalized to the expression of GAPDH. Values are the mean of triplicates and error bars represent the standard error. The experiment was performed in triplicate. Data generated using the methods described in Section 2.6 and Section 2.7.

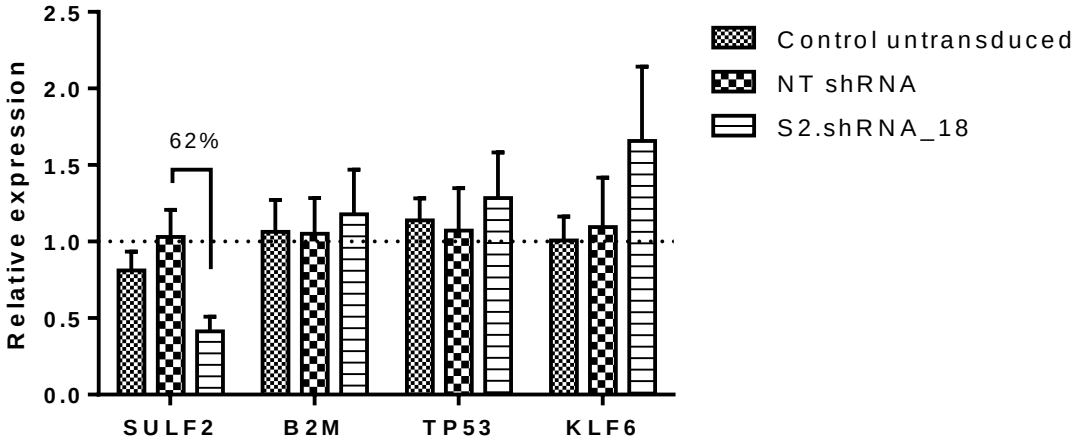

Figure 5.10: Effect of SULF2 gene silencing on the expression of selected genes in the HepG2 cell line: HepG2 cells were stably transduced with either S2.shRNA_18 or NT shRNA lentiviral particles. RT-qPCR was performed and the data normalized to the expression of GAPDH. Values are the mean of triplicates and error bars represent the standard error. The experiment was performed in duplicate. Data generated using the methods described in Section 2.6 and Section 2.7.

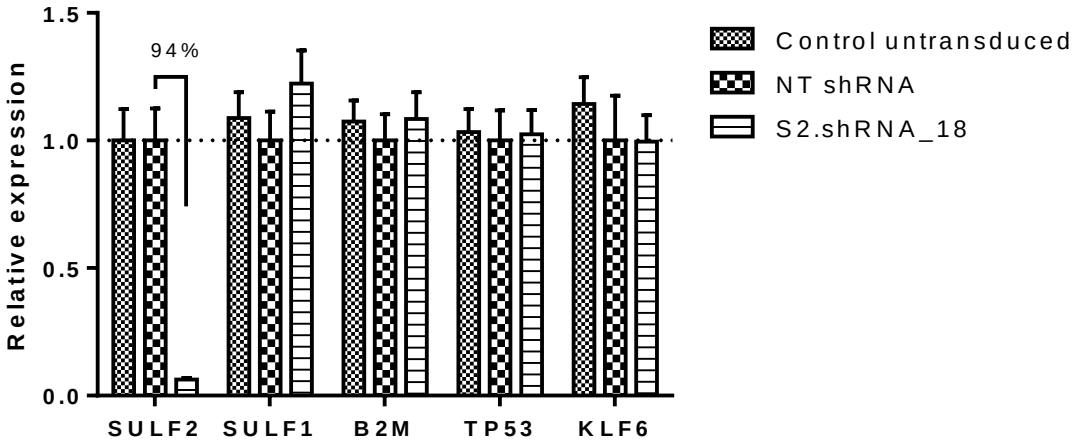

Figure 5.11: Effect of SULF2 gene silencing on the expression of selected genes in the SNU-182 cell line: SNU-182 cells were stably transduced with either S2.shRNA_18 or NT shRNA lentiviral particles. RT-qPCR was performed and the data normalized to the expression of GAPDH. Values are the mean of triplicates and error bars represent the standard error. The experiment was performed in duplicate. Data generated using the methods described in Section 2.6 and Section 2.7.

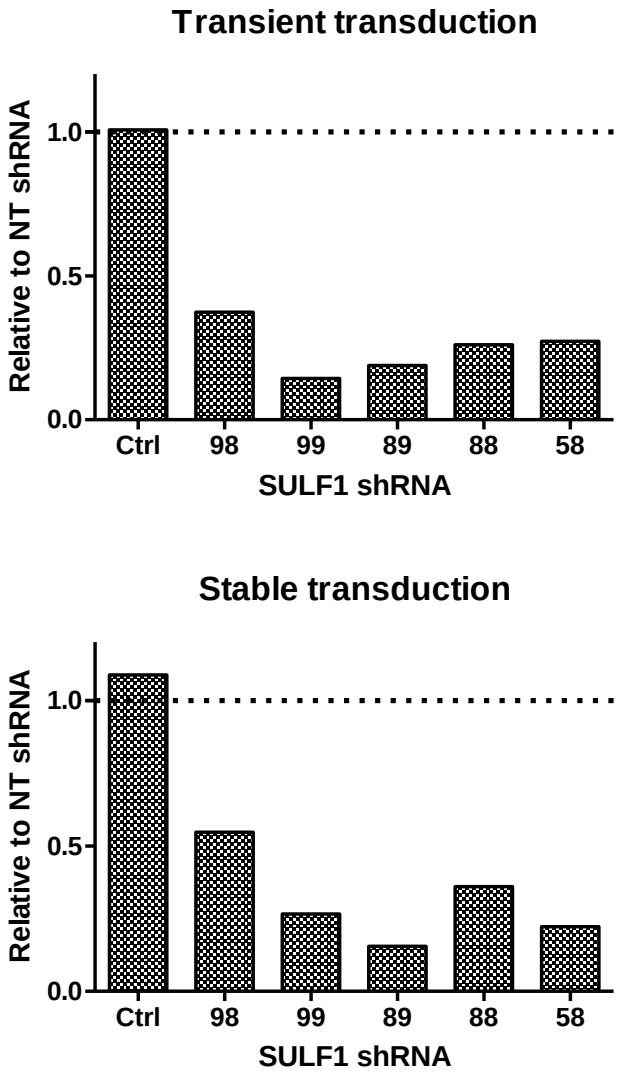

Figure 5.12: Identification of the optimal SULF1-targeting shRNA: SNU-182 cells were transiently transduced with 1 MOI for 48 hrs or stably transduced with different SULF1 targeting shRNA lentiviral particles or NT shRNA lentiviral particles. RT-qPCR was performed and the data normalized to the expression of GAPDH and presented relative to the SULF2 mRNA expression level in cells transduced with NT shRNA. Ctrl: control untransduced cells. Data are from a single experiment. Data generated using the methods described in Section 2.6 and Section 2.7.

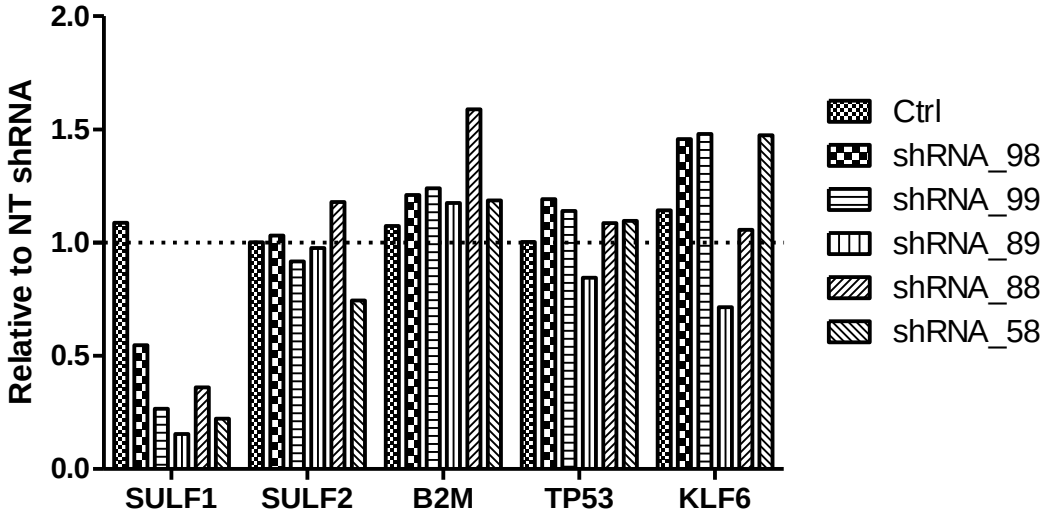

Figure 5.13: Effect of SULF1 gene silencing on the expression of selected genes in the SNU-182 cell line: SNU-182 cells were stably transduced with different SULF1 targeting shRNA lentiviral particles or NT shRNA lentiviral particles. RT-qPCR was performed and the data normalized to the expression of GAPDH and presented relative to the expression level in cells transduced with NT shRNA. Ctrl: control untransduced cells. Data are from a single experiment. Data generated using the methods described in Section 2.6 and Section 2.7.

Figure 5.14: SULF1/2 knockdown evaluation cascade (each assay was repeated at least 3 times)

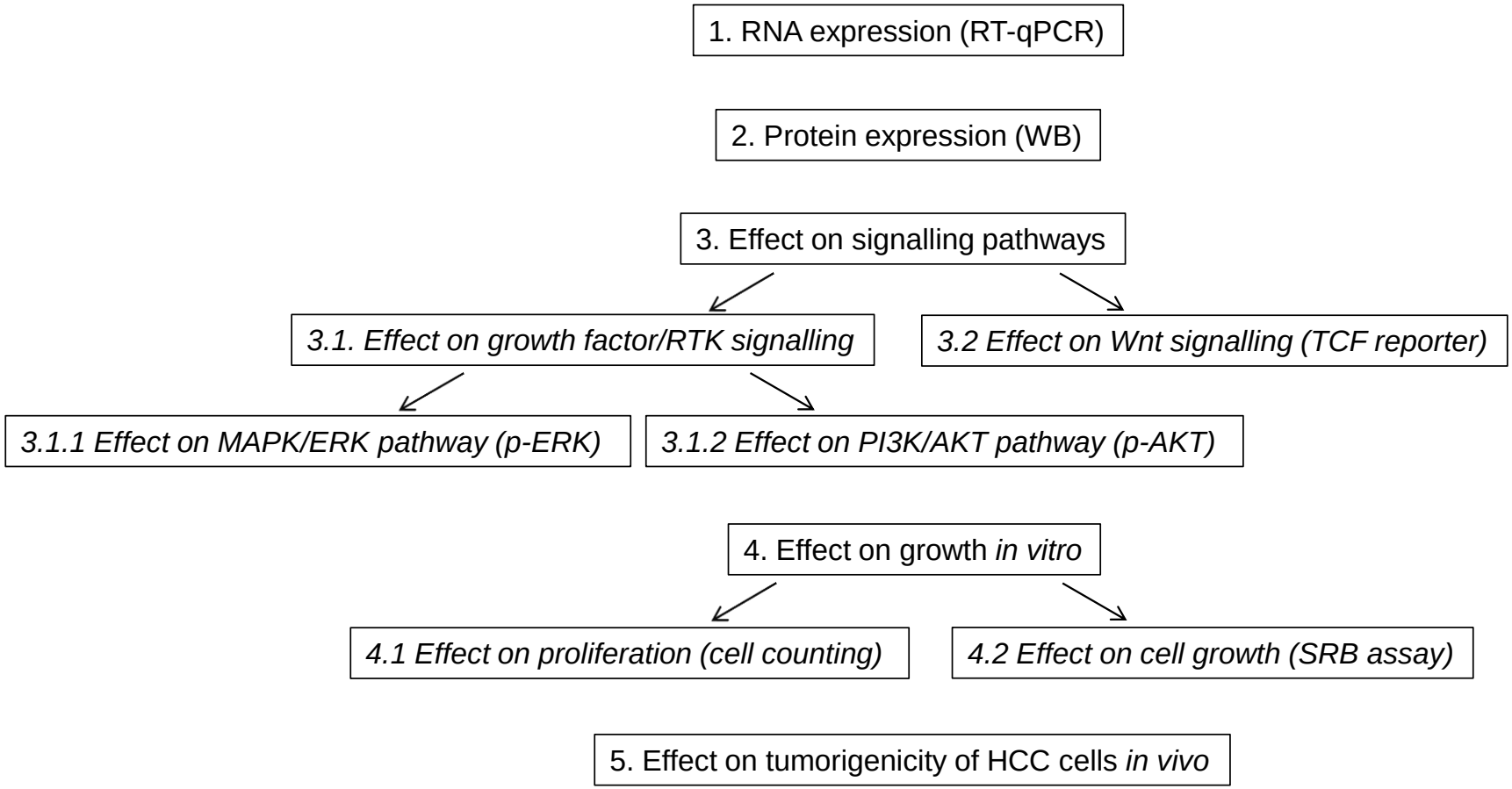

5.3.2. SULF2 gene silencing in HuH-7 cells and effects on signalling, cell growth and tumourigenicity

5.3.2.1. Effects of SULF2 gene silencing on signalling pathways in HuH-7 cells

5.3.2.1.1. Effect of SULF2 gene silencing on growth factor/RTK signalling in HuH-7 cells

HuH-7 cells that were stably transduced with NT shRNA or SULF2 shRNA (Figure 5.9) were serum-starved overnight and then stimulated with different concentrations of FGF-1, FGF-2 or IGF-I for 10 or 60 min. The cell lysates were extracted and WB was performed with antibodies against SULF2, p-ERK and p-AKT. WB membranes were then stripped and re-probed using total ERK and total AKT antibodies to serve as loading controls. WB showed expression of SULF2 protein in the NT shRNA-transduced cells but complete absence of SULF2 protein in the cells transduced with SULF2 shRNA, confirming the knockdown of SULF2 at the protein level in this cell line (Figure 5.15).

Both FGF-1- and FGF-2-stimulated p-ERK and p-AKT, while IGF-I stimulated p-AKT but not p-ERK in this cell line. Stimulation of p-ERK and p-AKT was concentration-dependent for all three ligands; however, no clear effect of SULF2 gene silencing was found on basal or stimulated ERK or AKT phosphorylation with any of the tested ligands after either 10 min (Figure 5.15) or 60 min (data not shown). The effect of SULF2 knockdown on IGF-II-stimulated ERK and AKT phosphorylation was also tested in this cell line and no clear effect was detected (data not shown).

A

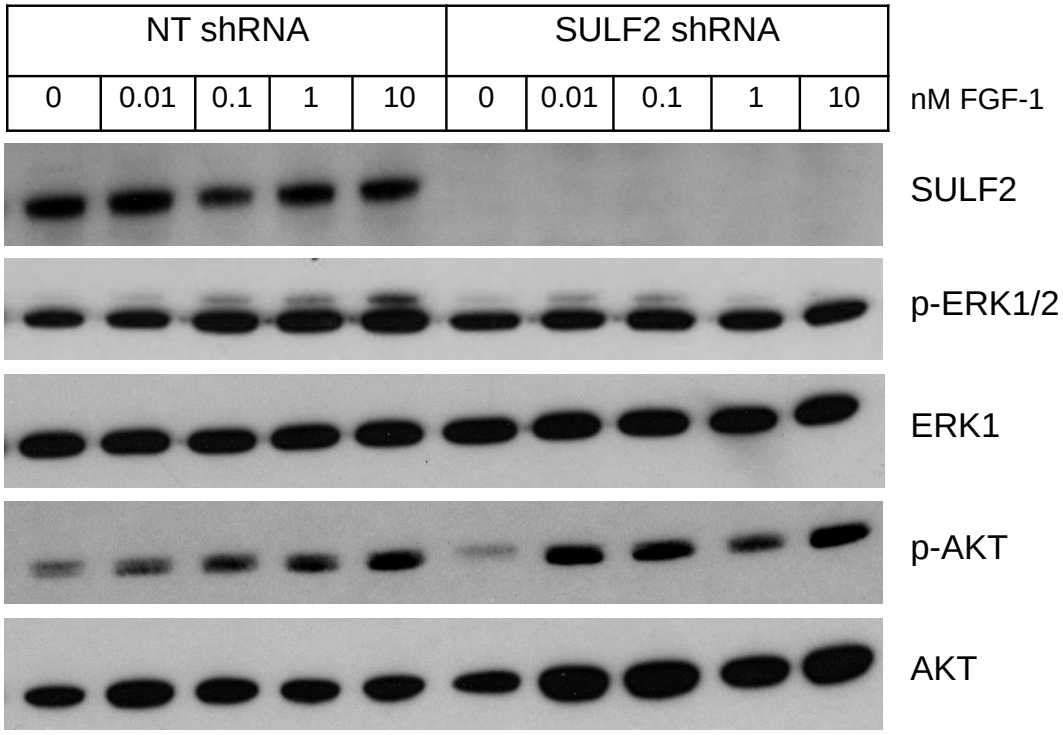
NT shRNA
SULF2 shRNA
0
0.01
0.1
1
10
0
0.01
0.1
1
10
nM FGF-1
SULF2
p-ERK1/2
ERK1
p-AKT
AKT

B

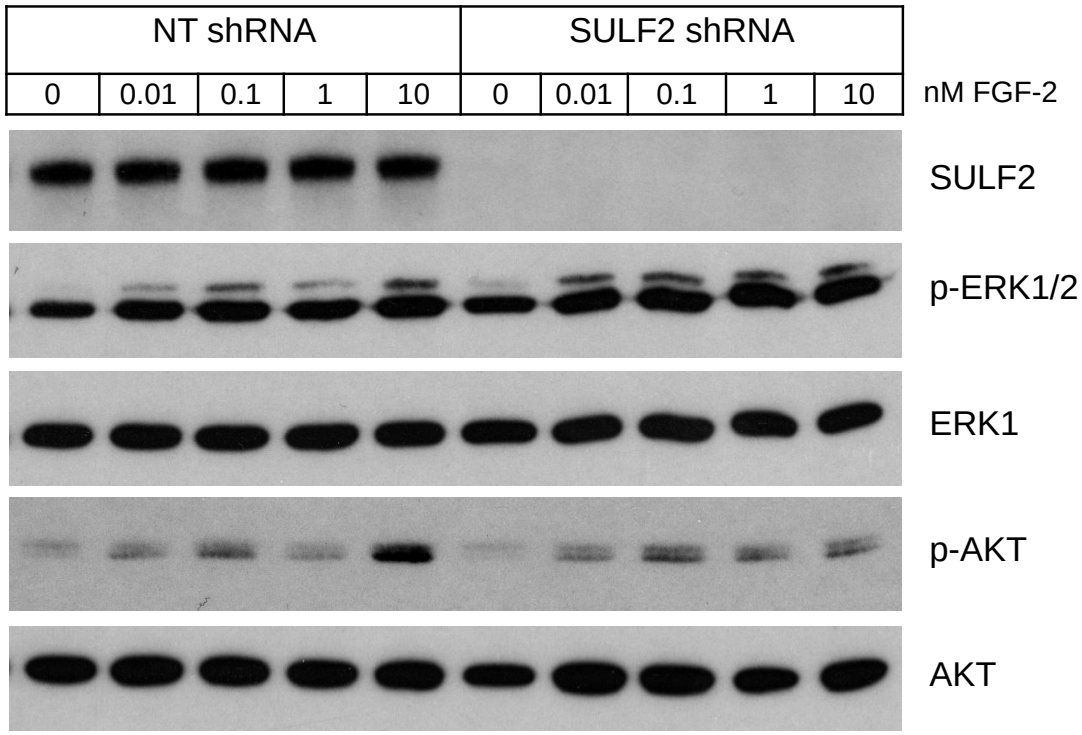
NT shRNA
SULF2 shRNA
0
0.01
0.1
1
10
0
0.01
0.1
1
10
nM FGF-2
SULF2
p-ERK1/2
ERK1
p-AKT
AKT

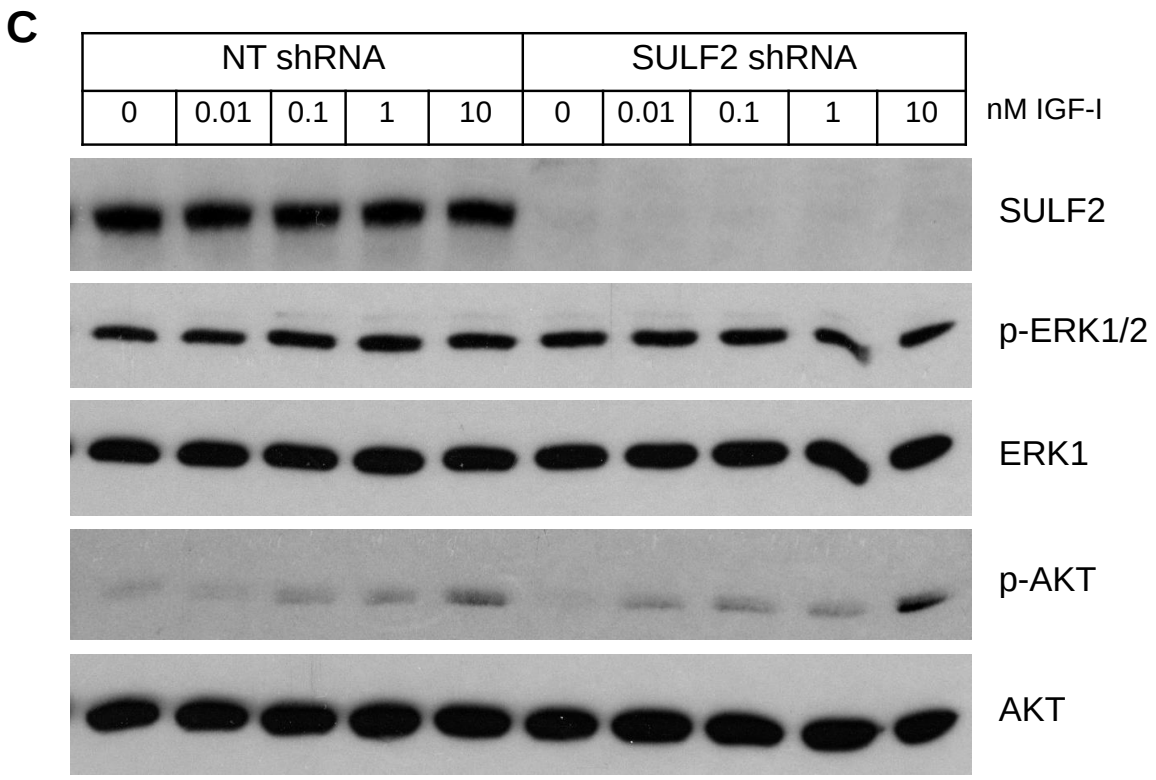

Figure 5.15: Effect of SULF2 gene silencing on FGF-1, FGF-2 and IGF-I signalling pathways in the HuH-7 cell line: HuH-7 cells were stably transduced with either NT shRNA or SULF2 shRNA lentiviral particles. The cells were serum-starved overnight and then treated with different concentrations of FGF-1 **(A)**, FGF-2 **(B)** or IGF-I **(C)** for 10 min. Whole cell lysates were prepared and WB was performed using antibodies against SULF2, p-ERK1/2 and p-AKT. The membranes were stripped and reprobed with antibodies against total ERK1/2 and total AKT serving as loading controls. The experiment was performed in triplicate and representative blots are shown. Data generated using the methods described in Section 2.6 and Section 2.10.

5.3.2.1.2. Effect of SULF2 gene silencing on Wnt signalling in HuH-7 cells

To study the effect of SULF2 gene silencing on Wnt signalling, HuH-7 cells stably transduced with NT shRNA or SULF2 shRNA (Figure 5.9) were transiently co-transfected with TOPflash and β-galactosidase constructs, and then stimulated with 100 ng/ml Wnt-3a for 6 hours. The cell lysates were extracted and the TOPflash luciferase activity was measured and normalized to the activity of β-galactosidase. The results showed that SULF2 gene silencing in this cell line caused a marked inhibition of Wnt-3a-induced β-catenin-dependent transcriptional activity (50% decrease and *p* value = 0.027, Figure 5.16).

Effect of SULF2 knockdown on Wnt signalling was confirmed by infecting the cells transduced with NT shRNA or SULF2 shRNA with the 7TFP lentiviral particles. The cells were treated with different concentrations of Wnt-3a for 6 hrs and the results showed marked inhibition of Wnt-3a-induced luciferase activity in the SULF2 knockdown cells (Figure 5.17; A). The Dvl-PDZ domain inhibitor II, compound 3289-8625, was used as positive control for inhibition. Incubation of the cells with 3289-8625 before treatment with 100 ng/ml Wnt-3a showed complete inhibition of luciferase activity (Figure 5.17; A).

To determine whether the effect of SULF2 knockdown on Wnt signalling was due to interfering with Wnt-3a ligand binding at the cell surface or downstream of the FZD/LRP receptors, the NT shRNA- and SULF2 shRNA-transduced cells were treated with BIO which inhibits GSK-3β, and hence activates Wnt signalling downstream of Wnt ligand receptor activation. The results showed that there was slight decrease of BIO-stimulated luciferase activity in the SULF2 knockdown cells (Figure 5.17; B), but much less than the decrease in Wnt3a-stimulated luciferase activity. This result suggests that SULF2 suppression led to reduced Wnt signalling predominantly by affecting Wnt-3a binding at the cell surface.

In an attempt to confirm the effect of SULF2 knockdown on Wnt signalling by another method, the level of total β-catenin was measured by sandwich ELISA both before and after stimulation with Wnt-3a for 24 hours, allowing enough time for the degradation of β-catenin. The results showed no change in the level of total β-catenin after SULF2 suppression (Figure 5.18; A). The lack of effect was possibly due to the high level of β-catenin that is present at the cell membrane in HuH-7 cells, where it has a role in cell-cell adhesion (Sangkhathat et al., 2006), masking changes in cytoplasmic/nuclear β-catenin. This hypothesis was confirmed by ICC, which showed that the majority of total β-catenin staining was at the cell surface with no detectable translocation of β-catenin to the nucleus after treatment with Wnt-3a in this cell line notwithstanding the changes in TCF reporter gene activity (Figure 5.19).

Therefore, the level of active β-catenin (ABC) was investigated by WB. WB showed that the increase in ABC levels in the NT shRNA-transduced cells was much higher

than that in the SULF2 shRNA-transduced cells after treatment with Wnt-3a for either 6 or 24 hrs (Figure 5.18; B). Unfortunately, the ABC antibody did not work for ICC or ELISA so it was not possible to visualize the cells or use ELISA to quantify the changes.

SULF2 knockdown in HuH-7 cells showed lack of an effect on the expression level of CCND1 and MYC, which are transcriptional targets of β-catenin-TCF complex, or on the expression of GPC3 (data not shown), which was previously reported to be affected by SULF2 gene silencing and to be required by Wnt signalling (Lai et al., 2008 a). However, signalling pathways other than Wnt signalling can regulate CCND1 and MYC, including the MAPK/ERK and PI3K/AKT signalling pathways, and these may have compensated for reduced Wnt signalling in the HuH-7 cells.

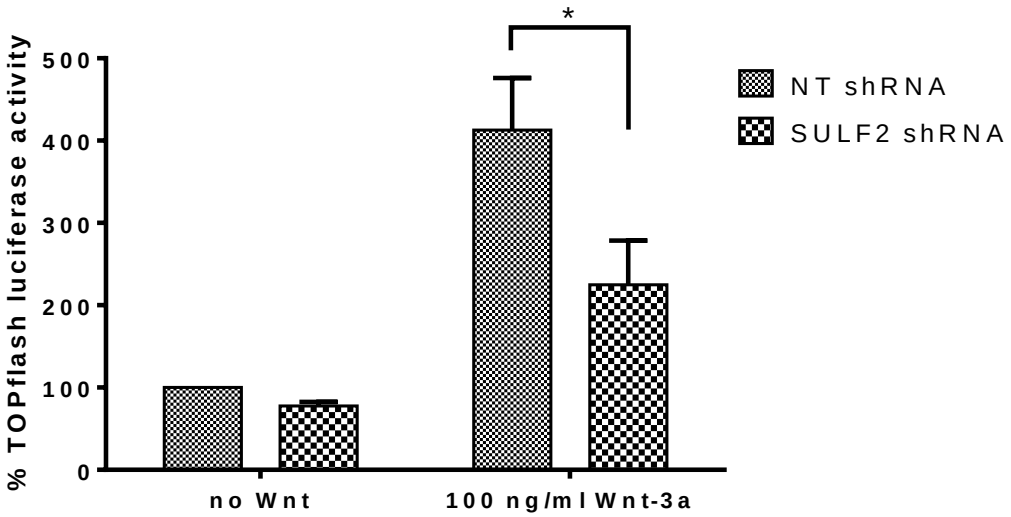

Figure 5.16: Effect of SULF2 gene silencing on Wnt signalling pathway in HuH-7 cells measured by the TOPflash reporter assay: HuH-7 cells were stably transduced with either NT shRNA or SULF2 shRNA lentiviral particles. The cells were then transiently co-transfected with TOPflash and β-galactosidase constructs in Opti-MEM medium followed by treatment with 100 ng/ml Wnt-3a for 6 hours. Whole cell lysates were prepared using RLB and luciferase activity was measured. Values are the mean of four different experiments and error bars represent the standard error. * p = 0.027, 2-sample t-test. Data generated using the methods described in Section 2.6 and Section 2.15.

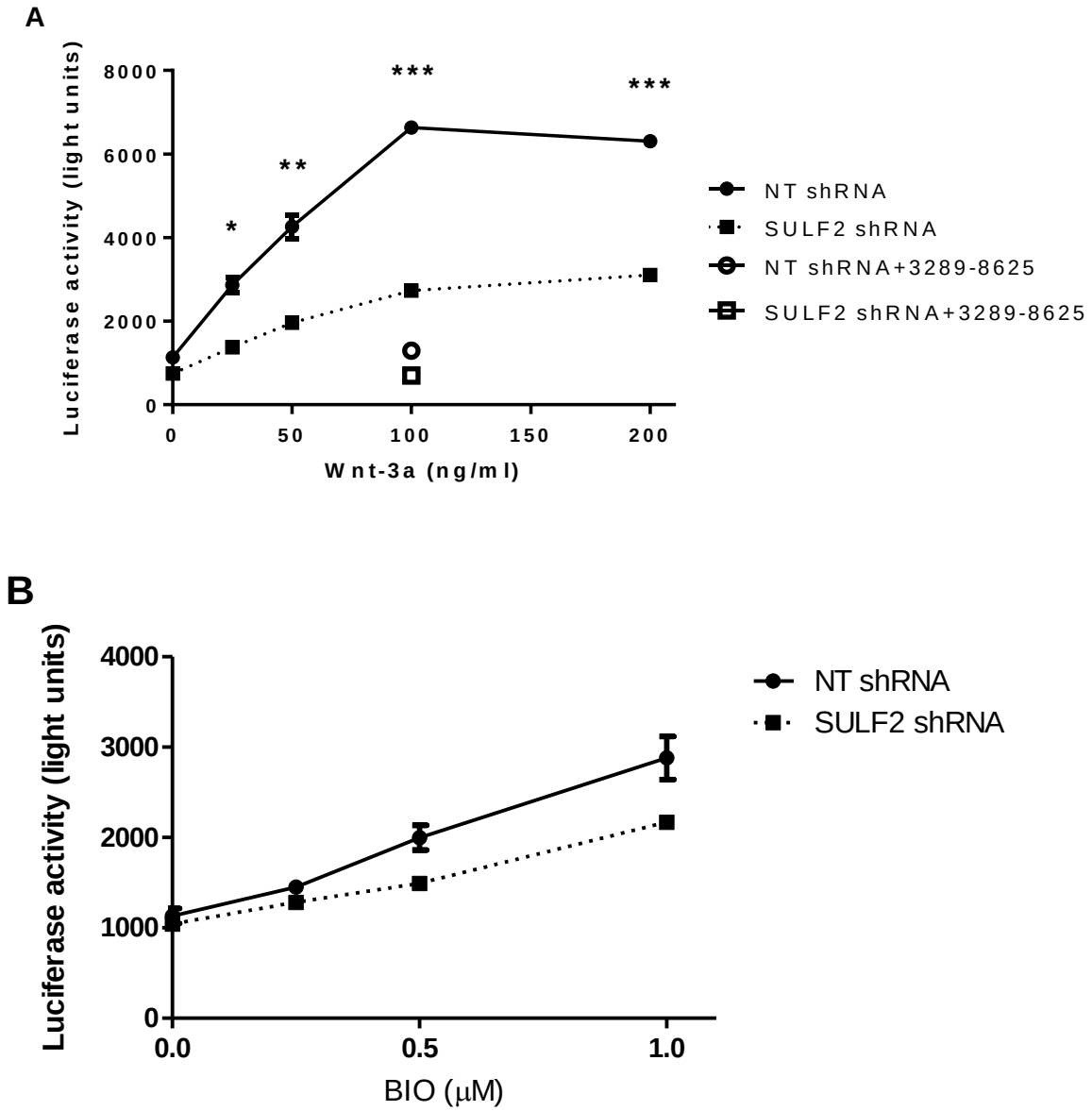

Figure 5.17: Effect of SULF2 gene silencing on Wnt signalling pathway in HuH-7 cells measured by the 7TFP reporter assay: HuH-7 cells were stably transduced with either NT shRNA or SULF2 shRNA lentiviral particles followed by transduction with 7TFP lentiviral particles. The cells were serum-starved overnight and then treated with different concentrations of Wnt-3a **(A)** or BIO **(B)** for 6 hours. ONE-Glo reagent was added and luciferase activity was measured. Values are the mean of triplicates and error bars represent the standard error. The experiment was performed in triplicate. * $p = 0.004$, ** $p = 0.001$, *** $p < 0.0001$, 2-sample t-test. Data generated using the methods described in Section 2.6 and Section 2.15.

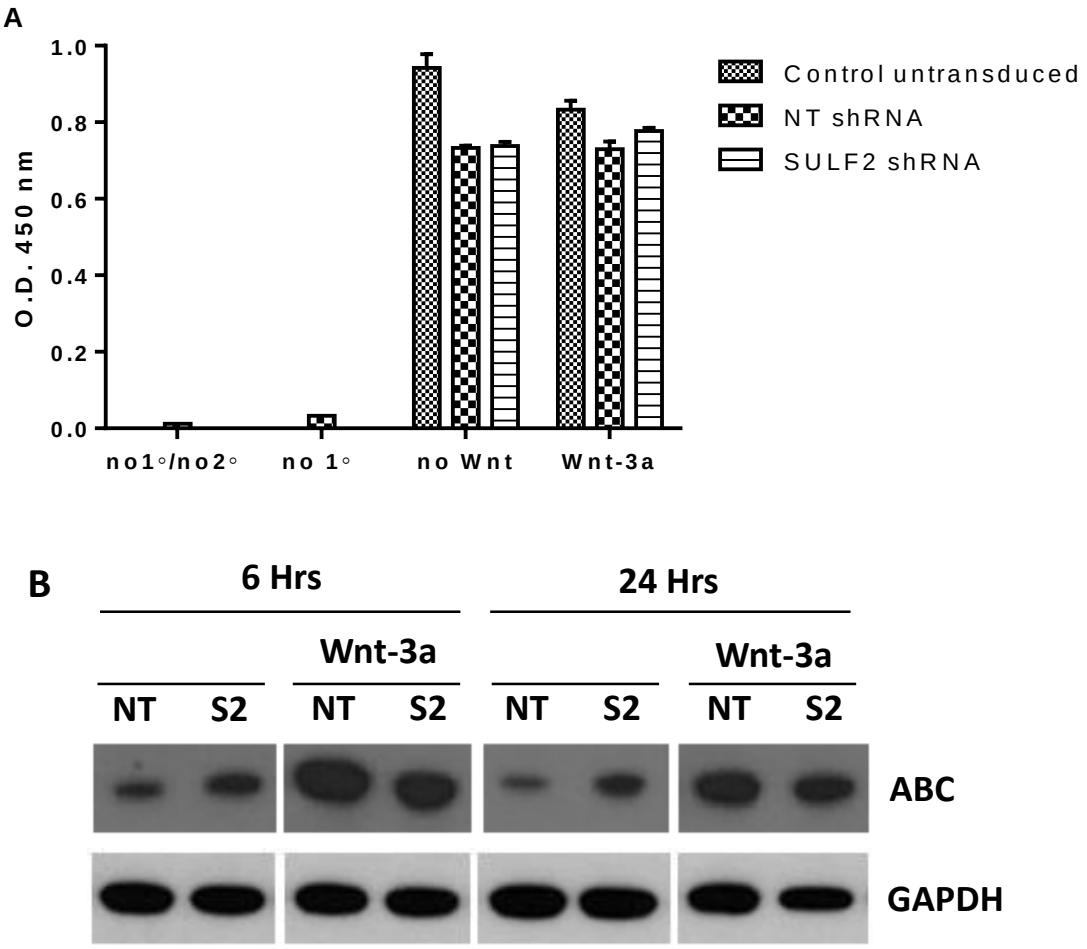

Figure 5.18: Effect of SULF2 knockdown on total β-catenin and ABC levels in HuH-7 cells: Control untransduced HuH-7 cells or those stably transduced with either NT shRNA or SULF2 shRNA lentiviral particles were serum-starved overnight and then treated with 100 ng/ml Wnt-3a for 6 or 24 hours. Cell lysates were prepared. **(A)** Total β-catenin ELISA was performed after treatment of cells with Wnt-3a for 24 hours. No1^{o}/no2^{o}: detection and secondary antibodies omitted. No 1^{o}: detection antibody omitted. Values are the mean of triplicates and error bars represent the standard error. **(B)** WB was performed using an ABC antibody. GAPDH was used as loading control. NT: NT shRNA-transduced cells. S2: SULF2 shRNA-transduced cells. The experiment was performed in duplicate. Data generated using the methods described in Section 2.10 and Section 2.16.

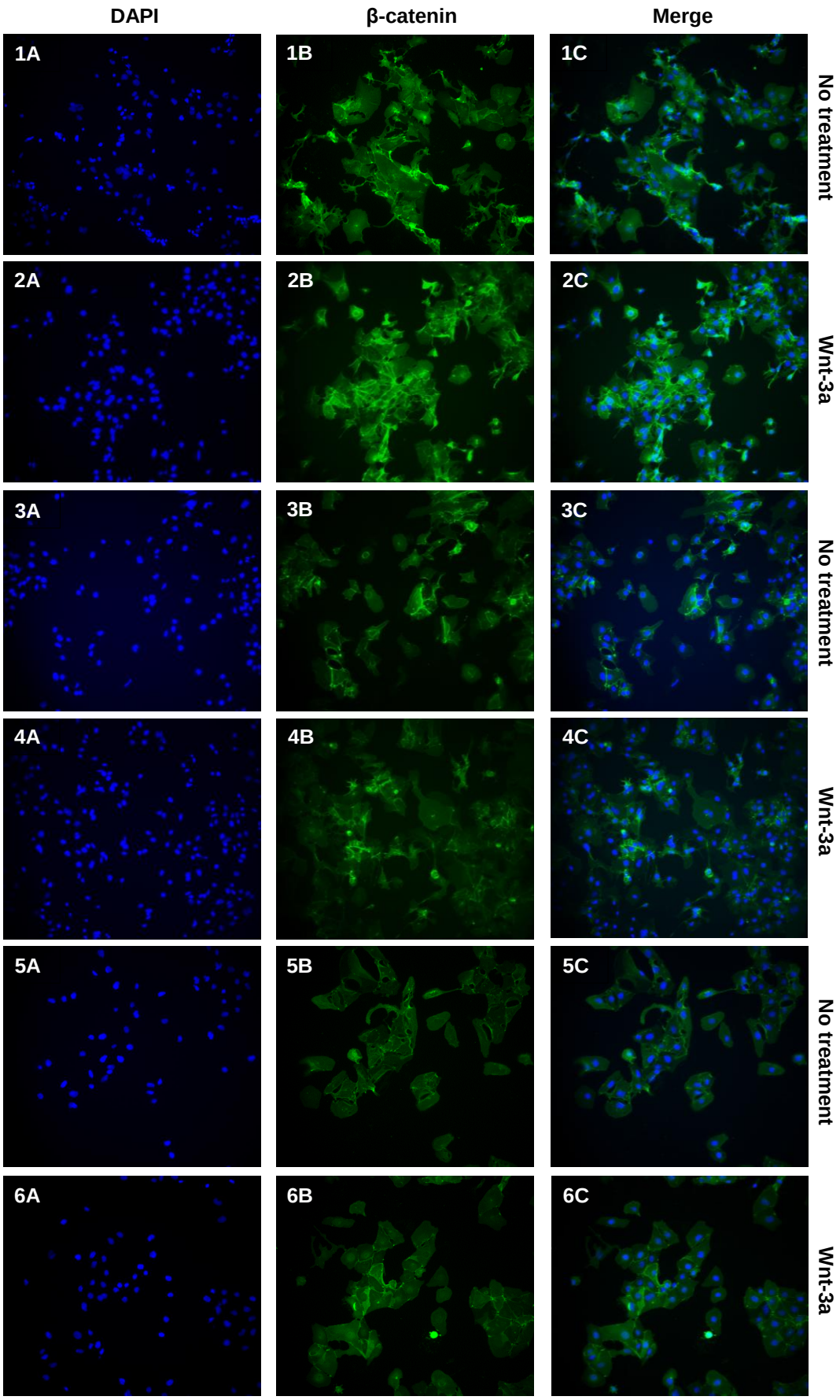
DAPI
β-catenin
Merge
1A
1B
1C
No treatment
2A
2B
2C
Wnt-3a
3A
3B
3C
No treatment
4A
4B
4C
Wnt-3a
5A
5B
5C
No treatment
6A
6B
6C
Wnt-3a

Figure 5.19: ICC staining of β-catenin in the HuH-7 cell line: Control untransduced HuH-7 cells or those stably transduced with either NT shRNA or SULF2 shRNA lentiviral particles were grown on glass coverslips and serum-starved overnight followed by treatment with or without 100 ng/ml Wnt-3a for 24 hours. The cells were incubated with total β-catenin antibody and then incubated with Alexa Fluor 488 conjugated secondary antibody. Mounting medium with DAPI was used to counter-stain the nuclei in blue. 1, 2: control untransduced cells. 3, 4: NT shRNA-transduced cells. 5, 6: SULF2 shRNA-transduced cells. **(A)** blue channel for DAPI, **(B)** green channel for Alexa Fluor 488, **(C)** merge picture. The experiment was performed in duplicate. Data generated using the method described in Section 2.11.

5.3.2.2. Effects of SULF2 gene silencing on growth of HuH-7 cells *in vitro*

To determine the effect of SULF2 knockdown and consequent Wnt signalling suppression on cell growth and proliferation, HuH-7 cells that were stably transduced with NT shRNA or SULF2 shRNA (Figure 5.9) were cultured in a 96-well plate and cell proliferation was evaluated by cell counting and measuring cellular protein content using sulforhodamine B (SRB) assay. The results showed that SULF2 suppression significantly inhibited the proliferation of HuH-7 cells as evidenced by a doubling time of 58 hours as opposed to 43 hours for both control untransduced and NT shRNA-transduced cells (Figure 5.20).

The effect of exogenous Wnt-3a on the growth of control untransduced and NT shRNA- and SULF2 shRNA-transduced HuH-7 cells was then investigated. The cells were cultured in 10% (v/v) FBS-containing medium due to the detrimental effect of the lack of FBS on the growth of HuH-7 cells. The SRB assay showed no effect of either Wnt-3a or BIO on cell growth of any of the three HuH-7 tested cell lines where BIO was used as a positive control for stimulation of Wnt signalling (Figure 5.21; A, B). The lack of an effect of Wnt-3a or BIO on cell growth could be due to the presence of growth factors in the FBS masking any stimulation resulting from the exogenous Wnt-3a. On the other hand, treating the cells with the Wnt signalling inhibitor, compound 3289-8625 completely inhibited the growth of all three HuH-7 cell lines (Figure 5.21; C). Inhibition of growth by 3289-8625 was partially rescued by the addition of BIO, but not Wnt-3a (Figure 5.21; D, E), presumably because compound 3289-8625 works downstream of Wnt-3a binding

to its receptors but not downstream of BIO-mediated inhibition of GSK-3β. Interestingly, and consistent with the proposed role of SULF2 in Wnt signalling, the BIO-rescued cells showed similar growth rates regardless of SULF2 expression status. Overall, these data suggest that Wnt signalling is involved in regulating the growth of HuH-7 cells, and that SULF2 has a role in controlling Wnt-3a binding at the cell surface.

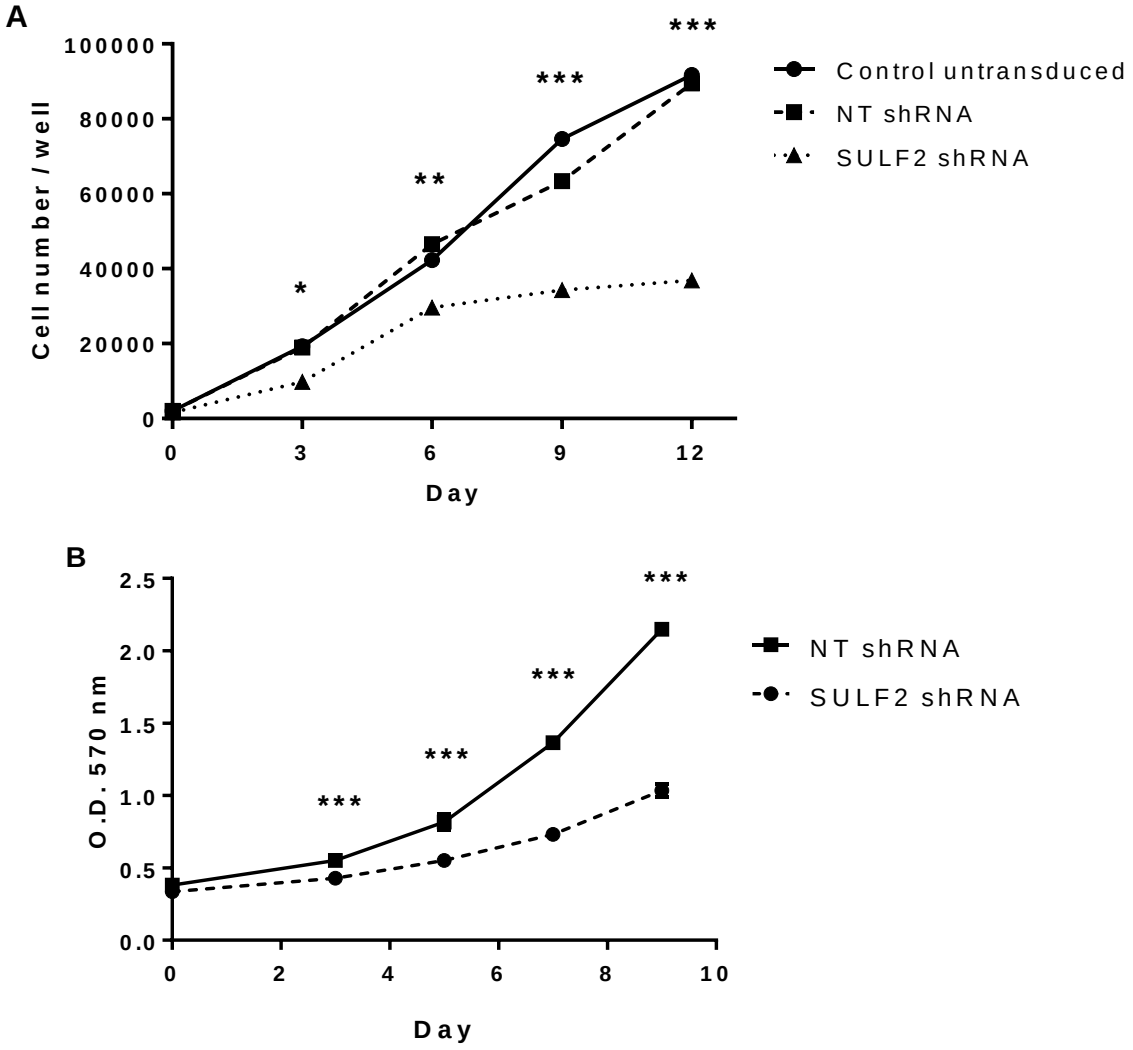

Figure 5.20: Effect of SULF2 gene silencing on cell growth and proliferation in HuH-7 cells: HuH-7 cells were stably transduced with either NT shRNA or SULF2 shRNA lentiviral particles. 2,000 cells were seeded per well for different time points and then either counted **(A)** or stained with SRB **(B)**. Values are the mean of triplicates for (A) and six replicates for (B) and error bars represent the standard error. The experiment was performed in quadruplicate. * $p = 0.002$, ** $p = 0.001$, *** p value < 0.0001, one-way ANOVA for (A) and 2-sample t-test for (B). Data generated using the methods described in Section 2.17 and Section 2.18.

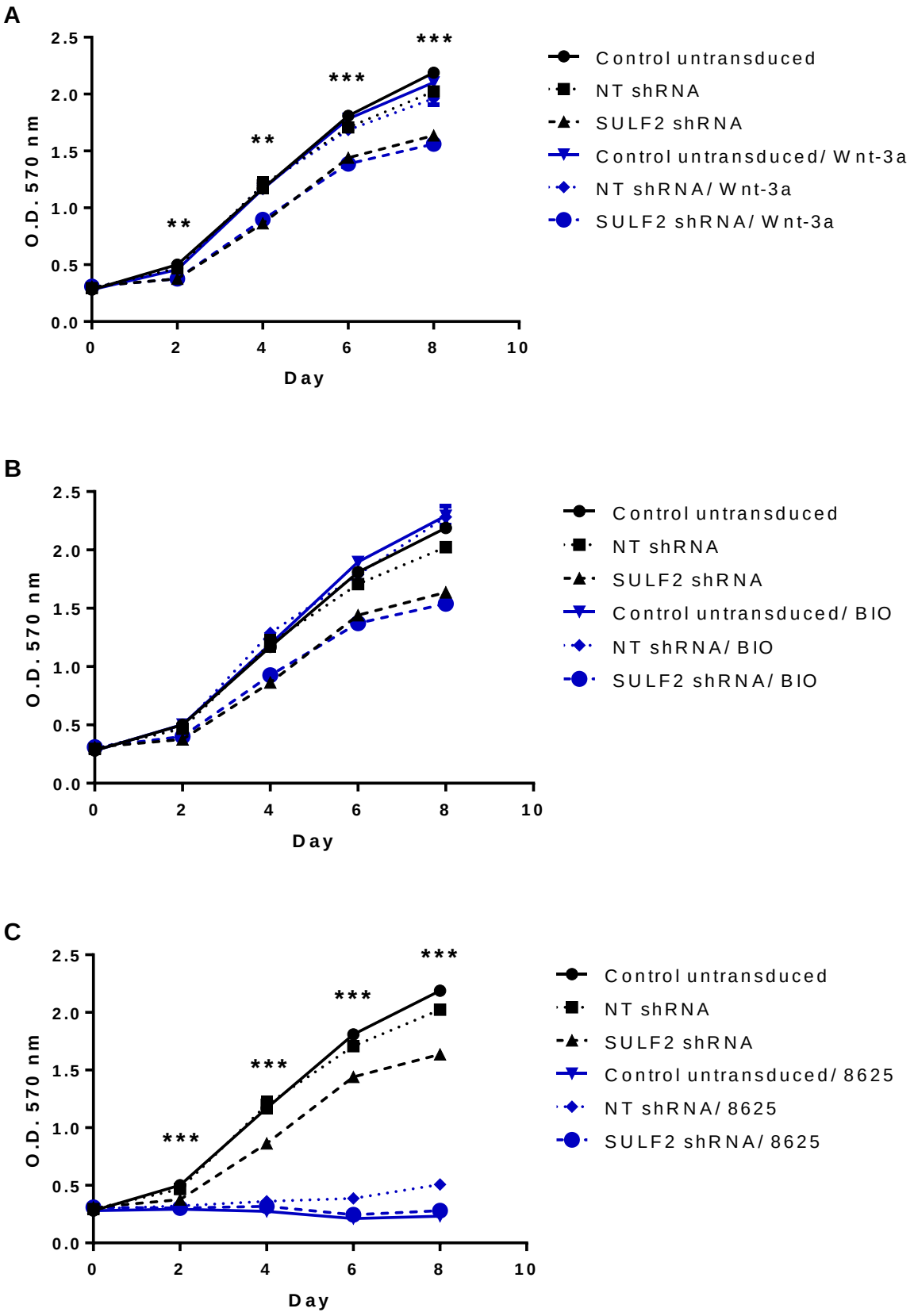
A
O.D. 570 nm
Day
**
**
***
***
Control untransduced
NT shRNA
SULF2 shRNA
Control untransduced/ Wnt-3a
NT shRNA/ Wnt-3a
SULF2 shRNA/ Wnt-3a
B
O.D. 570 nm
Day
Control untransduced
NT shRNA
SULF2 shRNA
Control untransduced/ BIO
NT shRNA/ BIO
SULF2 shRNA/ BIO
C
O.D. 570 nm
Day
***
***
***
***
Control untransduced
NT shRNA
SULF2 shRNA
Control untransduced/ 8625
NT shRNA/ 8625
SULF2 shRNA/ 8625

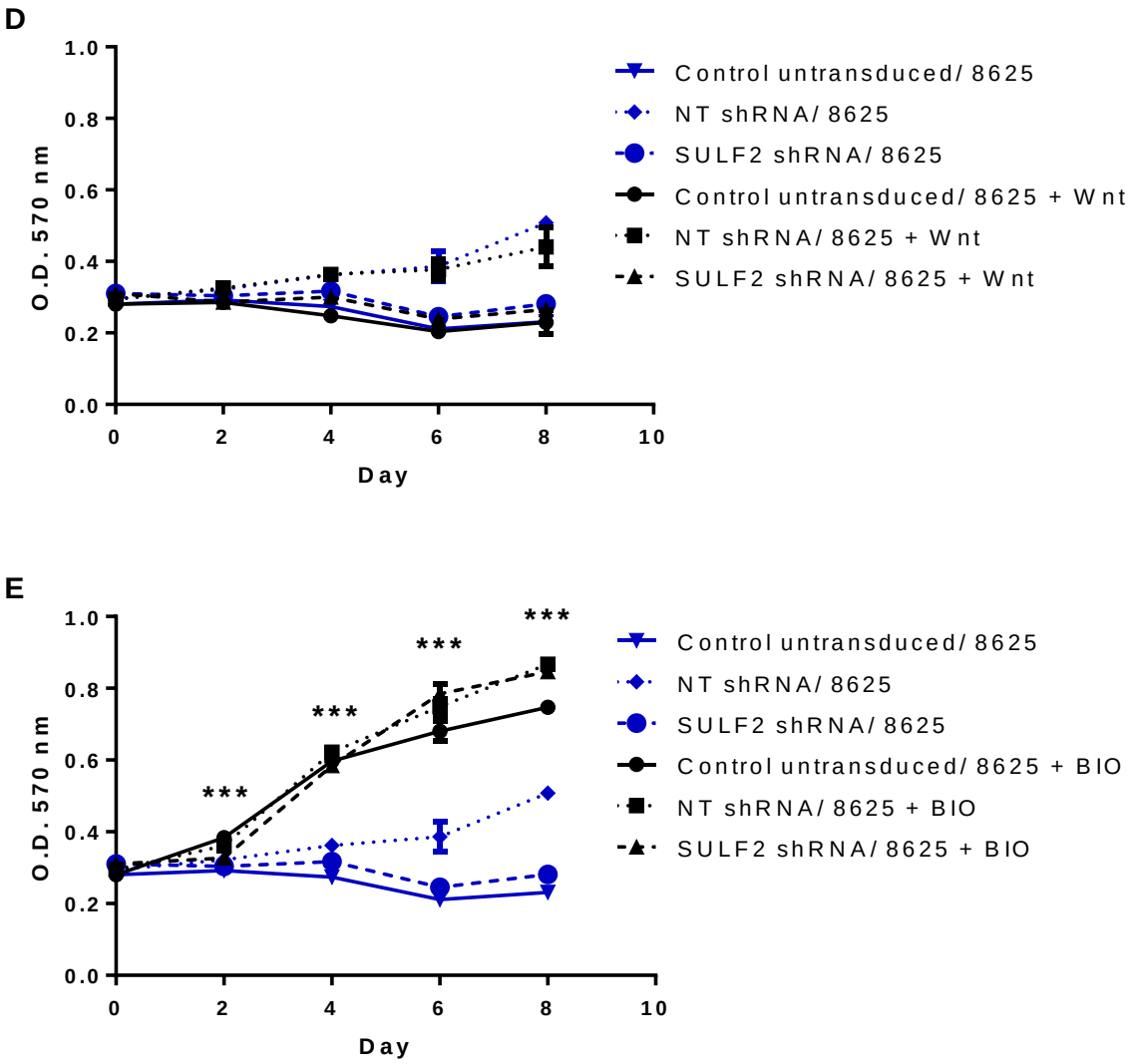

Figure 5.21: Effect of modulators of Wnt signalling on cell growth of HuH-7 cells after SULF2 knockdown: 2,000 HuH-7 cells (control untransduced and stably transduced with either NT shRNA or SULF2 shRNA lentiviral particles) were seeded per well in 96-well plates. The cells were treated with 100 ng/ml Wnt-3a **(A)**, 1 µM BIO **(B)**, 100 µM compound 3289-8625 **(C)**, a combination of Wnt-3a and compound 3289-8625 **(D)** or a combination of BIO and compound 3289-8625 **(E)**. Cells were fixed at different time points, stained using SRB and the optical density at 570 nm was measured. Values are the mean of triplicates and error bars represent the standard error. The experiment was performed in triplicate. ** *p* value = 0.001, *** *p* value < 0.0001, one-way ANOVA between untreated cell lines in (A), between untreated and 3289-8625-treated cell lines in (C) and between cell lines treated with 3289-8625 alone and cell lines treated with both 3289-8625 and BIO in (E). Data generated using the method described in Section 2.17.

5.3.2.3. Effects of SULF2 gene silencing on tumourigenicity of HuH-7 cells *in vivo*

After demonstrating the effect of SULF2 knockdown on HuH-7 cell signalling and growth *in vitro*, the impact on the tumourigenicity of HuH-7 cells *in vivo* was examined. A pilot study was conducted in which HuH-7 cells were implanted subcutaneously into CD1 female nude mice using cells that were stably transduced with either NT shRNA or SULF2 shRNA (5 mice per group). The results showed that within 32 days after implantation all 5 animals in the NT shRNA-transduced cells group had developed tumours (median time to tumour detection 28 days, range 25-32). The median time to reach a volume of 500 mm^3 was 35 days (range 28-42) from implantation or 8 days (range 5-10) from the first day tumours were measurable. In contrast, over a 100-day period, none of the animals implanted with the SULF2 shRNA-transduced cells developed tumours (Figure 5.22).

To confirm the pilot study data, the *in vivo* experiment was repeated and 10 mice were implanted per group. In addition to the two cell lines mentioned above, untransduced HuH-7 cells were also used serving as an additional control. The results showed that both control untransduced and NT shRNA-transduced cells formed tumours (8/10 and 9/10 mice, respectively) (Figure 5.23; A) with no difference in the mean time to reach a tumour volume of 500 mm^3 from implantation between the two groups (Figure 5.23; B). Importantly, SULF2 shRNA-transduced cells failed to form any tumours as before.

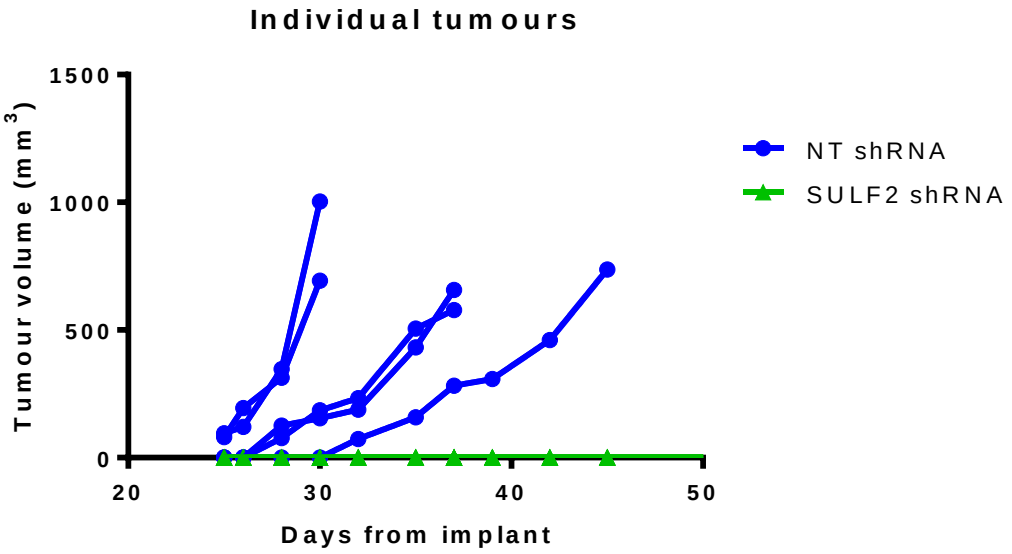

Figure 5.22: Pilot study of the effect of SULF2 gene silencing on tumourigenicity of HuH-7 cells in mice: $1x10^7$ NT shRNA- or SULF2 shRNA-transduced cells were implanted subcutaneously into the right flank of five CD1 female nude mice each, and the tumour volume was measured 3 times a week using a digital caliper. The data represent the tumour incidence and growth rate in mice. Data generated using the method described in Section 2.20.

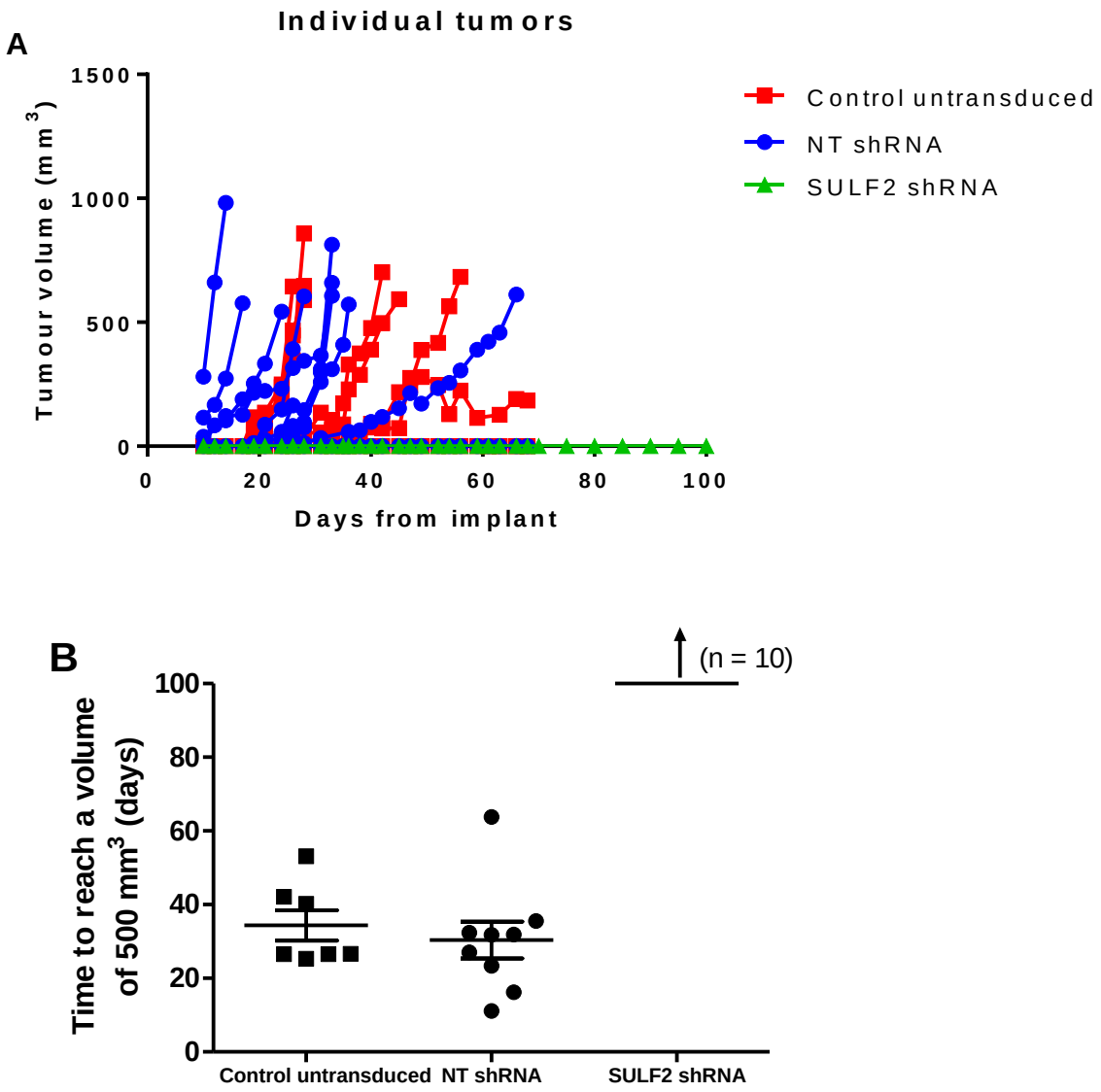

Figure 5.23: Repeat study of the effect of SULF2 gene silencing on tumourigenicity of HuH-7 cells in mice: $1x10^7$ control untransduced, NT shRNA-transduced or SULF2 shRNA-transduced cells were implanted subcutaneously into the right flank of ten CD1 female nude mice and the tumour volume was measured 3 times a week using a digital caliper. (A) Tumour incidence and growth rate in mouse. (B) Mean time to reach a volume size of 500 mm^3. The horizontal lines are the mean of the replicates and error bars represent the standard error. Data generated using the method described in Section 2.20.

5.3.3. SULF1/2 gene silencing in SNU-182 cells and effects on signalling, cell growth and tumourigenicity

SNU-182 is a poorly differentiated HCC cell line that expresses both SULF1 and SULF2 at high and comparable levels. Therefore, knocking down SULF1 and SULF2 in this cell line was investigated, in order to compare the biology and the roles of SULF1 and SULF2 in the context of HCC.

SNU-182 cells were stably transduced with NT shRNA, SULF1 shRNA or SULF2 shRNA. RT-qPCR results showed that after two weeks of selection of transduced cells with puromycin there was a 94% decrease of SULF2 and 85% decrease of SULF1 mRNA levels in the SULF2 shRNA-transduced cells and the SULF1 shRNA-transduced cells, respectively, as compared to NT shRNA-transduced cells (Figure 5.24; A). After two months of growing cells under selection (i.e., in puromycin) there was more suppression of the expression of SULF2 and SULF1 in their respective shRNA-transduced cells (98% and 89%, respectively) (Figure 5.24; B). However, there was also a 50% decrease of SULF2 expression in the SULF1 shRNA-transduced cells as compared to NT shRNA-transduced cells, suggesting a late effect of SULF1 suppression on the expression of SULF2 (Figure 5.24; B). However, no effect was detected on the expression of other genes tested, for example B2M, TP53 and KLF6, after either SULF1 or SULF2 knockdown in SNU-182 cells (data not shown).

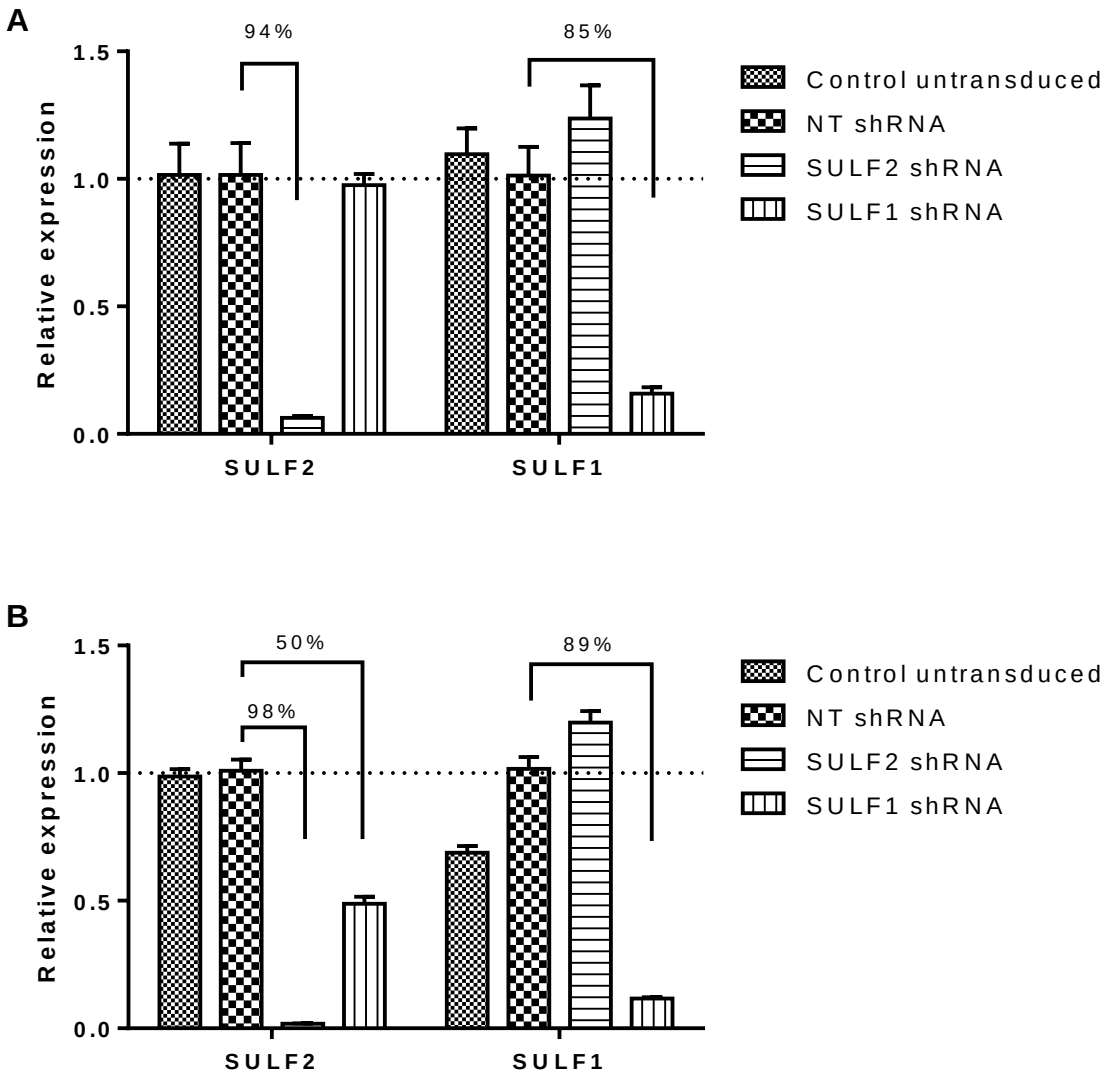

Figure 5.24: SULF1/2 mRNA levels in SNU-182 cells after transduction with shRNA lentiviral particles: SNU-182 cells were stably transduced with NT shRNA, SULF2 shRNA or SULF1 shRNA lentiviral particles. RT-qPCR was performed and the data were normalized using GAPDH as a reference gene. **(A)** Early effect (2 weeks) of transduction. **(B)** Late effect (2 months) of transduction. Values are the mean of triplicates and error bars represent the standard error. The experiment was performed in triplicate. Data generated using the methods described in Section 2.6 and Section 2.7.

5.3.3.1. Effects of SULF1/2 gene silencing on signalling pathways in SNU-182 cells

5.3.3.1.1. Effect of SULF1/2 gene silencing on growth factor/RTK signalling in SNU-182 cells

SNU-182 cells that were stably transduced with NT shRNA, SULF2 shRNA or SULF1 shRNA and grown for ≥ 2 months (Figure 5.24; B) were serum-starved overnight and then treated with or without the FGFR inhibitor PD173074 or the MEK inhibitor PD0325901 for 1 hour before stimulation with 10 nM FGF-1 or FGF-2 for 10 min. The cell lysates were extracted and WB was performed with antibodies against SULF1, SULF2, p-ERK1/2, p-AKT or actin. WB membranes were then stripped and re-probed using total ERK and total AKT antibodies as a loading control. WB showed the absence of SULF2 protein in the cells transduced with SULF2 shRNA (Figure 5.25; A) and the absence of SULF1 protein in the cells transduced with SULF1 shRNA (Figure 5.25; B).

There was no effect on the basal level of p-ERK or p-AKT as a result of SULF1 or SULF2 knockdown. However, both FGF-1 and FGF-2 could stimulate p-ERK in all cell lines except the SULF2 knockdown cells which showed marked inhibition of FGF-1- or FGF-2-stimulated p-ERK levels (Figure 5.25). Both PD173074 and PD0325901 reduced basal and FGF-1- or FGF-2-stimulated p-ERK levels without affecting p-AKT levels, and thus served as positive controls for inhibition of p-ERK (Figure 5.25). As WB is a semi-quantitative technique, a p-ERK1/2 sandwich ELISA was performed to quantify p-ERK levels. The results showed significant lower p-ERK levels after stimulation with either FGF-1 or FGF-2 in SULF2 knockdown cells (p value < 0.02, Figure 5.26). The positive controls for inhibition, PD173074 and PD0325901 treatment completely abrogated the phosphorylation of ERK in response to FGF-1 or FGF-2 in all 4 SNU-182 cell lines (Figure 5.26).

A similar approach was used to examine the effect of SULF1/2 knockdown on the IGF-I and IGF-II signalling pathways. The main downstream transducer of the IGF growth factors is the PI3K/AKT pathway resulting in the phosphorylation of AKT. Therefore, a p-AKT ELISA was used and the results showed no effect of SULF1/2 knockdown on the basal level of p-AKT or on IGF-I-stimulated p-AKT level (Figure

5.27**;** A). However, there was significant inhibition of IGF-II-stimulated p-AKT in the SULF2 knockdown cells only (*p* value < 0.05, Figure 5.27; B). Collectively, these results demonstrated the important role of SULF2, but not SULF1, in the SNU-182 cell line in the regulation of the signalling consequent to FGF-1, FGF-2 and IGF-II, but not IGF-I, treatment.

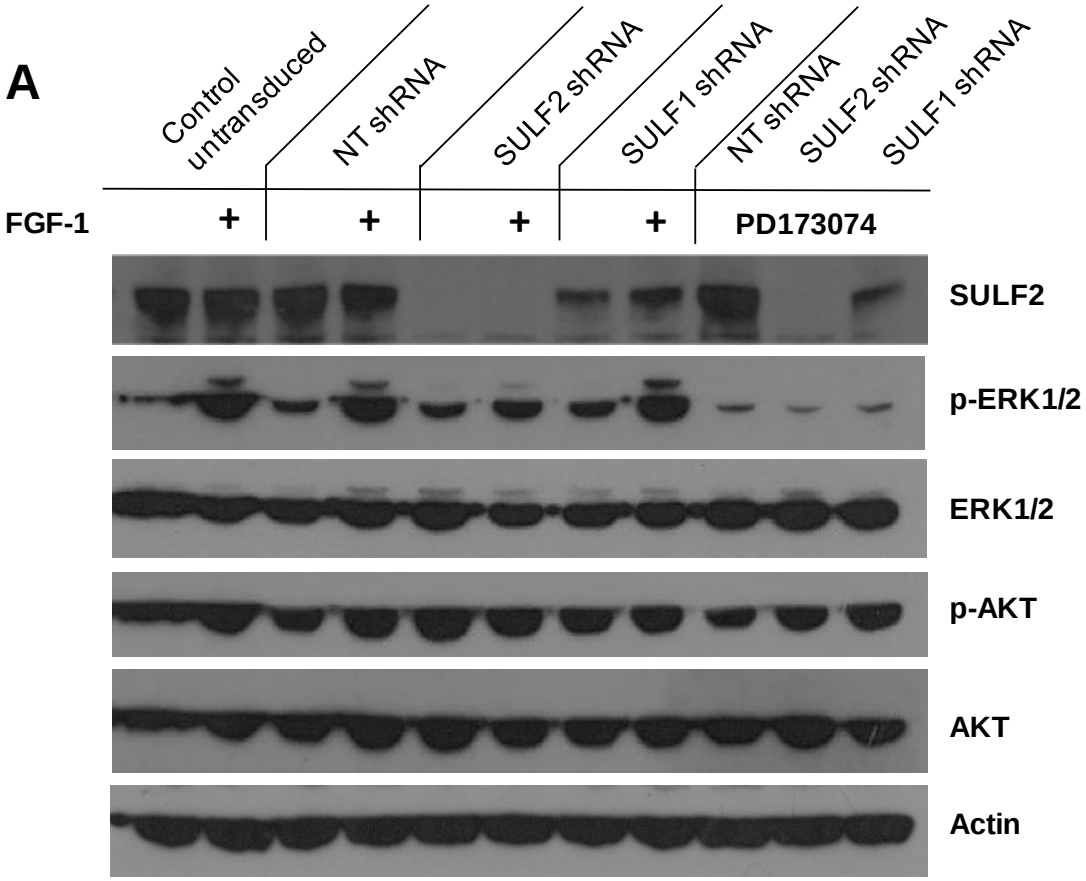

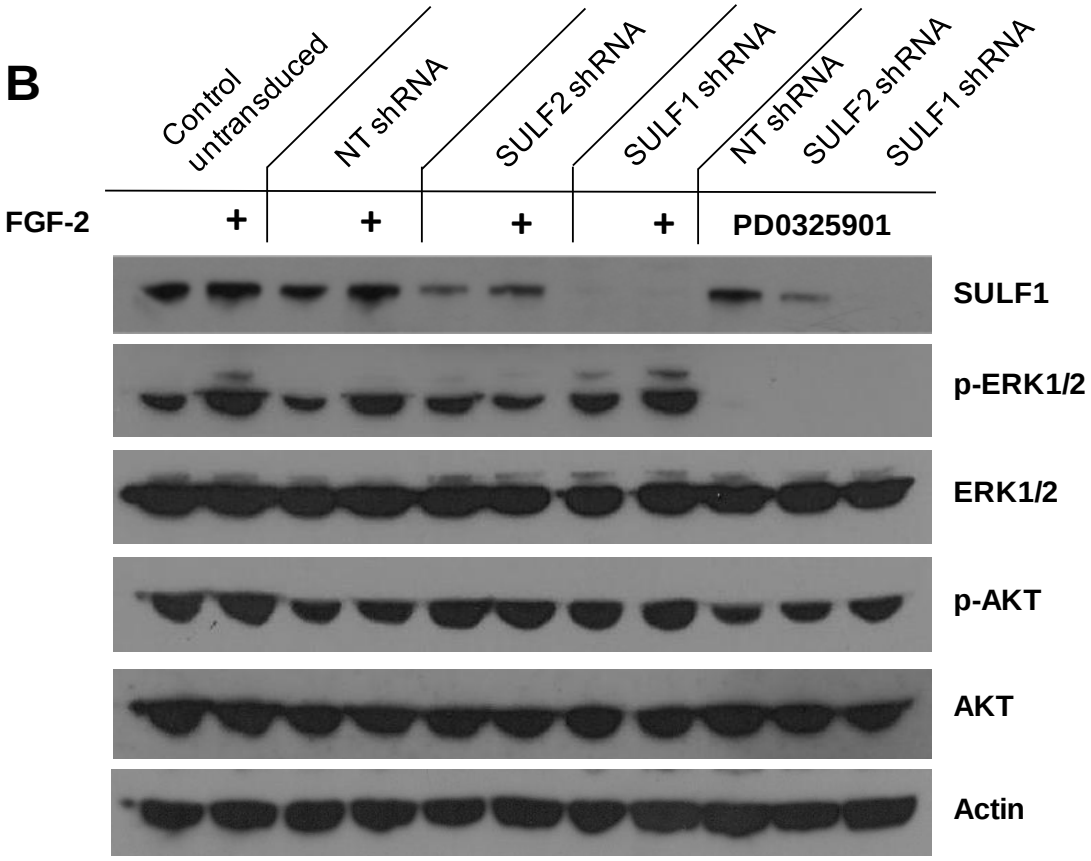

Figure 5.25: Effect of SULF1/2 gene silencing on FGF-1 and FGF-2 signalling pathways in SNU-182 cells measured by WB: SNU-182 cells were stably transduced with NT shRNA, SULF2 shRNA or SULF1 shRNA lentiviral particles. The cells were serum-starved overnight and then treated with 100 nM PD173074 or 1 µM PD0325901 for 1 hour before stimulation with 10 nM FGF-1 **(A)** or FGF-2 **(B)** for 10 min. Whole cell lysates were prepared and WB was performed using antibodies against SULF2, SULF1, p-ERK1/2, p-AKT or actin. The membranes were stripped and reprobed with antibodies against total ERK1/2 and total AKT serving as loading controls. The experiment was performed in triplicate and representative blots are shown. Data generated using the methods described in Section 2.6 and Section 2.10.

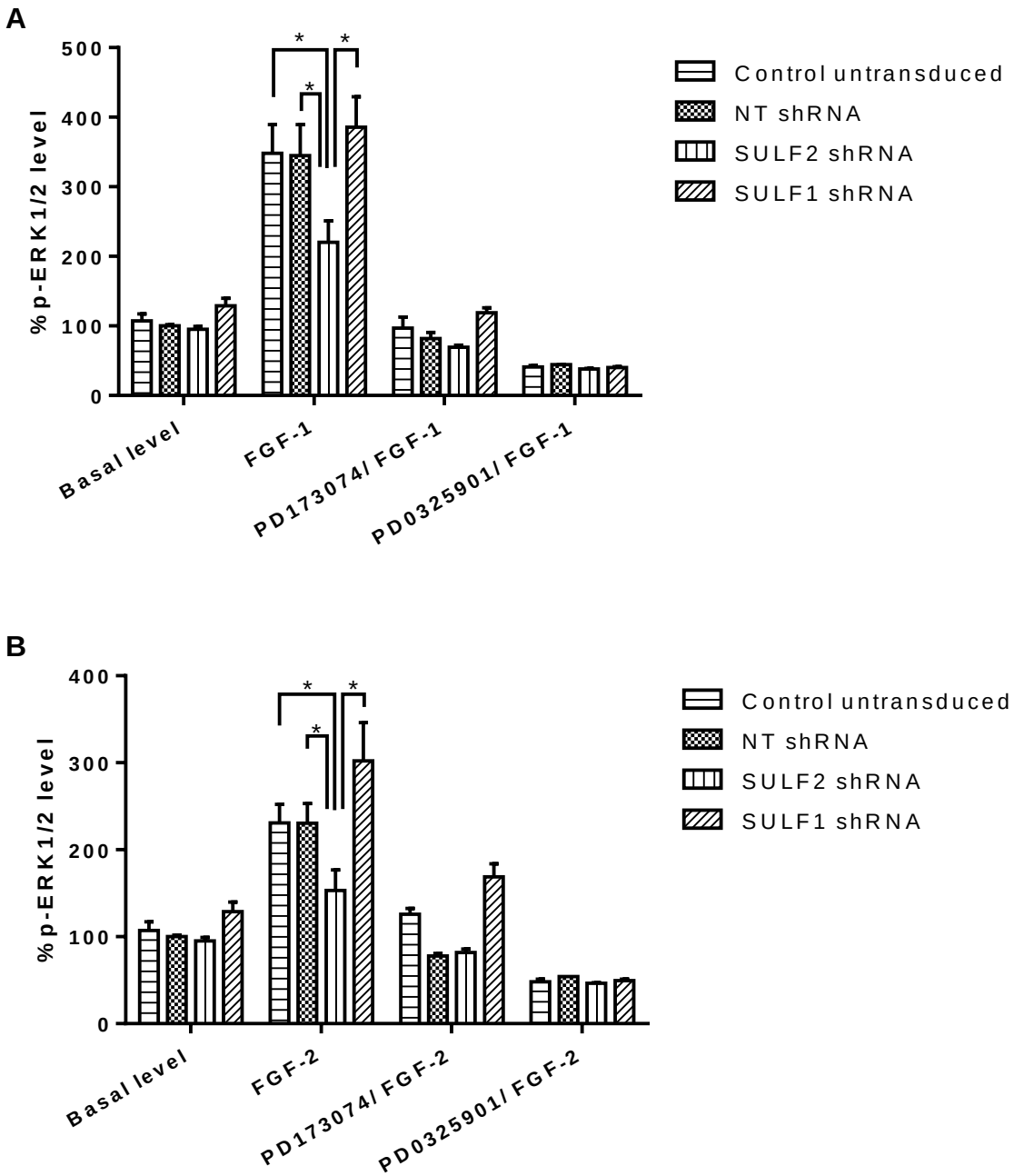

Figure 5.26: Effect of SULF1/2 gene silencing on FGF-1 and FGF-2 signalling pathways in SNU-182 cells measured by ELISA: SNU-182 cells were stably transduced with NT shRNA, SULF2 shRNA or SULF1 shRNA lentiviral particles. The cells were serum-starved overnight and then treated with 100 nM PD173074 or 1 µM PD0325901 for 1 hour before stimulation with 10 nM FGF-1 (A) or FGF-2 (B) for 10 min. Whole cell lysates were prepared and p-ERK1/2 sandwich ELISA was performed. 50 µg of cell lysates were loaded of each sample. Values are the mean of 5 different experiments for (A) and 3 different experiments for (B) and error bars represent the standard error. * *p* value < 0.05, 2-sample t-test. Data generated using the methods described in Section 2.6 and Section 2.16.

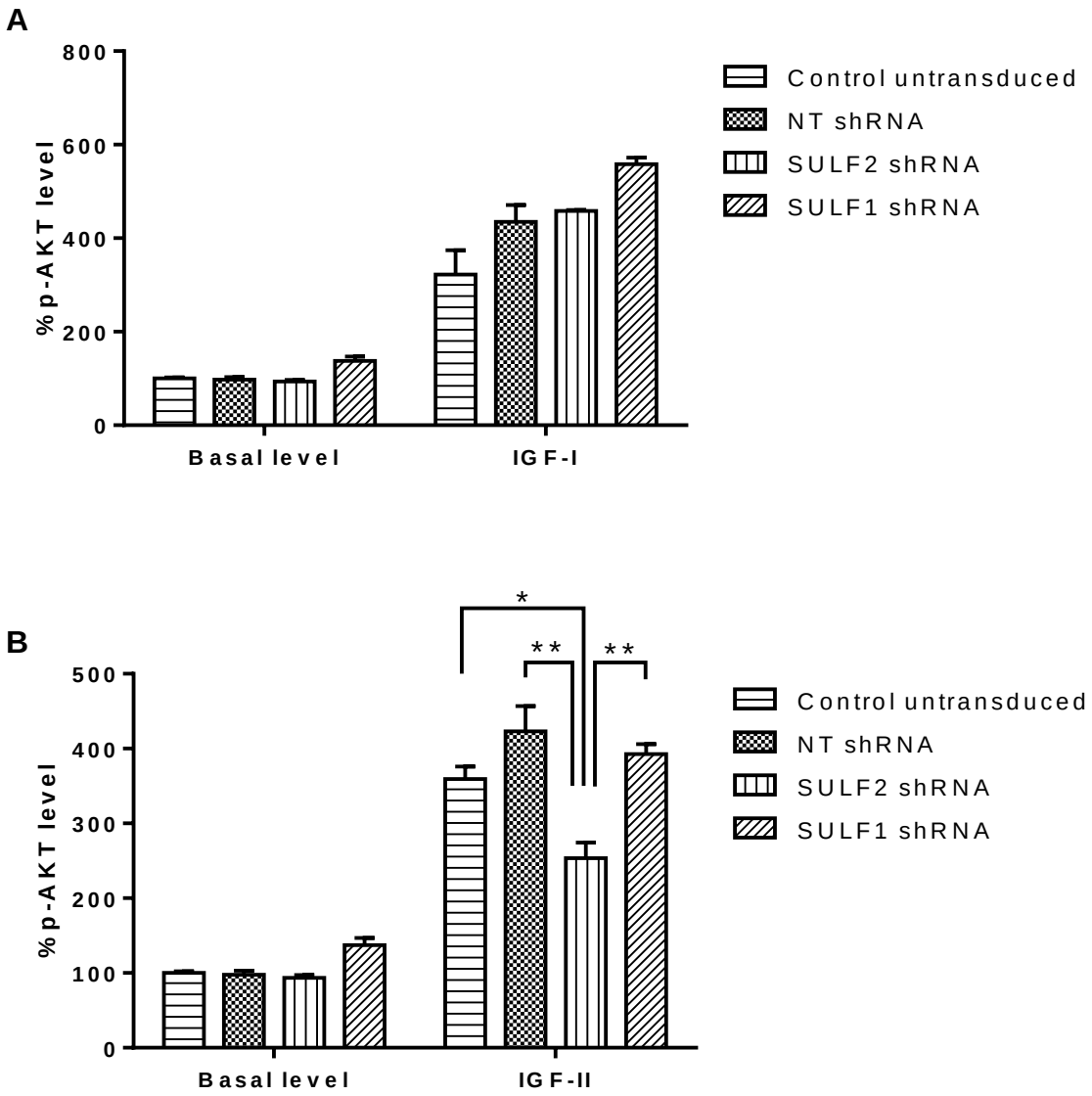

Figure 5.27: Effect of SULF1/2 gene silencing on IGF-I and IGF-II signalling pathways in SNU-182 cells measured by ELISA: SNU-182 cells were stably transduced with NT shRNA, SULF2 shRNA or SULF1 shRNA lentiviral particles. The cells were serum-starved overnight and then treated with 10 nM IGF-I (A) for 5 min or IGF-II (B) for 10 min. Whole cell lysates were prepared and p-AKT sandwich ELISA was performed. 50 µg of cell lysates were loaded of each sample. Values are the mean of 3 different experiments and error bars represent the standard error. * *p* value = 0.014, ** *p* value ≤ 0.005, 2-sample t-test. Data generated using the methods described in Section 2.6 and Section 2.16.

5.3.3.1.2. Effect of SULF1/2 gene silencing on Wnt signalling in SNU-182 cells

SNU-182 cells that were transduced with NT shRNA, SULF2 shRNA or SULF1 shRNA were transduced with 7TFP lentiviral particles, prior to stimulation with Wnt-3a. None of these cell lines were responsive to Wnt-3a (Figure 5.28), in keeping with a report that TCF activity was not detected in SNU-182, even after transfecting the cells with mutant β-catenin (Yuzugullu et al., 2009).

Neither SULF1 nor SULF2 knockdown in SNU-182 cells affected the expression level of CCND1 or MYC, two transcriptional targets of the β-catenin-TCF complex. However there was a late, rather than early, effect of SULF1 and SULF2 suppression on the expression of GPC3, resulting in 4- and 11-fold downregulation of GPC3, respectively (Figure 5.29).

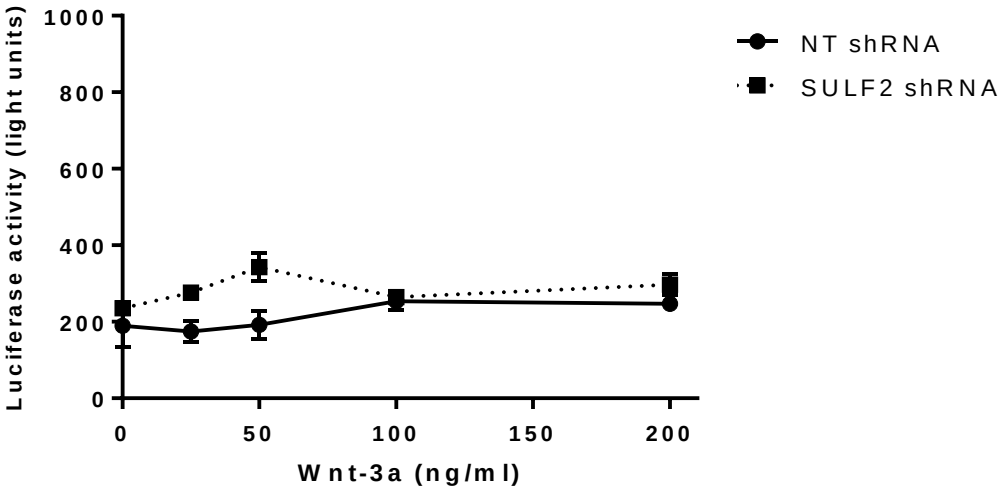

Figure 5.28: Effect of SULF2 gene silencing on Wnt signalling pathway in SNU-182 cells using 7TFP reporter assay: SNU-182 cells were stably transduced with either NT shRNA or SULF2 shRNA lentiviral particles followed by transduction with 7TFP lentiviral particles. The cells were serum-starved and then treated with different concentrations of Wnt-3a for 6 hours. ONE-Glo reagent was added and luciferase activity was measured. Values are the mean of triplicates and error bars represent the standard error. The experiment was performed in duplicate. Data generated using the methods described in Section 2.6 and Section 2.15.

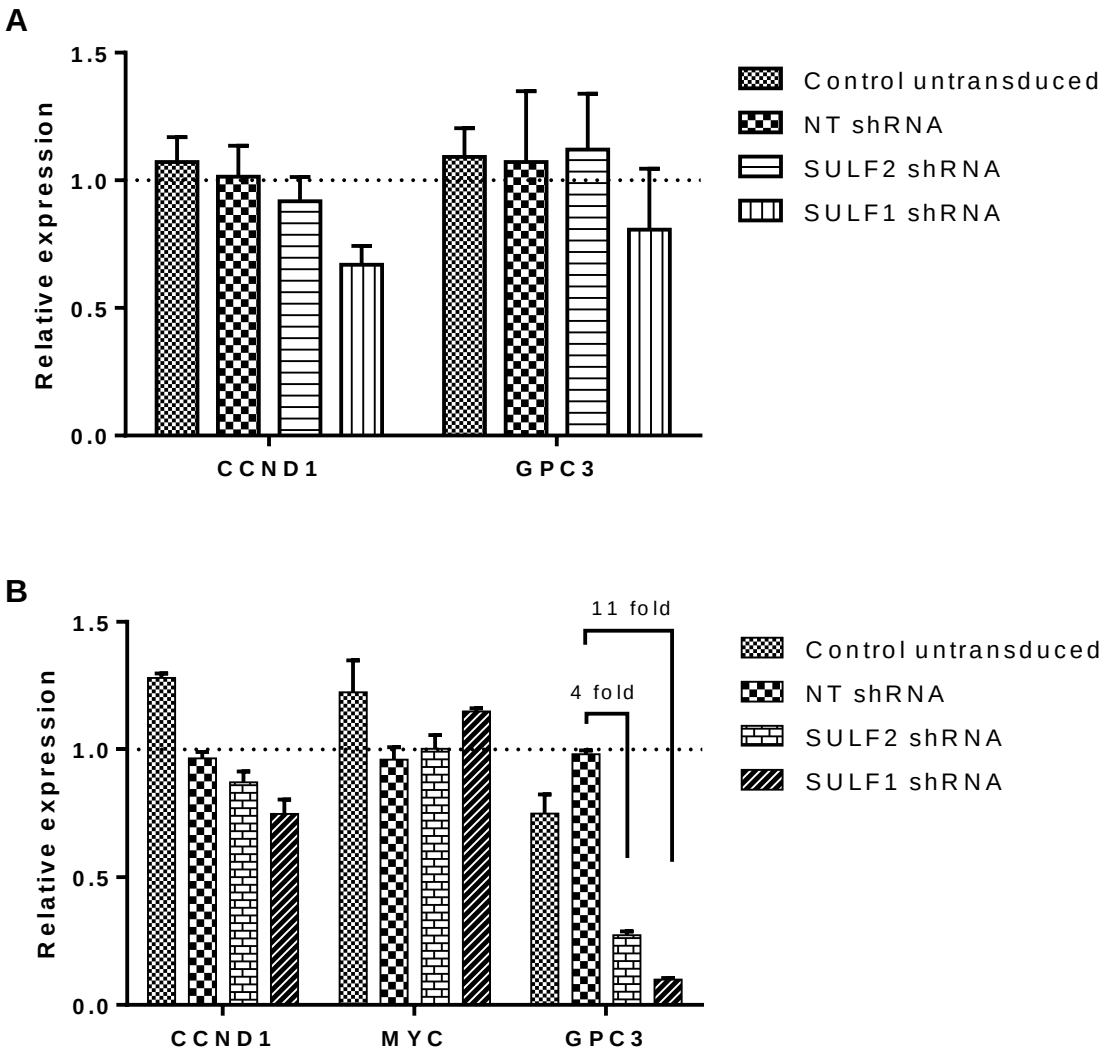

Figure 5.29: Effect of SULF2 gene silencing on Wnt signalling pathway-related genes in SNU-182 cells: SNU-182 cells were stably transduced with NT shRNA, SULF2 shRNA or SULF1 shRNA lentiviral particles. RT-qPCR was performed and the data were normalized using GAPDH as a reference gene. **(A)** Early effect (2 weeks) of transduction. **(B)** Late effect (2 months) of transduction. Values are the mean of triplicates and error bars represent the standard error. The experiment was performed in triplicate. Data generated using the methods described in Section 2.6 and Section 2.7.

5.3.3.2. Effects of SULF1/2 gene silencing on growth of SNU-182 cells *in vitro*

To investigate the effect of SULF2 knockdown and subsequent growth factor signalling suppression on cell proliferation, SNU-182 cells that were stably transduced with NT shRNA, SULF2 shRNA or SULF1 shRNA (Figure 5.24) were cultured in 96-well plates and cell proliferation was evaluated by cell counting. The results showed that SULF2 suppression increased the doubling time of 50 hours for both control untransduced and NT shRNA-transduced cells to 62 hours for the SULF2 knockdown cells. Interestingly, SULF1 suppression also reduced the proliferation of SNU-182 cells, and the doubling time of SULF1 knockdown cells was 60 hours (Figure 5.30).

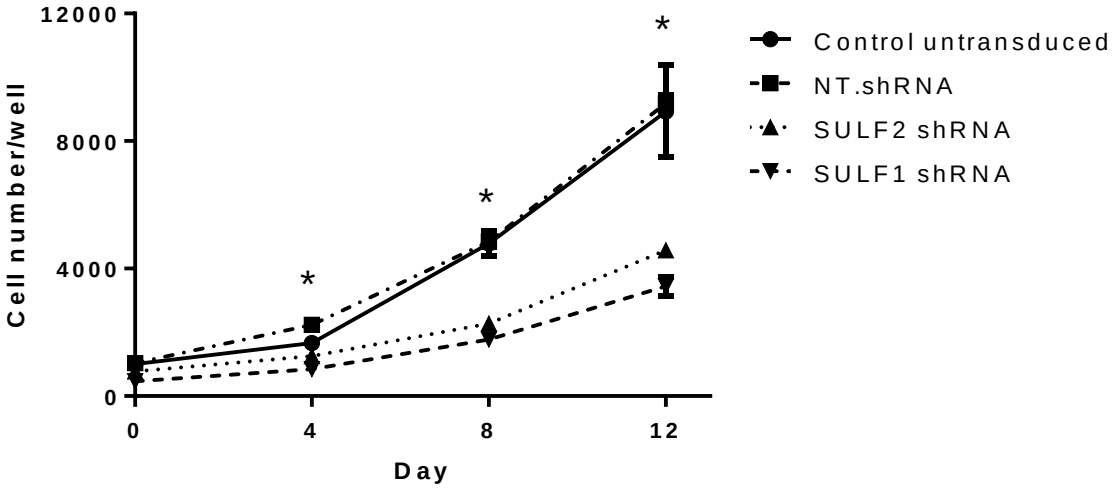

Figure 5.30: Effect of SULF1/2 gene silencing on cell proliferation in SNU-182 cells: SNU-182 cells were stably transduced with NT shRNA, SULF2 shRNA or SULF1 shRNA lentiviral particles. 1,000 cells were seeded per well and counted at different time points. Values are the mean of triplicates and error bars represent the standard error. The experiment was performed in quadruplicate. * *p* value < 0.05, 2-sample t-test between control untransduced or NT shRNA-transduced cells vs. SULF2 shRNA- or SULF1 shRNA-transduced cells. Data generated using the method described in Section 2.18.

5.3.3.3. Effects of SULF1/2 gene silencing on tumourigenicity of SNU-182 cells *in vivo*

None of the SNU-182 cell lines formed tumour xenografts in nude mice, even after re-suspending the cell pellet before injection in Matrigel basement membrane matrix. Matrigel contains a variety of growth factors and was used to promote cell-cell contact and enhance growth, with the goal of increasing the tumour-forming potential of the cells. Also, no tumours were formed when the cells were implanted into the more immunocompromised NSG (NOD scid gamma) mice. Therefore, it was not possible to investigate the effect of SULF1/2 knockdown on the tumourigenicity of SNU-182 cells.

5.3.4. SULF2 gene silencing in HepG2 cells and effects on signalling, cell growth and tumourigenicity

HepG2 cells express SULF2 at high level but not SULF1. To study the role of SULF2 in this cell line, SULF2 knockdown was performed using SULF2 shRNA (Figure 5.10) and the effect of SULF2 suppression on growth factor and Wnt signalling studied.

5.3.4.1. Effects of SULF2 gene silencing on signalling pathways in HepG2 cells

5.3.4.1.1. Effect of SULF2 gene silencing on growth factor/RTK signalling in HepG2 cells

To study the effect of SULF2 gene silencing on growth factor signalling pathway, the phosphorylation status of ERK1/2 and AKT was assessed by WB after stimulation with 10 nM FGF-1 or FGF-2 for 10 min, or IGF-I for 5 min, either in serum-free or serum-containing medium. WB showed no clear effect of SULF2 suppression on the basal or growth factor-stimulated levels of p-ERK1/2 or p-AKT (Figure 5.31).

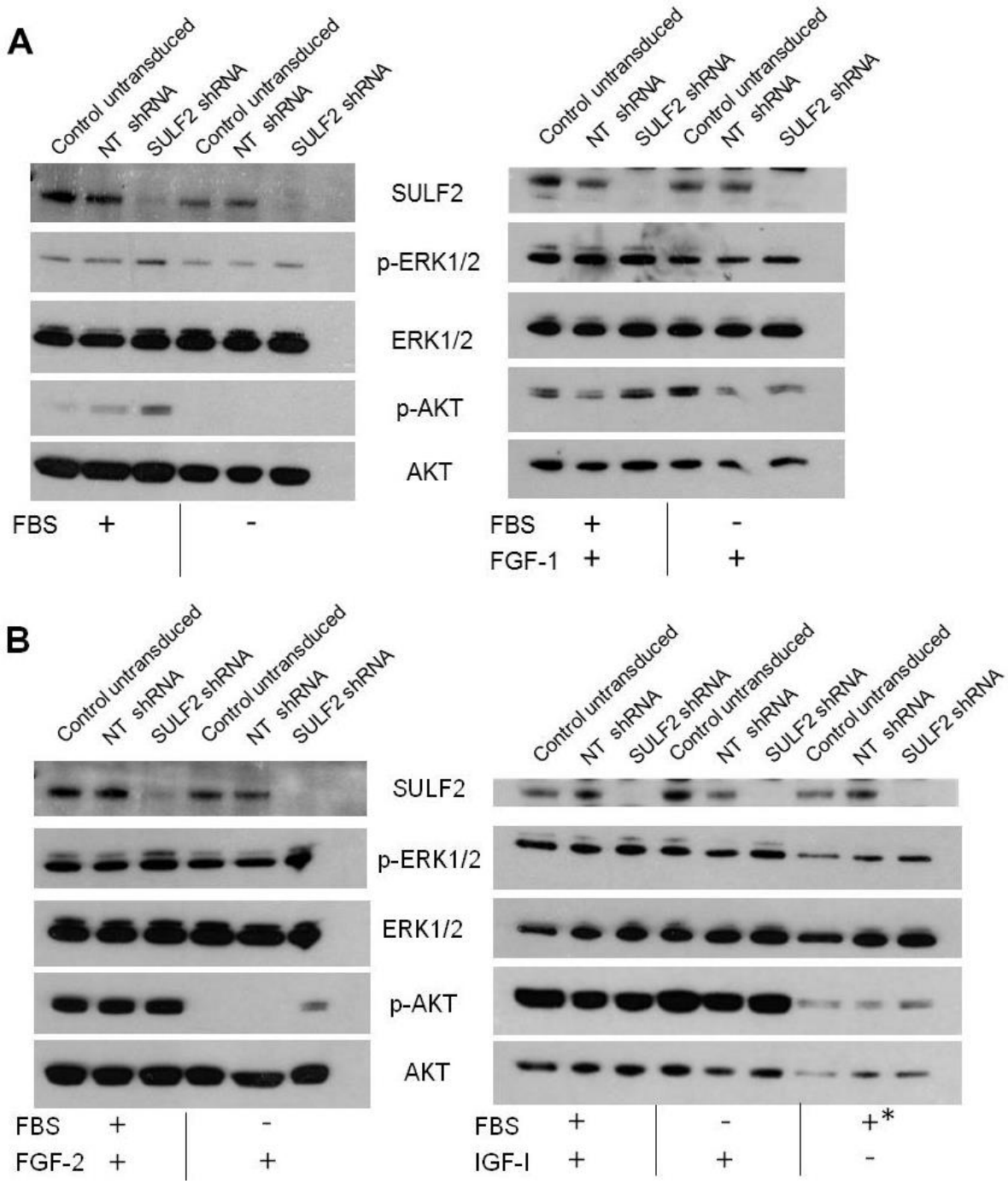

Figure 5.31: Effect of SULF2 gene silencing on growth factor signalling in HepG2 cells: HepG2 cells were stably transduced with either NT shRNA or SULF2 shNRA lentiviral particles. The cells were incubated in either serum-free medium (FBS -) or serum-containing medium (FBS +) overnight. Cells were then treated with 10 nM FGF-1 **(A; left)** or FGF-2 **(B; right)** for 10 min or IGF-I for 5 min **(B; left)**. Whole cell lysates were prepared and WB was performed using antibodies against SULF2, p-ERK1/2 and p-AKT. Total ERK1/2 and total AKT were used as loading controls. * denotes samples that were incubated with serum-free medium overnight and then treated with 10% FBS for 10 min. FBS: foetal bovine serum. The experiment was performed in duplicate and representative blots are shown.

5.3.4.1.2. Effect of SULF2 gene silencing on Wnt signalling in HepG2 cells

HepG2 cells have a wild-type and a truncated form of β-catenin that is constitutively active (Carruba et al., 1999). When these cells were treated with Wnt-3a, there was a small Wnt-3a concentration-dependent increase in the level of the wild type β-catenin as detected by WB (data not shown). Therefore, to determine whether there is any effect of SULF2 suppression on wild type β-catenin-dependent TCF activity, the TCF luciferase reporter assay was performed using the TOPflash reporter system.

The results showed that there was a very high luciferase activity in all 3 cell lines (i.e., control untransduced, NT shRNA or SULF2 shRNA-transduced cells) that was ≥ 9-fold the background level measured by the FOPflash construct that contains mutant TCF binding sites (Figure 5.32). The TOPflash TCF-dependent activity was not increased by treatment with Wnt-3a (data not shown), and the basal activity was not affected by SULF2 knockdown (Figure 5.32). Furthermore, no change was detected in the expression level of either CCND1 or GPC3 after SULF2 knockdown in this cell line (data not shown).

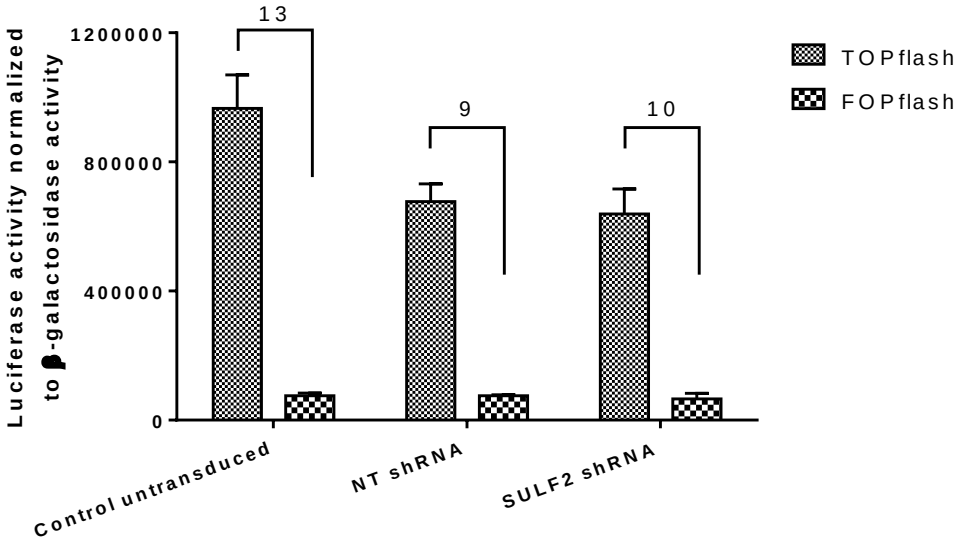

Figure 5.32: Effect of SULF2 gene silencing on Wnt signalling pathway in HepG2 cells: HepG2 cells were stably transduced with either NT shRNA or SULF2 shRNA lentiviral particles. The cells were then transiently co-transfected with either TOPflash or FOPflash and β-galactosidase constructs in Opti-MEM medium. Whole cell lysates were prepared using RLB and luciferase activity was measured. Values are the mean of triplicates and error bars represent the standard error. The experiment was performed in triplicate. Data generated using the methods described in Section 2.6 and Section 2.15.

5.3.4.2. Effects of SULF2 gene silencing on growth of HepG2 cells *in vitro*

Although SULF2 knockdown did not affect growth factor or Wnt signalling, SULF2 could still alter other signalling pathways and affect proliferation in HepG2 cells. The SRB assay was, therefore, performed to measure cell growth; however, the results showed no change in the growth of HepG2 cells after SULF2 gene silencing (Figure 5.33).

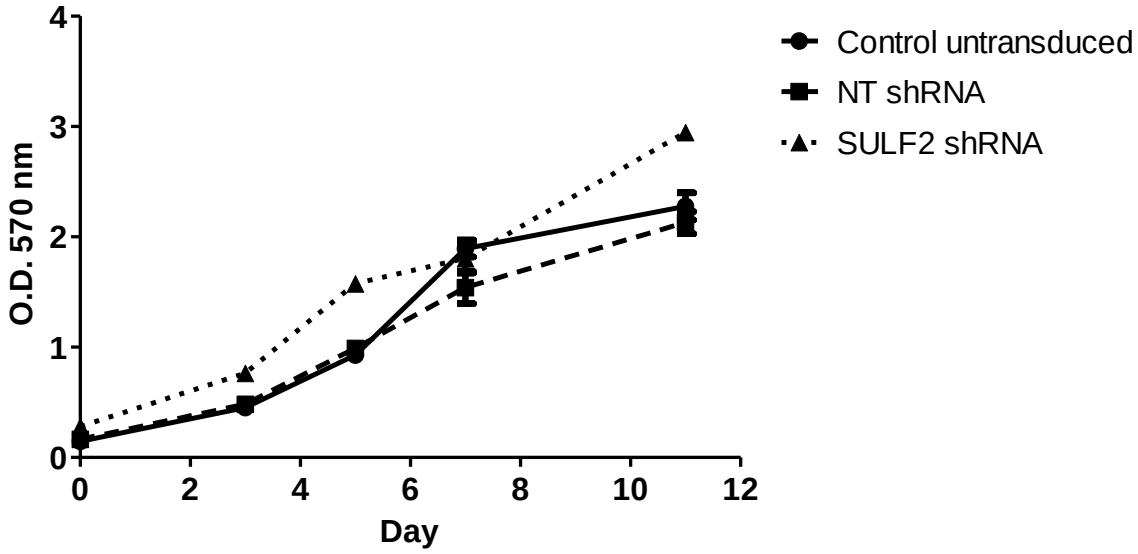

Figure 5.33: Effect of SULF2 gene silencing on the growth of HepG2 cells: HepG2 cells were stably transduced with either NT shRNA or SULF2 shRNA lentiviral particles. 1,000 cells were seeded per well for different time points and then stained with SRB. Values are the mean of quadruplicates and error bars represent the standard error. The experiment was performed in triplicate. Data generated using the methods described in Section 2.6 and Section 2.17.

5.4. Summary

Two of the most important signalling pathways that are involved in hepatocarcinogenesis were characterised in a panel of HCC cell lines; the Wnt and the growth factor/RTK signalling pathways. Well-validated inhibitors of these pathways were also tested; compound 3289-8625 and PD173074 that inhibit Wnt and RTK signalling pathways, respectively. These inhibitors were thus used as positive controls for inhibition of their respective pathways. The optimal shRNA sequences for gene silencing of either SULF2 or SULF1 were selected, and these were stably transduced into HCC cells and the downstream consequences were investigated. Mechanistically, the effect of SULF2 knockdown was cell-type specific, with inhibition of Wnt signalling in HuH-7 cell line, inhibition of FGF-1, FGF-2 and IGF-II signalling in SNU-182 cell line and no effect on either pathway in HepG2 cell line. Phenotypically, SULF2 knockdown had a detrimental effect on the proliferation of HuH-7 and SNU-182 cells *in vitro* and inhibited the tumourigenicity of HuH-7 cells *in vivo*. There was no effect of SULF2 knockdown on the proliferation of HepG2 cells.

SULF1 knockdown inhibited the proliferation of SNU-182 cells, but it did not affect the growth factor/RTK signalling pathway, in contrast to SULF2 knockdown in this cell line.

Chapter 6. Effects of Inducible SULF1/2 Suppression in HCC Cell Lines

The data presented in Chapter 5 demonstrated that SULF2 has a role in the regulation of cellular signalling and growth in HCC cell lines. The experiments described in this chapter were designed to further characterise the function of SULF1 and SULF2 by using inducible shRNAs to regulate expression. The S2.shRNA_18 and S1.shRNA_89 sequences were cloned into an isopropyl β-D-thiogalactoside (IPTG)-inducible shRNA lentiviral vector by Sigma. This vector contains one LacI and a U6 promoter with three LacO sequences (Figure 2.4). IPTG is an analogue of lactose and binds to the LacI protein, changing its conformation and releasing it from the LacO site, which promotes the expression of the shRNA. These non-targeting (NT), SULF2 and SULF1 inducible shRNA constructs were provided in the form of lentiviral particles, and will be referred to as iNT.shRNA, iSULF2.shRNA and iSULF1.shRNA throughout the rest of the thesis.

6.1. Optimisation of the Conditions for the Inducible Knockdown

To choose the best conditions to achieve maximum knockdown of SULF1/2, HuH-7 cells were stably transduced with either iNT.shRNA or iSULF2.shRNA and then treated with different concentrations of IPTG for different time periods with daily medium changes and replenishment of IPTG. WB showed that 1-2 mM IPTG caused silencing of SULF2 in the iSULF2.shRNA-transduced cells as early as one day after treatment with maximum reduction in SULF2 protein levels achieved after 3 days (Figure 6.1). No effect on the levels of SULF2 protein was detected in the iNT.shRNA-transduced cells even after 5 days (data not shown). In the SNU-182 cell line, 1 mM IPTG for 1-2 days caused almost complete absence of SULF1 or SULF2 proteins, and as in the HuH-7 cell line IPTG caused no change in the protein levels of either SULF1 or SULF2 in the iNT.shRNA-transduced cells (data not shown).

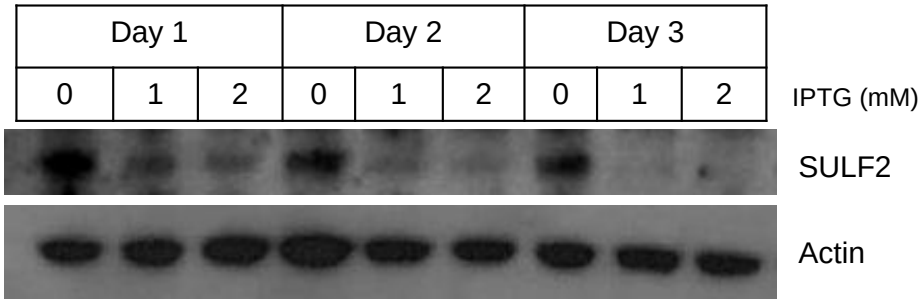

Figure 6.1: Optimisation of conditions for inducible SULF2 shRNA in HuH-7 cells: The inducible SULF2 shRNA-transduced HuH-7 cells were treated with different concentrations of IPTG for 1-3 days and WB was performed on whole cell lysates with SULF2 Ab (Serotec) or actin Ab (loading control). The experiment was performed in triplicate and a representative blot is shown. Data generated using the methods described in Section 2.6 and Section 2.10.

The duration of the effect of IPTG was assessed by RT-qPCR after treatment of iNT.shRNA- and iSULF2.shRNA-transduced HuH-7 cells with 1 mM of IPTG without any medium change or replenishment of IPTG. The results showed 75% and 86% decreases of SULF2 expression after treatment of iSULF2.shRNA-transduced HuH-7 cells with IPTG for 3 and 8 days, respectively. No effect on SULF2 expression was shown after treatment of iNT.shRNA-transduced cells with IPTG for 3 days, while there was a 2-fold upregulation after 8 days of treatment (Figure 6.2). In inducible iSULF2.shRNA-transduced SNU-182 cells, IPTG treatment caused 92% and 99% decreases of SULF2 expression after 3 and 8 days, while IPTG treatment caused 71% and 91% decreases of SULF1 expression in iSULF1.shRNA-transduced cells after 3 and 8 days, respectively. Interestingly, IPTG treatment for 8 days caused downregulation of SULF1 in iSULF2.shRNA-transduced cells (78%) and of SULF2 in iSULF1.shRNA-transduced cells (81%). However, no effect of IPTG on SULF1 or SULF2 mRNA levels was observed in iNT.shRNA-transduced cells (Figure 6.3). These data demonstrate that the effect of IPTG persists for at least 8 days, and that SULF1/2 knockdown increases over time during incubation of cells with IPTG.

To determine the specificity of knockdown, the expression of B2M was evaluated in both HuH-7 and SNU-182 cells transduced with the different inducible shRNAs.

The results showed no change in the expression of B2M in any of the cell lines tested before and after IPTG treatment (Figure 6.2) (Figure 6.3).

Finally, to confirm that iNT.shRNA was expressed after IPTG treatment and to compare the level of the inducibly expressed shRNAs to that of the constitutively expressed shRNAs previously used (Section 5.3), the expression of the different shRNAs was tested in SNU-182 cell line using the QuantiMir small RNA quantification system as described in Section 2.21 Using a forward primer corresponding to the siRNA effector sequence of S2.shRNA_18 and a universal reverse primer, the RT-qPCR results showed that the iSULF2.shRNA was expressed at high levels after treatment of SNU-182 cells with 1 mM of IPTG for 8 days. This expression level was close to that of the constitutively expressed SULF2 shRNA (6.4-fold for iSULF2.shRNA vs. 9.3-fold for SULF2 shRNA) (Figure 6.4).

However, the sequence of the constitutively expressed NT shRNA differed from that of the inducibly expressed iNT.shRNA. Using a forward primer corresponding to the siRNA effector sequence of NT shRNA, the RT-qPCR results showed 39-fold upregulation of NT shRNA while using a specific primer for iNT.shRNA, the analysis showed only 4-fold upregulation after IPTG treatment for 8 days (Figure 6.4). Regarding iSULF1.shRNA, the forward primer corresponding to the siRNA effector sequence of S1.shRNA_89 did not give any signal despite trying different optimisation conditions including changes to the qPCR program and the amount of cDNA used.

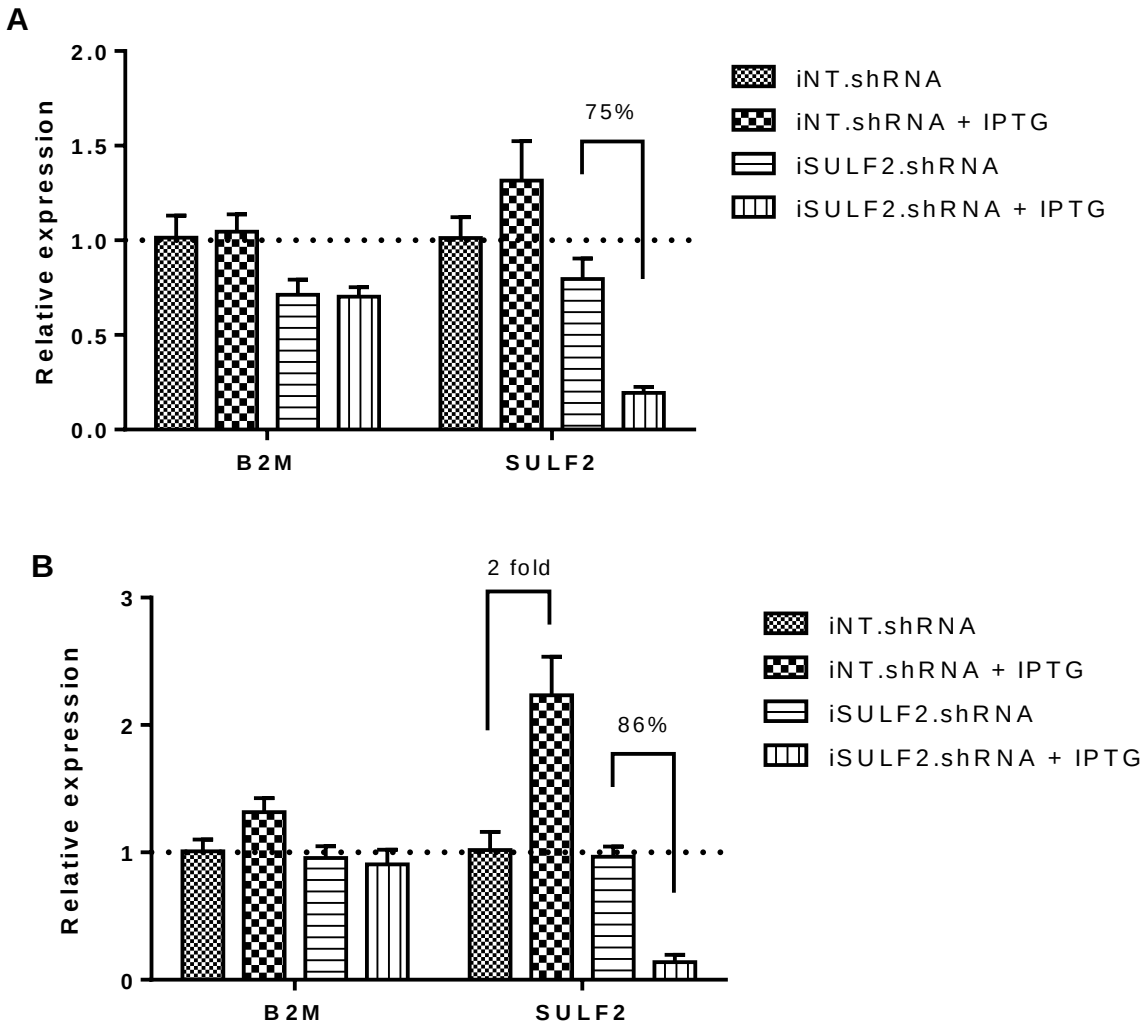

Figure 6.2: RT-qPCR analysis after treatment of inducible shRNA-transduced HuH-7 cells with IPTG: The iNT.shRNA- or iSULF2.shRNA-tranduced HuH-7 cells were treated with 1 mM IPTG for 3 days **(A)** or 8 days **(B)** without medium change, and RT-qPCR was performed using SULF2 and B2M primers. GAPDH was used as an endogenous control for normalization. Values are the mean of triplicates and error bars represent the standard error. The experiment was performed in triplicate. Data generated using the methods described in Section 2.6 and Section 2.7.

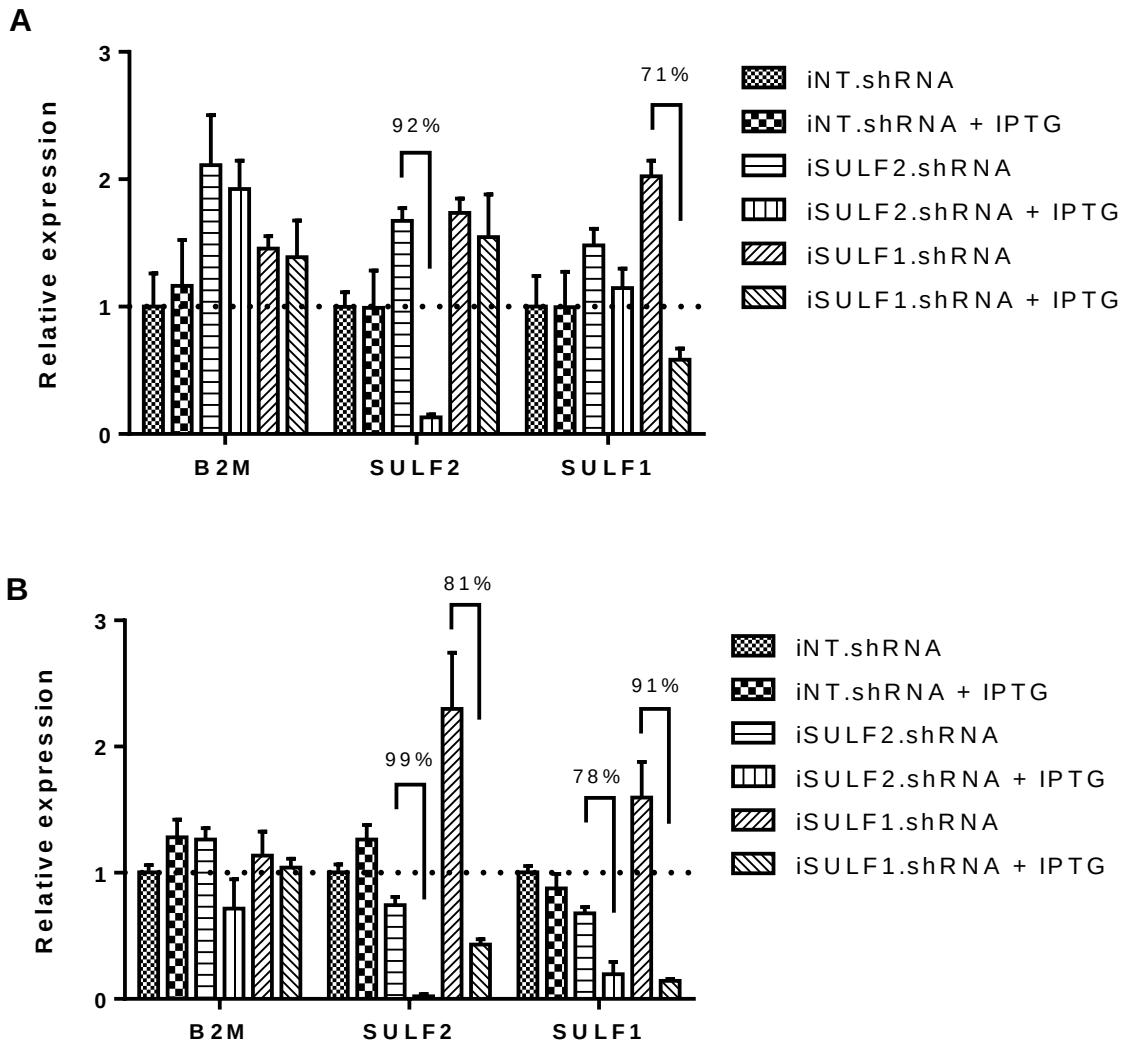

Figure 6.3: RT-qPCR analysis after treatment of inducible shRNA-transduced SNU-182 cells with IPTG: The iNT.shRNA-, iSULF2.shRNA- or iSULF1.shRNA-tranduced SNU-182 cells were treated with 1 mM IPTG for 3 days **(A)** or 8 days **(B)** without medium change and RT-qPCR was performed using SULF2, SULF1 and B2M primers. GAPDH was used as an endogenous control for normalization. Values are the mean of triplicates and error bars represent the standard error. The experiment was performed in triplicate. Data generated using the methods described in Section 2.6 and Section 2.7.

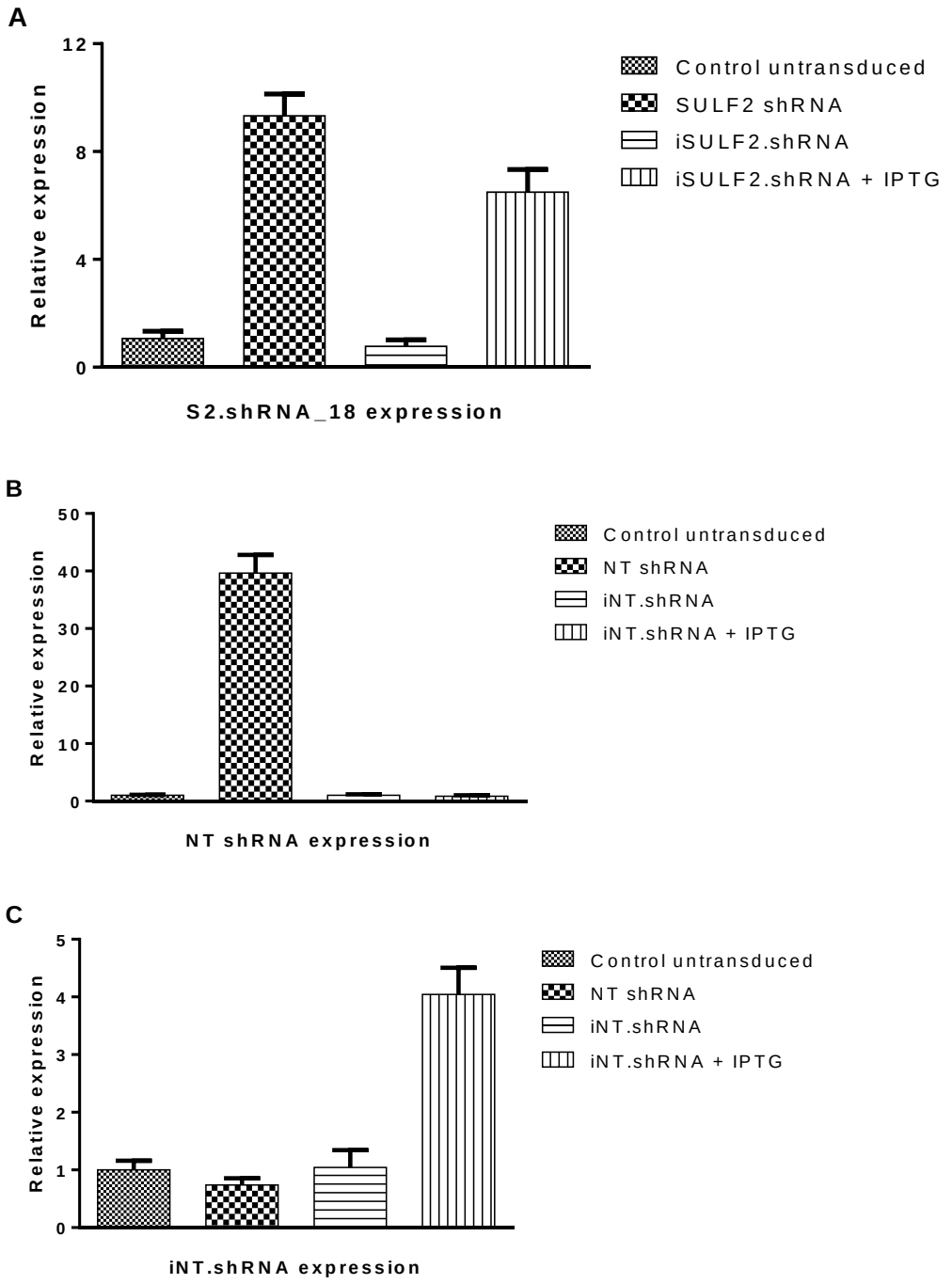

Figure 6.4: Comparison of shRNA expression in constitutive and inducible shRNA-transduced SNU-182 cells using RT-qPCR: RNA was extracted from the constitutively expressed shRNA-transduced SNU-182 cells and the inducibly expressed shRNA-transduced SNU-182 cells that were incubated with or without 1 mM IPTG for 8 days. RT-qPCR was performed using forward primers representing the siRNA sequences of S2.shRNA_18 **(A)**, NT shRNA **(B)** and iNT.shRNA **(C)** and the QuantiMir 3' universal reverse PCR primer. 5' human U6 snRNA forward primer was used as an endogenous control for normalization. Values are the mean of triplicates and error bars represent the standard error. The experiment was performed in triplicate. Data generated using the method described in Section 2.21.

Subsequently, the cell lines with inducible shRNAs were analysed for the effect of inducible SULF1 or SULF2 gene silencing by measuring cell signalling and proliferation.

6.2. Inducible SULF2 Gene Silencing in HuH-7 Cells and Effects on Signalling, Cell Growth and Tumourigenicity

6.2.1. Effects of inducible SULF2 gene silencing on signalling pathways in HuH-7 cells

As shown in Section 5.3.2, constitutive SULF2 knockdown resulted in inhibition of Wnt signalling in HuH-7 cell line, and hence the effect of inducible SULF2 suppression was investigated.

As measured by the TCF reporter gene assay, inducible SULF2 knockdown caused inhibition of Wnt-3a-induced β-catenin-dependent transcriptional activity (*p* value = 0.05, Figure 6.5; A). No effect on Wnt signalling was seen in the iNT.shRNA-transduced cells (Figure 6.5; A). This effect of SULF2 knockdown was attributed to the interaction of the Wnt-3a ligand with its receptor at the cell surface, as inducible SULF2 suppression did not diminish BIO-induced luciferase activity (BIO activates Wnt signalling by inhibiting GSK-3β, i.e. downstream of the frizzled receptor, as described in Section 5.1) (Figure 6.5; B).

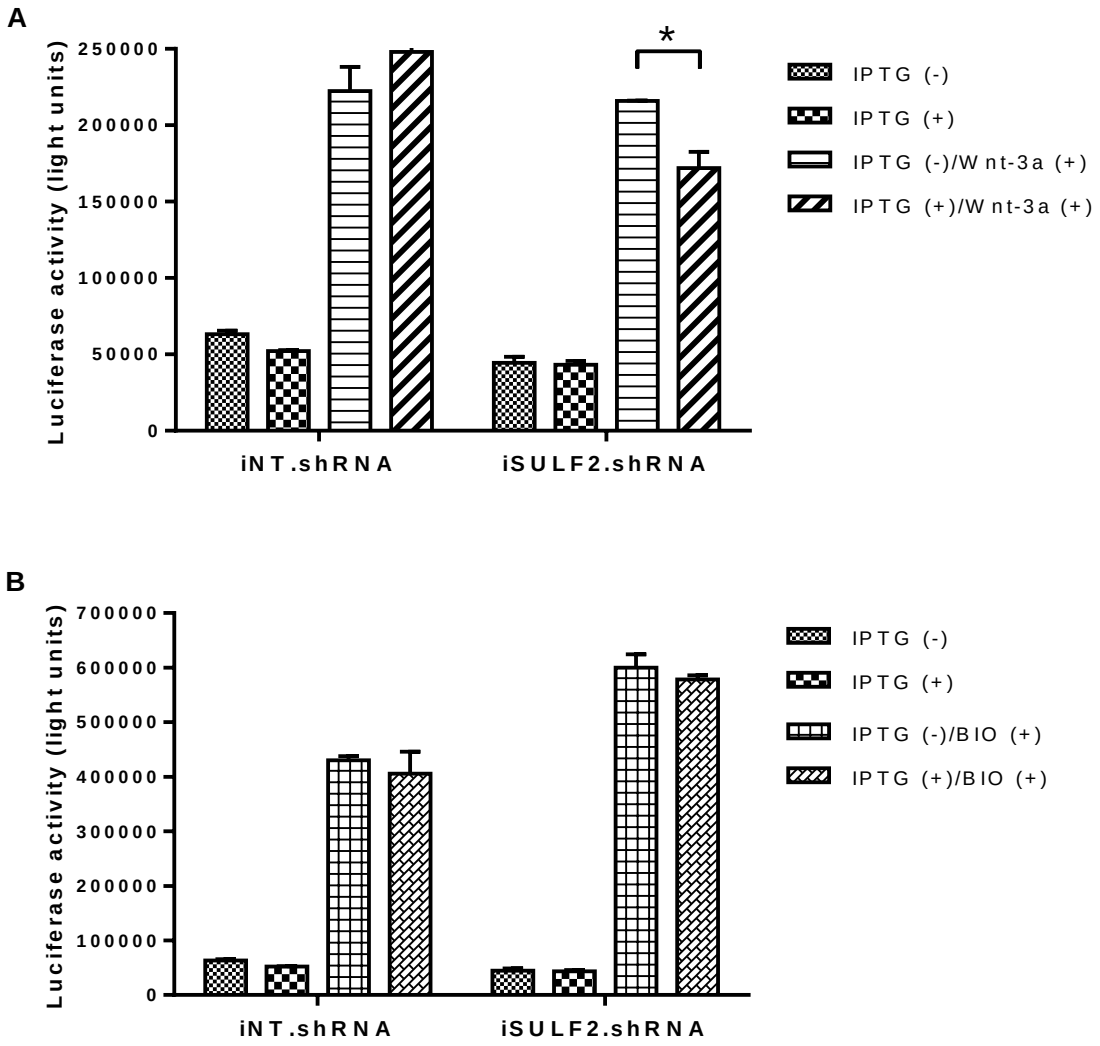

Figure 6.5: Effect of inducible SULF2 gene silencing on Wnt signalling pathway in HuH-7 cells: HuH-7 cells were stably transduced with either iNT.shRNA or iSULF2.shRNA lentiviral particles. The cells were treated with 1mM IPTG for 3 days, serum-starved overnight and then treated with 100 ng/ml Wnt-3a **(A)** or 1 µM BIO **(B)** for 6 hours. Whole cell lysates were prepared using RLB and luciferase activity was measured. Values are the mean of triplicates and error bars represent the standard error. The experiment was performed in triplicate. * p = 0.015, 2-sample t-test. Data generated using the methods described in Section 2.6 and Section 2.15.

6.2.2. Effects of inducible SULF2 gene silencing on growth of HuH-7 cells in vitro

The effect of inducible SULF2 knockdown on the growth of HuH-7 cells was investigated. The cells were treated with IPTG to induce shRNA expression. However, the results showed no effect of inducible SULF2 suppression on cell growth after treatment with IPTG at day 0 (data not shown) or at day 4 (Figure 6.6) following seeding cells.

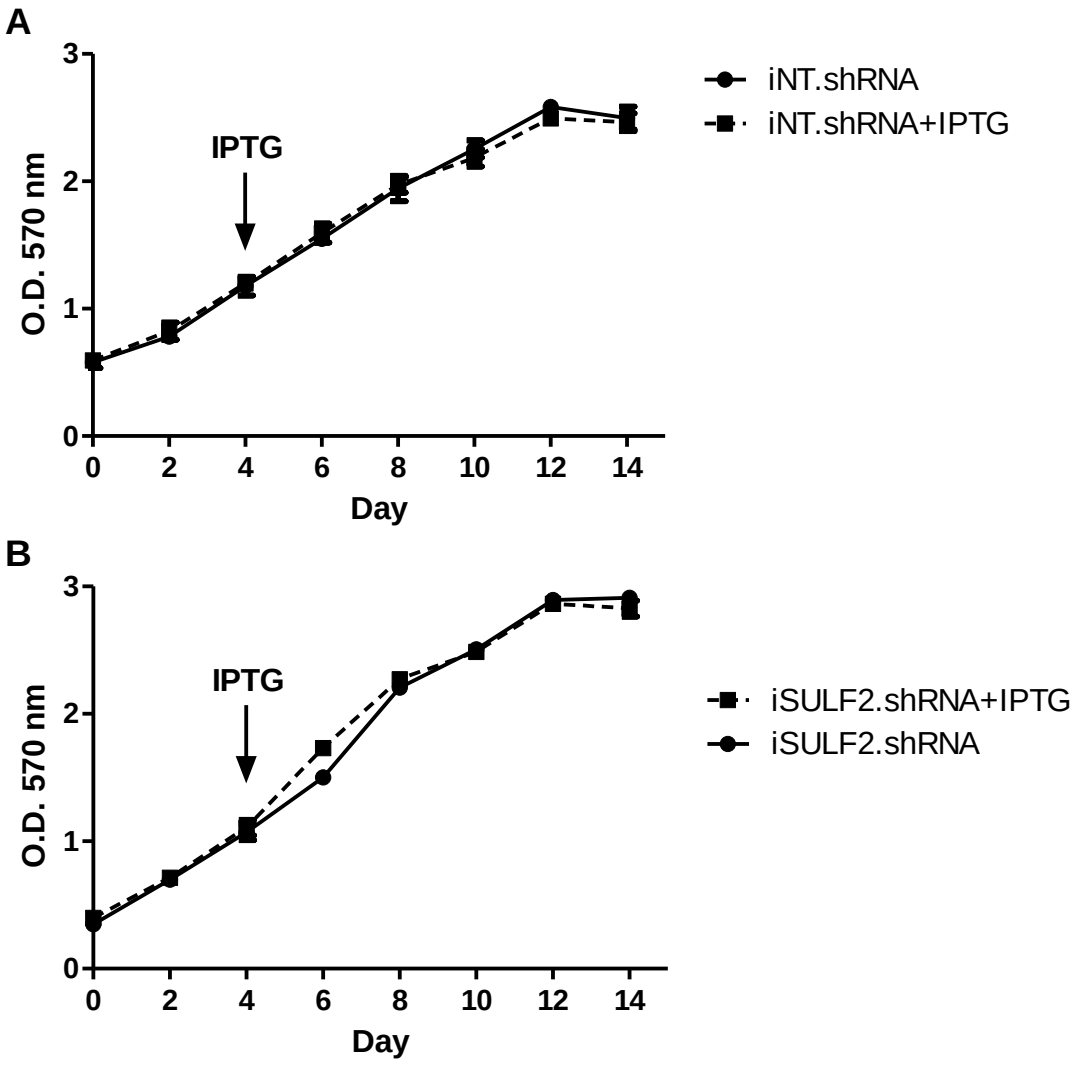

Figure 6.6: Effect of inducible SULF2 gene silencing on cell growth in HuH-7 cells: HuH-7 cells were stably transduced with either iNT.shRNA **(A)** or iSULF2.shRNA **(B)** lentiviral particles. 2000 cells/well were seeded in 96-well plates. Cells were treated with IPTG at day 4, or not (control), and stained with SRB every two days. Values are the mean of six replicates and error bars represent the standard error. The experiment was performed in triplicate. Data generated using the methods described in Section 2.6 and Section 2.17.

6.2.3. Effects of inducible SULF2 gene silencing on tumourigenicity of HuH-7 cells in vivo

Despite the lack of effect on growth *in vitro*, and given that the microenvironment *in vivo* is quite different from that in culture, the effect of inducible SULF2 knockdown was also investigated *in vivo*. iNT.shRNA- or iSULF2.shRNA-transduced cells were each implanted into 10 mice and 5 mice per cell line were given IPTG in the drinking water. IPTG was added from day 0 at a final concentration of 12.5 mM in the drinking water. This concentration was reported to strongly induce expression of tested genes as early as 24 hours in liver cell lines when implanted subcutaneously in mice (Wu et al., 1997). The mice developed tumour xenografts as follows: 2/5 of iNT.shRNA with no IPTG, 4/5 of iNT.shRNA with IPTG, 4/5 of iSULF2.shRNA with no IPTG, and 5/5 of iSULF2.shRNA with IPTG (Figure 6.7; A). Furthermore, there was no difference in the mean time to reach a tumour volume of 500 mm^3 between the four groups (Figure 6.7; B). The tumours were examined and SULF2 knockdown was confirmed in those tumours originating from iSULF2.shRNA-transduced cells after IPTG treatment (76% decrease of mRNA level vs. tumours from IPTG untreated iSULF2.shRNA-transduced cells), while no effect was detected on the expression level of B2M after IPTG treatment (Figure 6.7; C).

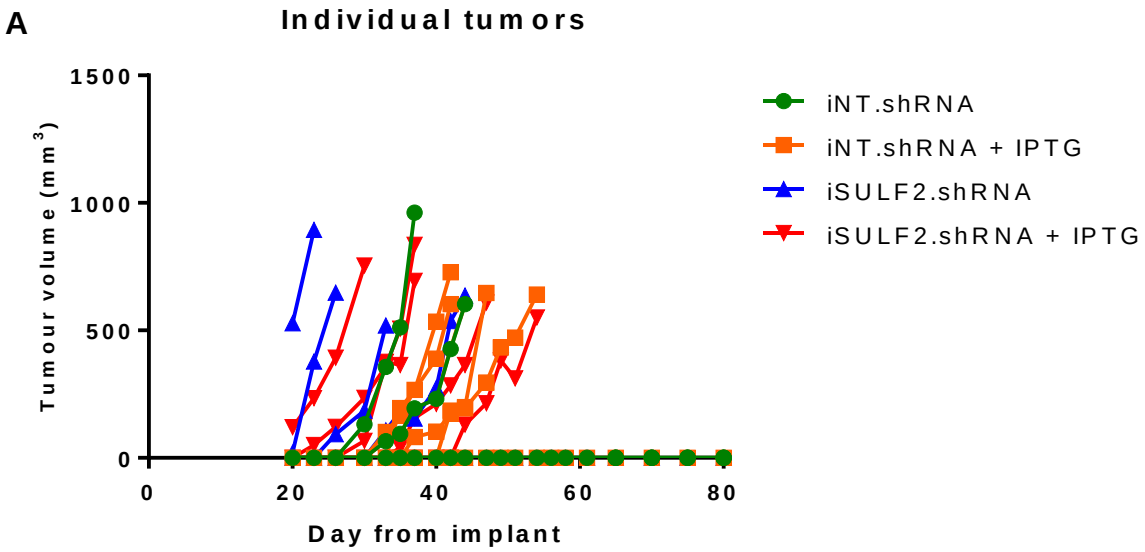

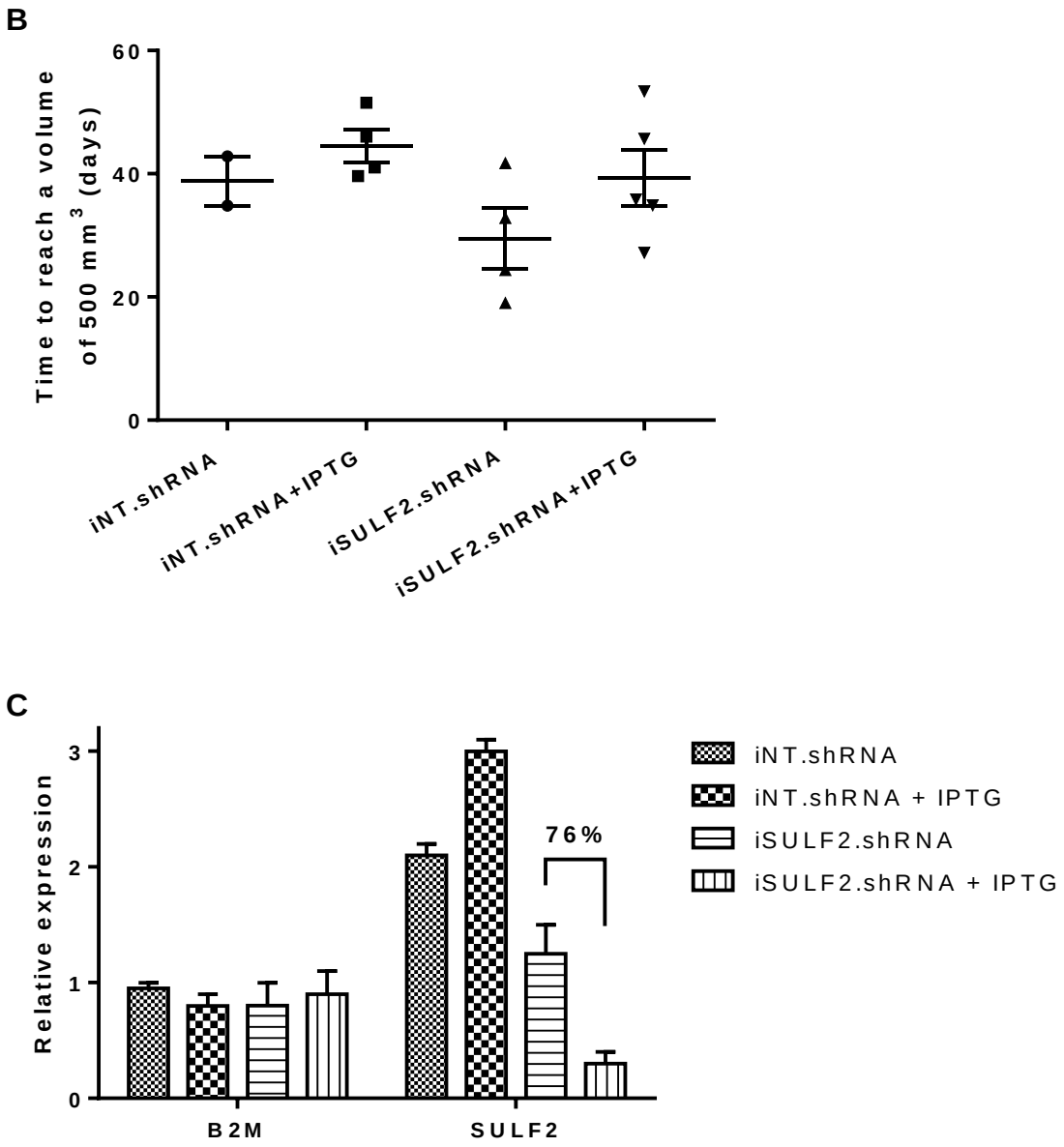

Figure 6.7: Effect of inducible SULF2 gene silencing on the tumourigenicity of HuH-7 cells: $1x10^7$ iNT.shRNA- or iSULF2.shRNA-transduced cells were implanted subcutaneously into the right flank of ten CD1 female nude mice each. 5 mice per group were supplied with drinking water containing 3 g/L (12.5 mM) IPTG that was prepared fresh every week. Tumour incidence and volume were measured 3 times a week using a digital caliper. **(A)** Tumour incidence and growth rate in mouse. **(B)** Mean time to reach a volume size of 500 mm^3 from implantation. The horizontal lines are the mean of the replicates and error bars represent the standard error. **(C)** RT-qPCR analysis using primers for SULF2 and B2M in tumours from each group removed when tumour volume reached 500 mm^3. GAPDH was used as a reference gene for normalization. Values are the mean of replicates and error bars represent the standard error. Data generated using the methods described in Section 2.7 and Section 2.20.

6.3. Inducible SULF1/2 Gene Silencing in SNU-182 Cells and Effects on Signalling and Cell Growth

6.3.1. Effects of inducible SULF1/2 gene silencing on signalling pathways in SNU-182 cells

As shown in Section 5.3.3, constitutive SULF2 knockdown resulted in inhibition of growth factor/RTK signalling in SNU-182 cell line, and hence the effect of inducible SULF2 suppression was investigated.

Constitutive SULF2 knockdown caused marked inhibition of FGF-1- and FGF-2-induced ERK and IGF-II-induced AKT phosphorylation in SNU-182 cells. However, inducible SULF2 knockdown failed to cause any effect on p-ERK levels induced by FGF-1 or FGF-2, or on p-AKT levels induced by IGF-I (Figure 6.8) or IGF-II (data not shown).

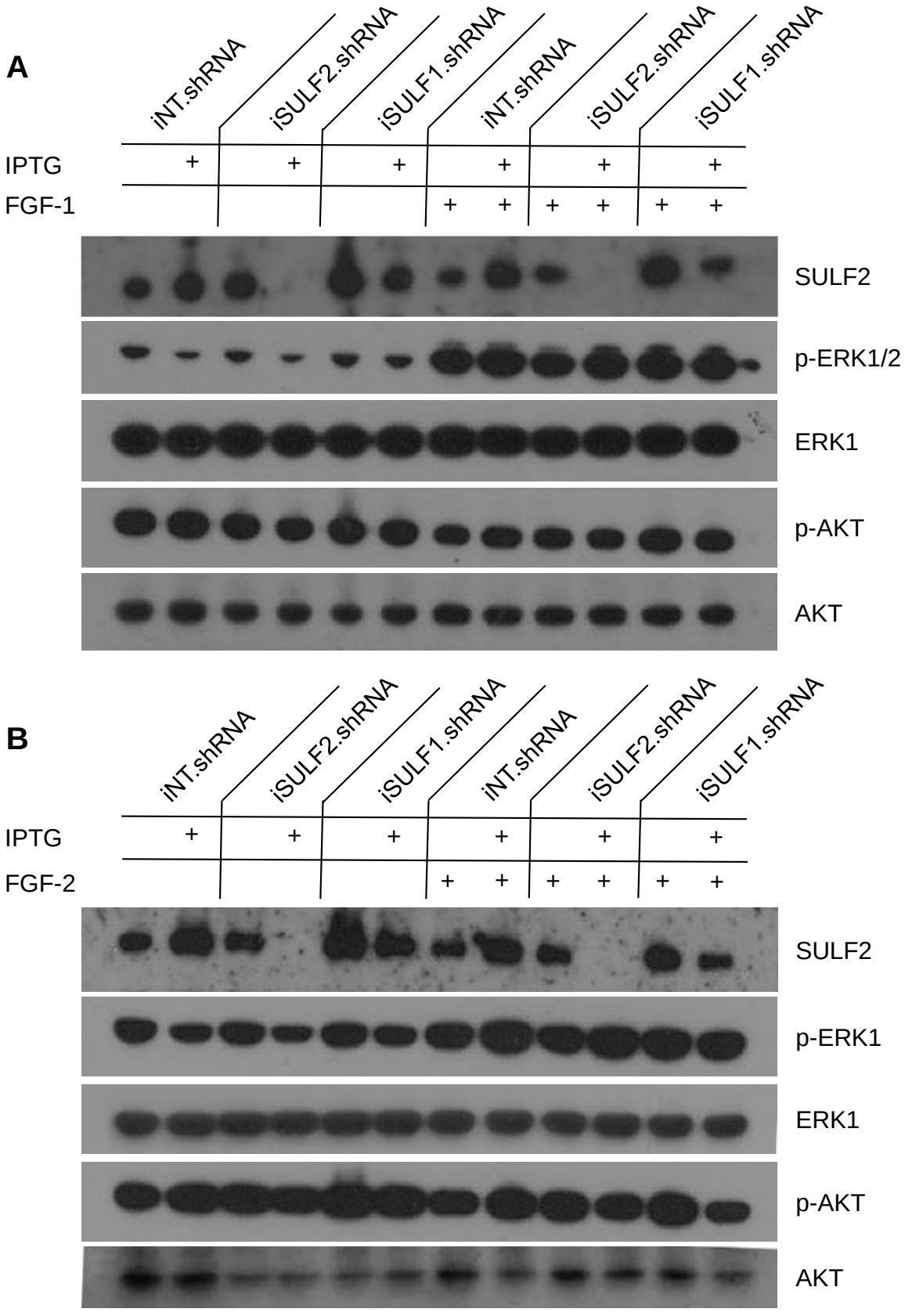
A
iNT.shRNA
iSULF2.shRNA
iSULF1.shRNA
iNT.shRNA
iSULF2.shRNA
iSULF1.shRNA
IPTG
FGF-1
SULF2
p-ERK1/2
ERK1
p-AKT
AKT
B
iNT.shRNA
iSULF2.shRNA
iSULF1.shRNA
iNT.shRNA
iSULF2.shRNA
iSULF1.shRNA
IPTG
FGF-2
SULF2
p-ERK1
ERK1
p-AKT
AKT

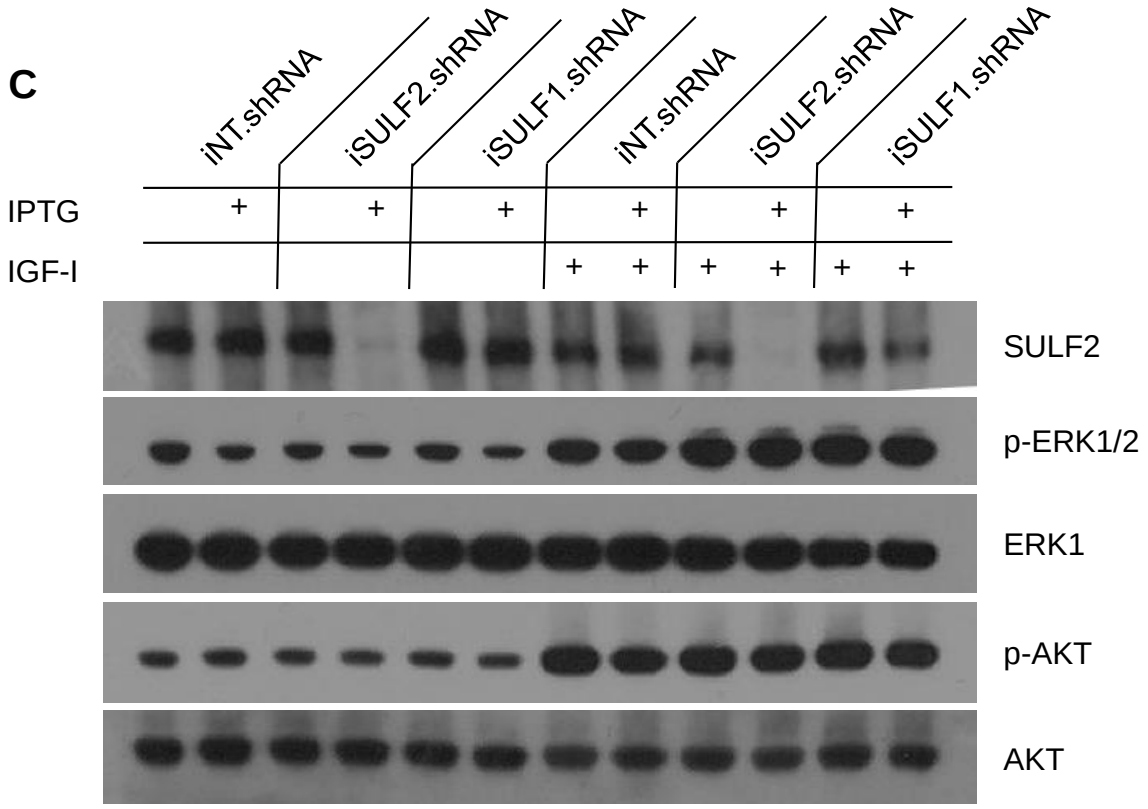

Figure 6.8: Effect of inducible SULF1/2 gene silencing on FGF-1, FGF-2 and IGF-I signalling pathways in SNU-182 cells: SNU-182 cells stably transduced with iNT.shRNA, iSULF2.shRNA or iSULF1.shRNA lentiviral particles were treated with 1 mM IPTG for two days. The cells were serum-starved overnight and then treated with 10 nM FGF-1 **(A)** or FGF-2 **(B)** for 10 min, or IGF-I **(C)** for 5 min. Whole cell lysates were prepared and WB was performed using antibodies against SULF2, p-ERK1/2 or p-AKT. The membranes were stripped and reprobed with antibodies against total ERK1/2 and total AKT serving as loading controls. The experiment was performed in triplicate and representative blots are shown. Data generated using the method described in Section 2.10.

6.3.2. Effects of inducible SULF1/2 gene silencing on growth of SNU-182 cells in vitro

The effect of inducible SULF1/2 knockdown on the growth of SNU-182 cells was also investigated. The cells were treated with IPTG at day 4 to induce shRNA expression. The results showed that neither SULF1 nor SULF2 suppression altered cell growth in 10% (v/v) FBS-containing medium (Figure 6.9) or 1% (v/v) FBS-containing medium (data not shown).

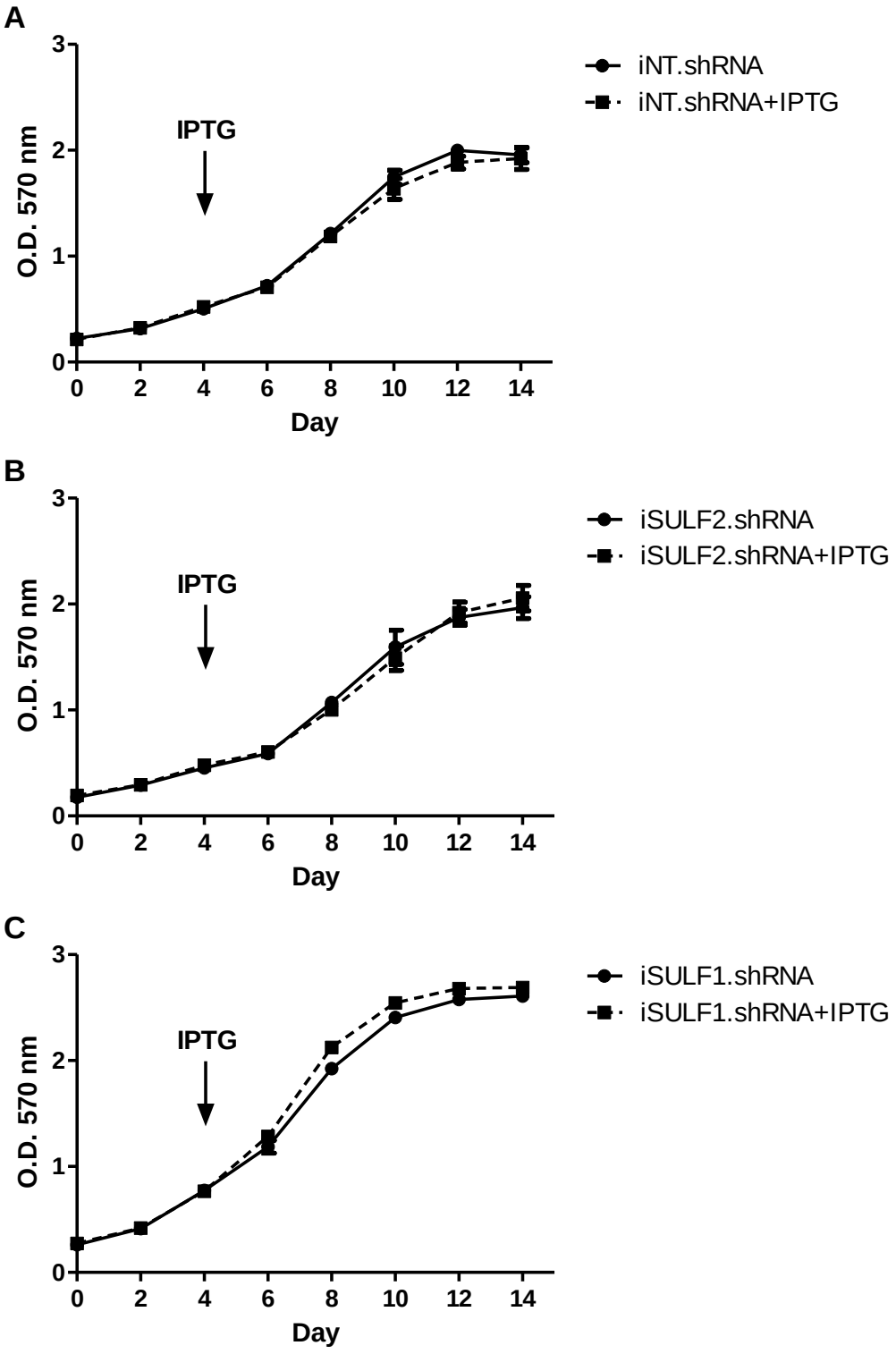

Figure 6.9: Effect of inducible SULF1/2 gene silencing on cell growth in SNU-182 cells: SNU-182 cells were stably transduced with iNT.shRNA **(A)**, iSULF2.shRNA **(B)** or iSULF1.shRNA **(C)** lentiviral particles. 1000 cells/well were seeded into 96-well plates. Cells were treated with IPTG at day 4 and stained with SRB every two days. Values are the mean of six replicates and error bars represent the standard error. The experiment was performed in triplicate. Data generated using the method described in Section 2.17.

6.4. Summary

In summary, the data in Chapter 5 demonstrated that SULF2 plays a role in regulating the growth of HCC cell lines. Further characterisation of the impact of SULF2 suppression using inducible knockdown of either SULF1 or SULF2 was therefore investigated. First, the conditions for inducing the expression of the different shRNAs using IPTG were optimised. The inducible SULF1/2 knockdown was confirmed at the mRNA and protein levels using RT-qPCR and WB. Second, the consequences of inducible SULF1/2 knockdown on signalling and cell growth were explored in HuH-7 and SNU-182 cell lines as these were the two cell lines where constitutive SULF2 knockdown reduced signalling and growth.

In the HuH-7 cell line, inducible SULF2 knockdown inhibited Wnt-3a-stimulated β-catenin-dependent transcriptional activity to a limited extent but had no effect on cell growth *in vitro* or tumourigenicity *in vivo*. In the SNU-182 cell line, neither SULF1 nor SULF2 inducible knockdown affected the growth factor/RTK signalling or cell growth *in vitro*. These results suggest that SULF2 knockdown should be maintained for long time before signalling or phenotypic effects are produced.

Chapter 7. Microarray Gene Expression Analysis Following SULF2 Knockdown in HCC Cell Lines

The data in the preceding chapters demonstrated that SULF2 suppression is clearly associated with biological effects in HCC cell lines. To explore the effect of SULF2 knockdown in HCC cells at the molecular level, as well as potentially identifying biomarkers for SULF2 inhibition, microarray gene expression analysis was performed, using Affymetrix human genome U133 plus 2.0 arrays, consisting of > 54,000 probe sets for the analysis of about 47,400 transcripts and variants including 38,500 characterised genes.

7.1. Effect of SULF2 Knockdown on Gene Expression in HuH-7 Cell Line

Control untransduced HuH-7 cells or the cells that were stably transduced with either NT shRNA or SULF2 shRNA were cultured for 48 hours before being harvested and sent for microarray analysis. The results represent the average of four biologically independent replicates. First, SULF2 knockdown was confirmed by RT-qPCR, and 97% decrease of SULF2 in the SULF2 shRNA-transduced cells demonstrated compared to SULF2 expression in NT shRNA-transduced cells. As noted before, there was upregulation (3-fold in this experiment) of SULF2 in NT shRNA-transduced cells compared to control untransduced cells (Figure 7.1; A), indicating that SULF2 expression may be induced by transducing cells with lentiviral particles or simply reflecting heterogeneity.

Analysis of the microarray experiment, as described in Section 2.22, showed that of the more than 54,000 tested probe sets:

- 1529 probe sets were differentially expressed between NT shRNA-transduced cells and control untransduced cells with ≥ 2-fold change and an adjusted *p* value ≤ 0.01.
- 2561 probe sets were differentially expressed between SULF2 shRNA-transduced cells and control untransduced cells with ≥ 2-fold change and an adjusted *p* value ≤ 0.01.

- 703 probe sets were differentially expressed between SULF2 shRNA-transduced cells and NT shRNA-transduced cells with ≥ 2-fold change and an adjusted *p* value ≤ 0.01.

These data suggest that there were considerable changes in the expression levels of many genes due to transduction with lentiviral particles and/or selection with puromycin, regardless of the expression level of SULF2, as shown by the principal component analysis, reflecting transcriptome differences among the samples (Figure 7.1; B). Therefore, only the genes that were differentially expressed in the SULF2 knockdown cells with ≥ 2-fold change and adjusted *p* value ≤ 0.01, compared to both NT shRNA and control untransduced cells, were taken into consideration for further analysis. This approach identified 444 differentially expressed probe sets, and of these 146 probe sets (representing 111 genes) were downregulated and 298 probe sets (representing 211 genes) were upregulated after SULF2 knockdown (Figure 7.2). A complete list of these differentially expressed probe sets that were downregulated or upregulated after SULF2 knockdown in HuH-7 cells can be found in Appendices A and B, respectively.

As one gene can be involved in more than one pathway, investigation of affected pathways was performed, using GeneSpring 12.6 software, based on WikiPathways analysis (Analysis, Reactome, GenMAPP and Other). Unsurprisingly, given the number of genes affected, SULF2 suppression was found to affect the transcript level of genes belonging to many different pathways (Table 7.1).

The most differentially expressed genes after SULF2 knockdown as compared to both NT shRNA-transduced cells and control untransduced cells are listed with their putative pathways in Table 7.2 (n = 26). To verify the microarray data prior to further study, the most differentially expressed genes that have a potential link to cancer were selected for RT-qPCR analysis (n = 18). These genes are listed in Table 7.2 and labelled in Figure 7.2; B. The RT-qPCR results confirmed the microarray data for all the genes tested, and genes with a potential role in liver carcinogenesis were selected for analysis at the protein level. Seven genes were chosen, five that were upregulated and two that were downregulated after SULF2

knockdown. The upregulated genes were ACE2 (angiotensin I converting enzyme (peptidyl-dipeptidase A) 2), PCDH20 (protocadherin 20), SLPI (secretory leukocyte peptidase inhibitor), TFPI2 (tissue factor pathway inhibitor 2) and WNT5A (wingless-type MMTV integration site family, member 5A). The two genes that were downregulated after SULF2 suppression were MYCN (v-myc myelocytomatosis viral related oncogene, neuroblastoma derived (avian)) and DLK1 (delta-like 1 homolog (Drosophila)).

Unfortunately, only the antibodies for ACE2 and MYCN performed satisfactorily in WB analysis (Figure 7.4). ACE2 was the most differentially expressed gene after SULF2 knockdown, with gene expression inversely correlated with SULF2, as evidenced by both microarray and RT-qPCR data (Figure 7.3; A and B). This effect was confirmed at the protein level, where ACE2 protein was only detected in the SULF2 knockdown cells (Figure 7.4). The expression of MYCN correlated with the expression of SULF2, with downregulation of MYCN mRNA levels (Figure 7.3; A and C) and a reduction in MYCN protein expression (Figure 7.4) after SULF2 knockdown.

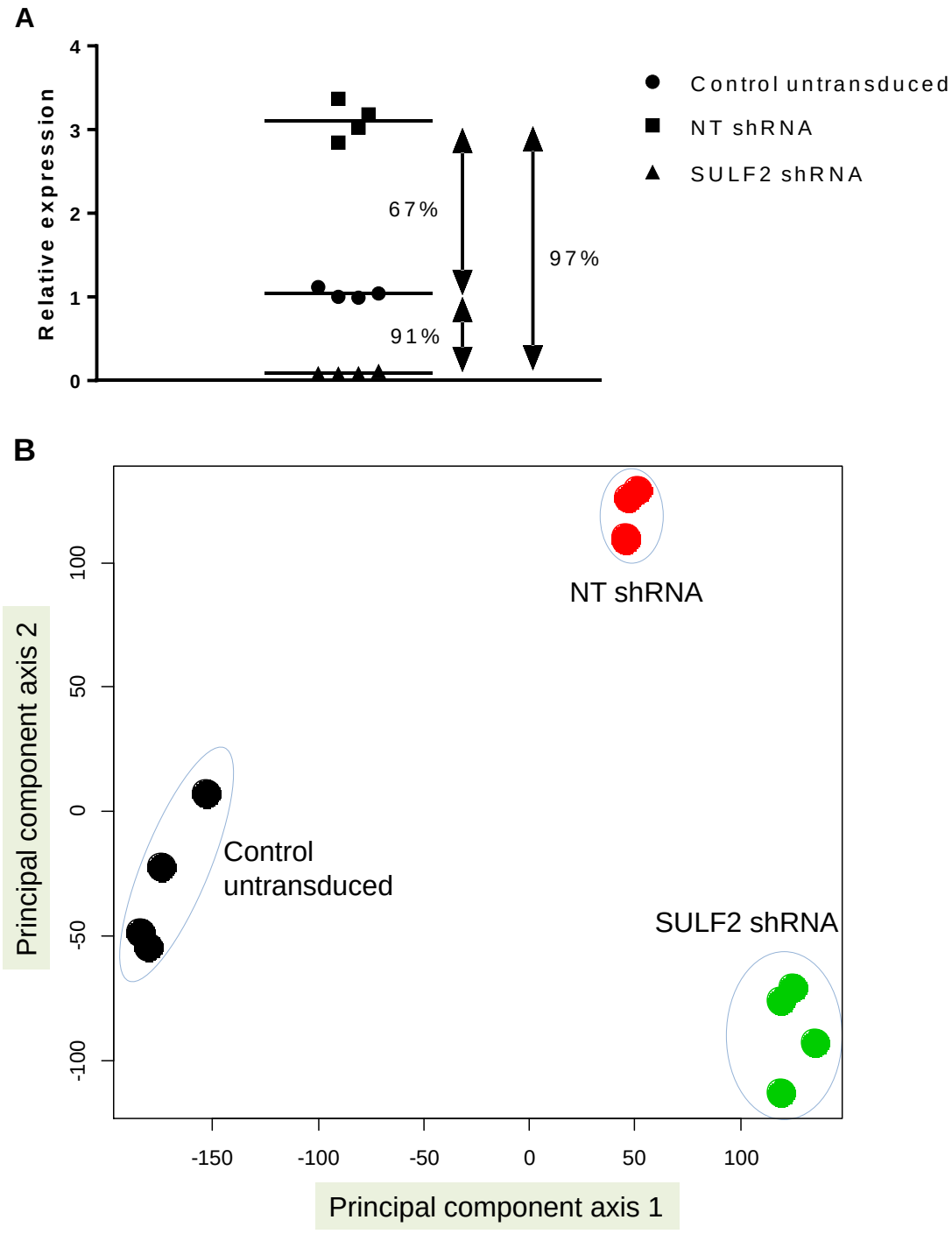

Figure 7.1: SULF2 expression and principal component analysis of HuH-7 cell lines: Control untransduced, NT shRNA-transduced and SULF2 shRNA-transduced HuH-7 cells were cultured for 2 days followed by mRNA extraction. **(A)** RT-qPCR analysis of SULF2 expression using GAPDH as a reference gene. Horizontal lines are the mean of 4 separate replicates of each cell line. **(B)** Principal component analysis plot provided as a 2-dimensional plot showing the transcriptome difference (variation in gene profile) of the samples. Each point is from a separate microarray analysis with 4 separate replicates for each cell line. Data generated using the methods described in Section 2.7 and Section 2.22.

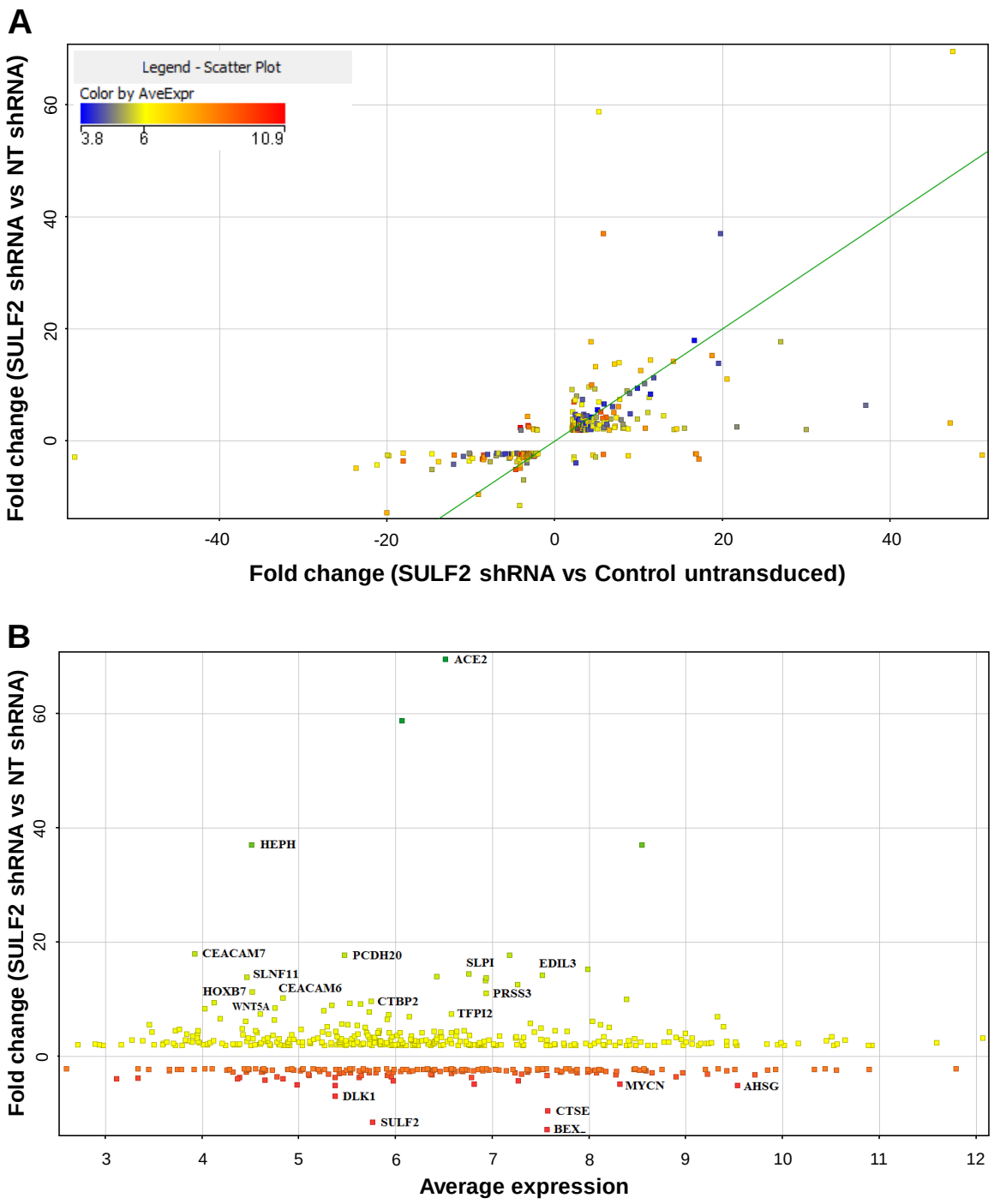

Figure 7.2: Scatter plot display of differentially expressed genes with ≥ 2-fold change and adjusted *p* value ≤ 0.01 after SULF2 knockdown in HuH-7 cells as compared to both NT shRNA-transduced cells and control untransduced cells: (A) Fold change (SULF2 shRNA vs. NT shRNA) was plotted against fold change (SULF2 shRNA vs. Control untransduced). Each dot represents one gene and the colour represents average expression where red colour represents high expression, yellow colour represents medium expression and blue colour represents low expression. **(B)** Fold change (SULF2 shRNA vs. NT shRNA) was plotted against average expression. Genes that were chosen for RT-qPCR analysis are labelled. Data generated using the method described in Section 2.22.

Table 7.1: Gene ontolgies enriched with differentially expressed transcripts after SULF2 knockdown in HuH-7 cell line with ≥ 2-fold change and adjusted *p* value ≤ 0.01 (only the pathways that contain ≥ two affected transcripts are listed).

Pathway	**Matched Entities (S2 vs. NT and Ctrl)**
Hs muscle cell TarBase	10
Hs epithelium TarBase	9
Hs lymphocyte TarBase	9
Hs focal adhesion	8
Hs neural crest differentiation	6
Hs myometrial relaxation and contraction pathways	6
Hs calcium regulation in the cardiac cell	5
Hs adipogenesis	4
Hs integrated pancreatic cancer pathway	4
Hs prostate cancer	4
Hs SIDS susceptibility pathways	4
Hs spinal cord injury	4
Hs metapathway biotransformation	3
Hs EGF-EGFR signalling pathway	3
Hs Wnt signalling pathway and pluripotency	3
Hs G protein signalling pathways	3
Hs GPCRs, class A rhodopsin-like	3
Hs Toll-like receptor signalling pathway	3
Hs microRNAs in cardiomyocyte hypertrophy	3
Hs leukocyte TarBase	3
Hs folate metabolism	3
Hs endochondral ossification	3
Hs GPCR ligand binding	2
Hs senescence and autophagy	2
Hs inflammatory response pathway	2
Hs BDNF signalling pathway	2
Hs regulation of actin cytoskeleton	2

Pathway	Matched Entities (S2 vs. NT and Ctrl)
Hs cell cycle	2
Hs TCR signalling pathway	2
Hs DNA damage response	2
Hs DNA damage response (only ATM dependent)	2
Hs TGF beta signalling pathway	2
Hs ErbB signalling pathway	2
Hs RANKL-RANK signalling pathway	2
Hs GPCR downstream signalling	2
Hs miRNA regulation of DNA damage response	2
Hs selenium pathway	2
Hs cytoplasmic ribosomal proteins	2
Hs integrated breast cancer pathway	2
Hs signalling pathways in glioblastoma	2
Hs vitamin B12 metabolism	2
Hs synaptic vesicle pathway	2
Hs nuclear receptors in lipid metabolism and toxicity	2
Hs matrix metalloproteinases	2
Hs drug induction of bile acid pathway	2
Hs integrin cell surface interactions	2
Hs sphingolipid metabolism	2
Hs Phase II conjugation	2
Hs response to elevated platelet cytosolic Ca2+	2

Ctrl: control untransduced cells; NT: NT shRNA-transduced cells; S2: SULF2 shRNA-transduced cells. Hs: Homo sapiens. SIDS: Sudden infant death syndrome.

Table 7.2: Summary of genes that were most differentially expressed at the mRNA level after SULF2 knockdown in HuH-7 cell line with their fold change values as measured by microarray and RT-qPCR analyses. The minus (-) symbol in front of the fold change value demonstrates gene downregulation. The data represent the mean of quadruplicate determinations.

Gene Symbol	Fold Change (Microarray)			Fold Change (qPCR)			Pathway
	NT vs. Ctrl	S2 vs. Ctrl	S2 vs. NT	NT vs. Ctrl	S2 vs. Ctrl	S2 vs. NT	
ACE2*	-1.5	47	70	-2.4	67	161	Renin-angiotensin system
CEACAM7	-1.2	42	46	high expression for S2 while undetermined expression for NT and Ctrl			Integral to membrane
HEPH	-1.9	20	37	-12	24	289	Mineral absorption
PCDH20	1.5	27	18	1.1	27	24	Cell adhesion
HOXB7*	1.1	15	15	-1.4	86	121	N/A
CA4*	-1.2	10	13				Nitrogen metabolism
CTBP2*	-2.5	4.4	11	-14	9.1	123	Notch and Wnt signalling pathways
GCC2	1.2	19	15				Golgi
PI3*	-1.9	7.7	14				Extracellular region
SLPI	-1.3	11	15	-2.2	38	83	Extracellular region
EDIL3	-1.0	14	14	-1.4	20	27	Cell adhesion
SLFN11	1.4	20	14	7.1	367	52	Nucleus
FAM198B	-2.0	7.1	14				Golgi membrane
PRSS3*	1.8	21	11	3.1	65	21	Protein digestion and absorption
CEACAM6*	1.0	11	10	-1.5	237	350	Integral to membrane
MUC13*	-1.1	8.6	9.0				Extracellular region
HOXB3	1.0	9.8	9.6				Nucleus
TFPI2*	1.0	7.7	7.6	-1.2	13	15	Extracellular region
CCL3 //CCL3L1 //CCL3L3	1.0	8.9	8.6				Senescence and autophagy
ESRP1	1.1	9.5	8.5				N/A
WNT5A*	-2.3	3.3	7.5	-4.4	5.2	23	Wnt and Hedgehog signalling pathways
MYCN	1.1	-4.2	-4.7	1.1	-4.0	-4.5	Transcriptional misregulation in cancer
AHSG*	1.1	-4.7	-5.0	-1.0	-5.8	-5.7	N/A
DLK1	1.8	-3.8	-6.9	1.7	-6.7	-11	N/A
CTSE	1.0	-9.2	-9.5	1.2	-54	-67	Lysosome
BEX1	-1.6	-20	-13	-1.7	-75	-44	N/A
SULF2*	2.8	-4.2	-12	3.0	-11	-34	N/A

* The values are the average of the fold change for the different probe sets used to detect the same gene in the microarray experiment. Ctrl: control untransduced cells; NT: NT shRNA-transduced cells; S2: SULF2 shRNA-transduced cells.

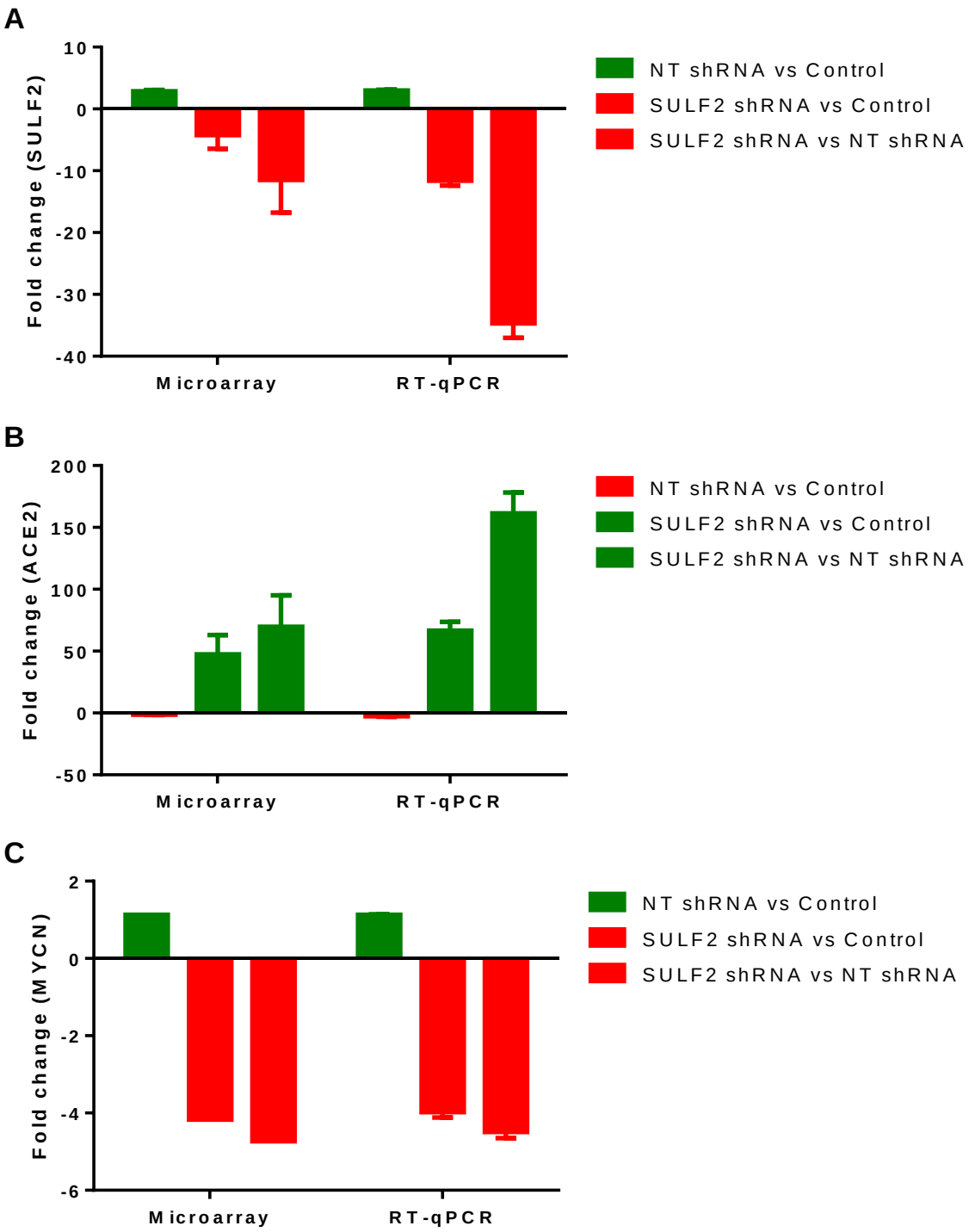

Figure 7.3: mRNA levels of ACE2 and MYCN after SULF2 knockdown in HuH-7 cells: mRNA expression analysis of control untransduced, NT shRNA-transduced and SULF2 shRNA-transduced HuH-7 cells by Affymetrix microarray or RT-qPCR. For RT-qPCR, GAPDH was used as a reference gene. **(A)** SULF2, **(B)** ACE2, **(C)** MYCN. Values are the average of the fold change for the different probe sets used to detect the same gene in the microarray experiment, and values are the mean of the fold change for 4 separate replicates in the RT-qPCR experiment. Error bars represent the standard error. Data generated using the methods described in Section 2.7 and Section 2.22.

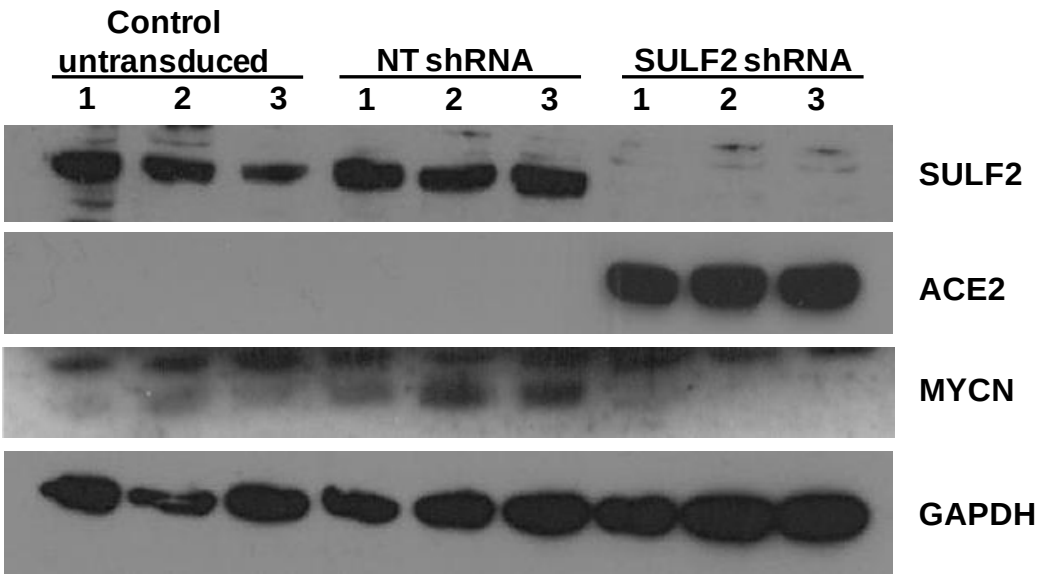

Figure 7.4: Protein levels of ACE2 and MYCN after SULF2 knockdown in HuH-7 cells: Analysis of control untransduced, NT shRNA-transduced and SULF2 shRNA-transduced HuH-7 cells by WB using antibodies against SULF2, ACE2 and MYCN. GAPDH was used as a loading control and samples were loaded as biological triplicates. The experiment was performed in triplicate and a representative blot is shown. Data generated using the method described in Section 2.10.

7.2. Effect of SULF2 Knockdown on Gene Expression in Other Cancer Cell Lines

To determine whether the effects of SULF2 knockdown in the HuH-7 cell line were cell type-specific, studies were performed in three additional cell lines. The first was the HCC cell line SNU-182, where there was inhibition of growth factor/RTK signalling pathway after SULF2 knockdown, and reduced cell proliferation after either SULF1 or SULF2 knockdown. The second cell line was the pancreatic cancer cell line BxPC3 that expresses high level of SULF2 but a low level of SULF1. SULF2 knockdown in this cell line was shown at the mRNA (Figure 7.6; A) and protein level (Figure 7.6; B). Cell growth *in vitro* was inhibited (Figure 7.6; C and D) and tumour growth was slightly delayed after SULF2 knockdown (Figure 7.6; E), in line with the findings of a previous study (Nawroth et al., 2007). The third cell line was the HCC cell line SNU-475. This cell line expresses both SULF1 and

SULF2 at low levels, and knockdown of either SULF1/2 genes had no effect on the proliferation of the SNU-475 cells (data not shown).

RT-qPCR analysis was performed in the 3 additional cell lines using primers for the genes that were differentially expressed after SULF2 knockdown in HuH-7 cell line, and had potential links to cancer. In the SNU-182 cell line, a small upregulation of SULF2 was observed in the NT shRNA-transduced cells in comparison to control untransduced cells (1.7-fold). SULF2 was markedly downregulated in the SULF2 shRNA-transduced cells, and there was a small downregulation of SULF2 expression in the SULF1 shRNA-transduced cells (98% and 68% vs. NT shRNA-transduced cells, respectively). Only SULF1 was downregulated in the SULF1 shRNA-transduced cells (70% vs. NT shRNA-transduced cells) (Table 7.3). SULF2 knockdown was confirmed at the protein level in these samples by WB (Figure 7.5).

Of these genes that were downregulated after SULF2 knockdown in the HuH-7 cell line, only three genes were affected in the SNU-182 cell line (i.e., ACE2, MYCN and DLK1). ACE2 was upregulated (≥ 1.5-fold) after SULF2 suppression and downregulated (≥ 1.9-fold) after SULF1 suppression in SNU-182 cell line, while both MYCN and DLK1 were downregulated (≥ 1.5-fold) after both SULF1 and SULF2 suppression (Table 7.3).

Other genes that have been reported to have role in liver carcinogenesis were also examined in SNU-182 cell line. GPC3 was dramatically downregulated after either SULF1 or SULF2 suppression, while GPC4 was downregulated (2-fold) and matrix metalloproteinase 9 (MMP9) was upregulated (> 2-fold) after SULF1 suppression only (Table 7.3). In addition, the gene encoding the angiotensin II type 1 receptor, AGTR1, was downregulated (> 2-fold), while the hedgehog-interacting protein (HHIP) that antagonizes hedgehog (Hh) signalling was upregulated (≥ 1.9-fold) after SULF2 knockdown (Table 7.3).

With respect to BxPC3 and SNU-475 cell lines, of the genes tested the only one that showed differential expression in either HuH-7 or SNU-182 cell lines that

showed any change after SULF1/2 knockdown was ACE2, and then only in BxPC3 cells where it was upregulated ≥ 2.2-fold after SULF2 knockdown (Figure 7.6; A).

Table 7.3: RT-qPCR analysis of the effect of SULF2 knockdown in SNU-182 cells. The minus (-) symbol in front of the fold change value demonstrates gene downregulation. The data represent the mean of quadruplicate determinations, and numbers in **bold** indicate the genes that were discussed in the thesis.

Gene Symbol	**Fold Change (qPCR)**						**Pathway**
	NT vs. Ctrl	S2 vs. Ctrl	S2 vs. NT	S2 vs. S1	S1 vs. Ctrl	S1 vs. NT	
ACE2	1.9	**2.7**	**1.5**	**5.3**	**-1.9**	**-3.6**	Renin-angiotensin system
CEACAM7	Not expressed						Integral to membrane
HEPH	Not expressed						Mineral absorption
PCDH20	Weakly expressed						Cell adhesion
HOXB7	1.4	1.0	-1.4	-1.3	1.3	-1.1	N/A
CTBP2	1.2	1.2	1.0	1.2	-1.1	-1.2	Notch and Wnt signalling pathways
SLPI	-1.6	-1.8	-1.1	1.2	-2.1	-1.3	Extracellular region
EDIL3	1.1	1.2	1.1	-1.2	1.4	1.3	Cell adhesion
SLFN11	Not expressed						Nucleus
PRSS3	Weakly expressed						Protein digestion and absorption
CEACAM6	Not expressed						Integral to membrane
TFPI2	1.2	-1.0	-1.3	-2.1	2.1	1.7	Extracellular region
WNT5A	1.5	1.3	-1.2	1.2	1.1	-1.5	Wnt and Hedgehog signalling pathways
MYCN	-1.2	**-1.7**	**-1.5**	1.2	**-2.1**	**-1.8**	Transcriptional misregulation in cancer
AHSG	Not expressed						N/A
DLK1	1.4	**-1.5**	**-2.1**	1.5	**-2.1**	**-3.0**	N/A
CTSE	Not expressed						Lysosome
BEX1	-7.9	-11	-1.4	-2.2	-4.9	1.6	N/A
SULF2	1.7	**-40**	**-66**	**-22**	-1.9	**-3.1**	N/A
SULF1	-1.3	-1.4	-1.1	**3.1**	**-4.3**	**-3.3**	N/A
GPC3	-1.6	**-23**	**-15**	2.8	**-65**	**-41**	Proteoglycans in cancer
GPC4	-1.2	-1.3	-1.1	**2.0**	**-2.7**	**-2.2**	Wnt signalling pathway
MYC	1.0	1.5	1.4	-1.0	1.5	1.4	Pathways in cancer
CCND1	1.3	1.0	-1.3	1.3	-1.3	-1.6	Pathways in cancer
ACE	1.2	1.3	1.0	1.5	-1.2	-1.4	Renin-angiotensin system

AGTR1	1.8	**-2.4**	**-4.3**	**-2.6**	1.1	-1.6	Renin-angiotensin system
FOXO1	-1.0	1.0	1.1	-1.2	1.2	1.2	Transcriptional misregulation in cancer
VEGFA	1.3	2.4	1.9	1.5	1.6	1.2	VEGF signalling pathway
Gene Symbol	**Fold Change (qPCR)**						**Pathway**
	NT vs. Ctrl	S2 vs. Ctrl	S2 vs. NT	S2 vs. S1	S1 vs. Ctrl	S1 vs. NT	
MMP2	1.2	-1.1	-1.3	-1.4	1.3	1.1	Pathways in cancer
MMP9	-1.0	-1.5	-1.5	**-3.9**	**2.7**	**2.7**	Pathways in cancer
HHIP	1.0	**2.4**	**2.4**	**1.9**	1.2	1.2	Hedgehog signalling pathway
GLI1	-1.9	-1.9	1.0	-1.1	-1.6	1.1	Hedgehog signalling pathway

Ctrl: control untransduced cells; NT: NT shRNA-transduced cells; S2: SULF2 shRNA-transduced cells.

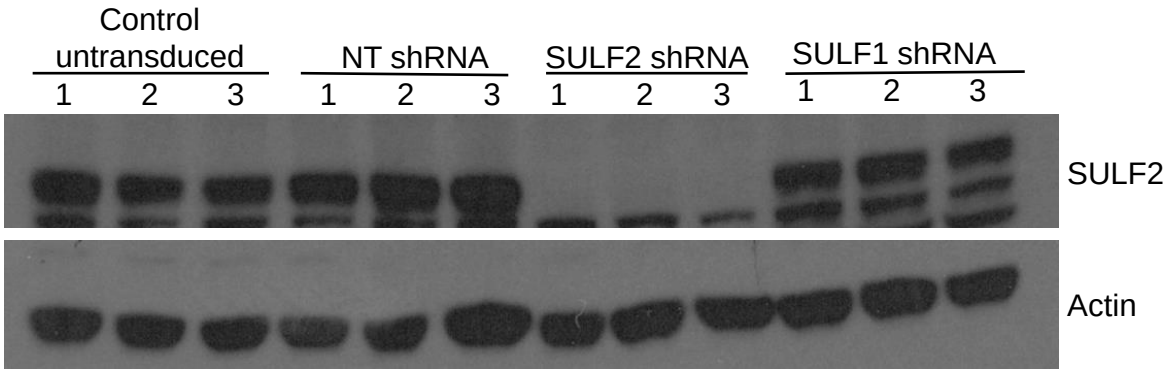

Figure 7.5: SULF2 protein levels after SULF1/2 knockdown in SNU-182 cells: Cell lysates were prepared from control untransduced, NT shRNA-transduced, SULF2 shRNA-transduced and SULF1 shRNA-transduced SNU-182 cells and WB was performed using antibody against SULF2 (Serotec). Actin was used as a loading control and samples were loaded as biological triplicates. The experiment was performed in triplicate and a representative blot is shown. Data generated using the method described in Section 2.10.

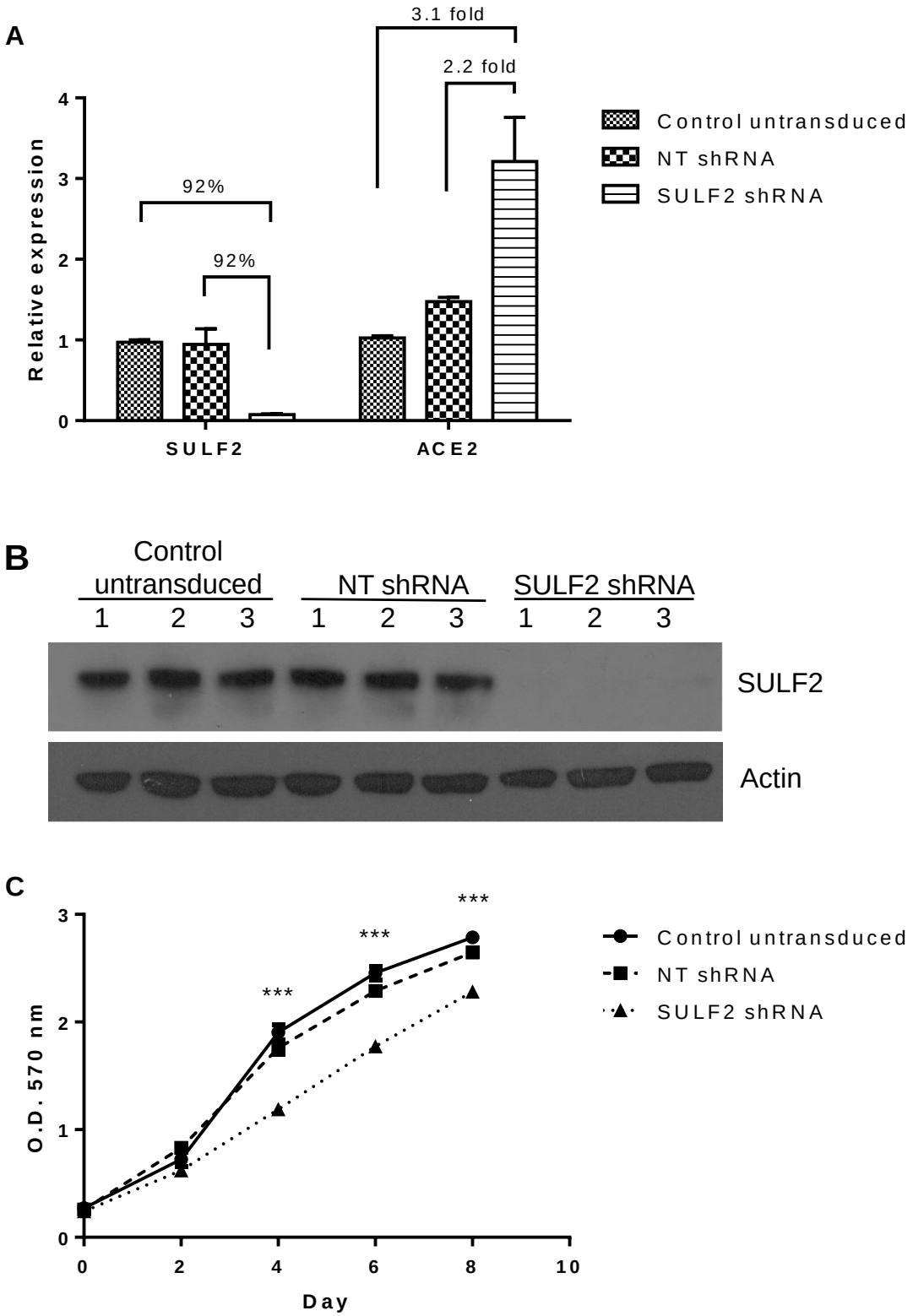
A
3.1 fold
2.2 fold
92%
92%
Relative expression
4
3
2
1
0
SULF2
ACE2
Control untransduced
NT shRNA
SULF2 shRNA
B
Control untransduced
NT shRNA
SULF2 shRNA
1 2 3 1 2 3 1 2 3
SULF2
Actin
C
***
***
***
O.D. 570 nm
3
2
1
0
0 2 4 6 8 10
Day
Control untransduced
NT shRNA
SULF2 shRNA

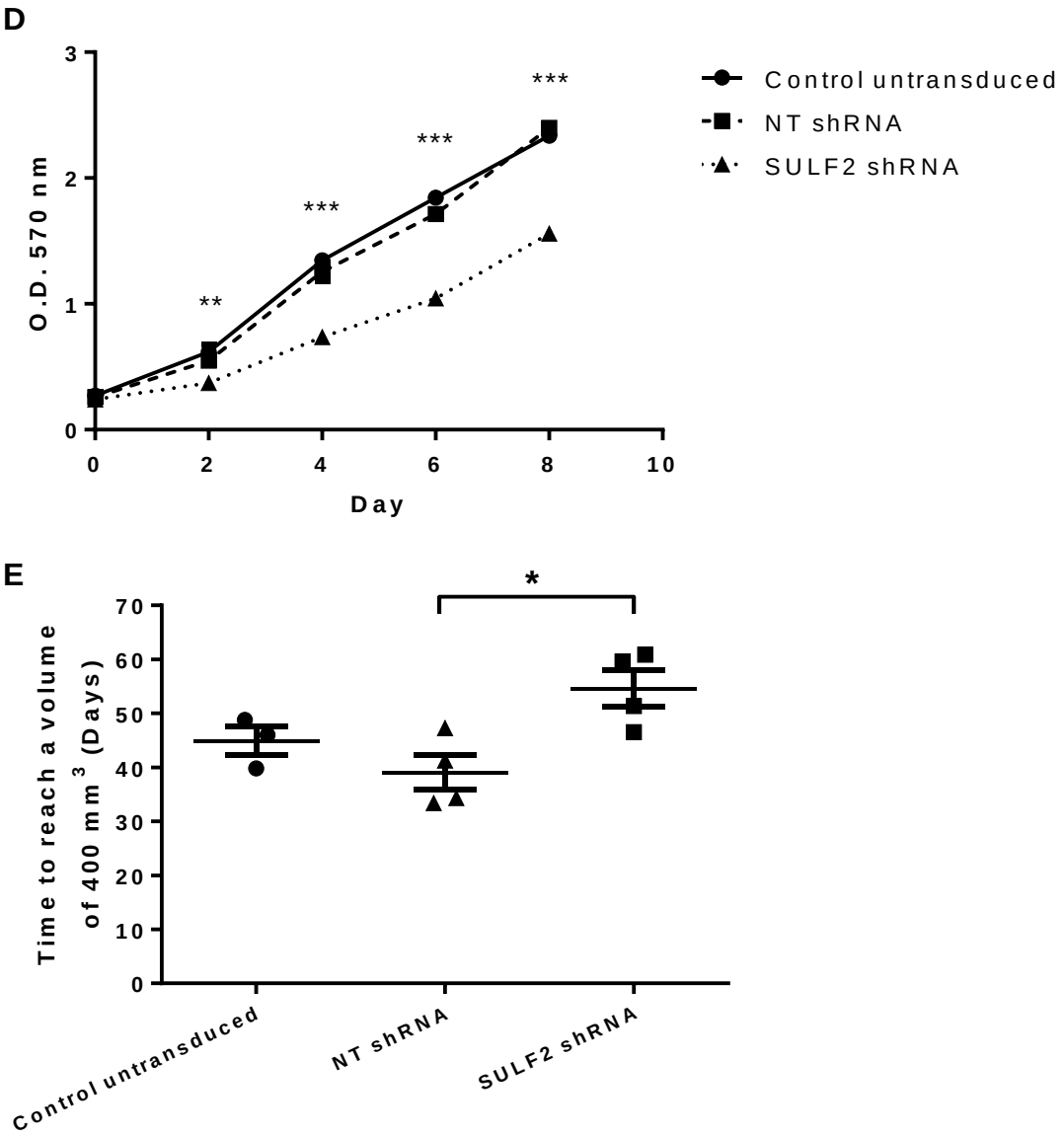

Figure 7.6: Effect of SULF2 gene silencing in BxPC3 cells: BxPC3 cells were stably transduced with either NT shRNA or SULF2 shRNA lentiviral particles. **(A)** RT-qPCR analysis using SULF2 and ACE2 primers. GAPDH was used as a reference gene for normalization. Values are the mean of triplicates and error bars represent the standard error. **(B)** WB analysis of cell lysates using SULF2 Ab (Serotec). Actin was used as a loading control. Samples were loaded as biological triplicates. **(C and D)** SRB assay of cell growth in 10% FBS **(C)** or 1% FBS **(D)** containing medium. Values are the mean of six replicates and error bars represent the standard error. ** *p* value = 0.003, *** *p* value < 0.0001, one-way ANOVA. Experiments (A-D) were performed in triplicate. **(E)** $5x10^6$ cells were resuspended in Matrigel and implanted subcutaneously into the right flank of 5 nude mice for each cell line, and the tumour volume measured 3 times a week using a digital caliper. The horizontal lines are the mean of replicates and error bars represent the standard error. * *p* value = 0.017, 2-sample t-test. Data are from a single experiment. Data generated using the methods described in Sections 2.6, 2.7, 2.10, 2.17 and 2.20.

7.3. Effect of the ACE2/Ang-(1-7)/Mas Receptor Axis in HuH-7 Cells

As shown in Section 7.1, there was a pronounced upregulation of ACE2 in SULF2 knockdown HuH-7 cells at both the mRNA and protein levels, hence experiments were performed to (1) determine the percentage of SULF2 knockdown cells overexpressing ACE2; (2) establish if the overexpressed ACE2 enzyme was catalytically active; and (3) explore the role of ACE2 in mediating the downstream biological consequences observed after prolonged SULF2 knockdown in HuH-7 cells.

ACE2 is an ectoenzyme that is present at the cell surface and can also be secreted. To determine the percentage of ACE2-positive cells and to explore the localization of the enzyme, cells were examined using the ImageStream^X imaging flow cytometer, as described in Section 2.23. Unfortunately, none of the SULF2 antibodies available were suitable for analysis using this equipment; however, the anti-ACE2 antibody worked well. Forty-five % of the SULF2 knockdown cells were ACE2-positive with a mean fluorescence intensity (FI) of 135,400 (median 105,195). This percentage was much higher than that of ACE2-positive cells in the control untransduced cells (10%), which had a mean FI of 110,753 (median 60,404), and also much higher than the NT shRNA-transduced cells (4%), which had a mean FI of 107,524 (median 60,199) (Figure 7.7; B-D). In addition, the analysis confirmed the membranous localization of ACE2 enzyme in all ACE2-positive cells (Figure 7.7; F).

A

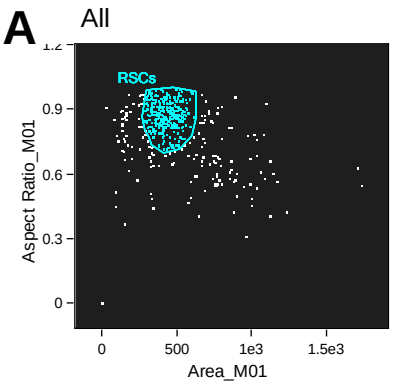

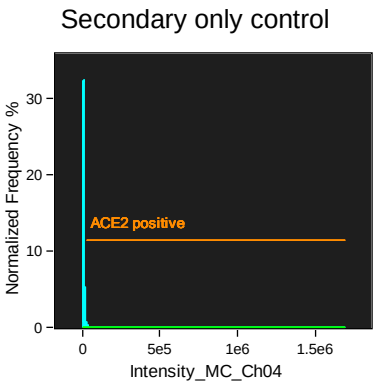

Area_M01, Aspect Ratio_M01

Population	Count	%Gated
All	487	100
RSCs	301	61.8

Intensity_MC_Ch04

Population	Count	%Gated
RSCs	301	100
ACE2 positive & RSCs	1	0.33

B

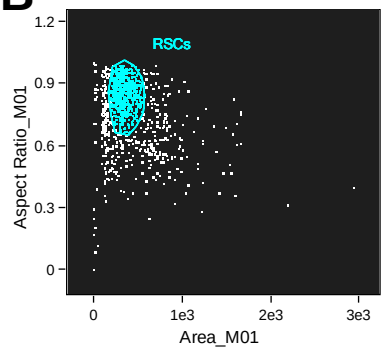

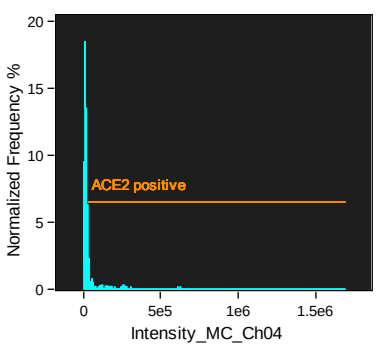

Area_M01, Aspect Ratio_M01

Population	Count	%Gated
All	1090	100
RSCs	621	57

Intensity_MC_Ch04

Population	Count	%Gated	Mean	Median
RSCs	621	100	26279.35	16520.78
ACE2 positive & RSCs	64	10.3	110752.55	60404.26

C

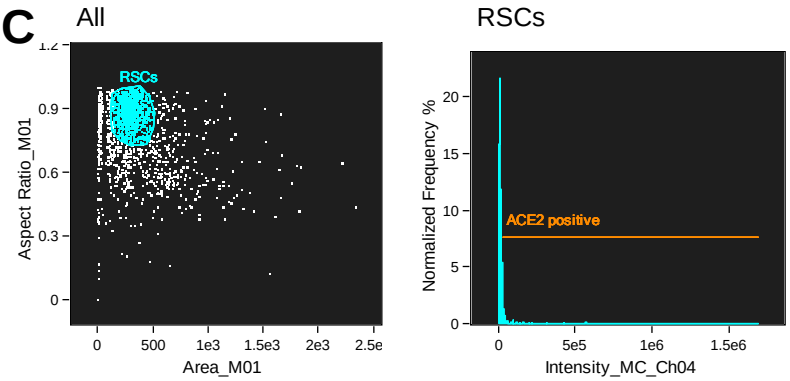

Area_M01, Aspect Ratio_M01

Population	Count	%Gated
All	1848	100
RSCs	911	49.3

Intensity_MC_Ch04

Population	Count	%Gated	Mean	Median
RSCs	911	100	17778.79	13569.87
ACE2 positive & RSCs	36	3.95	107523.53	60199.27

D

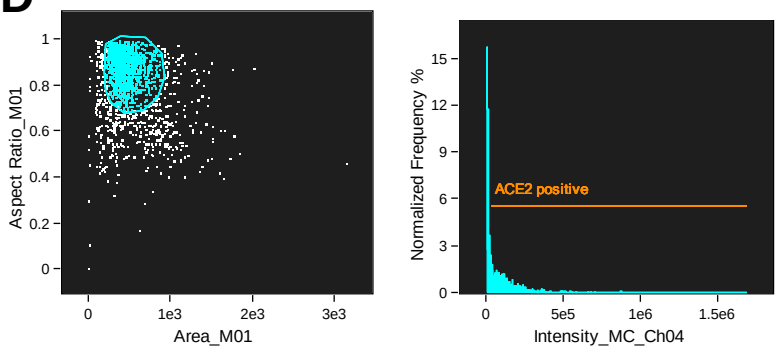

Area_M01, Aspect Ratio_M01

Population	Count	%Gated
All	1844	100
RSCs	1306	70.8

Intensity_MC_Ch04

Population	Count	%Gated	Mean	Median
RSCs	1306	100	68498.28	27964.14
ACE2 positive & RSCs	593	45.4	135400.19	105194.66

E

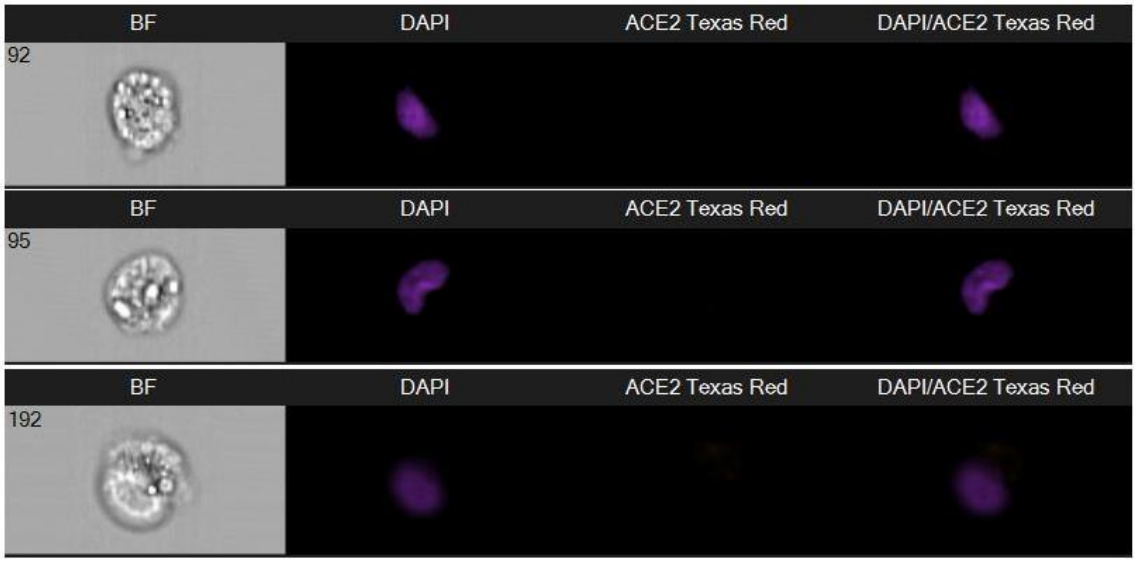

F

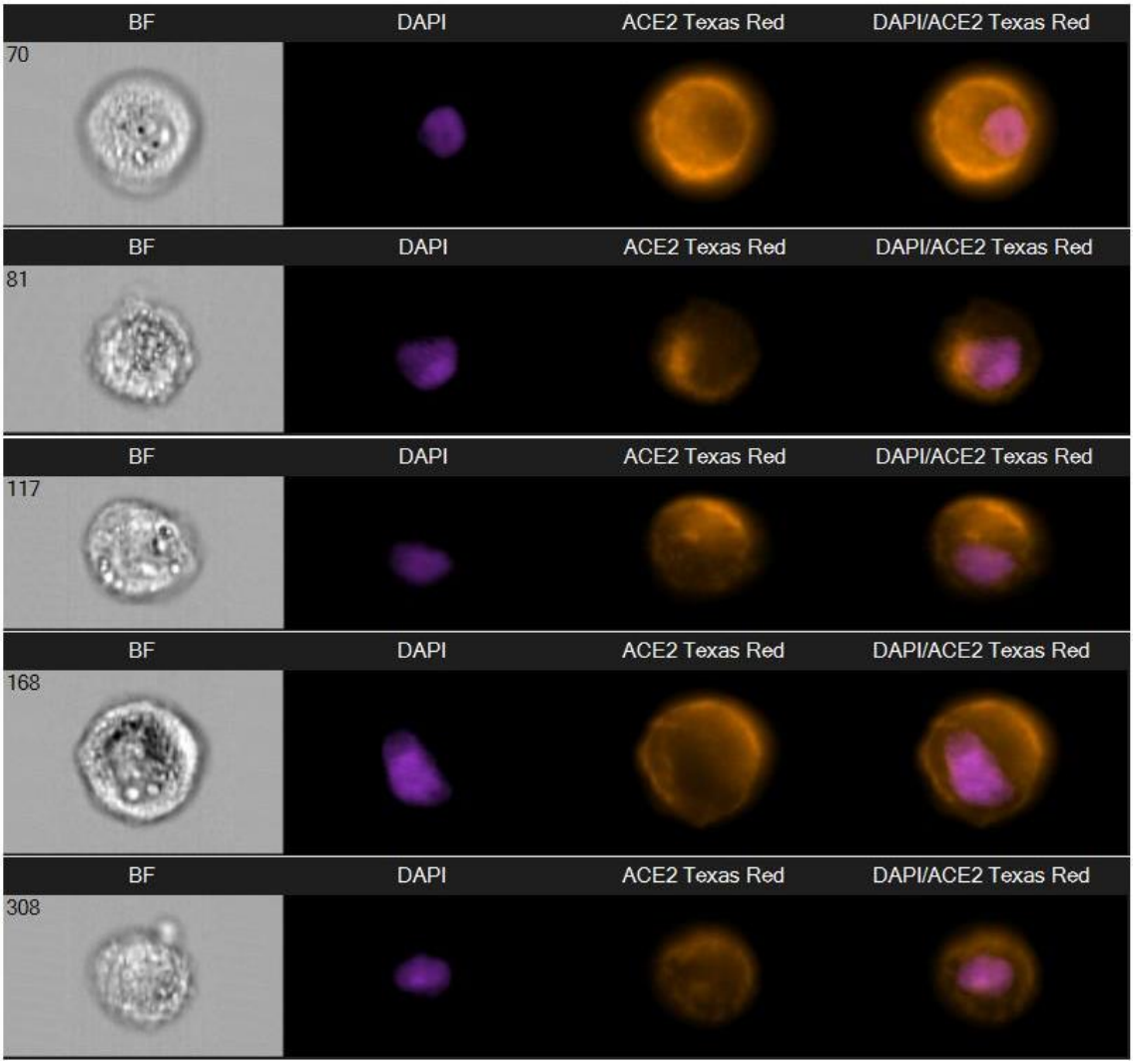

Figure 7.7: Flow cytometry analysis of the expression and localization of ACE2 after SULF2 knockdown in HuH-7 cells: Control untransduced, NT shRNA-transduced and SULF2 shRNA-transduced cells were trypsinized and a single cell suspension fixed, permeabilized, incubated with ACE2 antibody and then stained with Texas Red secondary antibody followed by analysis using ImageStream^X imaging flow cytometer. **(A-D)** Left panel is gating for round single cells (RSCs) using aspect ratio of cells on the y axis and cell area on the x axis. Right panel is frequency histograms of RSCs using frequency on the y axis and fluorescence intensity of Texas Red on the x axis. **(A)** Secondary antibody only control used to set the gate for ACE2 expression. **(B)** Control untransduced cells. **(C)** NT shRNA-transduced cells. **(D)** SULF2 shRNA-transduced cells. **(E)** Representative images of ACE2-negative SULF2 knockdown cells. **(F)** Representative images of ACE2-positive SULF2 knockdown cells. BF: Bright field, DAPI: Blue channel for DAPI staining of nuclei. The experiment was performed in triplicate. Data generated using the method described in Section 2.23.

Angiotensin II (Ang II) is a proliferation-promoting peptide that acts on the Ang II type 1 receptor (AT1R). ACE2 converts Ang II into another biologically active peptide called angiotensin 1-7 or Ang-(1-7). Ang-(1-7) stimulates the Mas receptor which is associated with an anti-proliferative effect (Santos et al., 2003) (Tallant and Clark, 2003) (Tallant et al., 2005). To test the enzymatic activity of ACE2 in HuH-7 cells, the fluorogenic peptide substrate Mca-Tyr-Val-Ala-Asp-Ala-Pro-Lys(Dnp)-OH was used as described in Section 2.24. This substrate has a highly fluorescent group, Mca (7-methoxycoumarin-4-yl acetyl), that is quenched by a Dnp (2,4-dinitophenyl) group. ACE2 can cleave the peptide bond between proline and lysine amino acids of the fluorogenic peptide, producing measurable fluorescence (Vickers et al., 2002). Firstly, this substrate was tested against recombinant human ACE2 (rhACE2). The experiment confirmed a concentration- and time-dependent increase in fluorescence, in keeping with ACE2 activity, that reached a plateau when a high concentration of the enzyme was used (Figure 7.8; A). Next, cell lysates of control untransduced, NT shRNA-transduced and SULF2 shRNA-transduced HuH-7 cells were incubated with this substrate and fluorescence was read in a kinetic mode. Assessment of the data revealed higher enzymatic activity of SULF2 knockdown cell lysate as compared to the control untransduced or NT shRNA-transduced cell lysates (Figure 7.8; B). As the Mca-Tyr-Val-Ala-Asp-Ala-Pro-Lys(Dnp)-OH substrate can also be cleaved by caspase-1 and interleukin-converting enzyme (Enari et al., 1996), a more specific ACE2 substrate was used, namely Mca-Ala-Pro-Lys (Dnp)-OH (Vickers et al., 2002). This latter substrate has a shorter peptide sequence and the same fluorochrome as the longer peptide substrate. The results were in line with the previous data and showed that SULF2 knockdown cells had higher ACE2 activity, in keeping with the overexpressed ACE2 being active in these cells (Figure 7.8; C).

Given that ACE2 converts Ang II into Ang-(1-7), the control untransduced HuH-7 cells and those transduced with NT shRNA or SULF2 shRNA were treated with or without Ang II and the level of Ang-(1-7) was measured in culture medium as described in Section 2.25. Serum-free medium was used to avoid any effect due to enzymes present in FBS that might metabolise Ang II. The study showed that basal levels of Ang-(1-7) were not detected in the culture medium of any of the 3

HuH-7 cell lines. However, in the cells treated with Ang II, the concentration of Ang-(1-7) was 3-fold higher in the culture medium from SULF2 knockdown cells (154 pg/ml) in comparison to medium from control untransduced cells (56 pg/ml) or NT shRNA-transduced cells (48 pg/ml) (Figure 7.9), further supporting the catalytically active nature of the overexpressed ACE2 enzyme in the SULF2 knockdown cells.

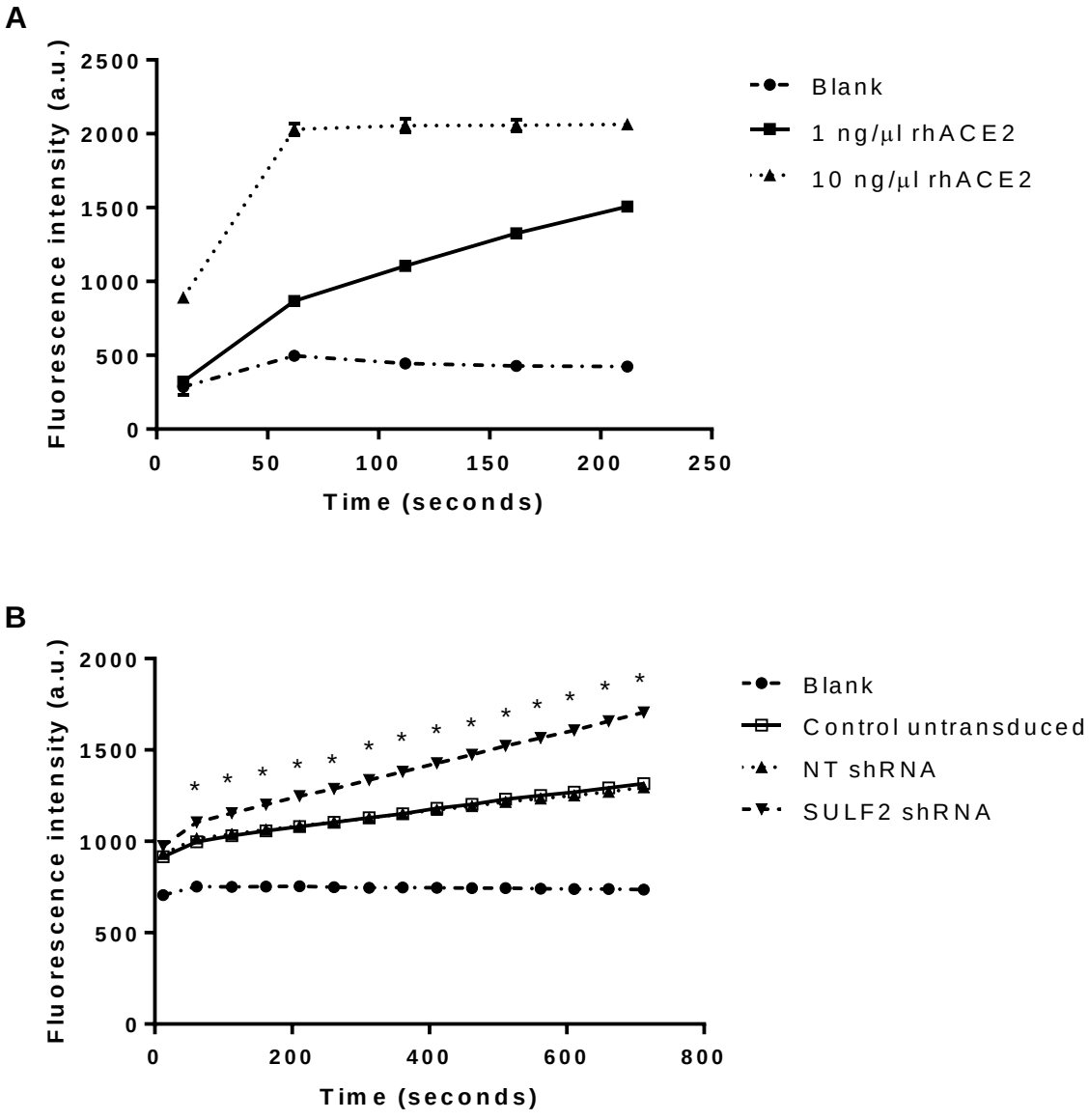

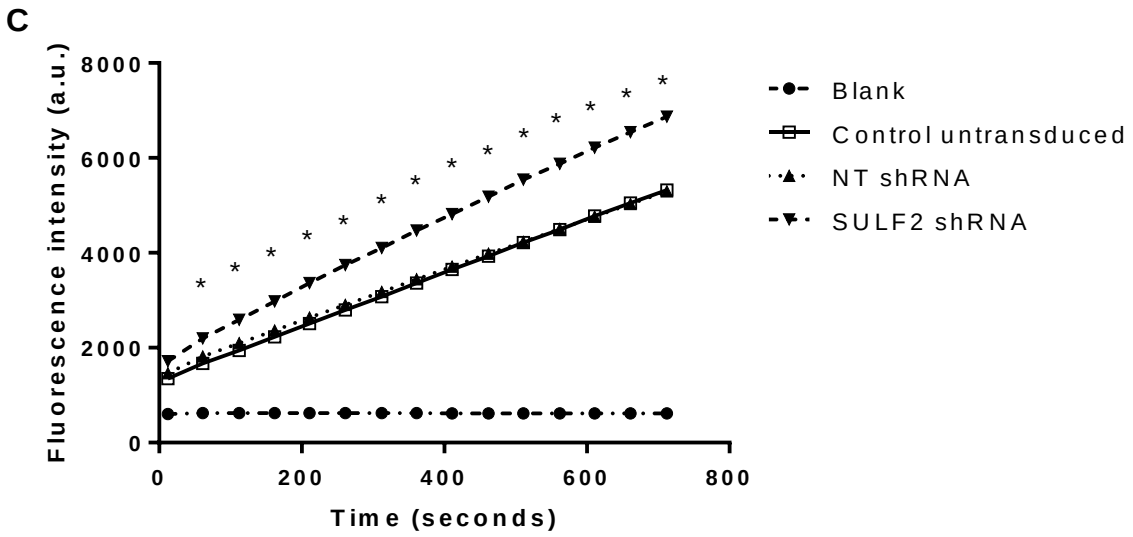

Figure 7.8: The activity of ACE2 after SULF2 knockdown in HuH-7 cells: 100,000 control untransduced HuH-7 cells or those transduced with NT shRNA or SULF2 shRNA were cultured in 12-well plate and cell lysates prepared. Substrate, either Mca-Tyr-Val-Ala-Asp-Ala-Pro-Lys(Dnp)-OH **(A and B)** or Mca-Ala-Pro-Lys(Dnp)-OH **(C)**, was diluted in assay buffer to give a concentration of 40 µM and added to recombinant ACE2 protein or cell lysates and the fluorescence was read at 450 nm after excitation at 355 nm. **(A)** rhACE2 at 1 or 10 ng/µl final concentration. **(B and C)** cell lysates. Blank is samples containing no cell lysates. Values are the mean of triplicates and error bars represent the standard error. The experiment was performed in triplicate. * *p* value < 0.05, one-way ANOVA. Data generated using the method described in Section 2.24.

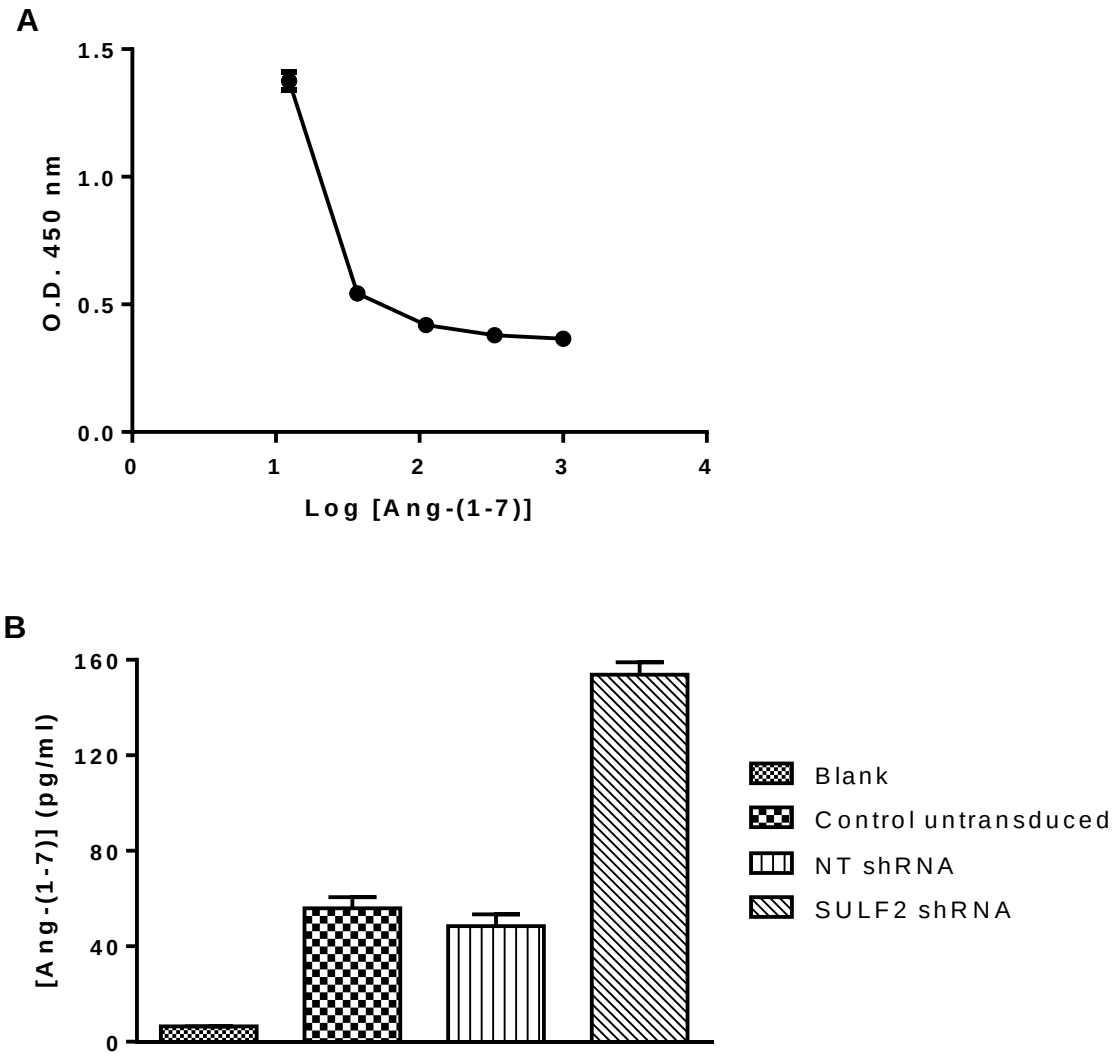

Figure 7.9: Metabolism of exogenous Ang II by the HuH-7 cell lines: 100,000 control untransduced HuH-7 cells or those transduced with NT shRNA or SULF2 shRNA were cultured in 6-well plates and serum-starved overnight followed by treatment with 10 µM Ang II for 1 hour. Culture medium was collected and filtered through a cellulose membrane with 10,000 kDa molecular weight cut-off. The Ang-(1-7) levels were measured using a competitive inhibition enzyme immunoassay. **(A)** Standard curve of Ang-(1-7) where the optical density readings at 450 nm were plotted against the log of standard concentrations in pg/ml. **(B)** Concentration of Ang-(1-7) in culture medium. Blank is medium that was not incubated with cells. Values are the mean of quadruplicates and error bars represent the standard error. The experiment was performed in triplicate. Data generated using the method described in Section 2.25.

The effect of Ang II and Ang-(1-7) on the growth of HuH-7 cells was investigated. It was hypothesized that Ang II would promote the proliferation of control untransduced and NT shRNA-transduced cells, but not SULF2 knockdown cells owing to its conversion into the anti-proliferative peptide Ang-(1-7) by ACE2 in these cells. Conversely, Ang-(1-7) would inhibit the proliferation of all 3 HuH-7 cell lines; control untransduced cells, NT shRNA-transduced cells and SULF2 knockdown cells. In fact, neither Ang II nor Ang-(1-7) had an effect on the proliferation of any of the HuH-7 cell lines, in 10% (v/v) or 1% (v/v) FBS-containing medium, at concentrations up to 10 µM of either peptide (Figure 7.10). It was not possible to culture these cells in serum-free medium due to the poor growth and survival of HuH-7 cells in the absence of FBS.

One possible explanation for the lack of effect of Ang-(1-7) in these cells is the low level of expression of the MAS1 gene, which encodes the Mas receptor, in the HuH-7 cell line, as shown by RT-qPCR analysis (Ct value of 36 for MAS1 compared to Ct value of 17 for GAPDH). However, the ACE2 enzyme expressed by SULF2 knockdown HuH-7 cells and its product Ang-(1-7) could still affect endothelial cells *in vivo*, and hence angiogenesis and this may explain the complete inhibition of tumourigenicity of SULF2 knockdown HuH-7 cells in nude mice.

Neither inducible nor transient SULF2 knockdown in the HuH-7 cell line caused any increase in ACE2 expression as assessed by RT-qPCR (data not shown), and this could explain, in addition to the weak inhibition of Wnt signalling resulting from inducible SULF2 suppression, the lack of inducible SULF2 knockdown effect on the tumourigenicity of HuH-7 cells *in vivo*.

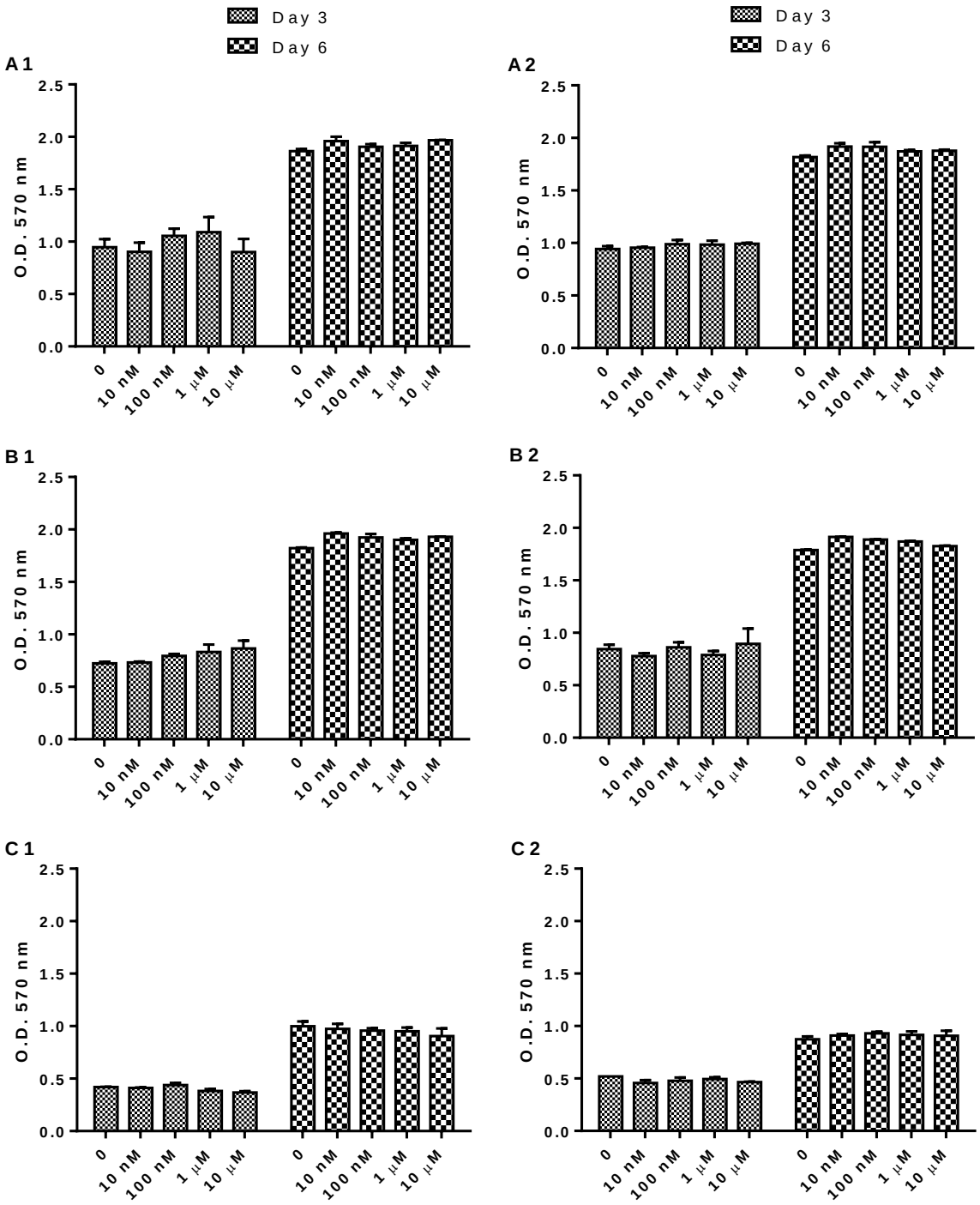

Figure 7.10: Effect of Ang II or Ang-(1-7) on the growth of HuH-7 cells: 2,000 control untransduced HuH-7 cells or those transduced with NT shRNA or SULF2 shRNA were cultured in 96-well plates in 10% (v/v) FBS-containing medium. The cells were treated with different concentrations of Ang II or Ang-(1-7) for 3 or 6 days. Cells were stained with SRB stain and the optical density at 570 nm was measured. **(A)** Control untransduced cells. **(B)** NT shRNA-transduced cells. **(C)** SULF2 shRNA-transduced cells. **(1)** Ang II-treated cells. **(2)** Ang-(1-7)-treated cells. Values are the mean of triplicates and error bars represent the standard error. The experiment was performed in triplicate. Data generated using the method described in Section 2.17.

7.4. Summary

Microarray gene expression analysis was performed in the HuH-7 cell line model to further understand the biology of SULF2 knockdown and also to identify biomarkers for SULF2 inhibition. Three hundred and twenty-two genes were found to be differentially expressed in the SULF2 knockdown cells as compared to both control untransduced and NT shRNA-transduced cells, with ≥ 2-fold change and adjusted *p* value ≤ 0.01. The changes in levels of mRNA from 18 genes most differentially expressed with a potential link to cancer were confirmed by RT-qPCR. Seven genes with a potential role in liver carcinogenesis were studied by WB. The gene most highly affected by SULF2 knockdown, ACE2, was further studied and ACE2 expression was found to be inversely related to SULF2 at the mRNA and protein levels. ACE2 expressed in SULF2 knockdown HuH-7 cells was enzymatically active and produced a higher level of its product, the anti-proliferative peptide Ang-(1-7), in medium from SULF2 knockdown cell cultures. Upregulation of ACE2 gene, albeit to a much lower level, was also shown after SULF2 suppression in SNU-182 and BxPC3 cell lines, suggesting a general role for SULF2 in controlling ACE2 expression.

Chapter 8. Discussion

One of the main goals of this project was to study the biology of SULF1/2 proteins in hepatocellular carcinoma (HCC) with particular focus on SULF2, which has previously been reported to be involved in hepatocarcinogenesis (Lai et al., 2008 a) (Lai et al., 2008 b) (Lai et al., 2010 a) (Lai et al., 2010 b). In order to do so, methods to investigate signalling pathways that are regulated by SULF1/2 were established, and as model systems a panel of HCC cell lines with differential patterns of SULF1/2 expression was established and characterised.

Characterisation of mRNA and protein expression in HCC cell lines

Six HCC cell lines were used in this study in which the expression of endogenous SULF1/2 was investigated at the mRNA and protein level. RT-PCR and RT-qPCR were performed using validated primers (Figure 3.2). The results showed that SULF2 was highly expressed in 3 cell lines (i.e., SNU-182, HuH-7 and HepG2), moderately expressed in the SNU-475 cell line, while it was weakly expressed in PLC/PRF/5 cell line and under the level of detection in the Hep 3B cell line (Figure 3.1) (Figure 3.3; A). With respect to SULF1, RT-qPCR showed that SULF1 was highly expressed in the SNU-182 cell line whereas modest expression was detected in the SNU-475 cell line, and no expression was detected in any of the other four cell lines (Figure 3.3; B).

This pattern of mRNA expression for SULF1/2 across cell lines was consistent with that reported in the literature (Lai et al., 2008 a) (Lai et al., 2008 c). It is noteworthy that the only cell lines that expressed SULF1 (i.e., SNU-182 and SNU-475) were derived from poorly differentiated HCC tumours and that they also expressed SULF2. None of the cell lines derived from well-differentiated tumours expressed SULF1. In the SNU-182 cell line, SULF1 expression was higher than that of SULF2 by 4-fold, while in the SNU-475 cell line SULF2 expression was higher than SULF1 expression by 16-fold.

Nawroth *et al.,* reported that SULF1 protein was not detected in certain pancreatic cancer cell lines even though SULF1 mRNA was expressed (Nawroth et al., 2007). Therefore, to investigate whether or not the mRNA for SULF1/2 was translated into proteins in HCC cell lines, western blot (WB) analysis was carried out using SULF1 and SULF2 antibodies. A panel of commercially available antibodies for both enzymes raised to different immunogens was used, and these antibodies are listed in Table 2.2. However, most of these antibodies were unsatisfactory, with multiple non-specific bands despite many attempts to optimise the concentration of the antibodies or the conditions of WB. Only one SULF1 antibody (Ab), namely SULF1 Ab (Abcam) that was raised against a peptide in the C-terminal domain, gave a band by WB corresponding to the full-length 125 kDa SULF1 protein. This band was detected only in SNU-182 cell lysates and not in the other 5 HCC cell lines (Figure 3.5). A similar band was detected in the lysate of HS766T pancreatic cancer cells that was used as a positive control in this experiment as this cell line expresses SULF1 at a high level (Nawroth et al., 2007) (Figure 3.5). However, the 50 kDa subunit that encompasses the C-terminal domain could still not be detected, even though SDS-PAGE was performed under reducing conditions (see Section 2.10).

As none of the commercially available SULF2 antibodies were satisfactory, a SULF2 antibody kindly provided by Prof. Lewis Roberts (Lai et al., 2008 a) was used in WB. This antibody, SULF2 Ab (LR), was generated in rabbits and raised against amino acids 421-444 within the hydrophilic domain (HD) of SULF2. The full-length 125 kDa SULF2 protein was detected in all HCC cell lysates except for Hep 3B (Figure 3.4; right). As WB was performed under reducing conditions, this antibody should also have detected the 75 kDa subunit that encompasses the N-terminal domain; however, it was not possible to distinguish the 75 kDa band from a large non-specific protein smear in this region (Figure 3.4; right).

According to the expression levels of SULF1/2 mRNAs and proteins that were revealed by RT-qPCR and WB, the panel of HCC cell lines that were tested could be divided into three groups: SULF1(+)/SULF2(+) - SNU-182 and SNU-475, SULF1(-)/SULF2(+) - HuH-7 and HepG2, and SULF1(-)/SULF2(-) - Hep 3B and

PLC/PRF/5. This pattern of expression was exploited to study the biology of SULF1/2, and in developing cell-based screening assays for small-molecule inhibitors of SULF2.

To generate a new SULF2 antibody, a somewhat similar peptide to that used to raise the SULF2 Ab (LR) was synthesized. The peptide included amino acids 421-435 of the HD domain of human SULF2 and, as the sequence did not have a cysteine residue, a terminal cysteine was added to the C-terminus to form the immunogen. The cysteine residue was added to conjugate the small peptide to carrier proteins to enhance the immune response and to immobilize the peptide on an affinity matrix for purification of the antibody. The production of this antibody, designated as SULF2 Ab (NCL), was performed by Eurogentec. Two rabbits were immunized and sera collected (1271 and 1272). These sera underwent affinity purification and were then tested by ELISA against the immunogen to which they were raised. However, neither purified antibody was suitable for WB.

During the course of these studies, a SULF2 Ab (Serotec) that was generated against the C-terminal domain by Lemjabbar-Alaoui *et al.* in 2010 became commercially available. Using this antibody in WB showed the expression of the full-length SULF2 protein in the cell lines that expressed high levels of SULF2 mRNA (i.e. SNU-182, HuH-7 and HepG2) with reduced non-specific binding compared with SULF2 Ab (LR) (Figure 3.4; left). However, the 50 kDa subunit could still not be detected in the cells that express endogenous SULF2.

To determine the subcellular localization of SULF1/2 proteins, immunocytochemistry (ICC) of permeabilized cells was performed using the antibodies that performed well for WB, namely, SULF1 Ab (Abcam) for SULF1 and SULF2 Ab (LR) and SULF2 Ab (Serotec) for SULF2. Immunofluorescence staining for SULF1 in the high SULF1-expressing HS766T cell line gave weak staining and there was no staining in the SNU-182 cell line, suggesting low affinity and unsuitability of this antibody for ICC. SULF2 Ab (LR) gave membranous but also non-specific cytoplasmic staining in HCC cells as indicated by the similar staining of SULF2-positive cell lines, HuH-7 and HepG2, and the SULF2-negative cell line, Hep 3B (Figure 3.6). However, SULF2 Ab (Serotec) produced dot-like

membranous staining of HuH-7 and HepG2 cells (Figure 3.7; 1B, 2B), rather than widespread staining of whole cells. This pattern of expression is in line with published data and the enrichment of SULF2 in lipid raft domains on the cell surface (Tang and Rosen, 2009). Hep 3B cells were completely negative on ICC with the SULF2 Ab (Serotec) (Figure 3.7; 3B).

Characterisation of the sulfatase enzymatic activities of HCC cell lines

After characterisation of SULF1/2 mRNA and protein expression in HCC cell lines, the next step was to evaluate catalytic activity, and in so doing explore potential test systems for screening small-molecule inhibitors of SULF2. SULF1/2 enzymes are known to have both arylsulfatase (ARS) and glucosamine 6-O endosulfatase activities (Morimoto-Tomita et al., 2002) (Uchimura et al., 2006 b). First, a fluorometric ARS assay using the fluorogenic substrate 4-methylumbelliferyl sulfate (4-MUS) was investigated. Upon desulfation of 4-MUS it is converted into the fluorescent product 4-methylumbelliferone (4-MU), whose fluorescence at 460 nm can be measured after excitation at 355 nm. Therefore, an ARS assay using 4-MUS as a substrate might represent a rapid method for screening inhibitors. However, a major drawback for this assay is related to the fluorescence of the product 4-MU which requires alkalization of the reaction mixture for complete ionization of 4-MU and optimal fluorescence. Hence, this alkalization leads to a discontinuous assay because the pH optimum for SULF1/2 activity is between pH 7 - 8, a drawback that prevents kinetic studies (Bilban et al., 2000) (Ahmed et al., 2005).

Therefore, the effect of pH on the fluorescence intensity (FI) and stability of 4-MU was investigated to determine whether it was possible to measure 4-MU fluorescence at a pH range of 7 - 8 with acceptable sensitivity. As expected, there was maximal 4-MU fluorescence at pH 10, that decreased gradually at lower pH values. However, the fluorometer was still able to detect 4-MU fluorescence at concentrations ≥ 0.1 µM in the pH range of 7 - 11 (Figure 3.8). Also, the fluorescence of 4-MU was found to be stable over at least 2 hours in aqueous solutions (Figure 3.9). Collectively, these observations indicated that it would be

possible to perform a continuous cell-based ARS activity assay at pH 7.4, the pH of culture medium, and a continuous cell-free ARS assay at pH value of 8.

After optimising the conditions for ARS activity measurement, the activity of SULF1/2 in HCC cells was investigated. It is important to note that the cell-based ARS assay does not differentiate between the ARS activity resulting from either SULF1/2 enzymes. Also, other members of the sulfatase family could contribute to the measured activity if these members are present at the cell surface or secreted into the medium, or if the substrate 4-MUS is internalized into the cells. Lysosomal sulfatases have been reported to be secreted and then re-internalized through the mannose-6-phosphate receptor (Buono and Cosma, 2010), while uptake of 4-MUS was reported to take place in isolated hepatocytes where it was hydrolysed by arylsulfatases (Kauffman et al., 1991). Therefore, to distinguish SULF1/2 activity, it would be necessary to inhibit other sulfatases before measuring the activity of SULF1/2. However, well-validated inhibitors are only available for steroid sulfatase (STS), also called ARSC, which is reported to be present in nearly all membrane compartments including the plasma membrane (Willemsen et al., 1988) (Stein et al., 1989). Deficiency of seven sulfatases (ARSA, ARSB, GALNS, GNS, SGSH, IDS, and ARSE) cause inherited disorders, for example lysosomal storage diseases, and inhibitors are not available (Hanson et al., 2004). STS/ARSC is implicated in steroid hormone biochemistry and, in addition to deficiency causing an inherited disorder; upregulation of STS/ARSC is involved in hormone-dependent breast cancer (Miyoshi et al., 2003) (Suzuki et al., 2003 b). Therefore, inhibitors of STS/ARSC have been developed. One of these STS/ARSC inhibitors is the irreversible inhibitor oestrone 3-O-sulfamate (EMATE) (Howarth et al., 1994) (Poirier et al, 1999), and HCC cells were incubated with EMATE for 1 hour before adding 4-MUS in all experiments to remove sulfatase activity due to STS/ARSC.

When equal numbers of cells were incubated with 4-MUS, ARS activity remaining after STS/ARSC inhibition was shown to be high in HuH-7 cells, HepG2 had some activity and no activity was detected in SNU-475, Hep 3B or PLC/PRF/5 cells (Figure 3.10). Surprisingly, SNU-182 cells did not show any ARS activity, even though both SULF1/2 proteins were highly expressed in this cell line. As only

SULF2, but not SULF1, was expressed in HuH-7 and HepG2 cells, the ARS activity that was measured in these two cell lines could be in part due to SULF2, and activity was also found to be proportional to the number of cells (Figure 3.12). No ARS activity was detected in any of the other 4 HCC cell lines even at very high cell densities. This result suggests that in some cell lines either SULF1/2 proteins are not presented on the cell membrane, or that SULF1/2 proteins are partially or completely inactive, i.e. ARS activity or both ARS and endosulfatase activities are absent, respectively. Lack of activity could be due to the complexity of SULF1/2 enzyme biosynthesis and the requirement for several processing steps for sulfatase activity. The absence of functional SULF1/2 on the cell membrane in SNU-182 cells could be investigated by measuring the ARS activity of SNU-182 cell lysates and membrane preparations. The results also showed that most of the ARS activity in HuH-7 and HepG2 cells was inhibitable by EMATE, and hence is attributed to STS/ARSC, while the remaining ARS activity that could result from SULF2 comprised about one third of the total activity only (Figure 3.11). This high level of STS/ARSC activity in selected HCC cell lines is consistent with other studies that have reported the expression of STS/ARSC in HepG2 cells (Hammer et al., 2005).

It is known that SULF1/2 proteins are extracellular enzymes that can be retained on the cell surface or secreted into the medium (Dhoot et al., 2001) (Morimoto-Tomita et al., 2002) (Ohto et al., 2002). However, no ARS activity was detected in the concentrated conditioned medium (CM) from cultures of HCC cell lines that exhibited cellular ARS activity (i.e., HuH-7 and HepG2), even though SULF2 protein could be detected by WB in the CM (data not shown). This result could be due to that the levels of SULF2 protein in the CM being insufficient to give detectable ARS activity with 4-MUS as a substrate, consistent with the low affinity of 4-MUS for SULF2 (Km = 2.6) (Figure 3.16).

As discussed in Section 1.4.2, SULF1/2 enzymes are synthesized in the endoplasmic reticulum (ER) where the signal peptide is removed (Tang and Rosen, 2009) and the Cα-formylglycine (FGly) is formed to generate a catalytically active protein (Dierks et al., 1997) (Dierks et al., 2003) (Cosma et al., 2003).

SULF1/2 enzymes are subsequently transported to the trans Golgi where they undergo cleavage by a furin-type proteinase to form a heterodimer that is linked by disulfide bonds (Thomas, 2002) (Tang and Rosen, 2009). At the same time, N-glycosylastion takes place in the ER and/or Golgi which is necessary for secretion of the protein, and possibly for endosulfatase activity (Morimoto-Tomita et al., 2002) (Ambasta et al., 2007). Ai *et al*. reported that SULF1/2 enzymes that were targeted to the ER or to the Golgi apparatus showed endosulfatase activity, and were as active as cell surface SULF1/2 against a heparan sulfate (HS) substrate (Ai et al., 2003). This latter observation is not surprising as the FGly residue required for the catalytic activity is generated early in the ER as a co-translational or early post-translational event. Therefore, to investigate the activity of total SULF1/2 proteins in HCC cell lines, and to explore whether some cell lines such as SNU-182 can express catalytically active SULF1/2 enzymes that are not localized to the cell surface, HCC total cell lysates were screened for ARS activity. The pattern of cell lysate activity using 4-MUS was not different from that of intact cell-based ARS activity. Thus, only HuH-7 and HepG2 cell lysates exhibited ARS activity while no activity was detected in any of the other 4 HCC cell lysates including SNU-182 (Figure 3.13). These data suggest that both SULF1/2 proteins in SNU-182 cell line do not have any arylsulfatase activity, although they may still possess endosulfatase activity.

Investigating ARS activity of cells or cell lysates using 4-MUS as a substrate does not exclude the possibility of members of the sulfatase family other than SULF1/2 contributing to the measured ARS activity. Therefore, it was important to attempt to purify SULF1/2 enzymes from HCC cell lysates before measuring their ARS activity. Purification was carried out by immunoprecipitation using SULF1/2 antibodies, namely, SULF1 Ab (Abcam) for SULF1 and SULF2 Ab (Abcam), SULF2 Ab (LR) or SULF2 Ab (Serotec) for SULF2, to give SULF1- and SULF2-Ab immunoprecipitates (IPs). These antibodies were used as they were raised against the C-terminal or HD domains that are unique to SULF1/2 enzymes and distinguish them from other sulfatases (Lai et al., 2008 c). Also, using antibodies that are raised against the N-terminal domain could block the enzymatic activity of SULF1/2.

ARS activity detected using SULF2-Ab (Abcam) IPs of HCC cell lysates were consistent with the ARS activity data generated using cells or cell lysates. The ARS activity of SULF2-Ab (Abcam) IPs showed that HuH-7 cells had the highest activity followed by HepG2 cells, with no activity detected in any of the other 4 HCC cell lines (Figure 3.14; A). These results suggest that the EMATE-uninhibited ARS activity measured in HuH-7 and HepG2 cells or cell lysates can possibly be attributed in part to SULF2. To confirm these results, SULF2 purification by immunoprecipitation using a different antibody, namely SULF2 Ab (LR) that was raised against the HD domain of SULF2, was performed. The results obtained were in line with the previous data and SULF2 Ab (LR) IPs of HuH-7 and HepG2 cell lysates showed ARS activity that was higher in HuH-7 (Figure 3.14; B). Also, the ARS activity of the purified SULF2 enzyme was concentration-dependent in SULF2 Ab (Abcam) IPs of HuH-7 cell lysates (Figure 3.15). Using the SULF2 Ab (Serotec) that was raised against the C-terminal domain, ARS activity similar to that found with SULF2-Ab (Abcam) IPs was observed (data not shown).

For SULF1 Ab (Abcam) IPs, IPs of SNU-182 cell lysates showed no ARS activity, consistent with the cellular and cell lysate data, and only a low level of activity was detected for IPs of HS766T cell lysates (Figure 3.14; C), even though the HS766T cell line expresses a very high level of SULF1 protein. These data are consistent with other studies showing that 4-MUS is a poorer substrate for SULF1 than SULF2 (Morimoto-Tomita et al., 2002).

Since it is possible to perform ARS activity assays using 4-MUS in a 96-well plate, this assay is a suitable fluorescence-based format for high-throughput screening of small-molecule inhibitors of SULF2. Therefore, the kinetics of the reaction between SULF2 and 4-MUS were investigated using this format with SULF2 Ab (Abcam) IPs of HuH-7 cell lysates as the enzyme source. The Michaelis constant (Km) of 4-MUS for SULF2 was calculated and found to be 2.6 mM (Figure 3.16). This value is not dissimilar to the Km value of 10 mM reported in other studies (Uchimura et al., 2006 b) (Rosen and Lemjabbar-Alaoui, 2010), and the high Km reflects the low affinity of SULF2 for 4-MUS.

The effect of the STS/ARSC inhibitor, EMATE, on SULF2 enzyme was investigated to determine whether it could also inhibit SULF2. The results showed that there was no effect of up to 100 µM EMATE on enzyme activity when SULF2 Ab IPs were used (Figure 3.17), and EMATE did not affect the kinetics of the reaction of purified SULF2 with 4-MUS (Figure 3.18). These results not only confirm that SULF2 is not inhibited by EMATE but also provide evidence that the ARS activity remaining in HCC cells or cell lysates after pre-incubation with EMATE is in part or totally due to SULF2, although the possibility that other sulfatases contribute to the measured ARS activity cannot be excluded. Thus, pre-incubation of HuH-7 cell lysate with up to 400 µM EMATE failed to inhibit at least one third of the total ARS activity measured without EMATE treatment (Figure 3.19). It is noteworthy that an EMATE concentration of 400 µM is high relative to the inhibition constant (K_i) for EMATE against purified human STS/ARSC (0.67 µM), and the IC_{50} of EMATE against STS/ARSC-expressing CHO cells (0.03 µM) using 4-MUS as a substrate (Nussbaumer et al., 2003) (Horvath and Billich, 2005).

In addition to arylsulfatase activity, the purified SULF1/2 proteins were shown to have endosulfatase activity using immobilized heparin as a substrate. This analysis was performed using the cMyc-tagged RB4CD12 phage display antibody whose preferred binding sequence is the trisulfated disaccharide composed of iduronic acid and glucosamine (Dennissen et al., 2002) (Jenniskens et al., 2002) (Uchimura et al., 2010). Removal of the 6-O sulfate by the endosulfatase activity of SULF1/2 prevents the binding of RB4CD12, which is detected using an HRP-conjugated cMyc secondary antibody. The results showed that both SULF1-Ab IPs of SNU-182 cell lysate and SULF2-Ab IPs of HuH-7 cell lysate using either SULF2 Ab (Serotec) or SULF2 Ab (Abcam) exhibited a concentration-dependent endosulfatase activity, while no activity was detected using STS/ARSC-Ab IPs of HuH-7 cell lysate (Figure 3.20). Interestingly, these results indicated that even though purified SULF1 from SNU-182 cell lysate had no ARS activity using 4-MUS as a substrate, it did have endosulfatase activity. SULF2 from HuH-7 cell lysate, on the other hand, had both activities. A summary of HCC cell lines used in this thesis with their characteristics and sulfatase activities is given in Table 8.1.

Table 8.1: Summary of HCC cell lines used in this thesis with their characteristics.

Cell line	SULF2 mRNA levels	SULF1 mRNA levels	SULF2 protein levels	SULF1 protein levels	Arylsulfatase activity	Endosulfatase activity
SNU-182	+++	+++	++	++	-	++ (SULF1)
SNU-475	+	+	-	-	-	n.t.
HuH-7	++	-	++	-	++	++ (SULF2)
HepG2	++	-	++	-	+	n.t.
Hep 3B	-	-	-	-	-	n.t.
PLC/PRF/5	+/-	-	-	-	-	n.t.

SULF2 protein levels tested using the SULF2 Ab (Serotec). n.t. = not tested.
Level or activity: +++, very high, ++, high; +, detectable; +/-, weak; -, absent.

Endosulfatase activity assays could be used to screen potential inhibitors of SULF2, with counter-screening of inhibitors using SULF1, in an ELISA format. However, there are two drawbacks to using this assay for screening. First, the RB4CD12 antibody detects an epitope, trisulfated disaccharide IdoA2S-GlcNS6S, which is not solely metabolised by SULF2 (Jenniskens et al., 2000), and SULF2 specificity could not be assumed as removal of the 6-O-sulfate by SULF2 or any of the other two sulfates by other sulfatases could affect the binding of the antibody to heparin, rendering the assay not specific for SULF2 activity unless purified enzyme is used. Second, current contractual limitations on the use of the RB4CD12 antibody would have to be resolved.

There are two other methods to measure the endosulfatase activity of SULF2 that do not require the RB4CD12 antibody, involving the use of either ^{35}S-radiolabelled or unlabelled synthetic heparan sulfates. The first approach measures the level of ^{35}S [SO_4] in the case of radiolabelled HS (Ai et al., 2003), and the second measures disaccharide fragments following enzymatic degradation in the case of unlabelled HS. The sulfation of the disaccharide fragments is measured using high performance liquid chromatography (HPLC) and compared with authentic disaccharide markers (Morimoto-Tomita et al., 2002). However, both methods

would require development and optimisation, and modification for use in the high throughput screening of inhibitors.

Generation of recombinant SULF2 enzyme

Although endogenous HuH-7 cell SULF2 activity could be measured, the level was low, and enrichment by SULF2-Ab IP was considered insufficiently robust for inhibitor screening. The specificity of the IP could not be assumed and because cell lysate and not CM was used for immunoprecipitation, the precipitate could be contaminated with other sulfatases with arylsulfatase activity not inhibited by EMATE. Ideally, recombinant SULF1/2 proteins should be generated that can be purified and used in an enzymatic assay for the screening of inhibitors.

In an attempt to generate recombinant SULF1/2 proteins, cells were transfected with two different constructs, one for each SULF. The open reading frame of either SULF1 or SULF2 was inserted under a CMV promoter in the pCMV6-Entry vector (Figure 2.1) to allow constitutive expression of SULF1/2 proteins which were fused with a C-terminal MYC/DDK tag for antibody detection and purification. A range of different cell lines were transfected including HCT (which is a human colon carcinoma cell line that grows quickly and is easy to transfect), Hep 3B and PLC/PRF/5 cell lines which are SULF1- and SULF2-negative and hence would allow SULF1/2 expression in a SULF-negative background. SULF2-transfected cells could also be used for the cell-based screening of inhibitors. As SULF1/2 enzymes are complex proteins, and their production requires a number of processing steps as discussed earlier, the SULF1/2 constructs were also transfected into the SULF2-positive HuH-7 and HepG2 cell lines, i.e. cells that had been shown to produce active SULF2 protein.

Transfection was performed using lipofection with two different transfection reagents (i.e., lipofectamine or FuGENE). Transfection conditions were optimised using the pCI-neo/EGFP plasmid that constitutively expresses EGFP, and FuGENE was shown to be superior to lipofectamine giving better transfection efficiency; however, transfection was in general poor. HuH-7 cells gave the highest transfection but only 5% of cells were successfully transfected (Figure 4.1).

However, the low transfection efficiency was circumvented to some extent by the use of SULF1/2 constructs containing a selectable marker that confers resistance to neomycin or its analogue G418.

After transfection with SULF1/2 constructs, cells were selected using G418 and multiple colonies were picked and expanded for each construct and each cell line. First, the clones were screened for SULF1/2 mRNA using RT-PCR or RT-qPCR. RT-PCR was used for cells that have a SULF-negative background while RT-qPCR was used for cells that express endogenous SULF1/2. For example, the RT-qPCR data showed the upregulation of SULF2 mRNA levels in two of SULF2-transfected HepG2 clones (4- and 80-fold increase) compared with untransfected control cells (Figure 4.2).

Additionally, the clones were screened for DDK-tagged recombinant SULF1/2 proteins by performing WB using an anti-DDK antibody. Either the secreted SULF1/2 proteins that were purified from the CM (Figure 4.3) or the total cell lysates of clones (Figure 4.4) were screened. In both cases, recombinant SULF1/2 proteins could be detected.

The SULF2-transfected HepG2 clone 15 showed 80-fold upregulation of SULF2 mRNA level over control untransfected HepG2 cells by RT-qPCR (Figure 4.2). The clone 15 cell lysate also showed high levels of recombinant SULF2 protein as demonstrated by WB using both anti-DDK and SULF2 (LR) antibodies (Figure 4.4), while WB of control untransfected HepG2 cell lysate showed no band and a much weaker band for SULF2 using anti-DDK Ab and SULF2 (LR) Ab, respectively (Figure 4.4). ICC showed membranous and cytoplasmic staining of SULF2 in HepG2 clone 15. However, only about 50% of the cells were SULF2 positive (Figure 4.5).

To investigate whether the recombinant SULF1/2 proteins were active. Clones were screened for their ARS activity using 4-MUS. Either cells or cell lysates were used; however, no more than a two-fold increase in ARS activity in transfected clones was detected, compared with that of corresponding untransfected cells. Furthermore, an increase in SULF2 activity was only seen in HuH-7 and HepG2

clones, i.e. in cells that express endogenous SULF2. Even the HepG2 SULF2-expressing clone 15 cell lysate did not show more than a 2-fold increase in ARS activity compared to untransfected HepG2 cell lysate (Figure 4.6).

Collectively, these results indicated that the recombinant SULF1/2 proteins generated were mostly inactive. Lack of activity was confirmed by measuring the ARS activity of purified SULF2 enzymes generated using SULF2-Ab IPs from equal quantities of clone 15 or untransfected HepG2 cell lysates (Figure 4.7). The slight increase in ARS activity of some cell lysates of HuH-7 and HepG2 clones compared with that of control untransfected cell lysates could be due to an increase in the level of endogenous SULF2 due to the different culture conditions, as the clones were maintained under a selection pressure of 400 µg/ml G418. However, another possibility for the slight increase in ARS activity is the presence of low levels of active recombinant SULF1/2 proteins in HuH-7 and HepG2 cells. Nevertheless, the amount of active recombinant protein was not enough for purification and subsequent applications such as screening of inhibitors.

Given that even the best SULF2-expressing clone, as assessed by RT-qPCR and WB, had only 50% SULF2-positive cells by ICC (Figure 4.5), another gene delivery method was used to improve the efficiency of gene delivery, namely, SULF2-containing lentiviral particles. The lentiviral construct used allows the expression of SULF2 and the blasticidin resistance gene under the same CMV promoter. This construct design ensures that all blasticidin-resistant cells are expressing SULF2. Infecting the SULF-negative Hep 3B cell line with SULF2 lentiviral particles led to high-level expression of SULF2 protein with full-length protein and the 50 kDa subunit detected by WB using the SULF2 Ab (Serotec) which was raised against the C-terminal domain. No SULF2 protein was detected in the control untransduced cells (Figure 4.8). ICC staining showed that the majority of the infected cells were SULF2-positive with no staining of the untransduced cells (Figure 4.9). Surprisingly, however, the cell lysates of the SULF2-transduced cells showed no ARS activity using 4-MUS as a substrate. Thus, colonies were picked to obtain clones that were highly enriched for catalytically active SULF2-expressing cells, and might therefore have enzymatic activity against 4-MUS. However, even

though the expression of SULF2 protein was confirmed by WB and ICC (Figure 4.10) (Figure 4.11**)**, none of the clones showed any measurable ARS activity (Figure 4.12).

The production of inactive recombinant SULF1/2 proteins could be due to defective post-translational processing, including insufficient cellular levels of the Cα-formylglycine generating enzyme (FGE) required to convert the cysteine residue into FGly at the active site of nascent SULF1/2 proteins. It has been reported that in arylsulfatase A (ARSA)-overexpressing cells a proportion of the ARSA generated enzyme still has the cysteine instead of FGly (Schmidt et al., 1995). Also, Anson *et al.* demonstrated that overexpression of arylsulfatase B (ARSB) led to a significant decline in the measured activities of other endogenous sulfatases (Anson et al., 1993), and these two studies suggest that the conversion of cysteine to FGly is carried out by a saturable mechanism, and that the level of FGE in the cells can be a limiting factor for sulfatase activity. A way to circumvent FGE insufficiency is by double transfection of cells with an FGE-expressing construct. A similar strategy has been described in other studies where the ARSA activity of ASRA-transfected COS-7 fibroblast-like cells or HepG2 cells was increased substantially by co-transfection of an FGE-expressing construct with the ARSA construct, compared with transfecting cells with the ARSA construct alone (Cosma et al., 2003) (Takakusaki et al., 2005).

The expression of endogenous SUMF1(sulfatase modifying factor 1), the gene encoding FGE, was measured and the results showed comparable expression of SUMF1 in all the HCC cell lines at a level that was about 2^5 - 2^8 fold higher than the expression of GAPDH (Figure 4.13). Therefore, to increase the expression of SUMF1 in the cells, a SUMF1 construct was co-transfected with the SULF2 construct either transiently or stably. The stably, but not the transiently, co-transfected cells rapidly lost the expression of SUMF1 as shown by RT-PCR (Figure 4.14; A), while the transiently co-transfected cells expressed both SULF2 and SUMF1 protein as evidenced by WB (Figure 4.14; B). However, no ARS activity was detected in these transiently co-transfected cells. Also, the HepG2 SULF2-expressing clone 15 showed no increase in ARS activity when it was

transiently transfected with the SUMF1 construct. A possible explanation for these results is that a high level of recombinant active SULF2 protein may affect or even kill cells in which it is present for a long time. Alternatively, the low transfection efficiency might have prevented any increase in ARS activity following transient transfection of SUMF1 into the SULF2-expressing clone 15. It may be possible to circumvent these two potential drawbacks by the transduction of inducible SUMF1 lentiviral constructs into cells or the expression of SUMF1 and SULF2 in alternative biological systems such as bacteria or insect cells.

Active SULF2 enzyme has been successfully generated using a plasmid supplied by the group that first cloned human SULF2 (Morimoto-Tomita et al., 2002). Transient expression of the wild-type SULF2 or a mutated form in which the cysteine in the active site is replaced by alanine, rendering the enzyme inactive, was performed in HEK 293T cells. Both forms were secreted into the conditioned medium (CM) at comparable levels as shown by WB (Figure 4.15; A). However, only the wild-type SULF2 had ARS activity against 4-MUS (Figure 4.15; B). This active SULF2 could be purified and enriched from CM by approximately 160-fold (Figure 4.15; C), but could not be eluted from agarose beads by standard conditions as these were found to inhibit SULF2 activity. Therefore, SULF2-bound beads will be used for screening of SULF2 inhibitors, and an analogous approach is being explored for the production of SULF1.

Characterisation of commercially available sulfatases for counter-screening SULF2 inhibitors

In the development of SULF2 inhibitors, it will be important to identify selective SULF2 inhibitors rather than general sulfatase inhibitors, given the important physiological roles of sulfatases as evidenced by the diseases resulting from their deficiency (Hanson et al., 2004). Where available, commercially produced sulfatases will be used for counter-screening of SULF2 inhibitors, and 9 members of the sulfatase family are available. These enzymes were purchased and activity using 4-MUS as a substrate was characterised in terms of pH optimum, concentration and time dependency. The Km values of the reaction were measured when possible. Three sulfatases could readily convert 4-MUS to 4-MU

(i.e., ARSA, ARSB, STS/ARSC) with pH optima in the acidic range for ARSA and ARSB (Figure 4.16) (Figure 4.19) consistent with their lysosomal localization, and in the neutral range for STS/ARSC (Figure 4.22) consistent with its localization in the microsomes (Hanson et al., 2004). The three enzymes showed concentration-dependent activities (Figure 4.17) (Figure 4.20) (Figure 4.23) and time-dependent activities with 4-MUS Km values of 2.2 mM, 415 µM and 82 µM for ARSA, ARSB and STS/ARSC, respectively (Figure 4.18) (Figure 4.21) (Figure 4.24) (Table 4.1). Other neutral pH-dependent sulfatases (i.e., ARSD, ARSF and ARSG) were also tested, but 4-MUS was not an efficient substrate (Figure 4.25) (Table 4.1). Only IDS of three acidic pH-dependent sulfatases tested showed any activity with 4-MUS as a substrate, while GNS and GALNS had no activity at all (Figure 4.26) (Table 4.1). Therefore, other assays were investigated for the latter two enzymes.

GNS is an exosulfatase that removes the 6-O-sulfate group from N-sulfated or N-acetylated glucosamine residues at the non-reducing end of HS chains or the N-acetylated glucosamine residues of keratan sulfate (Parenti et al., 1997). Therefore, a glucosidase-coupled assay which had been used before with flavobacterial 6-sulfatase (Myette et al., 2009) was evaluated. This assay depends on the intrinsically poor ability of β-glucosidase to hydrolyse the glycosidic bond between 4-MU and N-acetylglucosamine (GlcNAc) when the latter is 6-O-sulfated (Figure 4.27) (Figure 4.28). However, the activity of β-glucosidase is increased when the substrate MU-GlcNAc,6S is pre-incubated with GNS (Figure 4.29), and this two-stage assay could be used for GNS counter-screening of SULF2 inhibitors. A similar strategy was evaluated for GALNS which is another exosulfatase that removes the 6-O-sulfate group from N-acetylated galactosamine residues of chondroitin sulfate or from galactosamine in keratan sulfate (Parenti et al., 1997). The galactosidase-coupled assay has been used before with human GALNS (van Diggelen et al., 1990) and depends on the ability of GALNS to remove the 6-O-sulfate from galactosamine-6-sulfate (Gal,6S) allowing β-galactosidase to liberate 4-MU from the substrate MU-Gal,6S (Figure 4.30). However, the data generated showed no activity with commercial GALNS using MU-Gal,6S as a substrate in the coupled reaction (Figure 4.31).

In summary, the sulfatases ARSA, ARSB and STS/ARSC have sufficient affinity for 4-MUS to be used in the initial counter-screening of inhibitors of SULF2. ARSD, ARSF, ARSG and IDS have only weak affinity for 4-MUS, and large amounts of the enzymes would be required. These latter enzymes could only be used for limited counter-screening. Similarly, the glucosidase-coupled GNS assay could be used for testing selected inhibitors, as a high concentration of the enzyme is again required.

Biology of SULF1/2 enzymes in cancer

A complementary approach to SULF2 inhibition using small-molecule inhibitors in target validation is SULF2 knockdown using shRNA. In the studies described in this thesis, knockdown of SULF2 was performed to (1) understand the biology of SULF2, (2) serve as a positive control for the effects of SULF2 inhibition using small-molecule inhibitors and (3) validate the selectivity of SULF2 inhibitors by treating cells where the SULF2 gene had been silenced with the inhibitors and confirming the lack of any effect of the inhibitors under conditions of SULF2 knockdown.

Given that the response of cells to a particular stimulus is cell-type and hence context dependent, the effect of SULF2 knockdown in an HCC cell line depends on the dominant signalling pathways and the genetic changes that drive the proliferation and growth of the cell line. Also, it is important to note that signal transduction pathways are not linear but sophisticated networks of protein interactions with cross-talk between different signalling pathways. Therefore, the response to SULF2 suppression is expected to be variable and different between cell lines.

Two of the most important and well-characterised signalling pathways in HCC are the Wnt signalling pathway (Pez et al., 2013) and the growth factor/receptor tyrosine kinase (RTK) signalling pathway. Some of the most important growth factors that are involved in HCC are FGFs, IGFs and VEGF (Yang et al., 2011) (Min et al., 2011) (Wu and Zhu, 2011) (Cornellà et al., 2011) (Zhang et al., 2012). It has been reported that the 6-O sulfation of heparin sulfate proteoglycans (HSPGs)

is important for regulating Wnt and RTK signalling pathways in HCC, and in other types of cancer.

SULF2 has been shown to modify Wnt signalling both at the basal level and after stimulation with different Wnt ligands, such as Wnt-1, Wnt-3a and Wnt-4. Overexpression of SULF2 was shown to promote Wnt signalling in response to Wnt-1 or Wnt-4 in HEK 293T cells (Nawroth et al., 2007), and SULF2 suppression by knocking down the gene using shRNA or expressing a dominant-negative form of SULF2 was found to inhibit autocrine Wnt signalling in both pancreatic cancer and NSCLC (non-small-cell lung carcinoma) cell lines (Nawroth et al., 2007) (Lemjabbar-Alaoui et al., 2010). Directly relevant to the studies described in this thesis, in HCC SULF2 overexpression in Hep 3B cells increased Wnt-3a binding to the cell surface and upregulated basal and Wnt-3a-stimulated Wnt signalling (Lai et al., 2010 b).

In growth factor/RTK signalling, SULF2 has been shown to modify FGF-2 signalling in myeloma and HCC. Overexpressing SULF2 inhibited FGF-2-stimulated p-ERK levels in one myeloma cell line (Dai et al., 2005), but had the opposite effect in the HCC cell line Hep 3B, increasing FGF-2 binding to cells and promoting basal and FGF-2-stimulated ERK and AKT phosphorylation (Lai et al., 2008 a). In glioblastoma, SULF2 suppression reduced the phosphorylation of the receptor tyrosine kinases, PDGFRα and IGF1Rβ (Phillips et al., 2012).

In HEK 293T cells, overexpression of SULF1 was demonstrated to promote Wnt-1- or Wnt-4-stimulated Wnt signalling (Nawroth et al., 2007), whereas overexpression of SULF1 inhibited activation of growth factor/RTK signalling pathway in response to FGF-2, HB-EGF (heparin binding-epidermal growth factor) and HGF. For example, SULF1 overexpression inhibited FGF-2 and HB-EGF signalling in ovarian cancer, as evidenced by reduced HB-EGF-stimulated phosphorylation of EGFR (epidermal growth factor receptor), and FGF-2- and HB-EGF-stimulated p-ERK levels (Lai et al., 2003). In SCCHN (squamous cell carcinoma of the head and neck) and HCC, SULF1 overexpression also inhibited FGF-2 and HGF signalling, as shown by reduced FGF-2-stimulated p-ERK, HGF-stimulated p-ERK and p-AKT levels, and phosphorylation of the HGF receptor, c-Met (Lai et al., 2004 a) (Lai et al., 2004 b). Also, SULF1 overexpression inhibited FGF-2 signalling in pancreatic

cancer and myeloma cells (Li et al., 2005) (Dai et al., 2005), and HGF signalling in oesophageal cancer cells (Liu et al., 2013). Furthermore, SULF1 overexpression inhibited autocrine p-EGFR and p-ERK levels in breast cancer (Narita et al., 2007). Hence, in the above settings, SULF1 has functions normally associated with tumour suppressor, as opposed to oncogenic signalling.

The above studies emphasise the tumour- and cell type-dependency of the role of SULF1/2 in cancer, and hence the Wnt and growth factor/RTK pathways were characterised in the HCC cell lines used in this thesis, and then the effect of SULF1/2 gene silencing on these pathways was investigated.

Wnt signalling pathway in HCC

The canonical Wnt signalling is strongly implicated in hepatocarcinogenesis. β-catenin aberrant accumulation and activation is reported in a high percentage of HCCs ranging from 50-80% (Laurent-Puig and Zucman-Rossi, 2006) (Thompson and Monga, 2007) (Takagi et al., 2008). A small fraction of this activation is attributed to mutations in downstream mediators of Wnt signalling, such as the β-catenin-encoding gene CTNNB1 which is seen in 19% (610 of 3234) of cases, and mutations in the AXIN1 and APC genes are also uncommon, with 14% (64 of 458) and 4% (5 of 116) of cases, respectively (de La Coste et al., 1998) (Kondo et al., 1999) (Legoix et al., 1999) (Taniguchi et al., 2002) (Ishizaki et al., 2004) (Wellcome Trust Sanger Institute, COSMIC database, 2013). Additionally, no mutations in the AXIN2 gene were reported in HCC. These results suggest that other components of the Wnt signal transduction cascade are responsible for β-catenin activation. Dysregulation of the upstream elements of Wnt signalling are reported to be frequent in HCC, including upregulation of Wnt ligands (e.g., Wnt-3, Wnt-4 and Wnt-5a) and their frizzled (FZD) receptors such as FZD-3, FZD-6 and FZD-7, or downregulation of the Wnt antagonists secreted frizzled-related proteins (sFRP-1, sFRP-2, sFRP-5) (Merle et al., 2004) (Bengochea et al., 2008) (Takagi et al., 2008). These events increase the levels of Wnt ligands available to bind to the cells in the case of Wnt ligand overexpression or sFRP downregulation, or increase the sensitivity of cells to Wnt ligands in the case of frizzled receptor overexpression. SULF2 has been shown to increase the levels of Wnt ligands and

affect Wnt signalling by either removing the 6-O-sulfate from storage-type HSPGs, and hence releasing Wnt ligands (Lai et al., 2010 b), and/or by decreasing the affinity of Wnt binding to the co-receptor-type HSPGs (Ai et al., 2003) making Wnt ligands more available to bind to frizzled receptors. Therefore, SULF2 inhibition could potentially benefit a high percentage of HCCs.

In the panel of HCC cell lines studied in this thesis, HuH-7 cells were reported to have wild-type β-catenin and AXIN1, with β-catenin reportedly showing membranous staining with no cytosolic accumulation (Satoh et al., 2000) (Cagatay and Ozturk, 2002). However, HuH-7 cells were shown to have high levels of FZD-7 mRNA compared to other HCC cell lines and normal hepatocytes (Merle et al., 2004) (Yuzugullu et al., 2009). Also, expression of a dominant-negative mutant form of FZD-7 that lacks the intracellular domain in HuH-7 cells decreased β-catenin activation and cell motility (Merle et al., 2004). Thus, the HuH-7 cells were used in the studies reported here to characterise Wnt signalling, given the importance of Wnt signalling for this cell line. For stimulation of Wnt signalling, the canonical Wnt-3a ligand was used which showed a concentration-dependent increase in β-catenin-dependent transcriptional activity as measured using the TCF (T-cell factor) luciferase reporter assay as a readout. 100 ng/ml of Wnt-3a for 6 hours caused the highest increase in luciferase activity (Figure 5.3; A).

As a positive control for activation of Wnt signalling, BIO (6-bromo-indirubin-3'-oxime) was used (Figure 5.2; left). BIO inhibits the GSK-3β enzyme that is responsible for phosphorylation of β-catenin, leading to β-catenin ubiquitination and degradation by the proteasome (Meijer et al., 2003) (Polychronopoulos et al., 2004). Therefore, treating cells with BIO stabilizes β-catenin leading to its accumulation in the cytoplasm, translocation into the nucleus and transcription of downstream genes. The results showed concentration-dependent luciferase activity that was highest after treatment with 1 μM of BIO. Higher concentrations were toxic to the cells (Figure 5.3; B). As a negative control for activation of Wnt signalling, compound 3289-8526 was used (Figure 5.2; right). This compound is a dishevelled (Dvl)-PDZ domain inhibitor II that blocks the interaction between the scaffolding protein Dvl and the frizzled receptor, leading to inhibition of Wnt

signalling (Grandy et al., 2009). Incubation of HuH-7 cells with this compound inhibited Wnt-3a-induced luciferase activity in a concentration-dependent manner (Figure 5.3; C).

Growth factor/RTK signalling pathway in HCC

Growth factors bind to their cognate cell surface receptor tyrosine kinases (RTKs) which then transduce the signal predominantly via the RAF/MEK/ERK or the PI3K/AKT/mTOR cascades, depending on the growth factor and the cell type. The RAF/MEK/ERK axis has been reported to be constitutively activated in HCC as evidenced by the increased phosphorylation of MEK1/2 and ERK1/2 (Feng et al., 2001) (Huynh et al., 2003). Similarly, the PI3K/AKT/mTOR axis is also constitutively activated in HCC (Zhou et al., 2011 a) as shown by increased phosphorylation of AKT (Boyault et al., 2007) or mTOR and its substrate p70S6 kinase (Sahin et al., 2004). Also, phosphorylation of either ERK or AKT was found to correlate with poor prognosis of patients with HCC (Schmitz et al., 2008) (Nakanishi et al., 2005).

Activation of the growth factor/RTK pathway primarily involves either mutations in downstream mediators, or dysregulation of growth factors and their receptors. However, pathway mutations are rare in HCC; 3% (18 of 667) for KRAS, 2% (8 of 422) for NRAS, 0.3% (1 of 383) for HRAS, 3% (2 of 73) for ARAF, 4% (16 of 357) for BRAF and 3% (2 of 71) for CRAF, also called RAF1, in the RAF/MEK/ERK axis (Tannapfel et al., 2003) (Whittaker et al., 2010) (Wellcome Trust Sanger Institute, COSMIC database, 2013), and 6% (40 of 640) for PIK3CA (encoding the p110α catalytic subunit of PI3K) and 4% (20 of 452) for PTEN in the PI3K/AKT/mTOR axis (Tanaka et al., 2006) (Boyault et al., 2007) (Wellcome Trust Sanger Institute, COSMIC database, 2013). In contrast, overexpression of growth factors and their RTK receptors is more common in HCC and leads to constitutive activation of RAF1 in the RAF/MEK/ERK axis (Gollob et al., 2006) or mTOR in the PI3K/AKT/mTOR axis (Villanueva et al., 2008). Dysregulated growth factors include FGFs, IGFs and VEGF.

The FGF signalling pathway is stimulated by binding of one of the 22 different FGF ligands to one of four FGF receptors (FGFR1-4). Overexpression of ligands, such as FGF-1 (Hu et al., 1996), FGF-2 (Mise et al., 1996), FGF-9 (Miura et al., 2012), FGF-8, FGF-17, and FGF-18 (Gauglhofer et al., 2011), among others, and their receptors, FGFR1, FGFR2, FGFR3 or FGFR4 (Hu et al., 1996) (Ho et al., 2009) (Gauglhofer et al., 2011) has been reported in HCC. Similarly, the IGF signalling pathway, which is activated by IGF-I or IGF-II binding to the receptor IGF-1R, has been implicated in hepatocarcinogenesis (Alexia et al., 2004). Dysregulation of the IGF pathway is mostly through upregulation of IGF-II, found in 16-40% of HCC (Cariani et al., 1988), overexpression of IGF-1R (Breuhahn and Schirmacher, 2008) or downregulation of IGF-2R, found in about 60% of tumours (De Souza et al., 1995) (Yamada et al., 1997). IGF-2R is different from IGF-1R in that it does not have cytoplasmic kinase activity and regulates IGF2 degradation through receptor-mediated endocytosis (Oka et al., 1985). Also, the angiogenic factor VEGF was found to be upregulated at the mRNA and plasma protein level in patients with HCC (Ng et al., 2001) (Mas et al., 2007), and was associated with poor prognosis (Poon et al., 2004). Furthermore, mRNA levels for the VEGF receptors, VEGFR-1 (or FLT-1) (Ng et al., 2001), VEGFR-2 (or KDR/FLK-1) (Shimamura et al., 2000) and VEGFR-3 (Dhar et al., 2002), were found to be increased in HCC tumours.

A requirement for 6-O sulfation of HS chains for cell-surface signalling by growth factors, such as FGF-1 and FGF-2, has been described (Pye et al., 1998) (Pye et al., 2000). Using X-ray crystallography analysis, DiGabriele *et al*., demonstrated a direct role for the 6-O sulfation and 2-O sulfation of heparin in its binding to FGF-1 (DiGabriele et al., 1998), while no such requirement for 6-O sulfation was revealed for binding of heparin to FGF-2 (Faham et al., 1996). Nevertheless, the 6-O sulfation of HS was shown to be necessary for maximal FGF-2 activity (Guimond et al., 1993) (Pye et al., 1998), indicating a role in mediating the interaction between HS and FGFR1 (Kan et al., 1993) (Panteliano et al., 1994). In this latter case, HS functions as a bridge to form the ternary complex of FGF-2/HS/FGFR (Rusnati et al., 1994). Also, it has been shown that both the chain length and sulfation pattern (including 6-O sulfation status) of HS may be involved in the differential activation of FGF-1/FGF-2 signalling (Pye et al., 2000). These data were further supported by

the ability of SULF2 to greatly reduce FGF-1 but not FGF-2 binding to immobilized heparin (Uchimura et al., 2006 a).

Overexpression of SULF2 in the HCC cell line Hep 3B has been shown to increase FGF-2 binding to the cell surface, and to enhance the level of phospho-ERK (p-ERK) and phospho-AKT (p-AKT) (Lai et al., 2008 a). Collectively, these data suggest that excess ligand availability, or higher sensitivity to growth factors due to overexpression of RTK receptors, could be modulated by SULF2 inhibition in a high percentage of HCCs.

To study the role of SULF2 in the growth factor/RTK signalling pathway, p-ERK and p-AKT were used as readouts, and stimulation of ERK and AKT phosphorylation was characterised using a range of growth factors to identify the optimal concentration and exposure time. For stimulation of this pathway in the SNU-182 cell line, five growth factors were chosen: FGF-1, FGF-2, IGF-I, IGF-II and VEGF-165. The results showed stimulation of p-ERK and p-AKT in response to FGF-1, FGF-2 and IGF-I at concentrations as low as 0.1 nM, with maximum activation after 10 min exposure to FGF-1 or FGF-2 and after 5 min exposure to IGF-I. IGF-II caused an increase in p-ERK after 5 min of treatment, and in p-AKT after 10 min of treatment, but only at 10 nM. VEGF-165 did not affect the level of either p-ERK or p-AKT in the SNU-182 cell line even at 10 nM (Figure 5.4) (Figure 5.5). HuH-7 and Hep 3B cells showed similar results to SNU-182 cells (G. Beale personal communication).

As a positive control for inhibition of FGF/RTK signalling pathway, the potent and selective inhibitor of the FGF receptor kinase activity, PD173074, was used (Figure 5.6, left). This compound has an IC_{50} of 5 and 22 nM against FGFR3 and FGFR1, respectively (Mohammadi et al., 1998) (Kunii et al., 2008) (Pardo et al., 2009). Using the p-ERK ELISA, concentration-dependent inhibition of basal and FGF-1- and FGF-2-induced p-ERK levels was demonstrated in the SNU-182 cell line (Figure 5.7; A), and the IC_{50} values for inhibition of FGF-stimulated p-ERK levels by PD173074 were 84 nM for FGF-1 and 27 nM for FGF-2 (Figure 5.7; B). Also, the MEK inhibitor PD0325901 (Barrett et al., 2008) (Figure 5.6, right) was used at 1 µM

and caused complete inhibition of basal, FGF-1- and FGF-2-induced ERK phosphorylation in the SNU-182 cell line (data not shown).

The biology of SULF1/2 enzymes in HCC

Two approaches can be used to study the biology of SULF1/2, the first being overexpression of the enzymes, and this approach has been studied extensively by other groups in HCC and in other types of cancer. For instance, the effect of SULF1 overexpression has been studied in myeloma, ovarian cancer, SCCHN, breast cancer, pancreatic cancer, ESCC (oesophageal squamous cell carcinoma) and gastric cancer (Lai et al., 2004 b) (Lai et al., 2006) (Dai et al., 2005) (Lai et al., 2003) (Lai et al., 2004 a) (Narita et al., 2007) (Narita et al., 2006) (Li et al., 2005) (Liu et al., 2013) (Hur et al., 2012). These studies showed that SULF1 acts a tumour suppressor in all these types of cancers except for gastric cancer, where it was found to have tumour-promoting activity as discussed in Section 1.5.1. Also, SULF2 overexpression was studied in the models of HCC, myeloma, NSCLC and gastric cancer (Lai et al., 2008 a) (Lai et al., 2010 a) (Lai et al., 2010 b) (Dai et al., 2005) (Lemjabbar-Alaoui et al., 2010) (Hur et al., 2012) where it was found to have an oncogenic role with the exception of myeloma, as discussed in Section 1.5.2.

A complimentary approach to studying the biology of SULF1/2 is knockdown of SULF1/2 mRNA, also termed gene silencing, which also serves as a positive control for SULF2 inhibition using small-molecule inhibitors. For this purpose, SULF1/2 shRNA lentiviral particles were used due to the high efficiency of delivery and because integration into genomic DNA produces stable expression of the shRNA (Stovall et al., 2012). As controls, both untransduced cells and non-targeting shRNA (NT shRNA)-transduced cells were used. The NT shRNA contained four base pair mismatches to any known human or mouse gene, and controlled for the effect of transduction with lentiviral particles and for selection with the antibiotic puromycin. The shRNA that caused the greatest gene silencing of SULF1 or SULF2 was selected from a panel of 5 different shRNAs for each gene. For SULF2, SULF2 mRNA levels were measured by RT-qPCR after transient or stable transduction of shRNA lentiviral particles at different multiplicities of infection (MOIs) in HuH-7 cells and at different time points (Figure 5.8). The specificity of

knockdown was confirmed by stably transducing SULF2 shRNA that caused the best knockdown of SULF2 into HuH-7, HepG2 and SNU-182 cells and showing the lack of any effect on the expression of unrelated genes, including B2M (beta-2-microglobulin), TP53 and KLF6 (Figure 5.9) (Figure 5.10) (Figure 5.11). The same strategy was followed for selecting the shRNA sequence that causes the best gene silencing of SULF1 (Figure 5.12). The SNU-182 cell line was chosen for the studies on SULF1 as it is the only HCC cell line that expresses this gene at a high level, and specificity of SULF1 knockdown was confirmed as for SULF2, i.e. there was no effect of transduction of SULF1 shRNA on the expression level of B2M, TP53 or KLF6 genes, or SULF2 (Figure 5.13).

The effects of SULF1/2 suppression were studied in all the HCC cell lines that express SULF1/2 (i.e., HuH-7, HepG2, SNU-182, SNU-475) and in addition in one pancreatic cancer cell line (BxPC3) that expresses a high level of SULF2 and a low level of SULF1. For all of the cell lines a test cascade was followed to define the downstream consequences of SULF1/2 knockdown, and each experiment was repeated at least 3 times (Figure 5.14). First, the knockdown was confirmed at the mRNA level by RT-qPCR and at the protein level by WB. Second, the effect of SULF1/2 knockdown on growth factor/RTK (including the two main axes, RAF/MEK/ERK and PI3K/AKT/mTOR) and on Wnt signalling pathways was investigated by measuring p-ERK and p-AKT levels, or TCF reporter activity, respectively. Subsequently, the impact of signalling modulation was evaluated by measuring phenotypic effects *in vitro* and tumourigenicity *in vivo*.

Effects of SULF2 knockdown in the HuH-7 cell line

The downstream consequences of SULF2 knockdown was first studied in the HuH-7 cell line which is derived from a well differentiated HCC and expresses SULF2 but not SULF1. HuH-7 has a p53 point mutation at codon 220 position 2 (A → G), leading to replacement of tyrosine with cysteine (Hsu et al., 1993) and mutant Rb (retinoblastoma). Infecting HuH-7 cells with SULF2 shRNA lentiviral particles caused 37-fold downregulation of SULF2 expression in the SULF2 knockdown cells compared to NT shRNA-transduced cells (Figure 5.9). Suppression of SULF2 was confirmed at the protein level by WB using SULF2 Ab (Serotec), which

showed complete absence of SULF2 protein in the SULF2 knockdown cells (Figure 5.15). Stimulation of HuH-7 cells with FGF-1 or FGF-2 caused an increase in p-ERK and p-AKT levels (Figure 5.15; A and B), while stimulation with IGF-I caused an increase in p-AKT levels, at a high concentration of the ligand (Figure 5.15; C), which was also observed with IGF-II (data not shown). However, there was no clear effect of SULF2 knockdown on the phosphorylation of either ERK or AKT after stimulation with any of these ligands (Figure 5.15), suggesting that SULF2 suppression does not affect these growth factor/RTK signalling pathways in the HuH-7 cell line.

The effect of SULF2 suppression on Wnt signalling was also studied in HuH-7 cells, and no significant effect of SULF2 knockdown on the basal level of β-catenin transcriptional activity was observed; however, marked inhibition of Wnt-3a-induced activity was shown using both the TOPflash and 7TFP reporter systems with luciferase activity as a readout (Figure 5.16) (Figure 5.17; A). The effect of SULF2 suppression on Wnt signalling was found to be predominantly due to modulating Wnt-3a upstream signalling as treating cells with the GSK-3β inhibitor BIO, that works downstream of Wnt-3a-mediated activation of the frizzled and LRP5/6 receptors, activated luciferase activity in a manner that was independent of the SULF2 expression level (Figure 5.17; B). The effect of SULF2 knockdown on Wnt signalling was confirmed by WB using an antibody against ABC (active β-catenin), the non-phosphorylated form of β-catenin, which showed that SULF2 knockdown inhibited Wnt-3a-induced ABC accumulation (Figure 5.18; B). However, no change in the level of total β-catenin was observed after SULF2 knockdown (Figure 5.18; A). The lack of an effect could be due to small changes in total β-catenin, as a result of Wnt signalling, being masked by the high levels of β-catenin present at the cell membrane in HuH-7 cells, where it has a role in cell-cell adhesion (Sangkhathat et al., 2006). ICC studies showed that the majority of total β-catenin staining was at the cell surface in the HuH-7 cells with no detectable translocation of β-catenin to the nucleus after treatment with Wnt-3a or reduction of β-catenin staining after SULF2 knockdown (Figure 5.19). Unfortunately, the ABC antibody used in the WB experiments did not work for ICC. These results are in contrast with those of Lai *et al.* who have shown that SULF2 suppression in HuH-7

cells was associated with reduced basal levels of p-AKT, Wnt-3a, total β-catenin, cyclin D1 and GPC3 (Lai et al., 2010 a) (Lai et al., 2010 b), whereas the results presented here showed no clear effect on the mRNA or protein levels of these genes.

Phenotypically, SULF2 knockdown in HuH-7 cell line caused inhibition of cell growth as measured by the SRB (sulforhodamine B) assay and cell counting, with the doubling time of 43 hours for both control untransduced and NT shRNA-transduced cells increasing to 58 hours in the SULF2 knockdown cells (Figure 5.20). The effect of modulators of Wnt signalling on the growth of HuH-7 cells *in vitro* was investigated, and due to the sensitivity of HuH-7 cells to reduced FBS (foetal bovine serum) levels the effect of Wnt-3a, BIO and compound 3289-8625 could be only studied in 10% (v/v) FBS-containing medium. Neither Wnt-3a nor BIO had any effect on the growth of HuH-7 cells regardless of the SULF2 expression level (Figure 5.21; A and B), possibly due to other growth factors in the FBS masking any effect of Wnt signalling. However, incubating cells with compound 3289-8625 completely inhibited the proliferation of control untransduced, NT shRNA-transduced and SULF2 shRNA-transduced cells (Figure 5.21; C), indicating that Wnt signalling does have a role in driving the proliferation of HuH-7 cells. Importantly, growth inhibition was partially rescued by adding BIO but not Wnt-3a (Figure 5.21; D and E), presumably because compound 3289-8625 inhibits the binding of the scaffolding protein dishevelled to the frizzled receptor, and hence works downstream of Wnt-3a binding to the cell surface but upstream of BIO-induced inhibition of GSK-3β, such that BIO can rescue the phenotypic effects of compound 3289-8625. There was also no difference in the growth of BIO-rescued SULF2 knockdown HuH-7 cells compared to BIO-rescued control untransduced or NT shRNA-transduced cells (Figure 5.21; E). This result is again consistent with SULF2 affecting the binding of Wnt-3a at the cell surface and, as BIO acts downstream in Wnt signalling, the effect of SULF2 knockdown is not observed.

In addition to a detrimental effect on cell proliferation *in vitro*, SULF2 knockdown caused complete inhibition of the tumourigenicity of HuH-7 cells *in vivo* (Figure

5.22) (Figure 5.23; A). Both control untransduced and NT shRNA-transduced HuH-7 cells formed tumours with no difference in the mean time to reach a tumour size of 500 mm^3, while none of the mice implanted with the SULF2 knockdown cells formed tumours up to 100 days post-implantation (Figure 5.23; B). These data are in contrast to an independent study showing that SULF2 knockdown HuH-7 cells could form tumours in nude mice when 5 x 10^5 cells/mouse were implanted (Zheng et al., 2013), which is 20 times fewer than the number of cells implanted in the current study. This discrepancy could be due to the much lower downregulation of SULF2 mRNA (3.4-fold) in the cells generated by Zheng and colleagues after stable transfection with shRNA and the consequently modest downregulation of SULF2 at the protein level as shown by WB (Zheng et al., 2013). The study here and two others are consistent in reporting that SULF2 knockdown prevents or retards the growth of tumours, with inhibition of Wnt signalling implicated as an underlying mechanism (Nawroth et al., 2007) (Lemjabbar-Alaoui et al., 2010). SULF2 overexpression in gastric cells or the HCC cell line Hep 3B was found to activate Wnt signalling and increase the tumourigenicity of cells *in vivo* (Lai et al., 2008 a) (Lai et al., 2010 b) (Hur et al., 2012), and the results presented here together with previous data suggest that SULF2 facilitates Wnt signalling in some tumour cell lines and that SULF2 inhibition would be detrimental to cell growth *in vitro* and tumourigenicity *in vivo*.

Effects of SULF1/2 knockdown in the SNU-182 cell line

The effects of SULF1/2 knockdown were also investigated in the SNU-182 cell line. The SNU-182 cell line was derived from a poorly differentiated HCC and expresses both SULF1 and SULF2 at high and comparable levels. SNU-182 cells have wild-type β-catenin but a p53 mutation S215I (AGT → ATT) leading to the substitution of isoleucine for serine (Cagatay and Ozturk, 2002). Knocking down SULF1 and SULF2 in this cell line allows comparison of the biology and the roles of SULF1 and SULF2 in the context of HCC. Infecting cells with SULF1/2 shRNA lentiviral particles caused downregulation of SULF2 (16-fold) in the SULF2 shRNA-transduced cells and downregulation of SULF1 (6.5-fold) in the SULF1 shRNA-transduced cells, as compared to NT shRNA-transduced cells, after two weeks of

selection with antibiotic (Figure 5.24; A). After two months of growing the cells under selection pressure, the suppression of gene expression was further increased to 56-fold for SULF2 and 9-fold for SULF1 (Figure 5.24; B). Interestingly, there was a late effect of SULF1 suppression on the expression of SULF2 as shown by a 2-fold downregulation of SULF2 expression in the SULF1 knockdown cells (Figure 5.24; B). However, there were no late effects on the expression of the other genes tested, namely B2M, TP53 and KLF6, after either SULF1 or SULF2 knockdown in the SNU-182 cell line. The suppression of SULF1/2 mRNA expression was confirmed in all cases at the protein level by WB (Figure 5.25).

Mechanistically, SULF2 but not SULF1 knockdown in SNU-182 cells caused inhibition of FGF-1- and FGF-2-stimulated p-ERK levels as shown by WB (Figure 5.25) or p-ERK ELISA (Figure 5.26), but SULF2 knockdown did not affect the basal level of p-ERK in this cell line. Two positive controls were used for inhibition of ERK phosphorylation, namely, the FGFR inhibitor PD173074 and the MEK inhibitor PD0325901. Both compounds inhibited basal and FGF-stimulated levels of p-ERK regardless of the SULF2 expression status (Figure 5.25) (Figure 5.26). Also, SULF2 but not SULF1 knockdown inhibited IGF-II- but not IGF-I-stimulated p-AKT levels, but again there was no effect on the basal level of p-AKT as a result of SULF2 knockdown (Figure 5.27). This result is interesting as IGF-II but not IGF-I is overexpressed in up to 40% of HCCs (Cariani et al., 1988) (Breuhahn and Schirmacher, 2008).

Previous studies have shown that targeting one of the FGF receptors, FGFR4, using antibodies blocks the binding of FGF-1 and FGF-19, and inhibits the growth of HCC cells *in vitro* and *in vivo* (Bumbaca et al., 2011) (French et al., 2012). Also, antibodies against FGFR4 or FGF-19 prevented the development of liver cancer in a FGF-19 transgenic animal model of HCC (Desnoyers et al., 2008) (French et al., 2012). In other animal models of HCC, re-expression of IGF-II coincided with disease progression (Schirmacher et al., 1992). Conversely, inhibition of the IGF-II pathway by neutralizing antibodies against IGF-II or its receptor IGF-1R in HCC cell lines decreased cell proliferation and increased chemotherapeutic agent-induced apoptosis (Lund et al., 2004). Small molecule inhibitors of growth

factor/RTK pathways are already in Phase III clinical trials for HCC including BMS582664/brivanib (Bristol-Myers Squibb) that works against FGFR and VEGFR (Johnson et al., 2013), TSU-68/orantinib (Pfizer) that targets FGFR, PDGFR and VEGFR2 (Kanai et al., 2011) and PI-88 (Progen) that works against FGF-1, FGF-2 and VEGF (Liu et al., 2009). In addition, more selective inhibitors are now in Phase I trials for solid tumours including BGJ398 (Novartis) targeting FGFR1-3 and LY2874455 (Eli Lilly) against FGFR1-4 (Brooks et al., 2012). Collectively, these studies demonstrate the level of interest in targeting this pathway in the management of cancer, and there are potential applications for these and related drugs in HCC. Interference with FGF or IGF signalling pathways through inhibiting SULF2 could provide an alternative mechanism for preventing tumour growth in HCC that is dependent on RTK signalling.

Wnt signalling was not functional in SNU-182 cells as there was no response to exogenous Wnt-3a up to 200 ng/ml as measured by 7TFP luciferase reporter activity (Figure 5.28). This result is consistent with an independent study showing that TCF activity was not detected in SNU-182 cells and that transient transfection of SNU-182 cells with a mutant form of β-catenin lacking the GSK-3β phosphorylation site, Ser33, did not induce canonical Wnt signalling (Yuzugullu et al., 2009). The lack of response to Wnt-3a in this cell line cannot be attributed to the lack of canonical frizzled receptors as FZD1, 5, 7, 9 were shown by RT-PCR to be expressed in this cell line (Yuzugullu et al., 2009). Instead, it was proposed that SNU-182 cells are resistant to canonical Wnt signalling as a result of the high expression of non-canonical Wnt ligands, especially Wnt-5a (Yuzugullu et al., 2009), which can antagonize the canonical pathway (Liang et al., 2003) (Hu et al., 2007) (Yuzugullu et al., 2009).

Interestingly, there was a late but not an early effect of SULF1 and SULF2 knockdown on the expression of glypican 3 (GPC3), an HSPG that is anchored to the cell surface. SULF1 knockdown caused 11-fold and SULF2 knockdown caused 4-fold downregulation of GPC3 expression (Figure 5.29). However, downregulation of GPC3 cannot explain the inhibition of growth factor/RTK signalling in SNU-182 cells, given the lack of an effect of SULF1 knockdown on this pathway, even

though SULF1 knockdown caused greater GPC3 downregulation than SULF2 knockdown. However, this result does not rule out a possible detrimental effect of GPC3 knockdown on other signalling pathways, because either SULF1 or SULF2 knockdown inhibited the proliferation of SNU-182 cells (Figure 5.30). Unfortunately, the effect of SULF1/2 knockdown on the tumourigenicity of SNU-182 cells could not be tested due to the inability of SNU-182 cells to form tumours in either nude mice or more immunodeficient NSG (NOD scid gamma) mice, despite one report that SNU-182 cells are tumourigenic in nude mice (Song et al., 2006).

Effects of SULF1/2 knockdown in other HCC cell lines and the BxPC3 pancreatic cancer cell line

In the HepG2 cell line, which is derived from a well differentiated hepatoblastoma, SULF2 was downregulated by only 2.6-fold in the SULF2 knockdown cells as compared to NT shRNA-transduced cells (Figure 5.10). HepG2 cells have mutant β-catenin, mutant N-Ras at codon 61 position 2 (A → T) and mutant Rb, and SULF2 knockdown had no clear effect on the growth factor/RTK signalling pathway after stimulation with a range of growth factors (Figure 5.31). HepG2 cells express both a wild-type as well as the truncated mutant form of β-catenin produced by an interstitial deletion in the domain that is usually phosphorylated by GSK-3β, making β-catenin constitutively active (de La Coste et al., 1998) (Cagatay and Ozturk, 2002). HepG2 cells were found to be responsive to exogenous Wnt-3a (data not shown), presumably due to the wild-type allele, and the effect of SULF2 knockdown was investigated on Wnt-3a-induced β-catenin-dependent TCF activity. However, basal TCF activity was very high in the HepG2 cells, compared to the activity of the mutated form of the TCF reporter serving as a negative control (Figure 5.32), and treatment with Wnt-3a did not increase activity any further. Collectively, SULF2 seems not to play a role in the growth of HepG2 cells and this was confirmed by SRB growth assays where the SULF2 knockdown cells grew at a similar rate to the control untransduced and NT shRNA-transduced cells (Figure 5.33). It is most probable that in this cell line, due to the endogenous β-catenin mutation and activation of the Wnt signalling pathway, exogenous activation by Wnt ligands has no phenotypic effect.

SULF2 was also knocked down in the SNU-475 cell line which is derived from a poorly differentiated HCC. However, no phenotypic effect of either SULF1 or SULF2 knockdown was observed (data not shown). There was low expression of SULF1/2 genes in this cell line, and hence the cell line may not depend on SULF1/2 activity for proliferation. SULF2 knockdown in a pancreatic cancer cell line, BxPC3, that expresses high levels of SULF2 and low levels of SULF1, caused 12-fold downregulation of SULF2 mRNA levels, complete loss of SULF2 protein and reduction of cell growth *in vitro* and a small delay of tumour growth *in vivo*, as compared to control untransduced and NT shRNA-transduced cells (Figure 7.6). This effect of SULF2 knockdown in BxPC3 cells is consistent with the findings of an independent study that also showed inhibition of autocrine Wnt signalling (Nawroth et al., 2007). No effect of SULF2 knockdown on growth factor/RTK signalling pathways was observed in the BxPC cells studied here (data not shown), while the effect on Wnt signalling was not studied. A summary of the effects of SULF2 knockdown on cell signalling, growth and tumourigenicity is presented in Table 8.2.

Table 8.2: Summary of the effects of SULF2 knockdown on cell signalling, growth and tumourigenicity in HCC and BxPC3 pancreatic cancer cell lines.

Cell line	Effect on signalling	Effect on cell growth	Effect on tumourigenicity
SNU-182	↓FGF-1-stimulated p-ERK ↓FGF-2-stimulated p-ERK ↓IGF-II-stimulated p-AKT No effect on IGF-I signalling No functional Wnt signalling	↓Growth	Not applicable*
SNU-475	Not tested	No effect	Not tested
HuH-7	↓Wnt-3a-induced β-catenin-dependent transcriptional activity No effect on FGF-1, FGF-2, IGF-I or IGF-II signalling	↓Growth	Complete inhibition of tumourigenicity
HepG2	No effect on FGF-1, FGF-2, IGF-I or Wnt signalling	No effect	Not tested
BxPC3	No effect on FGF-1, FGF-2, IGF-I or IGF-II signalling Effect on Wnt signalling not studied	↓Growth	Minimal delay of tumour growth

* Parental SNU-182 cells are not tumourigenic in nude or NSG mice.

Inducible SULF1/2 knockdown in HCC cell lines

Due to the detrimental effects of constitutive SULF2 knockdown on the growth of both HuH-7 and SNU-182 cells, and to characterise further the downstream consequences of SULF1 and SULF2 knockdown on signalling pathways in these two cell lines, IPTG (isopropyl β-D-1-thiogalactopyranoside)-inducible shRNAs for SULF1 and SULF2 were evaluated. The shRNA sequences that caused the highest level of silencing of the SULF1 and SULF2 genes were used and cloned into the inducible constructs, designated iSULF1.shRNA and iSULF2.shRNA, respectively. Also, an inducible construct for an NT shRNA was used and this was called iNT.shRNA. The sequence of the inducible NT shRNA was different from that of the constitutive NT shRNA (Table 2.3), but nevertheless did not match any

known human gene. These inducible constructs have three LacO sequences in the U6 promoter instead of one (Figure 2.4) to ensure tight regulation and minimal leakiness of shRNA expression, while allowing the production of shRNA on addition of IPTG. Regulation of shRNA expression is based on the *lac* operator-repressor gene system, and in the absence of lactose or its analogue IPTG the protein encoded by the LacI (lac repressor) binds to the LacO (lac operator) sequences that are inserted in the U6 promoter, thus blocking transcription of the shRNA. On adding IPTG, the lactose analogue binds to the lac repressor protein modifying its affinity for LacO and thus allowing expression of the shRNA. This system is proven to work *in vitro* and *in vivo* and has the advantage of a fast response to IPTG induction that was observed as early as one day post-treatment in the two cell lines tested (i.e., HuH-7 and SNU-182) (Figure 6.1). One mM IPTG was found to be enough to induce SULF1/2 knockdown, and IPTG was shown to be stable in conditioned medium. In addition, it was found that knockdown was greater with longer incubation with IPTG (Figure 6.2) (Figure 6.3). Interestingly, treatment of SNU-182 cells with IPTG for 8 days caused 5-fold downregulation of SULF1 in iSULF2.shRNA-transduced cells and conversely SULF2 was downregulated in iSULF1.shRNA-transduced cells (Figure 6.3; B), while no effect on SULF1/2 expression was detected after treating iNT.shRNA-transduced cells with IPTG. Also, there was no effect of treating iNT.shRNA-, iSULF1.shRNA- or iSULF2.shRNA-transduced cells with IPTG on the expression of B2M, indicating the specificity of SULF1/2 knockdown (Figure 6.2) (Figure 6.3).

To confirm the expression of iNT.shRNA after IPTG treatment, and to compare the level of the inducible shRNAs expression to that of the constitutive shRNAs, the amount of shRNA was analysed using RT-qPCR in the SNU-182 cell line using the QuantiMir small RNA quantification system, which converts the shRNA species into cDNA. The results showed comparable expression of the inducible iSULF2.shRNA after 8 days of treatment with IPTG to that produced by constitutively expressed SULF2 shRNA (6.4- vs. 9.3-fold) (Figure 6.4; A). The RT-qPCR data also indicated expression of both the inducible iNT.shRNA and the constitutively expressed NT shRNA in SNU-182 cells (Figure 6.4; B and C). However, as these two NT shRNAs

have different sequences, it was not possible to directly compare their expression levels.

The effect of inducible SULF1/2 knockdown was investigated in the HuH-7 and SNU-182 cell lines. Inducing SULF2 knockdown in HuH-7 cells caused reduction of the β-catenin-dependent TCF transcriptional activity that was stimulated by Wnt-3a, but not that stimulated by BIO. No effect of inducing iNT.shRNA expression was seen on Wnt signalling (Figure 6.5). However, the effect of inducible SULF2 knockdown on Wnt signalling was much less than that observed after constitutive SULF2 knockdown, and this reduced effect could explain the lack of any impact of inducible SULF2 knockdown on the growth of HuH-7 cells *in vitro* (Figure 6.6). Given that the microenvironment *in vivo* is different from that in cell culture, and based on the finding that constitutive SULF2 knockdown caused complete inhibition of tumourigenicity of HuH-7 cells, the effect of inducible SULF2 knockdown *in vivo* was also investigated.

Induction of gene expression *in vivo* in mice has been reported 48 hours after adding IPTG to the drinking water, and shown to regulate the expression of the lac system in nearly all tissues (Wu et al., 1997) (Cronin et al., 2003) (Smith et al., 2004). Mice with subcutaneous implants of iNT.shRNA- or iSULF2.shRNA-transduced HuH-7 cells were split into two groups (n = 10 per group) and half the mice in each group received IPTG in the drinking water. However, IPTG treatment did not affect the tumourigenicity or change the mean time to reach a tumour volume of 500 mm^3 among the resulting four groups (Figure 6.7). The induction of SULF2 knockdown in the HuH-7 tumours originating from iSULF2.shRNA-transduced cells by IPTG treatment was investigated by RT-qPCR and a 4.2-fold downregulation of SULF2 expression was demonstrated, while there was no change in SULF2 expression in the iNT.shRNA group with or without IPTG treatment (Figure 6.7; C). This low level of SULF2 knockdown in the tumours could be the reason for the lack of an effect on tumourigenicity with inducible SULF2 knockdown in HuH-7 cells as it is far lower than that achieved using constitutive SULF2 knockdown (37-fold) (Figure 5.9). This result is consistent with an independent study where a 3.4-fold downregulation of SULF2 mRNA expression in

HuH-7 cells did not impede tumourigenicity in nude mice (Zheng et al., 2013). Therefore, a high level of SULF2 suppression may be required before any phenotypic effect is produced in the HuH-7 cell line. The duration of SULF2 suppression could also be an important factor as SULF2 was only knocked down after implantation in the case of inducible shRNA, while it was already knocked down for about two months before implantation in the case of HuH-7 cells with constitutive shRNA expression. Thus, prolonged SULF2 loss may be needed to inhibit tumourigenicity in HuH-7 cells.

Neither SULF1 knockdown nor SULF2 knockdown caused any effect on the p-ERK levels stimulated by FGF-1 or FGF-2, or on p-ERK or p-AKT levels stimulated by IGF-I (Figure 6.8) or IGF-II (data not shown) in the SNU-182 cell line. Also, no effect on the growth of these cells was observed after inducible SULF1/2 knockdown (Figure 6.9). This result is in contrast to the detrimental effects of constitutive SULF2 knockdown on growth factor/RTK signalling, and the effect of either SULF1 or SULF2 constitutive knockdown on the growth of SNU-182 cells.

Collectively, these data suggest that SULF1/2 knockdown in HuH-7 and SNU-182 cell lines must be maintained at a high level and for adequate time period before effects on cell growth and tumourigenicity are seen.

The effect of SULF2 knockdown on gene expression in HCC cell lines

To extend studies of the effect of SULF1/2 knockdown beyond growth factor/RTK and Wnt signalling pathways, microarray gene expression analysis was performed in HuH-7 cell lines using Affymetrix human genome U133 plus 2.0 arrays. In addition to understanding the biological impact of SULF2 suppression, the experiment could identify biomarkers for SULF2 inhibition. More than 54,000 probe sets were analysed corresponding to 47,400 transcripts and variants encoded by 38,500 characterised genes. Samples were provided as biological quadruplicates and SULF2 expression was first confirmed by RT-qPCR (Figure 7.1; A). There was 3-fold upregulation of SULF2 in the NT shRNA-transduced cells as compared to control untransduced cells, possibly due to infecting cells with lentiviral particles. In SULF2 shRNA-transduced cells, SULF2 expression was downregulated 34- and

11-fold compared to NT shRNA-transduced cells and control untransduced cells, respectively (Figure 7.1; A).

The microarray data revealed changes in the expression level of many genes in the control untransduced cells as compared to the NT shRNA- and SULF2 shRNA-transduced cells as shown by the principal component analysis plot (Figure 7.1; B). Changes could be due to transduction with lentiviral particles and/or selection with puromycin regardless of SULF2 expression status. These results suggest that NT shRNA-transduced cells could represent a better control for the effects of SULF2 knockdown than control untransduced cells. Only genes that were differentially expressed in the SULF2 knockdown cells with ≥ 2-fold change and adjusted *p* value ≤ 0.01 compared to both NT shRNA-transduced and control untransduced cells and that showed a similar trend in the NT shRNA-transduced and control untransduced cells (i.e., upregulation or downregulation in both cell lines) as compared to SULF2 knockdown cells were taken into consideration for further analysis. These criteria identified 444 differentially expressed probe sets representing 322 genes (Figure 7.2) (Appendices A and B). The genes are involved in a range of pathways, and pathways with at least two affected genes are listed in Table 7.1.

The most differentially expressed genes were chosen for further analysis (n = 26) (Table 7.2), and the expression of genes that have a potential link to cancer was confirmed by RT-qPCR (n = 18) (Table 7.2). Subsequently, seven genes that have been implicated in hepatocarcinogenesis were studied at the protein level; namely ACE2, PCDH20, SLPI, TFPI2, WNT5A, MYCN and DLK1. However, only the antibodies for ACE2 and MYCN performed satisfactorily in WB such that the effect of SULF2 suppression could be confirmed at the protein level (Figure 7.4).

ACE2 and Ang-(1-7)

Microarray data showed that the most highly upregulated gene after SULF2 knockdown in the HuH-7 cell line was angiotensin I converting enzyme (peptidyl-dipeptidase A) 2 (ACE2), using two different probe sets. The expression of this gene inversely correlated with SULF2 expression as evidenced by microarray and

RT-qPCR analyses (Figure 7.3). The relationship was also observed at the protein level where ACE2 protein was only detected in the SULF2 knockdown cells (Figure 7.4).

ACE2 is a newly discovered member of the renin-angiotensin system (RAS). In the past, RAS was thought to be a simple linear pathway that leads to the formation of the final active peptide angiotensin II (Ang II) through the catalytic activity of angiotensin I converting enzyme (peptidyl-dipeptidase A) 1 or ACE (Figure 8.1). Ang II then acts on the Ang II type 1 receptor (AT1R) (Figure 8.1) to exert its effects that were initially thought to be restricted to increasing blood pressure through vascular smooth muscle cells, inducing vasoconstriction and regulating electrolyte and fluid homeostasis. Subsequently, it was found that the ACE/Ang II/AT1R axis is also involved in promoting fibrosis, cell proliferation and inflammation (Mezzano et al., 2001) (Suzuki et al., 2003).

Understanding of the RAS was further revised by the discovery of the ACE homologue, ACE2 in 2000 (Donoghue et al., 2000) (Tipnis et al., 2000). ACE2 is a zinc metalloprotease with 40% homology to ACE in the catalytic domain and is a type I transmembrane ectoenzyme; it has a signal sequence at the N-terminus and is anchored to the cell membrane by its C-terminus (Warner et al., 2005). Furthermore, the ectodomain of the enzyme can be cleaved post-translationally by ADAM17 to give a soluble functional glycoprotein enzyme (Lambert et al., 2005).

Therefore, to determine the level and localization of ACE2 in the SULF2 knockdown cells, flow cytometry analysis was performed which demonstrated that 45% of SULF2 knockdown cells were ACE2-positive with higher fluorescence intensity compared to control untransduced and NT shRNA-transduced cells, where 10% and 4% of the cells were ACE2-positive, respectively. Also, ACE2 was shown to be expressed at the cell surface (Figure 7.7).

The importance of ACE2 arises from its ability to convert Ang II with very high efficiency into the biologically active peptide angiotensin 1-7 (Ang-(1-7)). Ang-(1-7) stimulates the Mas receptor (MasR) which is a separate G protein-coupled receptor to AT1R with completely opposite properties including vasodilation, anti-

fibrotic, anti-proliferative and anti-inflammatory effects (Figure 8.1) (Santos et al., 2003) (Tallant and Clark, 2003) (Tallant et al., 2005). Therefore, this second arm of RAS counterbalances effects resulting from the over-activation of the classical arm. Also, both Ang II and Ang-(1-7) stimulate to a lesser degree the Ang II type 2 receptor (AT2R) (Figure 8.1). Activation of the AT2R can induce apoptosis and inhibit cell proliferation (Nakajima et al., 1995) (Stoll et al., 1995) (Li et al., 2009).

To determine whether or not the overexpressed ACE2 enzyme is catalytically active in SULF2 knockdown cells, the enzymatic activity of cell lysates was tested using two fluorogenic substrates that generate the fluorescent molecule 7-methoxycoumarin. The assay showed higher activity in SULF2 knockdown cell lysates as compared to that of control untransduced and NT shRNA-transduced cell lysates (Figure 7.8). Also, the level of ACE2 product, Ang-(1-7), was measured by ELISA in the CM of cultures of these cells. The results showed that the level of Ang-(1-7) was 56 and 48 pg/ml for CM from control untransduced and NT shRNA-transduced cell cultures, respectively, which falls within the range of physiological levels in the plasma of healthy volunteers of 32 ± 27 pg/ml (Reyes-Engel et al., 2006). In contrast, the level of Ang-(1-7) was 3-times higher in the CM from SULF2 knockdown cells (154 pg/ml) (Figure 7.9), confirming that the overexpressed ACE2 was catalytically active in the SULF2 knockdown cells.

ACE2 is different to ACE in several ways. First of all, ACE2 has only one active site while ACE has two homologous active sites (Donoghue et al., 2000). Secondly, ACE2 acts as a carboxymonopeptidase, and hence removes one amino acid from the carboxy terminus in substrates like angiotensin I (Ang I) to produce angiotensin 1-9 (Ang-(1-9)) or Ang II to give Ang-(1-7). In contrast, ACE cleaves the C-terminal dipeptide from substrates like angiotensin I (Ang I) to produce Ang II, Ang-(1-9) to give Ang-(1-7), or the vasodilator bradykinin (Donoghue et al., 2000) (Tipnis et al., 2000) (Rice et al., 2004). However, the affinity of ACE2 for Ang I is much lower than that of ACE, whereas ACE2 has a high catalytic activity for Ang II that is 400-fold greater than that for Ang I (Vickers et al., 2002) (Rice et al., 2004). Thirdly, ACE2 is not inhibited by ACE inhibitors such as captopril and lisinopril that bind to both active sites of ACE (Ehlers and Riordan, 1991) (Donoghue et al., 2000)

(Tipnis et al., 2000). Fourthly, ACE2 is particularly expressed in heart, kidney and testis whereas the expression of ACE is more widespread in the endothelium of somatic tissues (Donoghue et al., 2000).

ACE2 knockout mice have been generated (Crackower et al., 2002), and the role of ACE2 studied in the context of cardiovascular physiology and the pathogenesis of cardiovascular disease, not cancer. ACE2 null mice are healthy and fertile with normal organ function. However, they show progressive severe contractile dysfunction of the heart that subsequently results in reduced blood pressure with no signs of cardiac fibrosis or hypertrophy. This effect was attributed to increased cardiac hypoxia as evidenced by the upregulation of hypoxia-inducible genes. Ang II and Ang I were also increased in ACE2 knockout mice, but no change in ACE expression was detected. All these observed changes were reversed in the ACE and ACE2 double knockout mice (Crackower et al., 2002), suggesting that the effects observed in the ACE2 knockout mice may be the result of dysregulated RAS system.

Role of ACE2 and Ang-(1-7) in liver fibrosis and cirrhosis

Recently, activation of the classical RAS arm was found to be associated with liver injury, fibrosis and cirrhosis (Paizis et al., 2002). It was also found that activated human hepatic stellate cells (HSCs), which play an essential role in hepatic fibrosis, express high levels of renin and ACE and secrete Ang II, as opposed to quiescent HSCs which only express these elements at low levels and do not secrete Ang II (Bataller et al., 2003 a). Also, it was shown that Ang II promotes the activation of HSCs and their transformation into extracellular matrix-producing myofibroblasts (Bataller et al., 2000) (Bataller et al., 2003 b). Administration of Ang II during liver injury in rat models caused liver fibrosis that was alleviated by blocking the AT1R by AT1R blockers including olmesartan and candesartan (Hirose et al., 2007). Furthermore, fibrosis was completely inhibited in AT1R knockout mice (Yang et al., 2005), but was enhanced in AT2R knockout mice (Nabeshima et al., 2006). These studies reveal the role of the classical RAS arm in liver fibrosis.

It has been reported that human ACE2 protein, which is usually only weakly expressed by endothelial cells, perivenular hepatocytes and bile duct cells in healthy livers, was overexpressed by parenchymal cells in cirrhotic livers (Paizis et al., 2005). Furthermore, hepatic ACE2 and MasR expression was increased in rats with cirrhosis, and plasma Ang-(1-7) levels elevated in rats and patients with cirrhosis (Herath et al., 2007) (Lubel et al., 2009). Ang-(1-7) improved fibrosis stage in a cirrhotic rat model and decreased expression of the fibrosis marker α-SMA (alpha-smooth muscle actin). Decreased α-SMA expression was also observed after treating rat HSCs with Ang-(1-7) or the MasR agonist AVE-0991, an effect that was reversed by the MasR antagonist, [D-Ala^7]-Ang (1-7) (also called A-779) where the amino acid proline in Ang-(1-7) is modified by D-alanine at position 7 (Lubel et al., 2009). Additionally, ACE2 knockout mice showed increased chronic liver damage and fibrosis compared to wild-type littermates, which was attenuated by treatment with recombinant human ACE2 (rhACE2) protein (Osterreicher et al., 2009). Collectively, these data suggest a role of the alternative RAS arm in counteracting aberrant RAS over-activation in liver disease.

Two strategies can be employed to manipulate the RAS system in liver disease. The first is to inhibit the classical arm by using an ACE inhibitor (ACEi) or an AT1R blocker (ARB). However, there is insufficient evidence to recommend this approach in liver fibrosis (Grace et al., 2012). The second strategy is to activate the alternative ACE2/Ang-(1-7)/MasR arm by administering ACE2, Ang-(1-7) or MasR agonists. In animals, rhACE2 administration was demonstrated to attenuate cardiovascular (hypertension) and renal (diabetic nephropathy) disease, and liver fibrosis (Oudit et al., 2010) (Wysocki et al., 2010) (Osterreicher et al., 2009). Also, in healthy human volunteers, rhACE2 was well-tolerated with no adverse effects in Phase I clinical trials (Haschke et al., 2013). Ang-(1-7) has a very short half-life in plasma (20 seconds) after intravenous (*i.v.)* administration in rats (Iusuf et al., 2008). However, in humans, the half-life is 29 - 30 min after *i.v.* or subcutaneous administration (Kono et al., 1986) (Rodgers et al., 2006). More stable oral formulations were developed for Ang-(1-7), such as hydroxypropyl β-cyclodextrin-coated Ang-(1-7), and this drug was found to have cardioprotective effects (Marques et al., 2011). Alternatively, the MasR could be stimulated using the

agonist AVE-0991 which has been shown to be effective in models of cardiovascular disease when given intraperitoneally or orally (Ferreira et al., 2007) (Benter et al., 2007) (Ebermann et al., 2008).

Role of ACE2 and Ang-(1-7) in cancer

In addition to treating liver fibrosis and cirrhosis, the alternative RAS arm has potential in treating HCC itself. Recent studies have indicated that the alternative RAS arm can be used as a treatment for cancer based on its anti-proliferative and anti-angiogenic effects. Overexpression of ACE2 in the NSCLC A549 cell line reduced invasion and expression of tumour metastasis-promoting enzymes, matrix metalloproteinases MMP2 and MMP9, *in vitro* and inhibited tumour growth and downregulated VEGF-A, ACE and AT1R expression *in vivo* (Feng et al., 2011).

ACE2 expression was found to be downregulated in pancreatic ductal adenocarcinoma (PDAC) compared to normal neighbouring tissues as opposed to ACE and AT1R expression, and Ang II levels were higher in PDAC (Arafat et al., 2007) (Feng et al., 2011). In addition, ACE2 expression was found to be inversely related to tumour stage (Zhou et al., 2009). Suppressing ACE2 expression in two pancreatic cancer cell lines with siRNA promoted cell proliferation *in vitro* (Zhou et al., 2009), while overexpressing ACE2 in the same cell lines inhibited their proliferation, migration and invasion and sensitized them to hypoxia *in vitro*, and reduced the growth of tumour xenografts and VEGF-A expression *in vivo*. Treating established pancreatic tumour xenografts with ACE2-carrying adenovirus reduced their growth and further enhanced the survival of the mice when combined with the chemotherapeutic agent gemcitabine (Zhou et al., 2011 b). Furthermore, ACE2 and ACE expression and activity were shown to be downregulated in renal cancer (Larrinaga et al., 2010). Lastly, clinical data in HCC showed that ACE2 expression was upregulated in 84 cases and downregulated in 196 cases with a deregulation ratio of 47% (Center for Bioinformatics and Computational Biology, East China Normal University, HCCNet database, 2013).

Collectively, studies investigating regulation of ACE2 in different types of cancer have shown that ACE2 may be a potential therapeutic target for cancer treatment due to its ability to suppress the growth of cancer cells and tumour angiogenesis.

Ang-(1-7), the main product of ACE2 activity, reduced the growth of three human NSCLC cell lines (SK-LU-1, A549 and SK-MES-1) *in vitro*, an effect that was mediated through activation of the MasR that is expressed in these cells; blocking the AT1R or AT2R or treatment with Ang II did not alter the inhibitory effect of Ang-(1-7). Ang-(1-7) treatment also reduced the phosphorylation of ERK in SK-LU-1 cells which could explain the growth inhibitory effect of Ang-(1-7) in this cell line (Gallagher and Tallant, 2004). Treating the A549 cell line with Ang-(1-7) inhibited their invasion and migration *in vitro* which was associated with reduced phosphorylation of p38 MAPK and JNK, and MMP2 and MMP9 activity (Ni et al., 2012). Treating mice with A549 human tumour xenografts with Ang-(1-7) reduced tumour growth *in vivo* which was accompanied by a reduction in cyclooxygenase-2 expression in the tumour. Thus, the growth inhibitory effect of Ang-(1-7) may be mediated through decreased pro-inflammatory prostaglandin synthesis (Menon et al., 2007). Treatment of orthotopic human breast tumour-bearing mice with Ang-(1-7) reduced the growth of stroma myofibroblasts and fibrosis in tumour microenvironment, which was associated with (1) reduced TGF-β1 (transforming growth factor-β1), that is responsible for fibroblast activation, and (2) increased DUSP1 (dual specificity phosphatase 1) which dephosphorylates, and hence deactivates ERK (Cook et al., 2010).

Furthermore, Ang-(1-7) decreased vascular smooth muscle cell growth *in vitro* and *in vivo* (Freeman et al., 1996) (Strawn et al., 1999), and microvessel density in lung tumour xenografts that was associated with a reduction in VEGF-A expression (Soto-Pantoja et al., 2009), revealing an important antiangiogenic role. In another study, Ang-(1-7) was found to inhibit the proliferation of prostate cancer cell lines that express the MasR *in vitro* and *in vivo*, and attenuated their metastatic potential. The inhibition was associated with a reduction in p-ERK levels, vessel density and expression of the two angiogenic factors VEGF-A and PIGF and the

FLT-1 receptor, and an increase of the inhibitory secreted form of the receptor sFTL-1 in tumour extracts (Krishnan et al., 2013 a) (Krishnan et al., 2013 b).

All the above studies are consistent with Ang-(1-7) exerting its anti-tumourigenic and anti-angiogenic effects through stimulating the MasR. This view was confirmed by a further study showing that Ang-(1-7) inhibited angiogenesis in sponge implants in mice, where inhibition was not affected by ACEi, ARB or AT2R inhibitors (Machado et al., 2001), while the potent and selective MasR antagonist A-779 abolished the Ang-(1-7) effect. The effect of Ang-(1-7) on vascularisation was found to be mediated by nitric oxide (NO) release as treating mice with NO synthase inhibitors attenuated Ang-(1-7) effect (Machado et al., 2001).

Clinically, Ang-(1-7) has been used in Phase I clinical trials in patients with advanced solid tumours. Ang-(1-7) was generally well-tolerated and caused a reduction in plasma level of PlGF (placental growth factor) in patients. There was also evidence of clinical benefit manifested as stabilization of the disease for more than 3 months (Petty et al., 2009).

In summary, several studies validate the RAS system as a target for cancer therapy. In addition, components of this system have been found to be expressed in the tumour environment (Ino et al., 2006) (Herr et al., 2008), and the RAS system may provide approaches to cancer chemoprevention. For instance, in retrospective analyses and follow-up studies of hypertensive patients, it was found that long-term use of ACEi reduced the risk of cancer compared to other types of antihypertensive drugs (Pahor et al., 1996) (Jick et al., 1997) (Lever et al., 1998) (van der Knaap et al., 2008). Moreover, combining ACEi or ARB with chemotherapy has been reported to increase the survival of pancreatic cancer and NSCLC patients (Wilop et al., 2009) (Nakai et al., 2010), and improve progression-free survival in pancreatic cancer and renal cell carcinoma (Nakai et al., 2010) (Keizman et al., 2011). Also, ACEi or ARB reduced the risk of breast cancer recurrence (Chae et al., 2011) and distant metastasis in colorectal cancer patients (Heinzerling et al., 2007). Such effects could be due to decreased Ang II concentrations or increased Ang-(1-7) levels.

There was no effect of Ang II treatment on cell growth of control untransduced, NT shRNA-transduced cells or SULF2 knockdown HuH-7 cells (Figure 7.10). This result is in line with an independent study showing an increase in HuH-7 cell proliferation after treatment with Ang II for 24 hrs that was no longer apparent at 48 hrs (Itabashi et al., 2008). These data suggest that Ang II has no mitogenic effects in HuH-7 cell lines even though AGTR1, the gene encoding Ang II receptor, is expressed in HuH-7 cells as analysed by RT-qPCR (Ct value of 25 compared to Ct value of 17 for GAPDH). AGTR1 was also shown to be expressed at the protein level in HuH-7 cells (Itabashi et al., 2008). Similarly, treatment with Ang-(1-7) did not cause any change in cell growth of any of the three cell lines, which could be due to the low expression of MAS1, the gene encoding Ang-(1-7) receptor, in HuH-7 cells (Ct value of 36 compared to Ct value of 17 for GAPDH).

It is conceivable that expression of the MasR in a tumour may be necessary for patients to benefit from Ang-(1-7) or a MasR agonist. However, given that MasR is expressed on endothelial cells (Tallant et al., 1997) and Ang-(1-7) directly inhibits endothelial cell tubule formation (Soto-Pantoja et al., 2008) (Soto-Pantoja et al., 2009), tumour cell MasR expression might not be required to inhibit tumour angiogenesis.

The effect of SULF1/2 knockdown on the expression of RAS elements was also studied in other cell lines. ACE2 was slightly upregulated (≥ 1.5-fold) after SULF2 suppression and downregulated (≥ 1.9-fold) after SULF1 suppression in the SNU-182 cell line. No change in ACE expression was shown, while > 2-fold downregulation of AGTR1 was detected after SULF2 knockdown in SNU-182 cells (Table 7.3). MMP9 but not MMP2 was found to be downregulated (≥ 1.5-fold) after SULF2 knockdown and upregulated (> 2-fold) after SULF1 knockdown in SNU-182 cells (Table 7.3). In the BxPC3 cell line, ACE2 expression was > 2-fold upregulated after SULF2 knockdown (Figure 7.6; A). These data suggest a general effect of SULF2 knockdown on the expression of ACE2 in tumour cells; however, the effect was only profound in the HuH-7 cell line.

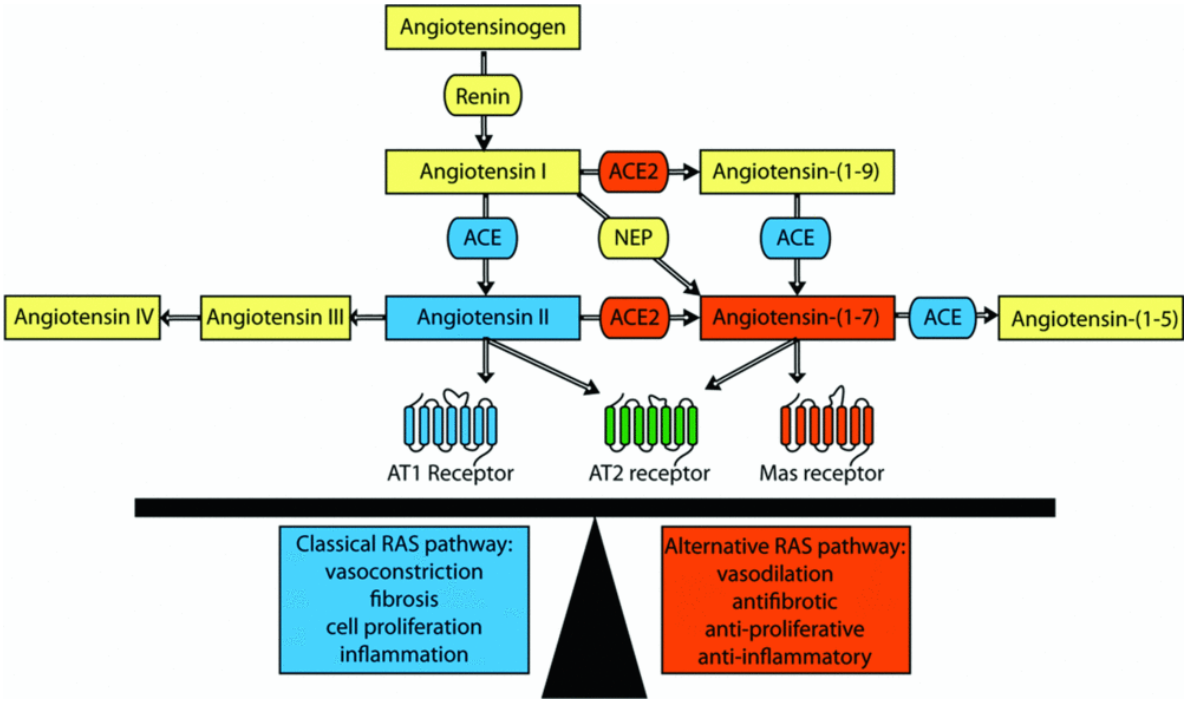

Figure 8.1: Renin-angiotensin system: The classical arm (ACE/Ang II/AT1 receptor) in blue leads to pro-inflammatory and pro-fibrotic responses, and the alternative arm in red (ACE2/Ang-(1-7)/Mas receptor) has anti-inflammatory and anti-fibrotic effects. The AT2 receptor in green can be activated by either Ang II or Ang-(1-7), and this often leads to similar effects to those resulting from Mas receptor activation. NEP: neprilysin. (Adapted from Grace et al., 2012).

Other genes differentially expressed after SULF2 knockdown

MYCN (v-myc myelocytomatosis viral related oncogene, neuroblastoma derived (avian)) was the other gene that showed changes at the mRNA and protein level after SULF2 knockdown in HuH-7 cells. The expression of MYCN correlated with the expression of SULF2, with ≥ 4-fold downregulation of MYCN mRNA expression (Figure 7.3) and a reduction in MYCN protein levels (Figure 7.4) after SULF2 knockdown. In the SNU-182 cell line, both SULF1 and SULF2 knockdown also caused downregulation of MYCN expression (≥ 1.5-fold) (Table 7.3). MYCN encodes the transcription factor N-Myc and overexpression of N-Myc is associated with different types of cancer especially neuroblastoma (Cheng et al., 1993). In neuroblastoma, MYCN expression has been reported to be related to advanced stages and metastasis of the disease, and associated with poor prognosis

(Brodeur et al., 1984) (Seeger et al., 1985). Overexpression of MYCN increased, and its suppression decreased, cell growth, invasion and migration in neuroblastoma cell lines (Burkhart et al., 2003) (Kang et al., 2006) (Tanaka and Fukuzawa, 2008). However, no studies have been reported on N-Myc in the context of HCC.

PCDH20 (protocadherin 20) showed ≥ 24-fold upregulation after SULF2 knockdown in HuH-7 cells (Table 7.2). PCDH20 is a member of the cadherin superfamily that encompasses over 80 members involved in cell-cell adhesion. However, little is known about protocadherin function and downstream signalling (Kim et al., 2011). Involvement of some protocadherins (protocadherin LKC, protocadherin 2 and protocadherin-PC) in carcinogenesis has been suggested in colon, renal and prostate cancer, and in HCC (Okazaki et al., 2002) (Stassar et al., 2001) (Chen et al., 2002). In established tumours there is only one study (Imoto et al., 2006) where PCDH20 was found to be expressed in normal lung tissues but epigenetically silenced in 53% (32 of 59) of NSCLC by promoter hypermethylation. Reduced PCDH20 expression was related to poor patient survival, and overexpression of PCDH20 in NSCLC cells inhibited cell growth *in vitro* (Imoto et al., 2006), suggesting a potential tumour suppressor role for PCDH20 in cancer.

SLPI (secretory leukocyte protease inhibitor) showed ≥ 38-fold upregulation after SULF2 knockdown in HuH-7 cells (Table 7.2). SLPI is secreted by epithelial and inflammatory cells of the digestive, respiratory and genital tracts, and SLPI has anti-protease, antibacterial and antiviral activities (Williams et al., 2006). Clinically, SLPI was found to be upregulated in 160 cases and downregulated in 203 cases in HCC with a deregulation ratio of 56% (Center for Bioinformatics and Computational Biology, East China Normal University, HCCNet database, 2013). The role of SLPI has been studied in different types of cancer and cancer-type dependent effects shown. For instance, in ovarian, lung and colon cancer cell lines, SLPI was found to have a tumour-promoting effect, and overexpression of SLPI increased cell proliferation *in vitro* and tumourigenicity *in vivo* (Devoogdt et al., 2003) (Devoogdt et al., 2009) (Amiano et al., 2013). In contrast, in oral squamous cell carcinoma (OSCC), SLPI was downregulated and inversely related to tumour progression,

with overexpression inhibiting the migration of OSCC cells *in vitro* (Wen et al., 2011). SPLI was also found to reduce the metastatic potential of lung carcinoma cells (Wang et al., 2006), and overexpression of SLPI in mammary cancer cells caused apoptosis *in vitro* and inhibited their tumourigenicity *in vivo* (Amiano et al., 2013). However, no studies have been reported on the role of SLPI in HCC.

TFPI2 (tissue factor pathway inhibitor 2) showed ≥ 13-fold upregulation after SULF2 knockdown in the HuH-7 cell line (Table 7.2). TFPI2 is a serine protease inhibitor and was found to inhibit the activation of MMPs (Rao et al., 1999). TFPI2 was reported to be downregulated in about 90% (38 of 42) of HCCs and silenced by promoter methylation in 47% (16 of 34) of HCC and in 62% (31 of 50) of colorectal cancers (Wong et al., 2007) (Hibi et al., 2010). Overexpression of TFPI2 in HCC cell lines (including HepG2 and Hep 3B) inhibited their proliferation and invasiveness *in vitro* (Wong et al., 2007) (Xu et al., 2011). Clinically, elevated TFPI2 methylation was detected in the sera of patients with HCC and in the tumours of colorectal cancer, especially in advanced cases, suggesting that TFPI2 may have a role in cancer progression (Hibi et al., 2010) (Sun et al., 2013). Given that TFPI2 expression increased after SULF2 knockdown, TFPI2 may be a biomarker for SULF2 inhibition.

Effect of SULF2 suppression on Wnt signalling-related genes

The microarray and RT-qPCR data for the HuH-7 cell line showed changes in the expression level of different Wnt signalling-related genes including the upregulation of WNT5A (wingless-type MMTV integration site family, member 5A) (> 5-fold) and CTBP2 (> 9-fold), and downregulation of DLK1 (delta-like 1 homolog (Drosophila)) (> 6-fold) (Table 7.2). In the SNU-182 cell line, both SULF2 and SULF1 knockdown caused ≥ 1.5-fold downregulation of DLK1 expression (Table 7.3). The WNT5A gene encodes Wnt-5a ligand that activates the non-canonical Wnt signalling pathway, and this ligand has been reported to antagonize the canonical Wnt signalling pathway in HuH-7 cells by inhibiting TCF reporter activity (Yuzugullu et al., 2009). Downregulation of Wnt-5a protein has been reported in 77% (65 of 85) and 81% (92 of 114) of HCCs, and was associated with weak β-catenin

membranous staining, high serum α-fetoprotein (AFP) and poor prognosis (Liu et al., 2008) (Geng et al., 2012).

The CTBP2 gene, which encodes the C-terminal binding protein 2 that functions as a transcriptional co-repressor of β-catenin-dependent Wnt signalling, has similar effects (Valenta et al., 2003) (Hamada and Bienz, 2004), and blocking DLK1 with an anti-DLK1 antibody also suppresses Wnt signalling (Zhu et al., 2012). Therefore the downregulation of DLK1 and upregulation of WNT5A and CTBP2 after SULF2 knockdown could also contribute to the inhibition of canonical Wnt signalling pathway that was observed in the HuH-7 cell line, in addition to the inhibition of Wnt-3a binding to its receptors at the cell surface, as a result of SULF2 suppression.

SULF2 knockdown in HuH-7 cells was shown to markedly inhibit Wnt-3a-induced β-catenin-dependent transcriptional activity as measured by both the TOPflash and 7TFP luciferase activity assays, and analysis of ABC levels by WB (Figure 5.16) (Figure 5.17; A) (Figure 5.18; B). Inhibition of Wnt signalling could be the cause of the inhibition of HuH-7 cell growth and proliferation *in vitro* (Figure 5.20) and tumourigenicity *in vivo* (Figure 5.22) (Figure 5.23) after SULF2 suppression. HuH-7 are a heterogeneous population of cells, and a subpopulation of HuH-7 cells can be sorted as a side population (SP) that behave as cancer stem cells. These cells divide asymmetrically *in vitro* and *in vivo* and have high tumourigenic potential; 1,000 of these cells forming tumours in comparison to 1,000,000 non-SP cells (Chiba et al., 2006). Canonical Wnt signalling has been implicated in the self-renewal of stem cells and in the malignant proliferation of some types of cancer cells, and HCC may arise from cancer stem/progenitor cells with dysregulated Wnt signalling (Reya and Clevers, 2005) (Ji and Wang, 2012). Thus, it is possible that SULF2 knockdown may have a particularly detrimental effect on HuH-7 cells *in vitro* and *in vivo* as a result of the inhibition of Wnt signalling in the cancer stem cells.

DLK1 is a transmembrane and secreted protein that is expressed in foetal but not neonatal or adult liver, except in hepatic stem/progenitor cells derived from adult livers, suggesting that DLK1 could be a potential marker of these cells (Oertel et

al., 2008) (Tanaka et al., 2009) (Xu et al., 2012). Sorted DLK1-positive HuH-7 cells (which constituted 4% of total cell population) formed larger colonies *in vitro* and were substantially more tumourigenic when 10,000 cells were injected into NOD/SCID mice (5/5 mice) as compared to DLK1-negative cells injected into the opposite flank of the same mice (1/5 mice) (Xu et al., 2012). DLK1-positive HuH-7 cells expressed other stem cell markers and were able to self-renew and regenerate the DLK1-negative cells *in vitro* and *in vivo*. Also, treating HCC cell lines (HuH-7, HepG2 and Hep 3B) with different chemotherapeutic drugs increased the percentage of DLK1-positive cells 5-fold, suggesting that they are more chemo-resistant (Xu et al., 2012).

DLK1 was found to be upregulated in hepatocytes and hepatic stellate cells after partial hepatectomy in mice (Zhu et al., 2012), and expression was upregulated at the mRNA level in 73% (60 of 82), and at the protein level in 57% (50 of 88) (Huang et al., 2007) and 72% (41 of 57) (Yu et al., 2010) of HCC cases, in addition to overexpression in other types of cancer including colon, pancreatic and NSCLC (Yanai et al., 2010). Overexpression of DLK1 was shown to promote cell growth and increase tumourigenicity of HCC cell lines (Huang et al., 2007) (Yu et al., 2010), while its knockdown by shRNA in HuH-7, HepG2 and Hep 3B cell lines was found to inhibit their growth *in vitro*. Also, DLK1 knockdown almost completely inhibited tumourigenicity of HuH-7 cells in nude mice *in vivo*, with 8/8 tumours developing after implantation of empty vector-transfected cells, and 2/8 and 0/8 tumours after implantation of two different DLK1 shRNA-transfected clones (Huang et al., 2007). Therefore, downregulation of DLK1 as a result of SULF2 knockdown in HuH-7 could reduce tumourigenicity.

In summary, 7 genes underwent marked changes after SULF2 knockdown in HuH-7 cells, and these are summarized in Table 8.3 with their expression changes after SULF2 knockdown and potential role in cancer, as indicated in the literature.

Table 8.3: Summary of genes that underwent changes after SULF2 knockdown in cancer cells studied in the thesis.

Gene	Fold change *	Role in cancer **
ACE2	↑ ≥ 67-fold (HuH-7) ↑ ≥ 1.5-fold (SNU-182) ↑ ≥ 2.2-fold (BxPC3)	Overexpression reduces invasion *in vitro* and inhibits tumour growth *in vivo* (NSCLC cells). Suppression promotes cell proliferation and overexpression inhibits proliferation, migration and invasion and sensitizes cells to hypoxia *in vitro*, and reduces tumour growth *in vivo* (pancreatic cancer cells). Expression inversely correlates with tumour stage (pancreatic cancer). Expression is upregulated in 84 and downregulated in 196 of cases (HCC).
MYCN	↓ ≥ 4-fold (HuH-7) ↓ ≥ 1.5-fold (SNU-182)	Promotes growth, invasion and migration (neuroblastoma cells). Expression correlates with advanced stages, metastasis and poor prognosis (neuroblastoma).
PCDH20	↑ ≥ 24-fold (HuH-7)	Overexpression inhibits growth *in vitro* (NSCLC cells). Reduced expression correlates with poor patient survival (NSCLC).
SLPI	↑ ≥ 38-fold (HuH-7)	Overexpression increases cell proliferation *in vitro* and tumourigenicity *in vivo* (ovarian, lung and colon cancer cells). Overexpression inhibits migration *in vitro* (OSCC cells). Overexpression reduces the metastatic potential (lung carcinoma cells). Overexpression causes apoptosis *in vitro* and inhibits tumourigenicity *in vivo* (mammary

		cancer cells). Expression inversely correlates with tumour progression (OSCC). Expression is upregulated in 160 and downregulated in 203 of cases (HCC).
TFPI2	↑ ≥ 13-fold (HuH-7)	Overexpression inhibits proliferation and invasiveness *in vitro* (HCC). Expression downregulated in ~ 90% (HCC). Silenced by promoter methylation in 47% (HCC) and in 62% (colorectal cancer). Elevated methylation detected in the sera of (HCC) or tumours (colorectal cancer) of patients. Potential biomarker for SULF2 inhibition.
WNT5A	↑ ≥ 5.2-fold (HuH-7)	Protein downregulation in 77% - 81% (HCC). Downregulation is associated with high AFP level and poor prognosis (HCC).
DLK1	↓ ≥ 6.7-fold (HuH-7) ↓ ≥ 1.5-fold (SNU-182)	Overexpression promotes and knockdown inhibits cell growth *in vitro* and tumourigenicity *in vivo* (HCC cells). Upregulation at the mRNA level in 73% and at the protein level in 57% - 72% (HCC)

*Fold change values of gene expression in SULF2 knockdown cells as compared to control untransduced and NT shRNA-transduced cells measured by RT-qPCR.
**References are included in the text.

Summary and Future Work

A. Summary

- SULF2 has higher expression in 3/6 HCC cell lines at the mRNA and protein levels.
- SULF2 is catalytically active as shown by arylsulfatase and endosulfatase activity assays using SULF2-Ab IPs of HCC cell lysates.
- Recombinant SULF2 protein is expressed and catalytically active, and can be used for screening of small-molecule inhibitors.
- Commercially available sulfatases are enzymatically active and can be used for counter-screening of SULF2 inhibitors.
- Constitutive SULF2 knockdown inhibits Wnt signalling and proliferation *in vitro* and tumourigenicity *in vivo* in the HuH-7 cell line.
- Constitutive SULF2 but not SULF1 knockdown inhibits FGF-1, FGF-2 and IGF-II signalling, while either SULF1 or SULF2 knockdown can inhibit proliferation in the SNU-182 cell line.
- Inducible SULF2 knockdown failed to reproduce the detrimental effects of constitutive SULF2 suppression in HCC cell lines.
- SULF2 suppression dramatically upregulates ACE2 and increases the level of the anti-proliferative, anti-angiogenic peptide, Ang-(1-7) in the HuH-7 cell line.
- SULF2 is a promising target for HCC therapy

B. Future Work

Screening of small-molecule inhibitors of SULF2 using the optimised assays according to the following test cascade:

1) SULF1/2 inhibition using recombinant SULF1/2 proteins.
2) Counter-screening of inhibitors using commercially available sulfatases: ARSA, ARSB and ARSC for the initial screening and IDS, ARSD, ARSF, ARSG and GNS for selected inhibitors.
3) Cell-based mechanistic studies (effect on FGF-1-stimulated p-ERK levels in the SNU-182 cell line using the p-ERK ELISA and Wnt-3a-induced β-catenin-dependent transcriptional activity in the HuH-7 cell line using the TCF luciferase reporter assay).
4) Cell-based phenotypic investigations (effect on proliferation using the SRB assay and cell counting, migration by measuring the number of cells traversing a porous membrane using cultrex 96-well cell migration assay (R and D systems), and invasion by monitoring cell movement through extracellular matrices using cultrex cell invasion assay (R and D systems).
5) *In vitro* ADME (plasma protein binding assessed by the rapid equilibrium dialysis method (BD Biosciences), metabolic stability analysed by incubating test compounds with liver microsomes (BD Biosciences), P-glycoprotein-mediated transport assessed by Caco-2 permeability (BD Biosciences) and cytochrome P450 inhibition (BD Biosciences)).
6) *In vivo* PK (bioavailability, half-life, C_{max}, T_{max}, clearance, elimination) and PD (turnover of sulfation of HSPGs, reduction of p-ERK and p-AKT levels or translocation of β-catenin to the nucleus, increase in Ang-(1-7) level in plasma) properties.
7) *In vivo* efficacy using HuH-7 cell tumour xenografts as a model and toxicity studies.

Investigation of the role of the alternative arm of RAS in mediating the effect of SULF2 knockdown on HuH-7 tumourigenicity *in vivo:*

1) Stimulation of the Mas receptor using the MasR agonist, AVE-0991, in mice bearing untransduced HuH-7 cell tumour xenografts as a model to evaluate the anti-tumour effect of AVE-0991.
2) Inhibition of ACE2 enzyme using MLN-4760 in SULF2 knockdown HuH-7 cells as a model to test the pro-tumourigenic effect of MLN-4760 by demonstrating the ability of SULF2 knockdown cells to form tumours in mice following inhibition of ACE2, at doses associated with an increase of Ang II and reduction in Ang-(1-7) levels in plasma.

Appendices

Appendix A

Differentially expressed probe sets (n = 146, representing 111 genes) that were downregulated in the SULF2 knockdown HuH-7 cells with ≥ 2-fold change and adjusted *p* value ≤ 0.01 as compared to both NT shRNA and control untransduced HuH-7 cells (alphabetically ordered). Data generated using Affymetrix microarray gene expression analysis as described in Section 2.22

CTRL: control untransduced cells

NT: NT shRNA-transduced cells

S2: SULF2 knockdown cells

Ave Expr: average expression

Probe Set ID	Gene Symbol	Gene Title	Entrez Gene	Fold Change			Ave Expr	Adjusted *p* value
				NT vs CTRL	S2 vs CTRL	S2 vs NT		
242110_at	---	---	---	-5.08	-15.85	-3.12	8.14	0.0000000005
230413_s_at	---	---	---	-1.26	-3.28	-2.60	5.27	0.0000460556
228835_at	---	---	---	-2.64	-5.84	-2.21	6.61	0.0000000000
242051_at	---	---	---	-1.65	-3.65	-2.21	5.46	0.0000000098
242096_at	---	---	---	-1.88	-4.09	-2.18	5.33	0.0000000126
240655_at	---	---	---	-3.08	-6.45	-2.09	5.81	0.0000000007
228734_at	---	---	---	1.01	-2.05	-2.08	6.78	0.0000010959
239253_at	---	---	---	-1.20	-2.44	-2.04	7.07	0.0000000584
205997_at	ADAM28	ADAM metallopeptidase domain 28	10863	-3.44	-6.97	-2.03	4.63	0.0000000001
210929_s_at	AHSG	alpha-2-HS-glycoprotein	197	1.06	-4.87	-5.14	10.41	0.0000000000
204551_s_at	AHSG	alpha-2-HS-glycoprotein	197	1.07	-4.58	-4.87	8.64	0.0000000000
201952_at	ALCAM	activated leukocyte cell adhesion molecule	214	-1.80	-4.02	-2.23	10.55	0.0000000000
203300_x_at	AP1S2	adaptor-related protein complex 1, sigma 2 subunit	8905	-1.34	-2.81	-2.10	7.27	0.0000000149
228415_at	AP1S2	adaptor-related protein complex 1, sigma 2 subunit	8905	-1.75	-3.63	-2.08	7.85	0.0000000001
230264_s_at	AP1S2	adaptor-related protein complex 1, sigma 2 subunit	8905	-1.45	-2.94	-2.02	8.25	0.0000000002
205216_s_at	APOH	apolipoprotein H (beta-2-glycoprotein I)	350	-1.52	-3.21	-2.11	10.89	0.0000000000
217936_at	ARHGAP5	Rho GTPase activating protein 5	394	-3.08	-10.22	-3.32	10.29	0.0000000000
233849_s_at	ARHGAP5	Rho GTPase activating protein 5	394	-2.86	-9.13	-3.19	10.46	0.0000000000
235635_at	ARHGAP5	Rho GTPase activating protein 5	394	-2.37	-6.65	-2.81	8.37	0.0000000000
228889_at	ARHGAP5-AS1	ARHGAP5 antisense RNA 1 (non-protein coding)	84837	-3.03	-8.55	-2.82	6.57	0.0000000000
224797_at	ARRDC3	arrestin domain containing 3	57561	1.05	-2.43	-2.56	8.17	0.0000000021
206743_s_at	ASGR1	asialoglycoprotein receptor 1	432	-1.89	-5.30	-2.80	7.23	0.0000000000
212599_at	AUTS2	autism susceptibility candidate 2	26053	-1.79	-4.10	-2.29	4.65	0.0000000039
235007_at	BBS7	Bardet-Biedl syndrome 7	55212	-1.22	-2.52	-2.07	5.90	0.0000000605
218332_at	BEX1	brain expressed, X-linked 1	55859	-1.59	-20.07	-12.63	7.56	0.0000000000

Probe Set ID	Gene Symbol	Gene Title	Entrez Gene	Fold Change			Ave Expr	Adjusted *p* value
				NT vs CTRL	S2 vs CTRL	S2 vs NT		
221478_at	BNIP3L	BCL2/adenovirus E1B 19kDa interacting protein 3-like	665	-1.42	-2.93	-2.07	10.43	0.0000000001
224719_s_at	C12orf57	chromosome 12 open reading frame 57	113246	-1.38	-2.98	-2.16	9.20	0.0000000001
227158_at	C14orf126	chromosome 14 open reading frame 126	112487	-4.37	-9.89	-2.26	9.31	0.0000000000
1553801_a_at	C14orf126	chromosome 14 open reading frame 126	112487	-4.73	-10.52	-2.22	6.93	0.0000000000
218802_at	CCDC109B	coiled-coil domain containing 109B	55013	-2.22	-4.90	-2.21	6.29	0.0000000828
220115_s_at	CDH10	cadherin 10, type 2 (T2-cadherin)	1008	13.55	4.85	-2.80	5.53	0.0000000000
214803_at	CDH6	cadherin 6, type 2, K-cadherin (fetal kidney)	1004	-4.96	-20.73	-4.18	6.94	0.0000000000
205532_s_at	CDH6	cadherin 6, type 2, K-cadherin (fetal kidney)	1004	-2.41	-7.15	-2.97	6.62	0.0000000001
226274_at	CLCN5	chloride channel, voltage-sensitive 5	1184	-8.77	-22.90	-2.61	6.38	0.0000000000
226273_at	CLCN5	chloride channel, voltage-sensitive 5	1184	-8.11	-17.10	-2.11	5.07	0.0000000003
223507_at	CLPX	ClpX caseinolytic peptidase X homolog (E. coli)	10845	-1.05	-2.09	-2.00	7.51	0.0000000055
225664_at	COL12A1	collagen, type XII, alpha 1	1303	-1.00	-2.05	-2.05	7.46	0.0000000290
201990_s_at	CREBL2	cAMP responsive element binding protein-like 2	1389	-1.50	-3.07	-2.04	6.57	0.0000000398
205927_s_at	CTSE	cathepsin E	1510	1.03	-9.19	-9.47	7.57	0.0000000085
201372_s_at	CUL3	cullin 3	8452	-1.79	-4.27	-2.39	4.64	0.0000000024
217028_at	CXCR4	chemokine (C-X-C motif) receptor 4	7852	-2.67	-8.51	-3.18	7.56	0.0000000008
228915_at	DACH1	dachshund homolog 1 (Drosophila)	1602	-2.91	-23.59	-8.09	5.31	0.0000000000
205471_s_at	DACH1	dachshund homolog 1 (Drosophila)	1602	-3.24	-6.73	-2.08	4.55	0.0000000583
205472_s_at	DACH1	dachshund homolog 1 (Drosophila)	1602	-3.01	-6.10	-2.03	4.07	0.0000000102
239425_at	DCUN1D5	DCN1, defective in cullin neddylation 1, domain containing 5 (S. cerevisiae)	84259	-1.16	-2.38	-2.05	4.10	0.0000026347
209560_s_at	DLK1	delta-like 1 homolog (Drosophila)	8788	1.82	-3.78	-6.89	5.37	0.0000000000
227708_at	EEF1A1 /// LOC100653236	eukaryotic translation elongation factor 1 alpha 1 /// uncharacterized LOC100653236	100653236 /// 1915	-1.30	-2.87	-2.21	9.50	0.0000000001
207257_at	EPO	erythropoietin	2056	1.06	-2.02	-2.15	5.26	0.0000002349
224833_at	ETS1	v-ets erythroblastosis virus E26 oncogene homolog	2113	-4.91	-10.26	-2.09	5.04	0.0000000005

Probe Set ID	Gene Symbol	Gene Title	Entrez Gene	Fold Change			Ave Expr	Adjusted *p* value
				NT vs CTRL	S2 vs CTRL	S2 vs NT		
205774_at	F12	coagulation factor XII (Hageman factor)	2161	-9.04	-18.16	-2.01	6.89	0.0000000000
219427_at	FAT4	FAT tumor suppressor homolog 4 (Drosophila)	79633	-1.25	-2.95	-2.36	6.17	0.0000000031
215245_x_at	FMR1	fragile X mental retardation 1	2332	-1.43	-4.70	-3.29	9.45	0.0000000000
203689_s_at	FMR1	fragile X mental retardation 1	2332	-1.41	-3.88	-2.74	8.98	0.0000000000
230645_at	FRMD3	FERM domain containing 3	257019	-1.34	-2.95	-2.21	5.53	0.0000000034
207345_at	FST	follistatin	10468	-1.22	-3.68	-3.01	7.38	0.0000000008
226847_at	FST	follistatin	10468	-1.18	-3.27	-2.77	9.00	0.0000000000
204948_s_at	FST	follistatin	10468	-1.35	-3.10	-2.30	9.55	0.0000000000
223257_at	G2E3	G2/M-phase specific E3 ubiquitin protein ligase	55632	-2.75	-6.80	-2.48	8.42	0.0000000000
223256_at	G2E3	G2/M-phase specific E3 ubiquitin protein ligase	55632	-2.56	-5.22	-2.04	8.90	0.0000000000
223255_at	G2E3	G2/M-phase specific E3 ubiquitin protein ligase	55632	-2.57	-5.15	-2.00	8.93	0.0000000001
222943_at	GBA3	glucosidase, beta, acid 3 (cytosolic)	57733	-21.11	-57.35	-2.72	5.92	0.0000000000
201667_at	GJA1	gap junction protein, alpha 1, 43kDa	2697	-1.27	-2.55	-2.01	11.79	0.0000000002
226510_at	HEATR5A	HEAT repeat containing 5A	25938	-3.47	-8.53	-2.45	9.42	0.0000000000
209398_at	HIST1H1C	histone cluster 1, H1c	3006	-5.33	-18.15	-3.40	8.89	0.0000000000
214290_s_at	HIST2H2AA3 /// HIST2H2AA4	histone cluster 2, H2aa3 /// histone cluster 2, H2aa4	723790 /// 8337	-5.29	-14.39	-2.72	9.15	0.0000000000
218280_x_at	HIST2H2AA3 /// HIST2H2AA4	histone cluster 2, H2aa3 /// histone cluster 2, H2aa4	723790 /// 8337	-4.48	-9.63	-2.15	8.01	0.0000000000
206697_s_at	HP	haptoglobin	3240	-1.02	-2.27	-2.23	5.53	0.0000000524
208470_s_at	HP /// HPR	haptoglobin /// haptoglobin-related protein	3240 /// 3250	-1.03	-2.09	-2.04	5.30	0.0000002489
227361_at	HS3ST3B1	heparan sulfate (glucosamine) 3-O-sulfotransferase 3B1	9953	-1.00	-4.16	-4.16	7.26	0.0000000006
230031_at	HSPA5	heat shock 70kDa protein 5 (glucose-regulated protein, 78kDa)	3309	-1.25	-2.93	-2.33	7.46	0.0000000027
211406_at	IER3IP1	immediate early response 3 interacting protein 1	51124	-1.35	-3.39	-2.51	6.34	0.0000003940

Probe Set ID	Gene Symbol	Gene Title	Entrez Gene	Fold Change			Ave Expr	Adjusted *p* value
				NT vs CTRL	S2 vs CTRL	S2 vs NT		
223071_at	IER3IP1	immediate early response 3 interacting protein 1	51124	-1.75	-3.94	-2.25	9.66	0.0000000000
202490_at	IKBKAP	inhibitor of kappa light polypeptide gene enhancer in B-cells, kinase complex-associated protein	8518	-1.32	-3.04	-2.30	5.49	0.0000000110
212859_x_at	LOC100505584 /// MT1E	metallothionein-2-like /// metallothionein 1E	100505584 /// 4493	-1.68	-3.74	-2.22	7.98	0.0000000000
238632_at	LOC100505946	uncharacterized LOC100505946	1.01E+08	1.09	-2.02	-2.20	6.59	0.0000011850
230057_at	LOC285178	uncharacterized LOC285178	285178	-1.43	-2.94	-2.06	6.93	0.0000008596
230930_at	LOC338620	uncharacterized LOC338620	338620	-1.31	-3.49	-2.67	7.70	0.0000000001
235497_at	LOC643837	uncharacterized LOC643837	643837	-2.29	-4.58	-2.00	4.47	0.0000000011
202998_s_at	LOXL2	lysyl oxidase-like 2	4017	-1.91	-4.08	-2.14	6.40	0.0000000014
204036_at	LPAR1	lysophosphatidic acid receptor 1	1902	-1.05	-3.38	-3.23	5.64	0.0000000103
226884_at	LRRN1	leucine rich repeat neuronal 1	57633	-2.78	-5.97	-2.14	4.28	0.0000000056
239960_x_at	LYRM7	Lyrm7 homolog (mouse)	90624	-1.12	-2.59	-2.30	4.94	0.0041715506
210302_s_at	MAB21L2	mab-21-like 2 (C. elegans)	10586	-5.13	-21.28	-4.14	5.97	0.0000000000
213627_at	MAGED2	melanoma antigen family D, 2	10916	-1.06	-2.62	-2.48	6.05	0.0000000047
212741_at	MAOA	monoamine oxidase A	4128	-8.13	-23.41	-2.88	6.90	0.0000000000
204388_s_at	MAOA	monoamine oxidase A	4128	-7.47	-16.35	-2.19	6.01	0.0000000000
224507_s_at	MGC12916	uncharacterized protein MGC12916	84815	-1.21	-3.26	-2.70	5.46	0.0000000353
217165_x_at	MT1F	metallothionein 1F	4494	-1.38	-2.86	-2.08	7.55	0.0000000039
204326_x_at	MT1X	metallothionein 1X	4501	-1.67	-3.65	-2.19	7.81	0.0000000001
208581_x_at	MT1X	metallothionein 1X	4501	-1.45	-3.10	-2.14	7.93	0.0000000003
212185_x_at	MT2A	metallothionein 2A	4502	-1.11	-2.29	-2.07	9.33	0.0000000005
209757_s_at	MYCN	v-myc myelocytomatosis viral related oncogene, neuroblastoma derived (avian)	4613	1.13	-4.17	-4.73	8.31	0.0000000000
225355_at	NEURL1B	neuralized homolog 1B (Drosophila)	54492	-1.59	-4.10	-2.58	5.97	0.0000000018
220176_at	NUBPL	nucleotide binding protein-like	80224	-3.02	-8.48	-2.81	8.07	0.0000000000
230883_at	NXPH2	neurexophilin 2	11249	1.11	-3.41	-3.79	4.83	0.0000000058

Probe Set ID	Gene Symbol	Gene Title	Entrez Gene	Fold Change			Ave Expr	Adjusted *p* value
				NT vs CTRL	S2 vs CTRL	S2 vs NT		
228959_at	PDK3	pyruvate dehydrogenase kinase, isozyme 3	5165	-3.57	-20.30	-5.69	7.34	0.0000000000
230085_at	PDK3	pyruvate dehydrogenase kinase, isozyme 3	5165	-2.97	-7.53	-2.53	5.01	0.0000000000
221957_at	PDK3	pyruvate dehydrogenase kinase, isozyme 3	5165	-1.40	-2.83	-2.02	5.50	0.0000285828
219165_at	PDLIM2	PDZ and LIM domain 2 (mystique)	64236	-1.07	-2.69	-2.52	7.36	0.0000000005
213469_at	PGAP1	post-GPI attachment to proteins 1	80055	-1.70	-4.48	-2.64	6.49	0.0000000002
241801_at	PGAP1	post-GPI attachment to proteins 1	80055	-1.55	-3.80	-2.45	5.79	0.0000004795
214717_at	PKI55	DKFZp434H1419	150967	-1.26	-2.76	-2.19	7.21	0.0000000017
235758_at	PNMA6A /// PNMA6B /// PNMA6C /// PNMA6D	paraneoplastic Ma antigen family member 6A /// paraneoplastic Ma antigen family member 6B /// paraneoplastic Ma antigen family member 6C /// paraneoplastic Ma antigen family member 6D	100287428 100287466 /// 728513 /// 84968	-1.10	-2.33	-2.13	6.52	0.0000000057
232424_at	PRDM16	PR domain containing 16	63976	-2.36	-5.21	-2.20	3.66	0.0000000230
205880_at	PRKD1	protein kinase D1	5587	-1.22	-3.21	-2.62	7.98	0.0000000005
201300_s_at	PRNP	prion protein	5621	-1.86	-3.76	-2.03	5.14	0.0000002133
238852_at	PRRX1	paired related homeobox 1	5396	-2.69	-6.24	-2.32	4.72	0.0000000547
205174_s_at	QPCT	glutaminyl-peptide cyclotransferase	25797	-2.76	-7.07	-2.56	5.21	0.0000000005
229300_at	RAB3C	RAB3C, member RAS oncogene family	115827	-1.14	-2.31	-2.02	4.43	0.0000018907
212706_at	RASA4 /// RASA4B	RAS p21 protein activator 4 /// RAS p21 protein activator 4B	100271927 /// 10156	1.07	-2.50	-2.68	4.61	0.0000001951
222026_at	RBM3	RNA binding motif (RNP1, RRM) protein 3	5935	-2.28	-5.05	-2.22	6.69	0.0000000001
208873_s_at	REEP5	receptor accessory protein 5	7905	-1.23	-3.34	-2.72	8.96	0.0000000000
204319_s_at	RGS10	regulator of G-protein signaling 10	6001	-1.09	-2.25	-2.06	5.55	0.0000042374
213397_x_at	RNASE4	ribonuclease, RNase A family, 4	6038	-1.83	-4.43	-2.42	8.06	0.0000000000
205158_at	RNASE4	ribonuclease, RNase A family, 4	6038	-1.86	-4.14	-2.22	7.27	0.0000000000
226885_at	RNF217	ring finger protein 217	154214	-1.83	-5.46	-2.99	5.30	0.0000000069
240806_at	RPL15	Ribosomal protein L15	6138	-1.29	-2.79	-2.15	5.81	0.0000050770
216247_at	RPS20	ribosomal protein S20	26795	-1.59	-3.38	-2.13	5.03	0.0000000118

Probe Set ID	Gene Symbol	Gene Title	Entrez Gene	Fold Change			Ave Expr	Adjusted *p* value
				NT vs CTRL	S2 vs CTRL	S2 vs NT		
228176_at	S1PR3	sphingosine-1-phosphate receptor 3	1903	-5.01	-23.73	-4.74	6.81	0.0000000000
212425_at	SCAMP1	secretory carrier membrane protein 1	9522	-1.09	-2.27	-2.08	4.92	0.0000042523
238078_at	SEC22A	SEC22 vesicle trafficking protein homolog A (S. cerevisiae)	26984	-1.15	-2.33	-2.03	5.52	0.0000060618
227038_at	SGMS2	sphingomyelin synthase 2	166929	-3.48	-8.07	-2.32	4.46	0.0000002306
225056_at	SIPA1L2	signal-induced proliferation-associated 1 like 2	57568	-6.91	-14.69	-2.13	6.11	0.0000000000
227506_at	SLC16A9	solute carrier family 16, member 9 (monocarboxylic acid transporter 9)	220963	-1.38	-4.25	-3.08	6.37	0.0000000012
235763_at	SLC44A5	solute carrier family 44, member 5	204962	-2.26	-11.43	-5.06	5.71	0.0000000005
1569112_at	SLC44A5	solute carrier family 44, member 5	204962	-1.87	-4.00	-2.14	5.03	0.0000000006
223748_at	SLC4A11	solute carrier family 4, sodium borate transporter, member 11	83959	-1.39	-3.13	-2.25	6.74	0.0000000004
226550_at	SLC9A7	solute carrier family 9, subfamily A (NHE7, cation proton antiporter 7), member 7	84679	-3.88	-12.03	-3.10	4.88	0.0000000008
1558105_a_at	SLC9A7	solute carrier family 9, subfamily A (NHE7, cation proton antiporter 7), member 7	84679	-4.74	-9.89	-2.09	4.35	0.0000000006
230782_at	SORD	sorbitol dehydrogenase	6652	-2.28	-4.98	-2.19	5.80	0.0000000011
222557_at	STMN3	stathmin-like 3	50861	-1.33	-3.84	-2.88	6.57	0.0000000457
213413_at	STON1	stonin 1	11037	-1.14	-2.37	-2.08	4.55	0.0000000276
224724_at	SULF2	sulfatase 2	55959	2.61	-6.43	-16.79	6.29	0.0000000000
233555_s_at	SULF2	sulfatase 2	55959	3.07	-2.00	-6.13	5.22	0.0000000003
227480_at	SUSD2	sushi domain containing 2	56241	-1.23	-2.65	-2.15	6.07	0.0000002287
232760_at	TEX15	testis expressed 15	56154	-1.36	-3.77	-2.77	7.87	0.0000000120
214476_at	TFF2	trefoil factor 2	7032	-1.11	-2.97	-2.68	7.36	0.0000000441
203786_s_at	TPD52L1	tumor protein D52-like 1	7164	-1.36	-3.31	-2.43	7.14	0.0000000003
202242_at	TSPAN7	tetraspanin 7	7102	-2.98	-14.73	-4.95	5.37	0.0000000003
235561_at	TXNL1	thioredoxin-like 1	9352	-2.45	-5.34	-2.18	5.20	0.0000000010

Probe Set ID	Gene Symbol	Gene Title	Entrez Gene	Fold Change			Ave Expr	Adjusted *p* value
				NT vs CTRL	S2 vs CTRL	S2 vs NT		
238462_at	UBASH3B	ubiquitin associated and SH3 domain containing B	84959	-3.25	-6.75	-2.08	5.66	0.0000000000
1556095_at	UNC13C	unc-13 homolog C (C. elegans)	440279	-2.93	-7.16	-2.44	4.69	0.0000000109
1556096_s_at	UNC13C	unc-13 homolog C (C. elegans)	440279	-2.61	-5.67	-2.17	6.63	0.0000000000
227399_at	VGLL3	vestigial like 3 (Drosophila)	389136	-3.25	-9.82	-3.02	6.36	0.0000000001
239680_at	WDR76	WD repeat domain 76	79968	-1.54	-3.39	-2.20	5.38	0.0000000082
243024_at	ZNF394	zinc finger protein 394	84124	-1.28	-4.58	-3.57	5.62	0.0000000177

Appendix B

Differentially expressed probe sets (n = 298, representing 211 genes) that were upregulated in the SULF2 knockdown HuH-7 cells with ≥ 2-fold change and adjusted *p* value ≤ 0.01 as compared to both NT shRNA and control untransduced HuH-7 cells (alphabetically ordered). Data generated using Affymetrix microarray gene expression analysis as described in Section 2.22

CTRL: control untransduced cells

NT: NT shRNA-transduced cells

S2: SULF2 knockdown cells

Ave Expr: average expression

Probe Set ID	Gene Symbol	Gene Title	Entrez Gene	Fold Change			Ave Expr	Adjusted *p* value
				NT vs CTRL	S2 vs CTRL	S2 vs NT		
235152_at	---	---	---	1.48	3.03	2.05	4.34	0.0000001040
236750_at	---	---	---	1.53	3.24	2.12	4.58	0.0000012971
239914_at	---	---	---	1.11	2.55	2.29	3.17	0.0000018992
222288_at	---	---	---	2.39	5.60	2.34	6.08	0.0000000137
237400_at	---	---	---	1.72	4.24	2.47	4.21	0.0000000125
232827_at	---	---	---	1.13	3.18	2.81	4.48	0.0000000030
239767_at	---	---	---	1.04	2.99	2.88	3.65	0.0000005319
1558871_at	---	---	---	-1.27	2.28	2.88	4.09	0.0000002019
1561195_at	---	---	---	-1.35	2.18	2.95	5.88	0.0001746303
1563494_at	---	---	---	-1.22	2.66	3.25	4.03	0.0000006241
231035_s_at	---	---	---	1.36	5.61	4.12	5.43	0.0000046434
242967_at	---	---	---	-1.04	23.58	24.57	4.50	0.0000000000
209993_at	ABCB1	ATP-binding cassette, sub-family B (MDR/TAP), member 1	5243	1.42	6.34	4.47	8.66	0.0000000000
209994_s_at	ABCB1 /// ABCB4	ATP-binding cassette, sub-family B (MDR/TAP), member 1 /// ATP-binding cassette, sub-family B (MDR/TAP), member 4	5243 /// 5244	1.37	5.71	4.18	8.99	0.0000000000
1554918_a_at	ABCC4	ATP-binding cassette, sub-family C (CFTR/MRP), member 4	10257	2.95	7.51	2.55	5.92	0.0000000000
1555039_a_at	ABCC4	ATP-binding cassette, sub-family C (CFTR/MRP), member 4	10257	1.63	4.91	3.01	4.29	0.0000000002
222257_s_at	ACE2	angiotensin I converting enzyme (peptidyl-dipeptidase A) 2	59272	-1.39	31.80	44.21	6.57	0.0000000000
219962_at	ACE2	angiotensin I converting enzyme (peptidyl-dipeptidase A) 2	59272	-1.51	63.03	95.13	6.45	0.0000000000
206262_at	ADH1C	alcohol dehydrogenase 1C (class I), gamma polypeptide	126	-1.33	2.75	3.66	3.90	0.0000000255
222458_s_at	AKIRIN1	akirin 1	79647	1.32	2.63	2.00	7.59	0.0000069899
215241_at	ANO3	anoctamin 3	63982	1.05	2.57	2.45	6.39	0.0000000015

289

Probe Set ID	Gene Symbol	Gene Title	Entrez Gene	Fold Change			Ave Expr	Adjusted *p* value
				NT vs CTRL	S2 vs CTRL	S2 vs NT		
208323_s_at	ANXA13	annexin A13	312	-3.08	2.42	7.43	5.92	0.0000000001
206632_s_at	APOBEC3B	apolipoprotein B mRNA editing enzyme, catalytic polypeptide-like 3B	9582	2.81	7.05	2.51	5.88	0.0000000000
205980_s_at	ARHGAP8 /// PRR5-ARHGAP8	Rho GTPase activating protein 8 /// PRR5-ARHGAP8 readthrough	23779 /// 553158	-1.11	2.66	2.95	3.80	0.0000023559
37117_at	ARHGAP8 /// PRR5-ARHGAP8	Rho GTPase activating protein 8 /// PRR5-ARHGAP8 readthrough	23779 /// 553158	-1.13	4.27	4.83	4.10	0.0000000000
242230_at	ATXN1	ataxin 1	6310	1.82	3.66	2.01	5.96	0.0000000858
225612_s_at	B3GNT5 /// LOC100505668	UDP-GlcNAc:betaGal beta-1,3-N-acetylglucosaminyltransferase 5 /// uncharacterized LOC100505668	100505668 /// 84002	1.04	3.06	2.95	7.56	0.0000000095
210347_s_at	BCL11A	B-cell CLL/lymphoma 11A (zinc finger protein)	53335	1.04	2.14	2.07	4.78	0.0000010982
222891_s_at	BCL11A	B-cell CLL/lymphoma 11A (zinc finger protein)	53335	1.09	2.49	2.28	4.82	0.0000001175
219497_s_at	BCL11A	B-cell CLL/lymphoma 11A (zinc finger protein)	53335	1.12	2.70	2.41	4.20	0.0000000566
205780_at	BIK	BCL2-interacting killer (apoptosis-inducing)	638	-1.30	3.30	4.28	6.04	0.0000000001
223631_s_at	C19orf33	chromosome 19 open reading frame 33	64073	-1.31	2.38	3.11	7.50	0.0000000040
228865_at	C1orf116	chromosome 1 open reading frame 116	79098	1.48	3.44	2.32	4.83	0.0000001162
219476_at	C1orf116	chromosome 1 open reading frame 116	79098	1.35	4.38	3.25	4.09	0.0000000000
238965_at	C21orf2	Chromosome 21 open reading frame 2	755	-1.17	2.14	2.51	5.90	0.0000000492
1552575_a_at	C6orf141	chromosome 6 open reading frame 141	135398	-1.18	2.15	2.54	5.23	0.0000017441
1552390_a_at	C8orf47	chromosome 8 open reading frame 47	203111	-1.15	2.76	3.18	6.76	0.0000000110
1552389_at	C8orf47	chromosome 8 open reading frame 47	203111	-1.17	3.39	3.96	5.16	0.0000000587
209301_at	CA2	carbonic anhydrase II	760	-1.29	2.25	2.90	8.40	0.0000000006
204865_at	CA3	carbonic anhydrase III, muscle specific	761	-1.13	5.07	5.71	3.45	0.0000000152
206208_at	CA4	carbonic anhydrase IV	762	-1.19	6.94	8.26	7.17	0.0000000000
206209_s_at	CA4	carbonic anhydrase IV	762	-1.27	13.51	17.19	7.34	0.0000000000

Probe Set ID	Gene Symbol	Gene Title	Entrez Gene	Fold Change			Ave Expr	Adjusted *p* value
				NT vs CTRL	S2 vs CTRL	S2 vs NT		
225627_s_at	CACHD1	cache domain containing 1	57685	-1.14	2.37	2.69	6.53	0.0000000077
212763_at	CAMSAP2	calmodulin regulated spectrin-associated protein family, member 2	23271	1.10	2.25	2.05	6.23	0.0000003004
205114_s_at	CCL3 /// CCL3L1 /// CCL3L3	chemokine (C-C motif) ligand 3 /// chemokine (C-C motif) ligand 3-like 1 /// chemokine (C-C motif) ligand 3-like 3	414062 /// 6348 /// 6349	1.03	8.86	8.62	4.75	0.0000000005
1553043_a_at	CD300LF	CD300 molecule-like family member f	146722	-1.01	3.34	3.38	4.47	0.0000000000
201925_s_at	CD55	CD55 molecule, decay accelerating factor for complement (Cromer blood group)	1604	1.14	2.27	2.00	7.14	0.0000004828
218451_at	CDCP1	CUB domain containing protein 1	64866	1.07	2.94	2.76	5.11	0.0000000212
207149_at	CDH12	cadherin 12, type 2 (N-cadherin 2)	1010	5.67	37.04	6.53	4.74	0.0000000000
209847_at	CDH17	cadherin 17, LI cadherin (liver-intestine)	1015	-6.42	5.77	37.09	8.54	0.0000000000
235287_at	CDK6	cyclin-dependent kinase 6	1021	1.21	2.96	2.44	4.20	0.0000013778
226187_at	CDS1	CDP-diacylglycerol synthase (phosphatidate cytidylyltransferase) 1	1040	-1.27	2.52	3.20	5.85	0.0000000426
226185_at	CDS1	CDP-diacylglycerol synthase (phosphatidate cytidylyltransferase) 1	1040	-1.29	3.20	4.12	7.05	0.0000000000
205709_s_at	CDS1	CDP-diacylglycerol synthase (phosphatidate cytidylyltransferase) 1	1040	-1.29	4.31	5.56	6.81	0.0000000016
206387_at	CDX2	caudal type homeobox 2	1045	-1.12	2.62	2.94	6.05	0.0000000019
211657_at	CEACAM6	carcinoembryonic antigen-related cell adhesion molecule 6 (non-specific cross reacting antigen)	4680	1.02	10.29	10.11	5.47	0.0000000002
203757_s_at	CEACAM6	carcinoembryonic antigen-related cell adhesion molecule 6 (non-specific cross reacting antigen)	4680	1.04	10.98	10.57	4.19	0.0000000000
211848_s_at	CEACAM7	carcinoembryonic antigen-related cell adhesion molecule 7	1087	-1.11	3.16	3.51	4.08	0.0000000007
206198_s_at	CEACAM7	carcinoembryonic antigen-related cell adhesion molecule 7	1087	-1.01	4.43	4.45	2.97	0.0000000106
206199_at	CEACAM7	carcinoembryonic antigen-related cell adhesion molecule 7	1087	-1.09	42.22	46.09	4.71	0.0000000000
203973_s_at	CEBPD	CCAAT/enhancer binding protein (C/EBP), delta	1052	-1.13	2.17	2.45	9.51	0.0000000028

Probe Set ID	Gene Symbol	Gene Title	Entrez Gene	Fold Change			Ave Expr	Adjusted *p* value
				NT vs CTRL	S2 vs CTRL	S2 vs NT		
202790_at	CLDN7	claudin 7	1366	1.61	4.47	2.78	5.84	0.0000000387
213317_at	CLIC5	chloride intracellular channel 5	53405	1.00	4.36	4.34	3.48	0.0000000046
217404_s_at	COL2A1	collagen, type II, alpha 1	1280	3.12	6.48	2.08	7.31	0.0000000000
215076_s_at	COL3A1	collagen, type III, alpha 1	1281	1.44	4.08	2.83	6.60	0.0000000000
201852_x_at	COL3A1	collagen, type III, alpha 1	1281	1.40	4.00	2.86	5.94	0.0000000000
211980_at	COL4A1	collagen, type IV, alpha 1	1282	1.50	3.07	2.05	4.90	0.0000001012
205713_s_at	COMP	cartilage oligomeric matrix protein	1311	2.63	8.09	3.08	5.15	0.0000000000
206212_at	CPA2	carboxypeptidase A2 (pancreatic)	1358	-1.17	3.70	4.33	6.46	0.0000000004
210262_at	CRISP2	cysteine-rich secretory protein 2	7180	2.01	6.13	3.05	4.64	0.0000000002
201219_at	CTBP2	C-terminal binding protein 2	1488	-1.29	2.69	3.48	4.59	0.0000000073
201220_x_at	CTBP2	C-terminal binding protein 2	1488	-1.86	3.22	6.00	6.41	0.0000000037
210554_s_at	CTBP2	C-terminal binding protein 2	1488	-2.40	4.50	10.79	6.48	0.0000000001
210835_s_at	CTBP2	C-terminal binding protein 2	1488	-2.74	4.63	12.66	5.96	0.0000000000
201218_at	CTBP2	C-terminal binding protein 2	1488	-3.10	5.20	16.14	5.26	0.0000000000
206085_s_at	CTH	cystathionase (cystathionine gamma-lyase)	1491	1.81	3.85	2.13	5.93	0.0000000080
225647_s_at	CTSC	cathepsin C	1075	1.16	2.42	2.08	8.60	0.0000000067
202901_x_at	CTSS	cathepsin S	1520	3.08	6.55	2.12	4.95	0.0000000040
202902_s_at	CTSS	cathepsin S	1520	3.46	9.95	2.87	6.61	0.0000000000
207852_at	CXCL5	chemokine (C-X-C motif) ligand 5	6374	1.39	2.89	2.08	3.65	0.0000000893
215101_s_at	CXCL5	chemokine (C-X-C motif) ligand 5	6374	2.49	6.66	2.67	8.43	0.0000000001
242138_at	DLX1	distal-less homeobox 1	1745	1.47	4.24	2.88	4.11	0.0000000107
204455_at	DST /// LOC100652766	dystonin /// dystonin-like	100652766 /// 667	1.31	3.42	2.61	6.40	0.0000000006
225275_at	EDIL3	EGF-like repeats and discoidin I-like domains 3	10085	-1.02	14.08	14.34	7.51	0.0000000000
222802_at	EDN1	endothelin 1	1906	1.08	2.73	2.54	8.88	0.0000000169
218995_s_at	EDN1	endothelin 1	1906	-1.03	2.53	2.62	9.12	0.0000000077

Probe Set ID	Gene Symbol	Gene Title	Entrez Gene	Fold Change			Ave Expr	Adjusted *p* value
				NT vs CTRL	S2 vs CTRL	S2 vs NT		
204271_s_at	EDNRB	endothelin receptor type B	1910	17.99	57.85	3.22	8.00	0.0000000005
206701_x_at	EDNRB	endothelin receptor type B	1910	10.58	36.31	3.43	6.47	0.0000000011
201842_s_at	EFEMP1	EGF containing fibulin-like extracellular matrix protein 1	2202	1.03	2.21	2.14	9.94	0.0000000005
210827_s_at	ELF3	E74-like factor 3 (ets domain transcription factor, epithelial-specific)	1999	1.03	2.34	2.26	7.01	0.0000000002
227803_at	ENPP5	ectonucleotide pyrophosphatase/phosphodiesterase 5 (putative)	59084	1.89	4.01	2.13	4.80	0.0000000264
214053_at	ERBB4	v-erb-a erythroblastic leukemia viral oncogene homolog 4 (avian)	2066	-1.38	3.41	4.71	5.09	0.0000000001
219121_s_at	ESRP1	epithelial splicing regulatory protein 1	54845	1.09	4.27	3.91	4.17	0.0000000013
225846_at	ESRP1	epithelial splicing regulatory protein 1	54845	1.11	9.45	8.53	4.72	0.0000000000
224453_s_at	ETNK1	ethanolamine kinase 1	55500	-1.01	2.36	2.39	5.22	0.0000000715
224454_at	ETNK1	ethanolamine kinase 1	55500	-1.04	2.88	2.98	4.09	0.0000002352
1554576_a_at	ETV4	ets variant 4	2118	1.13	2.41	2.14	6.86	0.0000000038
230147_at	F2RL2	coagulation factor II (thrombin) receptor-like 2	2151	1.20	4.29	3.58	5.39	0.0000000002
218510_x_at	FAM134B	family with sequence similarity 134, member B	54463	2.17	8.52	3.93	5.52	0.0000000000
218532_s_at	FAM134B	family with sequence similarity 134, member B	54463	2.63	11.06	4.20	5.69	0.0000000000
223204_at	FAM198B	family with sequence similarity 198, member B	51313	-1.97	7.06	13.87	6.93	0.0000000000
202766_s_at	FBN1	fibrillin 1	2200	-1.82	2.10	3.83	8.49	0.0000000000
232064_at	FER	fer (fps/fes related) tyrosine kinase	2241	1.39	2.85	2.05	5.26	0.0003999943
239178_at	FGF9	fibroblast growth factor 9 (glia-activating factor)	2254	1.09	2.18	2.00	2.83	0.0000056468
206404_at	FGF9	fibroblast growth factor 9 (glia-activating factor)	2254	1.29	3.55	2.75	4.36	0.0000000237
204437_s_at	FOLR1	folate receptor 1 (adult)	2348	1.55	4.97	3.21	4.79	0.0000000003
227475_at	FOXQ1	forkhead box Q1	94234	-1.23	2.28	2.80	6.66	0.0000000845
208782_at	FSTL1	follistatin-like 1	11167	1.55	3.24	2.08	10.52	0.0000000000
203988_s_at	FUT8	fucosyltransferase 8 (alpha (1,6) fucosyltransferase)	2530	1.08	2.19	2.02	7.90	0.0000000080

Probe Set ID	Gene Symbol	Gene Title	Entrez Gene	Fold Change			Ave Expr	Adjusted *p* value
				NT vs CTRL	S2 vs CTRL	S2 vs NT		
1554930_a_at	FUT8	fucosyltransferase 8 (alpha (1,6) fucosyltransferase)	2530	1.07	2.57	2.41	6.25	0.0000001497
209602_s_at	GATA3	GATA binding protein 3	2625	1.81	3.99	2.20	3.16	0.0000000460
202832_at	GCC2	GRIP and coiled-coil domain containing 2	9648	1.22	18.68	15.34	7.98	0.0000000000
221577_x_at	GDF15	growth differentiation factor 15	9518	1.14	2.32	2.03	10.01	0.0000000004
204472_at	GEM	GTP binding protein overexpressed in skeletal muscle	2669	-1.67	2.55	4.25	4.56	0.0000000017
214071_at	GNAL	guanine nucleotide binding protein (G protein), alpha activating activity polypeptide, olfactory type	2774	2.18	5.07	2.33	5.84	0.0000000020
204115_at	GNG11	guanine nucleotide binding protein (G protein), gamma 11	2791	1.14	2.96	2.60	6.34	0.0000000231
204324_s_at	GOLIM4	golgi integral membrane protein 4	27333	1.19	2.62	2.21	7.08	0.0000542395
217771_at	GOLM1	golgi membrane protein 1	51280	-2.31	4.37	10.11	8.38	0.0000000000
207174_at	GPC5	glypican 5	2262	-1.41	2.07	2.90	3.85	0.0000001952
235733_at	GXYLT2	glucoside xylosyltransferase 2	727936	2.62	5.36	2.04	5.47	0.0000000001
235371_at	GXYLT2	glucoside xylosyltransferase 2	727936	2.44	6.21	2.55	5.78	0.0000000002
214500_at	H2AFY	H2A histone family, member Y	9555	1.05	2.12	2.02	6.02	0.0000000098
205659_at	HDAC9	histone deacetylase 9	9734	-1.17	2.18	2.55	8.06	0.0000000034
242601_at	HEPACAM2	HEPACAM family member 2	253012	1.51	3.25	2.15	4.05	0.0000001032
203903_s_at	HEPH	hephaestin	9843	-1.88	19.74	37.14	4.51	0.0000000000
232271_at	HNF4G	hepatocyte nuclear factor 4, gamma	3174	1.09	2.40	2.20	7.64	0.0000000017
239153_at	HOTAIR	HOX transcript antisense RNA (non-protein coding)	1E+08	-1.28	3.65	4.67	3.72	0.0000000016
213150_at	HOXA10	homeobox A10	3206	-1.91	2.11	4.03	5.69	0.0000000017
209905_at	HOXA10-HOXA9	HOXA10-HOXA9 readthrough /// homeobox A9	100534589 /// 3205	-1.70	2.50	4.23	6.09	0.0000000023
214651_s_at	HOXA10-HOXA9 /// MIR196B	HOXA10-HOXA9 readthrough /// homeobox A9 /// microRNA 196b	100534589 /// 3205 /// 442920	-1.67	2.80	4.67	6.70	0.0000000007

Probe Set ID	Gene Symbol	Gene Title	Entrez Gene	Fold Change			Ave Expr	Adjusted *p* value
				NT vs CTRL	S2 vs CTRL	S2 vs NT		
231786_at	HOXA13	homeobox A13	3209	-1.43	3.39	4.84	3.76	0.0000000171
213844_at	HOXA5	homeobox A5	3202	-1.37	2.13	2.91	4.67	0.0000001983
228904_at	HOXB3	homeobox B3	3213	1.02	9.80	9.58	4.12	0.0000000000
205366_s_at	HOXB6	homeobox B6	3216	-1.16	5.81	6.74	4.18	0.0000000000
204778_x_at	HOXB7	homeobox B7	3217	-1.09	4.57	4.97	5.17	0.0000000017
216973_s_at	HOXB7	homeobox B7	3217	1.12	12.70	11.39	4.22	0.0000000000
204779_s_at	HOXB7	homeobox B7	3217	1.02	18.06	17.74	4.16	0.0000000000
229667_s_at	HOXB8	homeobox B8	3218	1.10	2.46	2.24	2.89	0.0000001374
226461_at	HOXB9	homeobox B9	3219	1.10	3.67	3.33	3.94	0.0000000008
205975_s_at	HOXD1	homeobox D1	3231	1.42	11.18	7.85	5.72	0.0000000000
229400_at	HOXD10	homeobox D10	3236	-1.21	3.80	4.60	4.55	0.0000000017
205522_at	HOXD4	homeobox D4	3233	1.12	4.65	4.16	5.82	0.0000000002
242042_s_at	HOXD-AS1	HOXD cluster antisense RNA 1 (non-protein coding)	401022	1.12	4.91	4.40	4.34	0.0000000005
228601_at	HOXD-AS1	HOXD cluster antisense RNA 1 (non-protein coding)	401022	1.11	4.89	4.40	6.14	0.0000000005
229493_at	HOXD-AS2	HOXD cluster antisense RNA 2 (non-protein coding)	1.01E+08	-1.30	3.49	4.53	5.38	0.0000000001
206172_at	IL13RA2	interleukin 13 receptor, alpha 2	3598	1.34	11.34	8.45	4.02	0.0000000000
206693_at	IL7	interleukin 7	3574	-1.43	2.86	4.07	3.84	0.0000000299
205376_at	INPP4B	inositol polyphosphate-4-phosphatase, type II, 105kDa	8821	-1.03	2.24	2.32	3.00	0.0000016223
235046_at	INPP4B	inositol polyphosphate-4-phosphatase, type II, 105kDa	8821	1.31	4.59	3.50	3.76	0.0000000359
225303_at	KIRREL	kin of IRRE like (Drosophila)	55243	6.46	14.17	2.19	5.64	0.0000000000
209211_at	KLF5	Kruppel-like factor 5 (intestinal)	688	1.08	2.85	2.63	8.94	0.0000000004
209212_s_at	KLF5	Kruppel-like factor 5 (intestinal)	688	-1.02	3.72	3.78	7.99	0.0000000001

Probe Set ID	Gene Symbol	Gene Title	Entrez Gene	Fold Change			Ave Expr	Adjusted *p* value
				NT vs CTRL	S2 vs CTRL	S2 vs NT		
204734_at	KRT15	keratin 15	3866	1.05	2.22	2.11	4.54	0.0000022952
202267_at	LAMC2	laminin, gamma 2	3918	-1.36	5.20	7.08	6.14	0.0000000000
205569_at	LAMP3	lysosomal-associated membrane protein 3	27074	1.70	5.83	3.42	5.78	0.0000000043
1554679_a_at	LAPTM4B	lysosomal protein transmembrane 4 beta	55353	1.40	3.19	2.28	10.56	0.0000000002
242006_at	LCA5	Leber congenital amaurosis 5	167691	1.68	3.62	2.16	4.94	0.0000000491
244401_at	LCA5	Leber congenital amaurosis 5	167691	1.53	4.40	2.88	5.28	0.0000001128
212325_at	LIMCH1	LIM and calponin homology domains 1	22998	-1.57	2.40	3.78	6.29	0.0000000905
1561367_a_at	LINC00540	long intergenic non-protein coding RNA 540	1.01E+08	1.99	7.86	3.95	4.92	0.0000000000
209465_x_at	LOC100287705 /// PTN	uncharacterized LOC100287705 /// pleiotrophin	100287705 /// 5764	1.76	6.13	3.49	6.15	0.0000000003
209466_x_at	LOC100287705 /// PTN	uncharacterized LOC100287705 /// pleiotrophin	100287705 /// 5764	1.36	5.18	3.82	6.92	0.0000000001
211737_x_at	LOC100287705 /// PTN	uncharacterized LOC100287705 /// pleiotrophin	100287705 /// 5764	1.74	6.89	3.96	7.20	0.0000000000
227452_at	LOC100499467	uncharacterized LOC100499467	1E+08	2.02	5.83	2.89	7.66	0.0000000000
227880_s_at	LOC100506234 /// TMEM185A	uncharacterized LOC100506234 /// transmembrane protein 185A	100506234 /// 84548	-1.37	2.47	3.39	5.56	0.0000000893
1560425_s_at	LOC100506247	uncharacterized LOC100506247	1.01E+08	1.59	3.56	2.24	3.55	0.0000000009
232504_at	LOC285628 /// MIR146A	uncharacterized LOC285628 /// microRNA 146a	285628 /// 406938	-1.02	2.09	2.14	3.59	0.0003179666
204298_s_at	LOX	lysyl oxidase	4015	4.60	10.76	2.34	8.05	0.0000000000
227688_at	LRCH2	leucine-rich repeats and calponin homology (CH) domain containing 2	57631	1.83	8.96	4.91	4.41	0.0000000002
231861_at	LRP10	low density lipoprotein receptor-related protein 10	26020	1.10	2.26	2.05	6.46	0.0000000886
219631_at	LRP12	low density lipoprotein receptor-related protein 12	29967	9.04	19.44	2.15	6.28	0.0000000000
220253_s_at	LRP12	low density lipoprotein receptor-related protein 12	29967	6.12	15.24	2.49	5.49	0.0000000000
220254_at	LRP12	low density lipoprotein receptor-related protein 12	29967	4.37	11.53	2.64	4.77	0.0000000000
220622_at	LRRC31	leucine rich repeat containing 31	79782	-2.00	4.71	9.43	5.52	0.0000000026

Probe Set ID	Gene Symbol	Gene Title	Entrez Gene	Fold Change			Ave Expr	Adjusted *p* value
				NT vs CTRL	S2 vs CTRL	S2 vs NT		
233499_at	LRRC7	leucine rich repeat containing 7	57554	-1.04	2.81	2.92	3.27	0.0000008869
218918_at	MAN1C1	mannosidase, alpha, class 1C, member 1	57134	1.21	3.23	2.68	5.03	0.0000000041
221884_at	MECOM	MDS1 and EVI1 complex locus	2122	-1.08	2.13	2.29	8.13	0.0000013594
206000_at	MEP1A	meprin A, alpha (PABA peptide hydrolase)	4224	1.02	5.40	5.30	9.38	0.0000000000
225478_at	MFHAS1	malignant fibrous histiocytoma amplified sequence1	9258	-1.01	2.87	2.91	8.99	0.0000000000
213457_at	MFHAS1	malignant fibrous histiocytoma amplified sequence1	9258	-1.10	2.97	3.27	8.90	0.0000000001
225102_at	MGLL	monoglyceride lipase	11343	1.14	6.64	5.84	8.05	0.0000000000
211026_s_at	MGLL	monoglyceride lipase	11343	1.29	8.47	6.56	8.01	0.0000000000
207233_s_at	MITF	microphthalmia-associated transcription factor	4286	-2.65	2.10	5.55	5.32	0.0000000001
226066_at	MITF	microphthalmia-associated transcription factor	4286	-3.63	2.97	10.76	5.18	0.0000000005
204918_s_at	MLLT3	myeloid/lymphoid or mixed-lineage leukemia (trithorax homolog, Drosophila); translocated to, 3	4300	3.06	14.26	4.65	5.38	0.0000000002
204917_s_at	MLLT3	myeloid/lymphoid or mixed-lineage leukemia (trithorax homolog, Drosophila); translocated to, 3	4300	2.08	10.42	5.01	6.97	0.0000000000
1569652_at	MLLT3	myeloid/lymphoid or mixed-lineage leukemia (trithorax homolog, Drosophila); translocated to, 3	4300	1.45	8.41	5.80	4.69	0.0000000015
209708_at	MOXD1	monooxygenase, DBH-like 1	26002	-1.24	2.18	2.71	6.73	0.0000000004
1554474_a_at	MOXD1	monooxygenase, DBH-like 1	26002	-1.22	2.26	2.76	6.72	0.0000000042
205675_at	MTTP	microsomal triglyceride transfer protein	4547	1.13	2.26	2.00	10.92	0.0000000014
222712_s_at	MUC13	mucin 13, cell surface associated	56667	1.06	8.02	7.58	4.24	0.0000000000
218687_s_at	MUC13	mucin 13, cell surface associated	56667	-1.14	9.13	10.42	6.43	0.0000000000
220196_at	MUC16	mucin 16, cell surface associated	94025	2.26	5.79	2.56	4.88	0.0000000013
206797_at	NAT2	N-acetyltransferase 2 (arylamine N-acetyltransferase)	10	1.25	3.51	2.81	6.42	0.0000000001
206964_at	NAT8B	N-acetyltransferase 8B (GCN5-related, putative, gene/pseudogene)	51471	-1.15	2.83	3.24	5.55	0.0000000076
211466_at	NFIB	nuclear factor I/B	4781	1.29	3.05	2.36	3.70	0.0000150754
223218_s_at	NFKBIZ	nuclear factor of kappa light polypeptide gene enhancer in B-cells inhibitor, zeta	64332	-1.03	2.20	2.27	10.23	0.0000000071

Probe Set ID	Gene Symbol	Gene Title	Entrez Gene	Fold Change			Ave Expr	Adjusted *p* value
				NT vs CTRL	S2 vs CTRL	S2 vs NT		
223217_s_at	NFKBIZ	nuclear factor of kappa light polypeptide gene enhancer in B-cells inhibitor, zeta	64332	-1.09	2.85	3.11	8.61	0.0000000090
202238_s_at	NNMT	nicotinamide N-methyltransferase	4837	-2.11	4.78	10.10	6.64	0.0000000000
202237_at	NNMT	nicotinamide N-methyltransferase	4837	-3.41	4.85	16.57	7.21	0.0000000000
229233_at	NRG3	neuregulin 3	10718	-1.07	2.10	2.25	4.36	0.0000000352
215020_at	NRXN3	neurexin 3	9369	1.46	3.05	2.09	4.12	0.0000000001
229649_at	NRXN3	neurexin 3	9369	5.26	13.06	2.48	6.86	0.0000000000
205795_at	NRXN3	neurexin 3	9369	3.25	8.06	2.48	5.40	0.0000000006
206291_at	NTS	neurotensin	4922	-10.33	-4.18	2.47	11.59	0.0000000000
205552_s_at	OAS1	2'-5'-oligoadenylate synthetase 1, 40/46kDa	4938	1.64	4.21	2.57	4.77	0.0000000005
1554524_a_at	OLFM3	olfactomedin 3	118427	1.70	3.60	2.12	4.01	0.0000000003
217525_at	OLFML1	olfactomedin-like 1	283298	1.19	2.71	2.27	4.31	0.0000000077
226140_s_at	OTUD1	OTU domain containing 1	220213	1.35	7.01	5.18	8.20	0.0000000000
203058_s_at	PAPSS2	3'-phosphoadenosine 5'-phosphosulfate synthase 2	9060	1.03	2.46	2.39	9.15	0.0000000672
242871_at	PAQR5	progestin and adipoQ receptor family member V	54852	1.71	7.29	4.27	6.27	0.0000000000
232054_at	PCDH20	protocadherin 20	64881	1.51	26.92	17.82	5.47	0.0000000000
205535_s_at	PCDH7	protocadherin 7	5099	-2.01	2.41	4.83	4.44	0.0000000027
239443_at	PCDHB6	protocadherin beta 6	56130	-1.09	2.03	2.22	5.83	0.0000006945
216867_s_at	PDGFA	platelet-derived growth factor alpha polypeptide	5154	-1.23	2.02	2.50	6.20	0.0000000147
218273_s_at	PDP1	pyruvate dehyrogenase phosphatase catalytic subunit 1	54704	1.34	4.23	3.16	4.52	0.0000064423
203691_at	PI3	peptidase inhibitor 3, skin-derived	5266	-1.87	6.97	13.02	6.67	0.0000000000
41469_at	PI3	peptidase inhibitor 3, skin-derived	5266	-1.82	8.33	15.19	6.17	0.0000000000
216218_s_at	PLCL2	phospholipase C-like 2	23228	1.42	3.28	2.32	5.49	0.0000000065
219756_s_at	POF1B	premature ovarian failure, 1B	79983	1.12	2.59	2.30	4.05	0.0000008710
1552670_a_at	PPP1R3B	protein phosphatase 1, regulatory subunit 3B	79660	1.08	2.17	2.01	4.84	0.0000002397

Probe Set ID	Gene Symbol	Gene Title	Entrez Gene	Fold Change			Ave Expr	Adjusted *p* value
				NT vs CTRL	S2 vs CTRL	S2 vs NT		
219127_at	PRR15L	proline rich 15-like	79170	-1.57	2.07	3.25	5.54	0.0000008616
216470_x_at	PRSS2	protease, serine, 2 (trypsin 2)	5645	1.27	4.73	3.72	5.82	0.0000000014
205402_x_at	PRSS2	protease, serine, 2 (trypsin 2)	5645	1.17	4.47	3.83	6.21	0.0000000008
207463_x_at	PRSS3	protease, serine, 3	5646	1.96	21.14	10.78	6.88	0.0000000000
213421_x_at	PRSS3	protease, serine, 3	5646	1.72	19.87	11.53	6.98	0.0000000000
215395_x_at	PRSS3P2	protease, serine, 3 pseudogene 2	154754	1.30	2.92	2.24	6.03	0.0000000118
222611_s_at	PSPC1	paraspeckle component 1	55269	1.23	2.51	2.04	6.05	0.0000007085
205171_at	PTPN4	protein tyrosine phosphatase, non-receptor type 4 (megakaryocyte)	5775	1.33	3.06	2.31	7.84	0.0000000005
214043_at	PTPRD	protein tyrosine phosphatase, receptor type, D	5789	20.59	51.00	2.48	5.99	0.0000000000
205712_at	PTPRD	protein tyrosine phosphatase, receptor type, D	5789	1.68	4.18	2.49	3.70	0.0000000019
213362_at	PTPRD	protein tyrosine phosphatase, receptor type, D	5789	3.47	9.94	2.86	5.30	0.0000000003
243001_at	RBFA	ribosome binding factor A (putative)	79863	1.09	2.62	2.42	5.66	0.0000000685
203498_at	RCAN2	regulator of calcineurin 2	10231	1.66	3.83	2.30	5.66	0.0000009286
218723_s_at	RGCC	regulator of cell cycle	28984	1.41	3.56	2.53	5.33	0.0000000020
202388_at	RGS2	regulator of G-protein signaling 2, 24kDa	5997	-1.06	2.37	2.52	9.26	0.0000000037
241703_at	RUNDC3B	RUN domain containing 3B	154661	1.28	3.71	2.89	5.50	0.0000000168
215321_at	RUNDC3B	RUN domain containing 3B	154661	-1.03	3.09	3.20	4.39	0.0000000034
1552367_a_at	SCIN	scinderin	85477	-1.22	2.64	3.22	3.91	0.0000029479
1552365_at	SCIN	scinderin	85477	-1.30	4.60	5.98	4.00	0.0000000002
223449_at	SEMA6A	sema domain, transmembrane domain (TM), and cytoplasmic domain, (semaphorin) 6A	57556	-1.34	2.06	2.76	6.51	0.0000000029
225660_at	SEMA6A	sema domain, transmembrane domain (TM), and cytoplasmic domain, (semaphorin) 6A	57556	-1.72	2.29	3.95	6.73	0.0000000023
215028_at	SEMA6A	sema domain, transmembrane domain (TM), and cytoplasmic domain, (semaphorin) 6A	57556	-1.95	2.28	4.43	5.24	0.0000000211
202376_at	SERPINA3	serpin peptidase inhibitor, clade A (alpha-1 antiproteinase, antitrypsin), member 3	12	1.78	5.29	2.97	6.31	0.0000000000

Probe Set ID	Gene Symbol	Gene Title	Entrez Gene	Fold Change			Ave Expr	Adjusted *p* value
				NT vs CTRL	S2 vs CTRL	S2 vs NT		
223196_s_at	SESN2	sestrin 2	83667	1.19	2.37	2.00	6.91	0.0000000684
206664_at	SI	sucrase-isomaltase (alpha-glucosidase)	6476	-11.37	5.18	58.88	6.06	0.0000000000
239345_at	SLC19A3	solute carrier family 19, member 3	80704	-1.36	3.10	4.22	8.17	0.0000000001
220736_at	SLC19A3	solute carrier family 19, member 3	80704	-1.17	4.35	5.09	7.12	0.0000000003
206143_at	SLC26A3	solute carrier family 26, member 3	1811	-1.81	2.11	3.82	5.71	0.0000000193
206354_at	SLCO1B3	solute carrier organic anion transporter family, member 1B3	28234	-4.62	2.01	9.30	5.63	0.0000000012
226743_at	SLFN11	schlafen family member 11	91607	1.39	19.46	13.98	4.46	0.0000000000
1553423_a_at	SLFN13	schlafen family member 13	146857	1.12	3.35	3.00	3.82	0.0000013893
203021_at	SLPI	secretory leukocyte peptidase inhibitor	6590	-1.28	11.36	14.50	6.75	0.0000000000
1568574_x_at	SPP1	Secreted phosphoprotein 1	6696	1.66	3.97	2.39	3.33	0.0000335438
209875_s_at	SPP1	secreted phosphoprotein 1	6696	3.29	10.30	3.13	10.49	0.0000000000
204011_at	SPRY2	sprouty homolog 2 (Drosophila)	10253	1.43	2.90	2.03	9.42	0.0000000006
233888_s_at	SRGAP1	SLIT-ROBO Rho GTPase activating protein 1	57522	1.03	2.57	2.50	6.18	0.0000000576
1554473_at	SRGAP1	SLIT-ROBO Rho GTPase activating protein 1	57522	-1.10	2.49	2.74	3.96	0.0000001127
227484_at	SRGAP1	SLIT-ROBO Rho GTPase activating protein 1	57522	1.12	3.85	3.44	7.35	0.0000000003
231969_at	STOX2	storkhead box 2	56977	-1.02	2.14	2.19	5.77	0.0000000362
203767_s_at	STS	steroid sulfatase (microsomal), isozyme S	412	1.65	3.30	2.00	7.74	0.0000000003
203768_s_at	STS	steroid sulfatase (microsomal), isozyme S	412	1.41	2.99	2.12	5.79	0.0000000368
219992_at	TAC3	tachykinin 3	6866	1.33	3.34	2.51	6.07	0.0000000362
209277_at	TFPI2	tissue factor pathway inhibitor 2	7980	1.05	6.75	6.43	5.74	0.0000000002
209278_s_at	TFPI2	tissue factor pathway inhibitor 2	7980	-1.00	8.71	8.72	7.41	0.0000000000
203167_at	TIMP2	TIMP metallopeptidase inhibitor 2	7077	1.34	3.10	2.30	6.62	0.0000000002
224560_at	TIMP2	TIMP metallopeptidase inhibitor 2	7077	-1.08	2.17	2.35	8.38	0.0000000002
231579_s_at	TIMP2	TIMP metallopeptidase inhibitor 2	7077	-1.10	2.20	2.43	8.89	0.0000000002
206271_at	TLR3	toll-like receptor 3	7098	1.98	4.30	2.17	4.37	0.0000001751

Probe Set ID	Gene Symbol	Gene Title	Entrez Gene	Fold Change			Ave Expr	Adjusted *p* value
				NT vs CTRL	S2 vs CTRL	S2 vs NT		
220639_at	TM4SF20	transmembrane 4 L six family member 20	79853	-1.36	2.91	3.97	4.42	0.0000000054
226489_at	TMCC3	transmembrane and coiled-coil domain family 3	57458	3.89	8.71	2.24	6.38	0.0000000000
1554105_at	TMEM185A	transmembrane protein 185A	84548	1.07	2.86	2.68	5.30	0.0000000003
226226_at	TMEM45B	transmembrane protein 45B	120224	-2.40	3.87	9.28	7.66	0.0000000003
230323_s_at	TMEM45B	transmembrane protein 45B	120224	-5.62	4.69	26.38	6.68	0.0000000000
228574_at	TMTC2	transmembrane and tetratricopeptide repeat containing 2	160335	1.45	3.50	2.41	4.80	0.0000000253
235775_at	TMTC2	transmembrane and tetratricopeptide repeat containing 2	160335	1.26	3.38	2.68	3.13	0.0000001297
201688_s_at	TPD52	tumor protein D52	7163	1.04	2.47	2.38	9.21	0.0000000007
243952_at	TPTEP1	transmembrane phosphatase with tensin homology pseudogene 1	387590	1.09	3.86	3.55	7.24	0.0000000000
202504_at	TRIM29	tripartite motif containing 29	23650	1.14	2.44	2.14	4.33	0.0000004942
210159_s_at	TRIM31	tripartite motif containing 31	11074	1.74	5.69	3.27	5.99	0.0000000003
215444_s_at	TRIM31	tripartite motif containing 31	11074	3.22	15.07	4.68	6.16	0.0000000001
208170_s_at	TRIM31	tripartite motif containing 31	11074	2.97	17.99	6.06	5.32	0.0000000000
203824_at	TSPAN8	tetraspanin 8	7103	-3.09	2.27	7.01	9.32	0.0000000000
227388_at	TUSC1	tumor suppressor candidate 1	286319	6.34	14.53	2.29	6.75	0.0000000000
211184_s_at	USH1C	Usher syndrome 1C (autosomal recessive, severe)	10083	-2.54	2.09	5.29	5.87	0.0000000002
205139_s_at	UST	uronyl-2-sulfotransferase	10090	1.05	2.10	2.00	2.97	0.0000004782
218806_s_at	VAV3	vav 3 guanine nucleotide exchange factor	10451	1.41	5.42	3.84	4.45	0.0000000003
218807_at	VAV3	vav 3 guanine nucleotide exchange factor	10451	1.82	7.76	4.27	6.15	0.0000000000
220528_at	VNN3	vanin 3	55350	-1.33	2.26	3.02	6.82	0.0000000070
210861_s_at	WISP3	WNT1 inducible signaling pathway protein 3	8838	-1.28	2.10	2.69	7.30	0.0000000083
221958_s_at	WLS	wntless homolog (Drosophila)	79971	-2.02	2.80	5.65	7.37	0.0000000000
228949_at	WLS	wntless homolog (Drosophila)	79971	-2.22	3.04	6.74	5.00	0.0000000032
228950_s_at	WLS	wntless homolog (Drosophila)	79971	-2.00	3.65	7.30	5.35	0.0000000008

Probe Set ID	Gene Symbol	Gene Title	Entrez Gene	Fold Change			Ave Expr	Adjusted *p* value
				NT vs CTRL	S2 vs CTRL	S2 vs NT		
213425_at	WNT5A	wingless-type MMTV integration site family, member 5A	7474	-1.99	3.26	6.48	4.18	0.0000000017
205990_s_at	WNT5A	wingless-type MMTV integration site family, member 5A	7474	-2.60	3.27	8.50	5.02	0.0000000000
1555800_at	ZNF385B	zinc finger protein 385B	151126	1.46	3.69	2.53	3.92	0.0000001228
1555801_s_at	ZNF385B	zinc finger protein 385B	151126	1.93	5.82	3.01	3.99	0.0000000024
228988_at	ZNF711	zinc finger protein 711	7552	13.99	29.98	2.14	5.33	0.0000000000

Appendix C

Affymetrix microarray gene expression analysis procedure:

For transcriptional profiling, Affymetrix Human Genome U133 plus 2.0 arrays were used, and this was preformed by the Center of Physiology and Pathophysiology, Institute of Neurophysiology, Cologne, Germany. The reagents and instrumentation regarding microarrays were acquired from Affymetrix (Affymetrix, Santa Clara, CA, USA, http://www.affymetrix.com). For biotin-labelling and RNA amplification, 100 ng total RNA was used with GeneChip 3' IVT Express kit according to the manufacturer's instructions (Affymetrix). The amplified RNA (aRNA) was purified using magnetic beads and 15 µg of aRNA was fragmented in fragmentation buffer. For hybridization (Affymetrix HWS kit) 12.5 µg fragmented aRNA was hybridized with Affymetrix GeneChip Human Genome U133 plus 2.0 arrays along with hybridization cocktail solution and then placed in Genechip Hybridization Oven-645 (Affymetrix), rotating at 60 rpm at 45°C for 16 hours (hrs). For staining with streptavidin-phycoerythrin and washing, the Affymetrix HWS kit was used according to the manufacturer's washing and staining protocol using a Genechip Fluidics Station-450 (Affymetrix). The stained arrays were scanned with Affymetrix GeneChip Scanner-3000-7G and the quality control analysis were performed with Affymetrix GCOS software.

To analyse the data, background correction, normalization and summarization were performed using Robust Multi-array Average (RMA) normalization method. Differential expression of probe sets has been determined by the linear model implementation of R Limma Package followed by a Benjamini Hochberg multiple testing correction and the corrected *p* value were provided as adjusted *p* value. Fold change value calculation between the conditions were provided in normal scale.

References

Abeijon, C., Mandon, E. C., Hirschberg, C. B. (1997). "Transporters of nucleotide sugars, nucleotide sulfate and ATP in the Golgi apparatus."Trends Biochem Sci.22: 203-207.

Ahmed, V., Ispahany, M., Ruttgaizer, S., Guillemette, G., Taylor, S. D. (2005)."A fluorogenic substrate for the continuous assaying of aryl sulfatases."Anal Biochem.340: 80-88.

Ai, X., Do, A. T., Lozynska, O., Kusche-Gullberg, M., Lindahl, U., Emerson, C. P. Jr. (2003). "QSulf1 remodels the 6-O sulfation states of cell surface heparan sulfate proteoglycans to promote Wnt signalling." J Cell Biol.162: 341-351.

Ai, X., Do, A. T., Kusche-Gullberg, M., Lindahl, U., Lu, K., Emerson, C. P. Jr. (2006). "Substrate specificity and domain functions of extracellular heparan sulfate 6-O-endosulfatases, QSulf1 and QSulf2." J Biol Chem.281: 4969-4976.

Alexia, C., Fallot, G., Lasfer, M., Schweizer-Groyer, G., Groyer, A. (2004). "An evaluation of the role of insulin-like growth factors (IGF) and of type-I IGF receptor signalling in hepatocarcinogenesis and in the resistance of hepatocarcinoma cells against drug-induced apoptosis." Biochem Pharmacol. 68: 1003-1015.

Ambasta, R., Ai, X., Emerson, C. P. Jr. (2007). "Quail Sulf1 function requires asparagine-linked glycosylation." J Biol Chem.282: 34492-34499.

Amiano, N. O., Costa, M. J., Reiteri, R. M., Payes, C., Guerrieri, D., Tateosian, N. L., Sanchez, M. L., Maffia, P. C., Diament, M., Karas, R., Orqueda, A., Rizzo, M., Alaniz, L., Mazzolini, G., Klein, S., Sallenave, J. M., Chuluyan, H. E. (2013). "Anti-tumor effect of SLPI on mammary but not colon tumor growth." J Cell Physiol 228: 469-475.

Amit, S., Hatzubai, A., Birman, Y., Andersen, J. S., Ben-Shushan, E., Mann, M., Ben-Neriah, Y., Alkalay, I. (2002). "Axin-mediated CKI phosphorylation of beta-catenin at Ser 45: a molecular switch for the Wnt pathway." Genes Dev. 16: 1066-1076.

Arafat, H. A., Gong, Q., Chipitsyna, G., Rizvi, A., Saa, C. T., Yeo, C. J. (2007). "Antihypertensives as novel antineoplastics: angiotensin-I-converting enzyme

inhibitors and angiotensin II type 1 receptor blockers in pancreatic ductal adenocarcinoma." J Am Coll Surg 204: 996-1005; discussion 1005-1006.

Barrett, S. D., Bridges, A. J., Dudley, D. T., Saltiel, A. R., Fergus, J. H., Flamme, C. M., Delaney, A. M., Kaufman, M., LePage, S., Leopold, W. R., Przybranowski, S. A., Sebolt-Leopold, J., Van Becelaere, K., Doherty, A. M., Kennedy, R. M., Marston, D., Howard, W. A. Jr., Smith, Y., Warmus, J. S., Tecle, H. (2008). "The discovery of the benzhydroxamate MEK inhibitors CI-1040 and PD 0325901." Bioorg Med Chem Lett. 18: 6501-6504.

Bataller, R., Ginès, P., Nicolás, J. M., Görbig, M. N., Garcia-Ramallo, E., Gasull, X., Bosch, J., Arroyo, V., Rodés, J. (2000). "Angiotensin II induces contraction and proliferation of human hepatic stellate cells." Gastroenterology. 118: 1149-1156.

Bataller, R., Sancho-Bru, P., Ginès, P., Lora, J. M., Al-Garawi, A., Solé, M., Colmenero, J., Nicolás, J. M., Jiménez, W., Weich, N., Gutiérrez-Ramos, J. C., Arroyo, V., Rodés, J. (2003 a). "Activated human hepatic stellate cells express the renin-angiotensin system and synthesize angiotensin II." Gastroenterology. 125: 117-125.

Bataller, R., Gäbele, E., Schoonhoven, R., Morris, T., Lehnert, M., Yang, L., Brenner, D. A., Rippe, R. A. (2003 b). "Prolonged infusion of angiotensin II into normal rats induces stellate cell activation and proinflammatory events in liver." Am J Physiol Gastrointest Liver Physiol. 285: G642-651.

Bataller, R., Brenner, D. A. (2005). "Liver fibrosis." J Clin Invest. 115: 209-218.

Beasley, R. (2009). "Rocks along the road to the control of HBV and HCC."Ann Epidemiol. 19: 231-234.

Belghiti, J., Carr, B. I., Greig, P. D., Lencioni, R., Poon, R. T. (2008). "Treatment before liver transplantation for HCC."Ann Surg Oncol.15: 993-1000.

Bengochea, A., de Souza, M. M., Lefrançois, L., Le Roux, E., Galy, O., Chemin, I., Kim, M., Wands, J. R., Trepo, C., Hainaut, P., Scoazec, J. Y., Vitvitski, L., Merle, P. (2008). "Common dysregulation of Wnt/Frizzled receptor elements in human hepatocellular carcinoma." Br J Cancer. 99: 143-150.

Benter, I. F., Yousif, M. H., Cojocel, C., Al-Maghrebi, M., Diz, D. I. (2007). "Angiotensin-(1-7) prevents diabetes-induced cardiovascular dysfunction." Am J Physiol Heart Circ Physiol 292: H666-672.

Bernfield, M., Götte, M., Park, P. W., Reizes, O., Fitzgerald, M. L., Lincecum, J., Zako, M. (1999). "Functions of cell surface heparan sulfate proteoglycans." Annu Rev Biochem.68: 729-777.

Bilban, M., Billich, A., Auer, M., Nussbaumer, P. (2000)."New fluorogenic substrate for the first continuous steroid sulfatase assay."Bioorg Med Chem Lett.10: 967-969.

Bilic, J., Huang, Y. L., Davidson, G., Zimmermann, T., Cruciat, C. M., Bienz, M., Niehrs, C. (2007). "Wnt induces LRP6 signalosomes and promotes dishevelled-dependent LRP6 phosphorylation." Science. 316: 1619-1622.

Bishop, J., Schuksz, M., Esko, J. D. (2007). "Heparan sulphate proteoglycans fine-tune mammalian physiology." Nature.446: 1030-1037.

Bosch, F., Ribes, J., Cléries, R., Díaz, M. (2005)."Epidemiology of hepatocellular carcinoma."Clin Liver Dis.9: 191-211.

Boyault, S., Rickman, D. S., de Reyniès, A., Balabaud, C., Rebouissou, S., Jeannot, E., Hérault, A., Saric, J., Belghiti, J., Franco, D., Bioulac-Sage, P., Laurent-Puig, P., Zucman-Rossi, J. (2007). "Transcriptome classification of HCC is related to gene alterations and to new therapeutic targets." Hepatology. 45: 42-52.

Brembeck, F. H., Rosário, M., Birchmeier, W. (2006). "Balancing cell adhesion and Wnt signalling, the key role of beta-catenin." Curr Opin Genet Dev. 16: 51-59.

Breuhahn, K., Schirmacher, P. (2008). "Reactivation of the insulin-like growth factor-II signaling pathway in human hepatocellular carcinoma." World J Gastroenterol. 14: 1690-1698.

Brodeur, G. M., Seeger, R. C., Schwab, M., Varmus, H. E., Bishop, J. M. (1984). "Amplification of N-myc in untreated human neuroblastomas correlates with advanced disease stage." Science 224: 1121-1124.

Brooks, A. N., Kilgour, E., Smith, P. D. (2012). "Molecular pathways: fibroblast growth factor signaling: a new therapeutic opportunity in cancer." Clin Cancer Res 18: 1855-1862.

Bumbaca, D., Wong, A., Drake, E., Reyes, A. E., 2nd, Lin, B. C., Stephan, J. P., Desnoyers, L., Shen, B. Q., Dennis, M. S. (2011). "Highly specific off-target binding identified and eliminated during the humanization of an antibody against FGF receptor 4." MAbs 3: 376-386.

Buono, M., Cosma, M. P. (2010). "Sulfatase activities towards the regulation of cell metabolism and signalling in mammals."Cell Mol Life Sci. 67: 769-780.

Burkhart, C. A., Cheng, A. J., Madafiglio, J., Kavallaris, M., Mili, M., Marshall, G. M., Weiss, W. A., Khachigian, L. M., Norris, M. D., Haber, M. (2003). "Effects of MYCN antisense oligonucleotide administration on tumorigenesis in a murine model of neuroblastoma." J Natl Cancer Inst 95: 1394-1403.

Cagatay, T., Ozturk, M. (2002). "P53 mutation as a source of aberrant beta-catenin accumulation in cancer cells." Oncogene 21: 7971-7980.

Cariani, E., Lasserre, C., Seurin, D., Hamelin, B., Kemeny, F., Franco, D., Czech, M. P., Ullrich, A., Brechot, C. (1988). "Differential expression of insulin-like growth factor II mRNA in human primary liver cancers, benign liver tumors, and liver cirrhosis." Cancer Res. 48: 6844-6849.

Carruba, G., Cervello, M., Miceli, M. D., Farruggio, R., Notarbartolo, M., Virruso, L., Giannitrapani, L., Gambino, R., Montalto, G., Castagnetta, L. (1999). "Truncated form of beta-catenin and reduced expression of wild-type catenins feature HepG2 human liver cancer cells." Ann N Y Acad Sci. 886: 212-216.

Chae, Y. K., Valsecchi, M. E., Kim, J., Bianchi, A. L., Khemasuwan, D., Desai, A., Tester, W. (2011). "Reduced risk of breast cancer recurrence in patients using ACE inhibitors, ARBs, and/or statins." Cancer Invest 29: 585-593.

Chang, M., You, S. L., Chen, C. J., Liu, C. J., Lee, C. M., Lin, S. M., Chu, H. C., Wu, T. C., Yang, S. S., Kuo, H. S., Chen, D. S.; Taiwan Hepatoma Study Group. (2009). "Decreased incidence of hepatocellular carcinoma in hepatitis B vaccinees: a 20-year follow-up study." J Natl Cancer Inst.101: 1348-1355.

Chang, M., You, S. L., Chen, C. J., Liu, C. J., Lee, C. M., Lin, S. M., Chu, H. C., Wu, T. C., Yang, S. S., Kuo, H. S., Chen, D. S.; Taiwan Hepatoma Study Group. (2009). "Decreased incidence of hepatocellular carcinoma in hepatitis B vaccinees: a 20-year follow-up study." J Natl Cancer Inst.101: 1348-1355.

Chen, M. W., Vacherot, F., De La Taille, A., Gil-Diez-De-Medina, S., Shen, R., Friedman, R. A., Burchardt, M., Chopin, D. K., Buttyan, R. (2002). "The emergence of protocadherin-PC expression during the acquisition of apoptosis-resistance by prostate cancer cells." Oncogene 21: 7861-7871.

Cheng, J. M., Hiemstra, J. L., Schneider, S. S., Naumova, A., Cheung, N. K., Cohn, S. L., Diller, L., Sapienza, C., Brodeur, G. M. (1993). "Preferential

amplification of the paternal allele of the N-myc gene in human neuroblastomas." Nat Genet 4: 191-194.

Chiba, T., Kita, K., Zheng, Y. W., Yokosuka, O., Saisho, H., Iwama, A., Nakauchi, H., Taniguchi, H. (2006). "Side population purified from hepatocellular carcinoma cells harbors cancer stem cell-like properties." Hepatology. 44: 240-251.

Clark, H., Carson, W. F., Kavanagh, P. V., Ho, C. P., Shen, P., Zagoria, R. J. (2005). "Staging and current treatment of hepatocellular carcinoma." Radiographics 25.

Cong, F., Schweizer, L., Varmus, H. (2004). "Wnt signals across the plasma membrane to activate the beta-catenin pathway by forming oligomers containing its receptors, Frizzled and LRP." Development. 131: 5103-5115.

Cook, K. L., Metheny-Barlow, L. J., Tallant, E. A., Gallagher, P. E. (2010). "Angiotensin-(1-7) reduces fibrosis in orthotopic breast tumors." Cancer Res 70: 8319-8328.

Cornellà, H., Alsinet, C., Villanueva, A. (2011). "Molecular pathogenesis of hepatocellular carcinoma." Alcohol Clin Exp Res. 35: 821-825.

Cosma, M., Pepe, S., Annunziata, I., Newbold, R. F., Grompe, M., Parenti, G., Ballabio, A. (2003). "The multiple sulfatase deficiency gene encodes an essential and limiting factor for the activity of sulfatases." Cell113: 445-456.

Crackower, M. A., Sarao, R., Oudit, G. Y., Yagil, C., Kozieradzki, I., Scanga, S. E., Oliveira-dos-Santos, A. J., da Costa, J., Zhang, L., Pei, Y., Scholey, J., Ferrario, C. M., Manoukian, A. S., Chappell, M. C., Backx, P. H., Yagil, Y., Penninger, J. M. (2002). "Angiotensin-converting enzyme 2 is an essential regulator of heart function." Nature. 417: 822-828.

Cronin, C. A., Ryan, A. B., Talley, E. M., Scrable, H. (2003). "Tyrosinase expression during neuroblast divisions affects later pathfinding by retinal ganglion cells." J Neurosci. 23: 11692-11697.

Cunningham, S., Tsai, S., Marques, H. P., Mira, P., Cameron, A., Barroso, E., Philosophe, B., Pawlik, T. M. (2009). "Management of early hepatocellular carcinoma in patients with well-compensated cirrhosis."Ann Surg Oncol.16: 1820-1831.

Dai, Y., Yang, Y., MacLeod, V., Yue, X., Rapraeger, A. C., Shriver, Z., Venkataraman, G., Sasisekharan, R., Sanderson, R. D. (2005). "HSulf-1 and HSulf-2 are potent inhibitors of myeloma tumor growth in vivo." J Biol Chem.280: 40066-40073.

de La Coste, A., Romagnolo, B., Billuart, P., Renard, C. A., Buendia, M. A., Soubrane, O., Fabre, M., Chelly, J., Beldjord, C., Kahn, A., Perret, C. (1998). "Somatic mutations of the beta-catenin gene are frequent in mouse and human hepatocellular carcinomas." Proc Natl Acad Sci USA. 95: 8847-8851.

De Souza, A. T., Hankins, G. R., Washington, M. K., Fine, R. L., Orton, T. C., Jirtle, R. L. (1995). "Frequent loss of heterozygosity on 6q at the mannose 6-phosphate/insulin-like growth factor II receptor locus in human hepatocellular tumors." Oncogene 10: 1725-1729.

Desnoyers, L. R., Pai, R., Ferrando, R. E., Hotzel, K., Le, T., Ross, J., Carano, R., D'Souza, A., Qing, J., Mohtashemi, I., Ashkenazi, A., French, D. M. (2008). "Targeting FGF19 inhibits tumor growth in colon cancer xenograft and FGF19 transgenic hepatocellular carcinoma models." Oncogene 27: 85-97.

Devoogdt, N., Hassanzadeh Ghassabeh, G., Zhang, J., Brys, L., De Baetselier, P., Revets, H. (2003). "Secretory leukocyte protease inhibitor promotes the tumorigenic and metastatic potential of cancer cells." Proc Natl Acad Sci U S A 100: 5778-5782.

Devoogdt, N., Rasool, N., Hoskins, E., Simpkins, F., Tchabo, N., Kohn, E. C. (2009). "Overexpression of protease inhibitor-dead secretory leukocyte protease inhibitor causes more aggressive ovarian cancer in vitro and in vivo." Cancer Sci 100: 434-440.

Dhar, D. K., Naora, H., Yamanoi, A., Ono, T., Kohno, H., Otani, H., Nagasue, N. (2002). "Requisite role of VEGF receptors in angiogenesis of hepatocellular carcinoma: a comparison with angiopoietin/Tie pathway." Anticancer Res. 22: 379-386.

Dhoot, G., Gustafsson, M. K., Ai, X., Sun, W., Standiford, D. M., Emerson, C. P. Jr. (2001). "Regulation of Wnt signalling and embryo patterning by an extracellular sulfatase." Science293: 1663-1666.

Dierks, T., Schmidt, B., von Figura, K. (1997). "Conversion of cysteine to formylglycine: a protein modification in the endoplasmic reticulum." Proc Natl Acad Sci U S A.94: 11963-11968.

Dierks, T., Schmidt, B., Borissenko, L. V., Peng, J., Preusser, A., Mariappan, M., von Figura, K. (2003). "Multiple sulfatase deficiency is caused by mutations in the gene encoding the human C(alpha)-formylglycine generating enzyme." Cell113: 435-444.

Diez-Roux, G., Ballabio, A. (2005)."Sulfatases and human disease."Annu Rev Genomics Hum Genet.6: 355-379.

DiGabriele, A., Lax, I., Chen, D. I., Svahn, C. M., Jaye, M., Schlessinger, J., Hendrickson, W. A. (1998). "Structure of a heparin-linked biologically active dimer of fibroblast growth factor."Nature393: 812-817.

Donoghue, M., Hsieh, F., Baronas, E., Godbout, K., Gosselin, M., Stagliano, N., Donovan, M., Woolf, B., Robison, K., Jeyaseelan, R., Breitbart, R. E., Acton, S. (2000). "A novel angiotensin-converting enzyme-related carboxypeptidase (ACE2) converts angiotensin I to angiotensin 1-9." Circ Res. 87: E1-9.

Ebermann, L., Spillmann, F., Sidiropoulos, M., Escher, F., Heringer-Walther, S., Schultheiss, H. P., Tschope, C., Walther, T. (2008). "The angiotensin-(1-7) receptor agonist AVE0991 is cardioprotective in diabetic rats." Eur J Pharmacol 590: 276-280.

Edwards, B., Ward, E., Kohler, B. A., Eheman, C., Zauber, A. G., Anderson, R. N., Jemal, A., Schymura, M. J., Lansdorp-Vogelaar, I., Seeff, L. C., van Ballegooijen, M., Goede, S. L., Ries, L. A. (2010). "Annual report to the nation on the status of cancer, 1975-2006, featuring colorectal cancer trends and impact of interventions (risk factors, screening, and treatment) to reduce future rates." Cancer116: 544-573.

Ehlers, M. R., Riordan, J. F. (1991). "Angiotensin-converting enzyme: zinc- and inhibitor-binding stoichiometries of the somatic and testis isozymes." Biochemistry. 30: 7118-7126.

El-Serag, H., Rudolph, K. L. (2007). "Hepatocellular carcinoma: epidemiology and molecular carcinogenesis." Gastroenterology.132: 2557-2576.

Enari, M., Talanian, R. V., Wong, W. W., Nagata, S. (1996). "Sequential activation of ICE-like and CPP32-like proteases during Fas-mediated apoptosis." Nature 380: 723-726.

Faham, S., Hileman, R. E., Fromm, J. R., Linhardt, R. J., Rees, D. C. (1996). "Heparin structure and interactions with basic fibroblast growth factor."Science271: 1116-1120.

Feng, D. Y., Zheng, H., Tan, Y., Cheng, R. X. (2001). "Effect of phosphorylation of MAPK and Stat3 and expression of c-fos and c-jun proteins on hepatocarcinogenesis and their clinical significance." World J Gastroenterol. 7: 33-36.

Feng, Y., Ni, L., Wan, H., Fan, L., Fei, X., Ma, Q., Gao, B., Xiang, Y., Che, J., Li, Q. (2011). "Overexpression of ACE2 produces antitumor effects via inhibition of angiogenesis and tumor cell invasion in vivo and in vitro." Oncol Rep 26: 1157-1164.

Ferreira, A. J., Jacoby, B. A., Araujo, C. A., Macedo, F. A., Silva, G. A., Almeida, A. P., Caliari, M. V., Santos, R. A. (2007). "The nonpeptide angiotensin-(1-7) receptor Mas agonist AVE-0991 attenuates heart failure induced by myocardial infarction." Am J Physiol Heart Circ Physiol 292: H1113-1119.

Forsten-Williams, K., Chua, C. C., Nugent, M. A. (2005). "The kinetics of FGF-2 binding to heparan sulfate proteoglycans and MAP kinase signalling."J Theor Biol.233: 483-499.

Freeman, E. J., Chisolm, G. M., Ferrario, C. M., Tallant, E. A. (1996). "Angiotensin-(1-7) inhibits vascular smooth muscle cell growth." Hypertension 28: 104-108.

French, D. M., Lin, B. C., Wang, M., Adams, C., Shek, T., Hotzel, K., Bolon, B., Ferrando, R., Blackmore, C., Schroeder, K., Rodriguez, L. A., Hristopoulos, M., Venook, R., Ashkenazi, A., Desnoyers, L. R. (2012). "Targeting FGFR4 inhibits hepatocellular carcinoma in preclinical mouse models." PLoS One 7: e36713.

Frese, M., Milz, F., Dick, M., Lamanna, W. C., Dierks, T. (2009). "Characterization of the human sulfatase Sulf1 and its high affinity heparin/heparan sulfate interaction domain." J Biol Chem.284: 28033-28044.

Fuerer, C., Nusse, R. (2010). "Lentiviral vectors to probe and manipulate the Wnt signalling pathway." PLoS One. 5: e9370.

Gallagher, J. (2001). "Heparan sulfate: growth control with a restricted sequence menu." J Clin Invest. 108: 357-361.

Gallagher, P. E., Tallant, E. A. (2004). "Inhibition of human lung cancer cell growth by angiotensin-(1-7)." Carcinogenesis 25: 2045-2052.

Gallagher, J. (2006). "Multiprotein signalling complexes: regional assembly on heparan sulphate." Biochem Soc Trans.34: 438-441.

Galli, L. M., Barnes, T., Cheng, T., Acosta, L., Anglade, A., Willert, K., Nusse, R., Burrus, L. W. (2006). "Differential inhibition of Wnt-3a by Sfrp-1, Sfrp-2, and Sfrp-3." Dev Dyn. 235: 681-690.

Gallo, et. al. (1998). "A new prognostic system for hepatocellular carcinoma: a retrospective study of 435 patients: the Cancer of the Liver Italian Program (CLIP) investigators." Hepatology28: 751-755.

Gauglhofer, C., Sagmeister, S., Schrottmaier, W., Fischer, C., Rodgarkia-Dara, C., Mohr, T., Stättner, S., Bichler, C., Kandioler, D., Wrba, F., Schulte-Hermann, R., Holzmann, K., Grusch, M., Marian, B., Berger, W., Grasl-Kraupp, B. (2011). "Up-regulation of the fibroblast growth factor 8 subfamily in human hepatocellular carcinoma for cell survival and neoangiogenesis." Hepatology 53: 854-864.

Geng, M., Cao, Y. C., Chen, Y. J., Jiang, H., Bi, L. Q., Liu, X. H. (2012). "Loss of Wnt5a and Ror2 protein in hepatocellular carcinoma associated with poor prognosis." World J Gastroenterol 18: 1328-1338.

Gollob, J. A., Wilhelm, S., Carter, C., Kelley, S. L. (2006). "Role of Raf kinase in cancer: therapeutic potential of targeting the Raf/MEK/ERK signal transduction pathway." Semin Oncol. 33: 392-406.

Gordon, M. D., Nusse, R. (2006). "Wnt signalling: multiple pathways, multiple receptors, and multiple transcription factors." J Biol Chem. 281: 22429-22433.

Grace, J. A., Herath, C. B., Mak, K. Y., Burrell, L. M., Angus, P. W. (2012). "Update on new aspects of the renin-angiotensin system in liver disease: clinical implications and new therapeutic options." Clin Sci (Lond). 123: 225-239.

Grandy, D., Shan, J., Zhang, X., Rao, S., Akunuru, S., Li, H., Zhang, Y., Alpatov, I., Zhang, X. A., Lang, R. A., Shi, D. L., Zheng, J. J. (2009). "Discovery and characterization of a small molecule inhibitor of the PDZ domain of dishevelled." J Biol Chem. 284: 16256-16263.

Grigoryan, T., Wend, P., Klaus, A., Birchmeier, W. (2008). "Deciphering the function of canonical Wnt signals in development and disease: conditional loss-

and gain-of-function mutations of beta-catenin in mice." Genes Dev. 22: 2308-2341.

Guimond, S., Maccarana, M., Olwin, B. B., Lindahl, U., Rapraeger, A. C. (1993). "Activating and inhibitory heparin sequences for FGF-2 (basic FGF). Distinct requirements for FGF-1, FGF-2, and FGF-4."J Biol Chem. 268: 23906-23914.

Habuchi, H., Tanaka, M., Habuchi, O., Yoshida, K., Suzuki, H., Ban, K., Kimata, K. (2000)."The occurrence of three isoforms of heparan sulfate 6-O-sulfotransferase having different specificities for hexuronic acid adjacent to the targeted N-sulfoglucosamine."J Biol Chem.275: 2859-2868.

Habuchi, H., Miyake, G., Nogami, K., Kuroiwa, A., Matsuda, Y., Kusche-Gullberg, M., Habuchi, O., Tanaka, M., Kimata, K. (2003). "Biosynthesis of heparan sulphate with diverse structures and functions: two alternatively spliced forms of human heparan sulphate 6-O-sulphotransferase-2 having different expression patterns and properties." Biochem J. 371: 131-142.

Habuchi, H., Habuchi, O., Kimata, K. (2004). "Sulfation pattern in glycosaminoglycan: does it have a code?" Glycoconj J.21: 47-52.

Hamada, F., Bienz, M. (2004). "The APC tumor suppressor binds to C-terminal binding protein to divert nuclear beta-catenin from TCF." Dev Cell 7: 677-685.

Hammer, F., Subtil, S., Lux, P., Maser-Gluth, C., Stewart, P. M., Allolio, B., Arlt, W. (2005). "No evidence for hepatic conversion of dehydroepiandrosterone (DHEA) sulfate to DHEA: in vivo and in vitro studies." J Clin Endocrinol Metab.90: 3600-3605.

Hanson, S. R., Best, M. D., Wong, C. H. (2004). "Sulfatases: structure, mechanism, biological activity, inhibition, and synthetic utility." Angew Chem Int Ed Engl. 43: 5736-5763.

Haschke, M., Schuster, M., Poglitsch, M., Loibner, H., Salzberg, M., Bruggisser, M., Penninger, J., Krahenbuhl, S. (2013). "Pharmacokinetics and Pharmacodynamics of Recombinant Human Angiotensin-Converting Enzyme 2 in Healthy Human Subjects." Clin Pharmacokinet.

Heckman, J., Devera, M. B., Marsh, J. W., Fontes, P., Amesur, N. B., Holloway, S. E., Nalesnik, M., Geller, D. A., Steel, J. L., Gamblin, T. C. (2008). "Bridging locoregional therapy for hepatocellular carcinoma prior to liver transplantation." Ann Surg Oncol.15: 3169-3177.

Heinzerling, J. H., Anthony, T., Livingston, E. H., Huerta, S. (2007). "Predictors of distant metastasis and mortality in patients with stage II colorectal cancer." Am Surg 73: 230-238.

Helenius, A. (1994). "How N-linked oligosaccharides affect glycoprotein folding in the endoplasmic reticulum." Mol Biol Cell.5: 253-265.

Helenius, A., Aebi, M. (2001). "Intracellular functions of N-linked glycans." Science291: 2364-2369.

Herath, C. B., Warner, F. J., Lubel, J. S., Dean, R. G., Jia, Z., Lew, R. A., Smith, A. I., Burrell, L. M., Angus, P. W. (2007). "Upregulation of hepatic angiotensin-converting enzyme 2 (ACE2) and angiotensin-(1-7) levels in experimental biliary fibrosis." J Hepatol. 47: 387-395.

Herr, D., Rodewald, M., Fraser, H. M., Hack, G., Konrad, R., Kreienberg, R., Wulff, C. (2008). "Potential role of Renin-Angiotensin-system for tumor angiogenesis in receptor negative breast cancer." Gynecol Oncol 109: 418-425.

Hibi, K., Goto, T., Kitamura, Y. H., Yokomizo, K., Sakuraba, K., Shirahata, A., Mizukami, H., Saito, M., Ishibashi, K., Kigawa, G., Nemoto, H., Sanada, Y. (2010). "Methylation of TFPI2 gene is frequently detected in advanced well-differentiated colorectal cancer." Anticancer Res 30: 1205-1207.

Hirose, A., Ono, M., Saibara, T., Nozaki, Y., Masuda, K., Yoshioka, A., Takahashi, M., Akisawa, N., Iwasaki, S., Oben, J. A., Onishi, S. (2007). "Angiotensin II type 1 receptor blocker inhibits fibrosis in rat nonalcoholic steatohepatitis." Hepatology. 45: 1375-1381.

Ho, H. K., Pok, S., Streit, S., Ruhe, J. E., Hart, S., Lim, K. S., Loo, H. L., Aung, M. O., Lim, S. G., Ullrich, A. (2009). "Fibroblast growth factor receptor 4 regulates proliferation, anti-apoptosis and alpha-fetoprotein secretion during hepatocellular carcinoma progression and represents a potential target for therapeutic intervention." J Hepatol. 50: 118-127.

Holst, C. R., Bou-Reslan, H., Gore, B. B., Wong, K., Grant, D., Chalasani, S., Carano, R. A., Frantz, G. D., Tessier-Lavigne, M., Bolon, B., French, D. M., Ashkenazi, A. (2007). "Secreted sulfatases Sulf1 and Sulf2 have overlapping yet essential roles in mouse neonatal survival." PLoS One 2: e575.

Honke, K., Taniguchi N. (2002). "Sulfotransferases and sulfated oligosaccharides."Med Res Rev.22: 637-654.

Horvath, A., & Billich, A. (2005)."Steroid sulfatase inhibitors."Expert Opin.Ther. Patents15: 1541-1553.

Howarth, N. M., Purohit, A., Reed, M. J., Potter, B. V. (1994). "Estrone sulfamates: potent inhibitors of estrone sulfatase with therapeutic potential." J Med Chem 37: 219-221.

Hsu, I. C., Tokiwa, T., Bennett, W., Metcalf, R. A., Welsh, J. A., Sun, T., Harris, C. C. (1993). "p53 gene mutation and integrated hepatitis B viral DNA sequences in human liver cancer cell lines." Carcinogenesis. 14: 987-992.

Hu, Z., Evarts, R. P., Fujio, K., Omori, N., Omori, M., Marsden, E. R., Thorgeirsson, S. S. (1996). "Expression of transforming growth factor alpha/epidermal growth factor receptor, hepatocyte growth factor/c-met and acidic fibroblast growth factor/fibroblast growth factor receptors during hepatocarcinogenesis." Carcinogenesis 17: 931-938.

Hu, M., Kurobe, M., Jeong, Y. J., Fuerer, C., Ghole, S., Nusse, R., Sylvester, K. G. (2007). "Wnt/beta-catenin signalling in murine hepatic transit amplifying progenitor cells." Gastroenterology 133: 1579-1591.

Huang, H., Fujii, H., Sankila, A., Mahler-Araujo, B. M., Matsuda, M., Cathomas, G., Ohgaki, H. (1999). "Beta-catenin mutations are frequent in human hepatocellular carcinomas associated with hepatitis C virus infection." Am J Pathol. 155: 1795-1801.

Huang, J., Zhang, X., Zhang, M., Zhu, J. D., Zhang, Y. L., Lin, Y., Wang, K. S., Qi, X. F., Zhang, Q., Liu, G. Z., Yu, J., Cui, Y., Yang, P. Y., Wang, Z. Q., Han, Z. G., (2007). "Up-regulation of DLK1 as an imprinted gene could contribute to human hepatocellular carcinoma." Carcinogenesis 28(5): 1094-1103.

Hur, K., Han, T. S., Jung, E. J., Yu, J., Lee, H. J., Kim, W. H., Goel, A., Yang, H. K. (2012). "Up-regulated expression of sulfatases (SULF1 and SULF2) as prognostic and metastasis predictive markers in human gastric cancer." J Pathol. 228: 88-98.

Huynh, H., Nguyen, T. T., Chow, K. H., Tan, P. H., Soo, K. C., Tran, E. (2003). "Over-expression of the mitogen-activated protein kinase (MAPK) kinase (MEK)-MAPK in hepatocellular carcinoma: its role in tumor progression and apoptosis." BMC Gastroenterol. 3: 19.

Imoto, I., Izumi, H., Yokoi, S., Hosoda, H., Shibata, T., Hosoda, F., Ohki, M., Hirohashi, S., Inazawa, J. (2006). "Frequent silencing of the candidate tumor

suppressor PCDH20 by epigenetic mechanism in non-small-cell lung cancers." Cancer Res 66: 4617-4626.

Ino, K., Shibata, K., Kajiyama, H., Nawa, A., Nomura, S., Kikkawa, F. (2006). "Manipulating the angiotensin system--new approaches to the treatment of solid tumours." Expert Opin Biol Ther 6: 243-255.

Ishizaki, Y., Ikeda, S., Fujimori, M., Shimizu, Y., Kurihara, T., Itamoto, T., Kikuchi, A., Okajima, M., Asahara, T. (2004). "Immunohistochemical analysis and mutational analyses of beta-catenin, Axin family and APC genes in hepatocellular carcinomas." Int J Oncol. 24: 1077-1083.

Itabashi, H., Maesawa, C., Oikawa, H., Kotani, K., Sakurai, E., Kato, K., Komatsu, H., Nitta, H., Kawamura, H., Wakabayashi, G., Masuda, T. (2008). "Angiotensin II and epidermal growth factor receptor cross-talk mediated by a disintegrin and metalloprotease accelerates tumor cell proliferation of hepatocellular carcinoma cell lines." Hepatol Res 38: 601-613.

Iusuf, D., Henning, R. H., van Gilst, W. H., Roks, A. J. (2008). "Angiotensin-(1-7): pharmacological properties and pharmacotherapeutic perspectives." Eur J Pharmacol 585: 303-312.

Jenniskens, G. J., Oosterhof, A., Brandwijk, R., Veerkamp, J. H., van Kuppevelt, T. H. (2000). "Heparan sulfate heterogeneity in skeletal muscle basal lamina: demonstration by phage display-derived antibodies." J Neurosci 20: 4099-4111.

Ji, J., Wang, X. W. (2012). "Clinical implications of cancer stem cell biology in hepatocellular carcinoma." Semin Oncol. 39: 461-472.

Jick, H., Jick, S., Derby, L. E., Vasilakis, C., Myers, M. W., Meier, C. R. (1997). "Calcium-channel blockers and risk of cancer." Lancet 349: 525-528.

Johnson, P. J., Qin, S., Park, J. W., Poon, R. T., Raoul, J. L., Philip, P. A., Hsu, C. H., Hu, T. H., Heo, J., Xu, J., Lu, L., Chao, Y., Boucher, E., Han, K. H., Paik, S. W., Robles-Avina, J., Kudo, M., Yan, L., Sobhonslidsuk, A., Komov, D., Decaens, T., Tak, W. Y., Jeng, L. B., Liu, D., Ezzeddine, R., Walters, I., Cheng, A. L. (2013). "Brivanib versus sorafenib as first-line therapy in patients with unresectable, advanced hepatocellular carcinoma: results from the randomized phase III BRISK-FL study." J Clin Oncol 31: 3517-3524.

Kalus, I., Salmen B, Viebahn C, von Figura K, Schmitz D, D'Hooge R, Dierks T. (2009). "Differential involvement of the extracellular 6-O-endosulfatases Sulf1 and

Sulf2 in brain development and neuronal and behavioural plasticity." J Cell Mol Med.13: 4505-4521.

Kan, M., Wang, F., Xu, J,. Crabb, J. W., Hou, J., McKeehan, W. L. (1993). "An essential heparin-binding domain in the fibroblast growth factor receptor kinase."Science.259: 1918-1921.

Kanai, F., Yoshida, H., Tateishi, R., Sato, S., Kawabe, T., Obi, S., Kondo, Y., Taniguchi, M., Tagawa, K., Ikeda, M., Morizane, C., Okusaka, T., Arioka, H., Shiina, S., Omata, M. (2011). "A phase I/II trial of the oral antiangiogenic agent TSU-68 in patients with advanced hepatocellular carcinoma." Cancer Chemother Pharmacol 67: 315-324.

Kane, R., Farrell, A. T., Madabushi, R., Booth, B., Chattopadhyay, S., Sridhara, R., Justice, R., Pazdur, R. (2009). "Sorafenib for the treatment of unresectable hepatocellular carcinoma."Oncologist.14: 95-100.

Kang, J. H., Rychahou, P. G., Ishola, T. A., Qiao, J., Evers, B. M., Chung, D. H. (2006). "MYCN silencing induces differentiation and apoptosis in human neuroblastoma cells." Biochem Biophys Res Commun 351: 192-197.

Kauffman, F., Whittaker, M., Anundi, I., Thurman, R. G. (1991). "Futile cycling of a sulfate conjugate by isolated hepatocytes."Mol Pharmacol.39: 414-420.

Keizman, D., Huang, P., Eisenberger, M. A., Pili, R., Kim, J. J., Antonarakis, E. S., Hammers, H., Carducci, M. A. (2011). "Angiotensin system inhibitors and outcome of sunitinib treatment in patients with metastatic renal cell carcinoma: a retrospective examination." Eur J Cancer 47: 1955-1961.

Kondo, Y., Kanai, Y., Sakamoto, M., Genda, T., Mizokami, M., Ueda, R., Hirohashi, S. (1999). "Beta-catenin accumulation and mutation of exon 3 of the beta-catenin gene in hepatocellular carcinoma." Jpn J Cancer Res. 90: 1301-1309.

Kim, S. Y., Yasuda, S., Tanaka, H., Yamagata, K., Kim, H. (2011). "Non-clustered protocadherin." Cell Adh Migr 5: 97-105.

Kono, T., Taniguchi, A., Imura, H., Oseko, F., Khosla, M. C. (1986). "Biological activities of angiotensin II-(1-6)-hexapeptide and angiotensin II-(1-7)-heptapeptide in man." Life Sci 38: 1515-1519.

Krishnan, B., Torti, F. M., Gallagher, P. E., Tallant, E. A. (2013 a). "Angiotensin-(1-7) reduces proliferation and angiogenesis of human prostate cancer xenografts

with a decrease in angiogenic factors and an increase in sFlt-1." Prostate 73: 60-70.

Krishnan, B., Smith, T. L., Dubey, P., Zapadka, M. E., Torti, F. M., Willingham, M. C., Tallant, E. A., Gallagher, P. E. (2013 b). "Angiotensin-(1-7) attenuates metastatic prostate cancer and reduces osteoclastogenesis." Prostate 73: 71-82.

Kulik, L. (2006). "Can therapy of hepatitis C affect the development of hepatocellular carcinoma?" J Natl Compr Canc Netw.4: 751-757.

Kunii, K., Davis, L., Gorenstein, J., Hatch, H., Yashiro, M., Di Bacco, A., Elbi, C., Lutterbach, B. (2008). "FGFR2-amplified gastric cancer cell lines require FGFR2 and Erbb3 signalling for growth and survival." Cancer Res. 68: 2340-2348.

Lai, J., Chien, J., Staub, J., Avula, R., Greene, E. L., Matthews, T. A., Smith, D. I., Kaufmann, S. H., Roberts, L. R., Shridhar, V. (2003). "Loss of HSulf-1 up-regulates heparin-binding growth factor signalling in cancer." J Biol Chem.278: 23107-23117.

Lai, J., Chien, J., Strome, S. E., Staub, J., Montoya, D. P., Greene, E. L., Smith, D. I., Roberts, L. R., Shridhar, V. (2004 a). "HSulf-1 modulates HGF-mediated tumor cell invasion and signalling in head and neck squamous carcinoma." Oncogene23: 1439-1447.

Lai, J., Chien, J. R., Moser, D. R., Staub, J. K., Aderca, I., Montoya, D. P., Matthews, T. A., Nagorney, D. M., Cunningham, J. M., Smith, D. I., Greene, E. L., Shridhar, V., Roberts, L. R. (2004 b). "hSulf1 Sulfatase promotes apoptosis of hepatocellular cancer cells by decreasing heparin-binding growth factor signalling." Gastroenterology.126: 231-248.

Lai, J., Yu, C., Moser, C. D., Aderca, I., Han, T., Garvey, T. D., Murphy, L. M., Garrity-Park, M. M., Shridhar, V., Adjei, A. A., Roberts, L. R. (2006). "SULF1 inhibits tumor growth and potentiates the effects of histone deacetylase inhibitors in hepatocellular carcinoma." Gastroenterology.130: 2130-2144.

Lai, J., Sandhu, D. S., Yu, C., Han, T., Moser, C. D., Jackson, K. K., Guerrero, R. B., Aderca, I., Isomoto, H., Garrity-Park, M. M., Zou, H., Shire, A. M., Nagorney, D. M., Sanderson, S. O., Adjei, A. A., Lee, J. S., Thorgeirsson, S. S., Roberts, L. R. (2008 a). "Sulfatase 2 up-regulates glypican 3, promotes fibroblast growth factor signalling, and decreases survival in hepatocellular carcinoma." Hepatology47: 1211-1222.

Lai, J., Sandhu, D. S., Shire, A. M., Roberts, L. R.(2008 b)."The tumor suppressor function of human sulfatase 1 (SULF1) in carcinogenesis."J Gastrointest Cancer.39: 149-158.

Lai, J., Thompson, J. R., Sandhu, D. S., Roberts, L. R. (2008 c). "Heparin-degrading sulfatases in hepatocellular carcinoma: roles in pathogenesis and therapy targets." Future Oncol.4: 803-814.

Lai, J., Sandhu, D. S., Yu, C., Moser, C. D., Hu, C., Shire, A. M., Aderca, I., Murphy, L. M., Adjei, A. A., Sanderson, S., Roberts, L. R. (2010 a). "Sulfatase 2 protects hepatocellular carcinoma cells against apoptosis induced by the PI3K inhibitor LY294002 and ERK and JNK kinase inhibitors." Liver Int.30: 1522-1528.

Lai, J., Oseini, A. M., Moser, C. D., Yu, C., Elsawa, S. F., Hu, C., Nakamura, I., Han, T., Aderca, I., Isomoto, H., Garrity-Park, M. M., Shire, A. M., Li, J., Sanderson, S. O., Adjei, A. A., Fernandez-Zapico, M. E., Roberts, L. R. (2010 b). "The oncogenic effect of sulfatase 2 in human hepatocellular carcinoma is mediated in part by glypican 3-dependent Wnt activation." Hepatology52: 1680-1689.

Lamanna, W., Kalus, I., Padva, M., Baldwin, R. J., Merry, C. L., Dierks, T. (2007). "The heparanome--the enigma of encoding and decoding heparan sulfate sulfation." J Biotechnol.129: 290-307.

Lamanna, W., Frese, M. A., Balleininger, M., Dierks, T. (2008). "Sulf loss influences N-, 2-O-, and 6-O-sulfation of multiple heparan sulfate proteoglycans and modulates fibroblast growth factor signalling." J Biol Chem.283: 27724-27735.

Landgrebe, J., Dierks, T., Schmidt, B., von Figura, K. (2003). "The human SUMF1 gene, required for posttranslational sulfatase modification, defines a new gene family which is conserved from pro- to eukaryotes." Gene316: 47-56.

Lang, L. (2008). "FDA approves sorafenib for patients with inoperable liver cancer." Gastroenterology.134: 379.

Larrinaga, G., Perez, I., Sanz, B., Blanco, L., Lopez, J. I., Candenas, M. L., Pinto, F. M., Gil, J., Irazusta, J., Varona, A. (2010). "Angiotensin-converting enzymes (ACE and ACE2) are downregulated in renal tumors." Regul Pept 165: 218-223.

Laurent-Puig, P., Zucman-Rossi, J. (2006). "Genetics of hepatocellular tumors." Oncogene. 25: 3778-3786.

Lee, J., Chu, I. S., Heo, J., Calvisi, D. F., Sun, Z., Roskams, T., Durnez, A., Demetris, A. J., Thorgeirsson, S. S. (2004). "Classification and prediction of survival in hepatocellular carcinoma by gene expression profiling."Hepatology40: 667-676.

Legoix, P., Bluteau, O., Bayer, J., Perret, C., Balabaud, C., Belghiti, J., Franco, D., Thomas, G., Laurent-Puig, P., Zucman-Rossi, J. (1999). "Beta-catenin mutations in hepatocellular carcinoma correlate with a low rate of loss of heterozygosity." Oncogene. 18: 4044-4046.

Lemjabbar-Alaoui, H., van Zante, A., Singer, M. S., Xue, Q., Wang, Y. Q., Tsay, D., He, B., Jablons, D. M., Rosen, S. D. (2010). "Sulf-2, a heparan sulfate endosulfatase, promotes human lung carcinogenesis." Oncogene29: 635-646.

Lever, A. F., Hole, D. J., Gillis, C. R., McCallum, I. R., McInnes, G. T., MacKinnon, P. L., Meredith, P. A., Murray, L. S., Reid, J. L., Robertson, J. W. (1998). "Do inhibitors of angiotensin-I-converting enzyme protect against risk of cancer?" Lancet 352: 179-184.

Li, J., Kleeff, J., Abiatari, I., Kayed, H., Giese, N. A., Felix, K., Giese, T., Büchler, M. W., Friess, H. (2005). "Enhanced levels of Hsulf-1 interfere with heparin-binding growth factor signalling in pancreatic cancer." Mol Cancer.4: 14.

Li, H., Qi, Y., Li, C., Braseth, L. N., Gao, Y., Shabashvili, A. E., Katovich, M. J., Sumners, C. (2009). "Angiotensin type 2 receptor-mediated apoptosis of human prostate cancer cells." Mol Cancer Ther 8: 3255-3265.

Liang, H., Chen, Q., Coles, A. H., Anderson, S. J., Pihan, G., Bradley, A., Gerstein, R., Jurecic, R., Jones, S. N. (2003). "Wnt5a inhibits B cell proliferation and functions as a tumor suppressor in hematopoietic tissue." Cancer Cell 4: 349-360.

Lingwood, D., Simons, K. (2010). "Lipid rafts as a membrane-organizing principle." Science327: 46-50.

Liu, C., Li, Y., Semenov, M., Han, C., Baeg, G. H., Tan, Y., Zhang, Z., Lin, X., He, X. (2002). "Control of beta-catenin phosphorylation/degradation by a dual-kinase mechanism." Cell. 108: 837-847.

Liu, X. H., Pan, M. H., Lu, Z. F., Wu, B., Rao, Q., Zhou, Z. Y., Zhou, X. J. (2008). "Expression of Wnt-5a and its clinicopathological significance in hepatocellular carcinoma." Dig Liver Dis 40: 560-567.

Liu, Y., Wu, F. (2010). "Global burden of aflatoxin-induced hepatocellular carcinoma: a risk assessment." Environ Health Perspect. 118: 818-824.

Liu, C. T., Zhu, S. T., Li, P., Wang, Y. J., Zhang, H., Zhang, S. T. (2013). "SULF1 inhibits proliferation and invasion of esophageal squamous cell carcinoma cells by decreasing heparin-binding growth factor signaling." Dig Dis Sci 58: 1256-1263.

Llovet, J., Ricci, S., Mazzaferro, V., Hilgard, P., Gane, E., Blanc, J. F., de Oliveira, A. C., Santoro, A., Raoul, J. L., Forner, A., Schwartz, M., Porta, C., Zeuzem, S., Bolondi, L., Greten, T. F., Galle, P. R., Seitz, J. F., Borbath, I., Häussinger, D., Giannaris, T., Shan, M., Moscovici, M., Voliotis, D., Bruix, J.; SHARP Investigators Study Group. (2008). "Sorafenib in advanced hepatocellular carcinoma."N Engl J Med.359: 378-390.

Lubel, J. S., Herath, C. B., Tchongue, J., Grace, J., Jia, Z., Spencer, K., Casley, D., Crowley, P., Sievert, W., Burrell, L. M., Angus, P. W. (2009). "Angiotensin-(1-7), an alternative metabolite of the renin-angiotensin system, is up-regulated in human liver disease and has antifibrotic activity in the bile-duct-ligated rat." Clin Sci (Lond). 117: 375-386.

Liu, C. J., Lee, P. H., Lin, D. Y., Wu, C. C., Jeng, L. B., Lin, P. W., Mok, K. T., Lee, W. C., Yeh, H. Z., Ho, M. C., Yang, S. S., Lee, C. C., Yu, M. C., Hu, R. H., Peng, C. Y., Lai, K. L., Chang, S. S., Chen, P. J. (2009). "Heparanase inhibitor PI-88 as adjuvant therapy for hepatocellular carcinoma after curative resection: a randomized phase II trial for safety and optimal dosage." J Hepatol 50: 958-968.

Lui, N. S., van Zante, A., Rosen, S. D., Jablons, D. M., Lemjabbar-Alaoui, H. (2012). "SULF2 expression by immunohistochemistry and overall survival in oesophageal cancer: a cohort study." BMJ Open. 2 (6). pii: e001624.

Lum, D. H., Tan, J., Rosen, S. D., Werb, Z. (2007). "Gene trap disruption of the mouse heparan sulfate 6-O-endosulfatase gene, Sulf2." Mol Cell Biol 27: 678-688.

Lund, P., Schubert, D., Niketeghad, F., Schirmacher, P. (2004). "Autocrine inhibition of chemotherapy response in human liver tumor cells by insulin-like growth factor-II." Cancer Lett 206: 85-96.

Machado, R. D., Santos, R. A., Andrade, S. P. (2001). "Mechanisms of angiotensin-(1-7)-induced inhibition of angiogenesis." Am J Physiol Regul Integr Comp Physiol 280: R994-R1000.

Mao, J., Wang, J., Liu, B., Pan, W., Farr, G. H., Flynn, C., Yuan, H., Takada, S., Kimelman, D., Li, L., Wu, D. (2001). "Low-density lipoprotein receptor-related protein-5 binds to Axin and regulates the canonical Wnt signalling pathway." Mol Cell. 7: 801-809.

Marques, F. D., Ferreira, A. J., Sinisterra, R. D., Jacoby, B. A., Sousa, F. B., Caliari, M. V., Silva, G. A., Melo, M. B., Nadu, A. P., Souza, L. E., Irigoyen, M. C., Almeida, A. P., Santos, R. A. (2011). "An oral formulation of angiotensin-(1-7) produces cardioprotective effects in infarcted and isoproterenol-treated rats." Hypertension 57: 477-483.

Mas, V. R., Maluf, D. G., Archer, K. J., Yanek, K. C., Fisher, R. A. (2007). "Angiogenesis soluble factors as hepatocellular carcinoma noninvasive markers for monitoring hepatitis C virus cirrhotic patients awaiting liver transplantation." Transplantation. 84: 1262-1271.

Meijer, L., Skaltsounis, A. L., Magiatis, P., Polychronopoulos, P., Knockaert, M., Leost, M., Ryan, X. P., Vonica, C. A., Brivanlou, A., Dajani, R., Crovace, C., Tarricone, C., Musacchio, A., Roe, S. M., Pearl, L., Greengard, P. (2003). "GSK-3-selective inhibitors derived from Tyrian purple indirubins." Chem Biol. 10: 1255-1266.

Menon, J., Soto-Pantoja, D. R., Callahan, M. F., Cline, J. M., Ferrario, C. M., Tallant, E. A., Gallagher, P. E. (2007). "Angiotensin-(1-7) inhibits growth of human lung adenocarcinoma xenografts in nude mice through a reduction in cyclooxygenase-2." Cancer Res 67: 2809-2815.

Merle, P., de la Monte, S., Kim, M., Herrmann, M., Tanaka, S., Von Dem Bussche, A., Kew, M. C., Trepo, C., Wands, J. R. (2004). "Functional consequences of frizzled-7 receptor overexpression in human hepatocellular carcinoma." Gastroenterology. 127: 1110-1122.

Mezzano, S. A., Ruiz-Ortega, M., Egido, J. (2001). "Angiotensin II and Renal Fibrosis." Hypertension 38: 635-638.

Millat, G., Froissart, R., Maire, I., Bozon, D. (1997). "IDS transfer from overexpressing cells to IDS-deficient cells." Exp Cell Res 230: 362-367.

Min, L., He, B., Hui, L. (2011). "Mitogen-activated protein kinases in hepatocellular carcinoma development." Semin Cancer Biol. 21: 10-20.

Mise, M., Arii, S., Higashituji, H., Furutani, M., Niwano, M., Harada, T., Ishigami, S., Toda, Y., Nakayama, H., Fukumoto, M., Fujita, J., Imamura, M. (1996). "Clinical significance of vascular endothelial growth factor and basic fibroblast growth factor gene expression in liver tumor." Hepatology 23: 455-464.

Mitsunaga-Nakatsubo, K., Kusunoki, S., Kawakami, H., Akasaka, K., Akimoto, Y. (2009). "Cell-surface arylsulfatase A and B on sinusoidal endothelial cells, hepatocytes, and Kupffer cells in mammalian livers." Med Mol Morphol. 42: 63-69.

Miura, S., Mitsuhashi, N., Shimizu, H., Kimura, F., Yoshidome, H., Otsuka, M., Kato, A., Shida, T., Okamura, D., Miyazaki, M. (2012). "Fibroblast growth factor 19 expression correlates with tumor progression and poorer prognosis of hepatocellular carcinoma." BMC Cancer. 12:56.

Miyoshi, Y., Ando, A., Hasegawa, S., Ishitobi, M., Taguchi, T., Tamaki, Y., Noguchi, S. (2003). "High expression of steroid sulfatase mRNA predicts poor prognosis in patients with estrogen receptor-positive breast cancer." Clin Cancer Res. 9: 2288-2293.

Mohammadi, M., Froum, S., Hamby, J. M., Schroeder, M. C., Panek, R. L., Lu, G. H., Eliseenkova, A. V., Green, D., Schlessinger, J., Hubbard, S. R. (1998). "Crystal structure of an angiogenesis inhibitor bound to the FGF receptor tyrosine kinase domain." EMBO J. 17: 5896-5904.

Mohammadi, M., Olsen, S. K., Ibrahimi, O. A. (2005). "Structural basis for fibroblast growth factor receptor activation."Cytokine Growth Factor Rev. 16: 107-137.

Morimoto-Tomita, M., Uchimura, K., Werb, Z., Hemmerich, S., Rosen, S. D. (2002)."Cloning and characterization of two extracellular heparin-degrading endosulfatases in mice and humans."J Biol Chem.277: 49175-49185.

Morimoto-Tomita, M., Uchimura, K., Bistrup, A., Lum, D. H., Egeblad, M., Boudreau, N., Werb, Z., Rosen, S. D. (2005). "Sulf-2, a proangiogenic heparan sulfate endosulfatase, is upregulated in breast cancer." Neoplasia.7: 1001-1010.

Myette, J. R., Soundararajan, V., Shriver, Z., Raman, R., Sasisekharan, R. (2009). "Heparin/heparan sulfate 6-O-sulfatase from Flavobacterium heparinum: integrated structural and biochemical investigation of enzyme active site and substrate specificity." J Biol Chem. 284: 35177-35188.

Nabeshima, Y., Tazuma, S., Kanno, K., Hyogo, H., Iwai, M., Horiuchi, M., Chayama, K. (2006). "Anti-fibrogenic function of angiotensin II type 2 receptor in CCl4-induced liver fibrosis." Biochem Biophys Res Commun 346: 658-664.

Nagamine, S., Keino-Masu, K., Shiomi, K., Masu, M. (2010). "Proteolytic cleavage of the rat heparan sulfate 6-O-endosulfatase SulfFP2 by furin-type proprotein convertases." Biochem Biophys Res Commun.391: 107-112.

Nagamine, S., Tamba, M., Ishimine, H., Araki, K., Shiomi, K., Okada, T., Ohto, T., Kunita, S., Takahashi, S., Wismans, R. G., van Kuppevelt, T. H., Masu, M., Keino-Masu, K. (2012). "Organ-specific sulfation patterns of heparan sulfate generated by extracellular sulfatases Sulf1 and Sulf2 in mice." J Biol Chem 287: 9579-9590.

Nakai, Y., Isayama, H., Ijichi, H., Sasaki, T., Sasahira, N., Hirano, K., Kogure, H., Kawakubo, K., Yagioka, H., Yashima, Y., Mizuno, S., Yamamoto, K., Arizumi, T., Togawa, O., Matsubara, S., Tsujino, T., Tateishi, K., Tada, M., Omata, M., Koike, K. (2010). "Inhibition of renin-angiotensin system affects prognosis of advanced pancreatic cancer receiving gemcitabine." Br J Cancer 103: 1644-1648.

Nakajima, M., Hutchinson, H. G., Fujinaga, M., Hayashida, W., Morishita, R., Zhang, L., Horiuchi, M., Pratt, R. E., Dzau, V. J. (1995). "The angiotensin II type 2 (AT2) receptor antagonizes the growth effects of the AT1 receptor: gain-of-function study using gene transfer." Proc Natl Acad Sci U S A 92: 10663-10667.

Nakanishi, K., Sakamoto, M., Yamasaki, S., Todo, S., Hirohashi, S. (2005). "Akt phosphorylation is a risk factor for early disease recurrence and poor prognosis in hepatocellular carcinoma." Cancer. 103: 307-312.

Naldini, L., Blömer, U., Gallay, P., Ory, D., Mulligan, R., Gage, F. H., Verma, I. M., Trono, D. (1996). "In vivo gene delivery and stable transduction of nondividing cells by a lentiviral vector." Science 272: 263-267.

Narita, K., Staub, J., Chien, J., Meyer, K., Bauer, M., Friedl, A., Ramakrishnan, S., Shridhar, V. (2006). "HSulf-1 inhibits angiogenesis and tumorigenesis in vivo." Cancer Res.66: 6025-6032.

Narita, K., Chien, J., Mullany, S. A., Staub, J., Qian, X., Lingle, W. L., Shridhar, V. (2007). "Loss of HSulf-1 expression enhances autocrine signalling mediated by amphiregulin in breast cancer." J Biol Chem.282: 14413-14420.

Nawroth, R., van Zante, A., Cervantes, S., McManus, M., Hebrok, M., Rosen, S. D. (2007). "Extracellular sulfatases, elements of the Wnt signalling pathway, positively

regulate growth and tumorigenicity of human pancreatic cancer cells." PLoS One.2: e392.

Ng, I. O., Poon, R. T., Lee, J. M., Fan, S. T., Ng, M., Tso, W. K. (2001). "Microvessel density, vascular endothelial growth factor and its receptors Flt-1 and Flk-1/KDR in hepatocellular carcinoma." Am J Clin Pathol. 116: 838-845.

Ni, L., Feng, Y., Wan, H., Ma, Q., Fan, L., Qian, Y., Li, Q., Xiang, Y., Gao, B. (2012). "Angiotensin-(1-7) inhibits the migration and invasion of A549 human lung adenocarcinoma cells through inactivation of the PI3K/Akt and MAPK signaling pathways." Oncol Rep 27: 783-790.

Nussbaumer, P., Geyl, D., Horvath, A., Lehr, P., Wolff, B., Billich, A. (2003). "Nortropinyl-arylsulfonylureas as novel, reversible inhibitors of human steroid sulfatase."Bioorg Med Chem Lett.13: 3673-3677.

Nusse, R. (2012). "Wnt signalling." Cold Spring Harb Perspect Biol. 4: pii: a011163.

Nuzzo, G., Giuliante, F., Gauzolino, R., Vellone, M., Ardito, F., Giovannini, I. (2007). "Liver resections for hepatocellular carcinoma in chronic liver disease: experience in an Italian centre." Eur J Surg Oncol.33: 1014-1018.

Oertel, M., Menthena, A., Chen, Y. Q., Teisner, B., Jensen, C. H., Shafritz, D. A. (2008). "Purification of fetal liver stem/progenitor cells containing all the repopulation potential for normal adult rat liver." Gastroenterology 134: 823-832.

Ohto, T., Uchida, H., Yamazaki, H., Keino-Masu, K., Matsui, A., Masu, M. (2002). "Identification of a novel nonlysosomal sulphatase expressed in the floor plate, choroid plexus and cartilage." Genes Cells.7: 173-185.

Oka, Y., Rozek, L. M., Czech, M. P. (1985). "Direct demonstration of rapid insulin-like growth factor II Receptor internalization and recycling in rat adipocytes. Insulin stimulates 125I-insulin-like growth factor II degradation by modulating the IGF-II receptor recycling process." J Biol Chem. 260: 9435-9442.

Okazaki, N., Takahashi, N., Kojima, S., Masuho, Y., Koga, H. (2002). "Protocadherin LKC, a new candidate for a tumor suppressor of colon and liver cancers, its association with contact inhibition of cell proliferation." Carcinogenesis 23: 1139-1148.

Osterreicher, C. H., Taura, K., De Minicis, S., Seki, E., Penz-sterreicher, M., Kodama, Y., Kluwe, J., Schuster, M., Oudit, G. Y., Penninger, J. M., Brenner, D. A. (2009). "Angiotensin-converting-enzyme 2 inhibits liver fibrosis in mice." Hepatology 50: 929-938.

Oudit, G. Y., Liu, G. C., Zhong, J., Basu, R., Chow, F. L., Zhou, J., Loibner, H., Janzek, E., Schuster, M., Penninger, J. M., Herzenberg, A. M., Kassiri, Z., Scholey, J. W. (2010). "Human recombinant ACE2 reduces the progression of diabetic nephropathy." Diabetes 59: 529-538.

Pahor, M., Guralnik, J. M., Salive, M. E., Corti, M. C., Carbonin, P., Havlik, R. J. (1996). "Do calcium channel blockers increase the risk of cancer?" Am J Hypertens 9: 695-699.

Paizis, G., Cooper, M. E., Schembri, J. M., Tikellis, C., Burrell, L. M., Angus, P. W. (2002). "Up-regulation of components of the renin-angiotensin system in the bile duct-ligated rat liver." Gastroenterology. 123: 1667-1676.

Paizis, G., Tikellis, C., Cooper, M. E., Schembri, J. M., Lew, R. A., Smith, A. I., Shaw, T., Warner, F. J., Zuilli, A., Burrell, L. M., Angus, P. W. (2005). "Chronic liver injury in rats and humans upregulates the novel enzyme angiotensin converting enzyme 2." Gut. 54: 1790-1796.

Pantoliano, M., Horlick, R. A., Springer, B. A., Van Dyk, D. E., Tobery, T., Wetmore, D. R., Lear, J. D., Nahapetian, A. T., Bradley, J. D., Sisk, W. P. (1994). "Multivalent ligand-receptor binding interactions in the fibroblast growth factor system produce a cooperative growth factor and heparin mechanism for receptor dimerization." Biochemistry.33: 10229-10248.

Pardo, O. E., Latigo, J., Jeffery, R. E., Nye, E., Poulsom, R., Spencer-Dene, B., Lemoine, N. R., Stamp, G. W., Aboagye, E. O., Seckl, M. J. (2009). "The fibroblast growth factor receptor inhibitor PD173074 blocks small cell lung cancer growth in vitro and in vivo." Cancer Res. 69: 8645-8651.

Parenti, G., Meroni, G., Ballabio, A. (1997). "The sulfatase gene family." Curr Opin Genet Dev. 7: 386-391.

Parkin, M., Bray, F., Ferlay, J., Pisani, P. (2005). "Global Cancer Statistics, 2002."CA Cancer J Clin55: 74–108.

Perrimon, N., Bernfield, M. (2000). "Specificities of heparan sulphate proteoglycans in developmental processes."Nature404: 725-728.

Petty, W. J., Miller, A. A., McCoy, T. P., Gallagher, P. E., Tallant, E. A., Torti, F. M. (2009). "Phase I and pharmacokinetic study of angiotensin-(1-7), an endogenous antiangiogenic hormone." Clin Cancer Res 15: 7398-7404.

Pez, F., Lopez, A., Kim, M., Wands, J. R., Fromentel, C. C., Merle, P. (2013). "Wnt signaling and hepatocarcinogenesis: molecular targets for the development of innovative anticancer drugs." J Hepatol.

Phillips, J. J., Huillard, E., Robinson, A. E., Ward, A., Lum, D. H., Polley, M. Y., Rosen, S. D., Rowitch, D. H., Werb, Z. (2012). "Heparan sulfate sulfatase SULF2 regulates PDGFRα signalling and growth in human and mouse malignant glioma." J Clin Invest. 10.1172: JCI58215.

Poirier, D., Ciobanu, L., Maltais, R. (1999)."Steriod sulfatase inhibitors."Expert Opin Ther Patents9: 1083-1099.

Polakis, P. (2012). "Wnt signalling in cancer." Cold Spring Harb Perspect Biol. 4: pii: a008052.

Polychronopoulos, P., Magiatis, P., Skaltsounis, A. L., Myrianthopoulos, V., Mikros, E., Tarricone, A., Musacchio, A., Roe, S. M., Pearl, L., Leost, M., Greengard, P., Meijer, L. (2004). "Structural basis for the synthesis of indirubins as potent and selective inhibitors of glycogen synthase kinase-3 and cyclin-dependent kinases." J Med Chem. 47: 935-946.

Pompili, M., Francica, G., Rapaccini, G. L. (2008). "Bridge treatments of hepatocellular carcinoma in cirrhotic patients submitted to liver transplantation." Dig Dis Sci.53: 2830-2831.

Pons, F., Varela, M., Llovet, J. M. (2005). "Staging systems in hepatocellular carcinoma." B (Oxford). 7: 35-41.

Poon, R. T., Ho, J. W., Tong, C. S., Lau, C., Ng, I. O., Fan, S. T. (2004). "Prognostic significance of serum vascular endothelial growth factor and endostatin in patients with hepatocellular carcinoma." Br J Surg. 91: 1354-1360.

Pye, D., Vives, R. R., Turnbull, J. E., Hyde, P., Gallagher, J. T. (1998). "Heparan sulfate oligosaccharides require 6-O-sulfation for promotion of basic fibroblast growth factor mitogenic activity." J Biol Chem.273: 22936-22942.

Pye, D., Vivès, R. R., Hyde, P., Gallagher, J. T. (2000). "Regulation of FGF-1 mitogenic activity by heparan sulfate oligosaccharides is dependent on specific

structural features: differential requirements for the modulation of FGF-1 and FGF-2." Glycobiology.10: 1183-1192.

Rao, C. N., Mohanam, S., Puppala, A., Rao, J. S. (1999). "Regulation of ProMMP-1 and ProMMP-3 activation by tissue factor pathway inhibitor-2/matrix-associated serine protease inhibitor." Biochem Biophys Res Commun 255: 94-98.

Ratzka, A., Kalus, I., Moser, M., Dierks, T., Mundlos, S., Vortkamp, A. (2008). "Redundant function of the heparan sulfate 6-O-endosulfatases Sulf1 and Sulf2 during skeletal development." Dev Dyn 237: 339-353.

Regimbeau, J., Colombat, M., Mognol, P., Durand, F., Abdalla, E., Degott, C., Degos, F., Farges, O., Belghiti, J. (2004). "Obesity and diabetes as a risk factor for hepatocellular carcinoma."Liver Transpl.10: S69-73.

Reya, T., Clevers, H. (2005). "Wnt signalling in stem cells and cancer." Nature 434: 843-850.

Reyes-Engel, A., Morcillo, L., Aranda, F. J., Ruiz, M., Gaitan, M. J., Mayor-Olea, A., Aranda, P., Ferrario, C. M. (2006). "Influence of gender and genetic variability on plasma angiotensin peptides." J Renin Angiotensin Aldosterone Syst 7: 92-97.

Ribes, J., Clèries, R., Esteban, L., Moreno, V., Bosch, F. X. (2008). "The influence of alcohol consumption and hepatitis B and C infections on the risk of liver cancer in Europe."J Hepatol.49: 233-242.

Rodgers, K. E., Oliver, J., diZerega, G. S. (2006). "Phase I/II dose escalation study of angiotensin 1-7 [A(1-7)] administered before and after chemotherapy in patients with newly diagnosed breast cancer." Cancer Chemother Pharmacol 57: 559-568.

Rosen, S., Lemjabbar-Alaoui, H. (2010). "Sulf-2: an extracellular modulator of cell signalling and a cancer target candidate." Expert Opin Ther Targets.14: 935-949.

Rusnati, M., Coltrini, D., Caccia, P., Dell'Era, P., Zoppetti, G., Oreste, P., Valsasina, B., Presta, M. (1994). "Distinct role of 2-O-, N-, and 6-O-sulfate groups of heparin in the formation of the ternary complex with basic fibroblast growth factor and soluble FGF receptor-1."Biochem Biophys Res Commun.203: 450-458.

Saad, O., Ebel, H., Uchimura, K., Rosen, S. D., Bertozzi, C. R., Leary, J. A. (2005). "Compositional profiling of heparin/heparan sulfate using mass spectrometry: assay for specificity of a novel extracellular human endosulfatase." Glycobiology.15: 818-826.

Sahin, F., Kannangai, R., Adegbola, O., Wang, J., Su, G., Torbenson, M. (2004). "mTOR and P70 S6 kinase expression in primary liver neoplasms." Clin Cancer Res. 10: 8421-8425.

Sallenave, J. M. (2010). "Secretory leukocyte protease inhibitor and elafin/trappin-2: versatile mucosal antimicrobials and regulators of immunity." Am J Respir Cell Mol Biol 42: 635-643.

Sangkhathat, S., Kusafuka, T., Miao, J., Yoneda, A., Nara, K., Yamamoto, S., Kaneda, Y., Fukuzawa, M. (2006). "In vitro RNA interference against beta-catenin inhibits the proliferation of pediatric hepatic tumors." Int J Oncol. 28: 715-722.

Santos, R. A., Simoes e Silva, A. C., Maric, C., Silva, D. M., Machado, R. P., de Buhr, I., Heringer-Walther, S., Pinheiro, S. V., Lopes, M. T., Bader, M., Mendes, E. P., Lemos, V. S., Campagnole-Santos, M. J., Schultheiss, H. P., Speth, R., Walther, T. (2003). "Angiotensin-(1-7) is an endogenous ligand for the G protein-coupled receptor Mas." Proc Natl Acad Sci U S A. 100(8258-63).

Sardiello, M., Annunziata, I., Roma, G., Ballabio, A. (2005). "Sulfatases and sulfatase modifying factors: an exclusive and promiscuous relationship." Hum Mol Genet. 14: 3203-3217.

Satoh, S., Daigo, Y., Furukawa, Y., Kato, T., Miwa, N., Nishiwaki, T., Kawasoe, T., Ishiguro, H., Fujita, M., Tokino, T., Sasaki, Y., Imaoka, S., Murata, M., Shimano, T., Yamaoka, Y., Nakamura, Y. (2000). "AXIN1 mutations in hepatocellular carcinomas, and growth suppression in cancer cells by virus-mediated transfer of AXIN1." Nat Genet. 24: 245-250.

Schirmacher, P., Held, W. A., Yang, D., Chisari, F. V., Rustum, Y., Rogler, C. E. (1992). "Reactivation of insulin-like growth factor II during hepatocarcinogenesis in transgenic mice suggests a role in malignant growth." Cancer Res 52: 2549-2556.

Schmidt, B., Selmer, T., Ingendoh, A., von Figura, K. (1995). "A novel amino acid modification in sulfatases that is defective in multiple sulfatase deficiency." Cell. 82: 271-278.

Schmitz, K. J., Wohlschlaeger, J., Lang, H., Sotiropoulos, G. C., Malago, M., Steveling, K., Reis, H., Cicinnati, V. R., Schmid, K. W., Baba, H. A. (2008). "Activation of the ERK and AKT signalling pathway predicts poor prognosis in hepatocellular carcinoma and ERK activation in cancer tissue is associated with hepatitis C virus infection." J Hepatol. 48: 83-90.

Schütte, K., Bornschein J, Malfertheiner P. (2009). "Hepatocellular carcinoma--epidemiological trends and risk factors."Dig Dis.27: 80-92.

Schwarz-Romond, T., Fiedler, M., Shibata, N., Butler, P. J., Kikuchi, A., Higuchi, Y., Bienz, M. (2007). "The DIX domain of Dishevelled confers Wnt signalling by dynamic polymerization." Nat Struct Mol Biol. 14: 484-492.

Seeger, R. C., Brodeur, G. M., Sather, H., Dalton, A., Siegel, S. E., Wong, K. Y., Hammond, D. (1985). "Association of multiple copies of the N-myc oncogene with rapid progression of neuroblastomas." N Engl J Med 313: 1111-1116.

Shimamura, T., Saito, S., Morita, K., Kitamura, T., Morimoto, M., Kiba, T., Numata, K., Tanaka, K., Sekihara, H. (2000). "Detection of vascular endothelial growth factor and its receptor expression in human hepatocellular carcinoma biopsy specimens." J Gastroenterol Hepatol. 15: 640-646.

Simonetti, R., Liberati A, Angiolini C, Pagliaro L. (1997). "Treatment of hepatocellular carcinoma: a systematic review of randomized controlled trials." Ann Oncol.8: 117-136.

Smith, R. S., Wolfgang, M. C., Lory, S. (2004). "An adenylate cyclase-controlled signalling network regulates Pseudomonas aeruginosa virulence in a mouse model of acute pneumonia." Infect Immun. 72: 1677-1684.

Song, T. J., Eisenberg, D. P., Adusumilli, P. S., Hezel, M., Fong, Y. (2006). "Oncolytic herpes viral therapy is effective in the treatment of hepatocellular carcinoma cell lines." J Gastrointest Surg. 10: 532-542.

Soto-Pantoja, D. R., Menon, J., Gallagher, P. E., Tallant, E. A. (2009). "Angiotensin-(1-7) inhibits tumor angiogenesis in human lung cancer xenografts with a reduction in vascular endothelial growth factor." Mol Cancer Ther 8(6): 1676-1683.

Staples, G. O., Shi, X., Zaia, J. (2011). "Glycomics analysis of mammalian heparan sulfates modified by the human extracellular sulfatase HSulf2." PLoS One. 6: e16689.

Starley, B., Calcagno, C. J., Harrison, S. A. (2010). "Nonalcoholic fatty liver disease and hepatocellular carcinoma: a weighty connection." Hepatology51: 1820-1832.

Tanaka, N., Fukuzawa, M. (2008). "MYCN downregulates integrin alpha1 to promote invasion of human neuroblastoma cells." Int J Oncol 33: 815-821.

Tang, R., Rosen, S. D. (2009). "Functional consequences of the subdomain organization of the sulfs."J Biol Chem.284: 21505-21514.

Stassar, M. J., Devitt, G., Brosius, M., Rinnab, L., Prang, J., Schradin, T., Simon, J., Petersen, S., Kopp-Schneider, A., Zoller, M. (2001). "Identification of human renal cell carcinoma associated genes by suppression subtractive hybridization." Br J Cancer 85: 1372-1382.

Stein, C., Hille, A., Seidel, J., Rijnbout, S., Waheed, A., Schmidt, B., Geuze, H., von Figura, K. (1989). "Cloning and expression of human steroid-sulfatase.Membrane topology, glycosylation, and subcellular distribution in BHK-21 cells."J Biol Chem.264: 13865-13872.

Stoll, M., Steckelings, U. M., Paul, M., Bottari, S. P., Metzger, R., Unger, T. (1995). "The angiotensin AT2-receptor mediates inhibition of cell proliferation in coronary endothelial cells." J Clin Invest 95: 651-657.

Stovall, D. B., Wan, M., Zhang, Q., Dubey, P., Sui, G. (2012). "DNA vector-based RNA interference to study gene function in cancer." J Vis Exp. e4129.

Strawn, W. B., Ferrario, C. M., Tallant, E. A. (1999). "Angiotensin-(1-7) reduces smooth muscle growth after vascular injury." Hypertension 33: 207-211.

Sun, F. K., Fan, Y. C., Zhao, J., Zhang, F., Gao, S., Zhao, Z. H., Sun, Q., Wang, K. (2013). "Detection of TFPI2 methylation in the serum of hepatocellular carcinoma patients." Dig Dis Sci 58: 1010-1015.

Suzuki, Y., Ruiz-Ortega, M., Lorenzo, O., Ruperez, M., Esteban, V., Egido, J. (2003 a). "Inflammation and angiotensin II." Int J Biochem Cell Biol. 35: 881-900.

Suzuki, T., Nakata, T., Miki, Y., Kaneko, C., Moriya, T., Ishida, T., Akinaga, S., Hirakawa, H., Kimura, M., Sasano, H. (2003 b). "Estrogen sulfotransferase and steroid sulfatase in human breast carcinoma." Cancer Res. 63: 2762-2770.

Takagi, H., Sasaki, S., Suzuki, H., Toyota, M., Maruyama, R., Nojima, M., Yamamoto, H., Omata, M., Tokino, T., Imai, K., Shinomura, Y. (2008). "Frequent epigenetic inactivation of SFRP genes in hepatocellular carcinoma." J Gastroenterol. 43: 378-389.

Takakusaki, Y., Hisayasu, S., Hirai, Y., Shimada, T. (2005). "Coexpression of formylglycine-generating enzyme is essential for synthesis and secretion of functional arylsulfatase A in a mouse model of metachromatic leukodystrophy." Hum Gene Ther. 16: 929-936.

Tallant, E. A., Lu, X., Weiss, R. B., Chappell, M. C., Ferrario, C. M. (1997). "Bovine aortic endothelial cells contain an angiotensin-(1-7) receptor." Hypertension 29: 388-393.

Tallant, E. A., Clark, M. A. (2003). "Molecular mechanisms of inhibition of vascular growth by angiotensin-(1-7)." Hypertension. 42: 574-579.

Tallant, E. A., Ferrario, C. M., Gallagher, P. E. (2005). "Angiotensin-(1-7) inhibits growth of cardiac myocytes through activation of the mas receptor." Am J Physiol Heart Circ Physiol. 289: H1560-1566.

Tanaka, Y., Kanai, F., Tada, M., Asaoka, Y., Guleng, B., Jazag, A., Ohta, M., Ikenoue, T., Tateishi, K., Obi, S., Kawabe, T., Yokosuka, O., Omata, M. (2006). "Absence of PIK3CA hotspot mutations in hepatocellular carcinoma in Japanese patients." Oncogene. 25: 2950-2952.

Tanaka, M., Okabe, M., Suzuki, K., Kamiya, Y., Tsukahara, Y., Saito, S., Miyajima, A. (2009). "Mouse hepatoblasts at distinct developmental stages are characterized by expression of EpCAM and DLK1: drastic change of EpCAM expression during liver development." Mech Dev 126(8-9): 665-676.

Tang, W., Morgan, D. R., Meyers, M. O., Dominguez, R. L., Martinez, E., Kakudo, K., Kuan, P. F., Banet, N., Muallem, H., Woodward, K., Speck, O., Gulley, M. L. (2012). "Epstein-barr virus infected gastric adenocarcinoma expresses latent and lytic viral transcripts and has a distinct human gene expression profile." Infect Agent Cancer.

Taniguchi, K., Roberts, L. R., Aderca, I. N., Dong, X., Qian, C., Murphy, L. M., Nagorney, D. M., Burgart, L. J., Roche, P. C., Smith, D. I., Ross, J. A., Liu, W. (2002). "Mutational spectrum of beta-catenin, AXIN1, and AXIN2 in hepatocellular carcinomas and hepatoblastomas." Oncogene. 21: 4863-4871.

Tannapfel, A., Sommerer, F., Benicke, M., Katalinic, A., Uhlmann, D., Witzigmann, H., Hauss, J., Wittekind, C. (2003). "Mutations of the BRAF gene in cholangiocarcinoma but not in hepatocellular carcinoma." Gut. 52: 706-712.

Taura, K., Ikai, I., Hatano, E., Yasuchika, K., Nakajima, A., Tada, M., Seo, S., Machimoto, T., Uemoto, S. (2007). "Influence of coexisting cirrhosis on outcomes after partial hepatic resection for hepatocellular carcinoma fulfilling the Milan criteria: an analysis of 293 patients." Surgery.142: 685-694.

Teh, S., Christein, J., Donohue, J., Que, F., Kendrick, M., Farnell, M., Cha, S., Kamath, P., Kim, R., Nagorney, D. M. (2005). "Hepatic resection of hepatocellular carcinoma in patients with cirrhosis: Model of End-Stage Liver Disease (MELD) score predicts perioperative mortality." J Gastrointest Surg.9: 1207-1215.

Thomas, G. (2002). "Furin at the cutting edge: from protein traffic to embryogenesis and disease." Nat Rev Mol Cell Biol.3: 753-766.

Thomas, M., Jaffe, D., Choti, M. M., Belghiti, J., Curley, S., Fong, Y., Gores, G., Kerlan, R., Merle, P., O'Neil, B., Poon, R., Schwartz, L., Tepper, J., Yao, F., Haller, D., Mooney, M., Venook, A. (2010). "Hepatocellular carcinoma: consensus recommendations of the National Cancer Institute Clinical Trials Planning Meeting." J Clin Oncol.28: 3994-4005.

Thompson, M. D., Monga, S. P. (2007). "WNT/beta-catenin signalling in liver health and disease." Hepatology. 45: 1298-1305.

Thorgeirsson, S., Grisham, J. W. (2002). "Molecular pathogenesis of human hepatocellular carcinoma."Nat Genet. 31: 339-346.

Tipnis, S. R., Hooper, N. M., Hyde, R., Karran, E., Christie, G., Turner, A. J. (2000). "A human homolog of angiotensin-converting enzyme. Cloning and functional expression as a captopril-insensitive carboxypeptidase." J Biol Chem. 275: 33238-33243.

Tokita, H., Fukui, H., Tanaka, A., Kamitsukasa, H., Yagura, M., Harada, H., Okamoto, H. (2005). "Risk factors for the development of hepatocellular carcinoma among patients with chronic hepatitis C who achieved a sustained virological response to interferon therapy."J Gastroenterol Hepatol.20: 752-758.

Uchimura, K., Morimoto-Tomita, M., Bistrup, A., Li, J., Lyon, M., Gallagher, J., Werb, Z., Rosen, S. D. (2006 a). "HSulf-2, an extracellular endoglucosamine-6-sulfatase, selectively mobilizes heparin-bound growth factors and chemokines: effects on VEGF, FGF-1, and SDF-1." BMC Biochem.7: 2.

Uchimura, K., Morimoto-Tomita, M., Rosen, S. D. (2006 b)."Measuring the activities of the Sulfs: two novel heparin/heparan sulfate endosulfatases."Methods Enzymol.416: 243-253.

Uchimura, K., Lemjabbar-Alaoui, H., van Kuppevelt, T. H., Rosen, S. D. (2010). "Use of a phage display antibody to measure the enzymatic activity of the Sulfs."Methods Enzymol.480: 51-64.

Umbhauer, M., Djiane, A., Goisset, C., Penzo-Méndez, A., Riou, J. F., Boucaut, J. C., Shi, D. L. (2000). "The C-terminal cytoplasmic Lys-thr-X-X-X-Trp motif in frizzled receptors mediates Wnt/beta-catenin signalling." EMBO J. 19: 4944-4954.

Valenta, T., Lukas, J., Korinek, V. (2003). "HMG box transcription factor TCF-4's interaction with CtBP1 controls the expression of the Wnt target Axin2/Conductin in human embryonic kidney cells." Nucleic Acids Res 31: 2369-2380.

van Amerongen, R., Nusse, R. (2009). "Towards an integrated view of Wnt signalling in development." Development. 136: 3205-3214.

van der Knaap, R., Siemes, C., Coebergh, J. W., van Duijn, C. M., Hofman, A., Stricker, B. H. (2008). "Renin-angiotensin system inhibitors, angiotensin I-converting enzyme gene insertion/deletion polymorphism, and cancer: the Rotterdam Study." Cancer 112: 748-757.

van Diggelen, O. P., Zhao, H., Kleijer, W. J., Janse, H. C., Poorthuis, B. J., van Pelt, J., Kamerling, J. P., Galjaard, H. (1990). "A fluorimetric enzyme assay for the diagnosis of Morquio disease type A (MPS IV A)." Clin Chim Acta. 187: 131-139.

Veeman, M. T., Axelrod, J. D., Moon, R. T. (2003). "A second canon. Functions and mechanisms of beta-catenin-independent Wnt signalling." Dev Cell. 5: 367-377.

Vickers, C., Hales, P., Kaushik, V., Dick, L., Gavin, J., Tang, J., Godbout, K., Parsons, T., Baronas, E., Hsieh, F., Acton, S., Patane, M., Nichols, A., Tummino, P. (2002). "Hydrolysis of biological peptides by human angiotensin-converting enzyme-related carboxypeptidase." J Biol Chem 277: 14838-14843.

Villanueva, A., Chiang, D. Y., Newell, P., Peix, J., Thung, S., Alsinet, C., Tovar, V., Roayaie, S., Minguez, B., Sole, M., Battiston, C., Van Laarhoven, S., Fiel, M. I., Di Feo, A., Hoshida, Y., Yea, S., Toffanin, S., Ramos, A., Martignetti, J. A., Mazzaferro, V., Bruix, J., Waxman, S., Schwartz, M., Meyerson, M., Friedman, S.

L., Llovet, J. M. (2008). "Pivotal role of mTOR signaling in hepatocellular carcinoma." Gastroenterology. 135: 1972-1983.

Vlodavsky, I., Goldshmidt, O., Zcharia, E., Atzmon, R., Rangini-Guatta, Z., Elkin, M., Peretz, T., Friedmann, Y. (2002). "Mammalian heparanase: involvement in cancer metastasis, angiogenesis and normal development." Semin Cancer Biol. 12: 121-129.

Waaijer, C. J., de Andrea, C. E., Hamilton, A., van Oosterwijk, J. G., Stringer, S. E., Bovée, J. V. (2012). "Cartilage tumour progression is characterized by an increased expression of heparan sulphate 6O-sulphation-modifying enzymes." Virchows Arch. 461: 475-481.

Wang, N., Thuraisingam, T., Fallavollita, L., Ding, A., Radzioch, D., Brodt, P. (2006). "The secretory leukocyte protease inhibitor is a type 1 insulin-like growth factor receptor-regulated protein that protects against liver metastasis by attenuating the host proinflammatory response." Cancer Res 66: 3062-3070.

Wellcome Trust Sanger Institute. Catalogue of somatic mutations in cancer (COSMIC) database http://www.sanger.ac.uk/genetics/CGP/cosmic/. Accessed 1 August 2013.

Wen, J., Nikitakis, N. G., Chaisuparat, R., Greenwell-Wild, T., Gliozzi, M., Jin, W., Adli, A., Moutsopoulos, N., Wu, T., Warburton, G., Wahl, S. M. (2011). "Secretory leukocyte protease inhibitor (SLPI) expression and tumor invasion in oral squamous cell carcinoma." Am J Pathol 178: 2866-2878.

Whittaker, S., Marais, R., Zhu, A. X. (2010). "The role of signaling pathways in the development and treatment of hepatocellular carcinoma." Oncogene. 29: 4989-5005.

Wild, C., Gong, Y. Y. (2010). "Mycotoxins and human disease: a largely ignored global health issue." Carcinogenesis31: 71-82.

Willemsen, R., Kroos, M., Hoogeveen, A. T., van Dongen, J. M., Parenti, G., van der Loos, C. M., Reuser, A. J. (1988). "Ultrastructural localization of steroid sulphatase in cultured human fibroblasts by immunocytochemistry: a comparative study with lysosomal enzymes and the mannose 6-phosphate receptor." Histochem J.20: 41-51.

Willert, K., Nusse, R. (1998). "Beta-catenin: a key mediator of Wnt signalling." Curr Opin Genet Dev. 8: 95-102.

Williams, S. E., Brown, T. I., Roghanian, A., Sallenave, J. M. (2006). "SLPI and elafin: one glove, many fingers." Clin Sci (Lond) 110: 21-35.

Wilop, S., von Hobe, S., Crysandt, M., Esser, A., Osieka, R., Jost, E. (2009). "Impact of angiotensin I converting enzyme inhibitors and angiotensin II type 1 receptor blockers on survival in patients with advanced non-small-cell lung cancer undergoing first-line platinum-based chemotherapy." J Cancer Res Clin Oncol 135: 1429-1435.

Wong, H. C., Bourdelas, A., Krauss, A., Lee, H. J., Shao, Y., Wu, D., Mlodzik, M., Shi, D. L., Zheng, J. (2003). "Direct binding of the PDZ domain of Dishevelled to a conserved internal sequence in the C-terminal region of Frizzled." Mol Cell. 12: 1251-1260.

Wong, C. M., Ng, Y. L., Lee, J. M., Wong, C. C., Cheung, O. F., Chan, C. Y., Tung, E. K., Ching, Y. P., Ng, I. O. (2007). "Tissue factor pathway inhibitor-2 as a frequently silenced tumor suppressor gene in hepatocellular carcinoma." Hepatology 45: 1129-1138.

Workman, P., Twentyman, P., Balkwill, F., Balmain, A., Chaplin, D., Double, J., Embleton, J., Newell, D., Raymond, R., Stables, J., Stephens, T. and Wallace, J. (1998) 'United Kingdom Co-ordinating Committee on Cancer Research (UKCCCR) Guidelines for the Welfare of Animals in Experimental Neoplasia (Second Edition).', Br J Cancer, 77, pp. 1-10.

Wu, J. D., Hsueh, H. C., Huang, W. T., Liu, H. S., Leung, H. W., Ho, Y. R., Lin, M. T., Lai, M. D. (1997). "The inducible lactose operator-repressor system is functional in the whole animal." DNA Cell Biol. 16: 17-22.

Wu, G., He, X. (2006). "Threonine 41 in beta-catenin serves as a key phosphorylation relay residue in beta-catenin degradation." Biochemistry. 45: 5319-5323.

Wu, J., Zhu, A. X. (2011). "Targeting insulin-like growth factor axis in hepatocellular carcinoma." J Hematol Oncol. 4:30.

Wysocki, J., Ye, M., Rodriguez, E., Gonzalez-Pacheco, F. R., Barrios, C., Evora, K., Schuster, M., Loibner, H., Brosnihan, K. B., Ferrario, C. M., Penninger, J. M., Batlle, D. (2010). "Targeting the degradation of angiotensin II with recombinant angiotensin-converting enzyme 2: prevention of angiotensin II-dependent hypertension." Hypertension 55: 90-98.

Xu, Y., Qin, X., Zhou, J., Tu, Z., Bi, X., Li, W., Fan, X., Zhang, Y. (2011). "Tissue factor pathway inhibitor-2 inhibits the growth and invasion of hepatocellular carcinoma cells and is inactivated in human hepatocellular carcinoma." Oncol Lett 2: 779-783.

Xu, X., Liu, R. F., Zhang, X., Huang, L. Y., Chen, F., Fei, Q. L., Han, Z. G. (2012). "DLK1 as a potential target against cancer stem/progenitor cells of hepatocellular carcinoma." Mol Cancer Ther 11: 629-638.

Yamada, T., De Souza, A. T., Finkelstein, S., Jirtle, R. L. (1997). "Loss of the gene encoding mannose 6-phosphate/insulin-like growth factor II receptor is an early event in liver carcinogenesis." Proc Natl Acad Sci U S A. 94: 10351-10355.

Yanai, H., Nakamura, K., Hijioka, S., Kamei, A., Ikari, T., Ishikawa, Y., Shinozaki, E., Mizunuma, N., Hatake, K., Miyajima, A. (2010). "Dlk-1, a cell surface antigen on foetal hepatic stem/progenitor cells, is expressed in hepatocellular, colon, pancreas and breast carcinomas at a high frequency." J Biochem 148: 85-92.

Yang, L., Bataller, R., Dulyx, J., Coffman, T. M., Gines, P., Rippe, R. A., Brenner, D. A. (2005). "Attenuated hepatic inflammation and fibrosis in angiotensin type 1a receptor deficient mice." J Hepatol 43: 317-323.

Yang, J. D., Sun, Z., Hu, C., Lai, J., Dove, R., Nakamura, I., Lee, J. S., Thorgeirsson, S. S., Kang, K. J., Chu, I. S., Roberts, L. R. (2011). "Sulfatase 1 and sulfatase 2 in hepatocellular carcinoma: associated signaling pathways, tumor phenotypes, and survival." Genes Chromosomes Cancer 50: 122-135.

Yu, F., Hao, X., Zhao, H., Ge, C., Yao, M., Yang, S., Li, J. (2010). "Delta-like 1 contributes to cell growth by increasing the interferon-inducible protein 16 expression in hepatocellular carcinoma." Liver Int 30: 703-714.

Yuzugullu, H., Benhaj, K., Ozturk, N., Senturk, S., Celik, E., Toylu, A., Tasdemir, N., Yilmaz, M., Erdal, E., Akcali, K. C., Atabey, N., Ozturk, M. (2009). "Canonical Wnt signaling is antagonized by noncanonical Wnt5a in hepatocellular carcinoma cells." Mol Cancer 8: 90.

Zhang, L., Wang, J. N., Tang, J. M., Kong, X., Yang, J. Y., Zheng, F., Guo, L. Y., Huang, Y. Z., Zhang, L., Tian, L., Cao, S. F., Tuo, C. H., Guo, H. L., Chen, S. Y. (2012). "VEGF is essential for the growth and migration of human hepatocellular carcinoma cells." Mol Biol Rep. 39: 5085-5093.

Zheng, X., Gai, X., Han, S., Moser, C. D., Hu, C., Shire, A. M., Floyd, R. A., Roberts, L. R. (2013). "The human sulfatase 2 inhibitor 2,4-disulfonylphenyl-tert-butylnitrone (OKN-007) has an antitumor effect in hepatocellular carcinoma mediated via suppression of TGFB1/SMAD2 and Hedgehog/GLI1 signaling." Genes Chromosomes Cancer. 52: 225-236.

Zhou, L., Zhang, R., Yao, W., Wang, J., Qian, A., Qiao, M., Zhang, Y., Yuan, Y. (2009). "Decreased expression of angiotensin-converting enzyme 2 in pancreatic ductal adenocarcinoma is associated with tumor progression." Tohoku J Exp Med 217: 123-131.

Zhou, Q., Lui, V. W., Yeo, W. (2011 a). "Targeting the PI3K/Akt/mTOR pathway in hepatocellular carcinoma." Future Oncol. 7: 1149-1167.

Zhou, L., Zhang, R., Zhang, L., Yao, W., Li, J., Yuan, Y. (2011 b). "Angiotensin-converting enzyme 2 acts as a potential molecular target for pancreatic cancer therapy." Cancer Lett 307: 18-25.

Zhu, N. L., Asahina, K., Wang, J., Ueno, A., Lazaro, R., Miyaoka, Y., Miyajima, A., Tsukamoto, H. (2012). "Hepatic stellate cell-derived delta-like homolog 1 (DLK1) protein in liver regeneration." J Biol Chem 287: 10355-10367.

Zufferey, R., Donello, J. E., Trono, D., Hope, T. J. (1999). "Woodchuck hepatitis virus posttranscriptional regulatory element enhances expression of transgenes delivered by retroviral vectors." J Virol. 73: 2886-2892.